SACLANTCEN CONFERENCE PROCEEDINGS SERIES CP-44

E. Pouliquen - A.D. Kirwan, Jr - R.T. Pearson - editors

Rapid Environmental Assessment

NATO SACLANT Undersea Research Centre

Rapid Environmental Assessment

SACLANTCEN Conference Proceeding CP – 44

Rapid Environmental Assessment

edited by

E. Pouliquen

SACLANT Undersea Research Centre, La Spezia, Italy

A.D. Kirwan, jr

Old Dominion University, Norfolk, VA

R.T. PEARSON

SACLANT, Norfolk, VA

NATO SACLANT Undersea research Centre
La Spezia, Italy

Proceedings of the conference on rapid environmental assessment, Lerici, Italy, 10-14 March 1997, organized and sponsored by:

NATO SACLANT Undersea Research Centre, La Spezia, Italy.

Office of Naval Research, Washington, D.C., U.S.A.

Old Dominion University, Norfolk, Virginia, U.S.A.

Supreme Allied Command, (SACLANT), Norfolk, Virginia, U.S.A.

Published by: NATO SACLANT Undersea Research Centre,
Viale San Bartolomeo 400,
19138 La Spezia, Italy.

email: library@saclantc.nato.int
Fax: +39 187 524 600

Distribution:

Requests for copies in the United Kingdom of Great Britain and Northern Ireland should be forwarded to:

Code 400
Office of Naval Research, European Office,
Edison House
223-231 Old Marylebone Road, London, NW1 5TH

Requests for copies in the United States should be forwarded to:

Office of Naval Research
United States National Liaison Officer (USNLO) to SACLANTCEN
800 North Quincy Street
Arlington VA 22217-5660
USA

British Library Cataloguing in Publication Data

A catalogue record for this book is available from the British Library.

Cataloguing in publication data:

Rapid environmental assessment
edited by Eric Pouliquen 1967-, Albert Denny Kirwan, jr and Robert Thomas Pearson
p. 24.5 cm.
Proceedings of a conference held in Lerici, (SP) Italy, 10-14 March 1997.
(SACLANTCEN Conference Proceedings Series CP-44)
ISBN 88-900194-0-9.

Contents

Preface

This volume contains the 43 papers presented at the conference on Rapid Environmental Assessment organized and sponsored jointly by the NATO SACLANT Undersea Research Centre, Old Dominion University, SACLANT and the U.S. Office of Naval Research.

The conference was held in the Villa Marigola in Lerici, Italy in March 1997 and attended by 100 scientists and senior naval officers.

The conference organizers would like to thank the following members of SACLANTCEN staff for their contributions to the success of the conference.

Claudio Di Prisa, Francesco Faggioni, Rosanna Giglione Gabrielli, Sabrina Matteuci, Francesco Serafini and Ferda Turgutcan.

E. Pouliquen
A.D. Kirwan
R.T. Pearson

Executive Summary

Introduction

The origins of *Rapid Environmental Assessment* (REA) lie in NATO's post-Cold War shift in military focus towards regional crisis response operations. NATO Maritime Forces are now likely to be the lead elements for any NATO involvement in crisis due to their inherent mobility. The uncertainty in the present strategic climate means that these forces may have little advance notice of the location, time or nature of the operation.

Conducting crisis response operations, possibly beyond the normal NATO areas of responsibility, has fundamentally changed the nature of Military Oceanographic (MILOC) support requirements. Future support must provide detailed and accurate information, in near real-time, to Operational Commanders preparing to deploy maritime forces, on short notice, into highly variable coastal waters that are not well known and may pose a significant threat.

In 1995 the Supreme Allied Commander, Atlantic (SACLANT) identified REA as a new Underwater Warfare operational requirement. This statement identified the Commander's requirement for a capability to accurately determine key features of the maritime littoral environment prior to NATO forces entering coastal operating areas. Responding to this requirement, SACLANT Undersea Research Centre designated REA as one of its five research Thrust Areas.

In that same year the NATO Group on Military Oceanography (NATO MILOC Group) agreed to focus on testing and evaluating REA during its next three MILOC Surveys, 1996-98. These surveys, Rapid Response 96, 97 and 98, were organized by the MILOC Group as a collaborative effort involving NATO maritime nations, commands and SACLANTCEN. The purpose of the surveys was to test emerging REA systems and procedures in an operational setting by employing the new capabilities to support NATO forces during military exercises.

As part of a cooperative investigation into areas of common interest, the Supreme Allied Commander, Atlantic (SACLANT) and Old Dominion University's Center for Coastal Physical Oceanography determined that an equivalent interest in REA exists in the civilian oceanographic community. A wide range of academic, business and government agencies have a growing requirement for near real-time monitoring of coastal areas, primarily for environmental protection and prediction.

Further investigation into this topic disclosed an array of initiatives currently underway on various aspects of REA. SACLANT and Old Dominion University agreed that a jointly sponsored conference co-hosted by SACLANTCEN and the Center for Coastal Physical Oceanography would provide an excellent forum for evaluating these initiatives. This conference will analyze current programs, define present status and propose future development of REA.

In his opening remarks to conference participants, Vice Admiral Ian Garnett, RN, Deputy SACLANT, challenged participants to produce a plan of action describing the way ahead for REA by addressing key questions such as:

- What are the most critical shortfalls in current capabilities and how do we make good the shortfalls?
- Which topic areas are most promising for future research?
- What new organizational structures must be created to implement REA?
- What is achievable now with our current technological capabilities?

Following the conference, a sub-committee of participants evaluated the results of the proceedings and prepared the following summaries addressing the Admiral's key issues as they relate to four principal REA functional areas:

- Assimilation and Modeling
- Measurement Systems
- Remote Sensing
- Geographic Information Systems

Assimilation and modelling

Albert D. Kirwan, Jr., Allan R. Robinson

Introduction

The three pillars of REA are data collection, data synthesis and assessment, and timely dissemination of assessment products to action groups. Assimilation and modeling methodologies are critical for successful synthesis and assessment. Although concern here is synthesis and assessment, it is important to note that these three components must not be viewed in isolation. In fact, the concept of an overall system for REA nowcasts and forecasts is essential. The system components are an observational network, a set of dynamical models, and a data assimilation scheme. The first effort to fuse these components into an environmental assessment in an operational setting was the NATO exercise RAPID RESPONSE 96. This exercise established that useful environmental assessments are now possible for some coastal and shallow water crisis response operations.

Two important perspectives on data synthesis and assessment for REA emerged from the conference. One was the realisation that environmental assessment requires physical, chemical and biological data. All environmental data can contribute to nowcasts or forecasts of specific variables such as currents or sound velocity. Environmental assessment truly is interdisciplinary.

The second issue brought out at the conference was the emergence of nowcasts, or dynamically adjusted melded data estimates, as an important product of rapid environmental assessment. Unprecedented quantities of high resolution data, such as obtained from HF radar, SAR, and passive remote sensing, now are required for many situations. The spatial resolution of these data may be finer than what is provided by existing nowcast and forecast models. Optimal blending of such data with models to provide useful products in operations will be one of the major challenges in coming years.

What are the most critical shortfalls in current capabilities and how do we make good the shortfalls?

Three critical shortfalls emerged from the conference. Perhaps the most urgent is for rapid nowcasts and forecasts of wave, current and bottom geotechnical properties in the vicinity of the surf zone and in the presence of tides. This will require developing methods to use HF radar, SAR, and optical data effectively. The second is to blend disparate data including biological and chemical data with nowcast and forecast models in an optimal fashion. Finally there is a need to further develop and automate adaptive sampling strategies.

Which topic areas are most promising for future research?

Four promising areas of research were identified at the conference. One is to continue development of methodologies that blend physical, acoustical, optical, biological and chemical data with dynamic models. The second is to develop methods to infer subsurface conditions from high resolution surface data. The third is to classify generic processes important in coastal and estuarine nowcasts and forecasts. Finally, comparative studies of coastal regions need to be made to identify dominant processes and to develop simplified models for these processes that could be used in data interpretation and assimilation. Important methodologies include the use of deterministic and statistical feature models and the carrying out of Observational System Simulation Experiments (OSSEs).

What new organizational structures must be created to implement REA?

Two permanent organisations are recommended. One is an oversight group whose function would be to monitor problems in data synthesis and assessment that arise during operations, and emerging technologies that could have an impact on REA. This body should establish standards and qualifications for procedures for operations. This group would also serve as an interface between the military users and those making the assessments. The other organisation would be a permanent data synthesis and assessment team with state of the art technology available on short notice.

What is achievable now with our current technological capabilities?

Successful nowcasts and forecasts for currents, sound speed, and density structure seaward of the surf zone in operational scenarios have been made. Application now of existing scientific knowledge and technical methodologies to the construction of an advanced REA overall system would lead to improved accuracy, efficiency and rapid deployability.

Measurement systems

Henrik Schmidt

Introduction

The general consensus of the REA conference can be summarized as follows:

- The increased emphasis on shallow water environmental assessment is associated with increased significance of small spatial scales and short time scales which were of no or little significance in the deeper ocean problem. Consequently, **high-resolution** and rapid data collection and **real-time analysis** has become extremely critical.
- The shallow water assessment problem cannot be addressed isolated as an environmental sampling problem. The ocean environment will always remain **under sampled** both spatially and temporally, and the measurements have to be interpolated without violating the fundamental physics of the ocean dynamics. The environmental assessment must therefore be performed by assimilating the data collected into accurate dynamical models.
- The environmental assessment is highly dependent on adequate sampling of the ocean measurements. Thus, accurate shallow water environmental assessment requires measurements at **multiple scales**, ranging from basin-wide circulation estimates to mapping of near-shore phenomena currents and fronts. Consequently, the measurement system must properly weigh the conflicting requirements to coverage and resolution. 'Layered' measurement systems covering all scales of significance must be operated in concert, to allow optimal environmental assessment through data assimilation and modeling.
- The **resources** will always be limited, and the combined measurement and modeling observation systems must take optimal advantage of their now-casting and fore-casting capabilities to provide feed-back to the measurement platforms to allow **adaptive** environmental sampling.
- The **technology** and **expertise** exists for developing fully integrated measurement and modeling systems. However, the solution requires a truly multi-disciplinary research and development effort, involving both *vertical integration* between basic ocean science and applied modeling and technology development, and *horizontal integration* between several science and technology disciplines. For example, the ocean physicists and numerical modelers must work closely with the sensor and measurement platform developers on designing adaptive sampling strategies which are optimal for the environmental assessment through assimilation. In terms of vertical integration, the scientists and system developers must work closely with the end-user to take advantage of the full potential of today measurement and communication technology within the context of operational environment.

What are the most critical shortfalls in current capabilities and how do we make good the shortfalls?

The most critical shortfall in current capability is a totally inadequate predictive capability for shallow and littoral environments. Thus, the theoretical performance limits for naval sonars and underwater communication systems are far from being reached in such environment due to lack of predictive skills. High-resolution sonar concepts and communication procedures are totally reliable on highly accurate and stable environmental estimates. The environment sensors and sensor systems used today are totally inadequate in this regard, both in terms of spatial and temporal resolution, as well as coverage.

How do we make good of the shortfalls?

The only viable solution is to develop an environmental observation systems which integrates environmental modeling directly with the sensors and measurement platforms to allow accurate now-and fore-casting through a synergy of **adaptive environmental sampling** and data **assimilation and modeling**. Such a new littoral observation paradigm shall include a wide spectrum of sensors, including acoustic, biological, chemical and other oceanographic sensors. Also, a synergy of platform technologies must be achieved, taking advantage of

new developments in small expendable sensor platforms, and inexpensive Autonomous Underwater Vehicle (AUV) technology. The latter, in particular as developed within the Autonomous Ocean Sampling Network (AOSN) paradigm is ideally suited for the adaptive sampling strategy which is a key to optimal environmental assessment with limited resources.

Which topic areas are most promising for future research?

The most critical first step towards achieving such an REA capability is to develop an infrastructure for data interchange between the measurement system and the various dynamical models, and for providing the real-time processing capability which is needed to successfully integrate the adaptive sampling on littoral environmental scales. The infrastructure shall take advantage in recent advances in communication technology and geographical information systems.

Another area where research is needed is adaptive sampling technologies using a synergy of different ocean sensor systems. An example is Acoustically Focused Ocean Sampling which uses acoustic tomography to provide a low-resolution environmental estimate which is then being used to adaptively deploy small AUV's with various oceanographic sensors to regions of high uncertainty or critical importance to the environmental assessment.

Acoustic communication is critical for adaptive sampling by underwater vehicles and expendable sensors. During the last decade significant progress has been made in regard to such systems operating in deep water. However, the temporal variability in littoral environments often makes such state-of-the-art technology virtually useless. For littoral observation systems, robust communication concepts and systems should be developed. **Robustness** is far more critical for such systems than **bit-rate**.

What new organizational structures must be created to implement REA?

The development of the information infrastructure crucial to the development of littoral REA systems should be guided by a multidisciplinary committee with participation of ocean scientists, underwater acousticians, numerical modelers, information technology specialists, platform/vehicle and sensor developers, and finally but not least, the various levels of end-users and operators.

This committee should provide guidance to the various communities, and facilitate the vertical and horizontal integration, e.g. by organizing regular workshops and symposia similar to REA-97.

What is available now with our current technological capabilities?

The various technologies for developing the combined measurement and modeling systems, with the potential of taking littoral environmental assessment one major step forward within the next decade. The most critical component missing is the development of the **infrastructure**. Another critical obstacle is **tradition**, both among scientists, and among the operators. If these obstacles can be overcome, all components are in place for vastly improving the littoral predictive capability which is so critical to operation of naval systems, but also to many civilian applications such as fisheries and coastal environmental management.

Remote sensing executive summary

Farid Askari, R. Mied

What are the most critical shortfalls in current capabilities and how do we make good the shortfalls?

The most critical current shortfall lies with the operator/warfighter capabilities in the areas of at-sea communication and processing power. While the current data fusion centers and laboratories posses adequate capabilities, the at-sea capabilities are limited in terms of data reception, visualization and user interactions. The cheapest and most versatile approach is to upgrade the processing capabilities of the fleet with PC-based hardware/software and to improve at-sea communications with portable down-link/LAN-based antennas.

Which topic areas are most promising for future research?

With the advent of new sensor technologies such as multifrequency/polarimetric SAR and hyper-spectral sensing, the volume of data available to the end-user is increasing substantially. Future research in remote sensing should be directed in the areas of data compression and automatic feature recognition. Data compression techniques are needed for maintaining information content during transmission while reducing the data bandwidth requirements. Automatic feature/pattern recognition techniques are necessary to aid the user in browsing through large volumes of data and to rapidly select and assess the desired information. Research should also be focused on deriving spatial/spectral signatures for oceanographic/atmospheric phenomena in the Littoral zone that can be automatically coupled to dynamical "feature models". In principle, our experience has shown that the synergistic use of more than one type of data field (e.g., SAR and AVHRR) can greatly reduce ambiguity in identifying the physics underlying a remote sensing signature. Using this approach, tactical decision aids can be assembled rapidly in denied regions using a host of feature models and remotely sensed signatures.

What new organizational structures must be created to implement REA?

A formal organizing body is needed to interface with the user community and data suppliers and to decide on formatting standards, data exchange, and data availability. Ideally, this organizing body would also provide "Value added" in the form of tactical decision aids resulting from the fusion of models and multiple data streams.

What is achievable now with our current technological capabilities?

Current spaceborne/airborne scatterometer techniques are capable of measuring the marine wind vector to +- 2m/s and +- 5 degrees. In the littoral environment however, wind stress is commonly observed to vary spatially by a factor of ten over the area, and semidiurnal variation of the magnitude and direction are the frequently observed. The spatial/temporal sampling required of the wind stress is thus incompatible with various fields obtained by other sensors. Because of this spatial/temporal variability of the wind field in the coastal environment, remotely sensed measurements must be coupled with in situ measurements in order to provide a comprehensive picture of the wind field. The most direct approach for spaceborne /airborne remote measurement of surface currents is via the Interferometric SAR (INSAR) technique. However, INSAR has been flown only a few times in space, and current capabilities are limited primarily to airborne platforms. Satellite altimeters have proven capabilities in measuring large-scale ocean currents, but their utility in the measuring coastal currents remains an open research topic. The reasons for this are that their relatively coarse resolution and spotty coverage immediately adjacent to land greatly reduce their utility in the littoral zone. This shortcoming is exacerbated by the nature of coastal motions themselves, the link between sea surface height and the velocity is not as simple as it is in the deeper ocean for scales in excess of the deformation radius. Current spaceborne/airborne SAR inversion techniques can provide an estimate of the directional wave height spectrum of ocean waves in the region extending from deep ocean into the littoral zone and up to the surf zone. As waves approach shallow water however, the increasing wave steepeness shifts the SAR imaging mechanisms into the non-linear imaging domain. This, coupled with the problem of high altitude orbits chosen for current commercial satellites (ERS, RADARSAT), makes the inversion problem more difficult. Current spaceborne/airborne remote sensing

techniques are capable of providing maps of locations of bathymetric obstacles and features. However, accurate (10 to 20%) estimates of bottom depths require the use of water penetrating sensors such as an active LIDAR or a passive hyperspectral instrument. No active LIDARs are currently in orbit, and far more accurate techniques than presently exist will have to be derived for deriving bottom depth from hyperspectral returns.

Now/Near term:

- Current shortfalls: at-sea communication and processing power.
- Solutions: PC-based hardware/software, and portable down-link/LAN-based antennas.
- Current capabilities for deriving parameters from remote sensing:
- Marine wind verctor: spaceborne/airborne scatterometer.
- Currents: interferometric SAR, altimeter.
- Directional wave height spectra: spaceborne/airborne SAR.
- Bathymetry: active LIDAR or a passive hyperspectral instrument.

Future:

Research:

- Data compression: maintaining information content while reducing bandwidth.
- Automatic feature recognition: rapid selection and quantification of signatures.
- Coupling of spatial/spectral signatures for ocean/atmosphere phenomena to dynamical feature models.

Organizational structures:

- A formal organizing body: to interface with the user community and data suppliers and to decide on formatting standards, data exchange, and data availability.

G.I.S. Executive summary

Farid Askari, Michael Max

What are the most critical shortfalls in current capabilities and how do we make good the shortfalls?

Currently, there are two critical shortfalls: first is the availability of at-sea communication and shipboard processing power to the operator/warfighter, and the second, is the availability of user friendly software that is optimized for data fusion and two-way communication. While the current data fusion centers and laboratories posses adequate capabilities, the at-sea capabilities are limited in terms of data reception, visualization and user interactions. For low data rates, Inmarsat and cellular phone communication can bring Geographic Information Systems (G.I.S.) capabilities to the operator at sea. However, for higher data rates, adding Asynchronous Transfer Mode (ATM) networking technology to existing communications capabilities will be necessary to alleviate the bandwidth problem. The cheapest and most versatile approach is to upgrade the processing capabilities of the fleet with PC-based hardware/software and to improve at-sea communications with portable down-link/LAN-based antennas.

Which topic areas are most promising for future research?

Future research should be directed in the areas of information fusion and data visualization techniques, as well as high-speed communication using large-scale/mesh-connected networks and distributed fusion centers. The goal of any sensor fusion and data visualization techniques should be to provide value-added information and to enhance data interpretation by the synergistic use of multiple data fields. For a mission critical operational REA, the distributed data mesh-connected networks should be capable of providing un-interruptable data streams, in the manner a power grid is resilient in the face of a source failure. In designing systems, considerations should be given to scalability in all dimensions, including data set size, number of users, number of server sites, and data delivery speeds.

What new organizational structures must be created to implement REA?

A formal organizing body is needed to interface with the user community and data suppliers and to decide on formatting standards, data exchange, and data availability. Ideally, this organizing body would also provide "Value added" in the form of tactical decision aids resulting from the fusion of multiple data streams.

What is achievable now with our current technological capabilities?

Current G.I.S. technology is capable of combining geo-spatial information layers (raster/vector) from the sea floor properties, to water column information, to remotely sensed sea surface and atmospheric parameters using various off-the-shelf software architectures. For satellite data requiring massive amounts of storage, processing power and network throughput, network-based G.I.S. capabilities have been implemented that rely on client/server interactions, near-real time image processing and high speed access to remotely stored data and processing power. For assembling low volume data and integrating environmental-operational data set archives in real-time, G.I.S. in navigational chart mode and object-linked electronic maps (E-Maps) have been implemented. These E-Maps are intended to be minimal data sets, optimized for individual missions, which hold much information in an abstracted form. Existing, relatively inexpensive off-the-shelf software and portable workstations using Internet technology are sufficient to provide interactive, distributed information systems. The challenge is to deliver to the end-user useful information faster and in a more automatic fashion using multiple distributed data sources.

Now/Near term

- Current shortfalls: at-sea communication and processing power, user friendly software.
- Solutions: PC-based hardware/software, ATM networking, and portable down-link/LAN-based antennas.

- Current capabilities for combining geo-spatial (vector/raster) layers.
- Networked-based GIS for high data rates: client/server interactions, near-real time image processing, and remote storage and processing power.
- Navigational chart mode for low data rates: object-linked E-maps.

Future

Research:

- Information fusion/visualization: provide value added/enhance interpretation through synergism.
- Distributed processing: mesh-connected networks and data fusion centers.

Organizational structures:

- A formal organizing body: to interface with the user community and data suppliers and to decide on formatting standards, data exchange, and data availability.

National Perspectives on Rapid Environmental Assessment

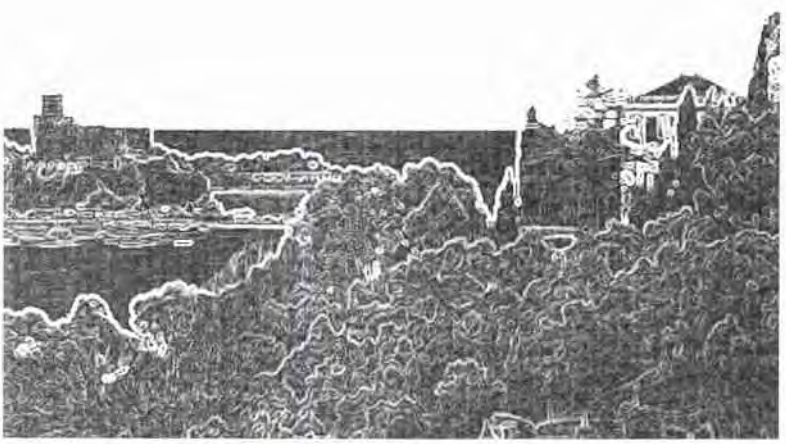

Evolving U.S. Navy Requirements for Rapid Environmental Assessment

Edward C. Whitman

Office of the Oceanographer of the Navy
U.S. Naval Observatory
3450 Massachusetts Avenue, NW
Washington, DC 20392-5421
Email: 096t@ocean.usno.navy.mil

Abstract

In re-orienting tactical meteorology and oceanography (METOC) for the post-Cold War era, the U.S. Navy is turning increasingly to Rapid Environmental Assessment for tactical support of both operational commanders and individual forces at sea. This requires a shift in emphasis from large scale, predictive, numerical models to "nowcasting", quick-reaction surveys, direct exploitation of remote and in situ observations, innovative processing techniques for satellite data, and through-the-sensor environmental measurements. Corresponding infrastructure requirements for direct assimilation of processed METOC data within the Navy command and control system are also discussed.

1. Introduction

The Oceanographer and the U.S. Navy's oceanography community are responsible primarily for understanding the effects of the natural environment on the planning and execution of naval operations and for interpreting atmospheric and ocean phenomena to the fighting forces. There are two basic motivations: first, to insure the safety of the Fleet and the shore establishment in the face of adverse ocean and weather conditions; and second, to provide warfighters a decisive tactical edge by accommodating meteorological and oceanographic processes in optimizing the performance of their platforms, sensors, and weapons.

With today's ongoing transition from the conditions of the Cold War to a "new world order" in which the likelihood of smaller-scale naval operations near shore becomes a primary concern, naval oceanography confronts an unfamiliar littoral environment that changes much more rapidly in time and space than the deep ocean venues of the past. This, in turn, demands a new emphasis on Rapid Environmental Assessment (REA) as the focus of future METOC support to the fighting forces. This paper will examine these new directions, identify promising opportunities, and propose corresponding new REA infrastructures.

2. Today's infrastructure for tactical oceanography

The top level concept of operations that has evolved as today's mechanism for assimilating observational data into ocean/atmosphere numerical models and generating tactical products for dissemination to the Fleet is shown in Figure 1. Synoptic scale guidance products are produced at two large supercomputer centers ashore: the Naval Oceanographic Office (NAVOCEANO - Stennis Space Center, MS) and the Fleet Numerical Meteorology and Oceanography Center (FNMOC - Monterey, CA). Both assimilate sensor data from a variety of sources and run large-scale numerical prediction models on a daily, scheduled basis. The model outputs are passed down the chain - normally as gridded fields of parameter estimates - for use as numerical guidance in more focused regional forecast centers at Norfolk, Pearl Harbor, Rota, and Guam. These centers, closely in touch with the area naval commanders they serve, add local value and produce forecast products tailored directly for afloat units and staffs in their areas of responsibility (AOR). In turn, at the tactical level, on-scene oceanographic staffs on command and aircraft-capable ships receive and display weather imagery from both DOD and NOAA satellites and produce local area forecasts for direct fleet support and processed data for insertion into tactical decision aids. At each stage, local and regional observations are forwarded back up the chain as input data for the next run of the synoptic-scale models at the shore "production centers." Both land-line and satellite communication links are used to tie together

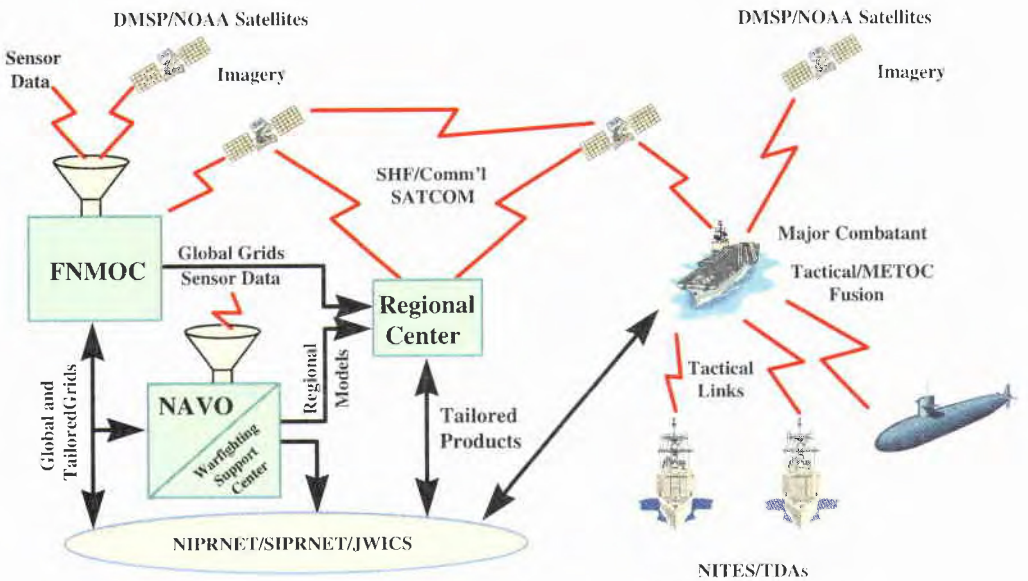

Figure 1. Today's infrastructure for the generation and dissemination of METOC products to the fleet

this infrastructure, and increasing use is being made of wide-band digital networks, for example, the Internet-like NIPRNET and SIPRNET.

This tiered approach to Fleet METOC support, beginning with a shore-generated, synoptic view and proceeding down the chain through successive stages of increasingly local focus, has served us well in the past. It continues to serve us well today for day-to-day weather and ocean "background forecasting" for aviation safety, Optimum Track Ship Routing (OTSR), storm avoidance, and theater-level operations planning. Under the changed conditions of supporting likely combat and contingency operations in the littoral, however, we need to do more.

3. Rapid Environmental Assessment—new neighborhood, new needs

In the new world of the littoral, where a multitude of closely inter-related natural processes vary rapidly in space and time, environmental modeling and prediction are much more complex and difficult than in the deep basins. Increasingly, our existing models and data bases are falling short. A whole new generation of algorithms and approaches is needed for these new scenarios, in which the rapid assimilation of more densely spaced observations will be key to predicting warfighting conditions on time scales commensurate with those of the littoral and its nearby hinterlands. Further, our existing Cold War infrastructure needs to be re-focused further forward, with REA as its primary goal.

3.1. Changing METOC requirements for littoral warfare

Today's littoral warfighters are demanding substantially more detailed characterization of the battlespace on smaller time and spatial scales. They are much less interested in long-term synoptic behavior than in knowing *today's* weather over the target and the details of near-shore thermal, current and salinity patterns. Thus, our earlier emphasis on long term weather and ocean forecasting on the theater scale, based heavily on global numerical models from half a world away, needs to be supplemented with a tighter focus at the tactical level.

This is the essence of Rapid Environmental Assessment. It comprises detailed and timely METOC characterization of a limited objective area, keyed to close support of an imminent military operation. All possible resources are brought to bear: ships and aircraft, *in situ* and satellite sensors, and dedicated analysis and interpretation cells capable of producing quick reaction products, including data base fills, paper charts, and quantitative and timely tactical advice.

In fact, REA calls for the sequential application of a repertoire of old and new techniques as H-hour nears. For early planning and preparation, the METOC CONOPS differs little from our traditional tiered approach, with its dependence on climatology, archival data bases, and synoptic numerical modeling. However, in the latter stages of preparation - in the hours leading up to the moment of commitment and during the operation itself - the new specifics of REA

come into their own. Principally, there is a growing dependence on the display and interpretation of direct observations, with less emphasis on numerical prediction models. Relatedly, forecasting - particularly more than a day into the future - yields increasingly to *nowcasting* - in which the interpolation and extrapolation of current sensor data within and beyond the sampling grid becomes the norm. Figure 2. attempts a rough conceptual representation.

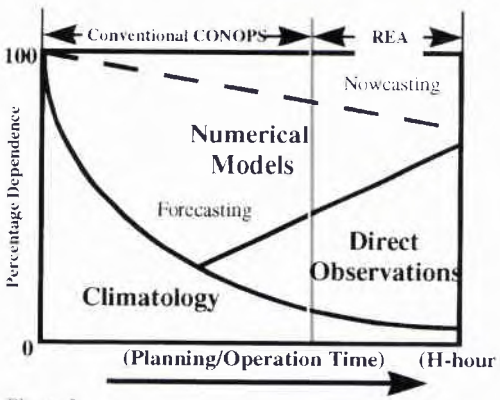

Figure 2.
The transition to rapid environmental assessment

The process is very much analogous to "intelligence preparation of the battlespace" but extends forward into the operational phase itself, providing engaged warfighters a stream of tailored, real time environmental updates, often incorporated adaptively into weapon and sensor settings directly.

Achieving the goal of seamless Rapid Environmental Assessment will be a continuing "work in progress." Our initial steps have been somewhat tentative, but the RAPID RESPONSE initiatives in the Mediterranean constitute an excellent beginning. There are several key aspects to consider. First is the need for a much denser grid of local area observations and correspondingly higher resolution data bases, both oceanographic and atmospheric. Second is a growing emphasis on local or "in stride" capabilities for direct assimilation of both raw and processed data into tactical decision aids in near real time, with continual adaptation to changing conditions. Finally, we need to evolve a responsive information infrastructure that targets the warfighters and not the METOC specialists.

4. Augmenting the sensor grid

4.1. New roles for old sensors

In achieving the density of measurements needed for Rapid Environmental Assessment, most of our customary sources of environmental data will remain a valuable resource. These include satellite sensors for sea surface temperature; visual, microwave, and radar imagery; radar altimetry; and atmospheric profiling of humidity and temperature. The U.S. Navy is funding a variety of studies on innovative processing techniques for existing satellite data, intended to extract oceanographic features and measurement parameters from space systems not originally planned for those purposes. The full range of *in situ* sensors will be useful also: radiosondes (weather balloons), bathythermographs (BTs) of ocean temperature, Conductivity/Temperature vs. Depth (CTD) casts, moored and drifting buoys, and direct ship and aircraft observations.

4.2. New and evolving sensor concepts

In addition, a number of promising new sources are under investigation. For example, several laser airborne bathymetry systems (LABS) are now in regular operation for shallow water hydrography from both fixed and rotary wing aircraft. These use blue-green laser radars for measuring bottom depths down to roughly 50 meters in water of average turbidity. Measurement precision and accuracy are essentially equivalent to that of acoustic methods, but the area coverage rate can be an order of magnitude higher. A major goal of ongoing development in this area is the ability to carry out beach or bottom surveys with similar laser systems pod-mounted on high speed tactical aircraft. Also, unmanned submersibles are in consideration both as adjuncts to conventional survey ships and as clandestine reconnaissance vehicles for beach surveys and mine countermeasure purposes.

4.2.1. The need for expendables

Significant progress has been made in extending state-of-the-art sonobuoy and oceanographic drifter technology toward a new generation of miniaturized, expendable sensors sufficiently inexpensive to allow widespread "seeding" of both land and water areas of interest. These instruments will provide both direct observations for immediate tactical exploitation and the density of input data necessary for initializing high resolution numerical models. Already, a miniaturized dropsonde, deployable from the chaff launchers of tactical aircraft has been demonstrated, and small, air-droppable micro-weather stations and chemical sensors are being examined as logical extensions.

4.2.2. Combatant data collection

Another promising road to REA is to make synergistic use for background measurements of the search, track, and fire control sensors already on board combatant ships and aircraft. In a program designated as "Combatant Data Collection" (CDC), the Navy is actively investigating the use of weapon system sensors for environmental characterization. The long-term goal is to make sensors and weapons environmentally adaptive in stride. Thus, outputs from the SQS-53C surface ship sonar have been

processed to estimate bottom and reverberation parameters, and significant success has been achieved using the SSQ-110 sonobuoy active source for characterizing bottom backscatter at low grazing angles. In the electromagnetic area, the SPQ-9 fire control radar has emerged as a useful tool for measuring near surface clutter, and the Aegis SPY-1 phased array has shown itself to be an excellent Doppler weather radar, with capabilities approaching those of the state-of-the-art Navy/NOAA NEXRAD system.

5. Fusion, interpretation, and infrastructure for REA

5.1. The need for in-theater fusion

More focused and intensive REA data collection by itself is of little use unless the "take" can be fused, analyzed, and interpreted into a form useful to decision-makers. There is still uncertainty about where this fusion should take place within the larger infrastructure, and likely it will take place to some degree everywhere. There is, however, growing enthusiasm for a central METOC tactical fusion center as far forward in theater as possible. This would serve as a clearing house for the entire range of METOC data that comes available from both remote and *in situ* sensors and be capable of running the more complex nowcast models, such as the Modular Ocean Data Assimilation System (MODAS) on local scales. A promising, near term opportunity is offered by commercially available geographic information system (GIS) software, which can be adapted to display registered oceanographic and meteorological information as a series of thematic layers over a background chart or topographical display. A successful example is the "E-Map" concept prototyped at the SACLANT ASW Center in La Spezia for several recent exercises.

A major role will still remain for the large ashore METOC production centers, such as NAVOCEANO and FNMOC, with their access to global synoptic data of all kinds and supercomputing power adequate for running the large scale models needed for bounding and initializing regional and local models for the theater. NAVOCEANO, in particular, with its Warfighting Support Center, fields a unique capability for the synthesis and detailed analysis of all-source oceanographic, satellite, and imagery data and the quick turn-around of highly focused, multidisciplinary products, such as the Special Tactical Oceanographic Information Chart (STOIC) and annotated imagery. The growing availability of wide-band satellite communications down to the tactical level will increasingly insure that even these specialized and labor-intensive products reach the warfighter in time to make a difference.

5.2. A new infrastructure

The more forward-leaning REA focus described above and its associated proliferation of sensor systems will require new concepts of operation and a new support architecture, both at sea and ashore. This is sketched out in Figure 3.

Key operational issues

While our traditional METOC products - derived as a fusion of gridded parameter fields (computed centrally) and local observations - will remain useful for long range planning, safety of operations, and protection of property, the new infrastructure must provide additional means to collect and assimilate a new dimension of local sensor data, as well as greater computational capacity in theater - and with the warfighter - for producing tactically useful products on scene. Global, synoptic numerical guidance will remain a key ingredient, but the preponderance of input will devolve to organically fused local observations and environmental satellite data downlinked directly.

5.2.1 Architectural implications

A number of architectural implications follow immediately. Principal among these is the need to "close the decision loop" for Rapid Environmental Assessment as far forward as possible. This in turn necessitates that more powerful tactical METOC fusion capabilities be deployed aboard ships and forward command facilities, with commensurate access to the local grid of tactical METOC sensors, guidance products from the ashore infrastructure, and satellite imagery and other relevant space-based observations. Computational resources need to be sufficient for assimilating all these data into tactical scale fusion and analysis models, whose outputs - in the form of nowcasts or near term forecasts - feed directly into tactical recommendations and decision aids. At the individual unit evel, tailored products from the local METOC "anchor desk" are ingested directly into the command and control system for tactical planning and execution, with own-ship support from environmentally self-adaptive radars, sonars, and weapons.

5.2.2 Communication needs

Communications are crucial, and although the evolution of modern digital communications provides an embarrassment of riches, serious shortfalls remain. Traditionally, the Achilles' heel of the METOC community has been the uneven availability of the bandwidth required for moving large gridded fields and satellite imagery on standard Navy point-to-point communication links, such as SHF SATCOM. Fortunately, this problem, at least, has been largely ameliorated by the availability of wide band, Internet-like data links, hosted on both fiberoptic landlines and commercial satellites. SIPRNET (the Secret Internet Protocol Router Network), in particular, now serves all of our major METOC shore facilities, including NAVOCEANO and FNMOC, and it has been extended to sea to provide wideband data access to major combatants, such as carriers and command ships. The METOC community is already a major user, and browseable World Wide Web home pages are now commonplace for disseminating data.

Unresolved issues remain at the tactical, local level, beginning with the communication needs of remote, *in situ* sensors of the type we hope to proliferate. Existing

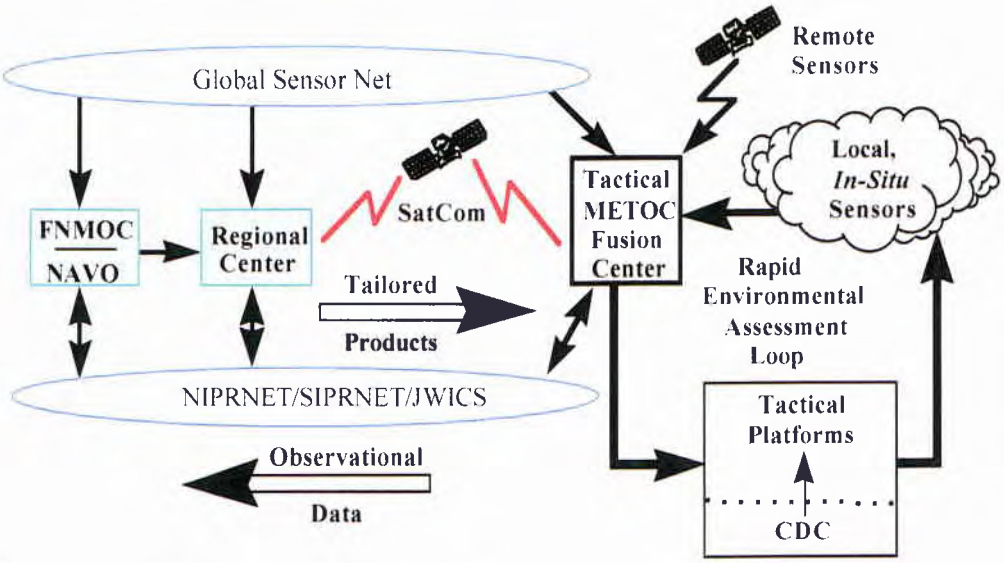

Figure 3. Target architecture for future METOC support.

prototypes have used line-of-sight sonobuoy and rawindsonde frequencies, but for over-the-horizon scenarios, other means need to be identified. A number of possibilities exist: derivatives of cellular communication systems, including those based on low earth orbiting (LEO) satellites; meteor burst; or even the long-neglected High Frequency (HF) band, if augmented by state-of-the-art error correcting and link establishment techniques. Under U.S. Navy sponsorship, there was recently a very promising demonstration of data-linking the METOC sensor "take" of an airborne P-3 aircraft via satellite to both NAVOCEANO's Warfighting Support Center and the Naval Atlantic METOC Center, from whence the resulting files were placed on the SIPRNET in virtually real time. These data included the output of several drifting buoys, compressed video cloud imagery, and processed data from a prototype laser airborne bathymetry system. A similar demonstration, in which miniature dropsondes will be deployed from the Predator UAV, is in final planning.

For the final stages of the METOC "retail chain" - reaching from the envisioned tactical fusion center to individual units in company - recent experience has shown that today's tactical communication nets, such as OTCIXS (the Officer-in-Tactical-Command Information Exchange System), are largely inadequate for even filtered METOC data. One assumes that similar needs for tactical intelligence and targeting information will maintain the momentum of the Fleet's evolving Joint Maritime Communications System (JMCOMS), which will provide all the warfighting and support communities much needed connectivity at the small ship level.

6. In conclusion...

Although the quality and scope of today's METOC support to the fighting forces is unprecedented, the underlying paradigm remains rooted largely in the needs of the Cold War. Recent contingencies in Somalia, Haiti, and the Adriatic have already defined new needs for which we are only partially prepared. This paper has sought to suggest the transitions that lie before us if the naval environmental community is to rise fully to the challenge of the "New World Order" and its likely proliferation of small-scale brushfire wars (and operations short of war) - in new and unfamiliar surroundings, near hostile and unknown coasts. The short time and spatial scales of littoral warfare demand fundamental changes in our operational posture. We need to move the "center of gravity" further forward toward the tip of the spear and prepare to take full advantage of the possibilities offered by Rapid Environmental Assessment

United Kingdom requirements for Rapid Environmental Assessment

Willis R.N.V.

Director of Naval Surveying, Oceanography & Meteorology
Room 2379, Main Building
Ministry of Defence
Whitehall, London SW1A 2HB
Fax: +44-171-807-0180

The UK strongly supports the REA concept which NATO has pioneered. Deputy SACLANT has signalled clearly that it is a means of applying research to achieve immediate operational benefit. We are pleased to see the focusing of SACLANTCEN skills and resources on this area, as indicated this morning by the Director.

The UK strongly supports the commitment of allies in this field, and we welcome the US emphasis this morning on the development of REA architecture, with increased focus on direct observations and nowcasting in theatre, close to the force commander, using tactical decision aids. I also note the impressive US development of crucial communications techniques. In fact, I believe this is the really critical and most challenging area that we need to address. Many people here will have experienced how, as the intensity of operations increases, it becomes progressively more difficult to get sufficient time on a communications circuit for environmental data and products. If REA is to work effectively, we need the products as far forward as possible in real, or near real, time.

In addition to the work being carried forward by the US, we are also aware of the significant contributions of our european colleagues and we are grateful and very willing collaborators with them. We plan to continue close liaison with France and the Netherlands during **Rapid Response 97** and we are examining with them, further options for REA tactical development during 1998, *The International Year of the Ocean* and in a joint maritime course in 1999.

So where is the UK putting its own resources? Our aim has been to focus on our areas of particular expertise:

We place great importance on generation and delivery of outputs in-theatre:

As in the USN, our METOC officers within the force use performance data from weapon system sensors to derive tactically significant information for the commander, standard practice during operation **Sharp Guard** in the Adriatic.

Our uniformed hydrographic specialists, operating from their warship surveying vessels, or from craft of opportunity, survey in-theatre and deliver a product, similar to the USN's standard tactical oceanographic information chart, direct to the commander, within a few hours of collection. This was demonstrated in operation **Strong Resolve 95** when fishing vessel density prevented use of the planned landing areas. This ***was*** REA in action.

Our commitment to the operational relevance of environmental data is demonstrated by the recent formation of the RN's new warfare "***HM***" specialisation, combining meteorological, oceanographic and hydrographic skills and placement of these environmentally aware, skilled warfare officers more widely throughout the fleet.

We are committed to expanding the expertise of the fleet weather and oceanographic centre at the Northwood HQ (the FWOC) as a data-fusion centre, broadly similar to the USN's regional centres about which you heard earlier, with the support of agencies such as the UK Hydrographic Office and the Meteorological Office to exploit model and remotely-sensed data for reactive operations. Our *ocean feature strategy*, developed from Defence Research Agency experiments during MILOC survey **Rocky Road**, was tested in the Mediterranean theatre in 1995, when HMS *Herald* was cued onto the Levantine front by the FWOC using satellite data.

FWOC supports permanent joint headquarters at Northwood, with data and products for deep water, littoral, air, and trafficability of beaches and hinterland.

We are constantly monitoring, and in some cases funding, research and development into techniques and technology which we believe will improve our capability to exploit the environment, multi-beam echo sounders, AUVS and new, more capable survey ships, are just a few examples.

Finally, I would like to echo what Dr Whitman has said about the need to push the point of data synthesis and tactical environmental decision-making as far towards

the front-line as possible. Furthermore, it is critically important that we demonstrate the operational benefit of REA to our senior commanders. The UK would also urge that REA be included as part of our exercise play at all levels of intensity, it should ***not*** be seen as a tool only used for the higher levels of conflict, after air and sea control have been achieved. Lastly, we believe the REA concept is perfectly suited to the uncertainties of the 1990s, when the next conflict may arise, where we least expect it, and where we are least prepared.

French exploratory development in REA

Michel EVEN
Etablissement Principal du
Service Hydrographique et Océanographique de la Marine
BP 426 - 29275 BREST CEDEX
FRANCE

Abstract

As a response to the needs of the French Navy for environmental knowledge in shallow waters, the french hydrographic office propose an exploratory development to model a system for fast production of coastal environmental data, in order to show the feasibility of such a system and to evaluate his interest for military use. In this exporatory development, existing or emergent techniques will be selected and tested, possibly adapted, and a first generation of products will be elaborated.

1. The context and the need of environmental data

As a result from the recent conflicts in which France was involved (Ex-Yougoslavia, Persian Gulf), one of the main roles attributed to the classical french naval forces is now the control of the communication routes and the projection of forces in the shallow waters. For the Navy, the amphibious and special operations, and the mine and anti-submarine warfare are concerned.

There is no precise definition of shallow waters: from the shoreline to the continental slope (when it exists) could be one. They are in fact generally characterized by the influence of the bottom: through its acoustical properties, its topography, its nature, its density ...

Until now, the major efforts were concentrated on deep waters, and even if some results can be transposed in shallow waters, our capabilities do not allow us to describe efficiently the environment. However, the forces need the best knowledge of it, to guide their choice in the use of their means and to assure the best performances of their weapon systems and sensors. The needs expressed by the french are very varied and concerne a very large domain of parameters, from meteoroly to the description of the bottom and the column of water.

All these parameters have spatial variations and sometimes temporal ones (tides, currents, sea-surface roughness, ...) Moreover, the interesting areas are very large and hardly accessible for the in situ observation. So, with the present means of acquisition, it can not be planed to collect enough data to describe precisely all the shallow waters. These limitations are experienced by all the great maritime nations and the concept of REA has emerged as a solution.

The French Service Hydrographique et Océanographique de la Marine (SHOM) has asked for the financing of an exporatory development to realize the mock-up of a system for fast production of coastal environmental data, in order to show the feasibility of such a system and to evaluate his interest for military use. The objectives of this exporatory development are to test in real size the performances and potential military abilities of selected means for production of data and to define and realize a first generation of products and services. Finally, a concept of use will be recommended by stating the capacities to acquire, the external capacities which the forces would have to rely on, the ways and time limits for the elaboration and diffusion of the products, and which products would have to be developped.

2. The production of data

The first important part of this exploratory development will be the evaluation of the different means to produce data. Three ways are concerned: teledetection, in situ measurements and models. The approach will generally consist in testing existing or emergent techniques. The aim is to define their operational use: density, temporal frequency, ...

2.1. Teledetection

During the last years, great progress were made in teledetection, due to the availability of new sensors and to scientific studies for the extraction of the environmental information from the signals. The large area covered and the fact that teledetection can be used without in situ intervention (except for a possible wedging) show the interest of such means.

Apart from AVHRR for the detection of oceanic features in deep waters, the SHOM produce in a routine way bathymetry in very shallow waters from SPOT imagery. The hydrographic criterions are not respected but it's a good evalution which for example could help the staff in the choice of a beach for amphibious operation. The figure 1 is an illustration of a treatment realized for the exercise Rapid Response in 1996.

This competences will have to be widen to other sensors (SAR, ...), to allow a maximum use of teledetection for the knowledge of the environment.

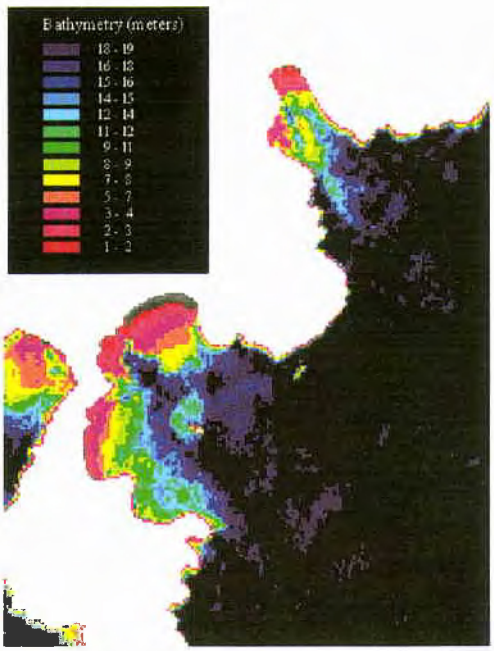

Figure 1: Assessment of the bathymetry from a SPOT imagery (Rapid Response 1996)

2.2 In situ measurements

Unfortunately, teledetection can not provide a sufficient description of the environment. In situ measurements are often necessary and sometimes the only source of data for some parameters: nature of the bottom, precise bathymetry, ... They could be done from ship, plane or submarine.

Some sensors (sediment sounder, speed sound profiler, ...) are already used by hydro-oceanographic ships but could also be deployed on war ships which are generally only equiped with expendable probes.

New sensors (XBP, laser bathymetry, ...) could be tested in the context of the exploratory development, to evaluate their interest and define their operational use.

2.3 Models

The third source of data is models. Hydrodynamics models are tested and used by the SHOM, for the study of circulation but also for production of data (for example, the figure 2 is the result of a model of currents in the Baie de Seine). Of course, they often need data from in situ measurements or teledetection to force and control them. The objective is to select the models which are the more suited to the different situations (closed seas, interaction of the rivers, ...) and define what types of data, and with what density and precision, are needed to perform them.

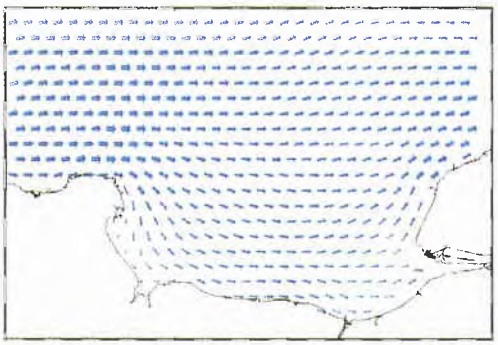

Figure 2: Model of the currents in the Baie de Seine

3. Elaboration of the products

The second important part of the exporatory development concerns the elaboration of products. The procedure used for the production of charts or nautical documents is not adapted, principally because of the necessity of very short time limits. New tools must be developped.

These tools will have to be able to accept different specific formats coming from a lot of sources (measurements, models, ...), not necessary in a unique reference system. An ability to merge data from different sources will probably be necessary, to present a coherent situation.

Each product realized will have to be adapted to its beneficiary, which means that the same set of data could be presented in different ways according to particular objectives. For example, the bathymetry must be general for the staff which wants a presentation of the whole area, but the more precise as possible in a limited area for the mine hunter.

Defining these tools and products is still difficult as we do not know exactly what will be the data, but our experience and the opinion of the users can guide us.

As examples, the figures 3 and 4 show a part of a product which was realized in february 1997 for the military exercise SPONTEX on the continental shelf of the Bay of Bisquay. The data were already treated and stocked in data bases, and the aim was to elaborate with reduced time limits a synthetic representation of all the knowledge.

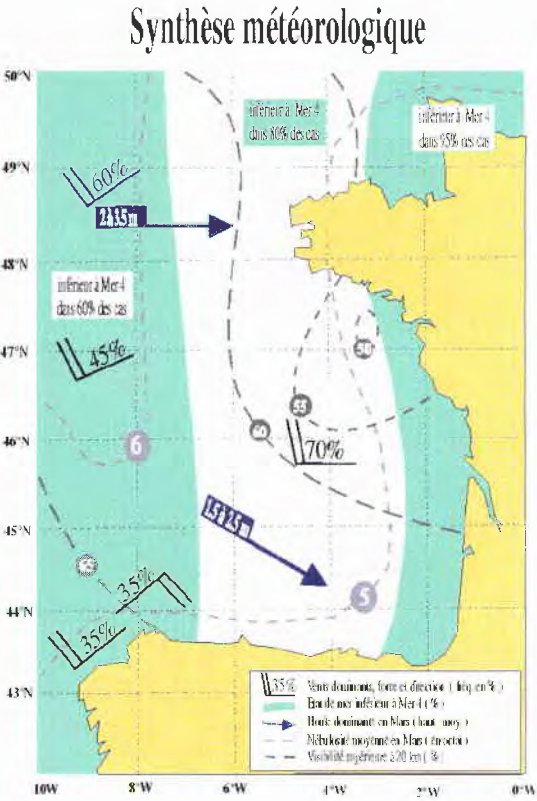

Figure 3: meteorological synthesis for the exercise SPONTEX

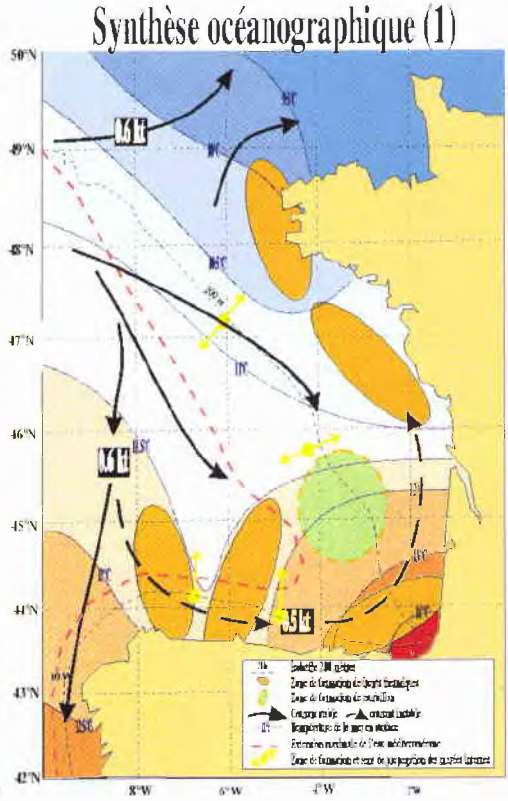

Figure 4: oceanographic synthesis for the exercise SPONTEX

For example, the figure 3 is a meteorological synthesis which shows the statistics of winds, swells, sea surface, nebulosity and visibility, with different symbols.

The interest of such products is to present a result directly exploitable by the users.

4. Conclusion

The exploratory development proposed by the SHOM is the french reponse to the shortage of data in foreign shallow waters. The two main parts will consist in evaluation of existing or emergent techniques and elaboration of products. In order to be confronted to the problems of time limits, interoperability, and diffusion of the information, the system will be tested during exercises. However, even if the exploratory development would not be credited this year, the SHOM will continue his studies linked with REA and will be present at Rapid Response 97, with the hydro-oceanographic ship D'Entrecasteaux.

United States Naval Meteorology and Oceanography Command Plans for Rapid Environmental Assessment

D. L. Durham and J. B. Boatman

COMNAVMETOCCOM
1020 Balch Boulevard
Stennis Space Center, MS, United States
Email: durham@cnmoc.navy.mil, boatman@cnmoc.navy.mil

Abstract

The shift in naval emphasis from the blue to brown water has resulted in increased need for NAVMETOCCOM's assessments and products in specific littoral regions. Use of widening communications pipes, the Internet, advances in Information Technology and visualization tools are being exploited to enable continued improvements in NAVMETOCCOM production. The Command is also partnering with academia, industry and other US governmental agencies to extend its capabilities.

1. Introduction

The U.S. Naval Meteorology and Oceanography Command (NAVMETOCCOM) executes oceanographic and meteorological data collection, processing, assessment, and product dissemination functions at activities worldwide; providing services for safety and readiness for US naval forces. The shift in naval emphasis to the dynamic littoral regions of the world has increased the challenges for timely production of NAVMETOCCOM centers, facilities and detachments.

2. Focus

NAVMETOCCOM has reshaped the various services to increase emphasis on support to expeditionary forces, which include amphibious, mine warfare, special and varied Marine Corps operations. Assets of the command are focused on analyzing the near shore meteorological and oceanographic (METOC) environment and its effects on operations in the planning and execution phases. Among the wide range of features reported are nearshore currents and bathymetry, water visibility for both mine warfare/countermeasure and special operations support; water column and seafloor characterization for shallow water ASW; and sea state, seafloor and beach descriptions for use in amphibious operations. As expected, interest areas generally lie in currently denied or inaccessible regions.

The focus of Rapid Response efforts has been on oceanographic effects, but equally important are nowcasts and forecasts of temperature, humidity, winds, and visibility on system performance and tactics. Choice of smart weapons, radar detection, chem/bio dispersion probabilities, and visibility over target represents a separate set of challenges with shorter time scales than ocean processes. Obviously, the atmospheric and oceanographic interactions are also more significant in the littoral where temporal and spatial scales are smaller as well as more variable. Impacts of sea state, current detection, shorelines/tidal flows, seafloor and beach - as well as the difficulties of modeling the coupled atmosphere and ocean are keeping both the operational and R&D communities scrambling to provide reliable solutions to operating forces.

3. Capabilities for Rapid Response

NAVMETOCCOM rapid response capabilities rely on the major production centers and Regional Centers for product consolidation and tailoring. The production centers at the Naval Oceanographic Office (NAVOCEANO) and the Fleet Numerical Meteorology and Oceanography Center (FLENUMMETOCCEN) generate products for both standard production flows and for ad hoc and quick response requirements. NAVOCEANO generates its products by collecting and merging data from NAVMETOCCOM's survey fleet, utilizing one of DoD's High Performance Computing Centers, merging data from the largest Oceanographic and MC&G database, and exploiting all-source imagery. FLENUMMETOCCEN collects atmospheric and oceanographic data from world wide sources, hosts and operates DoD's global numerical weather prediction models, describes the synoptic effects of weather on ocean areas, and works with NAVOCEANO to conduct oceanographic modeling. Production center products, used by NAVMETOCCOM Regional Centers(e.g. Naval European METOC Center (NEMOC), Rota, SP), and new analysis and forecast tools allow for merged and tailored tactical products provided to operating

forces.

NAVMETOCCOM's major assets dedicated to data collection has long been NAVOCEANO survey ships, gathering data for use on nautical charts and characterizing the water column, seafloor, and geodetic parameters. Traditionally, data collected is processed and sent forward to customers, and concurrently is incorporated into the massive oceanographic and geophysical databases at NAVOCEANO for on line use. Survey ships also have the capability to rapidly generate products in near real-time and forward to customers.

Other on-scene oceanographic collection platforms have been fleet aircraft, manned by NAVOCEANO scientists. Data collected by aircraft are often processed on-scene for fleet exercises and made available in near real time. This data is also incorporated into NAVOCEANO databases.

Remotely sensed data comprise a third and increasingly important collection method. An expanding range of satellite and tactical imagery is being used to collect information in areas denied to our ships and aircraft. Among satellites used are the geostationary and polar orbiting meteorological platforms, multispectral imagers, national systems, the Navy's operational GEOSAT follow on (GFO) and other commercial and research systems hosting such sensors as altimeters and scatterometers.

To supplement the sometimes sparse coverage of available data sets, ocean models are run on DoD's largest supercomputers at FLENUMMETOCCEN and NAVOCEANO to predict ocean circulation and temperatures. In addition, limited area models - using FLENUMMETOCCEN and NAVOCEANO boundary inputs, are run at Regional Centers, e.g., Modular Oceanographic Data Assimilation System (MODAS) runs at NEMOC. NAVMETOCCOM is taking advantage of advances in modeling of oceanographic and meteorological processes and in the development of advanced platform and instrumentation systems for the rapid collection of data to support the planning and execution of tactical operations in the littoral. MODAS, On-Scene Data Collectors and a variety of Sondes are being used together to provide near real time characterizations of the battlespace environment.

Finally, but most critically, Command activities work closely with on-scene fleet oceanographers and with deployed representatives from our activities to facilitate product delivery and help ensure the end user gets the maximum benefit from all products. The active involvement, interpretation, and product tailoring facilitated by this on-scene customer support is instrumental in the effective application of production efforts of the Command.

4. Issues

Rapid Environmental Assessment related issues facing NAVMETOCCOM are in collection platform response times, relocatable modeling solutions, and product communications to and from on-scene users.

Ships are our most effective data collectors, but the collection process is slow and relatively expensive. Although we generally keep ships deployed in theater, speed of response is still an issue as is access to denied areas. In addition we must ensure that these assets remain out of harms way.

The limiting factors in regional oceanographic models include site specific conditions and determination of boundary conditions without sufficient lead time. Such relocatable solutions are not yet part of the NAVMETOCCOM toolbox, but are a high priority R&D initiative.

Remotely sensed data are being exploited more effectively than ever before. Atmospheric and oceanographic models will soon assimilate satellite derived winds, vertical profiles of temperature and humidity, and sea surface temperatures, in addition to conventional data. However, direct analyses of remotely sensed data require algorithms that depend on manual intervention and interpolation and are often site specific to the point that local knowledge is required. Additional challenges remain in incorporation of surface winds data into models due to limitations in coverage and timeliness for sensors such as scatterometers.

Acoustic prediction modeling has been improved through the Naval Research Laboratory developed MODAS software, allowing a nowcasting of current oceanographic parameters by incorporating in-theater measurements with production model results. MODAS allows the on-scene tactical oceanographer to rapidly assimilate bathythermograph information into 3-D gridded temperature fields to create a near real-time physical oceanographic description of an operations area. MODAS derived sound speed fields can then be incorporated into acoustic models to produce 3-D range-dependent acoustic propagation assessments. However, even the existing range dependent models lack complete bottom model databases in the littorals. NAVOCEANO is working to overcome this shortfall, but a wide range of database population strategies is required. These efforts will certainly continue to improve acoustic predictive capabilities, but we must continue to grow in our understanding of shallow water acoustic propagation.

Most of the Command's products for Rapid Response have been hard copy. To meet production demands of speed and quality, increases in digital production capabilities are underway at all the

Centers. However, current on-scene processing and display capabilities, coupled with communications bandwidths, remain the limiting factor. The explosion of "Web" technology and DoD emphasis on robust communications networks appear to be solving some of the problem. The Web enables one to leverage the virtual production and dissemination capabilities of other sites with much less on-scene processing. The NAVMETOCCOM Regional Centers have developed the Smart Center concept to provide Web data fusion services to the afloat METOC divisions. Unfortunately, not all on-scene systems are capable of taking advantage of these advancements.

5. Solutions

As the NAVMETOCCOM community has pushed to provide improved rapid response, the best solutions are being provided by the efforts of individuals - NAVOCEANO quick turnaround on as Standard Tactical Oceanographic Intelligence Charts (STOICs) and close coordination with fleet aircraft operators; aggressive NEMOC personnel working hard to bring in additional data sources and working with the Command's communications managers to link into DoD communications initiatives; and the Naval Research Laboratory (NRL) response with timely MODAS modeling support and updates. However, the investment strategies in the R&D program of The Oceanographer of the Navy and operational collection improvements by NAVMETOCCOM are beginning to provide initial rapid response capabilities.

New collection systems include a new "fly away" survey system, which can be transported into theater and placed on a surface platform for almost immediate survey. This capability will augment the more robust ocean survey fleet.

NAVMETOCCOM, jointly with the U.S. National Imagery and Mapping Agency, is in the process of acquiring a Laser Airborne Bathymetric Survey (LABS) system for coastal survey in the 1-50 meter depth region. Laser bathymetry has been proven operationally successful around the world and will have immediate impact, but additional research will benefit world-wide LABS operations.

We are progressively preparing for future LABS operations, through a leased survey, conducted by NAVOCEANO and U.S. Army Corps of Engineers off the coast of Mexico. The experience gained by our hydrographers has already paid off in development of specifications and concept of survey operations. During this survey, we demonstrated significant payback in productive deployment and effective survey time. As might be expected, the most time consuming portion of the effort was in logistics support.

NAVMETOCCOM continues to improve its capabilities in processing of remotely sensed data and in product generation. NAVOCEANO has a variety of initiatives, both classified and unclassified, which have added to the effectiveness of the Warfighting Support Center (WSC). WSC analysts (who are regional experts) use a newly fielded acquisition and processing system to exploit satellite and tactical imagery; combine the data with ocean models, NAVOCEANO's ocean database and the ocean archives at the Maury Library; then provide detailed oceanographic products to a variety of customers. The WSC is currently developing collaborative products with other DoD agencies to provide a seamless depiction of the battlespace. In addition, the NAVOCEANO supercomputer visualization center and NRL are developing several flythrough approaches, from below the water up onto the beach. The flythrough scene is derived from merged remotely sensed data and charts, and is the type of capability requested for amphibious operations.

FLENUMMETOCCEN is also improving its model assimilation of remotely sensed scatterometry and satellite derived winds, vertical profiles of temperature and humidity, and sea surface temperature; and has already shown significant promise in improved tropical cyclone prediction accuracies.

NRL, in coordination with NAVOCEANO, has been exploring the capabilities of an Unmanned Underwater Vehicle (UUV), the (Oceanographic Remotely Controlled Automaton (ORCA)), to augment existing ship assets. NRL has developed several enhancements to enable Over The Horizon operation, obstacle avoidance, etc. There is much promise, but to date launch and recovery is an area in which we must work to improve. NAVMETOCCOM, NRL, the Office of Naval Research, and NAVOCEANO are currently working together to explore Unmanned Aerial Vehicle (UAV) technology which could be deployed or recovered from a survey launch and would be capable of data acquisition up to the shore

In response to the fielding of MODAS systems at Regional Centers, an expanded set of fleet platforms is targeted for receipt of MODAS fields. Shipboard Tactical Atmospheric Forecast Capability systems will also be soon fielded to provide some near real-time meteorological forecasts, using on-scene data such as Aegis radar.

NAVOCEANO supported the NATO exercise Rapid Response to develop methods for quicker product turnaround in support of tactical operations. Products included bathymetry charts incorporating

with "just surveyed" information, modeled dynamic current information, tactical charts, and satellite imagery from numerous sources.

NAVOCEANO is now fielding a capability to provide real time feed of survey data into the scientists at NAVOCEANO for in depth analysis and quick turnaround to on-scene customers. The Office has also exercised the remote in-theater production printing capabilities of NIMA, exploring this potential to disseminate paper products such as STOICs more rapidly. This effort provides an opportunity to speed production through more quickly applying the computing and analytical capabilities at NAVOCEANO to newly collected data. The result is a quick turnaround into products, returned on-scene digitally for rough print on NAVOCEANO collection platforms or for finish print on in theater NIMA systems.

The Internet has exploded to provide a wide range of opportunities. NAVMETOCCOM has been working with the leaders in technology to establish a common "look and feel" for the Command's home pages, and to explore possibilities in collaborative production via the Web. We have only scratched the surface for METOC, but our plans are in place for improvements in data access, product fusion, and collaborative production.

Open Systems, such as the Internet, have resulted in grass roots advances in NAVMETOCCOM, and more significantly within the fleet. Operators such as CINCPACFLT are modernizing their own assets, effectively linking together processing on board ship and throughout an entire fleet. The low cost solutions will likely have an impact on naval operations similar to that of the Personal Computer on Information Technology.

6. Needs for Research and Development

Though our capabilities are improving, there are additional areas which need R&D support, including:

- Improvements in rapid relocation of ocean models with reduced reliance on in-situ measurements for boundary conditions;
- Improvements in data collection, quality control and data bases, maximizing standard formats and archiving techniques;
- Effective code parallelization and coupling of the nearshore meteorological and oceanographic models, including improvements in efficient data assimilation schemes;
- Improvements in processing of remotely sensed data, focusing on automated feature detection and exploitation of hyperspectral data;
- More effective operation of UUVs/ Us for survey use;
- Incorporation of allied data collection assets into Navy production;
- Interoperable allied and Navy systems to take advantage of advanced communications and Web technology.

7. Conclusions

The US Navy continues to improve its responsiveness. Our production centers and Regional Centers play important roles in moving our products forward to the NATO community.

Technology infusion is making our advancements possible. Remote sensing and models and broadband communications are key tools in meeting today's challenges. We applaud the NATO community for working with us, exploiting new technologies, and addressing some of the significant opportunities for making further contributions to Rapid Environmental Assessment. With research addressing some of these issues discussed at this conference, we believe there will be additional advances in the REA concept, and we look forward to working with our allies to continue improvements.

NATO's Rapid Response Survey

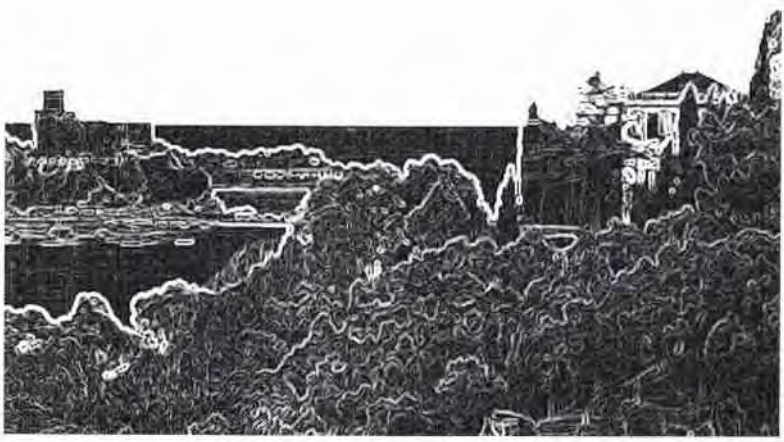

RAPID RESPONSE 96 - A Demonstration of NATO's Rapid Environmental Assessment Capability

N. Hammond

Royal Navy, Operations Division
HQ COMNAVSOUTH
Naples, ITALY

Abstract

In this paper I describe NATO's evolving doctrine for Rapid Environmental Assessment. In particular I look closely at RAPID RESPONSE 96, the first of a three year programme of REA development being conducted in the Mediterranean in conjunction with the SACLANT Undersea Research Centre at La Spezia, Italy. The paper concludes with some Lessons Learned and a quick look at the intentions for RAPID RESPONSE 97.

1. Introduction

During the summer of 1996 NATO achieved a first. A first in terms of the application of RAPID ENVIRONMENTAL ASSESSMENT or REA to a live situation. A demonstration of current REA technology took place in the central Mediterranean in support of the Southern Region LIVEX known as DYNAMIC MIX 96(DM96). This demonstration was known as RAPID RESPONSE 96(RR96).

2. Background

As NATO moved forward with its new NATO strategy to face the security environment of the late 90s a fresh approach to environmental support was clearly required. With the old, static scenario no longer valid NATO now has to cope with multiple risks, crisis management, humanitarian and non-Article V operations in littoral areas which may not necessarily be in the NATO Area of Responsibility.
Out of this requirement evolved RAPID ENVIRONMENTAL ASSESSMENT. REA is a new approach to environmental support, designed specifically to provide NATO's Reaction Forces or a CJTF(Combined Joint Tactical Force) with tactically useful environmental data in a tactically useable time scale.
REA is a SACLANTCEN Thrust Area and is attracting widespread interest both from the military and the civilian community.

The NATO MILOC(Military Oceanographic) community embraced this concept in 1995 and have now completed the first of a 3 year programme of REA development in conjunction with SACLANTCEN.
The principal aim of RAPID RESPONSE is:
to validate REA as a methodology and to show that it is capable of providing environmental support to ASW, MW, and AW operational commanders within tactically useable time scales for military operations.

The objective over the 3 year period is:
to produce a fully worked-up methodology package which can be applied to predict the environmental parameters of operational interest for ASW, MW, and AW operations. These operations may be in areas which have not been visited before, or where actual environmental knowledge is very limited.

MILOC's objective is to progress REA from 'experimental' to 'operational' and to incorporate validated REA procedures into NATO publications.

3. How is REA Different?

In the bad old days MILOC survey data was collected over a long period of time and eventually found its way into climatology, databases and reports.

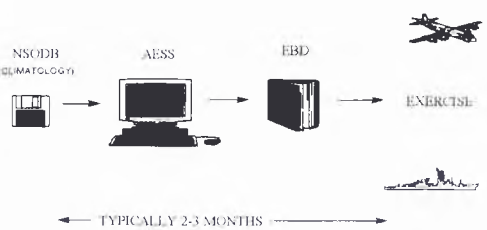

Fig 1. Exercise Support before REA

When required for an Exercise or Operation this data would be dusted down and fed into a Tactical Decision Aid(TDA), such as NATO's Allied Environmental Support System(AESS), to produce Environmental Briefing Dockets(EBD). These would then be distributed to the participants by post. The whole process would typically take 2-3 months and the end product would be neither timely or current.

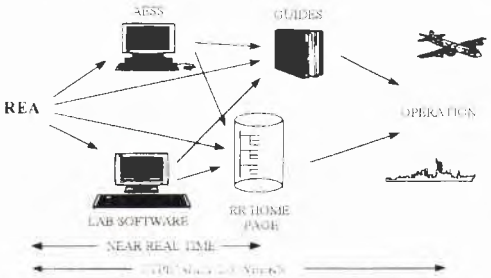

Fig 2. Operation Support with REA

With REA the support is based on in-situ, measured data. The data is passed through TDAs and then assimilated into User Guides in typically 2-3 weeks. More importantly by using modern communications technology support products can also be made available on an electronic Home Page in near real time.

4. Building the Knowledge Database

The concept of REA matches the possible data collection techniques with the politico-military situation. As Allied forces begin to exert greater dominance of the battlespace, more tools can be added to build the knowledge base.

Fig 3. Building the Knowledge Database

REA attempts to develop new tools to provide sufficient knowledge of the environment for battlespace dominance in a rapid time scale and at low risk. Integration and fusion of multiple data sources is one of the challenges of REA, as well as establishing the doctrine and infrastructure to rapidly put this information in the hands of the warfighters.

5. Participation and Assets

During RR96 satellite imagery from ERS-2, NOAA, AVHRR, SPOT, RADARSAT, and DMSP was used in near real time for SST depiction and feature analysis.

Raw imagery was processed by DRA in the UK, NRL in the US, and EPSHOM in France. This information was then used to cue further, and more specific, REA efforts using aircraft and ships.

Maritime Patrol Aircraft(MPA) from Canada, Netherlands, UK, and US flew 21 sorties from NAS Sigonella in Sicily and collected AXBT, AN, Reverberation, Geo Magnetic, and Surface Shipping disposition information. They also deployed drifting buoys and dropped SUS charges to support acoustic Transmission Loss measurements.

Ships from SACLANTCEN, Italy, UK, and US conducted Route, Bathymetric and Beach surveys, Bottom characterisation, XBP, XBT, CTD, and ADCP measurements as well as acoustic reverberation and transmission loss measurements.

Ship collected data was primarily used to 'ground-truth' the remotely sensed data.

During RR96 Canada, France, Germany, Greece, Italy, Turkey, UK, US, and SACLANTCEN provided manpower to sustain the effort.

6. Coordination

Military coordination was conducted from the USS La Salle, which also acted as an afloat operational fusion centre. Survey coordination, for scientific data collection, was undertaken from NRV Alliance.

7. RAPID RESPONSE 96 Execution

DM96 was a Mediterranean wide Exercise and did not allow the local concentration of ASW, AW, and MW forces that one would expect in a regional conflict. Accordingly RR96 was planned for the central Mediterranean, concentrating on unique operating areas for each warfare commander. As a Demonstration platform for NATO's current REA capabilities this offered interaction with all three warfare areas within a limited geographical area.

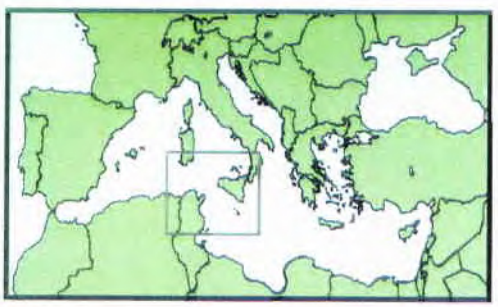

Fig 4. REA Area for RAPID RESPONSE 96

The AW area was set up to support amphibious landings at Capo Teulada, Sardinia.The MW area was established on Adventure Bank to support an Exercise Q-Route lead through for Task Groups transiting this area.
The ASW area was selected to support ASW operations south of Sicily, in particular a SHAREM Exercise conducted with STANAVFORMED Units in the Malta Channel.

Fig 5. ASW, AW, and MW Areas

8. The HOPS Model

The Harvard Oceanographic Prediction System(HOPS) model was set up for the ASW area and run at SACLANTCEN. This model is capable of producing a 7 day forecast of ocean conditions: SST; surface currents, vertical temperature profiles, and sound velocity profiles. Like any model the HOPS requires good initialisation data and the MPA programme was primarily driven by this requirement.

9. STOIC Charts

NAVOCEANO has developed a Special Tactical Oceanographic Information Chart(STOIC) which contains, on a paper product, all the environmental parameters of tactical significance within a small geographic area. During RR96 REA techniques were used to gather data for fusion onto STOICs covering the AW and the MW areas. REA data for inclusion on the STOIC was either sent to NAVOCEANO electronically by the Home Page, or physically by express carrier. This data was then fused into a STOIC, printed and hand carried to SACLANTCEN in time for the DM96 pre-sail briefings.

10. Warfare Guides

The culmination of the REA was assimilating all the raw data, and there was an awful lot of it, into ASW, MW, and AW Guides for presentation at the DM96 pre-sail briefings. This task was not easy, it had never been tried before in such a short period of time, so there was no template. In 5 days three tailored Guides were produced in large numbers at SACLANTCEN. Briefing teams then attended 4 DM96 pre-sail briefings and explained the REA concept, REA products in the Guides and how this demonstration of NATO's current REA capability was intended to support the war fighters.

11. Communications

RR96 was a success partly because of the rapid exchange of data that was possible and the communications that supported that data flow.
Internet technology was employed to allow large volumes of data to be exchanged between collecting platforms, processing sites and fusion centres.
SACLANTCEN established an Unclassified RAPID RESPONSE Home Page on a server at the Centre. Ships at sea had a lap top computer coupled to a cell phone through a modem as their workstation. From this they could dial into the Home Page and ftp data into the appropriate directory. They could also down load any data or E-Mail required for the operation. Sites as far afield as the UK, the US and USS La Salle, which happened to be in the Black Sea, were able to access the Home Page and exchange data through it.
This Internet communications technology was crucial to the concept of REA and exceeded expectations of its capability. Some where in the order of 400Mbytes of processed data were handled by the Home Page, which experienced 16,000 log-ons from 57 users.

Rapid Environmental Assessment, SACLANTCEN Techniques used during RAPID RESPONSE '96

Tuncay Akal
SACLANT Undersea Research Centre
Viale San Bartolomeo, 400
19138 La Spezia, ITALY
Email: akal@saclantc.nato.int

Abstract

Recently, the focus of undersea warfare has changed significantly. Operations for unpredictable areas have become central to potential military actions. In the MILOC context, Rapid Environmental Assessment (REA) encompasses the collection, assimilation and analysis of essential environmental parameters needed to support system performance assessment and operational decision making; all accomplished within a tactically acceptable time scale. In this context, the first demonstration of REA has been performed during MILOC operation RAPID RESPONSE-96. Here some of the results are presented.

Introduction

The objective of REA is to make a methodology package available which can be applied, in cases of crisis, to predict the environmental parameters of operational interest within a tactically useable time scale both for ASW, MW and AW operations in areas which have not been visited before, or where actual knowledge is very limited.

During 1996 this new concept has been implemented as part of the Mediterranean MILOC' operation Rapid Response 96 (RR-96) to demonstrate the available REA techniques within NATO community, to move new REA techniques from the "experimental" phase to the "operational" phase, and finally to introduce validated REA procedures into NATO's Allied Environmental Support System (AESS). RR-96 was a demonstration survey, designed to demonstrate NATO's current REA capability in a limited but complicated environment to assist in validating and developing the REA capability.

RR-96 took place in the Straits of Sicily and Sardinia between 12 August and 12 September 1996. Hear we present a summary of some of the SACLANTCEN REA products utilized in addressing different phases of REA.

2. SACLANTCEN REA techniques

2.1.Expendable Bottom Penetrometer (XBP)

During RR-96 a new REA tool developed jointly by SACLANTCEN and Lamont-Doherty Earth Observatory of Columbia University was used for assessing certain sea-floor geotechnical properties that are important in planning and carrying out navy operations. The new tool, called an XBP (Expendable bottom Penetrometer) [1,2], can be launched from a moving ship in exactly the same manner as an expendable bathythermograph (XBT) or it may be deployed from an aircraft or submarine in direct analogy to the launch methods currently available for XBT launching (Fig. 1).

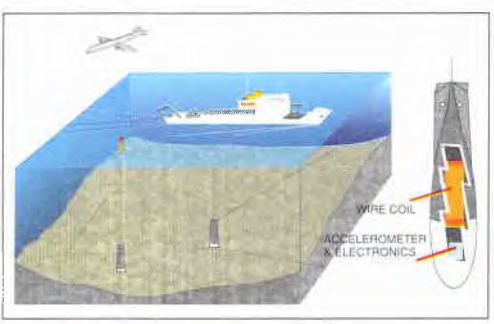

Figure 1: XBP system concept.

The XBP probes contain a sensitive accelerometer that measures the time-history of deceleration as it impacts and penetrates the sea-floor. This information is integrated to obtain the force exerted on the probe by the sediment as a function of depth of penetration. Since the force on the probe is a directly related to the undrained shearing strength of the sediment through well-known bearing capacity relationships, the shearing strength, which is one of the principal parameters necessary for evaluating mine burial potential, may be derived from the data in a direct way. Moreover, additional information about the Geo-acoustical characteristics of the sediment (e. g. whether it is granular or fine-grained) can also be determined from an analysis of the deceleration signature.

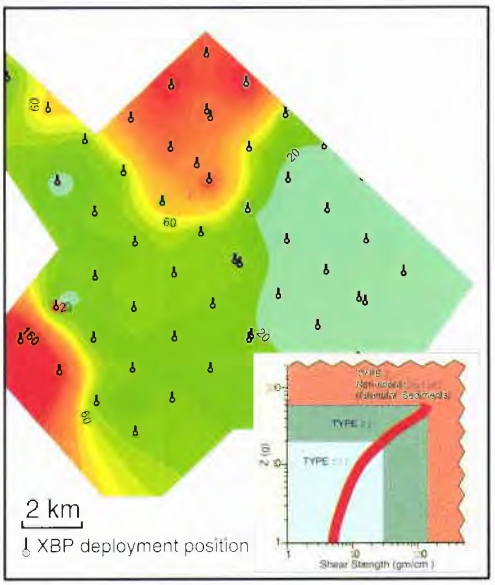

Figure 2: Sediment types within an area obtained by XBP.

During RR-96, XBPs were dropped in a rectangular pattern over a number of areas with the objective of defining sediment properties in certain regions of interest to the AW, MW and ASW community. These areas were then classified as to sediment type and certain parameters pertinent to mine burial studies such as shear strength were mapped in the regions where soft fine grained materials were found. Earlier work in the Mediterranean, Baltic and Black Seas suggested that the sediments could be divided into three more or less distinctive types designated I, II, and III. Figure 2 is an example of a chart showing sediment types within an area where 48 penetrometers were deployed. The quantitative information contained in this kind of chart is not available from any other kind of remote sensing technique currently in use and so illustrates the importance of this kind of reconnaissance.

2.2. 80 kHz Backscattering

Another new technique recently developed at the SACLANTCEN has been used onboard the R/V Alliance where acoustic data were collected at 80 kHz as part of the high frequency acoustic reverberation component of RR-96 (Fig. 3). With this technique we aim to describe the non-uniformity of the sea-floor environment whether it is made of areas of different sediment types, pockets of shells or fields of posidonia sea grass. The intent of the system described is to give a quick estimate of the acoustic properties of a site at frequencies relevant to mine hunting sonars.

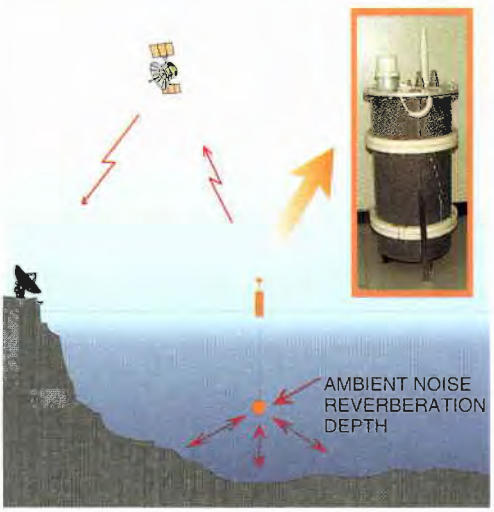

Figure 3: REA: Reverberation, Ambient Noise and Depth measurements.

During RR-96, fifteen sites were examined with this system and results are shown in Figure 4. Scattering strength as a function of grazing angle gives an indication of the average reverberation levels that can be expected with a 80 kHz system while the amplitude Probability Distribution Function (PDF) gives an estimate of clutter i.e. portions of the return that are consistently above the mean reverberation level [3].

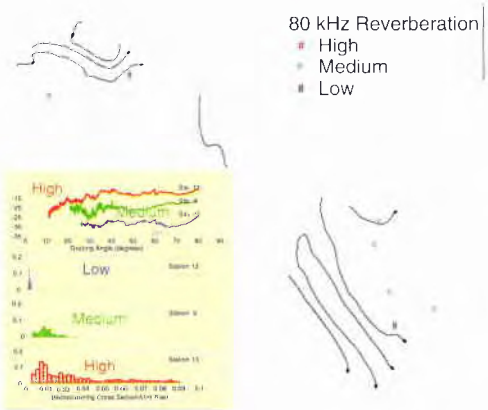

Figure 4: Description of an area according bottom reverberation characteristics.

Three sites were picked out as examples of three different reverberation regimes observed in the sites where measurements were taken. The expected mean reverberation levels can be estimated quickly from the graph with Station 13 giving the higher (Type: Red) and Station 12 (Type: Blue) giving the lower reverberation levels. The high scattering seen at Station 13 was the result of numerous shellfish covering the sea-floor while the video of Station 12 site revealed a very smooth featureless sea-floor. As an indicator of clutter the amplitude PDF of scattering cross section per unit area values was examined.

2.3. Ambient Noise

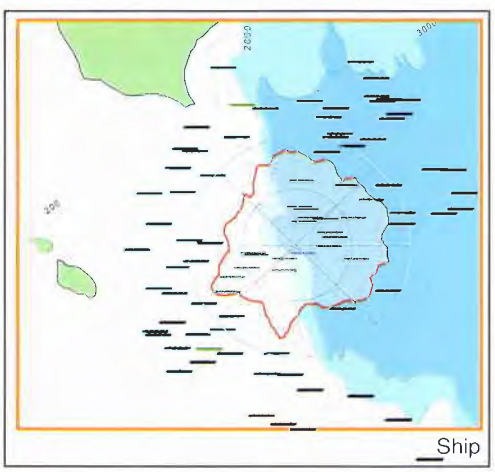

Figure 5: Shipping density and 50 Hz directionality pattern

The ambient noise field acts as an underlying limit on the detection ranges of passive sonar systems and active systems at long range. The objective of the noise field measurements conducted during Rapid Response was to determine the residual acoustic noise field in the RR-96 area, understand the physical processes generating the field and verify the prediction models for any given condition.

The measurement technique involves the performance of a polygon maneuver with a towed array, during which the beam noise levels are measured along each side of the polygon. An aerial shipping survey is conducted throughout the measurement period to provide near-to-intermediate range shipping data for modeling and interpretation of results.

The horizontal directionality measurements are presented in the form of polar plots at selected frequencies. The polar plot in Figure 5 represent the noise levels, relative to the omnidirectional levels. As an aid to interpretation of the results, the plots are overlaid on a nautical chart of the area, together with a plot of the aerial shipping survey.

The information obtained from shipping surveillance has been used to calculate the noise characteristics of the area. Figure 6 compares the measured data from Sonobuoys and SACLANTCEN towed array compared with RANDI 3-1[4] Ambient Noise Model outputs

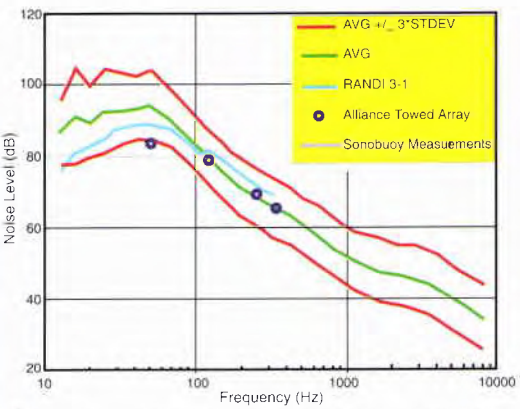

Figure 6: Measured and calculated Ambient Noise

2.4. Reverberation

Reverberation is the scattering of sound from the ocean volume, surface, and bottom. It limits active sonar performance by masking the target echo. At low frequencies (below 1 kHz) bottom reverberation tends to be stronger than surface and

volume reverberation; at higher frequencies surface reverberation is significant if the wind speed is high. Volume reverberation can be important when fish are present.

During Rapid Response 96, reverberation measurements were conducted from R/V Alliance using explosive sources, received on SACLANTCEN's towed array. These were used to characterize the areas, and by comparison with model predictions, to obtain estimates of bottom loss and scattering strengths.

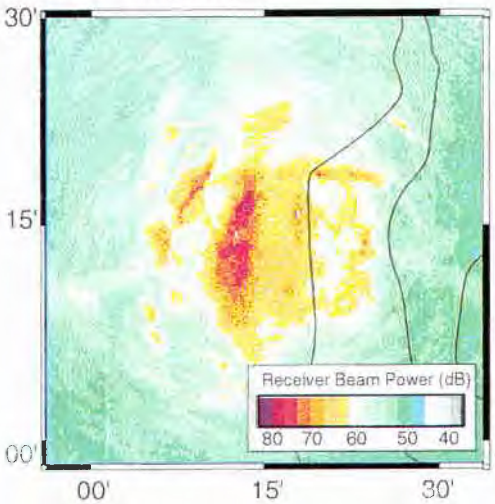

Figure 7: Reverberation field showing shallow water false targets

The reverberation data received on the towed array were formed into time series of spatial beams steered in different directions. By mapping time into range and beam angle into azimuth , the data displayed as intensity levels on a polar plot, similar to a radar display. Figure 7 shows an example of a polar display of reverberation field superimposed over the bathymetric chart of an area. This techniques provides the remote sensing of a large area to identify positions of false targets. Verification of reverberation models with this type of data permit to convert local bottom parameters to reverberation characteristics of an area [5].

2.5. Propagation

To a large extend the performance of a SONAR system can be described by a SONAR equation. Transmission Loss, Reverberation Level and Ambient-Noise Level are the parameters determined by the medium. As a SONAR parameter, Transmission Loss describes the magnitude of the energy lost while transmitted acoustic energy travels through the sea. As a parameter, it contains all the effects of different propagation phenomena.

The measurement technique involves deploying of an acoustic source (by a ship or aircraft), transmitting along a track and acquiring transmitted acoustic signals received at one end of the track with an array, during which the Transmission Loss levels are measured. Environmental parameters that effect acoustic propagation were also simultaneously to provide data for modeling and interpretation of results. Figure 8 shows the acoustic tracks covered during RR-96.

Figure 8: Transmission Loss measurement tracks covered during RR-96.

In support to the operation RR-96 broadband (50-3200 Hz) acoustic data from explosive and 3.5 kHz CW data from a towed sound source were acquired and processed onboard. During acoustic measurements sea-floor and oceanographic features have also been monitored, providing set of

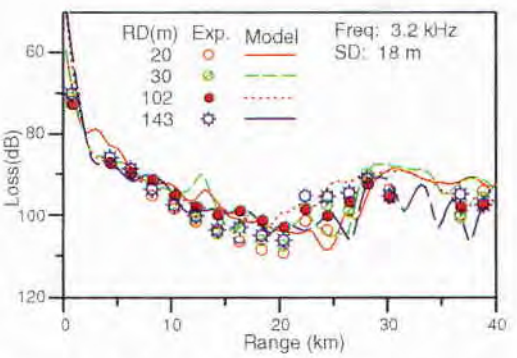

Figure 9: Measured and computed Transmission Losses at different receivers

parameters for acoustic propagation modeling. Figure 9 shows a comparison of measured and computed Transmission Losses for different receiver depths [6].

Due to the complexity of the environmental features affecting the acoustic propagation along the various tracks in this area, a suite of 2-D range dependent and range independent models had to be used to handle the various shallow and deep water scenarios at low and high frequencies. Ray based models as GSM [7], MOCASSIN [8] and HODGSON [9] were selected for deep water problems, while wave models such as PAREQ [10], RAM [11] and C-SNAP [12] were used for modeling in the shallow water regions. The computational speed, as well as the ability to treat bottom effects and sloping bottoms were among the main criteria for a choice between them.

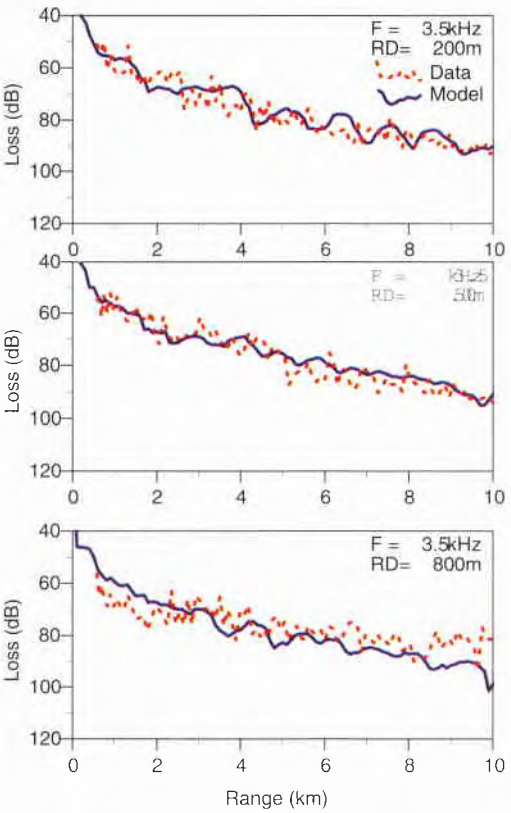

Figure 10: Data/model comparison for a CW source and receivers at different depths.

The model/data comparison presented here is intended to give a qualitative and quantitative illustration of the degree of predictability which can be obtained in the three areas. In figure 10 some examples are presented as propagation losses as a function of range for some selected tracks.

3. Conclusions

During the RR-96 the possibilities of the available SACLANTCEN REA methodology has been demonstrated.

As one can observe from the techniques presented, some of the methodology described depends on presence of special platforms and equipment on sight. These techniques have been used as ground-truth, to verify the capacity of forecasting acoustic parameters. These types of validations may not be possible during a crisis situation. Therefore remote techniques like, air/submarine deployed sensors, satellite remote sensing and reliable high resolution ocean and acoustic prediction models can provide the necessary information as REA methodology package which can be applied, in cases of crisis, to predict the environmental parameters of operational interest.

References

[1] T. Akal and R.D. Stoll: An Expendable Penetrometer for Rapid Assessment of Seafloor Parameters, pp 1822-1826, In OCEANS 95-Conference Proceedings, Oct. 1995

[2] T. Akal and R.D. Stoll: An Expendable Penetrometer for Rapid Assessment of Seafloor Parameters, pp 117-124, In UDT-96, Conference Proceedings, July 1996

[3] A. P. Lyons, D. A. Abraham, T. Akal, P. Guerrini: Statistical Evaluation of 80 kHz Shallow-water Seafloor Reverberation. SACLANTCEN Report SR-270, Sept. 1997

[4] J. E. Breeding, L. A. Pflug, M. Bradley, M. Hebert, M. Wooten: RANDI 3.1 User's Guide. NRL Report, NRL/MR/7176-94-7552, Aug. 1994

[5] Preston , Ellis, Akal (?)

[6] C.M. Ferla, F.B. Jensen and T. Akal: Rapid Response 1996: Modelling of Broad band Transmission Loss Along Selected Tracks in The Strait of Sicily. SACLANTCEN Memorandum: SM-334, July 1997.

[7,8,9,10,11] H. G. Schneider: Acoustic Models at Saclantcen. SACLANCEN Memorandum: SM-285 Mar. 1995.

Data Management and Exchange during RAPID RESPONSE '96: Problems and solutions

Alex Trangeled

SACLANT Undersea Research Centre
Viale San Bartolomeo, 400
19138 La Spezia, ITALY
E-mail: trangele@saclantc.nato.int

Abstract

For Rapid Response 96, a World Wide Web Internet server was established at Saclant Centre for exchange of data. It was connected to the Internet, but could be accessed only by authorized users from authorized sites. These included NRL and NAVO in the US, and DRA in the UK.

Four NATO naval vessels were issued with a portable computer, a modem with cellular capability and with a cellular phone. This allowed them to transfer data to/from the server via dial-in access through a Telebit Netblazer, and also provided an electronic mail capability.

Terrestrial installations also had dial-in access to the server. Both standard terrestrial connections and ISVN were used.

The system allowed for the timely exchange of measured and processed information between data collectors, processors and fusion cells.

A total of 216 Mb of data were uploaded during Rapid Response.

During the experiment, several problems of both technical and 'human-related' nature were encountered. We will address these issues and their potential solutions.

1. Introduction

In the summer of 1996, NATO conducted a major Sea trial, Operation *Rapid Response*.

Collected and processed data were stored centrally on a WWW-server located at Saclant Undersea Research Centre (SACLANTCEN) in La Spezia. The server was connected to the Internet, with access restricted to authorized sites. Authentication of users was based on the respective TCP/IP address. In addition, users were assigned a username and password.

Overall, the Operation was considered a success, albeit not error-free. Also, from a technical point of view, the overall performance, stability and 'user-friendliness' of such a system can be improved significantly, provided some measures are taken.

2. Communication methods

The following communications channels were utilized:

- Internet connection
- Cellular (TACS) dial-in
- PSTN/ISVN dial-in
- INMARSAT B/ISDN

Regardless of type, all dial-in computers became part of the SACLANTCEN domain. The communications setup is summarized in figure 1.

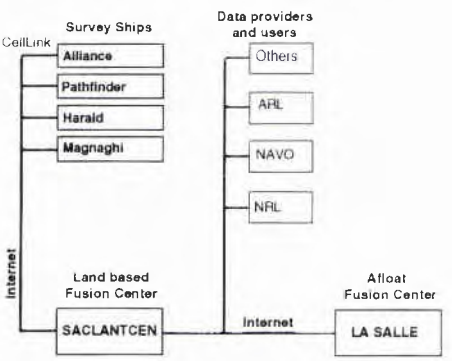

Figure 1: Data Flow RR96

2.1. Internet connectivity

Organizations, such as NAVOCEANO in the United States, and ARL in the United Kingdom established connections over the Internet. There were concerns, that SACLANTCEN's 128 Kbps connection would not be sufficient, so it was decided to upgrade to a T1 (2Mb) type connection for the duration of the Operation.

Although it did not live up to expectations with regard to speed (The average throughput never exceeded 512 Kbps), it did provide sufficient connectivity between the Centre and laboratories around the world.

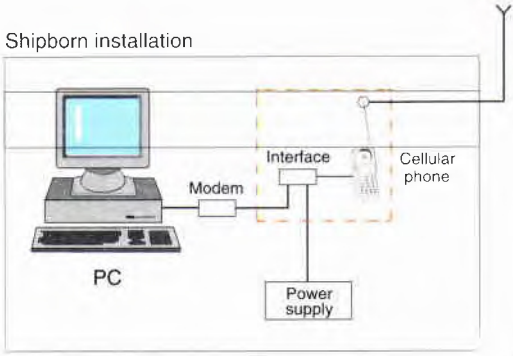

Figure 2: Ship portable equipment

The cellular phones were encapsulated in a water-tight box, and mounted next to their antennas in order to minimize loss through coaxial cables (Figure 2). A standard phone cable and power line were then run down to the PC's. Connections were established through the Italian analog cellular system(Figure 3).

Although connection speeds didn't exceed 9600 bps, these portable systems generally performed well. Connections were possible up to a distance of as much as 100 km from the Italian coast, depending on the placement of the antenna/cell-phone. This range is significantly larger then that possible with the GSM cellular network, where the maximum attainable range is in the order of 30-35 km.

2.3. PSTN/ISVN

NAVSOUTH connected via modem over the NATO ISVN or through the Italian Public Switched Telephone Network (PSTN), which is now largely digital except for the final connection to the subscriber.

Although the ISVN through-put is not impressive (Approximately 7200 Kb/s), it functioned reliably throughout the operation. PSTN connections can be twice as fast, but ISVN remained the primary choice, as no per-minute cost is involved in its operation.

2.4. INMARSAT A/B

In addition to a cellular connection, R/V Alliance utilized a high speed connection via Inmarsat A and B. Inmarsat B is a digital system, which on Alliance is connected to a Cisco router. The Inmarsat B ground

Figure 3: Data Flow RR96

station is connected to the European ISDN network and data transfers occur at 64Kbps.

On R/V Alliance, all computers on the Local Area Network have the option of connecting through the router. The Inmarsat systems were used when R/V Alliance was outside cellular range.

3. Data handling

It was decided to use standard off-the-shelf Internet hardware and software for data-exchange. First of all, it insured that a vast part of the participants were able to connect in a reliable fashion with already existing configurations, since the WWW-browsers exist for most computers. Secondly, we were able to choose the best hardware/software combinations for our needs. Emphasis was laid on security, ease of use, price and availability.

3.1. Web Structure/Security

Clients accessed the data structure through a WWW Home Page (Figure 4). Data requests were handled by a httpd daemon, *NCSA httpd*, running on a HP D350 computer. The software is freely down-loadable on the Internet, and proved sufficient, providing full support for password/ip-address access control, speed, reliability and CGI scripts. Access was further restricted by a Firewall.

3.2. Standards and Platform indepenancy

A data fusion center can only provide optimal performance and service, ie. *on-the-fly* data conversion, if provided and requested data types/formats are known in advance. In addition, data must also be independent of the systems on which the data are to be used.

Figure 4. Data Flow in R/R

A major problem encountered during Rapid Response was the many different file formats provided to us. For instance, five different platforms provided us with five different CTD file formats. The data formats were sometimes very poorly documented. In a few cases, one data provider even changed a **format** three times in two weeks.

The most widely used system-independent format used today remains ASCII. While this format is humanly readable, it is only appropriate for smaller files. Even though common data compression software can greatly reduce the size of an ASCII text file, and thus reduce the transfer time over a network, it is unsuitable for larger amounts of data, such as high resolution bathymetry data sets. Compression and decompression wastes both CPU time and disk space.

A better approach has been implemented by, for instance, MATLAB using 'MAT' format, and by *UNIDATA* with its Network Common Data Form (NetCDF). The NetCDF format is freely available via FTP, and represents scientific data via a machine-independent format. Together, the interface, library, and format support the creation, access, and sharing of scientific data. It is supported by hundreds of commercial and Public Domain software packages, and data files stored on one computer can be read directly from another with no time-consuming conversions involved.

3.3. Data transfers

3.3.1. Uploads

Data were uploaded to the server using the File Transfer Protocol (FTP). Data providers were issued an account and a directory, to which they could transfer their data. Providers were asked to provide an "info-file" accompanying each data file. This file would contain such information as data-type, longitude, latitude, date of acquisition, and finally the destination directory. A script running in a separate process would scan the upload-directories once an hour, read the information file, move the file to its destination directory, and finally update the main database.

This allowed us to index the data collected by position, time and data-type.

We encountered a number of problems with this approach. Due to erroneous information in the header files, data often ended up in the wrong directories, and would have to be moved manually when the mistake was noticed.

Clearly, a better approach needs to be investigated. In the future, we will try such strategies as enforcing users to enter data descriptions over, for instance, a forms-based interface, perhaps via a WWW-browser. Each WWW page will have an "upload button". When selecting this option, users can enter all information regarding a piece of data, including its whereabouts on the local file-system. Upon completion of the query, the file will immediately be uploaded to the relevant page.

3.3.2. Down-loads

The generally hierarchy of the server is shown in in figure 5.

Users could manually navigate through the hierarchy. A page with an interface to a search engine was implemented to search the database. A geographical clickable image map showing which data had been collected and where, was provided (Figure 6). We also provided a page where the latest entries in the database could quickly be accessed.

3.4. Page Content

3.4.1. Image formats

The data-type causing the heaviest load on any Internet Server is Image data. This was also the case on the Rapid Response Server.

In-lined images, while improving the visual impact, typically double or triple the total down-load time of a page. If a given image is used on several pages, it is an advantage to use an absolute reference to it, thus utilizing the cache-facility of the web-browser. A page will also load much faster, if the WWW-browser is given information regarding image size in advance.

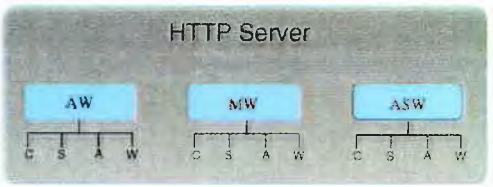

Figure 5: Web hierarchy

During Rapid Response, several different formats were utilized, the three most common being GIF, JPEG and TIFF.

Three items determine the size of a image file:

- Resolution
- Number of color entries
- Type of compression applied

In order to reduce the down-load time, irrespective of the format used, it is essential to reduce the file size of an image to its absolute minimum. In particular, this is the case when using sluggish connections such as cellular phones.

One way to do this is to reduce the usage of colors in the image file. This can often be done with little or no effect to the perceptibility of the image (Figures 7, since many graphics packages tend to allocate more colors then are actually used.

For larger images, such as satellite SPOT imagery in TIFF format, one should provide low-resolution, 16-color *thumbnail* preview images. This provides the user with a swift way of previewing a number of images, and aids him in deciding whether a full down-load is necessary. Furthermore, it dramatically reduces the overall load on a server.

3.4.2. tables

HTML tables , while improving visibility of a page, have the disadvantage, that a page cannot be displayed by the browser, until all code between the begin_table and end_table has been down-loaded. It is therefore an advantage to keep tables as small as possible.

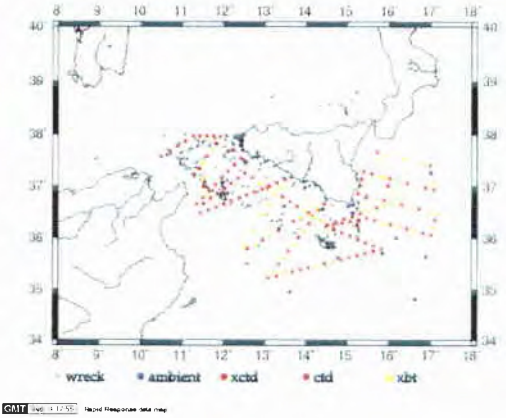

Figure 6: Area map

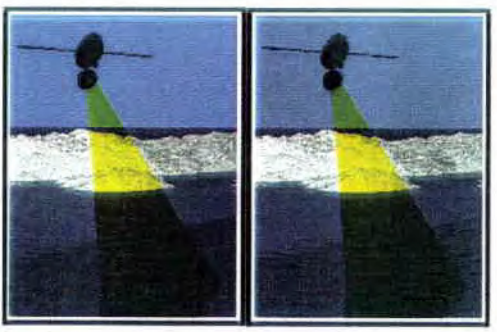

Figure 7: Gif file full color

4. Answers to questions

Should you require in-depth information, please contact

Alex Trangeled
Environmental Research Division
SACLANT Undersea Research Centre
Viale San Bartolomeo, 400
19138 La Spezia, Italy.
Email: trangele@saclantc.nato.int
Phone: (39) 187 540-296
Fax: (39) 187 540-331

5. Conclusion

It is essential that data providers supply full documentation for the data they intend to upload. Images should be kept as small as possible. Varying inlined images, except for where thumbnails are concerned, should preferably by avoided.

Describing and Forecasting Ocean Conditions during Operation Rapid Response

Jürgen Sellschopp*, Allan R. Robinson**

* SACLANT Undersea Research Centre
Viale San Bartolomeo, 400, 19138 La Spezia, ITALY

** Harvard University, Department of Earth and Planetary Sciences
Pierce Hall, 29 Oxford Street, Cambridge, MA 02138, USA

Abstract

Oceanographic conditions in the Sicilian Channel and western Ionian Sea were described in quasi real time by applying numerical dynamic modeling to survey results. The planning and execution of the hydrographic survey are described in the context of rapid data acquisition, evaluation, transmission and exchange with the Data Fusion Center and participating units. Examples of measured and modeled results are presented which illustrate the applicability and usefulness of the technique to naval operations.

1. Introduction

Rapid Response 96 was the first Military Oceanography (MILOC) survey designed for immediate support of a naval exercise with oceanographic and acoustic environmental data. The usual task to provide a reliable and comprehensive data set that strengthens the data base of environmental information systems, is preserved as in former surveys. But in addition and in contrast to any previous MILOC experiment, collected data and derived products were required to describe the actual environmental situation as at the end of September 1996.

The distinction between climate and actual weather is valid not only for the meteorological environment. The importance of mean against time variant aspects however varies with the type of environmental parameter. Obvious examples are the more static bottom characteristics *versus* ocean surface temperatures that change within synoptic time scales.

A motive for a Rapid Environmental Assessment survey can be the lack of sufficient data in a climate data base or a desire for updated actual data. The Sicilian Channel has been an area of major interest in the oceanographic research and military communities for many years. Climate data bases are therefore of good quality except for the southeastern part. The highest attention in Rapid Response 96 was given to the investigation of the actual "weather" and the methodology for a timely transfer of results to the naval exercise.

2. The Hydrographic Survey of *Alliance*

2.1. Design of the cruise

The part of the Rapid Response survey of *NRV Alliance* that was completely dedicated to oceanographic measurements was scheduled for 12 to 22 August with one week of on site hydrographic work, that is four to six weeks ahead of the naval exercise. Water mass distributions, sound velocity structures and ocean currents cannot be expected to be sustained for such a long period, but the changes can be predicted numerically, if the initial conditions and the acting forces are known in sufficient detail. Analogous to atmospheric weather forecast, degradation of numerical models of ocean dynamics is avoided by adaptive sampling and assimilation of fresh information at hand into the analysis and forecast system.

Previous knowledge of the area that was obtained in two cruises to the Sicilian Channel in 1994 and 1995 was applied to optimize the ship track for the expected mesoscale features. These are the cool and highly saline eddy centered on the southeastern edge of Adventure Bank and the jet stream through the Sicilian Channel into the Ionian Sea. During both autumn cruises, the Atlantic Ionian Stream changed direction from south to east near Pantelleria, crested near Sicily, crossed the Malta Plateau and turned northward to the Calabrian coast. The more sparse data in the oceanographic literature are consistent with this finding.

The track design for the survey, rather than covering the naval exercise area only in the Straits, took into account the needs for a sufficiently comprehensive area for ocean modeling.

The compromise between limited ship time and the need for dense information from a large area led to a zig-zag track through the Sicilian channel with as many crossings of the most important features as possible. Only the path from Adventure Bank in the west to the Calabrian coast in the northeast was preplanned. The track back to the west, essentially

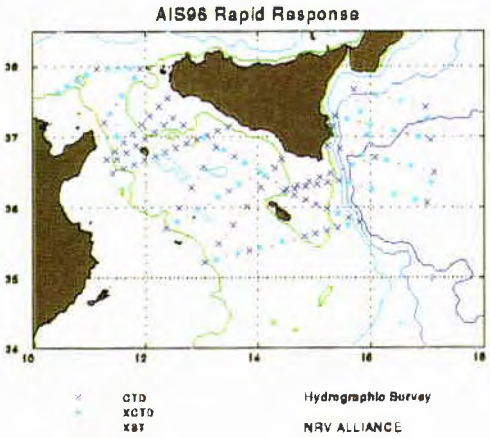

Figure 1 Stations in the Sicilian Channel and the western Ionian Sea. Depth contours indicate 200, 1000, 2000 and 3000 m.

parallel and some 50 km distant from the Sicilian coast was defined after inspection of the recently collected data. Hydrographic stations were separated by no more than 18 km, which is close to the internal Rossby deformation radius in the Sicilian channel.

Even if the probing instrument is not slacked down to the bottom every time, the stations are too many for the utilization of the high precision conductivity, temperature and depth (CTD) acquisition system. Expendable probes for temperature (XBT) or all three parameters (XCTD) were used instead for 89 of the 166 stations. The decision where it was tolerable to downgrade to an XCTD or an XBT was based on the degree of predictability of the salinity in that place. XCTDs very often and by an unknown amount, measure too low conductivity in the upper 50 m. Stations with less than 200 m water depth were always measured with the accurate CTD probe, because in shallow water, the salinity shows more variability than in deep water.

2.2. Survey data collection

Surface temperature was obtained from Advanced Very High Resolution Radiometers (AVHRR) of the NOAA12 and NOAA14 satellites. The images were processed at SACLANTCEN and included in the information on the Internet server of the Data Fusion Center.

Temperature and salinity profiles, the primary data set of the oceanographic survey, were the only data type assimilated into the numerical ocean prediction system. The Mk III CTD was calibrated before and checked after the cruise. Data acquisition was simultaneously accomplished on a PC and a workstation. Quality was checked, spikes removed, profiles filtered and formatted by an expert operator shortly after the measurement using a software package for the evaluation of high quality data.

Calibration checks had been made before deployment for all XBTs. Profiles of expendable probes were registered with a special hardware residing in a PC. They were transferred to the system on the workstation and treated similarly to the CTD profiles. A few hours after acquisition, all profiles were given to the numerical modelers and additionally, transmitted by radio-link to the Data Fusion Center at SACLANTCEN. Data were delivered in two formats: ASCII records every 1 m or dBar and inflection points coded in NATO's standard JJXX.

The measurement of temperature and salinity, and derived from these also density and sound velocity, were expanded by dynamic analysis to complete three-dimensional fields of these parameters. Geostrophic calculations also result in values of ocean current direction and strength. This represents one type of current measurements achieved during the AIS96 survey.

Ocean currents were also measured by three direct systems, by current meter moorings, by a ship-borne Acoustic Doppler Current Profiler (ADCP) and by satellite tracked surface drifters. While moored current meter data are interpreted after recovery and may be used for data base enlargement and model verification, the latter two of these systems provide data immediately useful to users of the Internet server during the exercise. Notice however that the Lagrangian motion of drifters can only be translated to streamlines of the calculated Eulerian flow as long as the current pattern does not change, and that ship-borne ADCP measurements represent a mixture of time- and space-dependent water motion.

Seven drifters were deployed by *NRV Alliance* in the western part of the Sicilian Channel during the AIS96 survey, and a second set by *ITS Magnaghi* three weeks later. Drifter positions were received from the Argos service via telephone. The limited daily information from single drifter motions cumulates into a relatively reliable image of the principal flow pattern in the Sicilian Channel An Acoustic current Profiler is permanently installed on *NRV Alliance*. In 1996 it was possible to create vector current plots as in Figure 2 and other data representations on board during the survey. Two years ago the complex software package CODAS3, written by scientists from the University of Hawaii, had been dowaloaded from the Internet. In the mean time, sufficient experience with the CODAS system was gained for rapid data evaluation. Therefore ADCP results were available every few days, after the data acquisition was halted and the ping data files were transferred to another computer for off-line processing. Channel.

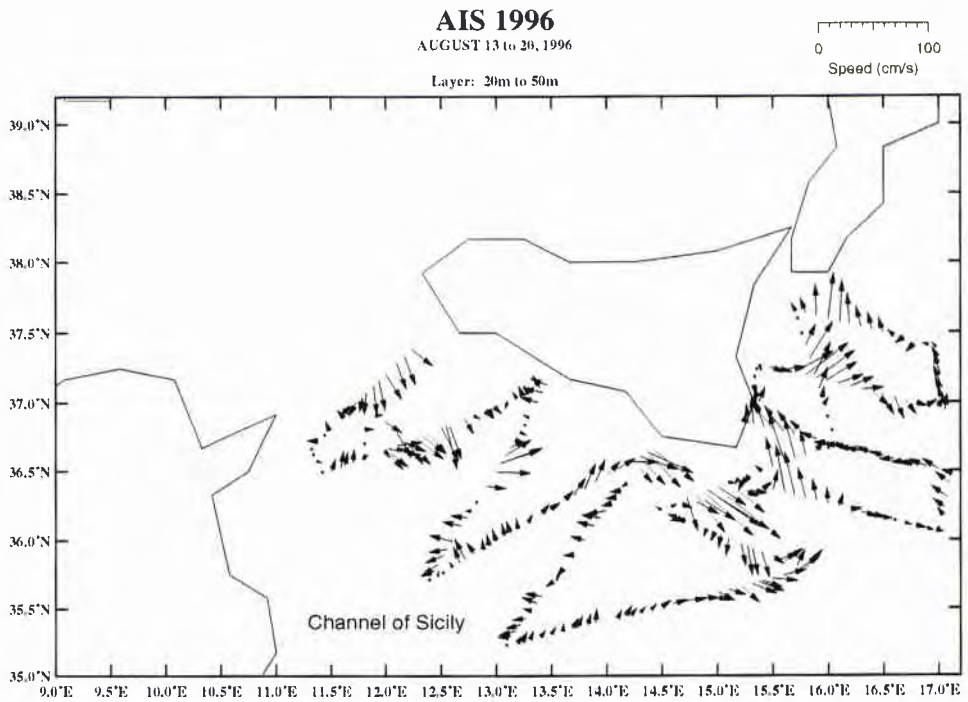

Figure 2 ADCP current vectors continuously measured in the upper layer by *NRV Alliance* on her way from Adventure Bank to the western Ionian Sea.

3. Ingesting Data from External Sources.

In addition to *Alliance's* AIS96 survey data, hydrographic measurements of further Rapid Response participants were necessary to drive the numerical models. The main supplement was airborne expendable temperature profiles. The flightpaths covered the tracks of *NRV Alliance* in the Sicilian Channel and western Ionian Sea and extended the area at its southeastern corner to 34° 30' N. The patrol aircraft were stationed on Sicily. AXBT data were made available shortly after the mission by the flight coordinator [2] and transmitted *via* cellular telephone to the Data Fusion Center. By Internet connection [3], the data were received on *Alliance* and merged with

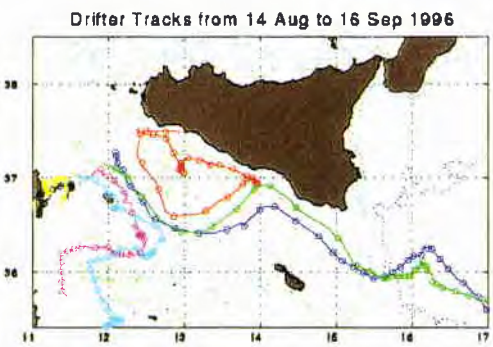

Figure 3 Drifters were deployed on a section crossing Adventure Bank and the Pantelleria Channel. Circles indicate midnight positions.

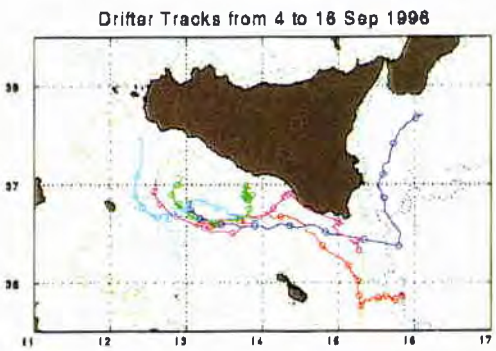

Figure 4 Drifters were deployed in the periphery of the Adventure Bank eddy. A current of 20 cm/s displaces a drifter by 10 miles per day.

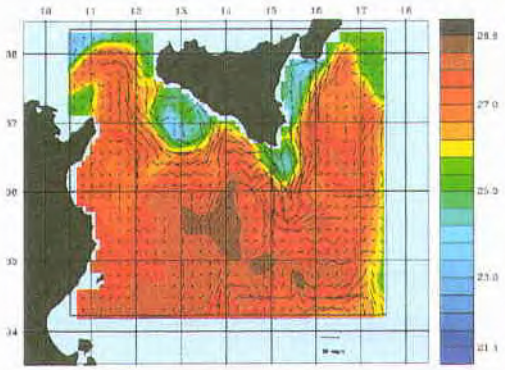

Figure 5 Dynamic analysis of 22 August showing surface temperatures and current vectors. The reference arrow indicates 25 cm/s

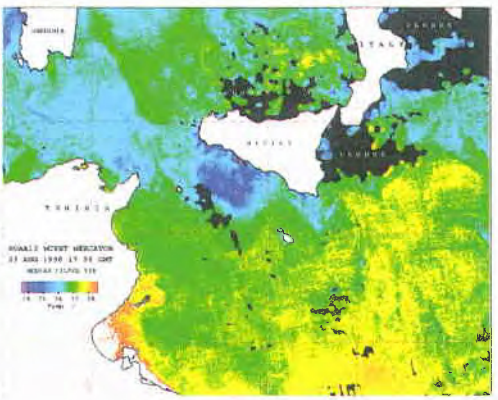

Figure 6 Surface temperature on 23 August measured from satellite

existing profiles. All AXBT profiles irrespective of the nation that provided the aircraft, were written in the same two formats, one for high vertical resolution and another for profile approximation by inflection points. A format description together with an example file had been supplied before the survey.

At the end of August, when the oceanographic survey concluded and oceanographic modeling was continued at SACLANTCEN, temperature profiles of air missions were the main source of data for assimilation into the system. There is always a desire for some salinity data in order to get the density fields right. As expected however, the survey ships were in confined areas during most of September and were therefore not able to meet the requirement for more CTD data sets in the modeling target area.

Of the CTD data that were received, only part was transferred to the modelers, because of unsolved decoding problems. It happened that a CTD data format was not understood or only after several days, too late for inclusion of the data in the prediction system.

Apart from sample data in the water column, the Ocean Prediction System needs surface fluxes of heat, momentum and water vapor. During the period of numeric modeling the wind was in general fairly moderate. Meteorological observations at airports in and around the Sicilian Channel reflect more the daily onshore-offshore cycle of the wind than the conditions at sea. Computed fields provided by the American Fleet Numerical Meteorology and Oceanography Center were the only data for surface stress, heating or cooling and evaporation. The absence of extreme weather situations made it easier to live without detailed local weather analysis.

4. The Hydrographic Situation during AIS96

The most striking feature in the observational period is the jet current that enters the Sicilian Channel from the north across Adventure Bank. It is apparent in the plots of ADCP measurements and drifter tracks as well as in the dynamic analysis output (Figure 5). Near 36° 30' N, 13° E the current turns NE. Close to the Sicilian coast, there is a bifurcation. Part of the stream is circulated back into the eddy which is centered on the eastern slope of Adventure Bank. The main branch turns SE and crosses the Malta Plateau. On the shelf break, at least during the survey of *Alliance*, the stream of modified Atlantic water into the Ionian (AIS) turns north and proceeds parallel to the Calabrian coast. The drifter tracks in Figure 3 seem to be in contradiction with the last mentioned detail. Remember however, that in a meandering current Langrangian (drifter) and Eulerian (streamline) velocity vectors differ, and that the surface current divergence which is coupled with the decrease of the mixed layer depth in the cyclonic motion, accounts for the escape of drifters from the main stream east of Malta.

The mine warfare area of Exercise Dynamic Mix lies at the northern edge of the Adventure Bank eddy, the position and structure of which are continuously changing. The exercise area may therefore on one day be exposed to the AIS inflow, on another day, lie in the higher salinity, westward back-circulation and soon after find itself in a local coastal current. With the given observational network, a precise forecast with a resolution of few miles is not possible. In the MCM environmental guide prepared for Dynamic Mix, it was however possible to discuss the situation and explain the currents and temperature and salinity profiles that must be expected.

The anti-submarine warfare areas south and southeast of Sicily were crossed by the meandering Atlantic-Ionian Stream (AIS). The lower AIS salinity and the layer depth variations caused by the current, directly influence the sound velocity structure in the Sicilian Channel and the Ionian Sea. One of the examples presented in the ASW environmental guide is given in Figure 7 and 8. It demonstrates changing sound propagation conditions within distances comparable to the sonar range. The profiles were taken from the section that starts on the shelf break and ends near 36° N, 17° E (see Figure 1). The shallowest profile is located in the cyclonic motion on the Malta Plateau edge. It demonstrates the reduced surface layer thickness mentioned earlier and an uplift of Levantine Intermediate Water, the water mass with the highest salinity, from 300 m to 100 m depth. Sound velocity profiles and therefore propagation conditions are strongly influenced by the water mass distribution in the western Ionian Sea. In the case under discussion only the three easternmost sound velocity profiles have the same characteristics.

The path of the AIS and the positions of eddies vary with time. The intention of dynamic modeling is to trace and predict changes of the physical fields including the sound propagation conditions. In order to do so, the numerical model extrapolates in time and assimilates observational data.

5. Experience with the Harvard Ocean Prediction System.

5.1. Initialization with CTD/XBT/AXBT data

The Harvard Ocean Prediction System (HOPS) [1] had been configured for Rapid Response 96 with matched five miles resolution bathymetry, Mediterranean Ocean Data Base climatology and the synoptic data sets of two previous cruises AIS94 and AIS95. The surface temperature in summer 1996 was significantly higher than summer climatology and old cruise data. The model ocean was initially heated up from the surface in order to meet the 1996 summer conditions. During AIS96 Rapid Response, cruise data and AXBT profiles were assimilated into the system as soon as they became available.

At the end of the 12-24 August time period when the oceanographic survey was completed, data base climatology and synoptic data from past years were no longer used in the forecast methodology. Figure 5 illustrates the dynamic analysis (nowcast) of surface temperature for 22 August. Conditions are generally warm, with the Atlantic-Ionian Stream (AIS) defining the boundary between cooler coastal waters and warmer off-shore waters.

Major features persisting in this region are: the inflow position of the AIS (Western Sill Jet), the Adventure Bank Vortex, the crest of the AIS in the Malta Channel, the Ionian Shelf Break Vortex and the East Sicilian Vortex. Significant variabilities of the major features of the region include: the size, position and shape of the vortices, the relative strength of the AIS, the location of the AIS and the tendencies of the motions.

The Malta Channel Crest of the AIS is located close to the coast of Sicily, with its closest proximity at 14° 30' E. The Ionian Shelf Break Vortex is small, centered at 36° 25' N, 15° 20' E.

5.2. Rapid Response nowcasting and forecasting

Over the period 24 August - 15 September, 520 additional profiles were added to the usable data set. This data was assimilated into the forecast system on an ongoing basis, leading to the issuance of dynamical nowcasts and forecasts on 28 and 31 August and 4 September.

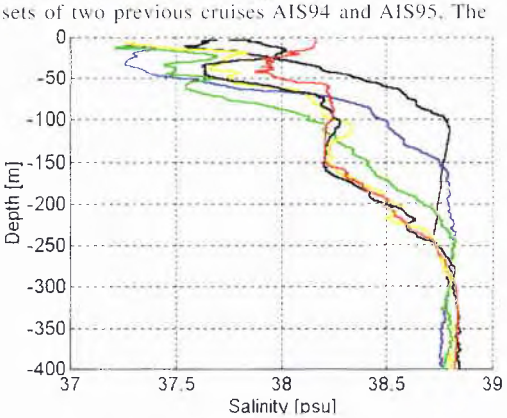

Figure 7 Salinity profiles of 18 August 1996 on a section from the Malta Plateau shelf break into the Ionian Sea. LIW rises to 100 m at the shelf break

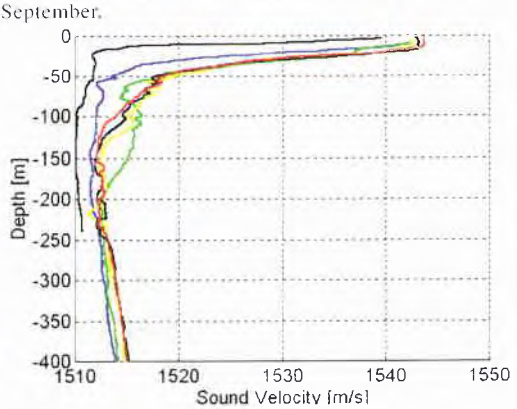

Figure 8 The sound velocity structure in the section in the Ionian Sea is influenced by upwelling in the cyclonic eddy on the shelf break and by the water mass composition in the AIS

A quick-look verification of predicted variations in the Sicilian Channel was performed for four instances of the Rapid Response survey. The satellite sea surface temperature images of 23AUG1736 (Figure 6), 25AUG1259, 27AUG1237 and 07SEP1218 and the HOPS nowcasts of 22, 28 and 31 August and 4 September have been selected and the position and shape of three dominant features are described in Tables 1 and 2, as well as their development in time. The quick-look comparison of actual development versus predicted development for 25 and 30 August and 3 and 7 September in Table 3 indicates that the HOPS forecasts successfully predicts conditions in approximately 70% of the instances.

Table 1 Satellite surface temperature

	Adventure Bank Vortex	Malta Channel Crest	Ionian Shelf BreakVortex
23-Aug	Medium size W of 14 E	Close to Sicily about 14.5 E	Small N of 36 N
25-Aug	Extends E to 14 E	Moves to SE	Enlarges extends S
27-Aug	A little more to S	Similar to 23 Aug moves N	Smaller or the same
07-Sep	A little more to S Indented meander	Moves to SE as 25 Aug	Extends E to 16 E

Table 2 HOPS nowcast (dynamic analysis of available data)

	Adventure Bank Vortex	Malta Channel Crest	Ionian Shelf Break Vortex
22-Aug	Medium size W of 14 E	High centered on 14 E	Small N of 36 N W of 15.75 E
28-Aug	Square, moves E across 14 E	14.5 E Moves to SE	Enlarges, moves S, extends E
31-Aug	Still straight on the W.	N at 14 E moves N	Similar to 28 on the E
04-Sep	Similar to 22 Aug	N at 14 E	Moves slightly NW

Table 3 HOPS forecast for 2 or 3 days

	Adventure Bank Vortex	Malta Channel Crest	Ionian Shelf Break Vortex
25-Aug	As nowcast ++	As nowcast ++	As nowcast ++
30-Aug	Square but wrong orientation	Remains SE of 14 E -	Similar +
03-Sep	Retains shape ++	N at 14 E ++	Slightly E -
07-Sep	W edge moves W ++	Perhaps slight SE ++	Extends to S -

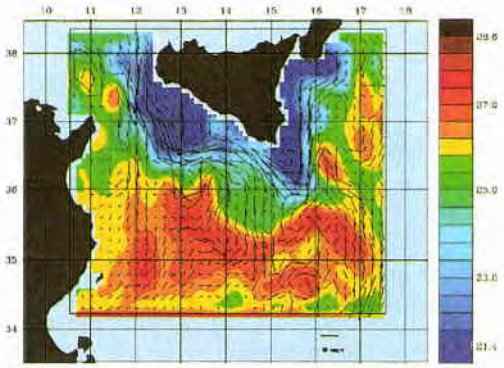

Figure 9 Dynamic analysis for 16 September

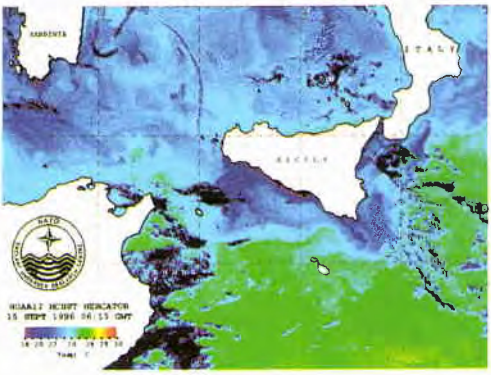

Figure 10 Surface temperature of 15 September

5.3. Nowcast (analysis) for 15 September 1996.

All data gathered up to 15 September has been used to create the dynamical analysis (nowcast) (Figure 9) for 16 September. This data set, is the data set used during the continuing Rapid Response period, augmented by an AXBT flight on 15 September. The general conditions have cooled in response to the seasonal changes and the major features have changed in size and shape (Figure 10), when compared to 22 August (Figure 6).

The crest of the AIS in the Malta Channel has flattened and moved southwards; with the AIS having more E-W orientation. The crest reaches its maximum at about 36° 30' N, 14° E. The Ionian Shelf Break Vortex is large, now reaching as far south as 36° N. The AIS has moved offshore, with its northward flowing branch located at 16° E.

5.4. Forecast with wind forced response

The forecast based on the situation of 16 September has been forced by internal dynamical processes and direct response to local surface forcing, which was derived from FNOC forecasted fields and is shown in Figure 11. The forcing pattern distributions are taken to be constant for the day. The wind stress pattern changes from a dominant north-south orientation on 20 September (Julian day 264) to an east-west distribution on 21 September (Julian day 265). Four and five day forecasts for the 20th and 21st of September are shown in Figure 12.

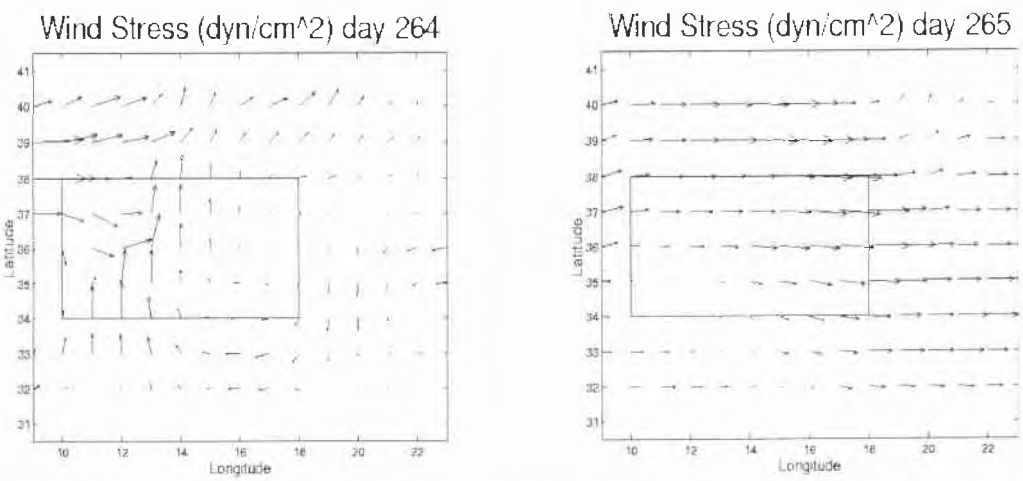

Figure 11 Surface forcing fields for 20 and 21 September provided by Fleet Numerical Meteorology and Oceanography Center

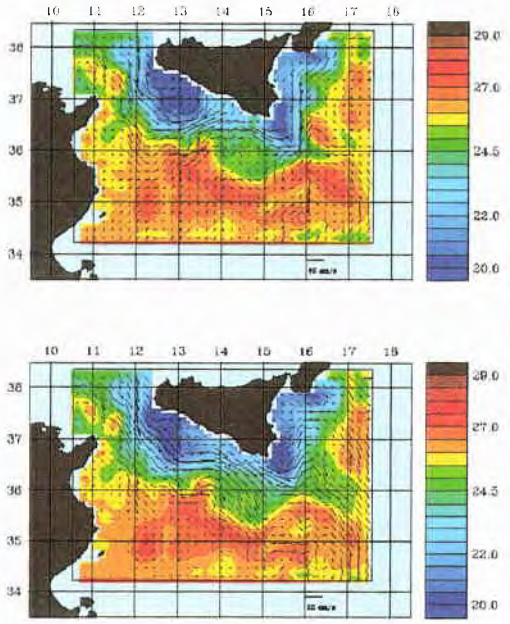

Figure 12 Surface temperatures and currents for 20 and 21 September, forced by predicted wind stress fields

We note the effect of the wind stress orientation on the surface flow (level 1) and the features that we have been following. The 20 September wind stress tends to drive the flow on shore. The 21 September distribution tends to push the flow to the right of the coast.

On 20 September, the Adventure Bank Vortex has moved onshore and has been further elongated in the NW-SE direction. The inflow of the AIS has a more onshore component than on 16 September. Surface temperatures are largely unchanged over the one-week period.

The crest of the AIS in the Malta Channel is moving back towards the Sicilian coast, the AIS has regained some of its 'arch' shape. The crest's maximum is now located at 36° 35' N, 14° 15' E. The Ionian Shelf Break Vortex is reduced slightly in size, now only reaching as far south as 36° 15' N. The northward flowing branch of the AIS is essentially unchanged in the ASW region. Figure 13 shows the radiation temperature of 20 September indicating the correctness of the prediction.

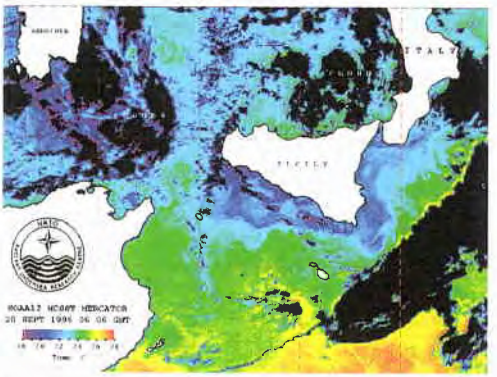

Figure 13 Surface temperature of 20 September

Acknowledgments

The work was made possible by the engagement and competence of numerous colleagues inside and outside SACLANTCEN.

This research was supported at Harvard University by the Office of Naval Research under contracts N00014-90-J-1612 and N00014-95-1-0371. Prof. Robinson thanks the tireless efforts of: Dr. Carlos J. Lozano, Mr. Wayne G. Leslie, Mr. Pierre F. J. Lermusiaux, Dr. Patrick J. Haley, Jr. and Dr. Lawrence A. Anderson.

References

[1] A.R. Robinson, "Real Time Regional Forecasting for Rapid Environmental Assessment with the Harvard Prediction System" in *Proceedings of the Conference on Rapid Environmental Assessment*, Lerici (1997).

[2] J. O'Neill, "Maritime Patrol Aircraft Operations during Rapid Response '96" in *Proceedings of the Conference on Rapid Environmental Assessment*, Lerici (1997).

[3] A. Trangeled, "Data Management and Exchange during Rapid Response '96: problems and solutions" in *Proceedings of the Conference on Rapid Environmental Assessment*, Lerici (1997).

Maritime Patrol Aircraft Operations During OPERATION RAPID RESPONSE 96

Charles J. O'Neill
1002 Balch Blvd
Stennis Space Center MS, 39522
Email: cjoneill@navo.navy.mil

Abstract

In August and September 1996, The NATO Military Oceanography Committee (MILOC) undertook OPERATION RAPID RESPONSE 96. This operation was the first proof of concept for a new idea called Rapid Environmental Assessment (REA). RAPID RESPONSE 96 directly preceded EXERCISE DYNAMIC MIX 96, and was designed to provide Navy Battle Group Commanders with additional environmental information specifically tailored to their warfare specialty needs during the exercise.

During OPERATION RAPID RESPONSE 96, a total of 22 Maritime Patrol Aircraft (MPA) flights were conducted to collect environmental data including oceanographic, acoustic, magnetic, and meteorological data. Flights included joint operations with surface ship data collection platforms and NATO combatant vessels.

1. Introduction

Twenty-two data collection flights were conducted by NATO Maritime Patrol Aircraft (MPA) during the period 12 August to 26 September. Nations providing MPA assets during RAPID RESPONSE 96 included Canada, Netherlands, United Kingdom, and the United States (Figure 1). During these flights, scientific crews aboard the aircraft collected oceanographic (temperature profile), acoustic (ambient noise and reverberation), magnetic, and meteorological data. These aircraft were also tasked to deploy drifting buoys, acoustic sound sources, and to record surface shipping densities to support the RAPID RESPONSE shipboard data collection efforts. All data collection flights were conducted from the NATO air base at NAS Sigonella IT on the island of Sicily. Data fusion centers were established at the NATO SACLANT Undersea Research Center (SACLANTCEN) and aboard USS LASALLE (COMSTRIKEFORSOUTH) to assess and analyze the data collected by MPA and survey ships. Data were transferred to a World Wide Web (WWW) home page at the data fusion center at SACLANTCEN using standard Internet protocols via the Italian telecommunications infrastructure.

Date	Aircraft	Mission
12 August	NL P-#C	AXBT, A/N
15 August	US P-3C	AXBT, A/N
17 August	US VP-45	AXBT, A/N
19 August	NL P-3C	AXBT, A/N
22 August	NL P-3C	(Cancelled)
24 August	NL P-3C	AXBT, A/N
26 August	US VP-45	AXBT, A/N
28 August	US VP-45	AXBT, A/N
31 August	NL P-3C	AXBT, A/N
2 September	US NRL	RVB, A/N, AXBT
3 September	CAN CP-140	SUS, AXBT, A/N
4 September	US NRL	SURV, RVB
5 September	CAN CP-140	SUS,AXBT
6 September	CAN CP-140	Magnetics
7 September	US NRL	SURV, RVB
8 September	CAN CP-140	SUS, AXBT
9 September	CAN CP-140	AXBT, A/N
10 September	US NRL	SURV, AXBT
15 September	NL P-3C	AXBT, A/N
18 September	US VP-64	AXBT, A/N
22 September	UK NIMROD	AXBT, A/N
24 September	UK NIMROD	AXBT, A/N
26 September	UK NIMROD	AXBT, A/N

Table 1:Rapid Response 96 MPA flight schedule

2. Survey Planning

Survey tracks for the first three survey flights were planned and constructed prior to the start of RAPID RESPONSE 96. Tracks for subsequent flights were designed using the analysis of data collected on previous flights by the fusion centers at SACLANTCEN and aboard USS LASALLE. Scientists merged these data with remotely-sensed data from satellites and with historical and modeled data. Detailed analyses indicated where additional data were needed to obtain and maintain a good overview of the oceanographic and acoustic conditions in the area-of-interest. Proposed survey tracks from the fusion centers were forwarded via E-mail to the Air Operations Coordinator at Sigonella, where the tracks were modified to meet operational constraints imposed by the aircraft limitations and the "real-world" situation in the exercise area.

Close cooperation and coordination were required between the Air Coordinator and personnel at the

TSC/MACA at NAS Sigonella to ensure that proper clearances and flight authorizations were obtained prior to each survey flight. Before each survey flight, aircrews and scientists were briefed by the Air Coordinator and provided with tasking and track lines for their flight. After completion of each survey flight, the Air Coordinator debriefed the aircrews to determine any problems that occurred during the flight and to solicit suggestions for improving the survey process.

3. Data Acquisition

Oceanographic and acoustic data were collected using air deployed expendable sonobuoys. The Airborne Expendable Bathythermograph (AXBT) buoy was used measure the temperature structure of the water to a depth of 400 m, and telemeter this information to the aircraft via a radio link. The AN/SSQ-57B sonobuoy (or its equivalent) was used to measure ambient noise. This buoy will deploy an omnidirectional hydrophone at a pre-launch selectable depth of either 27 m. (90 ft.) or 122 m. (400 ft.). Acoustic data between 10 Hz. and 20000 Hz. are telemetered to the aircraft via a radio link.

Magnetic data were collected by the Canadian CP-140 Aurora using its Magnetic Anomaly Detection (MAD) sensors and special collection and analysis equipment installed aboard the aircraft.

The Portable Data Acquisition and Processing System (PDAPS) was installed aboard each aircraft to perform the actual data collection and processing of AXBT and ambient noise data. PDAPS was developed by the Naval Oceanographic Office (NAVOCEANO) for use onboard fleet aircraft during naval exercises. The system will collect and process data telemetered to the aircraft from air-deployed expendable sensors. It is capable of processing data from up to three AXBT buoys simultaneously as well as providing calibrated ambient noise spectrum levels from 12 to 8000 Hz using air-deployed buoys. The system is contained in a single transportable case with a weight of 250 lb. and dimensions of 24"W X 24"D X 36"H. Connections to aircraft systems include 110 VAC 400 Hz power and the sonobuoy receiver system. PDAPS is also equipped with a Global Positioning System (GPS) receiving system for precision navigation data. The GPS is installed in the sextant port of each aircraft. The aircraft remained fully ASW mission capable with PDAPS installed. Approximately two to three hours were required for PDAPS installation aboard each aircraft and calibration of the aircraft sonobuoy receiving system.

PDAPS was installed aboard each aircraft except for the NRL and NIMROD aircraft. The NRL aircraft was equipped with onboard data collection and processing systems that replicated PDAPS with the additional capability for collecting and processing narrow band ambient noise and reverberation data. Clearances for installing PDAPS aboard the NIMROD were not obtained in time for this exercise.

4. Data Processing

NAVOCEANO scientists flew aboard the MPA on all survey flights to operate the PDAPS equipment. They were able to perform real-time data collection, processing, editing, and quality control while the flight was in progress. Final editing and quality control of the data were performed at the conclusion of the flight.

The temperature profile data received aboard the aircraft were processed to provide results in two formats. The data were processed into a JJXX format which gives inflection point information from the profile. This format is easily ingested into NATO tactical decision aids and models. The data were also processed to provide digital data files giving temperature values at 1-meter depth intervals along the profile for more detailed analysis by scientists at the fusion centers.

Ambient noise data were processed to yield calibrated spectrum levels at standard 1/3 octave center frequencies between 12 Hz and 8000 Hz. These data were corrected for sonobuoy receiver and sonobuoy calibrations by PDAPS. Ambient noise data collected by the NRL aircraft were processed in 1 Hz bands from 10 Hz to 5000 Hz to provide a detailed look at the structure of the noise field. Reverberation data were processed as _ second time-series records for various frequencies of interest.

Magnetic data were processed by special equipment aboard the CP-140 Aurora aircraft to provide charts indicating the expected performance of Magnetic Anomaly Detection (MAD) equipment in one portion of the RAPID RESPONSE survey area.

Data from the NIMROD flights were not collected and processed using PDAPS in real time. Tape recordings of the data were replayed after these flights in the TSC/MACA into PDAPS and were then processed in the normal fashion.

Following processing and quality control, the data from each flight were uploaded to the RAPID RESPONSE home page using standard INTERNET protocols. Both tabular and graphical digital data were uploaded. Data were normally available on the home page within three hours of the completion of the flight. These data were further analyzed by scientists at SACLANTCEN and aboard USS LASALLE for inclusion into tactical decision aids and acoustic and oceanographic models used to determine the oceanographic and acoustic properties of the RAPID RESPONSE survey area.

These analyses also yielded an insight into where and what types of additional data were required to fully understand the ocean dynamics in the survey area. Recommended survey tracks for future flights were forwarded to the Air Coordinator by scientists at SACLANTCEN. These recommendations were evaluated by the Air Coordinator, modified as necessary for aircraft and operational considerations,and flight plans were constructed. Operations and scheduling personnel at the TSC/MACA were briefed concerning the flight plans, the plans were modified as required and TSC/MACA personnel obtained the appropriate flight and area clearances. These procedures were very effective in ensuring that MPA assets and flight hours were optimally used for collection of the highest priority data.

5. Lessons Learned

5.1. Explosives

Signals Underwater Sound (SUS) were used during the exercise as acoustic sources for reverberation and propagation loss measurements. SUS contain 1.8 lb. of TNT and are designed to detonate at a pre-determined depth. As would be expected, extreme care must be taken to ensure that only trained personnel handle these explosives.

Logistics can also pose several problems when SUS are involved. All SUS should be prepositioned at the required locations at least 60 days in advance of the commencement of the exercise. Quite often, as was the case for RAPID RESPONSE, shipments of SUS are disrupted or postponed for a myriad of reasons. Personnel at the Weapons Department at the air base must be notified well in advance of the arrival of the SUS, and a constant monitoring of the shipment is required. Once the SUS are delivered to the air base, the problems are not over. Every movement of the explosives must be closely coordinated with the Weapons Department, including delivery of the SUS to the flight line. Any movement of SUS requires considerable advance preparation including obtaining approval of local government and police officials with the inherent delays for processing these approvals.

Training for shipboard personnel on SUS handling and safety and on the SUS launchers provided by the US was conducted at NAS Sigonella. An explosives expert from the Weapons Station Yorktown VA was brought to Sigonella to conduct this training. If SUS and SUS launchers are to be used in future exercises, provisions must be made for training appropriate personnel.

5.2. Expendables

Expendables including AXBT, ambient noise, and other air deployed buoys must be identified early in the exercise planning process. Firm commitments are required from all nations concerning the quantity and type of buoys they can provide. All sonobuoys should be pre-positioned at the air base prior to commencement of the exercise. Expenditure of sonobuoys allocated to the exercise should be controlled by the Air Coordinator.

Sonobuoys used by various nations have similar operational capabilities, but may be slightly different in their configuration and/or electronics. All details concerning sonobuoys from each nation should be forwarded as soon as possible to the Air Coordinator who will ensure that the buoys will perform the desired data collection missions. The Air Coordinator will also make sure that all details of the buoys are available for incorporation into the data processing hardware/software to be used.

All participants should make every effort to obtain clearances for the deployment of expendables provided by other nations. This greatly increases the flexibility of survey flight planning and will allow the optimal use of all MPA aircraft and expendables.

5.3. Data Collection and Processing

5.3.1. Survey Planning

Near-real-time analysis of the oceanographic and acoustic data by the data fusion center at SACLANTCEN had many benefits. Combining the survey data with remotely-sensed and historical data gave a much better view of the conditions in the area than could be obtained with the survey data alone. Proposed flight tracks, designed to acquire data where most needed in a changing environment, were forwarded to the Air Coordinator following each flight. The fusion center also provided graphical presentations of the data from AESS and Harvard Ocean Prediction System (HOPS), which gave the scientists and aircrews at Sigonella a better view of the MPA operational data requirements.

This program of data analysis and data exchange allowed the Air Coordinator to make the most effective use of the aircraft and expendables dedicated to the exercise. Flight planning, TSC/MACA personnel, and aircrews had to be flexible to accommodate these changing data requirements. During RAPID RESPONSE 96, all personnel involved in the MPA operations were most cooperative, and the Air Coordinator and the NAVOCEANO scientists on the flights had an outstanding relationship with all personnel involved.

5.3.2. Data Collection/Processing Equipment

During RAPID RESPONSE 96, all MPA oceanographic and acoustic data were collected and processed using PDAPS. Using one system for collecting and processing data gathered by various

types of aircraft from different nations has many advantages. Collection and real-time processing of the data are standardized, providing greater reliability in the accuracy of the data. The data are always handled using the same formats, making quality control a manageable task and simplifying the uploading of the data to the "home page" in standardized formats. The built-in GPS system in PDAPS ensured that all data were collected to the same navigational accuracy and standard.

If possible, PDAPS or a similar system should be used for MPA data collection in future REA exercises.

5.3.3. Data Collection/Processing Personnel
Using the same scientific personnel aboard all survey flights also simplifies the operation and gives greater control over the accuracy and quality control. Three NAVOCEANO scientists installed the PDAPS aboard the aircraft scheduled for each survey flight, calibrated the aircraft sonobuoy receiver system, attended the pre-flight crew briefings, flew aboard the aircraft performing the in-flight data collection and processing tasks, and removed the equipment from the aircraft. These same peraonnel performed the post-flight data processing, editing, and quality control, and uploaded the data to the "home page". This continuity of personnel handling the data throughout each flight, and from flight-to-flight, was invaluable, although it meant many long and arduous days for these personnel.

5.3.4. Coordinated Operations with survey Ships
During several flights, MPA aircraft conducted coordinated operations with survey ships participating in RAPID RESPONSE 96. During these coordinated operations, the aircraft and surface ships were involved in joint acoustic data collection efforts requiring a high level of coordination and communication. Prior to the briefings for these flights, the Survey Director aboard the ship and the Air Coordinator must agree via INMARSAT or cellular telephone that the joint operation will take place and resolve any conflicts and/or delays with the platforms that would affect aircraft scheduling. In the event that problems arise with either the ship or aircraft, a back-up flight plan should be already approved and necessary flight clearances obtained.

5.4 Communications

For REA to be successful, robust communications between all platforms and personnel is a necessity. During RAPID RESPONSE 96, communications between the Air Coordinator, survey ships, SACLANTCEN, and USS LASALLE were handled by cellular and INMARSAT telephones aboard the ships, and the Italian telephone system for shore-based units. Extensive use of E-mail between the various participating units helped to keep all units informed concerning the various phases of the operation. Situation reports (SITREPs) were provided daily to the Military Coordinator aboard USS LASALLE by all participants. These reports were collated and a daily status report was issued by the Military Coordinator. This report kept all involved up-to-date concerning RAPID RESPONSE 96 issues.

A portable cellular telephone is needed for the Air Coordinator during the exercise period. While coordinating operations with the squadrons involved, TSC/MACA, Weapons and logistics personnel at Sigonella, the Air Coordinator was often hard-to-reach. A portable cellular telephone would eliminate this difficulty at a minimal cost.

6. Conclusions

MPA operations during RAPID RESPONSE 96 proved to be very successful. This was due to the cooperation and professionalism of all personnel involved, from all participating nations. 22 of 23 scheduled missions were completed as scheduled. Over 700 AXBT and 27 ambient noise measurements were collected and processed. MPA operations completed all tasking to provide support for acoustic measurements made from the RAPID RESPONSE survey ships.

For RAPID RESPONSE 97, MPA operations are again scheduled to be conducted from NAS Sigonella. Hopefully these operations will be as successful or even more successful than last year based upon the knowledge and experience all participants have acquired.

Rapid Environmental Assessment Capabilities of the Naval Oceanographic Office

William Currie
Michael Carron
Steve Haeger

Naval Oceanographic Office
1002 Balch Boulevard
Stennis Space Center, MS 39522-5001

Abstract

The Naval Oceanographic Office (NAVOCEANO) provides Oceanographic and Mapping, Charting & Geodesy products and services to United States, NATO, and allied warfighters. NAVOCEANO addresses rapid response product requirements by utilizing its unique survey assets, data sources, expertise, and communication pathways to rapidly assess the oceanographic battlespace environment and produce individually tailored and tactically relevant products.

1. Introduction

The mission of the Naval Oceanographic Office (NAVOCEANO) is to acquire and analyze global ocean and littoral data for specialized operational products and services. Our customer base is primarily US Military and other national and international organizations. Our vision is to be the world leader in providing quality oceanographic products and services.

As an operational command NAVOCEANO is under the direction of the Chief of Naval Operations and we maintain strong relationships with organizations such as the Naval Research Laboratory (NRL) and NATO's Supreme Allied Commander, Atlantic Center (SACLANTCEN). Participation in multinational exercises such as Rapid Response 97 expands our capabilities.

The ability of NAVOCEANO to participate effectively in exercises which involve multiple players requires each participant to understand how we operate. The following illustrates who we are and how we provide products and support to our customers.

NAVOCEANO is responsible for the collection, data basing, and analysis of a large variety of oceanographic and geophysical parameters in support of the Department of Defense and other government customers. Products from these efforts range from hydrographic surveys to specialized reports supporting mine warfare, anti-submarine and undersea warfare, amphibious operations, special operations, and strategic systems, among others. To meet our customers' needs

NAVOCEANO has a fleet of eight ships, specially outfitted P-3 aircraft operated jointly with NRL, and an extensive satellite and remote sensing data processing facility. Additionally, a rapid response capability is continually evolving to deliver custom products quickly. Rapid response products are tailored to meet the operational needs of the customer making the request. Most rapid response products range form composite analyses of various oceanographic, hydrographic, geophysical, and biological factors, annotated imagery, and ocean model results.

The quality and quantity of information provided to customers depends on the time available for analysis, the availability of data, imagery, and previously analyzed information resident in climatologies, and standard products, many of which are stored 'on-line.' All internal efforts and procedures are designed to react to the receipt of a rapid Request For Product (RFP).

2. Preparation Phase

Upon determination that a situation exists which may require intervention of US armed forces, a Crisis Action Team (CAT) is established at the direction of the Commanding Officer. The CAT team is the initiating force for RFP capabilities. CAT membership, roles, and responsibilities are documented in a formal NAVOCEANO instruction. Members of the CAT represent those groups in NAVOCEANO that will play a major role in a crisis response. The CAT assesses our readiness to respond and assures that all production codes are ready to respond. The following example actions would be initiated by the CAT upon initial indication of an imminent conflict.

Our dynamic ocean modeling capability in the crisis area is assessed to provide wave, thermal,

tidal, and circulation forecasts. These model computations are given priority on the Cray supercomputers in the Department of Defense High Performance Computing Major Shared Resource Center located at NAVOCEANO. Literature searches are conducted using the resources of the Maury Oceanographic Library, the world's foremost military collection of oceanographic reference materials. Publications, hardcopy and digital, are inventoried.

Warfighting Support Center (WSC) personnel inventory imagery for the Area of Operations (AO), which includes SPOT, LANDSAT, and other National imagery assets. Data bases containing bathymetry, hydrography, geophysical parameters, and physical properties are assessed for coverage in the AO.

Geographic area subject matter specialists may be mobilized to assist in responding to the anticipated RFP.

Naval Meteorology and Oceanographic Command (NMOC) Regional Centers and Facilities are contacted to establish defined communications links and to agree upon the products to be supplied.

Proximity of NAVOCEANO survey assets to the crisis area is assessed. Survey requirements are determined and recommendations are made concerning the use of these assets in obtaining data in the AO.

3. RFP Request

RFPs are received in NAVOCEANO's Warfighting Support Center (WSC) from fleet commands and NMOC Centers and Facilities. Tasking is distributed to the appropriate NAVOCEANO codes initiating product development and construction. Steps in this evolution include:

a. WSC imagery analysts begin to study imagery on hand and submit tasking/requests for additional imagery, if needed.

b. WSC regional analysts continue literature searches and begin compiling an Environmental Support Package (ESP), a narrative description of expected environmental parameters in the AO.

c. Ocean modelers begin initializing models in the AO if they are not already in operation. If no models are currently operational, project officers from the modeling groups at NAVOCEANO attempt to initiate models in the desired region. Often assistance is given by modelers from NRL co-located with NAVOCEANO at Stennis Space Center.

d. A message is sent to the regional NMOC Center or Facility responsible for support in the crisis area, listing products and services available from NAVOCEANO and procedures to pull products from the NAVOCEANO servers. In addition, aircraft carriers and amphibious command ships with embarked oceanographers or Mobile Environmental Teams are contacted.

e. A listing of available products for the AO is placed as appropriate on NAVOCEANO's unclassified and classified home pages.

f. Bathymetric and hydrographic data coverage is assessed. Queries are initiated to the National Imagery and Mapping Agency (NIMA), the National Oceanic and Atmospheric Administration (NOAA), and NAVOCEANO's Hydrographic Cooperative Program (HYCOOP) for hydrographic data.

g. Data analysts begin to build Essential Elements of Information (EEIs) for compilation into Special Tactical Oceanographic Information Charts (STOICs) if required.

h. Within two days to a week, annotated images are posted on NAVOCEANO's home pages. Analysis includes fronts and eddies, wrecks, obstructions, and shoal areas.

I. Ocean model forecasts are posted on the home pages. While relying initially on historical and satellite date, these models will continually increase in accuracy with the infusion of on-scene data from naval platforms.

j. Existing STOICs in the AO will have been mailed or hand carried to regional NMOC Centers, facilities, and ships immediately. Additionally, STOIC data files would have been posted on NAVOCEANO home pages. Within two weeks new STOICs will be built and disseminated in theater.

By the final step a complete oceanographic, meteorological and geophysical picture of the AO will be available in either hard copy or digitized format. After initial establishment of a data link to users, near real time information is made available.

4. Long Term Support

Longer term efforts may include:

a. Software updates for the Geophysical Fleet Mission Program Library (GFMPL), a collection of sensor and weapon performance prediction software, may be accelerated to support specific warfare requirements in the AO.

b. Geophysical, acoustic, and oceanographic data base updates may be accelerated to support on-scene sensor and weapon performance prediction systems.

c. New ocean models may be rapidly transitioned to NAVOCEANO from R&D

organizations and universities as requirements dictate.

d. NAVOCEANO ships may deploy to the AO to conduct hydrographic and oceanographic surveys. Hydrographic field charts may be produced on-scene for immediate use by military planners.

e. NAVOCEANO personnel may deploy aboard NAVOCEANO/NRL or fleet P-3 aircraft to conduct airborne oceanographic and acoustic data collection.

f. A 'fly-away survey system' may be rapidly deployed in-theater aboard a platform of opportunity to conduct oceanographic, hydrographic, and geophysical surveys.

g. Opportunities for data acquisition through cooperative programs with foreign governments may be pursued through the Navy International Programs Office.

5. Conclusion

While NAVOCEANO's capabilities and efforts alone are a major contributor to the overall characterization of the battlespace environment, there is also an abundance of environmental data and expertise resident within NATO. By working and learning together through NATO exercises such as RAPID RESPONSE, we will achieve our common goal of providing accurate, timely, and collaborative environmental characterizations to NATO warfighters.

Remote Sensing

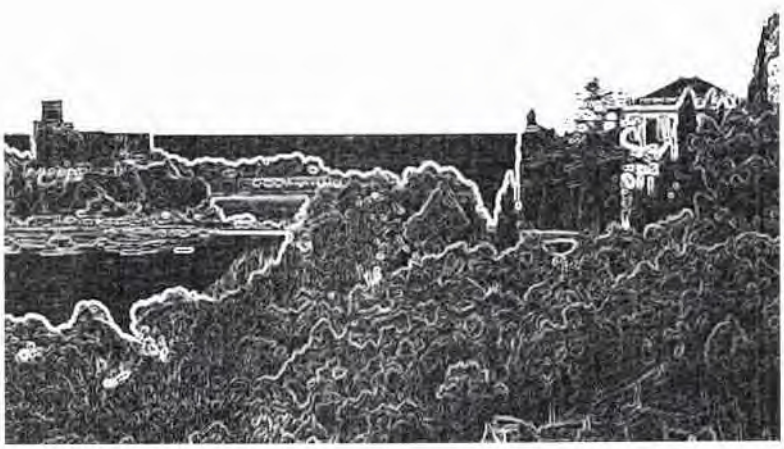

A review of the potential contributions - and limitations - of Earth Observing satellites.

T. D. Allan

Satellite Observing Systems
15 Church Street Godalming, Surrey GU7 1EL UK
email: tom @satobsys.co.uk

Abstract

The monitoring of sea surface conditions from polar-orbiting satellites equipped with fine resolution microwave, infra-red and optical sensors has continued for almost 2 decades. It was NASA's Seasat that first demonstrated that winds, waves, slicks, currents and eddies could be measured to useful accuracy by a suite of satellite-borne microwave instruments. Today there are up to 10 spacecraft circling the Earth dedicated to observing the state of the sea surface. Many more are in the pipeline. With the launch of the US Navy's Geosat Follow-On the number of satellites carrying a wave-measuring altimeter rose to 4.

This paper presents a brief review of the potential value of satellite-derived information to naval operations. The statistics that can now be derived on average and extreme values from the archive of satellite data will be demonstrated using the results of Wavsat - a 12-year archive of global wind and wave statistics. A wave atlas to assist in the planning of exercises was prepared from Wavsat for the Royal Navy.

The concept of using a cluster of purpose-built mini-satellites to relay information of sea state to ships in real-time which is now under study is also discussed and illustrated.

1. Background

The technology for measuring sea surface parameters from polar-orbiting satellite has altered little since the launch of the 3 pioneering spacecraft in 1978 - Seasat with a suite of microwave sensors, Nimbus-7 carrying the Coastal Zone Colour Scanner, and the NOAA satellites with the Advanced Very High Resolution Radiometer (AVHRR) for measuring sea surface temperature. Two decades ago it became clear that the number of surface features that could be observed to useful accuracy from space was limited to four - roughness, slope, temperature and colour. The same can be said today. Neither salinity nor surface pressure can be estimated to good accuracy and the volume of the ocean is virtually impervious to electromagnetic radiation.

The operational limitations have also remained more or less unchanged over the last two decades. Cloud cover remains a serious obstacle to the reliable operation of optical or infra-red sensors; the satellite still views only the surface; for narrow swath instruments such as an altimeter or synthetic aperture radar (SAR) a single satellite (despite its speed over the ground of 7km/s) still cannot provide the frequency of sampling required for day-to-day marine operations. Where some real progress has been made, however, is in the accuracy and resolution of sensors.

In the summer of 1978 there were 3 satellites designed to monitor the behaviour of the sea surface. Between them they observed wind, waves, slicks, internal waves, ships, pigment concentration and sea surface temperature. One, however, failed after 100 days (Seasat) and it was to be 13 years before a satellite with a comparable suite of microwave sensors was launched (ESA's ERS-1). Today one can count at least 10 spacecraft from 6 space agencies orbiting the earth with the prime purpose of observing the ocean. A comprehensive list of what is flying at present and what is planned for the future is presented in [1].

An evaluation of their potential contribution to REA tasks can now be made based on past performance.

2. Rapid Environmental Assessment

It is essential to distinguish between two distinct operational modes for generating useful satellite-derived information. In the past, the various claims made by space agencies and space-related industries of the benefits of Earth Observation to a wide variety of marine applications have sometimes confused the two. The first is in building up an *archive* of observations over the months and years of operation that enable good statistical inferences to be drawn on spatial and temporal variability. The second is the application of *real-time* measurements to marine operations. Here it seems obvious that satellite sampling must be matched to the rate of change of the phenomena being monitored; yet, that point is not always fully appreciated. At present the re-visit period for ESA's ERS-2 is 35 days for the US Navy's

for the US Navy's Geosat it will be 17 days (Figure 1). But many naval operations require to be updated on environmental conditions on a daily basis at least, if not more frequently.

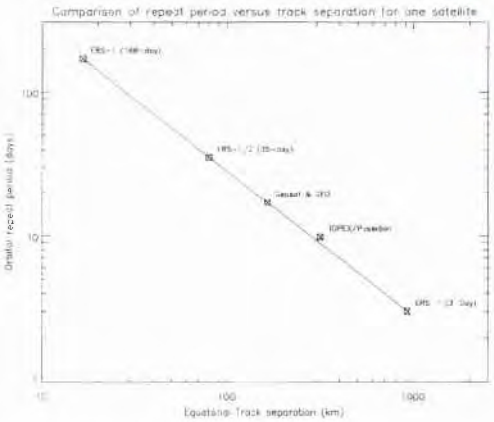

Figure 1: Track separation v repeat period

This would require a multi-satellite system in the fashion of GPS. Studies of real-time operational systems such as GANDER proposed by SOS (Global Altimeter Network Designed to Evaluate Risk) are presently underway but in reality it will be some years before the concept of clusters of custom-built satellites could become operational.

3. Optimising the present satellite configuration

i) Synergy

There are presently 4 SAR's, 3 altimeters, 4 infra-red sounders and 2 colour imagers in orbit around the earth. The missions of the satellites carrying these sensors were planned more as one-off operations to meet the specific objectives of the individual space agencies than as a co-ordinated effort. There is therefore a requirement on users to maximise the potential benefits of having so many observations beamed from the skies by seeking synergy between the different data sets.

Figure 2: AMIS sites in the Mediterranean

A group of specialist remote sensing laboratories in Europe (including Saclantcen) has agreed to take the first steps towards an Automated Marine Information System (AMIS) by co-ordinating their efforts on the processing and analysis of radar, colour and infra-red imagery over 4 selected sites in the Mediterranean Sea (see Figure 2) where special efforts will be made to back up the satellite data streams with reliable "in situ" data including meteorological analysis. The type of information that will be gathered each day by the satellites passing overhead is demonstrated in Figure 3 for the Strait of Sicily.

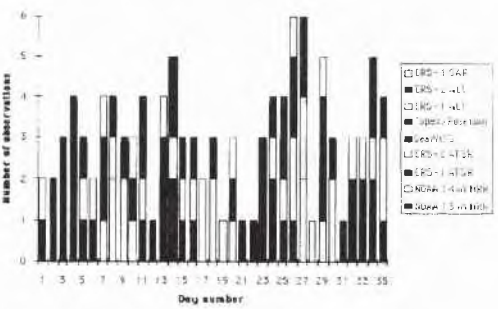

Figure 3: Strait of Sicily - 35-day schedule

(Note: The Japanese OCTS colour sensor has now taken the place of SeaWiFS which is not yet launched). It will be interesting to note in a more systematic way than has been possible in the past the relationships between the colour, temperature and roughness signatures of a potential surface feature such as an eddy or gyre.

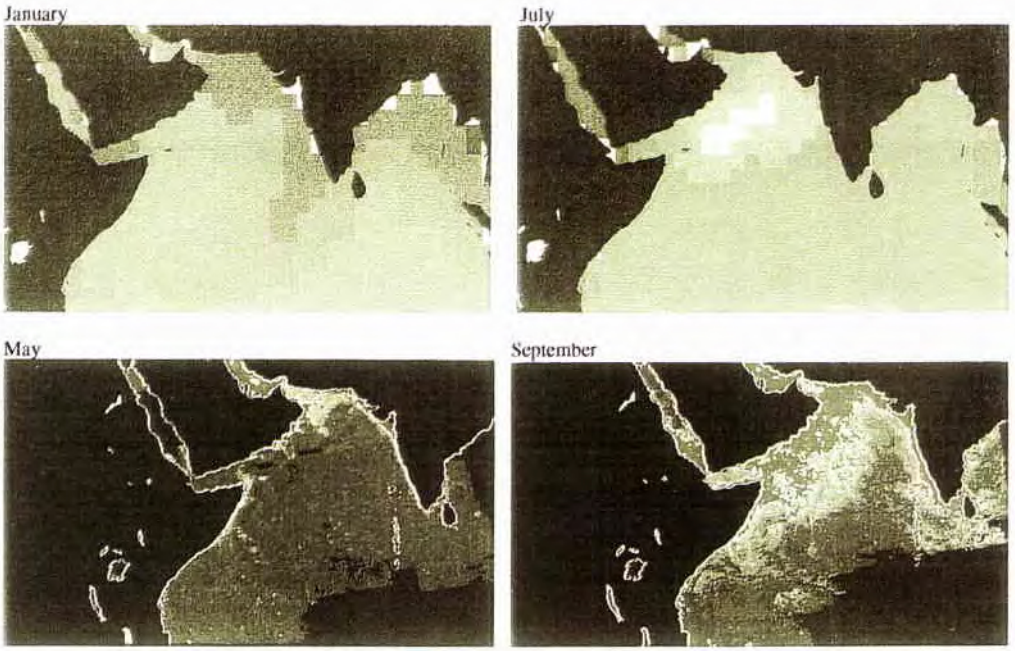

Figure 4: The top figures show the increase in mean monthly wave heights measured by the radar altimeter (lighter colour represents H_S > 3m). The bottom figures demonstrate the consequent upwelling of nutrients in September as measured by the CZCS.

Synergy is not necessarily confined to single features. Ocean processes observed from satellites have also been shown to be related. In a study carried out for the United Nations Development Programme* SOS demonstrated that the increasing wind speed and wave heights brought on by the monsoon and measured by the Geosat radar altimeter caused an upwelling of nutrients along the northern coastline of the Indian Ocean and Arabian Gulf which was observed by the Coastal Zone Colour Scanner of Nimbus-7. (See Figure 4).

ii) Archives

Since the first ocean observing satellites were launched in 1978 useful archives of data have been built up which allow statistical analysis to be made of such quantities as expected value, standard deviation, extreme values, seasonal range and inter-annual trends. The AVHRR record was started in 1978 and has continued uninterrupted to the present day though, of course, cloud obscures the sea surface for much of the time in some areas. The record of ocean colour imagery continued for almost 8 years after its launch in 1978. Two other colour scanners (German/Indian and Japanese) were launched in 1996. The ERS twins have provided a continuous altimeter record since 1991 plus a sequence of infra-red (ATSR) and radar imagery (SAR). ERS-2 continues today and will give way in 1999 to Envisat.

The US/French dual frequency altimeter carried on Topex/Poseidon was designed for the accurate configuration of sea surface topography from which geostrophic currents and tides can be extracted. The record has continued since 1992 and a replacement (JASON) has been approved.

In the case of the altimeter observations of surface wind speed and significant wave height the record has continued almost without interruption since 1985. Wavsat is an archive of calibrated 1-second observations maintained by SOS which is being added to at a rate of about 1 million observations per week. Statistics on wave behaviour are derived for cells of 2° x 2° over the surface of the globe. For any particular month or season mean values can be extracted as shown in Figure 5. A plot of the likely value of the highest wave in one year is shown for the Mediterranean in Figure 6 while an analysis of winter wave heights in the North Atlantic for 5 years before and after 1990 revealing a significant increase over the decade, is shown in Figure 7.

* *'Applications of Satellite Remote Sensing over the Indian Ocean'*

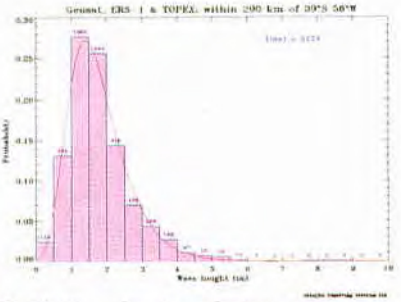

Figure 5: Wavsat - histogram of measurements

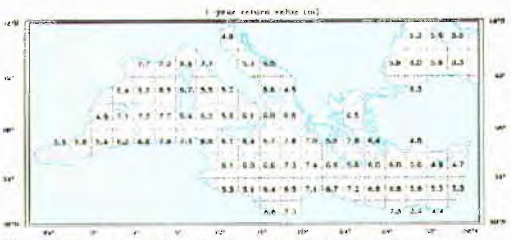

Figure 6: 1-year return value in the Mediterranean

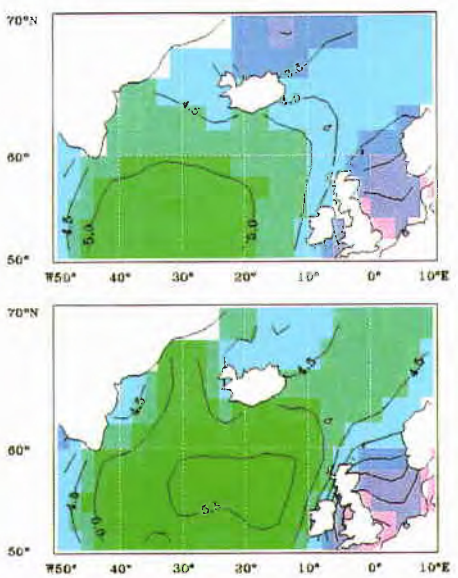

Figure 7: N Atlantic. The upper plot shows the average winter (Dec - Feb) significant wave height in the period 1985 - 89 derived from the radar altimeter. The lower plot for the period 1990 - 95, for the same quantity, shows a 10% increase.

Such a comprehensive global description of wave behaviour is unique and represents an important first step in establishing a more comprehensive marine or coastal information system capable of delivering statistics on the occurrence of fronts, SST cycles, phytoplankton concentration, upwelling, waves, winds, slicks, ship traffic and other features identified in the SAR record. To this satellite data could be added other 'in situ' data such as bathymetry, tides and meteorology.

4. Clean Seas

An experiment is currently underway supported by ESA (ERS-2 SAR), NASA (Radarsat) and the EC (part funding) to study the environmental conditions under which satellite sensors can detect and distinguish surface pollutants such as oil spills. Sites in the North Sea, Baltic and the Gulf of Lyons (Mediterranean) have been selected. Again, as for the synergy experiment AMIS, the idea behind Clean Seas is to assess the effectiveness of satellite sensors to detect and track marine pollutants under relatively well-observed conditions. It is not generally realised that almost ten times as much oil finds its way into the sea through deliberate discharges than from accidental spills. Future detection systems, based on a satellite observing the oil slick followed by interrogation of the ship's identity transponder, is technically (if not yet politically) within reach.

5. GANDER - an operational sea state alarm system

Losses at sea are still too high. In the last decade some 3,500 ships of over 500 tonnes foundered with the loss of 12,750 lives. About 30% were caused by bad weather. The SOS Sea State Alarm System placed on the Web each day is derived from the fast-delivery ERS-2 data stream. It demonstrates how an operational system could function if there were a sufficient number of satellites in orbit around the earth transmitting in real-time. At present the SOS Web site attracts the interest of about 7,000 visitors a week at times of hurricane activity. An example of a North Atlantic storm captured in near -real time by ERS-2, is shown in Figure 8.

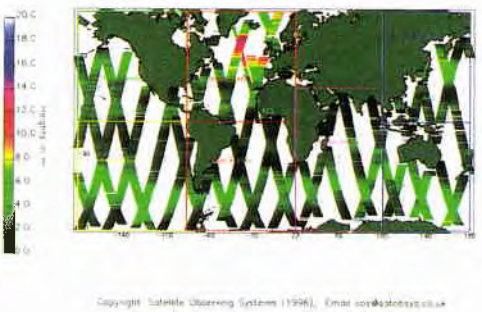

Figure 8: Sea state alarm - North Atlantic

Figures 9(a) and 9(b) demonstrate the coverage achieved over the North Atlantic in 1 day by ERS-2 and the 1-day coverage that would be achieved if ERS-1, ERS-2, Topex/ Poseidon and Geosat Follow-On were activated.

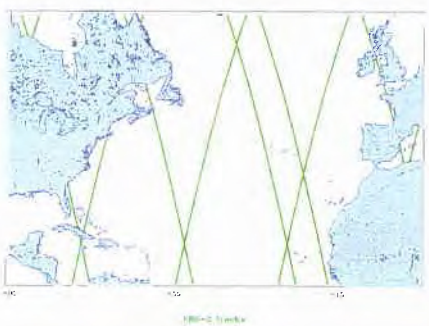

Figure 9(a): 1-day over the North Atlantic by ERS-2

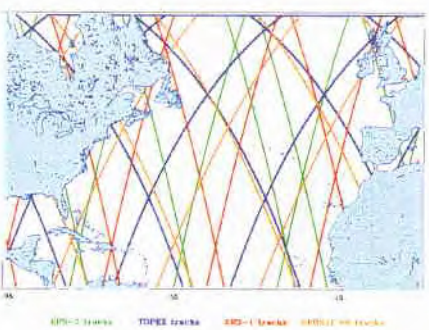

Figure 9(b): 1-day tracks over the North Atlantic by ERS-1, ERS-2, TOPEX and Geosat Follow-On

6. Conclusions

•Global archives of satellite data are now being rapidly expanded by adding data derived from 3 altimeters, 4 SAR's 2 colour sensors and 3 infra-red devices.

•In some cases, such as wave heights and surface winds the archive is now extensive enough to allow good statistical estimates to be made of average and extreme conditions.

•Lacking any direct co-ordination between individual satellite missions there is a need now to study synergistic relationships between the different sensor records.

•For adequate monitoring from satellites of most rapidly-evolving situations at sea, purpose-built, multi-platform systems must be designed and put into operation.

•In this regard, dedicated mini-satellites can be designed at a comparatively modest cost.

•If the present rather tight community of users of satellite data would widen its membership to include commercial, public sector and defence operations, and not limit itself to environmental research, a way might be found to achieve joint funding between national authorities, international agencies and private venture to design and launch purpose-built systems.

Reference

[1] J. C. Scott 'Satellite Remote Sensing in Rapid Environmental Assessment - the Optimum Use of Available Data', in *Proceedings of Rapid Environmental Assessment Conference*, 1997

New Remote Sensors for Application to Rapid Response Environmental Assessment

Dennis B. Trizna

Space & Remote Sensing Team
Office of Naval Reseach, Code 321
800 North Quincy Street
Arlington, VA 22015 USA
Email: triznad@onrhq.onr.navy.mil

Two new sensors currently under development by the Space & Remote Sensing Team, ONR Code 321, that have application toward littoral expeditionary warfare and rapid environmental assessment are discussed. These include a multifrequency HF Current Sensing Radar, and an ultrawideband multifunctional synthetic aperture radar (SAR),. Examples some results and future plans for each are discussed.

1. Introduction

Code 321 of the Office of Naval Research sponsors research into the understanding of the physics of remote sensing signatures of active and passive electromagnetic sensors from optical through microwave to HF bands. As an integrated program, it is also taken on new responsibilities for development of concepts for new sensors. This new thrust is sponsored under advanced development (6.2) funding, while the understanding of signatures is sponsored using basic research (6.1) funds.

2. Sensor Description

2.1. Single frequency OSCR Results

The commercial Ocean Surface Current Radar, built currently by Marconi in the UK, has been operated by Prof. Hans Graber at the University of Miami in a series of ONR sponsored field experiments. These began with the joint ONR/NRL High Resolution Accelerated Research Initiative (ARI) to study oceanic frontal features off the Coast of Cape Hatteras, NC, [1] and currently includes the NRL Physics of Coastal Remote Sensing ARI Chesapeake Bay Outflow Plume Experiment (COPE). The radar measures a depth integrated current over a range that is related to the depth of penetration of the fluid volume that is advected by the orbital wave motion of the Bragg resonant ocean wave for the operating radar frequency used. For the 25 MHz, 6-m Bragg ocean wavelength, the depth is suggested as integrated over roughly 80 cm. The first order Bragg lines in the Doppler spectrum are shifted from their expected frequency by an amount corresponding to the radial velocity component (along the radar look relative to the vector current direction). Two radial components are derived using two radars with near orthogonal looks onto a coverage area. A matrix of current vectors is mapped with 1-km spatial resolution to provide a map of currents each twenty minutes for 700 cells out to ranges of the order of 45 km offshore.

During the High Res ARI, an opportunity arose to intercompare such a current map with that derived from an overflight of the JPL along-track interferrometric AIRSAR system. The latter measures radial components of surface current as well, but using a different principle. It is based on the scene translation-induced electromagnetic total phase path shift of the sum signal from the scatterers in a single pixel from two successive complex images. These are collected using two different receive antennae spaced several meters or so apart for L-band on the aircraft fuselage. The primary contribution is typically dominated by the orbital wave motions of long waves. However, when average spatially across several long ocean wavelengths, the mean current averages out the orbital motions and the remainder can be separated into contributions of the surface current and the microwave Bragg resonant phase velocity. The latter can present a problem as it can be weighted by the approach and recede Bragg waves, and is an area under intensive study. When the radar look is into the wind, the Bragg waves along that direction typically are primarily in the direction of the wind and the Bragg contribution is straightforward.

Figure 1 shows the result of this intercomparison that were recently published [1].

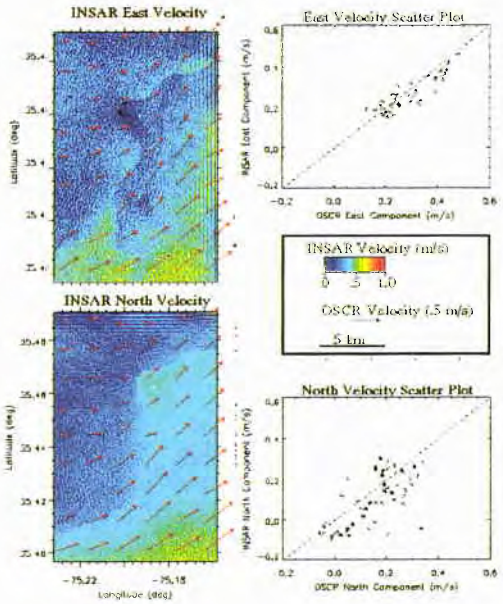

Figure 1. INSAR current components shown in color and OSCR vectors superimposed are also plotted in regression analyses to the right

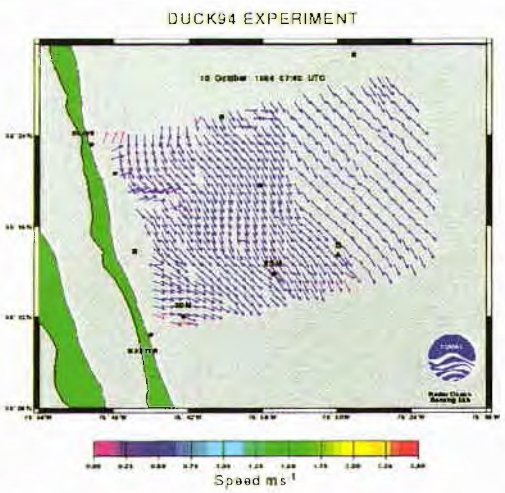

Figure 2. Intensive coverage available from an OSCR in the littoral zone is demonstrated in this Graber analysis of near shore currents during the Duck'94 experiment

The INSAR results of Fig. 1 are in color at 25-m resolution, while OSCR data are plotted as vectors at 1-km spacing. The INSAR data were further averaged over 1-km areas for comparison with the OSCR data and the results are plotted to the right of the images as regression analyses.

In Figure 2 is shown a map of currents offshore and north of the US Army Coastal Engineering Research Center Field Research Facility at Duck, NC, during the Duck '94 sediment transport experiment. This collection was cosponsored by the Space & Remote Sensing and Coastal Dynamics Teams of the ONR 32 department. These maps were available each 20 minutes from OSCR in real time. This University of Miami system has been also operated from aboard ship as a single site, and motion compensation corrections appear to be a manageable problem.

2.2. 3D HF Current Sensing Radar

A new multifrequency HF current sensing radar is currently under development by Prof. John Vesecky, of the University of Michigan, and elements of the system are undergoing final testing through the summer of 1997 at the MBARI test site in Monterey Bay, CA. A commercial development of this prototype is planned under an ONR sponsored STTR program just launched. An intercomparison experiment is planned for the fall of 1997 at the mouth of the Chesapeake Bay to compare OSCR and this new 3-D radar, possibly along with a CODAR system, all operating concurrently in the same area. Additional measurements there will also be made by the NUWSAR system discussed next.

The Multifrequency HF radar will provide more information than can be gotten from a single frequency, namely, vertical current shear maps. As indicated above, the 6-m Bragg waves at 25 MHz sample the currents over the top 80 cm. Choosing a frequency at 20 MHz, with a Bragg wavelength of 7.5 m then samples proportionately 25% deeper, to 100 cm, so that the vertical shear can be measured down to 2.5-m depth using a 4-MHz minimum operating frequency. The azimuthal resolution decreases inversely proportional to the decreasing radar frequency, however, using a fixed aperture received antenna. Nonetheless, the additional information provided over such a large vertical depth will provide a powerful tool for studying volume current fields. In particular, a method has been proposed that could utilize such measurements to estimate the current field over the entire volume in a shallow water environment (C.Y. Shen, this proceedings).

2.3. Naval Ultra-Wideband SAR (NUWSAR)

Under ONR SBIR funding a synthetic aperture radar is being developed for light aircraft and UAV platform applications for imaging the littoral ocean

A flexible system design is planned that will allow simultaneous operation using pulse-to-pulse switching across a number of system parameters. These include frequency (for pulse compression, as described below), radar frequency band (0.2 to 16 GHz), polarization (fully polarimetric), and cross- and/or along-track SAR operation. Such a combination is obviously data storage intensive, and this parameter currently limits the choices from the above selection.

The primary issues being addressed are package size and motion compensation limitations on spatial resolution. The system design methodology is based on stepped frequency technology, which allows pulse compression in processing. For example, using a fundamental 10-MHz operating bandwidth (100 nsec or 15-m pulse length), the radar is stepped pulse-to-pulse across in 50 10-MHz steps to cover a 500 MHz bandwidth, sampling each 100 nsec both in phase (I) and quadrature (Q) signals. For a given range bin set, the I/Q pair set of 50 are Fast Fourier Transformed to produce an output of 50 range bins with 30-cm range resolution (15m/50 samples). If motion compensation is not of sufficient quality to allow full resolution to be achieved for a given data set, then the multiple set of frequencies can be used to produce independent images at a lower resolution that can be summed to reduce speckle. The planned radar-range to along track velocity (R/V) ratio is of the order of 5 to 10 so that short integration times of the order of a small fraction of a second can be used with less blurring than is typical for ocean wave images for higher altitudes.

A prototype flight aboard an NRL P3 was made during September of 1996 during the first COPE experiment, simultaneous with the NRL RAR, currently undergoing upgrade modification. The dual polarized RAR capability under development will have higher sensitivity and larger swaths than is shown here. Using a dual polarized RAR antenna and vertically polarized SAR, the image shown in Figures 3 and 4 were made, of a ship wake crossing a front under study in the NRL ARI. To the author's knowledge, this is the first known simultaneous SAR/RAR image at the same frequency. Both were taken at X-band, with 10-m RAR resolution, and 1-m SAR resolution with range-extent limitation due to current data recording limits. The SAR is imaging just a fraction of the RAR coverage its shortest, but the same wake features can be seen in each image.

The traces of surfactant are seen to be much more complicated at the 1-m resolution. The frontal feature has a reasonable amount of fine structure at this higher resolution as well. These are four-look images with 50% overlap and 39 ms coherent integration each, which appears to be supported by the decorrelation time of the scene.

An interesting effect in the SAR image is the apparent rotation of the small scale wake features due to azimuthal translation/smearing effects. In particular, at the lower R/V ratio condition use here, the effect is one of translation rather than smearing, thus causing the rotation.

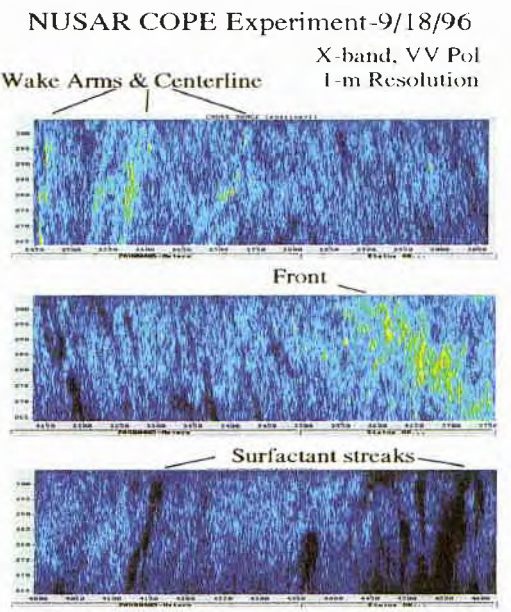

Figure 3. SAR image taken at 1-m resolution at R/V of 5 shows details of ship wave at top, front at center, and surfactant slicks in lower portion

RAR Dual Polarization Imagery

In the RAR images of Figure 4, the differences between the HH (upper) and VV (lower) images are striking. These are hypothesized to be due to different scattering mechanisms at these lower grazing angles, the HH being dominated by small scale breaking effects associated with the frontal structure. These have been seen previously in shipboard marine radar polarization studies [2]. A model that explains many of the observed differences in polarization results at low grazing angle has been published that introduces small scale breaking features as a scatterer that dominates the HH echo at low grazing angles below 20 deg. [3].

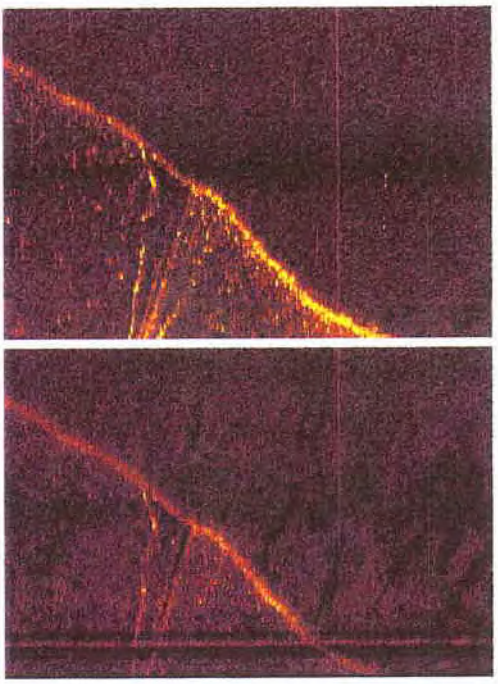

Figure 4. Horizontal (top) and vertical (bottom) polarized images from the NRL X-band RAR show striking differences in their response to breaking waves associated with the front and ship wake, as well as to surfactant streaks that suppress the Bragg free waves, suggesting quite different scattering mechanisms for the two cases

When the radar imagery is co-registered, as is done in Figure 5, the RAR and SAR image resolution differences become more apparent, as do the rotation of the Kelvin wake arm periodic components and their rotation. A pair of components are seen to be nearly vertical in the left arm, and about 20 deg from horizontal in the right arm, with a just single element apparent in the latter case.

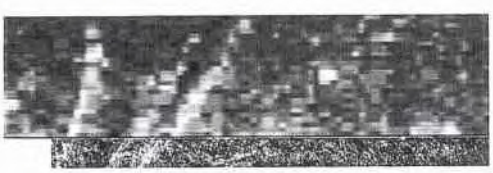

Figure 5. The RAR and SAR images are registered at the same image resolution, indicating the high resolution SAR wave imaging capabilities when flown with a low R/V ratio of 5

3. REA APPLICATIONS

3.1 3D Current Profiles; 3D HF radar can be used to directly determine the surface current shear by a measure of mean currents through a least three different depths, using three different operating frequencies and using the radar wavelength-current depth relationship discussed above. More than three radar frequencies allows a least squares fit of a model function for depth dependence to be made for improved accuracy.

Alternatively, current shear could be inferred using RAR image sequences in the following manner. Co-registered and geo-referenced imagery collected using a sequence of aircraft platform passes with tens of minutes spacing could be used to map surface tracer features, such as surfactant slicks, from one pass to another. From such a measurement sequence from several passes, a surface current vector could be derived averaged over pixels tens of meters on a side. Using the calibrated backscatter echo and existing scatterometry models and those being developed at NRL for low grazing angle applications appropriate to stand-off operations, estimates of wind stress could be derived. At lower grazing angles, HH polarization may provide a better wind stress measure, based on marine radar results [2]. From this pair of measurements, and a data assimilation and modeling approached proposed by Shen (this conference), three dimensional currents could be derived over the entire coverage area flown by the platform.

3.2 Internal Wave Pattern Maps for Acoustic Propagation Model Assimilation: While not shown here, it is well known that internal gravity waves can be mapped extremely well at low grazing angles (<30 deg) by HH polarization. It is also known that such wave patterns can cause problems for littoral acoustic propagation, introducing multipath and attenuation. Real time measures of internal wave patterns and their propagation characteristics using image sequencing could provide valuable inputs into acoustic propagation models. Real time assimilation into such models is limited only by lack of the communication link of imagery products between the airborne platform and a ship using the acoustic models for real time propagation assessment.

3.3 Bathymetric Estimates. Much work has been done in estimating bathymetry from the surface roughness variations due to the enhanced small scale surface roughness that results from wave current interactions. Tidal flow over variable bathymetry causes enhanced surface currents over shallower waters demanded by conservation of water mass flux.

The increased short wave spectral density that causes the radar echo intensity to vary spatially is a result of such tidal flow variations at the surface due to these wave-current interactions. (See, for example, Alpers, et al, [4], Vogelsang, [5]). Bathymetric maps could be developed from vertically polarized RAR imagery shown here, as well as much higher resolution SAR products planned for the future.

4. Summary

We have discussed two new remote sensing instruments that have under development by the Space & Remote Sensing Team, Code 321, of the Office of Naval Research. These are the new 3D Ocean Current Sensing Radar, and NUWSAR, a flexible research synthetic aperture radar with a multiplicity of capabilities including both cross and along-track spatial resolution in processing, radar frequency band, polarization, and cross and along track interferrometry. A newly modified NRL dual-polarized real aperture X-band imaging radar is also coming available and showing promise for rapid environmental assessment applications in the near term. Examples were given of these systems. Applications that were discussed included three dimensional current volume mapping, internal gravity wave mapping for assimilation into acoustic propagation models using a communication link between aircraft and ship, and bathymetry determination using surface radar echo intensity variations.

5. References

[1] Graber, H.C., D.R. Thompson, & R.E. Carande, Ocean surface features and currents measured with SAR interferrometry and HF radar, JGR, 101, 25813-25832, 1996.

[2] Trizna, D.B., & D. Carlson, Studies of low grazing angle radar seascatter in nearshore regions, IEEE Trans. Geosciences and Remote Sensing, **34**, pp. 747-757, 1996.

[3] Trizna, D.B., A model for Brewster angle damping and local multipath effects on low grazing angle sea scatter studies, IEEE Trans. Geosciences and Remote Sensing, accepted for publication.

[4] Alpers, W. & I. Hennings, A theory for the imaging mechanism of underwater bottom topography by real and synthetic aperture radar, JGR, **89**, 10529-10546, 1984.

[5] Vogelsang, J., G.J. Wensink, C.J. Calkoen, M.W.A. Van der Kooij, Mapping submarine sand waves with multiband imaging radar, JGR, 102, 1183-1192, 1997.

Satellite Remote Sensing in Rapid Environmental Assessment The Optimum Use of Available Data

John C. Scott

Defence Evaluation Research Agency
Winfrith Technology Centre
Dorset DT2 8XJ, UK
Email: jcscott@dra.hmg.gb

Abstract

The effective use of satellite earth observation data by naval ships and command authorities depends on a large variety of complex considerations. These range from limitations of the imaging physics through data fusion and oceanographic understanding matters to vital questions of data acquisition, processing and handling. Application of satellite techniques to Rapid Environmental Assessment (REA) brings in a number of additional complexities. Not least amongst the issues needing to be addressed is the ability to secure access to important data at all phases of a conflict. Additional factors concern the optimum use of remote sensing in the context of historical data, both in-water and remotely sensed. This paper attempts to bring all of the questions together with the aim of establishing an optimum utilization of the wide variety of potential benefits of satellite data.

1. Introduction

Satellite remote sensing is an established part of modern fleet operations. Visible light images from geostationary satellites are a mainstay of the weather forecasting process, both as direct input to the forecasting bench, as real-time monitoring information, and via sophisticated forecasting models, as vital synoptic assimilation data.

From the oceanographic viewpoint, polar orbiting satellites such as those from the NOAA (National Oceanic and Atmospheric Administration), DMSP (Defense Meteorological Satellite Program) and the Russian OKEAN and RESURS series have provided high resolution (~1km or better) sea surface temperature (SST) data. Particularly in ASW, these data have allowed reasonably precise monitoring of the ocean features which influence sonar performance, and they now make a routine and valued contribution to forecasts.

Although epoch-making satellites such as Seasat (1978), Nimbus 7 (1978) and Geosat (1985) gave tantalizing indications of the additional possibilities made possible with radar imagers, colour imagers, altimeters and passive microwave imagers, it is only in the few years since the launch of ERS-1 and Topex/Poseidon in 1992 that the potential is approaching realization. In these few years we have seen the launch of four synthetic aperture radar (SAR) imagers (ERS-1, JERS-1, ERS-2 and Radarsat) - three precision radar altimeters (ERS-1, Topex/Poseidon and ERS-2) and two microwave scatterometers, also on the two ERS satellites. The emergence into the scientific community of passive microwave imager data has also taken place during this period, as has increased access to data from satellites launched by countries of the Former Soviet Union, such as the OKEAN real aperture radar (RAR) satellites and the RESURS visible/infra-red imagers.

At this point it should be noted that the military application of sensors does not necessarily require the sensor performance that is essential for scientific studies. This is particularly true for thermal infra-red; the poorer performance of OLS compared with AVHRR is not operationally significant. The key requirements relate to the ability to detect ocean features.

The varieties of sensor now or imminently available and those potentially available in future are dealt with in other papers in this proceedings [1,2]. The reader of the present paper should look to these other papers for details of the sensors mentioned here.

In the present context it need only be noted, therefore, that remote sensing is already capable of providing a major input to REA, via existing operational practices, and that there is considerable scope for enhancing this input as a result of developments in sensor availability and data interpretation.

This paper starts from this knowledge and highlights some of the issues related to data availability and data usage which are likely to play important roles in the effective use of satellite data:

- constraints on the availability of data for military purposes;
- data synergy and data fusion;
- the optimum use of databases, both in-water and remote sensing.

DERA coordinated remote sensing activity for *RAPID RESPONSE 96*, and provided high resolution data to the exercise on operationally relevant time scales.

indicating the potential REA role of even high density remote sensing data.

2. Data Availability Constraints

2.1. General Issues

Since REA requires data that are timely, it makes sense, first of all, to examine how reliable are the sources of the data required. It can be seen that remote sensing data involves complications that are not common to other forms of data collection for REA.

The problem which used to dog remote sensing, that the quantities of data involved are simply to great to allow transfer from receiving stations to operational commands, has largely disappeared as a result of the advances allowed by the Internet. It appears reasonable to expect that the Internet will be available for use in future conflicts, as these are not likely to affect global communications networks.

For any operational satellite there are two essential elements of the data supply chain: having the sensors switched on; and having the data supplied to the operational user.

Switching On. For the sensors which are currently of greatest operational value: the km-resolution infra-red and visible imagers of the NOAA (AVHRR) and DMSP (OLS) satellite series the sensors operate continuously, but for some of the sensors now appearing as alternatives, such as SAR, current technology will not allow this, and data acquisition must be scheduled.

Data Supply. Two modes of operation are possible: the direct transmission of data as they are acquired; and on-board recording for later downloading. Many systems (including NOAA and DMSP) allow both modes. The direct transmission mode clearly allows real-time use of the data, and it is the preferred option for data which it is intended to make freely available. On-board recording is ideal for situations in which it is intended to supply the data commercially, and it involves placing a delay between data acquisition and onward data transfer, which adversely affects use in real time. A further factor relates to the fact that the use of direct transmission, although it facilitates free use by anyone with a suitable receiver, does not guarantee free use; encryption of the data stream is now a routine procedure for environmental data, even for some meteorological data sources.

2.2. Military Usage

If we look in more detail at these influences on data availability we uncover some interesting facts. The satellites of interest are not only overwhelmingly civilian in their funding and purpose, they present a very complex picture of National and International ownership.

Our present picture of future conflicts is largely based on the unpredictability of those conflicts. This is the main driving force behind the need for REA. This unpredictability generates considerable uncertainty concerning what National alliances might be involved, both with and against any particular participant. The presently rapidly shifting political picture could quickly lead to complex loyalty conflicts on the part of data providers. The data ownership issue could become very important in such a situation.

Military usage can really only be guaranteed for satellites that are owned and operated by military authorities. In our present context, applied strictly, this limits the data available to that coming from the US DMSP satellites (visible, infra-red and passive microwave imagers), and limits the favoured nations to just one.

The point is important for assessing military accessibility because even when we broaden the 'military' restriction to simply 'national', the data supply situation is still quite limited in extent. Again strictly applied, this restriction would still leave the majority of NATO nations without guaranteed access to the visible/infra-red core of naval forecasting systems.

The situation becomes particularly complex when we consider the extent to which civilian and commercial alliances have resulted in joint ownership or operation of satellites. The Multi-National European Space Agency (ESA) probably represents the most complicated case.

Table 1 (below) provides a summary of present and imminent earth-observation satellites, their data attributes, and their ownership.

The fact that there is a current trend towards commercialization of satellite observation data adds a further complication. Presumably a host country might be able to prevent one of its companies from supply data contrary to National interests, and this may remove the problem. However, modern trends towards multi-national companies, combined with the ease with which data may be moved electronically around the globe might obstruct such simple solutions.

It is relevant to point out that the timely supply of data to REA requires the wholehearted participation of all of those involved in the many relevant stages of data provision, from satellite scheduling to dispatch of the data.

Participation by DERA in the *NATO RAPID RESPONSE 96* operation, which involved close and effective co-operation with Naval Research Laboratory, Washington showed what can be achieved. This involved the co-ordination of a number of links - data handling, data processing and interpretation - all of which were vital to supply of the data on an operationally relevant time scale.

It would not be fair to suggest that any of the present

Satellite	Attributes	Ownership
Meteorological (Geostationary) Satellites		
Meteosat-6	Europe & Africa	ESA
GOES-8	North & South America	USA
GOES-9	Pacific Ocean	USA
GMS-5	Australia, SE Asia, W Pacific	Japan
INSAT	India	India
ELEKTRO/GOMS	Indian Ocean	Russia
{FENGYUN-2}	Indian Ocean, SE Asia	China
Polar-Orbiting Satellites		
NOAA-12, -14	AVHRR (Visible/IR) Imager	USA
SPOT	High Resolution Visible Imager	France
DMSP	OLS (Visible/IR Imager)	USA
	SSM/I (Passive Microwave)	
ERS-1, -2	ATSR (IR Imager) SAR Altimeter Scatterometer	ESA
JERS-1	SAR Optical Imager (Visible)	Japan
METEOR-2, -3	Visible/IR Imagers	Russia
OKEAN-01-7	RAR Visible Imager Passive Microwave Imager	Russia
RESURS-01-3	MSU-E (Visible Imager) MSU-SK (IR Imager)	Russia
IRS-1C	LISS (Visible/IR Imager)	India
Radarsat	SAR	Canada
Topex/Poseidon	Altimeter	USA/France
ADEOS-1	OCTS (Colour/IR Imager)	Japan
	NSCATT (Scatterometer)	Japan/USA
{SeaStar}	Sea WIFS (Colour Imager)	USA
{Geosat Follow-On}	Altimeter	USA

Table 1: Attributes and Ownership of Current and Imminent Satellites/Sensors

data-sharing privileges enjoyed by the military community might be under threat. At the same time, however, we should remember that if remote sensing data should emerge as a key element in any National (or NATO) REA strategy, risks such as have been identified here must be taken into account.

2.3. Access to Data by Potential Adversaries

At the same time as recognizing the possible fragility of remote sensing data supply routes, we should also be aware of the fact that the data supply situation faced by potential adversaries may not be very much poorer.

Perusal of Table 1 shows the wide variety of National and International interests which are involved. Implicit data supply agreements, if not already in place, could be swiftly negotiated, and data could be transmitted anywhere on the globe easily, quickly, and possibly covertly, with or without value-added interpretation of the data.

Again, the increasing commercialization of satellite data, while making a guaranteed data supply harder for one country, may make it easier for another.

3. Data Synergy and Data Fusion

The majority of research (and applications) of remote sensing for ocean monitoring has been focused, to date, on single sensors. This can be seen as a result of sensor development being carried out without adequate reference to the oceanographic research and applications communities, but it is also a result of the time needed by these communities, working with any particular sensor, to develop its potential fully. It has not been possible to provide good guidance to the satellite design community on the benefits of sensor combinations. The application of the sensor science and satellite technology are clearly still immature.

That said, the potential benefits of sensor combinations are now becoming clearer, and we are now in a position to influence satellite design. The past and present are packed with examples of single sensors that are now starting to be seen by the operational community to be severely limited by an out-of-date approach

In the past we have had both a SAR (Seasat) and colour imager (CZCS), neither of which was supported by thermal imagery. Currently we have a SAR satellite (Radarsat) which carries no other sensors; we have other SARs (ERS) which, although they have accompanying infra-red imagers, manage not to have overlapping data, and also have scatterometers that cannot be used simultaneously. We are about to launch a sophisticated colour imager (SeaWIFS) which, like CZCS, does not have a thermal infra-red channel. Fortunately, the single sensor trend is being reversed in the OCTS sensor of the Japanese ADEOS satellite, which combines colour and thermal sensors: the NSCATT scatterometer is also carried. It is to be hoped that the synergy potential of such multi-sensor approaches is realized quickly, to influence future payload designs.

Some synergy aspects are already quite well established. Altimetry is being used in the USA as an all-weather complement to infra-red imagery in Gulf Stream forecasts. SAR images have been used to complement SSM/I passive microwave in ice forecasts. The unique combination of co-located visible, passive microwave and real-aperture radar (RAR) sensors on the Russian OKEAN satellites, particularly useful for the main operational use of the satellite for ice monitoring, also provides a range of possibilities for open ocean monitoring.

The co-existence of complementary sensors on the same platform has the advantage that the time-variability of the ocean, not yet fully understood because of inadequate sampling by both in-water and remote sensing techniques, ceases to become an unknown. Without co-incidence of data it becomes impossible to relate sensor outputs, particularly when they rely on completely different physics to image the same features.

This is most evident in the case of understanding radar imagers, particularly SAR, which has the potential, being an all-weather technique, to resolve the cloud-limitation problem of thermal and visible light imagers. The literature contains a considerable number of examples (see, e.g. [3]) in which similarities can be drawn between SAR and IR images obtained with only a few hours separation. How many more of these vital co-incidences would there have been if ATSR - or even a coarse, badly calibrated thermal imager had covered even part of the SAR swath? We are now in the **fifth year** of highly successful SAR imaging by ERS platforms.

It could be contended that the unfortunate sensor mismatch on ERS is what is holding back the much needed assessment of SAR as an operational sensor. The sensor continues to offer great promise on the basis of the co-incidences obtained so far, but all SAR investigators have a large number of image examples which may be usefully interpretable, but for which we have no conclusive proof. Part of the problem resides in the greater sensitivity of radar imagers to atmospheric variability than to oceanographic variability; this might have been resolved if the satellite had allowed the simultaneous operation of a scatterometer with the SAR.

Synergy possibilities which are currently evident include:

- **Infra-red imagers and altimeters.** Altimetyry can detect ocean fronts and eddies, and in cases such as the Gulf Stream, which has a large dynamic height signature, it provides an all-weather indicator of its location. In low to medium latitudes even the coarse spatial resolution

allowed by the 10-day repeat of Topex/Poseidon allows the tracking of eddies. At higher latitudes, however, and with small (<10cm signature) features, the height signature is not sufficiently clear of the noise to allow stand-alone operation as a feature detector [4].

- **Infra-red and colour.** Although completely disabled by cloud cover, IR images provide the mainstay of the forecasting bench. However, thermal signatures deteriorate in high latitude summers, and there is evidence from CZCS that colour imagers can offer synergy for feature detection in such situations.
- **Infra-red and passive microwave.** Although this synergy is available in the DMSP OLS+SSM/I combination, inaccessibility of these data for the civilian community (and the lower specification of OLS relative to AVHRR) have led to the neglect of synergy in this case. Since IR images can only be obtained with clear skies, false IR signatures can result from low wind speed patches on the ocean surface. Poorer surface mixing in the patches can lead to the surface skin temperature becoming locally unrepresentative of the 'mixed layer' as a whole; wind speeds derived from passive microwave data can indicate the presence of conditions under which this may be happening. [This possibility should be realized with the planned co-existence of the AMSU-A passive microwave imager on future NOAA satellites.]
- **Infra-red and SAR.** This possibility would solve most of the ASW requirements of REA if the SAR sensor were developed into a state of reliability in feature detection. Possible on-going developments in SAR sensors (e.g. polarization and frequency versatility), together with improved data interpretation, could make this synergy a reality. IR is likely still to be needed, however, unless the ocean structure characteristics were very well known in the area in which REA is required.
- **SAR and scatterometry.** As was indicated above, the sensitivity of SAR image interpretation to confusion from spatial wind speed variations makes it important to have a good knowledge of wind variability, although the coarse spatial resolution of scatterometers will limit this potential source of synergy.

Clearly, combinations of the above could give even more productive possibilities.

4. Optimum Use of Databases

4.1. Remote Sensing Databases

Historical remote sensing data are not normally the concern of operational forecasting authorities: data for any area will only stay 'current' until it has been adequately replaced. This is a wholly reasonable approach to forecasting in areas in which the forecasters have experience in interpreting images, and an understanding of the oceanographic variability of a region.

The REA situation is significantly different. It is of the essence of REA that the most critical time for forecasting will be right at the start, when a forecaster is coming in 'cold' to a potentially unfamiliar region. It is in this situation that remote sensing databases come into their own. Particularly in the case of AVHRR (IR) images, we now have access to almost two decades of data in some regions, and in the global context there are still impressive quantities of data covering all seasons.

Such databases provide a detailed and thorough grounding in the spatial variability expected in a region, and even in the absence of any in-water data they can provide the necessary training both in the region's basic oceanography and in the interpretation of new remote sensing data.

It is, however, not practical to expect that forecasters should do all of the necessary groundwork to reach the optimum level of interpretation expertise, starting cold on 'Day 1' of an emergency. It is **essential** for REA that those Nations and Commands which expect to fulfil a forecasting role in any geographical region should achieve a state of preparedness well in advance of an emergency arising.

Such work clearly needs to incorporate all of the available in-water knowledge appropriate to the area concerned, including the relevant parts of hydrographic databases. Some further considerations on this will be addressed in the next section; it is here intended only to stress the central role that can be played by remote sensing archives in the familiarization process.

AVHRR databases are the first priority for REA. Secondly, if colour data are anticipated operationally then even though we do not yet have substantial databases from the new colour sensors it may be possible to gain experience with the freely available CZCS database. For SAR, ERS databases are steadily increasing in size, although their data density for any particular region depends critically firstly on the presence of a ground station to cover the region and secondly on to what extent the ground station has been tasked to collect data. The Radarsat (commercial) database might also be expected to make a contribution, although at present its ocean coverage is generally disappointingly small.

4.2. In-Water Databases

The previous section indicated that databases of in-water data would be needed, along with remote sensing databases, as part of the process of familiarization necessary to bring forecasting authorities quickly up to speed in the early stages of REA.

Traditionally, hydrographic databases have been constructed on a climatological basis, individual profiles being accumulated according to some gridded or geography based principle. In the ASW part of REA what we need is information on the locations and structures of tactically exploitable ocean features, and these databases are not configured to provide this information.

The approach already adopted for solving this problem is to derive ocean structure, at a level of detail suitable for acoustic propagation calculation, from predictive ocean models. Such models, at least ideally, would be initialized with historical data and then assimilate new information, including that from remote sensing, as it becomes available.

Remote sensing information can be very well suited to assimilation into models. Images are normally large-area synoptic views, potentially providing a full two dimensions of high resolution input to the three dimensional model. Altimeters provide an input which represents the integral of vertical ocean structure along a line through a model, again providing essentially multi-dimensional data. The success of the input of such data depends on the extent to which the final result, after assimilation, has been able to adapt to the new information.

Models which are able to respond fully to synoptic data are therefore preferred, and it appears that feature-based models, allowing features such as frontal boundaries and eddies to be moved bodily to fit with new surface data, may be the best way of achieving this result. Feature models are also preferred for assimilating remote sensing data because not all of the forms of such data offer parameters that are easily assimilated. Thus, whilst SST and dynamic height are normally model input parameters which can be used directly to force models, it is unlikely that any SAR information, or even ocean colour information, could be used directly as a model input. These sensors are expected to provide **feature detections,** including information such as size and location, and feature-based models are one vehicle capable of dealing with this form of input.

Another, simpler form of modelling of the environment is possible, one which uses historical data, but in a new way. Climatology-based databases, although they tend to be dominated by isolated CTD or XBT profiles, usually contain clearly defined tracks of data - straight lines of relatively dense sampling stations. These can usually be seen by visual inspection of database data position plots.

It is a reasonable objection that such data are still historical in nature, but such data tracks have the considerable virtue that they contain ocean structure information - similar to that required by sonar propagation calculations, and that the structure contained did actually occur at some point in time. Since most of the frontal and eddy systems found in any region are the result of confluences of water masses with reasonably distinct properties, it is likely that the horizontal variation found in the data will be to some extent similar to structures in approximately the same area at a similar season.

The biggest change between the historical data and current conditions might reasonably be expected to be in the position of the feature. This is precisely the information most likely to come from a number of remote sensing techniques. Having deduced a feature position and shape remotely, forecasts on range variability of sonar performance could be produced quickly from archived data.

It is suggested, therefore that this approach offers a low technology alternative to sophisticated ocean modelling. If areas of potential conflict should be identified for which databases do not contain adequate information, then the technique provides a rationale for data collection - feature-based - more effective than grid-based surveys.

It should be noted that this sort of low technology approach may be the approach of choice or even necessity for a potential adversary, particularly one without access to high-power computing facilities and reliable meteorological forcing data. The in-water data found in open-access databases are likely to be reinforced by an adversary's local knowledge. A potential adversary with even a limited technical capability could have access to remote sensing data of a quantity and quality equal to, perhaps greater than, that of a more technology-based opponent.

5. Conclusions

This paper has reviewed several aspects of the use of remotely sensed data in REA for Naval purposes which may be as crucial to the effective exploitation of the data source as the more scientific and technical aspects of data interpretation and tactical advice derivation dealt with elsewhere in this Proceedings.

Three topics have been addressed:

Firstly, it has been demonstrated that the present supply situation for remotely sensed earth observation data is complex, both technically, in the range of ocean monitoring possibilities available and planned, but also operationally, in the problem of ensuring a timely data supply in spite of potentially disruptive multi-national loyalty conflicts.

Secondly, it has been indicated that operational use of remote sensing data is expected to benefit, perhaps more than more scientific aspects of satellite data use, from synergy of different data sources. Such possibilities would be fostered if future satellite missions carried multi-sensor payloads designed to optimize such possibilities.

Thirdly, two aspects of database use have been highlighted. One concerns the use of historical remote sensing data as a familiarization or learning aid, to accelerate the adaptation of forecasting facilities to an unfamiliar area of operations in the earliest stages of REA. This requires the adoption of a programme of preparation aimed at operations globally. The second aspect considered involves a relatively simple means of enhancing the value of existing in-water databases, using remotely sensed data to locate tactically exploitable features whose properties can be estimated using historical data.

Finally, it must be emphasized that although satellite remote sensing is potentially capable of influencing the success of naval conflicts, several of the aspects considered above could act in favour of adversaries who do not have access to the high technology available to NATO nations.

References

[1] T.D. Allan, "The potential contributions - and limitations - of earth observing satellites", in *Proceedings of Rapid Environmental Assessment Conference*, 1997

[2] D. Trizna, "New remote sensors for applications to rapid environmental assessments", in *Proceedings of Rapid Environmental Assessment Conference*, 1997

[3] J.A. Johannessen, G. Digranes, H. Espedal, O.M. Johannessen, P. Samuel, D. Browne and P. Vachon, "SAR ocean feature catalogue", ESA Publications ESA SP-1174, October 1994

[4] J C Scott and A.L. McDowall, "Cross-frontal cold jets near Iceland: In-water satellite infra-red and Geosat altimeter data", Journal of Geophysical Research, C, Vol.95, pp.18005-18014 (1990)

Deduction of subsurface structures from satellite measured sea-surface temperature

H.-H. Essen
Universität Hamburg, Institut für Meereskunde
Troplowitzstr. 7
22529 Hamburg, Germany
E-mail: essen@ifm.uni-hamburg.de

February 5, 1997

Abstract

This paper reviews some work of the remote sensing project at SACLANTCEN (1991-1996) concerning the extraction of subsurface features from satellite-borne measurements of sea-surface temperature (SST). The satellite data are from the Advanced Very High Resolution Radiometer (AVHRR) of the series of NOAA satellites. The SSTs are related to (a) geostrophic currents in Norwegian coastal waters, and to (b) vertical sound speed profiles in the Iceland-Faeroe frontal region and in the Mediterranean.

1 Introduction

It is apparent that satellite remote sensing is an appropriate tool in the context of rapid environmental assessment. However, most of the information from satellites is restricted to the sea surface, but it is mainly the subsurface sound speed which is needed for acoustic modelling, i.e. the prediction of sonar performance. Since 1991, SACLANTCEN has paid increasing attention to relating satellite surface measurements to subsurface structures of the ocean. Two examples are presented, both in context with satellite-measured sea-surface temperature (SST). The first shows the relation between gradients of SST and geostrophically balanced currents. The second investigates the dependence of vertical profiles of sound-speed on SST.

Starting in 1994, research at SACLANTCEN has moved from the open ocean in the Greenland-Iceland-Norwegian seas to coastal areas of the Mediterranean. For this presentation, data from both areas are used. The application of satellite remote sensing in coastal areas requires sensors of high resolution. The AVHRR allows a resolution of about 1 km and is, beside others, an appropriate sensor for coastal application.

2 Geostrophic currents

Satellite images cover an extended area and reveal the horizontal variability, while in-situ measurements are available only at single points or from time-consuming surveys. For example, this is valid for conventional methods of current measurements like moored current meters or drifters. More suitable for ground truth of satellite imagery is the land-based HF radar, which measures surface currents in an area of up to 40 km × 40 km with a resolution of some 2 km. It does not only yield the two-dimensional distribution of current velocity but has also the same spatial resolution as the AVHRR.

In March 1985 and March 1988, surface currents have been measured by the HF radar of the University of Hamburg in Norwegian coastal waters. This region is characterized by high horizontal variablity. Because of the predominant cloud-coverage, the experiments provided only three satellite images for comparison with surface current maps. However, these images show strong temperature gradients. Fig. 1 displays the surface current field of an eddy, observed during low-wind conditions and clear sky. A coincident satellite SST image (not shown) reveals a warm water core at the center of the eddy.

Introducing a number of simplifying assumptions, the geostrophic portion of surface currents can bee derived by means of the "thermal wind equation" [1],

$$\rho f \left(\frac{\partial u}{\partial z}, \frac{\partial v}{\partial z} \right) = g \left(\frac{\partial \rho}{\partial y}, -\frac{\partial \rho}{\partial x} \right), \qquad (1)$$

with, (u, v) = horizontal vector of current velocity, ρ = density, f = Coriolis paramter, g = gravity acceleration.

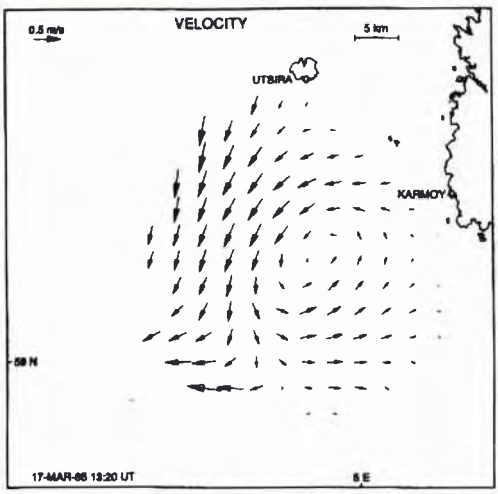

Figure 1: Surface currents as measured by an HF radar on 17-March 1985.

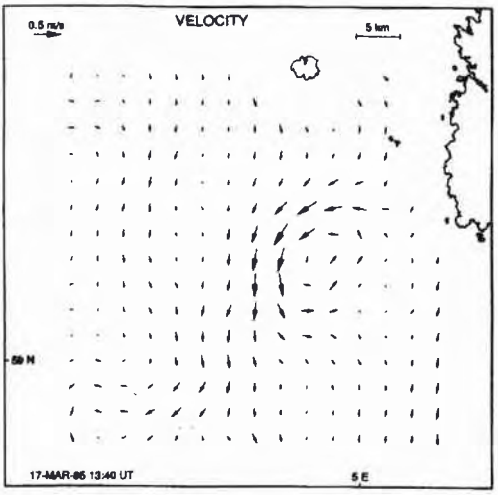

Figure 2: Surface currents derived from SST gradients of an AVHRR image (not shown), coincident with Fig. 1.

In order to determine the density gradient from the SST field, the dependence of salinity on temperature has to be known, which is assumed to be linear. The current velocity is obtained by vertically intergrating the thermal wind equation (1), which requires a model of the depth-dependence of density. Assuming a linear decrease of the density gradient with depth and vanishing currents at the sea-floor (250 m), the current velocity is quantitatively determined from the SST gradient. Fig. 2 shows surface currents as retrieved from the SST field. Maximum current speeds agree well with the measured ones (Fig. 1). However, the retrieved geostrophic currents occur in narrow jets, while those measured by HF radar cover more extended areas. It should be mentioned that the retrieval method does not account for homogeneous currents like tides.

Also the 1988 experiment, performed at a different area, revealed similar agreement between observed and retrieved surface currents [1]. In addition, two successive AVHRR images with 4 h separation allowed the estimate of the homogeneous current by means of feature tracking.

The geostrophic model used oversimplifies the oceanographic conditions. Temporal accelerations are neglected but are present due to tides or changes in wind (not present during the experiments reported). Also advective accelerations are not always negligible. In addition to the uncertain validity of the geostrophic model, the model itself requires assumptions on parameters, which, in general, are not known. However, despite all the problems mentioned, the experimental findings suggest that with some a priori knowledge of an oceanographic area, satellite SST images can supply quantitative information on ocean currents.

In the case of a-priori information available on the density stratification, equation (1) allows to compute the current field as function of depth. If in addition, the magnitude of surface current is known, the penetration depth of currents can be estimated from the SST gradients.

3 Sound-speed profiles

As proved for different oceanic regions, sound-speed profiles may be represented by a small number of so-called EOFs (Empirical Orthogonal Functions), which account for the major part of sound-speed variance. Individual profiles are determined by the EOF amplitudes.

$$c(z) = c_0(z) + a_1 \times e_1(z) + a_2 \times e_2(z) + \ldots, \qquad (2)$$

with, $c_0(z)$ = mean sound speed profile, $e_i(z)$ = normalized EOFs, a_i = EOF amplitudes.

Surveys of SACLANTCEN in the Iceland-Faeroe frontal (IFF) region by means of thermistor chains and CTD casts revealed that already the 1st EOF accounts for 94 % of the sound speed variance for profiles extending to 100 m depth [2] and for 90 % for profiles extending to 600 m [3]. From surveys in the Mediterranean, the highest percentage values for the 1st EOF have been found in the area south of Sicily, 88 % for 75 m profiles and 85 % for 300 m profiles [4]. The other areas surveyed, south of Elba and Strait of Otranto, revealed less dominant 1st EOFs. Fig. 3 shows the survey area south of Sicily and the positions of the CTD casts.

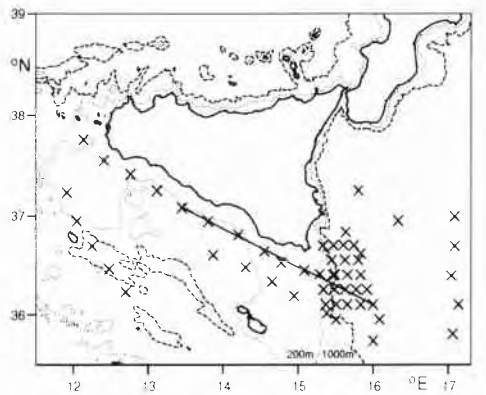

Figure 3: Locations of CTD casts (crosses) south of Sicily (13-22 November 1994).

Recent investigations from the Gulf Stream area showed a strong correlation between 1st- and 2nd-order EOF amplitudes and dynamic height. Dynamic height is a feature of the sea surface, which can be recorded by satellite altimetry. For the IFF area, similar correlation have been found. However, the variability of dynamic height is only ±10 cm and just about the same as the accuracy of presently operating altimeters. For this reason, the correlation between EOF amplitudes and SST has been investigated. High correlation has been found for the 1st EOF (in the IFF area as well as in the Mediterranean), which allows to relate the 1st-order EOF amplitude to SST by,

$$a_1 = A_1 + B_1 \times T + C_1 \times T^2 + \ldots, \qquad (3)$$

with, T = SST.

The method of constructing synthetic sound-speed profiles from satellite measured SSTs requires the knowledge of the EOFs in (2) and the coefficients in (3). Both are provided by CTD surveys and depend on the area and the time of year. The EOFs are determined by the covariance matrix of the sound speed profiles and the coefficients by regression between EOF amplitudes and SST, represented by the uppermost level of the CTD profile.

Fig. 4 displays measured and reconstructed sound-speed profiles along the section indicated in Fig. 3. Due to the relatively shallow water in this area a profile length of 75 m was selected. The sound speed profiles change considerably with distance, as becomes clear by the comparison with the mean profile. Reconstruction by means of the 1st EOF already yields a good fit of the overall features. The inclusion of the 2nd and 3rd EOF accounts for more variability.

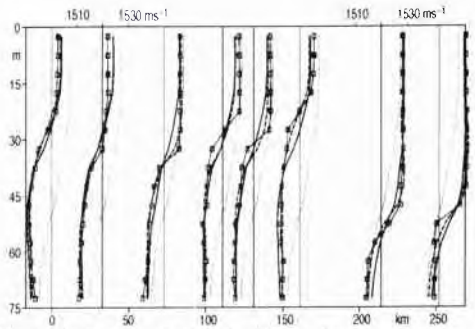

Figure 4: Representation by EOFs of sound-speed profiles. Lines marked by squares are the original data, thin dotted lines are the mean profile, full lines are the reconstruction by only the 1st EOF, dashed lines by 1st through 3rd EOF.

The upper part of Fig. 5 displays satellite measured SST along the section indicated in Fig. 3. The SSTs are the channel-4 brightness temperatures corrected by the difference to the ship measurement during the satellite overpass. The crosses represent near-surface temperatures measured by the CTD sonde. Because these measurements have been taken several days before the satellite image, no exact agreement can be expected. However, there should be general agreement as our method assumes that the SST is representative for the subsurface sound speed.

The satellite SSTs have been used to synthesize the sound-speed profiles in the lower part of Fig. 5. Correlation between EOF amplitudes and SST is significant only for the 1st EOF, with correlation of 92 %, and only the 1st EOF has been used.

Though comparison with measured data reveals considerable smoothing, some important features become visible, e.g. the sound-speed duct at the beginning of the section. For the purpose of acoustic modelling, artificial variability can be added by using further information from satellite SST images like the autocorrelation function [5].

Reasonable results, similar to those presented for the Sicily area, have been found for synthesized sound-speed profiles of the IFF region [2]-[3]. However, no reliable sound-speed features from SST could be determined south of Elba and the Strait of Otranto [4]. The SST gradients in the Elba area were too small and in addition, biased by seasonal warming. The Otranto survey revealed a very complex hydrography, less variance for the 1st EOF and only weak correlation with SST.

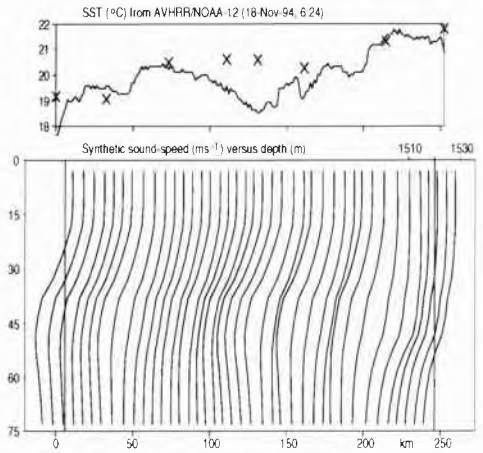

Fig. 5: Synthetic sound-speed profiles along the section indicated in Fig. 3. Satellite SSTs are displayed in the upper panel, the crosses represent the CTD measurements. Sound-speed profiles every 6 km have been derived from the mean profile and the 1st EOF, the amplitude of which has been determined from SST via a regression curve.

4 Conclusions

Satellite sensed data map large areas of the ocean and are (for most sensors) available in nearly real-time. The disadvantage is that the information is limited to parameters such as: ocean colour, sea-surface temperature, sea-surface roughness, and sea-surface topography, i.e. predominantly to the sea surface. For sonar performance prediction, information on the inner ocean is required, the spatial and temporal variability of sound speed. The examples presented here demonstrate that there exist relations between sea-surface temperature, which may be sensed from space, and subsurface features like currents and sound-speed profiles. However, a quantitative determination of these features requires the knowledge of additional parameters. These can be obtained from in-situ surveys, historical data and other satellite sensors.

References

[1] H.-H. Essen, "Geostrophic surface currents as derived from satellite SST images and measured by a land-based HF radar", *Int. J. Remote Sensing*, vol. 16, pp.239-256, 1995.

[2] H.-H. Essen and J. Sellschopp, "Three-dimensional distribution of sound speed in the Iceland-Faeroe area, retrieved from a CTD survey, thermistor-chain measurements and satellite SST images", *SACLANTCEN SR-226*, La Spezia (Italy), 1994.

[3] A. Warn-Varnas, H.-H. Essen, E. Gezgin, "Deduction of synthetic temperature profiles from SST observations in the Iceland-Faeroe frontal region", *SACLANTCEN SR-246*, La Spezia (Italy), 1996.

[4] H.-H. Essen, "On the predictability of subsurface sound speed from satellite-measured sea-surface temperature in the Mediterranean", *SACLANTCEN SR-245*, La Spezia (Italy), 1996.

[5] Essen, H.-H., "Horizontal scales of sound velocity at the Iceland-Faeroe front as deduced from satellite measured sea-surface temperatures", *SACLANTCEN SR-194*, La Spezia (Italy), 1992.

SPOT bathymetry and bottom type mapping for Rapid Response 96

F. Jourdin, J. R. Camus

Centre Militaire d'Océanographie
EPSHOM, B.P. 426
29275 Brest Cedex, FRANCE
Email: jourdin@shom.fr

Abstract

During the Rapid Response 96 experiment, SPOT 3 satellite acquired an image in multi-spectral mode for the aims of the amphibious warfare. The surveyed area is located in south Sardinia. From the image, the bathymetry and bottom types are evaluated in water areas shallower than 20m depth. These parameters are processed with the analysis of the upwelling light stream coming from bottom that reflects the solar illumination. The absence of clouds and turbid waters were favourable conditions. A simple index allowed delineation of sandy areas and vegetated bottom covers. On the other hand, a principal component analysis allowed extraction of the bathymetry. Comparing with in situ measurements, the depth accuracy is 2.5m r.m.s over sandy areas. The results are perturbed over vegetated areas.

1. Introduction

In less well-known coastal areas, SPOT and LANDSAT satellites can give quick, discreet and useful information in an REA military scenario. Here, we deal with mapping of bathymetry and bottom. Even under good conditions, the information is generally not accurate but it is synoptic. For instance, processed images of a relatively wide area can help in choosing the best beach to land troops. Otherwise it can help to optimally route ships during REA data collection phase. Moreover, this technique well benefits from only a few sea truth data, and makes it a good tool for REA. Here, we are focussing on SPOT satellites, in particular the conditions for observation, common processing methods and results obtained during the RR96 experiment.

2. Conditions for using SPOT

SPOT satellites carry a pushbroom imager. In multispectral (XS) mode, the equivalent to three thousand photocells are aligned. Each cell views along a line parallel to the subsatellite track. The imager collects the radiant flux in three spectral bands:

Band	Wavelenght (µm)	Color
XS1	0.50 - 0.59	green
XS2	0.61 - 0.68	red
XS3	0.79 - 0.89	near infrared

Table 1: SPOT multispectral bands.

Each SPOT satellite is on a sun-synchronous orbit (descending node at 10h30am local time) at an altitude of 830 km. When the satellite-borne instrument looks downward, the image characteristics with regard to the ground are:

Pixel size	20m x 20m
Image size	60km x 60km

Table 2: Image characteristics in XS mode.

At request, the instrument can look to the left and to the right, perpendicularly to the direction of the satellite. The view is said nearly vertical when the off-nadir angle is between -12° and +12°, and oblique when it is between -31° and +31°. SPOT orbit repetitivity is 26 days. With two satellites usually in orbit, the same area can be surveyed quite often, depending on latitude:

View angle	Return times
Nearly vertical	2 days
Oblique	1 day

Table 3: Average time period while surveying an area at latitude 45°, using two SPOT satellites.

The environmental conditions to evaluate bathymetry and bottom type are quite restrictive:

Atmosphere	no clouds low rate of water vapor no clouds of dust/smoke
Sunniness	no shadows (of clouds, montains,...)

	sun enough high above the horizon
	no sun glitter, low glittering
Water column	low rate of turbidity (due to suspendous sediments near estuaries, emissions of pollutants,...)
	no oil slicks....
Bottom type	few different bottom types (<4)
	enough reflecting bottom types
SPOT view angle	nearly vertical

Table 4. Qualitative conditions.

Depending on the photocell's sensitivity, SPOT can sounds depths until 20 m:

Band	Penetration depth
XS1	20 m
XS2	5 m
XS3	0.2 m

Table 5: Penetration depths.

3. A quick review of several methods

Remotely sensed bathymetry from multispectral imagery generally is based on a simple reflectance model [1] under the assumptions given in table 4. The radiance in wavelength band i at water depth z is given by:

$$L_i = L_i\infty + c_i R_i \exp(-2 k_i z) \quad (1)$$

where L_i is the remote radiance seen at the sensor in narrow band i, $L_i\infty$ is the average radiance observed over deep water, c_i includes solar irradiance, atmospheric and water surface effects, R_i is the bottom reflectance and k_i is the water attenuation coefficient. The exponential depth dependance suggests the use of the transformation:

$$X_i = \ln(L_i - L_i\infty) \quad (2)$$

3.1. The single band model

This model assumes that the atmosphere and sea state are uniform at all places in the image (constant c_i), bottom reflectance is unchanged over bottom types (constant R_i) and water characteristics are homogeneous (constant k_i). Hence, water depth becomes a simple function of the observed radiances:

$$Z = \alpha_{0i} + \alpha_{1i} \cdot X_i \quad (3)$$

where α_{0i} and α_{1i} are constant coefficients. For instance, the bathymetry of a region at the northern end of the Red Sea has been charted applying (3) to LANDSAT MSS green and red bands data [2]. The α coefficients were fitted to sea truth measurements of the bathymetry. Nevertheless, this method is restricted to homogeneous bottom types.

3.2. The two-band model

To reduce errors due to varying bottom reflectances, this model combined the radiances observed in two bands (i=1 and i=2):

$$Z = \alpha_0 + \alpha_1 (X_1 - X_2) \quad (4)$$

where α_0 and α_1 are independent of bottom type variations. Here, the assumption is that changes in bottom reflectance occur so that the ratio R_1/R_2 remains constant. For instance, the bathymetry of a small area of the Great Bahamas Bank has been charted applying (4) to LANDSAT TM blue and green bands data [3]. The blue band provides with improved water penetration and can reach depths up to 30 m. Once again, α_0 and α_1 were fitted to sea truth data. Nevertheless, the constant ratio assumption proves wrong in case of high different reflecting bottom types like vegetated and non-vegetated bottom covers.

3.3. The multiband model

This model generalizes the two-band model and extends it to several bands:

$$Z = \alpha_0 + \alpha_1 X_1 + \alpha_2 X_2 + \ldots \quad (5)$$

under the assumption that a relation links all the bottom reflectances R_i [4]. For instance, the bathymetry of an island of the Carribean Sea has been charted applying (5) to LANDSAT TM blue and green bands data [5]. In theory, (5) requires as many bands as bottom types to be exact. In practice, the method is quite efficient [6].

3.4. The statistical approach

First, this approach aims at reducing effects of noise and unmodelled physical phenomena in the results. Second, it aims at better classifying the bottom types. For an N-band system, the values of X_i in all pixels are considered as realizations of the random variable $\{X_i\}$ defined in the N-space. Analysing scatter plots of X_i-values, one can identify the direction k_i of the linear variation of X_i due to bathymetry [7]. Then, the depth invariant distribution of X_i perpendicularly to that direction can be put into conventional maximum likelihood classification algorithms. However, the processing of the bathymetry needs extra-information on the different bottom types identified. For instance, the bathymetry of an atoll of the Cook Islands has been charted applying this method to SPOT green and red bands data, with the help of in situ measurements [8]. This method gives better results than previous ones even though it excessively discriminates the bottom types. Other such image segmentation methods suggest more advanced schemes [9].

3.5. The physical approach

Here, the aim is to take into account the various physical phenomena that do not fit (1). For instance, a model [10] over the blue-green range of the visible spectrum has been developed for Case 1 waters (no

suspended sediments). It simulates the effects of water volume scattering and absorption, fluorescence and Raman scattering. Using more relevant formulae, all the new unknown parameters introduced in the problem can be obtained from remotely sensed chlorophyll concentration. Nevertheless, purely physical models will not be easily used in an REA scenario due to the high diversity and different amplitudes of the natural phenomena encountered.

3.6. Future prospects

Improvements will be performed with the following studies. Readers can find also a complete discussion on all these methods in [11].

3.6.1. Better spectral resolution
Observing with high spectral resolution is one way to better separate the several components (atmospheric, water volume and bottom reflectances and transfers) of the observed radiant flux. Hence, LANDSAT (high spectral resolution, blue band) and SPOT (high spatial resolution) combined, might give enhanced information. We may use also the panchromatic mode of SPOT.

3.6.2. Improved physics
As seen in the previous chapter, the radiative tranfer model (1) must be improved while restricting unknown parameters.

3.6.3. Improved statistics
The radiative transfer model must be included in a statistical evaluation scheme. Some assumptions will be made such as: a finite number of typical bottom covers, a spatially smothed bathymetry. The results may be less sensitive to noise and unmodelled physical phenomena.

3.6.4. Assimilation
To satisfy REA aims, the software must run with and without merging remote sensing images with in situ measurements.

4. SPOT for RR96

SPOT has evaluated the bathymetry and bottom type of an area for the purpose of the amphibious warfare part of RR96. It took about one month to supply the results. But all these tasks can be done in two weeks. The SPOT scene reference is K/J 060/272 23 August 96 Level 1A Mode XS SPOT 3.

Tasks	Date	Centre
Ask for specific satellite instrument configuration	7 August	SHOM Brest
Image acquisition	23 August	SPOT Image Toulouse
Image processing	12 Sept.	SHOM Brest
Presentation of results	16 Sept.	SACLANTCEN La Spezia

Table 6: SPOT for RR96, timescales.

The area is located in Golfo di Teulada, South Sardinia. Here, we are focussing on an area displaying two beaches:

Area	Coordinates
Porto Scudo (north beach)	38°52.5'N - 38°55'N
and	8°38.5'E - 8°41'E
Porto Zafferano (south beach)	

Table 7: Area of interest.

4.1. Image preprocessing

Before processing the bathymetry and bottom types, a level 1A SPOT scene needs three steps of preprocessing, decribed in the following.

4.1.1. Stripping noise removal
This noise comes from the relative gain differences among the photocells. The removal must be done properly. The slight changes in radiometric units we are looking for must not be affected. Therefore, SHOM has developed an interactive computing software for this purpose. A skilled user visually compares the radiometry over deep water, out of atmospheric perturbations, and corrects.

4.1.2. Geometrical rectification
Initially, the SPOT scene is geo-referenced with a typical and absolute error of 500 m at ground level. Based on a thorough model of image distortion using orbital and attitude parameters of the satellite, a software (Matra/Prodigeo) fits the image in with at least one ground referenced spot [12]. Here, several remarkable spots (piers, points, islets) were selected. They were geo-referenced according to four Italian maps (SHOM references are IT299, IT294, IT311, 7332). Biases are adjusted by least squares:

Number of spots	16
Spots discarded	4
Mean residuals (distance)	40 m

Table 8: Typical absolute error in location.

Then, a bicubic interpolation over 16 neighbouring pixels resamples all the pixels to conform the image with the desired coordinate system (here UTM32-WGS84).

4.1.3. Coastline and clouds
A threshold detection on XS3 (mainly) allows delineation of coastline, clouds boundaries and shadows of clouds. A skilled user adjust the contouring line with an interactive software (Matra/Multiscope). In this example, the area of interest is free of clouds.

4.2. Process bathymetry and bottom types

Usually, at SHOM, we chart the bathymetry applying the multiband method [13], [14]. Here, because of the presence of two different reflecting bottom covers, the lack of in situ information, possible turbid waters, and limited period of time, we opted for another purely empirical method. We transform the radiances L_i through a linear combination:

$$L_i^{\sim} = \sum_{j=1}^{3} A_{ij} L_j \qquad (6)$$

where A_{ij} is a constant matrix of rotation.

A principal component analysis gives the matrix A. The criterion is to maximize the variance. The maximum is assumed to be the effect of bathymetry. $L_1^{\sim}$ represents the bathymetry, $L_2^{\sim}$ represents the bottom type and $L_3^{\sim}$ the turbidity. Then, we assume that the images of bottom type, water turbidity and bathymetry are linear and spatially uncorrelated. However, at least for bathymetry, we know that this hypothesis is false.

Concerning the bottom, instead of $L_2^{\sim}$, we chose B as a better index [8]:

$$B = (XS1)^2 / XS2 \qquad (7)$$

The latter is visually more satisfactory. Concerning the turbidity, the water proved to be very clear in the area. Hence, we assumed $L_3^{\sim}$ not representing this parameter, and we did not chart it.

4.3. The results

Figure 1 displays the bathymetry $L_1^{\sim}$ of the area defined in table 7. Each radiance level was linked to a bathymetric level while we were quickly and visually comparing the shape of $L_1^{\sim}$ with the one of an Italian bathymetric chart. The deep water limit was delineated while we assumed to reach the noise level.

Figure 2 displays the bottom type B. It shows broadly two different types. The limits of the two corresponding areas are particularly well identified in Porto Zafferano. Nevertheless, the weak penetration of XS2 perturb analysis of bottom composition in areas deeper than 7 m. Observers in the area have defined bottom types as sand and posidonia. There are also rocky areas but their corresponding color may be to close to the sand to be identified.

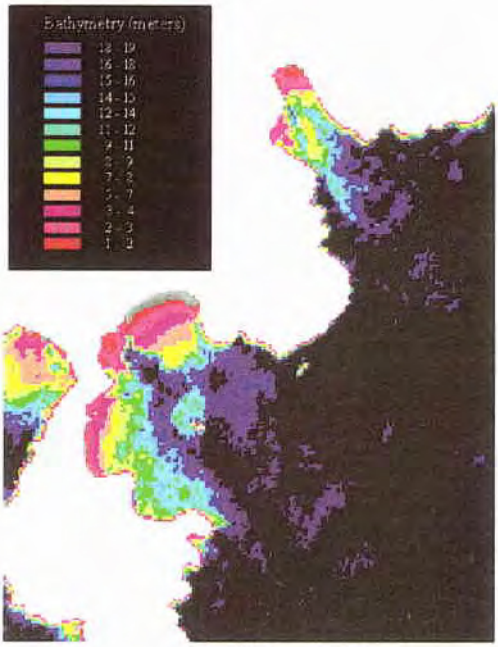

Figure 1: SPOT Bathymetry. Deep water is put in black. Land white. ©SPOT Image.

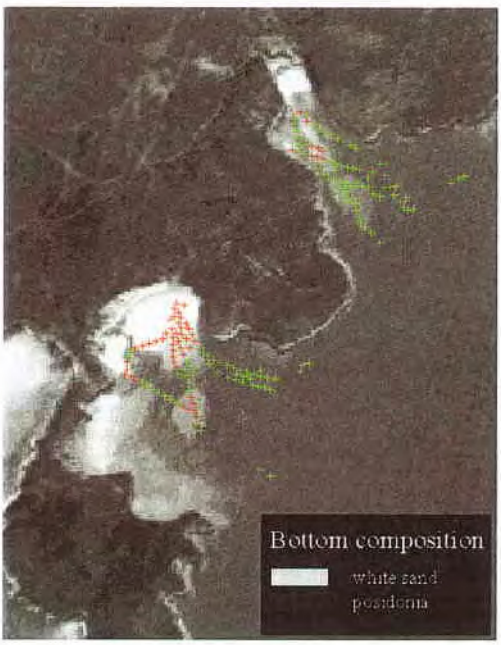

Figure 2: SPOT Bottom types. ©SPOT Image.

The bathymetric scale given in figure 1 is designed for the sandy areas only. Actually, the method does not separate bottom type and bathymetry. Therefore, over posidonia areas, color levels do not necessarily link to bathymetric range. We see the posidonia area affecting the bathymetric information in Porto Zafferano.

The Manning (a SACLANTCEN research ship) has performed a bathymetric survey in the area during the RR96 data collection phase. We superimposed some of the data on figure 2 and assigned them a bottom type according to B. Red and blue crosses have been classified as sand and posidonia respectively. The comparison between SPOT and in situ measurements shows better agreement over sandy areas. SPOT overestimate the depth over posidonia covers

Parameter \ Area	Sand	Posidonia	Total
Number of crosses	53	117	170
Mean deviation (m)	-0.1	2.5	1.6
Standard deviation (m)	2.4	4.2	3.9
RMS (m)	2.4	4.9	4.2

Table 9: Accuracy of the resulting bathymetry.

Over sandy areas, the bathymetric error is about 2.5 m.

5. Conclusion

Despite the low accuracy, SPOT gives a quick evaluation of the bathymetry of a relatively wide area. Bottom covers are also broadly identified. Here, vegetated and non-vegetated areas are delineated. Because there are highly different reflecting bottom covers, an improved method than the one used here will give more accurate results.

Acknowledgements

The authors wish to thank Sylvie Cacaux for help with the evaluation of the accuracy of the solutions and Cecilie Mauritzen for writing advice.

Glossary

LANDSAT	:	Land Satellite
MSS	:	Multi-Spectral Scanner
REA	:	Rapid Environment Assessment
RR96	:	Rapid Response 96
SPOT	:	Satellites pour l'Observation de la Terre
TM	:	Thematic Mapper

References

[1] F.C.Polcyn, W.L.Brown and I.J.Sattinger, "The measurement of water depth by remote sensing techniques," *Report 8973-26-F*, Willow Run Laboratories, The University of Michigan, Ann Arbor 1970.

[2] A.H.Benny and G.J.Dawson, "Satellite imagery as an aid to bathymetric charting in the Red Sea," *The Cartographic Journal*, vol. 20, N° 1, pp.5-16, June 1983.

[3] W.A.Hallada, "Mapping bathymetry with LANDSAT Thematic Mapper, preliminary findings," *9th Canadian Symposium on Remote Sensing, August 14-17 1984, St.John's, Newfoundland*, Edited by S.M.Till and D.Bajzak, pp.277-285, 1984.

[4] J.M.Paredes and R.E.Spero, "Water depth mapping from passive remote sensing data under a generalized ratio assumption," *Appl.Opt.*, vol. 22, 1134, 1983.

[5] R.Kent Clark, Temple H.Fay and Charles L.Walker, "Bathymetry calculations with LANDSAT 4 TM imagery under a generalized ratio assumption," *Appl.Opt.*, vol. 26, pp.4036-4038, 1983.

[6] D.Spitzer and R.W.J. Dirks, "Shallow water bathymetry and bottom classification by means of the LANDSAT and SPOT optical scanners," in *Proceedings of the Earth Remote Sensing Using the Landsat TM and Spot Sensor Systems, 15-17 April 1986, Innsbruck, Austria*, Edited by Philip N. Slater, pp.136-138, 1986.

[7] David R. Lyzenga, "Passive remote sensing techniques for mapping water depth and bottom features," *Appl.Opt.*, vol. 17, pp.379-383, 1978.

[8] L.Loubersac, P.Y.Burban, O.Lemaire, F.Chenon et H.Varet, "Nature des fonds et bathymétrie du lagon de l'atoll d'Aitutaki (Iles Cook) d'après des données SPOT-1," *Photo-Interpretation*, N° 5 et 6, pp.29-40, 1989.

[9] P.Masson, G.Dubois, G.Le Lann, A.Hillion and C.Roux, "Classification d'images du satellite SPOT pour la cartographie bathymetrique du littoral," in *Proceedings of OSATES 24-27 September 1991, Brest, France*, 11p., paper B7, 1991.

[10] L.Estep, "A suggested approach to the passive optical bathymetry problem by a component analysis of the upwelling remote sensing signal," *The Hydrographic Journal*, N° 69, pp. 25-29, July 1993.

[11] William D. Philpot, "Bathymetric mapping with passive multispectral imagery," *Appl.Opt.*, vol. 28, pp.1569-1578, 1989.

[12] François James, Georges Dubois et Thierry Garlan, "Rectification géométrique des images SPOT par modélisation de la prise de vue," *Rapport d'étude*, N° 005/90, EPSHOM-BREST, France, 34 p., juillet 1990.

[13] Thierry Garlan, "The nautical space chart," in *Proceedings of the US Hydrographic Conference'90, 1-4 Mai 1990, Norfolk, Virginia*, The Hydrographic Special Publication, N°25, Hydrographic Society, Rockville, Maryland, 1990.

[14] Thierry Garlan, "Cartographie spatiale du littoral corralien: topographie et bathymétrie," *Rapport d'étude*, N°006/89, EPSHOM-BREST, France, 29p., août 1989

Inferring Subsurface Current Structure in a Coastal Ocean From Remote Sensing Data

Colin Y. Shen

Code 7250, Remote Sensing Division
Naval Research Laboratory
Washington, D.C. 20375, USA
Email: shen@ccf.nrl.navy.mil

Abstract

In shallow coastal water, currents tend to be viscously dominated by vertical eddy momentum diffusion. This vertical transfer of momentum is shown to provide a dynamic link with which subsurface currents can be inferred from remote sensing measurements of surface currents. The inference method is described, and its applicability to the coastal ocean is demonstrated with field data. The issues related to the application of the method are discussed as well.

1. Introduction

Remote sensing technology presently exists to measure velocities on the surface of the coastal ocean, as well as wind stresses and sea surface height/pressure gradients that force the current. The challenge to the oceanographer is to find a way to use these remotely sensed observations to infer the current structure below the sea surface, so that an assessment can be made of the subsurface ocean environment, especially, in regions where in situ current measurements are lacking. The purpose of this paper is to show for a shallow coastal ocean that the vertical viscous coupling of current motions through eddy momentum diffusion can be exploited to obtain subsurface current estimates from surface data. In Sec. 2, the methodology is described, beginning with dominant scales of motion and vertical processes in coastal circulation, proceeding on to the surface-to-subsurface viscous link, and then the specific procedure for inferring the current structure. In Sec. 3, application of the method to an ocean experiment is presented. The results are compared with in situ current data, and related remote sensing data issues are addressed. The paper concludes in Sec. 4 with remarks assessing the status of the present approach to infer subsurface currents.

2. Methodology

Physical processes of all scales are operative within the ocean volume and give rise to the spatial/temporal relationship among different scales of motions. The present methodology for inferring subsurface flow in essence seeks this relationship but from the point of view that the most relevant dynamics to coastal currents occurs on space/time scales commensurable with those of the forcing - a view consistent with that of present day coastal circulation modeling. The specifics of the circulation dynamics are given next, with special attention to the role of vertical viscous momentum transfer. From the dynamics, the surface momentum equations are deduced and used to relate observed surface motion to the interior flow.

2.1 Dynamic basis

Coastal currents are driven by tides, winds, alongshore buoyancy fluxes, as well as by baroclinic and barotropic pressure gradients from the open ocean. The resulting coastal circulation thus necessarily evolves on space/time scales of these forcings, i.e., O(km) or more and O(day) or longer. In coastal water of tens of meters depth, km-scale and larger currents are constrained by the shallow depth to be predominantly horizontal and, hence, currents are in approximate vertical hydrostatic balance, or

$$\frac{\partial p}{\partial z} = -g\rho, \qquad (1)$$

where p is the pressure, g is the gravitational acceleration constant, ρ is the water density, and z is the vertical coordinate, positive upward.

The other important simplification of the physics on the scales of coastal currents is the parameterization of small-scale high frequency motions as eddy momentum fluxes (Reynolds stresses); these are represented as the product of an eddy viscosity, ν_d, and a mean current shear. In shallow water, a representation of only the vertical flux generally suffices, because the vertical mean shear is typically orders of magnitude lager than the large-scale horizontal shear. Thus, the eddy momentum flux is given by

$$F = -\nu_d \frac{\partial}{\partial z}(u, v) \qquad (2)$$

where u and v are the two horizontal components of the surface velocity.

Various semi-empirical models exist for estimating the eddy viscosity, which can vary depending on ambient flow conditions [1]. For current speeds of tens of cm/s, a ν_d of hundreds of cm^2/s can be expected typically. For $\nu_d \sim 100$ cm^2/s, eddy induced vertical momentum flux can produce a stress Ekman boundary layer that has a depth, $d = (2 \cdot \nu_d / f)^{1/2} \sim O(10\ m)$ for a Coriolis frequency, $f = 2\pi/24$ hrs. It is easy to see that the surface and bottom Ekman boundary layers thus can overlap in coastal water of tens of meters depth, and the surface and bottom stresses can be

transmitted through the whole water column. Moreover, the e-folding time scale for viscous transmission is, $d^2/(4 \cdot \nu_d) \leq 0.5$ day. Thus, on the time scales of coastal currents, eddy momentum diffusion dominates the vertical processes. In this sense, the current motions can be said to be viscously coupled in the vertical.

The foregoing characterization is consistent with the accepted view of coastal circulation physics; in particular, the emphasis on dominant scales of motion, the hydrostatic approximation, and the diffusive parameterization of vertical eddy momentum flux are all ingredients in today's customary coastal circulation models [2]. The equations for surface current motion are now deduced within this framwork.

2.2 Surface momentum balance

The surface pressure gradient under the hydrostatic approximation (1) can be expressed in terms of the sea surface slope as

$$\frac{1}{\rho_o}\left(\frac{\partial}{\partial x}, \frac{\partial}{\partial y}\right) p = g\left(\frac{\partial}{\partial x}, \frac{\partial}{\partial y}\right)\eta \qquad (3)$$

assuming constant atmospheric pressure, where the reference density ρ_o is taken to the sea surface density, η is the sea surface height, and x and y are the two Cartesian horizontal spatial coordinates.

The vertical diffusion of momentum is given by the divergence of the flux (2), where the vertical z-derivative is taken to be normal to a level sea surface. The sea surface elevation changes insignificantly relative to the km-scale of the current and can be viewed essentially as flat. Nevertheless, the sea surface slope is always dynamically important as shown in (3). The eddy viscosity in (2) can be treated as approximately constant near the surface, since in the proximity of the sea surface, water is almost always well mixed under high frequency surface gravity wave motions. (The discussion here and the subsequent formulation of the inference approach are not fundamentally altered, if for any reason, ν_d varies rapidly near the surface that warrants the addition of a flux term containing $\partial\nu_d/\partial z$.) Thus, the vertical divergence of (2), with constant ν_d, is

$$D = -\frac{\partial}{\partial z} F = \nu_d \frac{\partial^2}{\partial z^2}(u, v) \qquad (4)$$

The horizontal surface fluid acceleration is determined by the balance between the Coriolis forces, $f(-v, u)$, the pressure gradients (3), and vertical momentum diffusion (4). The vertical advective part of acceleration at the surface may be set to zero under the level sea surface approximation stated above. Thus, the surface momentum balance is

$$\left\{\frac{\partial u}{\partial t} + u\frac{\partial u}{\partial x} + v\frac{\partial u}{\partial y} - f v = -g\frac{\partial \eta}{\partial x} + \nu_d \frac{\partial^2 u}{\partial z^2}\right\}_{\text{surface}} \qquad (5)$$

$$\left\{\frac{\partial v}{\partial t} + u\frac{\partial v}{\partial x} + v\frac{\partial v}{\partial y} + f u = -g\frac{\partial \eta}{\partial y} + \nu_d \frac{\partial^2 v}{\partial z^2}\right\}_{\text{surface}} \qquad (6)$$

As the subscript indicates, these two balance equations are applicable only to the sea surface current motion. The validity of the two equations is not limited to a uniform density ocean, as the form of the equations appears to suggest. Both surface equations are valid for oceans with density stratification; the stratification effect enters implicitly into the surface balance through the pressure gradient terms.

The three variables u, v and η in (5) and (6) are quantities measurable with remote sensing. It is evident that with these measurements, the process represented by each of the terms in the balance equations can be evaluated, with the exception of momentum diffusion that must be obtained indirectly as the residual of the balance. The fact that (5) and (6) allow momentum diffusion to be deduced from the surface measurements is of significance, as momentum diffusion is the only process here that couples the surface to subsurface motions. In particular, terms for momentum diffusion contain vertical curvatures of u and v, and since the vertical gradients, $\partial u/\partial z$ and $\partial v/\partial z$ are already estimable from remote sensing of surface winds, the change of these gradients with depth is now known, thereby sharpening the description of the u and v variation from the surface. Because the viscous diffusion process is solely responsible for transmitting the wind energy from the surface into the water column, the magnitude of diffusion estimated above as a residual from the balance will most likely to be physically meaningful. The estimated velocity curvatures from diffusion will thus similarly be meaningful provided that ν_d is reasonably chosen.

The surface velocity gradients and curvatures characterize the initial vertical change of velocity with depth and are clearly useful for the inference of the subsurface velocity. These surface velocity derivatives hereinafter will be referred to as boundary conditions or constraints for the velocity profile to be inferred. A summary of available surface velocity boundary conditions/constraints are given in the following subsection including an additional condition derivable from surface shear balance equation.

2.3 Kinematic/dynamic boundary conditions

The surface velocity boundary conditions that presently can be obtained from remote sensing are (7) and (8) below. Those derivable from surface momentum equations using the remote sensed data are (9) and (10). The 2nd z-derivative condition is the one discussed in the foregoing subsection. The terms on the right hand side of (9) are to be evaluated from remotely sensed u, v and η, and the evaluation involves only the first derivatives in t, x, and y. The third derivative condition comes from differentiating the full three-dimensional u and v momentum equations once with respect to z and then taking the surface expressions of the differentiated form, assuming the density uniform at the surface. For this boundary condition, the terms on the right hand side are to be evaluated with remotely sensed velocities (7) and shears (8). Again, the evaluation involves only first derivatives in t, x, and y. Lastly, the current velocity at the sea floor is taken to be zero. Thus, at the surface, $z = 0$,

measured

$$(u, v), \tag{7}$$

$$\frac{\partial}{\partial z}(u, v), \tag{8}$$

derived

$$\frac{\partial^2}{\partial z^2}(u,v) \tag{9}$$
$$= \frac{1}{\nu_d}\frac{D}{Dt}(u,v) + \frac{f}{\nu_d}(-v,u) + \frac{g}{\nu_d}\left(\frac{\partial \eta}{\partial x}, \frac{\partial \eta}{\partial y}\right)$$

$$\frac{\partial^3}{\partial z^3}(u,v)$$
$$= \frac{1}{\nu_d}\frac{\partial}{\partial z}\frac{D}{Dt}(u,v) + \frac{f}{\nu_d}\frac{\partial}{\partial z}(-v,u) \tag{10}$$

where $D/Dt = \partial/\partial t + u\partial/\partial x + v\partial/\partial y$, and, provided that the water depth H is known, at the bottom, $z = -H$,

$$u = v = 0. \tag{11}$$

The remaining question now is whether or not these five constraints are sufficient to bound the problem, i.e., to characterize adequately the velocity variability with depth. The answer depends on how strongly viscous diffusion and Ekman layer dynamics affect the current. For a strongly affected current, the velocity profile will vary gradually with depth and can be expected to be characterized well by low order derivative boundary conditions. This is expected to be the case for shallow coastal currents, where the surface and benthic Ekman boundary layers can often overlap, as pointed out in subsection (2.1).

2.4 Vertical modal representation

It is known that a given continuous function in a finite spatial interval can be expressed as a linear sum of orthogonal basis functions with suitably chosen weights. Expressing the depth dependence of the current velocity in terms of orthogonal basis functions has the appeal that it reduces the problem of determining the profile to adjusting the weights to satisfy the boundary constraints. As there is no unique set of basis functions for a finite depth interval, such a modal approach necessitates a choice to be made as to the appropriate basis set for describing velocity variation with depth. The choice made here is a practical one based on this author's own experience with viscous flow calculations using Chebyshev polynomials, which generally gives efficient and accurate representation of flow profile. Ideally, one would like to have available basis functions that are also natural modes of the dynamics of the motion, in which case a more efficient representation of the flow profile would be possible than, say, with algebraically motivated basis functions. The possibility that a natural basis set could be obtained with climatology data including depth dependent eddy viscosity is being investigated by the author.

The important point here is that the present methodology does not depend on any specific choice ofbasis functions, although the final shape of the velocity profile will be influenced to some extent by the choice made. The first five modes of the Chebyshev polynomial basis set used here for the subsurface inference are shown in Fig. (1).

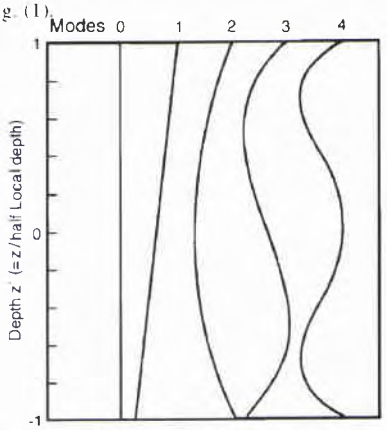

Figure 1: The first five Chebyshev polynomial modes as a function of normalized depth.

By requiring the linear combination of these modes to satisfy the five boundary constraints (7)-(11), the weights for these modes can be determined and hence, the velocity profile constructed. It is of interest to note that for a water column dominated by the viscous Ekman layer dynamics, horizontal flow seldom exhibits vertical scales smaller than that shown by mode 4; in situations like this, the five Chebyshev modes in Fig. (1) are essentially all that required to characterize the vertical structure.

2.5 The inverse solution and errors

The procedure for obtaining the velocity profile is straightforward, once a suitable modal representation is chosen. In the case of the Chebyshev modal expansion, the modes are most conveniently defined within a dimensionless interval, +1 to -1. This necessitates a simple conversion, $z' = 1 + 2z/H$, from the dimensional depth z to a dimensionless one z' for $0 > z > -H$. Let $F_i(z')$ denote the i-th order Chebyshev mode spanning the interval, $1 > z' > -1$. The representation of u and v in terms of the first five such modes are thus

$$u(\mathbf{x}, z', t) = \sum_{i=0}^{4} \alpha_i(\mathbf{x}, t) F_i(z') = \mathbf{A} \bullet \mathbf{F}^T \tag{12}$$

$$v(\mathbf{x}, z', t) = \sum_{i=0}^{4} \beta_i(\mathbf{x}, t) F_i(z') = \mathbf{B} \bullet \mathbf{F}^T \tag{13}$$

where **A**, **B**, and **F** are row vectors for the modal coefficients α_i, β_i, and the basis functions F_i, respectively. Because of the change of variable, the z-derivatives become

$$\frac{\partial^n}{\partial z^n} = \left(\frac{2}{H}\right)^n \frac{\partial^n}{\partial z'^n} \quad , \text{ with n = 1, 2, and 3,} \qquad (14)$$

and the z-derivative boundary conditions (9) and (10) need to be adjusted accordingly for use in the z' coordinate. An additional step is needed to treat the coefficient for the depth-independent, zeroth mode as the sum of the surface velocity and a correction, namely,

$$\alpha_0 = u(z' = 1) + \alpha'_0$$

and

$$\beta_0 = v(z' = 1) + \beta'_0 \qquad (15)$$

This helps to retain the depth-independent mode, which is absent in the derivative boundary conditions.

Applying the boundary conditions (7) - (11) to (12) and (13) with the vertical derivatives suitably adjusted as in (14), the following two linear systems of equations are obtained:

$$\mathbf{G} \bullet \mathbf{A}_* = \mathbf{U}$$

and

$$\mathbf{G} \bullet \mathbf{B}_* = \mathbf{V} \qquad (16)$$

where G is a 5x5 matrix containing the derivative values of the Chebyshev modes at z' = +1, -1; U and V are column vectors containing the five boundary conditions for u and v, and

$$\mathbf{A}_* = \left\{\alpha'_0, \alpha_1, \alpha_2, \alpha_3, \alpha_4\right\}^T$$

and

$$\mathbf{B}_* = \left\{\beta'_0, \beta_1, \beta_2, \beta_3, \beta_4\right\}^T \qquad (17)$$

are the unknown coefficients. The coefficients can be readily solved by standard matrix inversion procedure, and the u and v profiles can be assembled from (12) and (13). In passing, it may noted that although, in principle, more than 5 modes can be included in (12) and (13), and the resulting underdetermined system (16) solved using the method of single value decomposition, this does not necessarily yield a better result as the additional higher modes can weaken the constraining effect of low order derivative boundary conditions.

For the linear systems in (16), the errors on the subsurface u and v estimates due to errors in the input boundary values can also be readily assessed. Let $\mathbf{E} = \{E_i\}$ be the error vector in the boundary values, where i=1 refers to the surface velocity , 2 the shear, 3 the curvature, 4 the third z-derivative, and 5 the bottom velocity which is taken here to be error free. Consider u only since v is treated the same way. The error vector $\delta = \{\delta_j\}$ for the modal coefficients are thus, with j = 1, 2,.., 5,

$$\delta = \mathbf{G}^{-1} \bullet \mathbf{E} \qquad (18)$$

The error in the subsurface u velocity estimate is

$$\varepsilon_u = \delta \bullet \mathbf{F}^T \qquad (19)$$

In Fig. 2, the error profile ε_u versus depth is shown separately for each input surface errors. The error range has been normalized to unity. It is seen that the u error is the largest toward the bottom for surface derivative errors, while the surface u error propagates mostly undiminished toward the bottom.

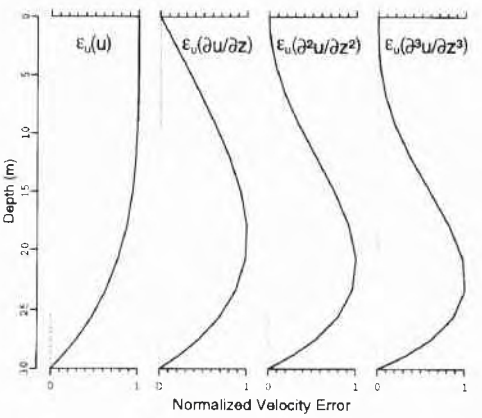

Figure 2: Normalized velocity error ε_u as a function of depth. Each curve represents the error from an individual surface source in the parentheses. The 30 m depth is used as an example.

3. Application to an ocean experiment

The methodology has been applied to the surface velocity data obtained during the High Resolution Remote Sensing - 2 experiment (HIRES-2), which is a field program sponsored jointly by the U.S. Office of Naval Research and the Naval Research Laboratory [3]. The experiment was conducted on the continental shelf off the coast of Cape Hatteras. During the experiment, from 11 June-8 July, 1993, the surface velocity was remotely measured with two shore-based, high frequency Ocean Surface Current Radars (OSCR) [4]. The radar sites and the area imaged by OSCR (dots) within the experimental area are shown in Fig. 3. Each dot in the imaged area represents the location at which a velocity vector is measured. The separation distance between the measurements is ~1.2 km, and the velocity in the entire area is sampled at 20 min intervals during the month long period. The OSCR experimental area is approximately 35 km by 40 km, and the water depth ranges between ~20 m and ~30 m. In situ measurements of current velocities below the sea surface were made from the ship using an Acoustic Doppler Current Profiler (ADCP) at various times during the experiment.

The surface wind speed during the experiment was measured at two discus buoy sites and from a moving ship; remote sensing of the wind with scatterometry was also attempted. Unfortunately, only the data from the buoy site referred to as D_w (35°25'N, 75°15'W) is of sufficiently good quality to be used for the wind stress calculation. The wind speed was sampled at 10 min intervals at this site, and the wind stress calculated from this data is used for the entire area. Attempts to measure sea surface elevation with subsurface pressure sensors mounted on the discus buoy moorings were not successful during the

experiment, and satellite altimetry data for the sea surface height was not available during the experimental period.

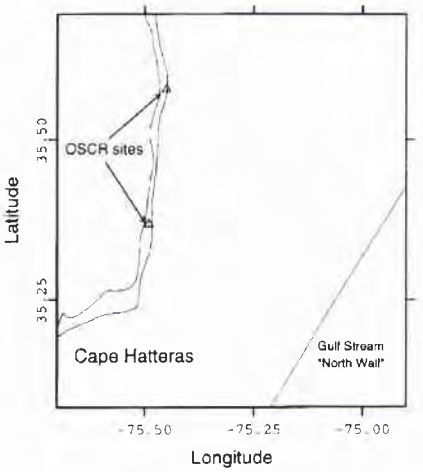

Figure 3. Area of the HIRES-2 Experiment and the area imaged by OSCR (dots). The continental shelf break is just to the west of the OSCR area and runs approximately parallel to the Gulf Stream "north wall".

In the absence of the sea surface height data, some model assumptions have to be made about the sea surface slope in (5) and (6). The assumption made for the HIRES-2 area is that the surface slope pressure force and the viscous force contribute equally to the balance of the inertial forces on the left-hand side of (5) and (6), and so the surface slope pressure term and the viscous term on the right-hand side of (5) and (6) each equals to 1/2 of the left-hand side sum, i.e., a distribution that biases neither term. Other assumptions are also possible, such as treating the Coriolis force as a part of the slope pressure, or to bound the slope pressure with tidal model calculations, with data from tidal gauges, or with additional dynamic constraints. These possibilities are presently under investigation.

From the sea surface velocities, wind stresses, and surface slopes obtained as described above, subsurface velocities as a function of depth have been calculated using the inference method for the whole OSCR area. Here, the results for two contrasting flow situations will be shown to demonstrate the applicability of the method.

The results to be shown are for currents at 1300 GMT and 1500 GMT, 23 June 1993. Figs. 4a and 5a show the current velocity vectors at these two times. It is seen that the overall circulation patterns in both figures are quite similar: a relatively strong and broad northeast flow in the western part of the domain, a cyclonic turning of a portion of this flow near the northern boundary, and a returning weak south-southwest flow on the eastern side. The details of two flow fields differ, however, reflecting the influence of the wind which is blowing to the southwest; this influence is evidenced in the strengthening of the southwest flow and weakening of the northeast flow from 1300 GMT to 1500 GMT. For the subsurface inference, the sea surface velocity vectors, as well as the wind

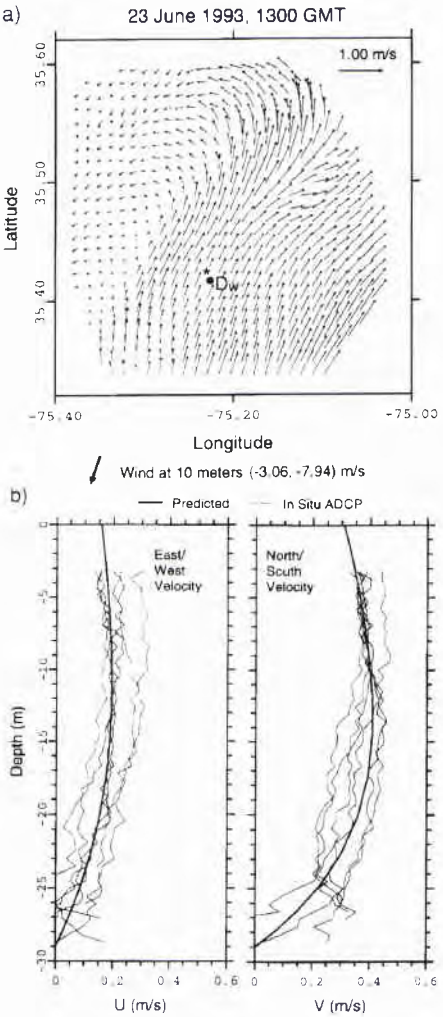

Figure 4: a) Sea surface current velocity vectors from OSCR, b) Comparison of inferred (predicted) and directly measured (ADCP) velocity profiles. The * symbol denotes location of the inferred profile. Within a km radius the ADCP velocity profiles were obtained. D_w denotes the location of the discus buoy where wind speed was measured

velocity vectors, have been low-passed filtered with a 6-hr cosine window.

At 1300 GMT, the velocity inference is made near D_w as marked in Fig. 4a, where direct ADCP measurements of the subsurface velocity from a ship are available. The inferred (predicted) velocity profiles and the directly measured profiles are compared in Fig. 4b. Except for the considerable scatter in the measured profiles near the bottom as a result of the bottom acoustic interference, the measured profiles can be seen generally clustered around the predicted profiles. It is noteworthy that the in situ profiles show that the velocity varies slowly with depth, giving a hint of maximum in the v-velocity around the mid depth, and this behavior is captured by the predicted profiles. The eddy viscosity used for this inference is 100 cm^2/s. This value is deemed reasonable for the HIRES-2 area and is used in all subsurface inference here. Increasing/decreasing this value decreases/increases the amplitudes of the predicted profiles.

At 1500 GMT, in situ velocity measurements were obtained in the region of weaker southwest flow near the location marked in Fig. 5a. The subsurface inference made at this location and time is compared to the in situ velocity profiles in Fig. 5b. It is seen that the measured u, in contrast to that in the previous stronger flow region, changes direction below the surface at about the 10 m depth. Although this change is predicted in the inferred u profile, the u speed is significantly underestimated. This discrepancy is primarily due to under estimation of the velocity curvature in the boundary condition (9). Presumably, this error could be reduced if the sea surface slope for u in (9) could be provided by direct measurements instead of the model assumption of the present method stated earlier. To indicate the kind of accuracy required of the surface slope measurement, the magnitudes of the velocity terms in the u balance (6) estimable from the surface u and v data for this case are listed, in m/s^2: $\partial u/\partial t \approx 4.4\times10^{-6}$, $u\partial u/\partial x+v\partial u/\partial y \approx 2.7\times10^{-6}$, and $-fv \approx 1.2\times10^{-5}$. This suggests a slope, $\partial\eta/\partial x$, of $O(10^{-6}\text{-}10^{-5})$ or 1-10 cm elevation change over a 10 km horizontal distance. The error in the predicted profile may be estimated using (18) and (19), if the measurement errors of the input surface parameters are known. The nature of the measurement error presently is still an issue and is being investigated.

4. Summary remarks

In this paper a method for inferring subsurface current velocities from remote sensing observation of the surface flow field has been described. The method exploits the strong viscous coupling between the surface and subsurface motions that exists in shallow water to obtain surface boundary conditions in terms of the vertical derivatives of the surface velocity. From these derivative conditions, the subsurface velocity is inferred based on a vertical modal representation of the velocity variation with depth.

The velocity profiles inferred with the present method are found to be generally consistent with those given by direct measurements, but, because the sea surface slope is

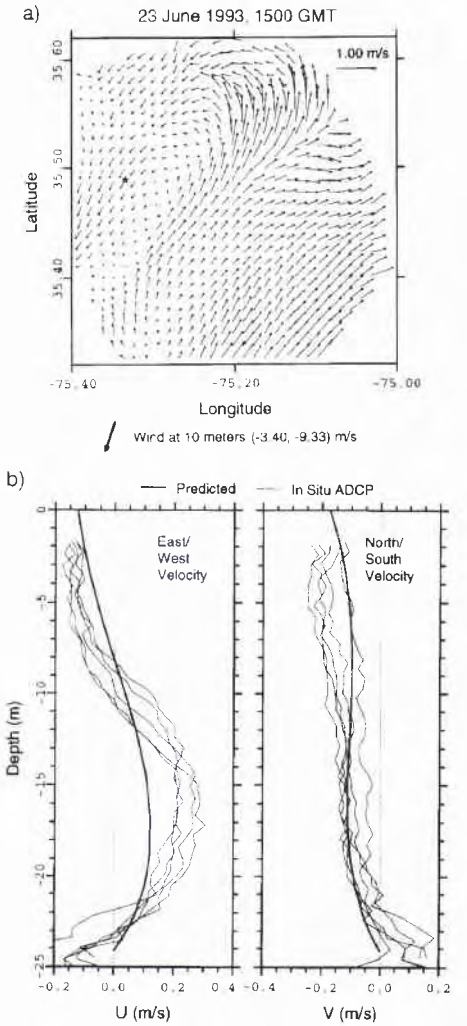

Figure 5: Same as Fig. 5, except at 1500 GMT and comparison made at another location denoted by the * symbol in (a).

unknown and has to be estimated based on a model assumption, there are cases where inferred profile amplitudes are in significant error. Whether or not coastal altimetry can eventually provide the needed sea surface height/slope is presently an issue. A possible long-term solution may lie in the direct measurement of surface derivative boundary conditions, which now appears possible with the new generation of multi frequency HF

radars presently being developed by the Office of Naval Research (see Trizna in this volume). Such direct measurements could make sea surface slope /wind stress measurements irrelevant for the application of the inference method here.

Although the surface data has been exclusively used, the present method can make use of in situ subsurface data, if available, to augment the remote sensing inference, by treating the subsurface data as additional constraints; alternately, the subsurface data can be assimilated into the inferred current field by standard assimilation techniques to improve the accuracy of subsurface description. It is not uncommon for a coastal region to be observed over a wide area with remote sensing and at the same time, sampled locally with in situ instruments, such as in the case of the HIRES-2 experiment. The combined use of the subsurface inference method and in situ data potentially allow a greater accuracy to be achieved in the description of the subsurface environment.

Acknowledgments. The author thanks Richard Mied for the many valuable discussions and Arnold Cooper for his helpful comments during the course of this work. It is a pleasure to thank Tom Evans for his valuable help with computer programming and graphics. Thanks also go to Cliff Trump for providing the ADCP data and Gloria Lindemann for assisting in the preparation of the manuscript. Lynn Shay and Hans Graber of University of Miami made available the OSCR data and wind speed data for analysis. The author is grateful to them. The author also gratefully acknowledges funding support by the Ocean Modeling and Prediction Program at the U.S. Office of Naval Research.

References

[1] G.L. Mellor, "Retrospect on Oceanic Boundary Layer Modeling and Second Moment Closure," in *Proceedings of 'Aha Huliko'a Hawaiian Winter Workshop on "Parameterization of Small-Scale Processes"*, University of Hawaii, Honolulu, Hawaii, 1989.

[2] *Coastal Ocean Prediction*. Editor: CNK Moores, Coastal and Estuarine Studies Monograph Series, American Geophysical Union, in press.

[3] F. Herr, C.A. Luther, G.O. Marmorino, R.P. Mied, and D.R. Thompson, "Ocean Remote Sensing Program Planned," *EOS*, vol. 72, p.214, 1991.

[4] L.K. Shay, H.C. Graber, D.B. Ross, and R.D. Chapman, "Mesoscale Ocean Surface Current Structure Detected by High-Frequency Radar," *J. Atmos. Oceanic Tech.*, vol. 12, pp.881-900, August 1995.

Remote Sensing in the Surf Zone - Non-traditional Methods

R. Holman*, T. Holland†, H. Stockdon* and C. Church†

*COAS-OSU
104 Ocean Admin Bldg
Corvallis, OR 97331-5503
Email: holman@oce.orst.edu
hstockdo@oce.orst.edu

†Naval Research Lab
Code 7442, Building 2438
Stennis Space Center, MS 39529
Email: holland@nrlssc.navy.mil
cchurch@gm7400.nrlssc.navy.mil

Abstract

Naval forces have developed an increasing interest in very shallow water and surf zone regions. Optimum use of the environment requires knowledge of a range of properties from depth profiles to wave heights and current strengths. These usually must be measured remotely, a challenge given the large spatial gradients of the nearshore.

Techniques have been developed based on video imagery from fixed platforms. Generalities of the sampling problem are discussed along with the concepts underlying each technique. The main complications of transition to moving platforms are related to the statistical consequences of the different sampling capabilities.

1. Background

The navy has long had an interest in the capability for remote measurement of environmental parameters in very shallow waters and the surf zone. Experiences during World War II painfully demonstrated the need for greatly improved reconnaissance in order for operations to be successful. This spawned a chain of research in the immediate post-war years that waned during the cold war but has seen increased recent interest as limited intensity conflict has become an increasing focus.

Reconnaissance needs have not changed substantially since W.W.II. The principle variables of interest include depth profiles (for both direct operational and indirect modeling purposes), wave and current characteristics, water clarity and, potentially, bioluminescence. Since these quantities change spatially, either a suite of spatially-spread samples are required or alternately a few samples with a model to allow interpolation. For many purposes, the importance of variables on operations increases as the surf zone is approached

For most purposes, clandestine techniques are required. In situ sampling has high reliability but also very high risk. Instead, remote sensing approaches by a variety of platforms are preferred. Fortunately, waves are quite visible and even currents can be inferred from foam drift. Thus a number of remote techniques may be available.

2. Technical Constraints

2.1. The Geophysical Problem

A geophysical description of the nearshore includes two components. The physical oceanography problem addresses the fluid dynamics of waves on a shoaling bathymetry. The complementary marine geology problem studies the response of loose sand grains to those fluid motions. The combination involves a great deal of feedback and the potential for chaos.

In order to constrain the sampling problem, we need to know the time and space scales of the variables of interest. Bathymetry gradients on some beaches can be large, often as much as 1:10. Bathymetry can include sand bars in the cross-shore direction and rip channels spaced along the beach. Important length scales of variation can be as little of tens of meters in the cross-shore and a hundred meters in the longshore direction. These bathymetric features can change on a daily basis, especially during storms.

Wave motions, with offshore periods of 10 s and wavelengths of 150 m, can shoal quite dramatically in the nearshore, with substantial changes in properties over one wavelength. Nonlinearities abound. Some are obvious, for example wave breaking, while others may not be as visually apparent, such as the generation of longshore currents or infragravity waves.

2.2. Sampling Issues

Issues of sampling the nearshore bathymetry and wave field include those questions concerning the relationship between imaged measurements and known geophysical quantities, and those that are sensor-independent. The techniques in this article will concentrate on visual band signals (how the eye sees waves).

Clearly the visual signature of waves is not constant. For example, wave crests are relatively dark outside the break point but are white once the waves start to break.

This can be quantified by cross-spectral techniques. Offshore, sea surface elevation and image intensity time series are highly coherent in the incident band and have a particular phase that is fairly constant in the cross-shore

direction. In the surf zone they are also very coherent but have a different, but also nearly constant, phase. In the region of occasional breaking, the mixing of these two different phases (when some waves break and others don't) yields very low coherences and unstable phase.

The visual signature of a wave passage may be related to sea surface elevation in a very nonlinear way. For example, waves that are just breaking appear as a narrow white band of foam at the wave crest. At the fundamental frequency of the wave, video signals should provide a good proxy for wave phase. However, higher frequencies can easily be dominated by these nonlinearities; therefore, video signals do not provide a faithful rendition of the high frequency sea surface.

Other sensors may have their own complications. For example, the modulation transfer function of different types of radars may depend on different details of the ocean wave form. We will generally omit these potentially important issues from the following discussion so that we can focus on the fundamentals of the techniques.

The techniques discussed below largely rely on signal processing tools to work: imaged data must be analyzed using statistical tools to yield an estimate of the geophysical quantity of interest. It is vital that the problem be treated as a statistical one. A necessary part of each result is a confidence interval so that a user can tell reliable from unreliable values.

Because techniques are statistical, standard sampling criteria apply. For example, sampling of the wave field involves a mix of both temporal and spatial data, the extents of which help determine error bars. In all cases, more data yields smaller confidence intervals on derived estimates.

3. Fixed Platform Solutions

At the Coastal Imaging Lab (CIL) at Oregon State University, we have developed a suite of techniques based on video imagery from fixed platforms, usually towers but including light houses and building roofs.

3.1. General Aspects of Fixed Platform Sampling

Sampling from a fixed platform has two distinct advantages. First, the geometry usually can be considered steady and need only be solved once. Thereafter, repeat samples require only a knowledge of the sampling pixel list.

Because the orientation is fixed and known, long time series can be collected, usually only limited by statistical needs or possible non-stationarity, for example due to tides. In this method, pixels can be imagined as equivalent to fixed instruments.

On the other hand, fixed platform imagery is often taken at near horizontal view angles and pixel resolution can be poor.

In general, images can be sampled in one of three ways. The traditional method is to consider either the entire image or a sub-region of interest. Alternately, several of the techniques consider intensity variations along a single line of pixels on the image, usually oriented in the cross-shore or longshore direction. Finally, time series of image intensity can be collected at individual pixels or at arrays of individual pixels. In this case, pixels are considered equivalent to fixed instruments in the water.

3.2. Fixed Platform Sampling Capabilities

We have developed or are developing techniques to estimate both fluid and bathymetric properties. These include:

Fluid Properties:	Bathymetric Properties:
• wave period	• shoreline and sand bar morphology
• angle of incidence	• foreshore beach slope
• wave celerity	• wave celerity
• runup	• bathymetric depths from celerity
• longshore currents	

3.2.1. *Wave Period and Angle of Incidence*

The high coherence of visual signals and the sea surface lets us estimate wave quantities. Thus, wave period can be found from the location of the peak in spectra of pixel intensity time series. Similarly, because the phase between waves and intensity does not change in the longshore direction, phase comparisons of longshore arrays of pixel time series (Figure 1) can be used to measure wave angle in a completely analogous approach to the usage of longshore arrays of pressure sensors. Estimation of wave angle at different depths or longshore locations

Figure 1. Example pixel array at Duck, NC, 10/08/90. Cross-shore spacing of sampled pixels is 5 m, with longshore arrays every 25 m. Arrays such as this allow estimation of wave period, angle of incidence, celerity and bathymetry

is as simple as sampling different pixels at those locations.

3.2.2. Wave Celerity

Wave celerity is defined as the speed of passage of wave phase in the direction of propagation, usually the cross-shore direction. With in-situ instruments, this is found from phase comparisons along a cross-shore array of fixed sensor, say pressure gages. The same analysis can be carried out with a cross-shore array of pixel time series (Figure 1).

In regions where the relationship between wave and intensity phases is roughly constant (outside the break point or inside the surf zone), wave celerity can be well estimated from imagery. In regions of rapid relative phase change (near the break point), estimates of celerity are poor.

The principle use for celerity data is as an intermediate product in estimating water depths (below).

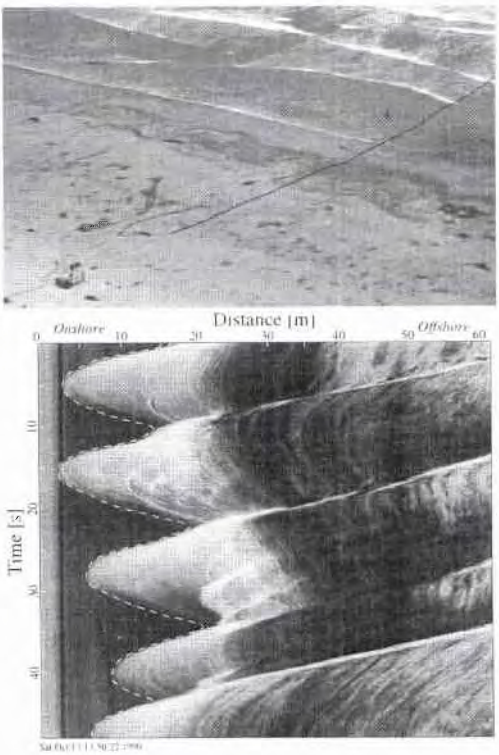

Figure 2. Measurement of wave runup using the time stack technique. Upper oblique image from San Onofre, CA, shows the location of the transect of interest. The lower time stack shows the time variation (down-page) of intensity of each pixel (cross-page) along the transect. Runup is marked by dashed white line

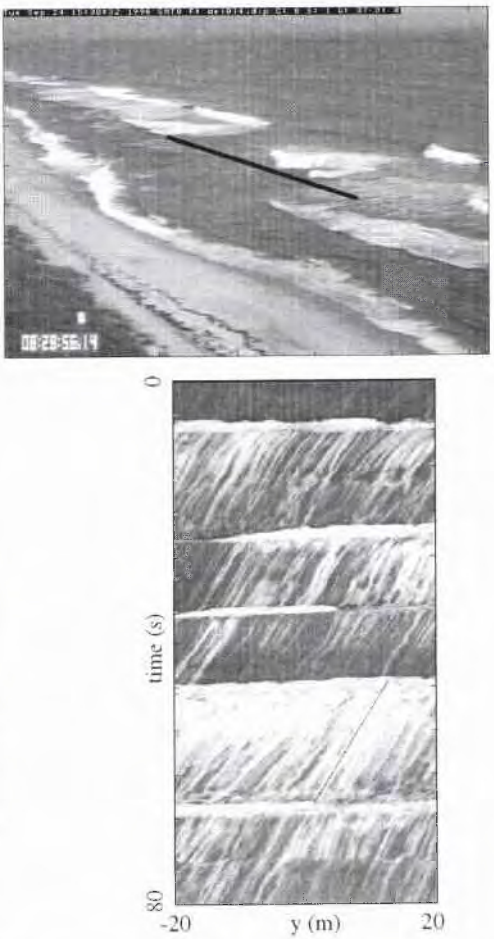

Figure 3. Longshore pixel arrays (upper) can be used to generate longshore time stacks (lower). Horizontal bands in the stack correspond to the passage of individual breakers, while oblique streaks are foam advected by the longshore current

3.2.3. Wave Runup

Wave runup, or swash, can be important both for operational reasons and as a diagnostic measure for the study of nearshore fluid dynamics. Robust estimation of the time dependent location of the water's edge can be difficult to do "on the fly" so it is usually important to return the data to the lab for analysis.

For analysis of runup at a location the entire image is not needed, only intensity values along the line of interest. Time variations of intensity along the line can be compactly represented in a "time stack" image, with pixel location plotted across-page and

time dependence down-page (Figure 2). From a time stack, a variety of measures can be made including swash characterization and measurement of the location of groundwater surfacing 2.

3.2.4. Longshore Currents

Figure 3 shows a time stack collected from a line of surf zone pixels oriented parallel to the beach. White horizontal bands correspond to the passage of individual breaking waves. Oblique streaks show the longshore drift of foam patches carried by the longshore current. Development of objective measures of the slope of the foam patches allows estimation of the strength of the longshore current.

3.2.5. Shoreline and Bar Morphology/Foreshore Slope

Waves break preferentially in regions that are relatively shallow. Thus, submerged sand bars can often be revealed by regions of concentrated wave breaking. While a snapshot (Figure 4a) will suggest the presence of a bar, it has been found that a time exposure image (Figure 4b) provides a good proxy for the location and morphology of a bar system. Knowing the geometry of a fixed camera installation, rectified views can be calculated (Figure 4c) and relevant length scales measured.

There also usually exists a band of concentrated breaking at the shoreline. This provides a good proxy for shoreline location. Variations of this location with the tide allows measurement of the foreshore slope, a technique that was first explored during W.W.II.

3.2.6. Nearshore Bathymetry

In shallow water, wave celerity is simply a function of depth and (for large amplitude waves) potentially wave height. Celerity measurements can therefore be inverted to allow estimation of depths at any point.

Research issues associated with this developing topic include proper estimation of confidence intervals, methods to deal with finite amplitude dispersion effects and methods to deal with regions where the relationship between wave and image phase change (particularly at the break point)

Figure 4a. Oblique snapshot from Duck, NC, 11/07/94.

Figure 4b. Ten minute time exposure of same.

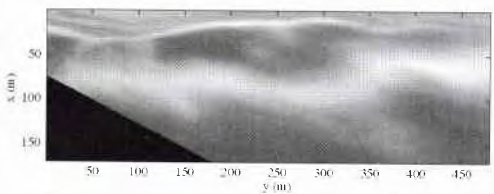

Figure 4c. Rectified view of a sub-region of the above time exposure

4. Application to Moving Platforms

For Navy purposes, sampling from fixed platforms is not an option. However, a variety of moving platforms are potentially available ranging from piloted and unmanned aircraft to satellites. Application of the above techniques to moving platforms may be largely associated with understanding the signal processing consequences of the different sampling characteristics.

4.1. General Aspects of Moving Platform Sampling

Air photos have different strengths than fixed, oblique images. Usually they allow excellent spatial resolution due to their near vertical views and large region of coverage. On the other hand, temporal sampling is usually limited to the time of overflight, while the frequency of sampling within that time depends on the sampling system. In addition, the geometry of every image is different and each must be navigated individually.

4.2. Problems in Transition from Fixed Platform

In principle, all techniques described for fixed platforms can be transitioned to a mobile platform scheme. Problems are tied to the consequences of the different spatial and temporal sampling of mobile schemes to subsequenct statistical analyses and complications due to varaiations of signals with view angle.

Spatial sampling requires knowledge of the geometry of every frame. For fixed platforms, small errors in geometry are usually not critical since the every point in a time series will have the identical error, thus there is only a slight offset in the position of a final estimate. On the other hand, for moving platforms, errors in each frame can be independent. Analysis that incorporates information from many frames (time series analyses) can be severely degraded. A careful study of the consequences of navigation errors on the final analysis is needed

Temporal issues usually revolve around the shortness of available records. An aircraft overpass might typically allow a record length of one minute, in contrast to the 17 minute records often used for fixed video. The consequences of short records to the analysis statistics must be examined.

Improvements in the temporal statistics may be improved by averaging realizations, for example including multiple overhead passes. If multiple passes are available at different stages of the tide, it may be possible to work around problems mentioned in previous sections associated with the breakpoint.

Moving platform sampling can also be complicated by potential variations in signatures with look angle. An obvious example might be the loss of clean imagery when an aircraft passes through the region of high sun reflectance or sun glitter.

5. Summary

Waves and currents in the nearshore are usually visually apparent. Thus, imagery of the nearshore can often be inverted to estimate a number of fluid and bathymetric quantities of interest. In university research, a number of such techniques have been developed and exploited, based on cameras that are installed on fixed platforms. Fluid properties that can be estimated include wave period and angle of incidence, wave celerity, runup and longshore current strength. The presence and morphology of sand bars can also be measured as well and the foreshore slope and nearshore bathymetry.

In principle, the same techniques can be transferred to a moving platform such as an airplane. However, care must be taken to determine how results are affected by the different spatial and temporal sampling parameters.

6. Acknowledgments

The authors would like to acknowledge ongoing support from the Office of Naval Research, Coastal Dynamics Program , grant N00014-96-J1118. Randi Miller continues to provide inspiration to our efforts.

References

T.C. Lippmann and R.A. Holman, *Phase speed and angle of breaking waves measured with video techniques*, in *Coastal Sediments '91*, N. Kraus, Editor, New York, ASCE, 1991, pp. 542-556.

[2] K.T. Holland and R.A. Holman, *Measuring run-up on a natural beach II*, in *EOS Transactions, American Geophysical Union*, 1991, p. 254.

[3] R.A Holman and M.H. Freilich, "Estimation of longshore currents on complex topography: A video technique," *Transactions, American Geophysical Union*, vol. 76, pp. 293, 1995.

[4] T.C. Lippmann and R.A. Holman, "Quantification of sand bar morphology: A video technique based on wave dissipation," *Journal of Geophysical Research*, vol. 94, pp. 995-1011, 1989.

[5] N.G. Plant and R.A. Holman, "Intertidal beach profile estimation using video images," *Marine Geology*, in press.

[6] H.F. Stockdon and R.A. Holman, "Accuracy of depth estimation techniques based on video observations of wave celerity," *Transactions, American Geophysical Union*, vol. 77, pp. 399, 1996.

Measurement of Mesoscale Oceanic and Atmospheric Phenomena by ERS-1/2 SAR

Werner Alpers

Institute of Oceanography, University of Hamburg,
Troplowitzstr. 7, D-22529 Hamburg, Germany,
Tel: +(49) 40 4123-5432, Fax: +(49) 40 4123-5713,

E-Mail: alpers@ifm.uni-hamburg.de

Abstract

Radar images acquired over the ocean by the synthetic aperture radar (SAR) aboard the two European Remote Sensing satellites ERS-1 and ERS-2 delineate oceanic as well as atmospheric phenomena. The mesoscale oceanic phenomena visible on ERS-1/2 SAR images include oceanic internal waves, eddies, oceanic fronts, underwater bottom topography, and surface slicks. The atmospheric phenomena include katabatic wind fields, convective cells, atmospheric boundary layer rolls, atmospheric internal waves, vortex rows (Karman vortex streets) behind islands, and atmospheric undular bores. Examples of ERS SAR images showing sea surface manifestations of mesoscale oceanic and atmospheric phenomena are presented.

1. Introduction

The two European Remote Sensing satellites ERS-1 and ERS-2 of the European Space Agency (ESA) were launched on July 17, 1991 and April 21, 1995, respectively. They both carry a C-band (5.3 GHz) synthetic aperture radar (SAR) operating at vertical polarization for transmission and reception. In the full SAR mode (geometric resolution: 25 m, swath width: 100 km) SAR data can be collected for a period of 10 minutes per orbit (period: about 100 minutes). As up to March 1997, more than one million SAR frames have been acquired by 25 receiving stations.

ERS SAR images acquired over the ocean often show sea surface manifestations of mesoscale oceanic as well as atmospheric phenomena. These phenomena become visible on radar images because they are associated with variations of the small-scale sea surface roughness caused by

(1) a varying wind field at the sea surface,

(2) a change of the temperature difference between air and water,

(3) a variable surface current,

(4) petroleum oil or natural films floating on the sea surface, and

(5) turbulence in the upper water layer.

The modulation of the Bragg waves caused by (1) render atmospheric phenomena visible on radar images of the sea surface, while the modulations caused by (3) - (4) render oceanic phenomena visible. The modulations caused by (2) and (5) can be of oceanic as well as atmospheric origin. A change of air-sea temperature difference may result from a change in the water temperature which occurs, e.g., in upwelling regions of the ocean where cold deep water rises to the surface or from a change in the air temperature associated with an atmospheric front. The air-sea temperature difference affects the stability of the air-sea interface. The more stable this interface (i.e., the warmer the air and/or the colder the water), the harder it is for the wind to generate small-scale surface waves. Similarly, turbulence in the upper water layer can be generated by oceanic as well as by atmospheric processes, e.g., by the propeller of a ship or by rain drops impinging on the sea surface.

2. Oceanic Phenomena

In this section we present two examples of sea surface manifestations of mesoscale oceanic phenomena visible on ERS SAR images caused by internal solitons and surface current fields. For a more detailed description of the observation of internal solitons in the Andaman Sea by ERS SAR the reader is referred to [1]. In other investigations ERS SAR images have been used to study the generation and propagation of internal waves in the Straits of Gibraltar and Messina [2],[3],[4].

2.1 Internal Solitary Waves in the Andaman Sea

The Andaman Sea of the Indian Ocean is known to be one of the sites in the world's ocean where extraordinarily large internal solitons are encountered [5]. The ERS receiving station in Singapore, which became operational in Sept. 1995, has captured a large number of ERS-1/2 SAR images showing sea surface manifestations of internal solitary waves in the Andaman Sea.

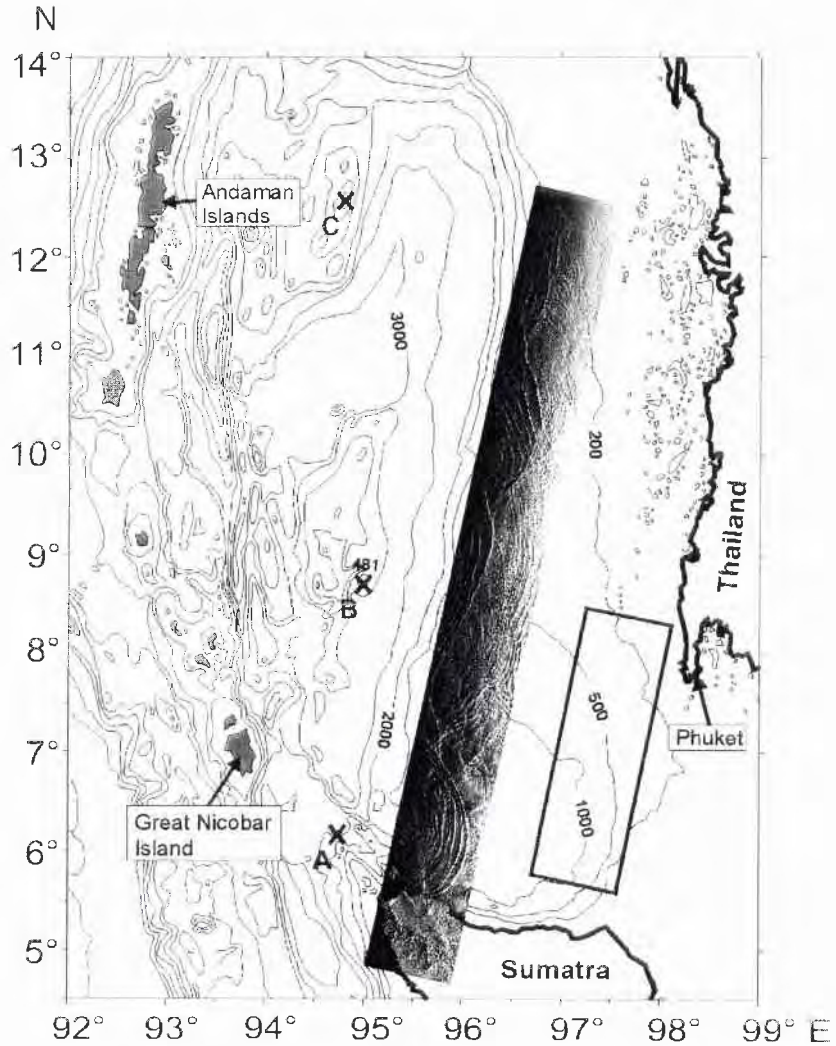

Fig. 1. A 900 km long and 100 km wide ERS-2 SAR strip inserted into a map of the Andaman Sea which was acquired on Feb. 11, 1997. Visible are sea surface manifestations of several internal solitary wave packets having their origin in three locations of shallow sea areas which are marked by A, B and C. Inserted is also the location of the ERS-2 SAR strip shown in Fig. 2 (rectangle).

Fig. 1 shows a SAR strip inserted into a map of the Andaman Sea which was acquired by the ERS-2 satellite during orbit 9477 on February 11, 1997, between 03:58 UTC and 04:00 UTC. It is a composite of 9 ERS-2 SAR frames (3357, 3375, 3393, 3411, 3429, 3447, 3465, 3483, and 3501). On this SAR strip sea surface manifestations of several internal solitary wave packets are visible. From the curved shape of these patterns one can estimate the position of their focal points and thus locate the generation areas of the internal solitons. At least

three generation areas, which are marked in Fig. 1 by A, B, and C, can be identified. They are located approximately at

(1) the shallow reefs off the northwest coast of Sumatra, around 6°10'N, 95°0'E (Indonesian name: Alur Pelayaran Bengala), where, near the 1000 m depth line, a coral reef rises up to a depth of 30 m below the sea surface (position A),

(2) the seamounts at 8°50'N, 94°56'E; 9°04'N, 94°34'E; and 8°42'N, 94°30'E, which rise up to depth of 481 m, 671 m, and 680 m below the sea surface, respectively, and which are located in an ambient sea area which has a depth of more than 2500 m (position B), and

(3) a submarine bank located at 12°34'N, 94°40'E which rises from a 1800 m to 2500 m deep ocean floor to a depth of 88 m below the sea surface (position C).

Fig. 2 shows another ERS-2 SAR strip on which sea surface manifestations of internal solitary wave packets can be delineated. It was acquired by ERS-2 during orbit 5426 on May 4, 1996, between 03:53 UTC and 03:54 UTC. It is a composite of the 5 SAR frames (3429, 3447, 3465, 3483 and 3501). Visible is in the central section of this image a long-crested ring-shaped roughness pattern which has a crest length of approximately 300 km. In the upper section a second wave pattern is visible which we interpret as sea surface manifestations of an internal solitary wave packet which was generated at the same location as the first one, but one tidal cycle earlier. In this second solitary wave packet the separation between the solitons is much smaller than in the first wave packet, which results from the interaction of the internal solitons with the shallow bottom topography in this area (close to the 200 m depth line). When dividing the distance between the leading solitons of these two internal solitary packets by the semi-diurnal tidal period (12 hours and 25 minutes) we obtain for the propagation velocity the value 1.43 m/s.

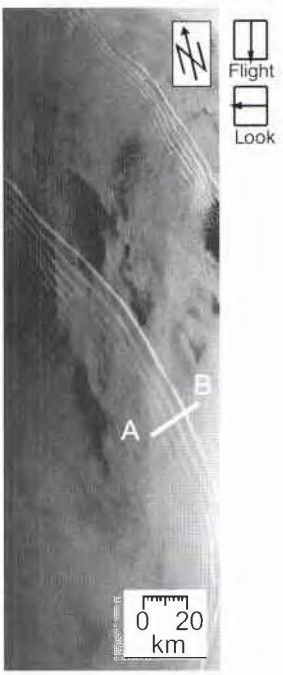

Fig. 2: ERS-2 SAR strip whose location is inserted in Fig. 1. It was acquired on May 4, 1996, and shows sea surface manifestations of two internal solitary wave packets in the Andaman Sea.

Fig. 3 shows a scan through the wave pattern along the line A-B marked in Fig. 1. Plotted is the variation of the normalized radar cross section (NRCS) in decibels (dB). Clearly visible is that the NRCS modulation pattern starts with an increase of the NRCS at the front (at the right-hand section in the plot) which indicates that the solitons in the wave packet are solitons of depression.

If an internal soliton propagates in stratified waters where the upper (lighter) layer is thinner than the lower

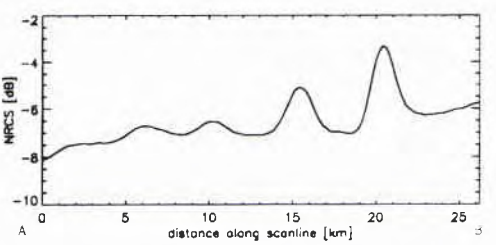

Fig. 3: Variations of the normalized radar cross section (NRCS) in dB along the scan line A-B shown in Fig 2.

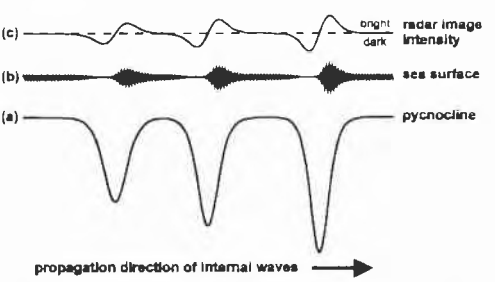

Fig. 4: Shape of the pycnocline (a), sea surface roughness pattern (b) and SAR image intensity (c) associated with an internal solitary wave packet consisting of solitons of depression of decreasing amplitude.

(heavier) one, then soliton theory predicts that the solitonshave to be solitons of depression. In this case the front of the internal soliton is associated with a region of convergent surface flow and the rear with a region of divergent surface flow. Thus the amplitudes of the short surface waves which are responsible for the radar backscattering (the Bragg waves) are increased in the front section and decreased in the rear section. The radar signature of an internal soliton of depression consists therefore of a narrow band of increased NRCS at the front followed by a band of decreased NRCS [6]. This is depicted schematically in Fig. 4.

2.2 Oceanic Current Patterns in the Caspian Sea

Mesoscale upper ocean circulation features often become visible on SAR images because they entrain surface slicks. In coastal areas biogenic slicks, which are produced by marine plants and animals, in particular by plankton, are frequently encountered. Fig. 5 shows an ERS-1 SAR image of the Northern Caspian Sea which was acquired on October 12, 1993, at 22:17 UTC (orbit 11724, frame 891). The imaged area is located slightly south of the delta of the river Volga (corner coordinates: 44.20°N, 48.58°E / 44.39°N, 49.80°E / 45.09°N, 48.29°E / 45.28°N, 49.53°E). The river Volga is known to discharge with its waters large amounts of nutrients, especially phosphorus, into the Northern Caspian Sea. These nutrients stimulate plankton growth and increase the biological productivity due to eutrophication. As a consequence, more surface active material is produced, which rises to the sea surface and covers there large sea areas. These films, which are usually monomolecular, follow the surface current field and thus render the upper ocean current features visible on radar images. Some very impressive features are visible on this ERS-1 SAR image shown in Fig. 5, e.g., the mushroom-shaped feature in the central left-hand section of the image.

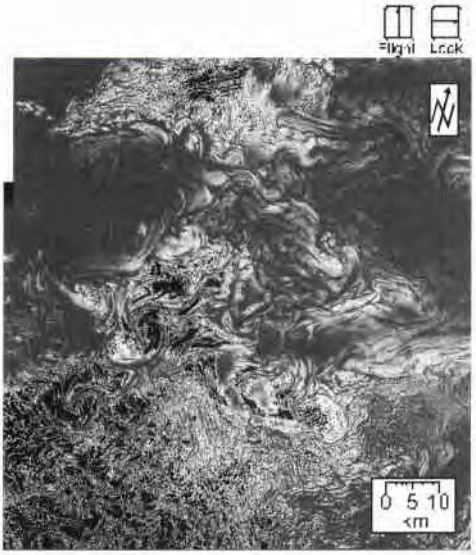

Fig. 5: ERS-1 SAR image of the Northern Caspian Sea acquired on Oct. 12, 1993, showing sea surface manifestations of current patterns which become visible by the entrainment of surface slicks.

3. Atmospheric Phenomena

In this section we present examples of sea surface manifestations of two mesoscale atmospheric phenomena: of (1) katabatic wind-fields and (2) atmospheric boundary layer rolls. For more details on sea surface manifestations of katabatic wind fields visible on ERS SAR images, the reader is referred to [7], and on atmospheric boundary layer rolls to [8],[9]. Other papers dealing with mesoscale atmospheric phenomena visible on ERS SAR images are [10],[11],[12].

3.1. Katabatic Wind Fields

Figures 6 shows a SAR image that was acquired on Feb. 20, 1995, at 21:12 UTC (orbit 18839, frame 765) by ERS-1 over the Mediterranean Sea off the western Calabrian coast (southern Italy). The SAR image shows, on the left-hand side, at the bottom the northeastern part of Sicily and on the right-hand side a part of the southern Italian province of Calabria. They are separated by the Strait of Messina. The most noticeable feature visible on this SAR image is, in the central right-hand section, a bright patch which is

Fig. 6: ERS-1 SAR image acquired on Feb. 20, 1995, over the Tyrrhenian Sea (Mediterranean) showing sea surface manifestations of a katabatic wind field (bright blob in the center)

located in the Tyrrhenian Sea adjacent to the valley of Gioia, Tauro. This valley opens at the western side to the Gulf of Gioia and is bordered at the eastern side by mountains of the Calabrian Apennine which have heights of up to 1800 m.

The bright patch is an area of increased sea surface roughness caused by katabatic winds that blow from the mountains through the valley onto the sea. Katabatic winds are caused by gravitational flow of cold air off high terrain. The cold air that is formed at night near the ground in sloping terrain flows downslope due to the differential cooling between the ground surface and the free atmosphere at the same height level some distance away. The direction of the cold air flow is controlled almost entirely by orographic features. Katabatic winds occur late in the evening and at night after the air in the mountains has cooled down. When the air flow hits the sea surface, it increases its roughness, which is detectable by radar. On the radar images, sea surface manifestations of katabatic wind fields appear as bright patches whose shapes sometimes resemble "tongues", "mushrooms" or broad "blobs" emanating from coastal valleys. The areal extent and shape of the sea surface roughness pattern depends, among others, on the orography of the valley, the synoptic weather situation, the thermal state of the air in the valley and the sea-land temperature difference.

Note that a part of the front of the roughness pattern is fringed. We have noticed this phenomenon also in many other SAR images showing sea surface manifestations of katabatic wind fields. The fringed structure is generated very likely by advancing lobes in the head of the gravity current, which are separated by deep clefts [13]. Another feature faintly visible in the upper left-hand section of this SAR image is the alignment of the sea surface manifestations of atmospheric convective cells in the NNW-SSE direction, i.e., in the direction into which the ambient wind is blowing. It is a well known fact that atmospheric convective cells tend to align in wind direction (see section 4).

4. SAR Image of Atmospheric Boundary Layer Rolls

Figure 7 shows an ERS-1 SAR image that was acquired over the Greenland Sea near Spitsbergen on March 24, 1993, at 19:54 UTC (orbit 8833, frames 1611 and 1629). The corner coordinates are 79.93° N, 0.88° E / 80.47° N, 5.07° E / 78.47° N, 6.88° E / 78.95° N, 10.55° E. In the upper part of the image, the fissured ice edge can be delineated. Areas covered with sea ice have a low NRCS and thus appear dark on the SAR image.

The area exhibiting a streaky pattern is open-water area. The streaky pattern is caused by variations of the short-scale sea surface roughness associated with atmospheric boundary layer rolls, which are frequently observed during cold-air outbreaks from land or ice over a warm sea surface. If the boundary-layer depth exceeds the height of the lifting condensation level, the upward branches of the roll circulations are marked by so-called cloud streets, frequently seen on satellite images acquired in the visible band. Observational data

Fig. 7: ERS-1 SAR image acquired on March 24, 1993, over the Greenland Sea near Spitsbergen showing sea surface manifestations of atmospheric boundary layer rolls

indicate that the rolls can persist for several hundred kilometers. The orientation of the roll axes to the mean boundary layer wind ranges from -20° to +30°. The aspect ratio, i.e., the ratio of the roll spacing (lateral wavelength) to the boundary layer height, typically ranges from 2 to 6, but values of up to 15 have also been observed [14]. Farther downwind, a transition from the roll regime to a three-dimensional cellular convective regime takes place in most cases.

Figure 8 shows the variation of the NRCS along the scan line A-B marked in Figure 7. From this scan we see that the wavelength of the roughness pattern varies between 2.7 km and 4.6 km and that the average wavelength is 3.5 km. If the wind direction at the sea surface is known, then the NRCS values can be converted into wind speed by using a wind scatterometer model. Here, we assume that the mean wind direction as well as the main component of the wind speed fluctuation associated with the boundary layer rolls are parallel to the direction of the streaks in the SAR image. For the conversion of NRCS values into sea surface wind speeds we

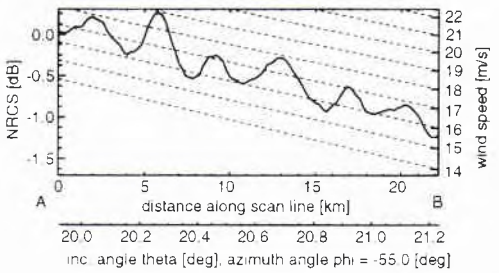

Fig. 8: Variation of the mean NRCS obtained from a scan from A to B in the area marked in Figure 7. The right-hand vertical axis shows the associated sea-surface wind speed calculated from the CMOD4 wind scatterometer model. The dashed lines are lines of constant wind speed.

use again the CMOD4 model [15]. Exactly speaking, this wind scatterometer model converts NRCS values into wind speeds at a reference height of 10 m above the sea surface for a neutrally stable air-sea interface. In the present case, the air-sea interface was highly unstable since at the ice edge the air-sea temperature difference was around -30 K and decreased to about -20 K at a distance 140 km downwind from the ice edge. Nevertheless, we use the CMOD4 model also in this case, because scatterometer measurements carried out from a sea-based platform in the North Sea have shown that the wind speed dependence of the NRCS does not change significantly when the air-sea interface changes from neutrally stable to unstable [16]. The wind speed calculated in this way is depicted on the right-hand vertical coordinate axis in Figure 8. Note that the curve in Figure 8 is tilted because, at constant wind speed, the NRCS increases with decreasing incidence angle. We see from Figure 8 that the average wind speed decreases slightly from 17 m/s at point A to 16 m/s at point B. The maximum (minimum) wind speed in direction of the streaks is approximately 19 m/s (15,5 m/s).

The atmospheric boundary layer rolls visible on the SAR image shown in Fig. 7 have been simulated by using a 3-D, time dependent, non-hydrostatic atmospheric model originally developed by Chlond [17] and later modified by Müller and Chlond [18]. In [9] it is shown that the sea surface wind speed derived from the ERS SAR image of Fig. 7 and plotted in Fig. 8 agrees quite well with wind speed calculated from the atmospheric model.

5. Conclusions

Investigations carried out with ERS SAR imagery acquired over the sea show that they can provide valuable information on mesoscale atmospheric phenomena in the marine boundary layer. If the wind direction is known, then the wind speed can be extracted from the SAR images by using a wind scatterometer model. The wind direction can sometimes be obtained from the SAR image itself, e.g., from the direction of the wind streaks or from the wind shadow behind isolated islands. SAR images of sea areas are also well suited for validating mesoscale atmospheric models whose model domain extends over the sea.

6. Acknowledgments

We thank ESA for supplying the ERS SAR images. This investigation was supported by the Deutsche Agentur für Raumfahrtangelegenheiten (Dara) under contract 50 EE 9413.

7. References

[1] W. Alpers, H. Wang-Chen, and Lim Hock, "Observation of internal waves in the Andaman Sea by ERS SAR", Proceedings of 3rd ERS Symposium, Florence, 1997.

[2] P. Brandt, W. Alpers, and J.O. Backhaus, "Study of the generation and propagation of internal waves in the Strait of Gibraltar using a numerical model and synthetic aperture radar images of the European ERS-1 satellite", J. Geophys. Res., 101, pp. 14,237-14,252, 1996.

[3] P. Brandt, A. Rubino, W. Alpers, and J.O. Backhaus, "Internal waves in the Strait of Messina studied by a numerical model and synthetic aperture radar images from the ERS-1 satellite", J. Phys. Oceanogr., in press.

[4] W. Alpers, P. Brandt, A. Rubino, and J.O. Backhaus, "Recent contributions of remote sensing to the study of internal waves in the Straits of Gibraltar and Messina", in: Dynamics of mediterranean straits and channels, F. Briand ed., CIESM Science Series no.2, Bulletin de l'Institut Océanographique, Monaco, no. spécial 17, pp. 21-40, 1996.

[5] A.R. Osborne and T.L. Burch, "Internal solitons in the Andaman Sea", Science, 208, pp. 451-460, 1980.

[6] W. Alpers, "Theory of radar imaging of internal waves", Nature, 314, No.6008, pp. 245-247, 1985.

[7] W. Alpers, U. Pahl, G. Gross, and D. Etling, "Study of katabatic wind fields by using ERS-1 synthetic aperture radar imagery of the ocean surface", Proceedings of the 1996 International Geoscience and Remote Sensing Symposium (IGARSS'96), Lincoln, Nebraska, USA, 27-31 May, Vol.III, pp. 1478-1480, 1996.

[8] W. Alpers and B. Bruemmer, "Atmospheric boundary layer rolls observad by the synthetic aperture radar aboard the ERS-1 satellite", J. Geophys. Res., 99, pp. 12613-12621, 1994.

[9] G. Mueller, B. Bruemmer and W. Alpers, "Roll convection within an Arctic cold-air outbreak: Three- dimensional numerical simulation, in situ aircraft measurements and spaceborne SAR imagery", submitted to Monthly Weather Review, April 1997.

[10] T.W. Vachon, O.M. Johannessen, and J.A. Johannessen, "An ERS-1 synthetic aperture radar image of atmospheric lee waves", J. Geophys. Res., 99, pp. 22483-22490, 1994.

[11] T.D. Sikora, G.S. Young, R.C. Beal, and J.B. Edson, "Use of spaceborne synthetic aperture radar imagery of the sea surface in detecting the presence and structure of the convective marine atmospheric boundary layer", Monthly Weather Review, 123, pp. 3623-3632, 1995.

[12] W. Alpers and G. Stilke, "Observation of a nonlinear wave disturbance in the marine atmosphere by the synthetic aperture radar aboard the ERS-1 satellite", J. Geophys. Res., 101, pp. 6513-6525, 1996.

[13] J.E. Simpson, Sea breeze and local winds, Cambridge Univ. Press, 234 pp., 1994.

[14] Y. Miura, "Aspects ratios of longitudinal rolls and convection cells observed during cold air outbreaks", J. Atmos. Sci., 43, pp. 26-39, 1986.

[15] A. Stoffelen and D.L.T. Anderson, "ERS-1 scatterometer data characteristics and wind retrieval skill", Proceedings First ERS-1 Symposium, Cannes, March 1993, ESA SP-359, pp. 41-47, 1993.

[16] W.C. Keller, V. Wismann, and W. Alpers, "Tower-based measurements of the ocean C-band radar backscattering cross section", J. Geophys. Res., 94, pp. 924-930, 1989.

[17] A. Chlond, "Three-dimensional simulation of cloud street development during a cold air outbreak", Boundary-Layer Meteorol., 58, pp. 495-527, 1992.

[18] G. Müller and A. Chlond, "Three-dimensional numerical study of cell broadening during cold-air outbreaks", Boundary-Layer Meteorol., 81, pp. 298-323, 1996

The use of radar for bathymetry assesment

J. Aardoom and H. Greidanus

TNO Physics and Electronics Laboratory
P.O. Box 96864, 2509 JG The Hague, The Netherlands
Fax +31 70 328 0961 Email: aardoom@fel.tno.nl

Abstract

The bottom topography in shallow seas can be observed by air- and spaceborne imaging radar. Bathymetric information derived from radar data is limited in accuracy, but radar has a good spatial coverage. The accuracy can be increased by assimilating the radar imagery into existing or in-situ gathered bathymetric data. The paper reviews the concepts of bathymetry assessment by radar, the radar imaging mechanism, and the possibilities and limitations of the use of radar data in rapid assessment.

1. Introduction

Radar radiation does not penetrate into the sea; on the contrary, all radiation is reflected off the surface. Therefore, only information about the sea *surface* can be extracted from radar images. Nevertheless, bathymetric features are sometimes expressed in radar images, as was first noticed in airborne radar images of the North Sea in 1969 [6,7]. At the time, the effect was quite unexpected. Since then, the effect has been routinely observed by numerous space and airborne systems, including the SEASAT (L-band, 1978) and ERS-1 (C-band, 1991-1996) radar satellites.

Due to developments in operational earth observation, radar imagery is becoming more easily available these days, the instrument of choice being the Synthetic Aperture Radar (SAR). Therefore, it would seem justified to investigate the possibilities for the use of radar for (rapid) bathymetry assessment. When doing so, it turns out that, although radar certainly has disadvantages with respect to the usual bathymetry mapping techniques, it in fact also has some very special advantages. These are found primarily in synoptic overview, speed, cost reduction, and the ability to survey from a safe distance. Main disadvantage is the fact that the radar produces only partial information, which has to be supplemented by data from other sources.

Figure 1 *Radar image from the ERS-1 satellite showing the North Sea and a part of the southwestern Netherlands coast. Most of the structures in the open sea are bottom topography.*

This paper aims at discussing some aspects of the use of radar images for bathymetry assessment. The paper first describes, in section 2, the concepts of bathymetry assessment, including the physical processes that lead to the imaging of bathymetric features by radar, the modeling techniques for simulating these radar images, and the use of inversion and assimilation schemes to extract quantitative bathymetric information from radar data. More detailed information on the various elements that play a role is given in section 3, including a review of the instrumentation. Examples of implementation and results are presented in section 4. The paper concludes, in section 5, with a brief summary of the current status of the research.

2. Concepts

2.1. Forward model

The reason that bathymetry can be observed by radar is because the bathymetry influences the sea surface. The amount of backscatter reflected from the sea surface (and thereby its radar image brightness) is proportional to its roughness: the rougher a patch of surface, the brighter it will be in a radar image. It is indeed the changes in sea surface roughness, caused by the sea bottom topography, that result in bathymetric signatures becoming visible in radar images. The way this happens is through a three-step process. First, it is necessary that a water flow is present, such as a tidal current. This current will be modulated by the bathymetry, and the resulting variations in current speed will also be present at the surface. The second step of the process is that these surface current variations influence the surface roughness. The third step is the radar imaging of the surface: as outlined above, the smoother areas will become darker in the image, and the rougher areas brighter.

This whole process can presently be quantitatively modeled, at least with certain approximations. Based on the physics of the problem, algorithms are available that can produce a simulated radar image, given a bathymetry. The radar signatures induced by the bathymetry are strongly dependent on the ambient hydro-meteorological conditions. Shape, location and amount of radar contrast associated with bathymetric features depend, e.g., on current and wind speed and direction. Furthermore, the system parameters of the radar are important, including viewing geometry.

2.2. Inversion

Although it is possible to compute the radar image given the bathymetry, this computation cannot, in fact, be directly inverted. This is due to the complexity of the relation between the magnitude of the radar contrast and the water depth. From a radar image *alone* it is, at least for now, impossible to extract a bathymetry chart. Radar, therefore, will probably never completely replace *in situ* depth measurements by conventional techniques (including sonar). Nevertheless, radar data can be utilized in several ways for bathymetry purposes. Distinction can be made between use in a qualitative and quantitative sense. In the first way, the radar images are interpreted for the presence, shape and location of bathymetric features. This interpretation has to be performed on the basis of knowledge of the forward modeling process, and the actual hydrometeo conditions. For the purpose of this paper, the result of this kind of analysis is denoted as a reconnaissance survey. As was described above, the relation between the contrasts in the radar image and the bathymetric features such as ridges or slopes is not fixed, but depends on parameters such as current and wind speed and direction. On the basis of modeling, the radar image can be analyzed to yield a more precise geometric location of the bathymetric features.

For quantitative use, it is necessary to employ an inversion scheme (figure 2). The inversion process can be summarized as an iterative adjustment of the bathymetry to minimize the difference between simulated and measured radar images. From an initial depth chart, a simulated radar image is computed using the forward model and the actual hydrometeo conditions. The differences between the simulated and observed image are used to adjust the depth chart. The procedure is repeated until the simulated results are consistent with the measured image.

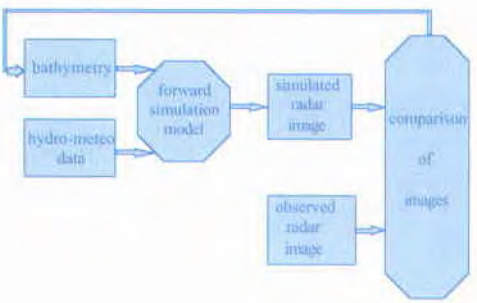

Figure 2 *Inversion scheme. From left to right: data input, forward simulation, and comparison of simulated and observed images. The process is repeated until the difference between the images is minimized.*

In such an inversion process, the radar data can be combined with bathymetric data from other sources, and the inversion process can thereby be extended to an assimilation scheme [4]. Assimilation of radar data for bathymetry assessment can involve the fusion of data from a range of sensors or data bases. The goal is to optimize the result, in this case bathymetric accuracy, by combining sensor data with different performance aspects. These may include echo soundings, ADCP-measured velocity profiles, existing bathymetric information or depth charts, and space and airborne SAR data. The main advantages for these types of data are: for the sounding and ADCP data their accuracy, for the bathymetry charts their instantaneously availability, and for the radar data their all-weather acquisition capability, extended spatial coverage and possibility for continuous update (for satellite data). Disadvantages are: the sparseness and local confinement of the sounding and ADCP data,

possible obsoleteness of the depth chart (depending on the time scales associated with the dynamics of the sea bottom), and the indirect and partial nature of the information in the radar images, plus the fixed orbit of the spaceborne platforms. The use of an assimilation scheme with input from different sensors can lead to more robust results, to more accurate results, and also to cost reduction by lowering the relative contribution of the more expensive types of data.

3. Components

3.1. Instruments

There are various types of radar that can be used to image sea bottom topography. From an aircraft, a "SLAR" (Sideways Looking Airborne Radar) may be utilized. SLAR, however, is becoming replaced by "SAR" (Synthetic Aperture Radar; also for airborne use). The data recorded by a SAR are not in the form of an image right away, but need numerical processing ("SAR processing") first. The advantage of SAR is that the image produced has a constant spatial resolution, whereas a SLAR (or any other type of conventional radar) has a resolution that decreases linearly with distance. For this reason, a SAR can also be operated from a satellite in earth orbit. Indeed, next to airborne SAR, satellite SAR promises to be a suitable instrument for bathymetry applications.

There are two main differences between the use of airborne and of satellite SAR systems. The first difference lies in the scales of the image. A satellite system will in general image a larger area (typically 100 x 100 km), but with less detail (typically 30 x 30 m); an airborne system will image a smaller area (of the order of 10 x 10 km), but with more detail (typically 3 x 3 m resolution). The second difference lies in the scheduling. A satellite will have a fixed orbit, giving it a fixed repeat period for imaging a particular area on the ground. An airborne system can be deployed much more flexibly. Given that the successful imaging of bathymetry depends rather strongly on hydrometeo conditions, and that a satellite needs to be scheduled in advance, satellite imagery typically needs to be collected during a period of time, waiting for a coincidence of favorable hydrometeo conditions with the satellite overpass. An airborne sensor, on the other hand, is typically kept on stand by and is flown once, as soon as the favorable conditions occur. Furthermore, it can be noted that, in general, airborne data is more expensive per square km than satellite data.

Presently, there are a number of satellite SARs in operation. These include ESA's ERS-2 (successor to ERS-1), Japan's JERS-1 and the Canadian RADARSAT. In the past, ERS-1 has produced useful data. Concerning airborne SAR, several systems are nowadays available for (semi-)operational use throughout the world. Many offer a choice of radar frequency and/or polarization, some are even multi-frequency or multi-polarization.

3.2. Details of the forward model

The first of the three steps of the forward modeling is the calculation of surface currents. Flow models have the bathymetry as a boundary condition at the bottom, and are typically driven by much larger-scale flow models that provide, e.g., a tidal and wind-driven current averaged over the entire area of interest. When the bottom topography is one dimensional, as in the case of parallel long-crested sand waves, a simple model suffices. Such parallel sand waves are found, for example, in front of the Dutch coast. In such a simple model the component of the surface current perpendicular to the sand wave crests can be approximated by simple flux conservation law, while the component parallel to the crests is constant. When the sea bottom topography is more complicated, however, more sophisticated two dimensional flow models are needed, or, in order to relate the surface current to the depth-averaged current, even three dimensional ones. The comparison of the simulated results with radar images requires flow data on a extremely fine grid (ERS-1 image comparison leads to 12.5 m) and the flow model must pass the assimilation loop not once but a (large) number of times. These requirements constrain the flow model complexity since there is only a limited computer capacity available.

The second step of the modeling describes the influence of the current, and in particular the current variations associated with the bathymetry, on the surface roughness. This description is in terms of the wave directional spectrum. The spectrum needs to be described over a very large range of wavelengths, from tens or hundreds of meters down to centimeters. Among the short (centimetric) waves are the so-called "Bragg" waves, which are in first instance responsible for the radar backscatter; these are in turn modulated by the longer waves upon which they ride. The modeling is of a perturbation/relaxation type. Starting with the equilibrium wave spectrum, the local changes in wavelength and amplitude of each wave in the spectrum due to the variations in current are computed. Again, this is done on the basis of conservation laws: conservation of apparent frequency and conservation of wave action. The conservation of apparent frequency yields the wavelengths of the waves as they are subject to the current variations while traveling on the water surface; the

conservation of action yields the wave amplitudes. This leads to a wave spectrum away from equilibrium. The evolution of the wave spectrum in time is then computed as a relaxation back toward its equilibrium. In this way, a wave spectrum is computed on each location of the surface [1,3,8,9,11,12].

The third step of the modeling is the computation of the radar backscattering from the local wave spectrum. The simplest model for this is the Bragg scattering model. In this model, the radar backscattering is simply proportional to the spectral value at the Bragg wavelength in the radar look direction. More sophisticated models average the local Bragg scattering contributions over all tilts that occur due to the long waves; as a further refinement they may also include contributions of specular reflection, which occurs when the water surface is locally tilted so much as to be aligned perpendicular to the radar. These types of models are called two-scale and composite models, respectively [10]. A different approach is also possible, computing the backscatter from the basic Maxwell equations of electromagnetics, resulting in so-called Kirchhoff-type models [*e.g.*, 5]; in order to get practical results, however, rather strong approximations need to be applied.

The various backscatter models have their advantages and disadvantages. The Bragg model is simplest and fastest, and often quite accurate. The two-scale and composite models in addition give polarization dependence. The Kirchhoff-type models are more accurate for steep incidence angles, but not very simple to compute.

3.3. Assimilation/inversion scheme

An assimilation scheme as outlined in section 2.2 can be implemented on the basis of a cost function that has to be minimized. The cost function quantifies the difference between simulated and observed image. Such a cost function can, *e.g.*, be defined as the sum of the squared differences between model predictions and measurements at all positions. Different weights may be assigned to all of the input data, to reflect their reliability [2,4].

4. Applications and results

4.1. Reconnaissance survey

In qualitative use, the foremost aspect of a radar is the synoptic overview it provides of a large area. This can be used to asses information about previously unknown areas, or to quickly detect changes in the bathymetry when such an overview is compared with a previous image or map. A radar image can thus be used for a preliminary survey leading to information about the occurrence of the type of bathymetric features as sand banks or shoals, sand waves, and channels.

Areas of particular interest can be identified with such a reconnaissance survey. If, consequently, a comprehensive survey is favored, this information can be used to optimize the gathering of *in situ* data. In this way, the *in situ* measurement capacity can be deployed in an economical way. Such an approach can lead to considerable cost reduction, possibly as high as a factor of ten [4]. In addition, radar bathymetry assessment can lead to a reduction in measuring time. In military applications sometimes the cost factor is less important than the ability to deliver results fast. In a reconnaissance phase, radar images are a valuable information source that can be used for rapid assessment; in this context, one can also think of using (recent) spaceborne data that are available from archives.

4.2. Quantitative survey

For a quantitative analysis, the inversion/assimilation process needs an initial depth map (section 2.2). For this, an existing bathymetric chart may be used, such as a digitized Admiralty Chart. The assimilation of an old Admiralty Chart with a recent radar image will lead to an updated bathymetric chart, with an accuracy depending on the deviations between the two and the quality of the radar image.

It is also possible to extract a map from a radar image with the help of a number of bathymetric cross-cuts through the image. A limited number of ship soundings are needed to determine large scale depth variations and to adjust model parameters. The cross-cuts help to locally "calibrate" the radar contrasts to the bathymetry. In this way, radar data can be applied to substantially reduce the *in situ* measurement effort by ships. For example, while a ship would conventionally need to survey a block by covering it with cross-cuts 50 meter apart, the same result may be obtained by having the ship measure cross-cuts 500 meter apart, and combining these measurements with a radar image. Inversion of the radar image using the 500 m-separated cross-cuts can yield a bathymetric map with similar depth accuracy. Accuracies achieved in this way depend on the complexity of the area, on the spacing of the in-situ cross-cuts, and, of course, on the quality of the input data. With a 500 m spacing, accuracies of better than 30 cm have been claimed, going down below 10 cm with closer spacing [4]. Experiments show that a bathymetry with curved or forked channels results in lower accuracies than a smooth sea floor or straight channels. Cost reductions that can be attained depend strongly on the situation, but a factor of three has been reported in a specific case [4].

4.3. Military context

In case of a rising conflict, radar observations can be used in several stages. First, they can be used in a reconnaissance survey. The achieved accuracy will not match that of the conventional method of (multi beam) echo sounding, but it is faster and there is no need for a vessel on location. A satellite can be used, or, when higher spatial resolution is needed, also an airborne radar: with the latter it is in principle possible to observe from a considerable distance by making use of a low grazing angle, enabling reconnaissance without violating a country's territory. When there is a need for more accurate and quantitative bathymetric information, the SAR images can be assimilated in existing depth charts. Ultimately, an even higher accuracy can be obtained by assimilation of *in situ* gathered data and radar data into a comprehensive survey. These methods make for a gradual refinement of the bathymetry assessment.

4.4. Limitations

Limitations on the use of radar images are imposed by water depth, hydrometeorological conditions, image positioning, and the radar image noise.

Concerning depth limitations, the technique only works in relatively shallow seas; typically, features of a few meters height are detectable down to a few tens of meters depth. Given optimal conditions, such features would still be detectable at considerably greater depth, while larger features or a faster current would in principle still further extend that depth range.

The hydrometeorological conditions impose rather strict limitations on the imaging of the bathymetry.

When the wind speed is too low, the sea surface will be too smooth to produce radar backscatter, and all radar measurements are precluded. When, on the other hand, the wind speed is too high, the bathymetry contrasts are drowned in the background of waves, white caps and radar image noise. In practice, wind speeds between 2 and 8 m/s seem to be optimal, though this also depends on the radar frequency used. The second requirement is the existence of an overall current through the area of interest. No fixed minimum for the current speed can be specified; the higher the current, the easier the bathymetry can be measured (i.e., the smaller the features and the larger the depth range); typical figures are a few tens of cm/s. In practice, a current is often present in shallow waters in the form of a tidal current. In contrast to the wind, the time of favorable current can be known beforehand on the basis of the tidal cycle; this limitation need therefore not severely limit practical applicability. Apart from the aspects of wind and current, the bathymetry has to compete with a number of other atmospheric and maritime features that can produce contrasts in the radar image. These include, *e.g.*, ocean waves, slicks, ships and their wakes, fronts, and internal waves. (Some of these features can be found in figure 1.) If any of these features happen to be present, it is possible that they (locally) preclude the use of the radar data for bathymetry purposes; this may also be expected in case a strong thermocline is present.

For the assimilation of satellite or airborne radar imagery with in-situ data, accurate geopositioning of the radar data is a necessity. The positional accuracy of space-measured SAR imagery is of the order some 100 m. For airborne data this can be of the same order, based on GPS (higher for differential or military GPS). This is not accurate enough for assimilation, and therefore ground control points need to be used. The number of ground control points required depends on the quality of the SAR image.

The fourth limitation is imposed by the, unavoidably present, radar image noise (or "speckle"). The occurrence of the speckle precludes detection of the weaker bathymetric contrasts, and is the main cause for the operational limitations on depth range and hydrometeo conditions. The speckle noise level can be reduced, but generally at the expense of spatial resolution.

Some of these limitations can be partly overcome by performing multi-temporal analysis [2]. By making use of more than one radar image of the same scene, the chance on optimal hydro-meteorological conditions is increased, true bathymetric signatures are more easily distinguished from other maritime features, and the impact of noise is diminished.

The rather indirect way in which the bathymetric features are expressed at the sea surface, combined with the speckle noise and the limited spatial resolution, gives rise to the fact that small objects on the sea bottom are not readily imaged. It is not expected that objects like containers or small ship wrecks will be reliably imaged by radar. If one needs to find objects like these, conventional surveys will still be needed. However, radar images are able to indicate those areas that are dynamic, where sunken objects can be expected to become covered or re-exposed.

5. Present research

The research efforts of the past twenty years have come far in understanding and describing the radar bathymetry imaging mechanism, and in delineating the boundaries for practical applications. On the one hand, it is on the basis of this work that the use of radar for bathymetry purposes can now begin to enter the operational domain. On the other hand, certainly a number of problems still perseveres. Most of the physical models used are merely approximations, at

times close to their limits of validity. In general, the modeling is characterized by the use of *ad hoc* parameters for black box descriptions of low-level physical processes. (This approach is of course in itself not at all unsuitable for practical purposes.) The most outstanding questions that are still open at the moment, and have a consequence for practical use, pertain to the shape of the equilibrium gravity-capillary directional wave spectrum, and to the rate by which deviations from equilibrium in this wave spectrum decay. Furthermore, several processes that are probably under most circumstances of minor consequence are not taken into account in the modeling so far, such as the role of wave breaking. Also, no proper model has yet been implemented to describe the radar imaging under very low grazing angles (< 80 degrees), precluding the quantitative use of surface-based radar data for bathymetry as yet.

Extensions and improvements of the models and their numerical implementations are subjects of current research. Other current developments are aimed at recognition and exclusion of non-bathymetric features from the SAR images, at improved techniques for the inversion and assimilation of the radar data, and at obtaining better quality radar images. The latter aspect concerns improvement of the image quality by applying dedicated SAR processing for bathymetry purposes, as opposed to the usual standardized processing (the same for all scenes, either over land or over water) [13]. As these developments will be finding their way into the operational process, the role of radar in bathymetry applications can be expected to be constantly further consolidated.

References

[1] Alpers, W., and Hennings, I., 1984, *A theory of the imaging mechanism of underwater bottom topography by real and synthetic aperture radar*, J. Geophys. Res. 89 (C6), 10529-10546.

[2] Calkoen, C.J., Wensink, G.J., Vogelzang, J., Heinen, P.F., 1995, *Efficiency Improvement of Bathymetric surveys with ERS-1*, BCRS report 95-01

[3] Hennings, I, 1990, *Radar imaging of submarine sandwaves in tidal channels*, J. Geophys. Res. 95 (C6), 9713-9721.

[4] Hesselmans, G.H.F.M., Wensink, G.J., Calkoen, C.J., and Sidhu, H., 1993, *Application of ERS-1 SAR data to support the routing of offshore pipelines*, BCRS-report 93-34.

[5] Holliday, D., St-Cyr, G., and Woods, N.E., 1986, *A radar ocean imaging model for small to moderate incidence angles*, Int. J. Remote Sens. 7, 1809-1834.

[6] de Loor, G.P., and Brunsveld van Hulten, H.W., 1978, *Microwave measurements over the North Sea*, Boundary Layer Meteor. 13, 119-131.

[7] de Loor, G.P., 1981, *The observation of tidal patterns, currents and bathymetry with SLAR imagery over the sea*, I.E.E.E. J. Oceanic Eng. OE6, 124-129.

[8] Romeiser, R., and Alpers, W., 1996, *An improved composite surface model for the radar backscattering cross section of the ocean surface. 2. Model response to surface roughness variations and the radar imaging of underwater bottom topography*, J. Geophys. Res. (submitted).

[9] Shuchman, R.A., Lyzenga, D.R., and Meadows, G.A., 1985, *Synthetic aperture radar imaging of ocean-bottom topography via tidal-current interactions: Theory and observations*, Int. J. Remote Sens. 6, 1179-1200.

[10] Valenzuela, G.R., 1978, *Theories for the interaction of electromagnetic and ocean waves - a review*, Boundary Layer Meteor. 13, 61-85.

[11] Vogelzang, J, 1989, *The mapping of bottom topography with imaging radar. A comparison of the hydrodynamic modulations in some existing models*, Int. J. Remote Sens. 10, 1503-1518.

[12] Vogelzang, J., Wensink, G.J., Calkoen, C.J., and van der Kooij, M.W.A., 1996, *Mapping submarine sandwaves with multi-band imaging radar. 2. Experimental results and model comparison*, J. Geophys. Res., submitted.

[13] Greidanus, H., de Vries, F.P.Ph, Aardoom, J., 1997, *Speckle reduction in low-contrast areas by dedicated SAR processing*, in Proc. 3rd ERS Symposium, March 1997, Florence, (submitted).

Estimates of Seabed Topography from Synthetic Aperture Radar Images

G. A. Keramidas, L. J. Du, T. Ainsworth, R. Jansen

Code 7260
Remote Sensing Division
Naval Research Laboratory
Washington, DC 20375
e-mail: keram@ccf.nrl.navy.mil

Abstract

While there is clear evidence that characteristics of the seabed topography can be seen as surface expressions in Synthetic Aperture Radar (SAR) images of coastal, shallow water regions, it remains to be shown that these surface expressions can be characterized rigorously with algorithms. This study focuses on three elements of the bathymetry effects observed in SAR images and uses first principles to develop an algorithm for estimating bathymetry from SAR image data. The first part of the study explores the conditions under which there is a hydrodynamic coupling of seabed features through the water column to the ocean surface. The second part uses an ocean model to simulate bathymetry effects under various wave conditions. The third part explore the possibility of using wave fields and wave spectra as a means of deriving seabed topography from shoaling effects on wave fields.

1. Introduction

The objective in deriving estimates of seabed topography is to enable the use of SAR image data to aid the characterization of probable obstacles and hazards to amphibious landing forces in coastal, shallow water regions.

The present study covers four approaches to be used in investigating the mechanisms by which seabed topography is expressed as modulations of sea surface roughness, namely:

1. Using a simulation model determine the limitations of SAR to image near-shore waves and submerged obstacles, as a function of the SAR operating parameters and the sensor viewing geometry.
2. Study the sensitivity of the surface roughness distribution to variations in ambient wave conditions and bottom topography using a non-linear wave motion model. This model will be used to calculate the surface height spectrum responsible for the modulation in SAR-derived surface signatures over near-shore obstacles and in shoaling waters, as well as determine the sensitivity of small-scale height distributions to bottom conditions.
3. Simulated SAR images of coastal wave refraction patterns will be used to assess the ability of SAR in deriving bottom topography conditions.
4. Using simulated SAR images, an algorithm will be developed to provide estimates of variable bottom topography.

2. Parametric Study

The conditions under which there is hydrodynamic coupling between seabed features and the modulated ocean surface can be derived through a parametric study. The variation of certain physical parameters is used to determine limits on wave/bottom interactions, namely: a) wave refraction, diffraction, reflection and evolution due to depth changes and b) environmental interactions and variability (wave-wave interactions). In addition the variation of sensor (SAR) parameters will be included to provide a realistic assessment.

To carry out the parametric study an extensive set of simulations was performed for two types of bathymetry and a range of values for the water depth, wave height, wave-length, ambient wind speed, and SAR frequency, polarization and look direction.

The first type of bathymetry used in the parametric study was a half sphere placed at the bottom of otherwise constant water depth. The geometry is shown in Figure 1.

A wave propagating over this type of bathymetry will be refracted and diffracted due to the presence of the half sphere. The choice of this type of bathymetry was based on the fact that theory and analytical results fully describe wave refraction/diffraction due to a spherical obstacle. The wave refraction/diffraction can be computed using an available numerical model.
An example of a wave of constant wavelength, amplitude and direction, refracted by the half sphere is shown in Figure 2, for two depths of 5 and 15 meters. The complete simulation geometry used for the simulations in the present study, including sensor geometry, is shown in Figure 3.

The number and type of simulations performed for the parametric study were obtained for the following range of parameters:

1. Two wavelengths 50 m (WL050) and 100 m (WL100).
2. Two wave amplitudes 2 m (WA02) and 4 m (WA04).
3. Five water depths 5 m (D05), 10 m (D10), 15 m (D15), 19 m (D19), and 20 m (D20).
4. Four wind speeds at 2 m/s (W02), 5 m/s (W05), 10 m/s (W10), and 15 m/s (W15).
5. Three radar frequencies at vertical polarization (CVV, LVV and XVV) and constant look direction (LD90) and incidence angle (IA45).

A representative set of results from the parametric study is included in order to demonstrate the dependence and coupling of hydrodynamic parameters to bottom topography. The included cases are shown in Figures 5 through 8, with their parameters listed in Table 1.

The results presented are variations of Signal to Noise Ratio (SNR) with respect to depth at CVV SAR frequency and polarization, and for a range of wind speeds. Comparing the parametric study results it is clear that the wind speed is a major factor in imaging any surface effects due to variations in depth. For all cases wind speeds greater than 5 m/s will have a strong effect on observing any significant wave refraction due to changes in bottom topography.

In addition to the analytical type of bottom topography, parametric study results were obtained for three coastal bathymetry data sets. The bathymetry used is shown in Figures 9-11. In each of these data sets the water depth ranged from very shallow (1 m) to depths over 100 m and the data range from simple sloping bottom (Case 1) to complicated shallow topography (Case 3).

To demonstrate the coupling of a propagating wave (swell) to bottom topography we used a non-linear wave propagation model to simulate the refraction and diffraction of a swell with mean height of 1 m. The results are shown in Figure 12, where the wave refraction/diffraction and the non-linear effects due to the shallow bathymetry can be clearly seen.

The hydrodynamic results shown above were used as input to the SAR model to obtain simulated images for two cases. For each of the cases the wind speed used was 6 m/s, the wind direction 45° and the frequency/polarization used was XVV. The only parameter that is different between the two cases is the sensor look direction, in Figure 13 the look direction is 0° or along the wave crests and in Figure 14 is 90°, which is perpendicular to the wave crests.

The above two figures clearly demonstrated the importance of the sensor look direction in the imaging of waves. One sensor parameter that did not changed in the parametric study, but it is a critical sensor parameter, is the sensor resolution. SAR sensors with low resolution, such as the ERS-1/2, may not be suitable for bathymetry effects imaging in coastal waters.

In assessing the results of the parametric study we concluded that bottom topography affects the propagation of free surface waves under an optimum range of conditions. The ability to observe these effects depends on three major parameters, namely: water depth, wave height and wind speed, and limitations are imposed by the following relationships:

1. Wavelength < Effective water depth,
2. Wave height (mean swell amplitude) < Mean wind wave height,
3. Bottom slope - Wavelength relationship,
4. Non-linear effects due to wave breaking and complex (sharp) depth changes.

In addition limitations imposed by sensor characteristics can further affect the ability to observe and image wave refraction and diffraction. Assuming that optimum conditions exist, bathymetry estimates can be obtained by measuring changes in wavelength and wave direction from the wave spectrum peak values. This is demonstrated in Figure 15 for one of the cases of the parametric study and in Figure 16 for one of the coastal bathymetry cases. In Figure 15 the smearing of the power density spectrum demonstrates the effect of the wind waves on the wave refraction/diffraction. As a result the wave spectrum peak values are not clearly detected and wavelength estimates are not easily obtained. Similar results are obtained in the case of real bathymetry, Figure 16. Although from the obtained results it easy to distinguish between the wave propagation direction and the wind propagation direction, wave spectrum peak values are not clearly detected.

3. Algorithm Development

Estimates of coastal bathymetry can be derived from SAR image data as long as optimum conditions exist, which in return allow for estimates of wavelength changes through the wave spectrum. The wavelength and the refraction coefficient are two of the main parameters that are needed to estimate water depth changes. The basic equations required for the development of the bathymetry estimation algorithm are the equations that describe wave refraction and diffraction.

For a monochromatic wave propagating along a sloping bottom the basic equations for deep and shallow water are given in Figure 17 and the resulting Dispersion relationship in Figure 18.

The function $f(k,d)$ relates the wave height between deep and shallow water for wave diffraction/refraction. These relationships together with the definition of the refraction coefficient are shown in Figure 19.

The described equations form the basis for developing the bathymetry estimation algorithm. Examples of wavelength and refraction coefficient estimates using wave spectra are given in Figures 20 and 21 for an incoming wave propagating at 0^0 and 30^0 respectively. These examples clearly demonstrated the advantage of using the wave spectrum to estimate the refraction coefficient and wavelength of the incoming waves.

The basic ingredients in developing the bathymetry algorithm include the dispersion relationship and the wave spectra derived parameters (wavelength and direction and refraction coefficient). In addition we use a rectangular mesh over the SAR image data and an iterative scheme over this mesh to derive the wavelength and wave umber at each mesh point and the refraction coefficient at each point. The values of these parameters are then used to calculate the effective water depth through the dispersion relationship. The iterative scheme requires the selection of the mesh size and resolution and an optimum window size to correctly resolve and derive the required wavelength at each point. The algorithm can be further enhanced by special processing of the SAR image data, such as speckle reduction, before the iterative scheme is applied.

The development of any computational tool requires that some form of testing should be performed in order to assess its validity and usefulness. Testing can be performed on either simulated data or available real data. In the present study the bathymetry estimation algorithm will be applied to simulated data to evaluate the overall algorithm performance. SAR image data that are suitable for applying the bathymetry algorithm were not available at the present time. As the first step of the evaluation process two sets of simulated data were used to assess the validity of the algorithm. A third set is also included as an additional example.

4. Derived Bathymetry Results

The first set is for the simple case of a wave with constant wavelength, amplitude and direction, propagating over bathymetry, with the geometry shown in Figure 21. The second set is for a wave of constant wavelength, amplitude and direction, shown in Figures 20 and 21, propagating over the complex geometry shown on the same figures. The last set is for the bathymetry shown in Figure 11 and for a wave of constant wavelength, amplitude and direction.

In deriving depth estimates for the three cases presented here two basic criteria were used for the optimum window size: 1) its size should extend at least one and one half wavelengths, and 2) enough points are used so that the wave spectrum provides good estimates for the wavelength.

The first case was considered for its simplicity in order to test the develop algorithm. As one can see from Figure 23 the estimation of depth from the simulated results is a close match of the actual depth of Figure 22. The obtained results in Figure 23 do not extend the full length of the domain. The zero depth in the beginning and end of the estimated depth corresponds to the half size of the window used to obtain the wave spectrum. The same is true for all results presented here. All figures that show depth estimates from simulated results have a box of zero depth with the width of the box equal to the half size of the wave spectra window.

Results for the second case are shown in Figures 24 through 29 and for the third case in Figures 30 through 36. Figure 24 shows depth contours of the actual bathymetry used to simulated wave propagation at 0^0, Figure 20, and wave propagation at 30^0, Figure 21. Obtained results of bathymetry estimates based on these simulations are shown in Figures 25 and 26. The same results of Figures 24-26 are shown in Figures 27-29 but with contours of specific values of the estimated depth to demonstrate the accuracy of the developed algorithm.

The additional example uses the bathymetry shown in Figure 11 to demonstrate the performance of the algorithm for a rather complicated bathymetry case. Figure 30 shows the image of simulated wave propagation over this bathymetry where the complexity of the bottom topography is apparent from the wave refraction/diffraction. Contours of the actual bathymetry are shown in Figure 31 and estimates of the depth as calculated from the simulations in Figure 32. Figures 33-34 shown the same results but with contours of specific values of the estimated depth to demonstrate the accuracy of the developed algorithm. Comparing these two figures the agreement of actual versus estimated depth in not as close as in the previous case. This can be attributed to the very complex bathymetry of this example. As a last comparison we show a cut along the length of the domain for the actual bathymetry, Figure 35, and estimated bathymetry Figure 36.

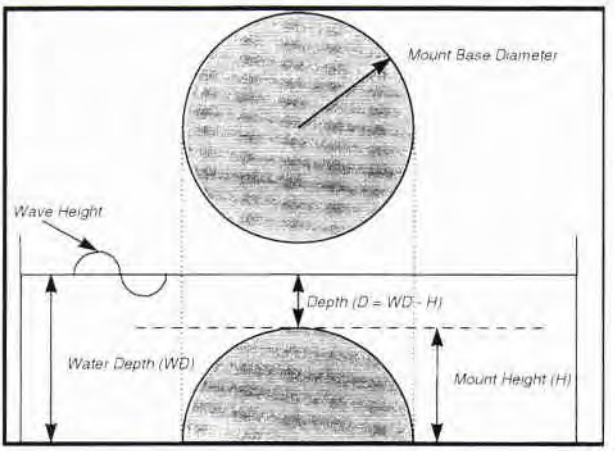

Figure 1. Simulation Geometry

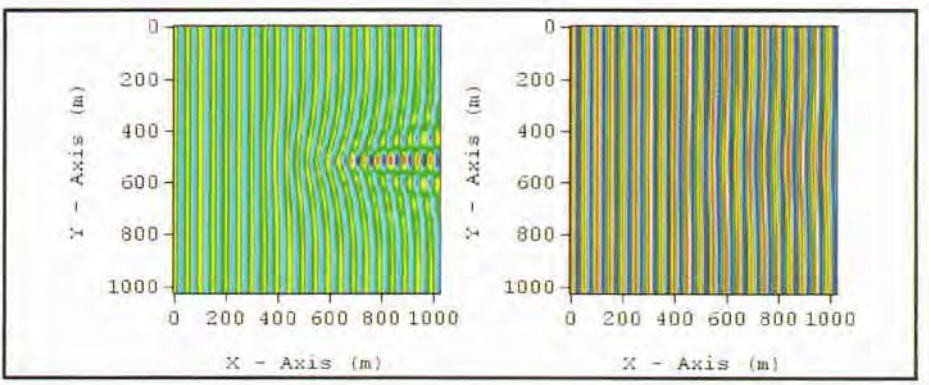

Figure 2. Wave refraction for 5 m and 15 m depths

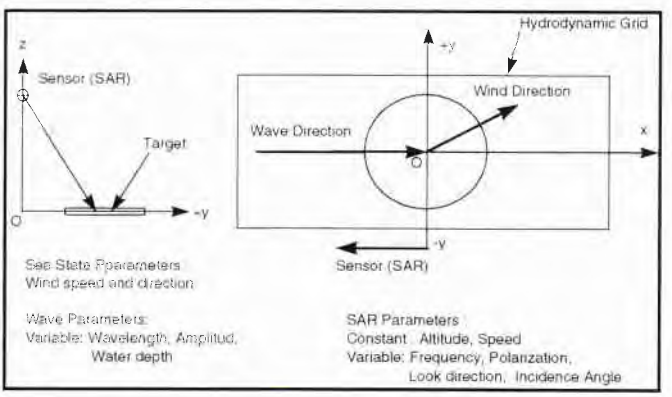

Figure 3. Simulation Geometry

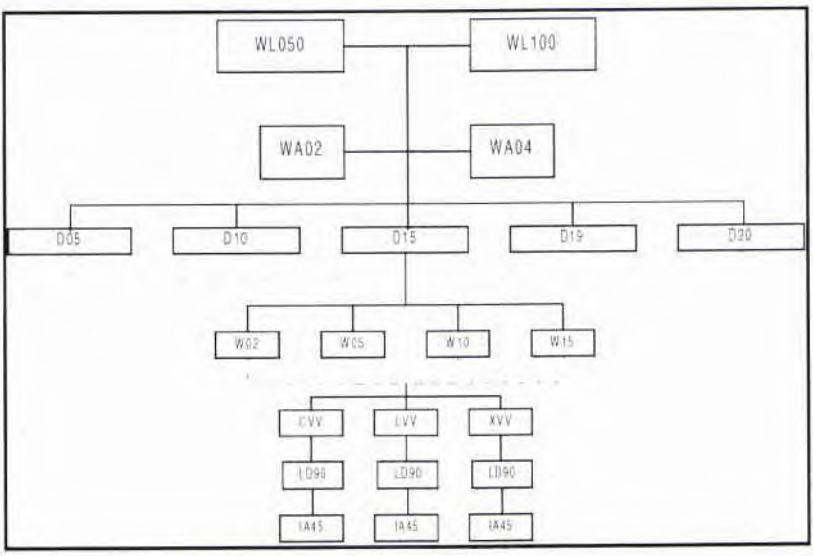

Figure 4. Simulation cases

Figure Number	Wavelength (m)	Wave Amplitude (m)	Depth (m)	Wind Speed (m/s)	Frequency, Polarization
5	50	2	5-20	2, 5, 10, 15	CVV
6	50	4	5-20	2, 5, 10, 15	CVV
7	100	2	5-20	2, 5, 10, 15	CVV
8	100	4	5-20	2, 5, 10, 15	CVV

Table 1. Simulation Cases

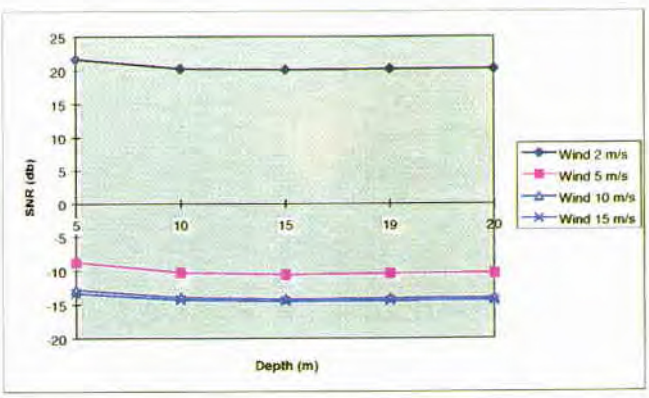

Figure 5. Wavelength 50 m, wave amplitude 2 m, CVV

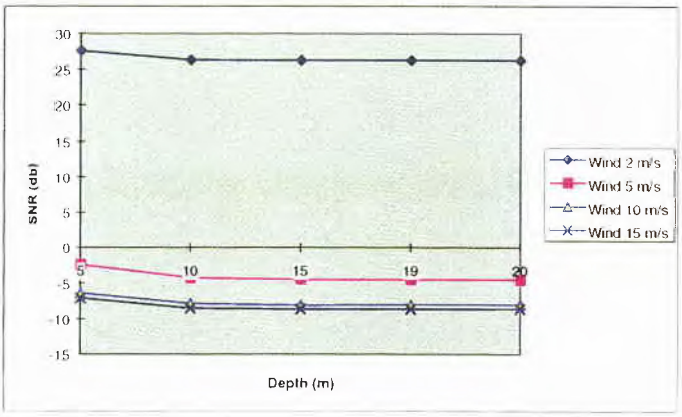

Figure 6. Wavelength 50 m, wave amplitude 4 m, CVV

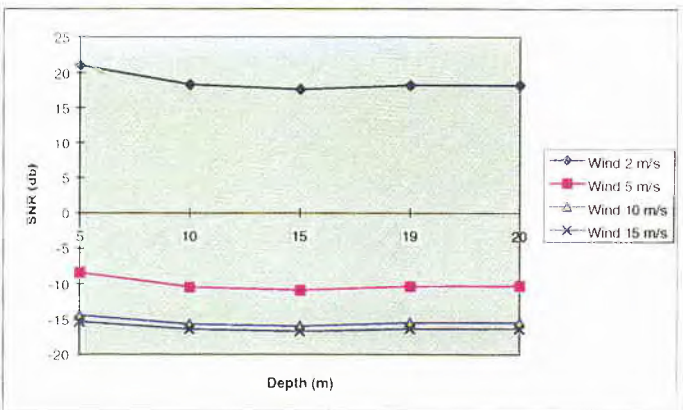

Figure 7. Wavelength 100 m, wave amplitude 2 m, CVV

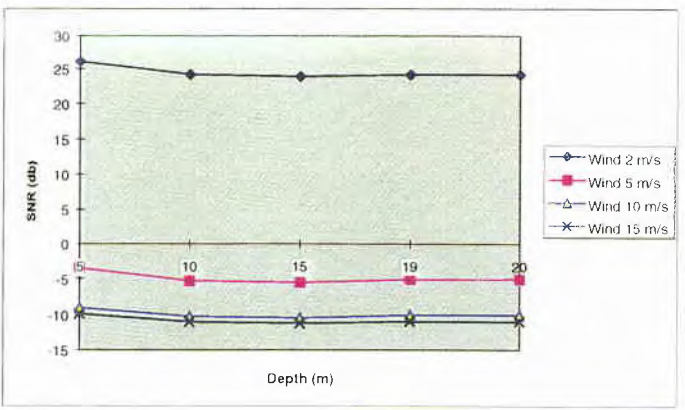

Figure 8. Wavelength 100 m, wave amplitude 4 m, CVV

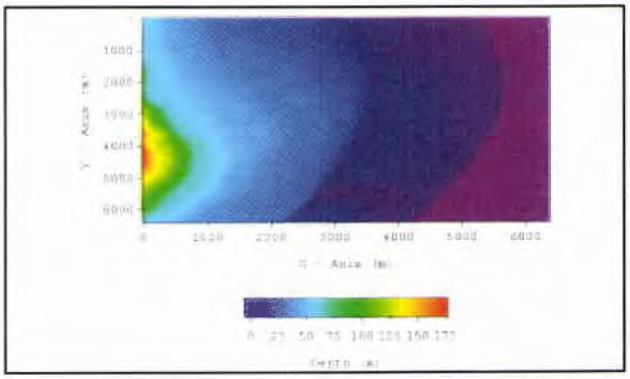

Figure 9. Bathymetry map for Case 1.

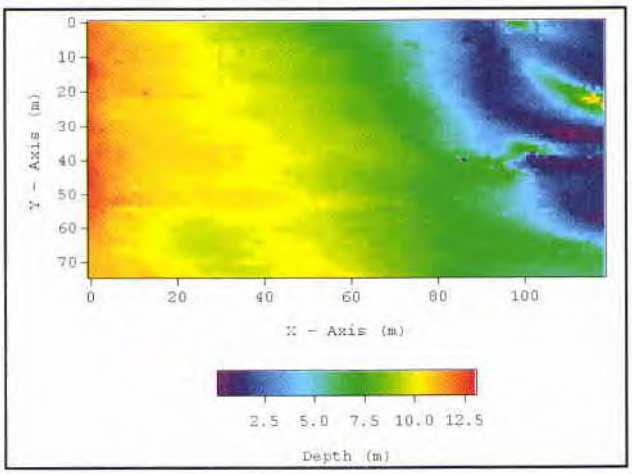

Figure 10. Bathymetry map for Case 2.

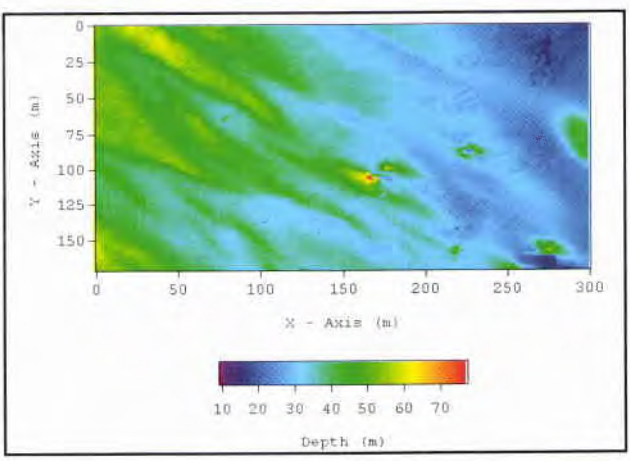

Figure 11. Bathymetry map for Case 3.

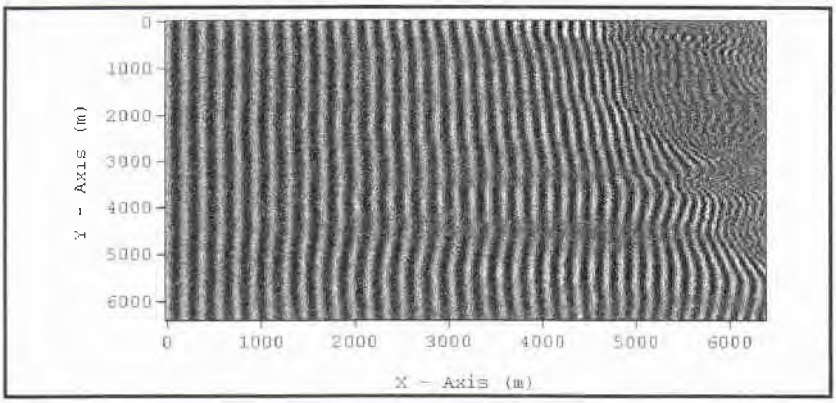

Figure 12. Wave propagation over Case 3 bathymetry.

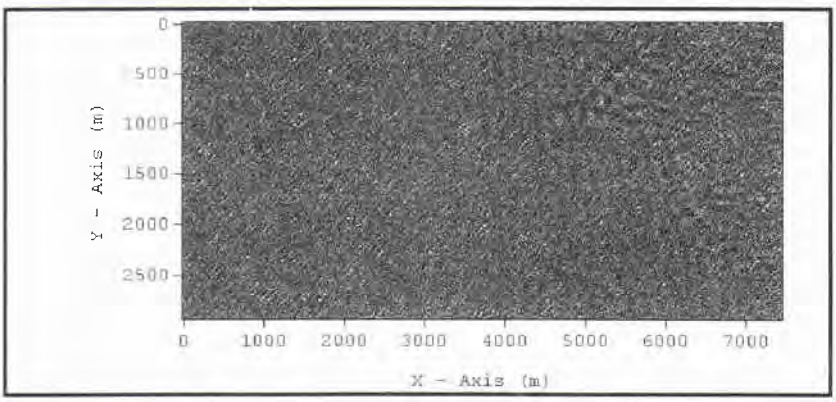

Figure 13. SAR image intensity, look direction = 0^0.

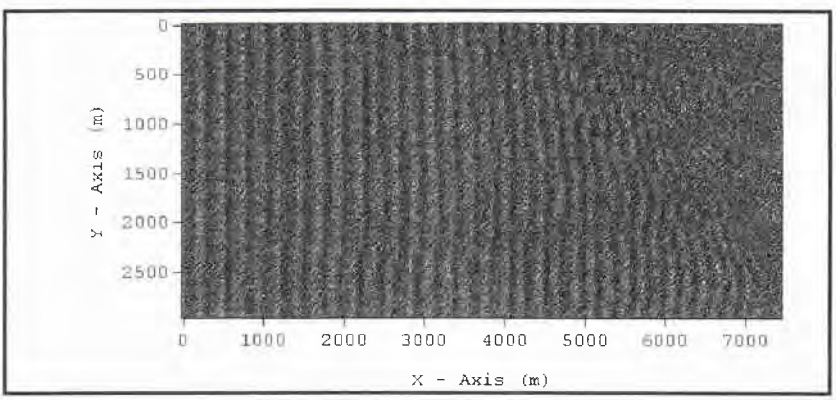

Figure 14. SAR image intensity, look direction = 90^0.

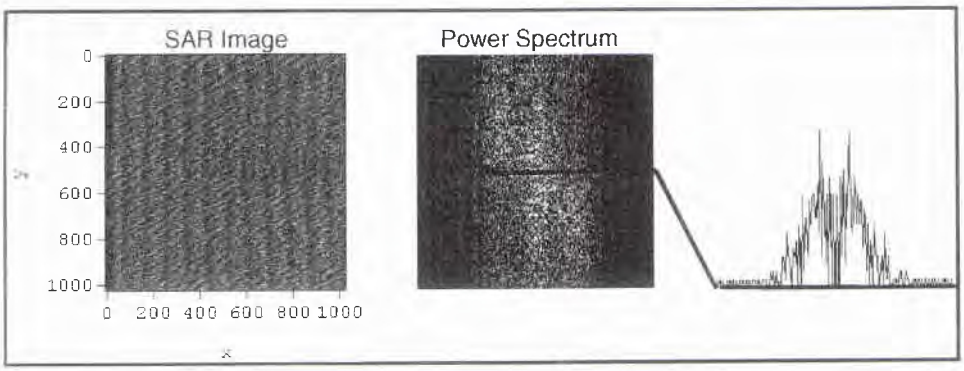

Figure 15. Power density spectrum for refracted/diffracted wave.

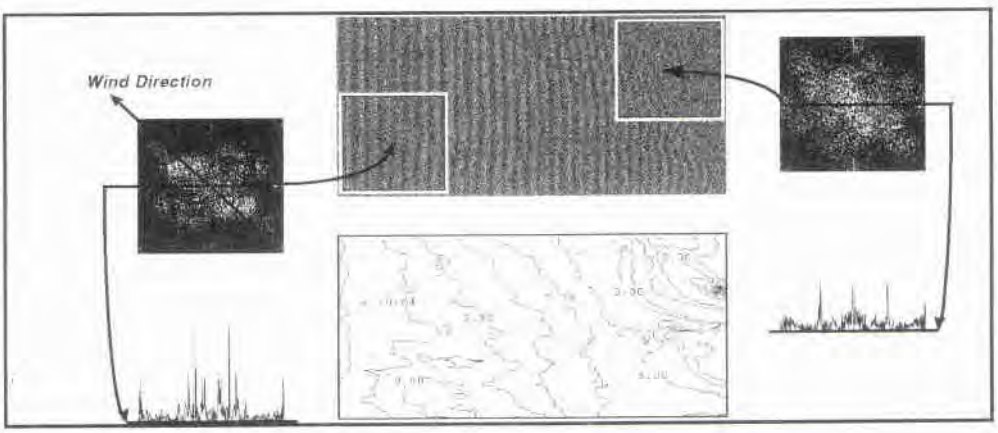

Figure 16. Wavelength estimates for refracted/diffracted wave.

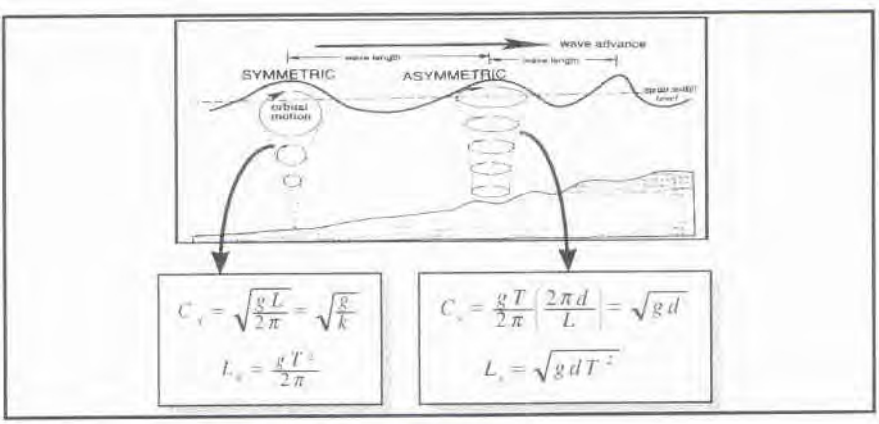

Figure 17. Wave refraction/diffraction for deep and shallow water.

$$k = \frac{2\pi}{L} \qquad \omega = \frac{2\pi}{T} \qquad C = \frac{L}{T}$$

Dispersion Relationship

$$L = \frac{g T^2}{2\pi} \tanh\left[\frac{2\pi d}{L}\right]$$

or

$$\omega^2 = g k \tanh\left[k d\right]$$

$$f(k,d) = \tanh(kd)\sqrt{\left[1 + \frac{2kd}{\sinh(kd)}\right]}$$

Figure 18. Wave dispersion relationships.

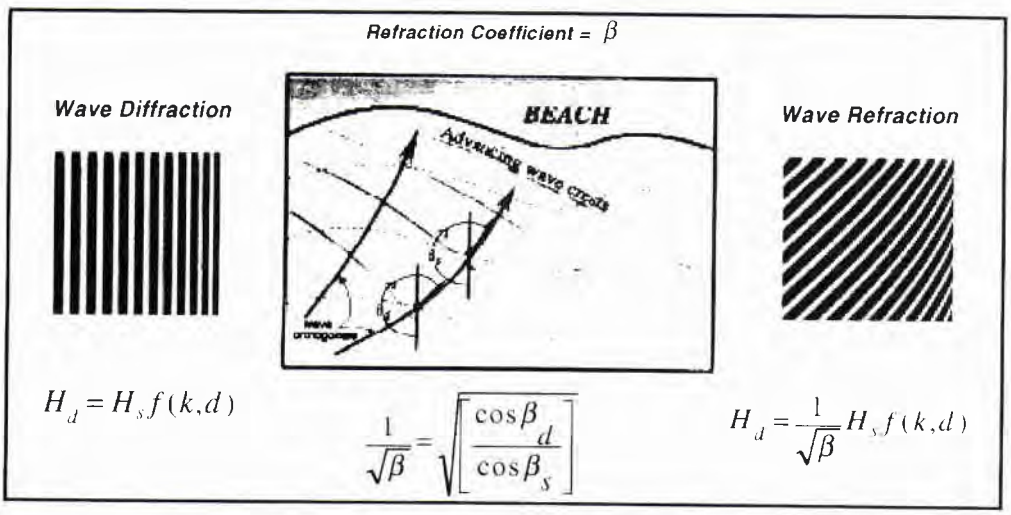

Figure 19. Wave diffraction/refraction relationships.

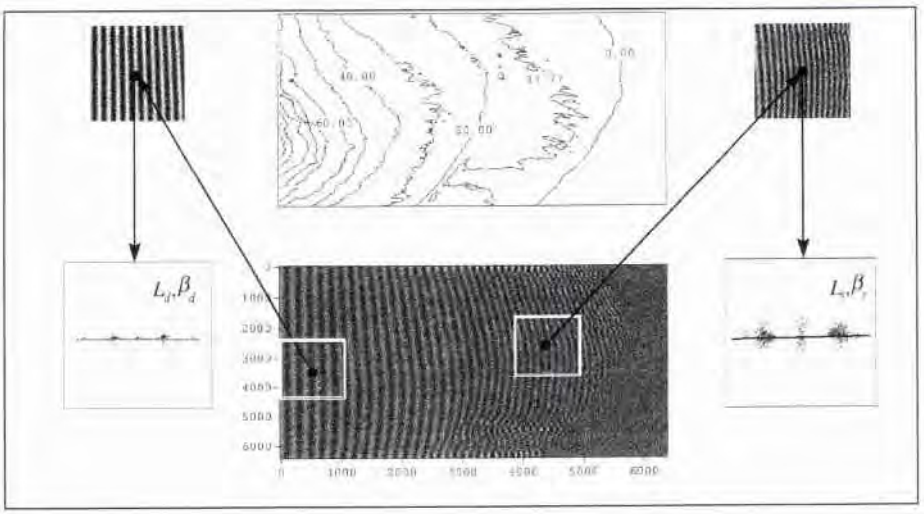

Figure 20. Wavelength and direction estimates from wave spectrum.

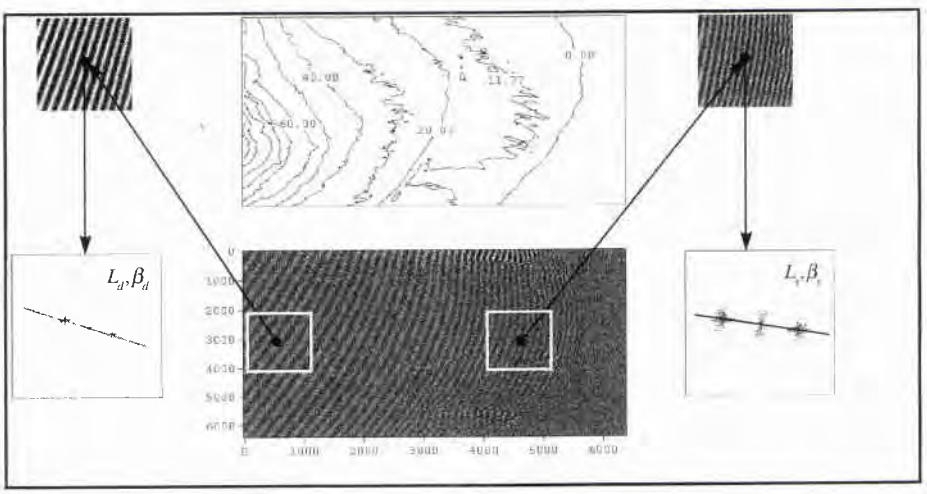

Figure 21. Wave length and direction estimates from wave spectrum.

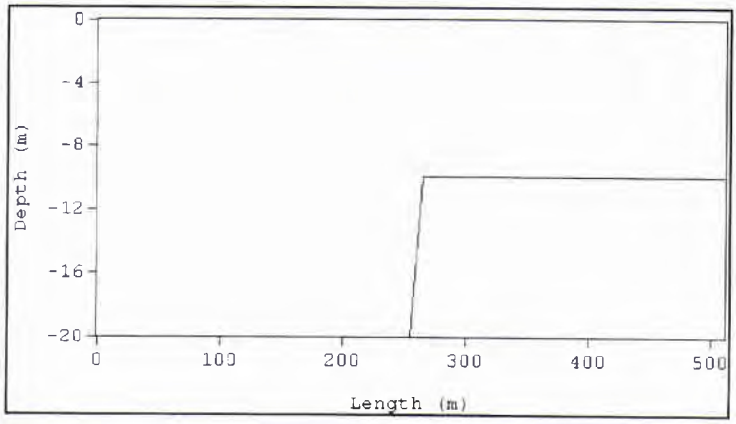

Figure 22. Water depth for first set of results.

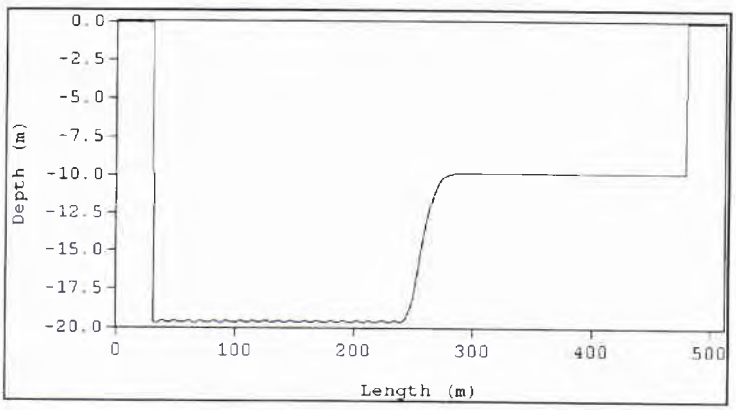

Figure 23. Estimated water depth from simulated results.

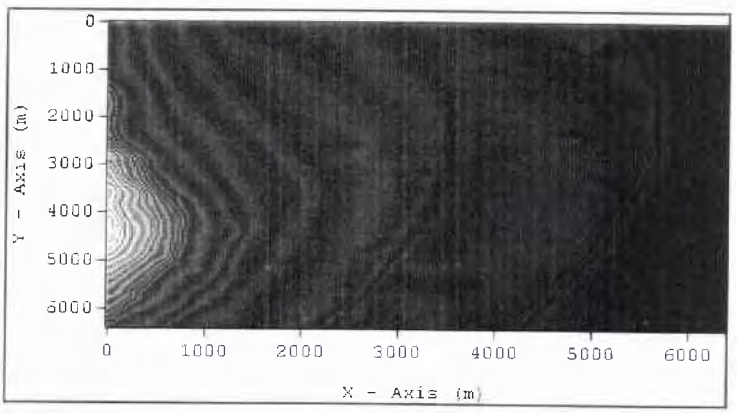

Figure 24. Water depth for second set of results.

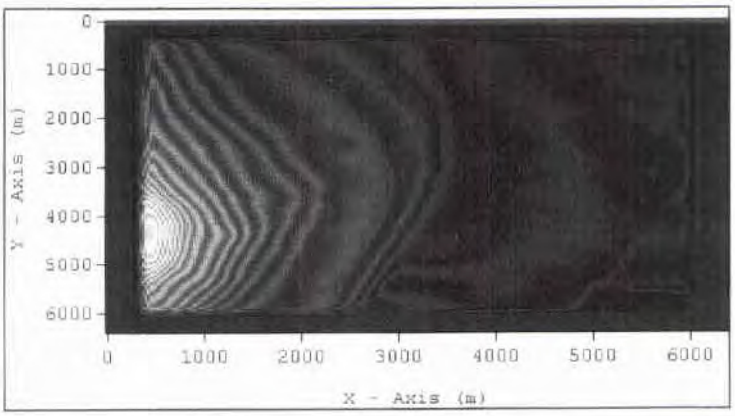

Figure 25. Estimated water depth for second set of results, waves at 0^0.

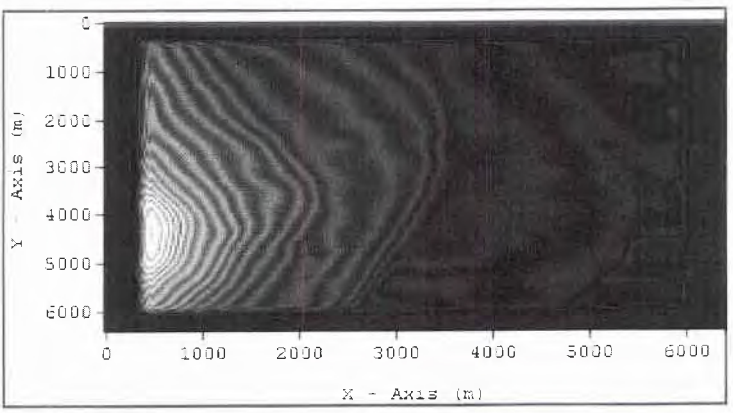

Figure 26. Estimated water depth from simulated results, waves at 30^0.

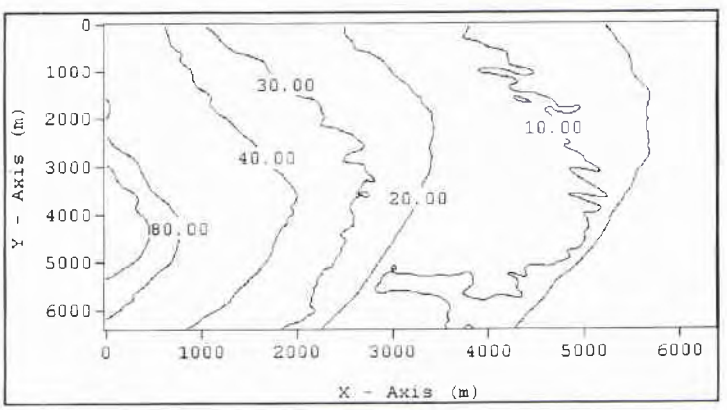

Figure 27. Water depth for second set of results.

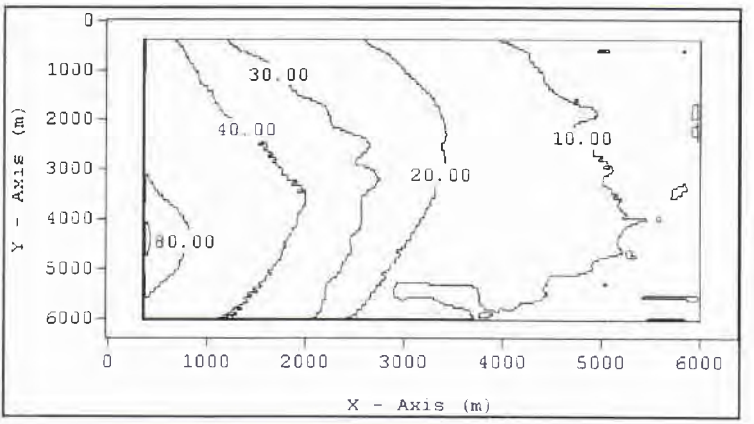

Figure 28. Estimated water depth from simulated results, waves at 0^0.

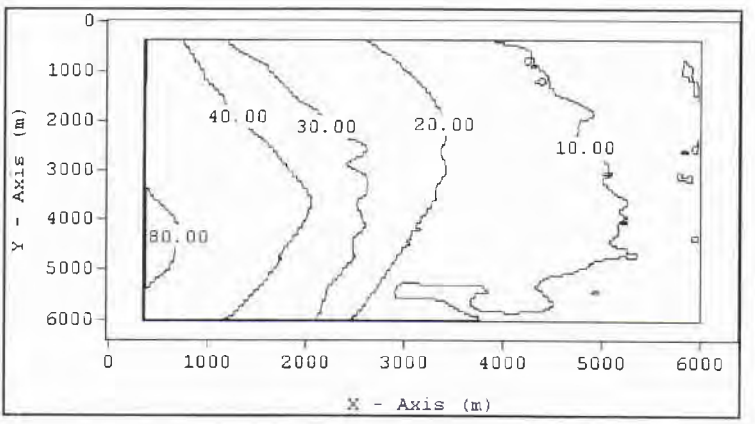

Figure 29. Estimated water depth from simulated results, waves at 30^0.

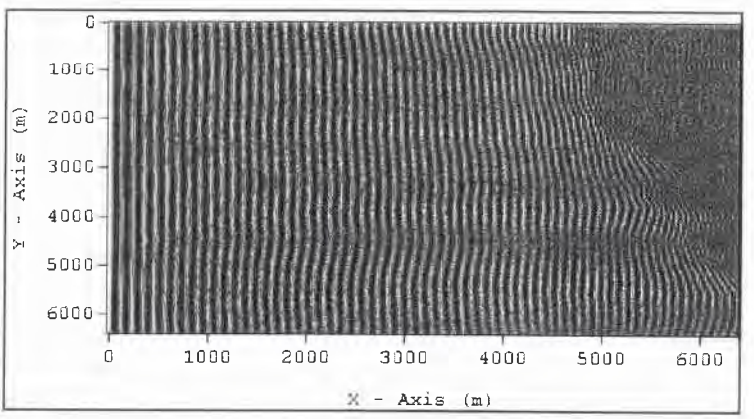

Figure 30. Wave propagation over Case 3 bathymetry.

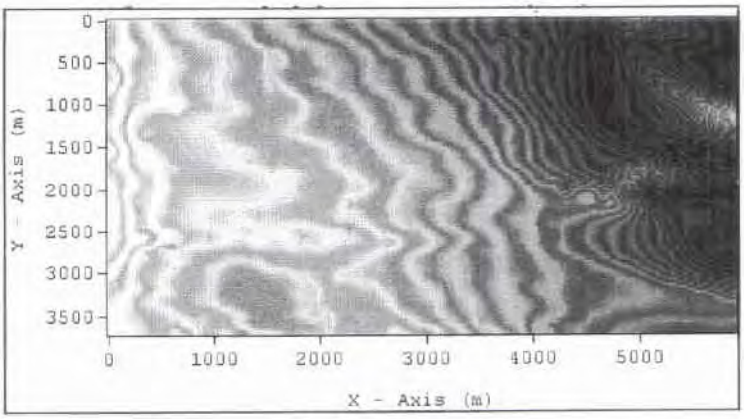

Figure 31. Water depth for Case 3 bathymetry.

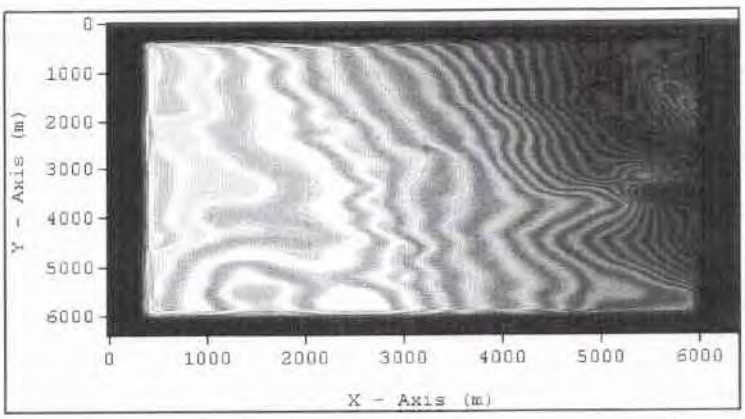

Figure 32. Estimated water depth from simulated results, Case 3 bathymetry.

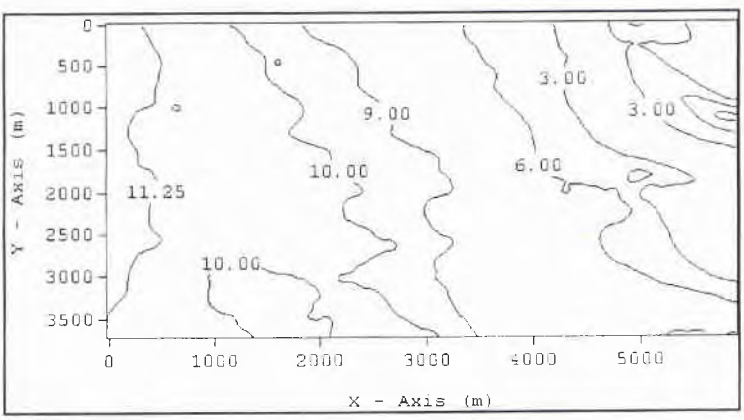

Figure 33. Water depth for Case 3 bathymetry.

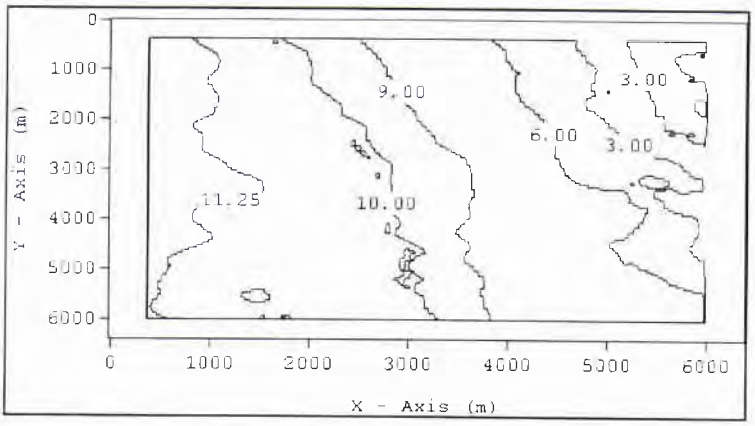

Figure 34. Estimated water depth from simulated results, Case 3 bathymetry.

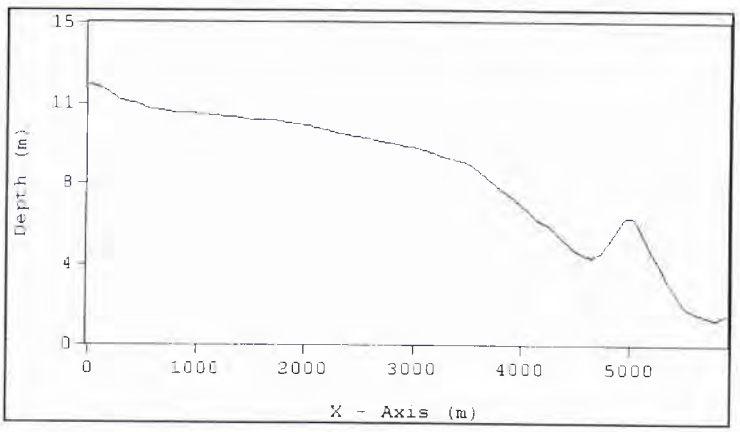

Figure 35. Water depth for Case 3 bathymetry, y = 3000.

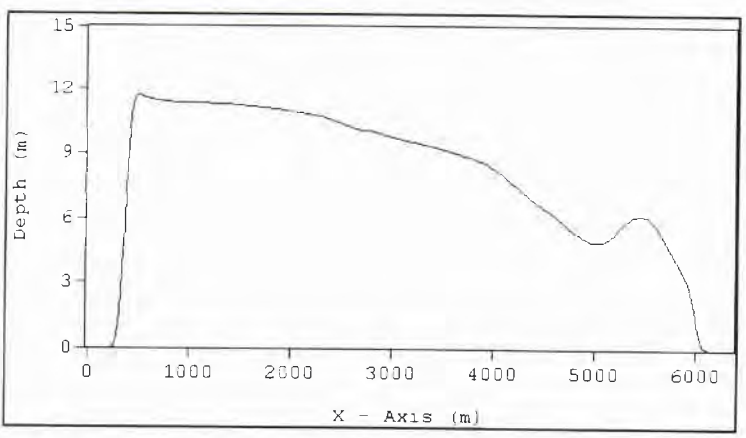

Figure 36. Estimated water depth from simulated results, y = 3000.

Use of Remote Imagery to Obtain Flow Information in the Littoral Zone

Richard P. Mied

Remote Sensing Division
Naval Research Laboratory
Washington, D.C. 20375
E-mail: mied@ccf.nrl.navy.mil

Abstract

Radar remote sensing provides synoptic, high-resolution images of estuaries and coastal regions, particularly the energetic hydraulic jumps generated at current meander boundaries and tidal plume edges. Radar image maps of these features are sensitive to surface roughness variations resulting from wave-current interactions around the density outcrop lines. We summarize results of NRL research to obtain flow information by merging image maps and model calculations to obtain velocity and hydrographic information about the jump. Future research on interpreting information encoded in the instabilities is discussed.

1. Introduction

Strong, propagating fronts are frequently observed to form in coastal and estuarine regions. They are bores or propagating hydraulic jumps, and are most often generated as a result of a strong or impulsive motion occurring in one water mass, where it touches a different body of water. For example, tidal plumes which occur on a semidiurnal basis are frequently observed to exhibit a steepening of their horizontal density gradient in the vicinity of the free surface, so that the isopycnal outcrop lines are grouped together in a small region, and the density is observed to change over a spatial scale which is effectively discontinuous. A similar phenomenon is seen to occur when the Gulf Stream makes a shoreward meander off of Cape Hatteras. As the northern edge of the cyclonic eddy (shingle) associated with the meander moves onto the continental shelf, a bore is formed between the continental shelf water and the Gulf Stream fluid (Figure 1). And finally, hydraulic jumps have been observed along shipping channels at the mouths of estuaries (Figure 2) under conditions of flood tide

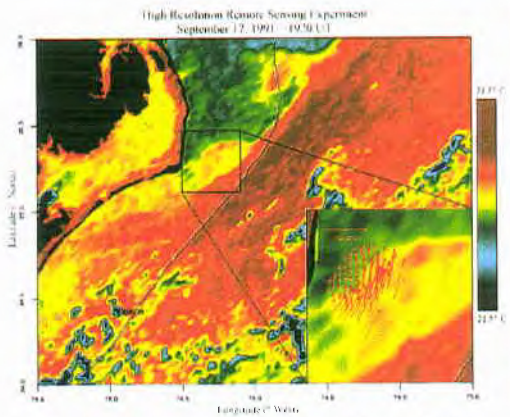

Figure 1. A combined AVHRR and Ocean Surface Current Radar (OSCR) map showing sea surface temperature and current velocities when a filament of the Gulf Stream meanders onto the continental shelf. The change in velocity and the temperature are coincident, and represent the location of a propagating hydraulic jump. OSCR data provided by Pro. L. Shay (University of Miami)

Figure 2. An ERS-1 SAR image of the lower Chesapeake Bay and adjoining continental shelf off the coasts of Maryland and Virginia. The jump associated with the tidal plume out of the estuary is marked with an "A" while the shipping channel fronts are labelled "B." This image is ESA copyrighted and was provided by Dr. Robert Beal (Johns Hopkins University Applied Physics Laboratory) as part of his US8-2c data set.

It is generally true that these hydraulic jumps are among the most intense phenomena occurring in the littoral region. Their strong current gradients render them excellent candidates for study by radar imaging methods, and their enhancement in radar cross section accounts for many of the bright lines so ubiquitious in the coastal environment. It is the current gradients and convergence rates that make them so important in a military context as well. With measured convergence rates approaching 0.05 s^{-1} and downwelling velocities of 15 cm s^{-1}, they are important in a variety of military contexts. First, the wave current interactions generate a much enhanced breaking wave climate, so that entrained air bubbles substantially alter the acoustic environment in the vicinity of the jump. Second, the intense downwelling constitutes an environment in which swimmers should not be deployed. And third, the strong fluid convergences make these flows very attractive locations to search for drifting mines.

2. The Imaging Mechanism

The radar image is essentially a map of the reflected radar signal, which is spatially and temporally modulated by the ocean surface wave field. The surface waves are modulated in turn through their interactions with the current field that is a manifestation of the broader meso- and submesoscale motions. This connection between the waves, currents, fluid motions, and image formation must be adequately modeled if we are to predict the radar cross section. The following sections outline these three types of models.

2.1. Surface Wave Spectrum

The evolution of wave action spectral energy density $N(x, y, \underline{k})$ is governed by

$$\frac{DN}{Dt} = \frac{\partial N}{\partial t} + \dot{x}\frac{\partial N}{\partial x} + \dot{y}\frac{\partial N}{\partial y} + \dot{k}\frac{\partial N}{\partial k} + \dot{\theta}\frac{\partial N}{\partial \theta} = S \qquad (1)$$

while the kinematic relations are written

$$\begin{aligned} \dot{x} &= \frac{\partial \omega_0}{\partial k} + u, \\ \dot{y} &= \frac{\partial \omega_0}{\partial k} + v, \\ \dot{k} &= -\hat{k} \cdot \nabla(\omega_0 + \underline{k} \cdot \underline{U}), \\ \dot{\theta} &= -\hat{\theta} \cdot (\omega_0 + \underline{k} \cdot \underline{U}) \end{aligned} \qquad (2)$$

and the source function contains the Plant-Hughes input from the wind, the Phillips resonant regrowth, the damping, and the wave breaking terms respectively

$$S = -\beta \frac{N}{N_0}(N - N_0) + \Pi - \gamma N + S_B \qquad (3)$$

These equations are solved with a finite difference formulation, rather than with the simpler and more familiar ray tracing technique. N_0 is taken to be the background Bjerkaas-Riedel spectrum appropriate to the particular windspeed being simulated. The damping term incorporates the effects of surfactants and viscosity [1], [2], [3].

2.2. Background Currents

The current $\underline{U}$ in the wave action spectral energy density equation is the surface manifestation of the underlying larger scale flow. Its evolution is governed by

$$\frac{\partial}{\partial t}\nabla^2\psi = J(\psi, \nabla^2\psi) + f\frac{\partial v}{\partial z} + \frac{g}{\rho_0}\frac{\partial \rho}{\partial x} + \nu\nabla^2(\nabla^2\psi) \qquad (4)$$

$$\frac{\partial v}{\partial t} = J(\psi, v) - f\frac{\partial \psi}{\partial z} + \nu\nabla^2 v \qquad (5)$$

$$\frac{\partial \rho}{\partial t} = J(\psi, \rho) + \nu\nabla^2\rho \qquad (6)$$

where ψ, v, and ρ are the stream function, along-front velocity, and density. Additionally,

$$J(A, B) = \frac{\partial A}{\partial x}\frac{\partial B}{\partial z} - \frac{\partial A}{\partial z}\frac{\partial B}{\partial x} \qquad (7)$$

while the (x,z) velocity (u, w) is given as

$$u = \frac{\partial \psi}{\partial z} \text{ and } w = -\frac{\partial \psi}{\partial x}, \qquad (8)$$

so that

$$\nabla^2\psi = \frac{\partial u}{\partial z} - \frac{\partial w}{\partial x}. \qquad (9)$$

Equations (4, 5, 6) are solved subject to the boundary conditions

$$\frac{\partial u}{\partial z} = \frac{\partial v}{\partial z} = \frac{\partial \rho}{\partial z} = w = 0 \quad \text{at the surface,}$$

and

$$u = v = w = \frac{\partial \rho}{\partial z} = 0 \text{ at the bottom.}$$

The ERIM ocean model [4], [5], [6] uses the tilted-Bragg approximation to calculate the change in radar cross section due to variations in the surface roughness. In order to accomplish this, a spatially variable spectrum is calculated, and the tilt of the long waves is computed from the small wavenumber components of the spectrum. However, we have found that the occurrence of breaking waves plays a large role in determining the rcs contrast of the scene. This poses a challenge to our deterministic approach in calculating the rcs, because wave breaking is an intrinsically stochastic occurrence. We have dealt with the problem by treating the rcs as the sum of a part given by the ERIM model (EOM) and a part arising from the wave breaking. Thus, we write

$$\sigma(x,y) = \left[1 - P_{WB}(x,y)\right]\sigma_{EOM} + P_{WB}(x,y)\sigma_{WB} \quad (10)$$

where P_{WB} is the probability of wave breaking calculated from the local acceleration criteria [7], [8], [9] derived from a spatial realization of the acceleration derived from the wave action spectral energy density $N(x, y, \underline{k})$. σ_{EOM} is the contribution to the rcs from the EOM and σ_{WB} is the contribution to wave breaking, which is derived from the rcs of a feature model of a spilling breaker [10], [11].

The results of the end–to–end simulation are shown in Figure 3. Of particular interest is the enhancement to the rcs due to the inclusion of the breaking formulation. Without it, the modeled rcs increase would be only about 5 dB. With it, we have the observed 10–12 dB response

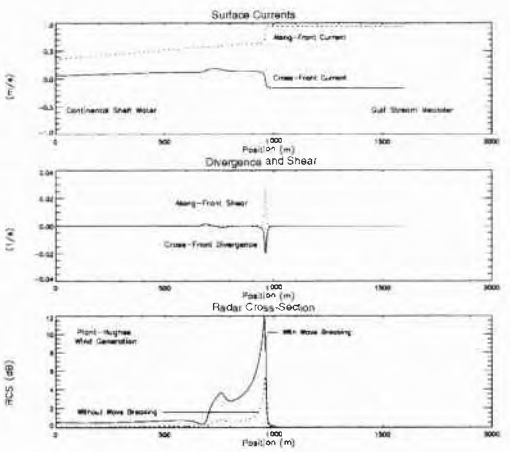

Figure 3 A three–panel figure showing the model-generated along–front and cross–front currents (top panel), along-front shear and cross-front convergence (middle), and the radar cross section (rcs) with and without breaking (bottom). The rcs calculated with wave breaking is about 12 dB, which is the observed magnitude of the jump in Figure 5.

3. Image Inversion

The details of the "forward" calculation have been shown in the previous section. That is, we have shown how to simulate an image from coupled hydrodynamic/electromagnetic calculations using first principles. However, the more immediate problem facing the warfighter is the need to interpret the imagery and obtain the associated velocities and convergences; that is, we need to invert the image to obtain flow quantities. If we understand the physics responsible for the creation of the image, this is not a formidable task.

For the case shown, we may take the increase of the rcs above the background to be ~12 dB. Even in denied regions, one has a crude idea of the magnitude of the depth and densities. In this particular case, we know the water depth and density difference are about 30 m and 0.9 kg m^{-3} respectively. Experience has shown us that the end result of these simulations is almost always a propagating hydraulic jump, irrespective of the details of the initial conditions. An indication of the error incurred in incorrectly specifying these input parameters can be appreciated by considering speed (c) of bore propagation in a simple two-layer fluid with density contrast ($\Delta\rho$),and upper layer depth (h):

$$c^2 = \frac{gh(\Delta\rho)}{2\rho_0} \quad (11)$$

We see that the layer depth and density enter the speed (and associated velocity field) as square roots. The error in specifying these quantities is thus halved by the occurrence of the square root.

It is a simple procedure to run the calculations with the assumed depth, density difference, and representative along-front velocity (v) to yield a rcs for the hydraulic jump. By iterating on the calculation until the assumed parameters produce the observed rcs magnitude, we may reproduce the naturally occurring scenario. The convergence velocity and propagation speed will result from this procedure (Figure 3).

4. Future Directions

The technique described above is the product of a straight–forward investigation which proceeds along the lines of the imaging mechanism. It requires that certain things be assumed regarding the environmental conditions. In the future, such restrictions may not be

necessary. By taking advantage of the ancillary properties of these flows, we may be able to invert the imagery without the benefit of these additional data. For example, we know that propagating fronts of this sort can undergo hydrodynamic instabilities of at least two types. Evidence of the first type can be seen in Figure 4 which shows a comparison between a smoothly evolving front and one with a symmetric baroclinic instability. In the latter case, a vortex is shed from the vicinity of the front and propagates away from the generation region near the density surface outcrop lines. The conditions under which this occurs are larger values of $\Delta\rho$ and v, and early experiments indicate that the rate of propagation of the shed vortex away from the nose of the jump is a monotonic increasing function of these two variables (given a known depth.)

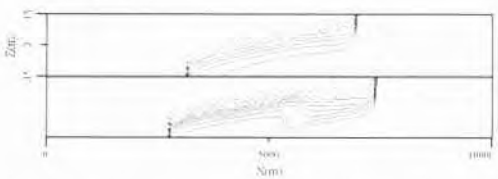

Figure 4. A comparison of the two hydraulic jump evolutions. The upper picture is of a hydraulic jump smoothly evolving from rest after 4.89 h. The lower plot shows a jump after evolving for 4.71 h and having shed a vortex.

A second—and more widely seen—type of instability is the series of corrugations (Figure 5) with wavelengths of 200 m–2 km. Investigations of the physics of the instability mechanism are just now beginning, but it seems likely that the wavelength and amplitude are determined by the environmental parameters and flow variables associated with the propagating front. As our knowledge of this process increases, we may be able to use the observed quantities to determine the desired flow variables.

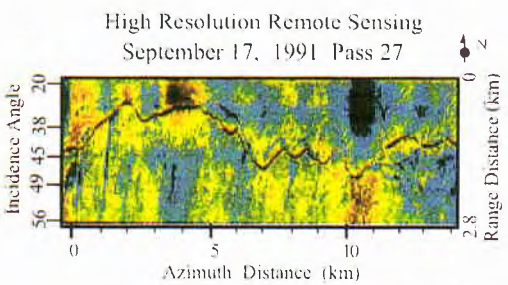

Figure 5. A false color res map of the propagating hydraulic that exists at the boundary between the Gulf Stream and continental shelf fluid in Figure 1. This image was provided by Dr Farid Askari (NATO SACLANT Center).

This note has dealt with hydraulic jumps, which are among the most energetic features in the littoral zone; their radar signatures are correspondingly strong. We have described a procedure to invert radar remote sensing imagery to obtain the convergence velocity and propagation speed of a propagating hydraulic jump, and indicated two possible future directions that could prove fruitful in inverting the imagery with fewer inputs

5. Acknowledgments

The work described in these proceedings has been the result of collaborations among scientists within the NRL-funded Accelerated Research Initiative "High Resolution Remote Sensing." Principal collaborators have been Drs. Farid Askari, George Marmorino, Colin Shen, and Dennis Trizna.

References

[1] Dorrestein, R., 1951A: "General theory of the effect of surface films on water ripples. I." *Proc. Acad. Sci. Amst.*, pp 260–272.

[2] Dorrestein, R., 1951A: "General theory of the effect of surface films on water ripples. II." *Proc. Acad. Sci. Amst.*, pp 350–376.

[3] Levich, V.G., 1962, **Physicochemical Hydrodynamics**, Chapter XI, Prentice Hall, New Jersey.

[4] Wright, J.W., 1968: "A new model for sea clutter." *IEEE Trans. Antennas Propag.*, **AP-14**, 749.

[5] Brown, G.S., 1978: "Backscattering from a Gaussian-distributed perfectly conducting rough surface," *IEEEE Trans Ant Prop*, **AP–26**, 472.

[6] Lyzenga, D.R., and J.R. Bennett, 1988: "Full–spectrum Modeling of synthetic aperture radar internal wave signatures," *J. Geophys Res.*, **93**, 12345–12354.

[7] Snyder, R.L., and R.M. Kennedy, 1983a: "On the formation of whitecaps by a threshold mechanism. Part I: Basic formalism," *J. Phys. Ocean.* **13**, 1482-1492.

[8] Snyder, R.L., and R.M. Kennedy, 1983b: "On the formation of whitecaps by a threshold mechanism. Part II: Monte Carlo experiments.", *ibid.*, 1493–1504.

[9] Longuet–Higgins, M.S., 1963: "The generation of capillary waves by steep gravity waves," *J. Fluid Mech.*, **16**, 138–159.

[10] Wetzel, L.B., 1990: "Electromagnetic scattering from the sea at low grazing angles" in **Surface Waves and Fluxes Volume II–Remote Sensing,** Geernaert, G.L., and W.J. Plant, eds., Kluwer, Dordrecht, Netherlands, pp. 146–171.
Wetzel, L.B. 1986: "On microwave scattering by breaking waves" in **Wave Dynamics and Radio Probing of the Ocean Surface**, Phillips, O.M., and K. Hasselmann, eds., Plenum Press, NY, pp 273–284.

Rapid Assessment of Current Velocities in the Coastal Ocean

Arnoldo Valle-Levinson
Center for Coastal Physical Oceanography
Old Dominion University
Norfolk, Virginia, USA 23529
Email: arnoldo@ccpo.odu.edu

Kamazima M.M. Lwiza
Marine Sciences Research Center
State University of New York
Stony Brook, New York, USA, 11794-5000
E-mail: kamazima@kafula.msrc.sunysb.edu

The circulation off the mouth of a coastal plain estuary, the Chesapeake Bay, was assessed under conditions of weak freshwater discharge. Current velocity observations obtained with an acoustic Doppler current profiler during 25 hours in September 1995 were separated into tidal and subtidal contributions. The subtidal flow was dominated by wind forcing. The tidal flow was presented as ellipses that illustrated the preferred orientation of this flow, which was influenced by the coastal morphology.

1. Introduction

The rapid assessment of coastal current velocities in a given area has important implications for environmental and military applications. The present study illustrates one example of describing the coastal circulation in a region influenced by buoyant discharges. The region of the Chesapeake Bay outflow is used as a test case. The Chesapeake Bay is located on the eastern coast of the United States and is the largest estuary of the country. Its plume is derived from a mean annual discharge of approximately 2000 m^3/s. The hydrography of the plume has been described in several studies [1], [2], [3] that show the importance of wind forcing on the fate of the buoyant discharges. The plume spreads offshore with southwesterly winds and remains close to the mouth of the estuary and to the coastline with northeasterly winds. The circulation associated with this plume, however, has not yet been described in detail. This paper begins to address this issue.

The overall objective of this study is to rapidly assess the coastal circulation off the mouth of an estuary under weak river discharge conditions, and in particular, to determine the influence of wind forcing on that coastal circulation. In order to accomplish this objective, an acoustic Doppler current profiler (ADCP) was towed for 25 hours between September 25 and 26, 1995 off the mouth of the Chesapeake Bay along the track shown in Figure 1. This rapid sampling of the area allowed the assessment of the coastal circulation within a period of 30 hours after the experiment started.

2. Data Collection

The survey was carried out during the time of the year of weakest discharge and in the driest year of the decade. The mean river discharge into Chesapeake Bay in September 1995 was less than 500 m^3/s, considerably less than the climatological mean of 1000 m^3/s for that month. The survey also took place under the influence of northerly winds, and after a period of relatively strong (~0.1 Pa) northeasterly winds as recorded at the Chesapeake Light Tower and at the Chesapeake Bay Bridge Tunnel by the U.S. National Oceanic and Atmospheric Administration (NOAA).

The current velocity data were obtained with a 600 kHz broadband ADCP manufactured by RD Instruments. The instrument was mounted on a catamaran and towed from the NOAA *R/V Ferrel*. The vertical resolution (or bin size) of the velocity measurements was 0.5 m so that the first usable bin was centered at approximately 2.25 m. The velocity data were collected in ensembles of 30 s, which gave a horizontal resolution of 75 m towing at a speed of ~2.5 m/s. The collection of ADCP data was combined with conductivity-temperature-depth (CTD) profiles obtained every 2 nautical miles along the ship track to characterize the potential influence of freshwater in the area. Navigation was performed with the aid of differential Global positioning system (DGPS). The grid over which the survey took place was approximately 60 km in the along-shelf direction from Cape Charles, Virginia, to False Cape, at the border between Virginia and North Carolina, and 20 km in the cross-shelf direction.

3. Data Description

3.1. Instantaneous Data

Given the river discharge and wind forcing conditions prevailing at the time of this survey, a very weak plume was observed off the mouth of the Chesapeake Bay. The salinity difference between plume and ambient waters was around 2 as indicated by instantaneous measurements (Fig. 1a).

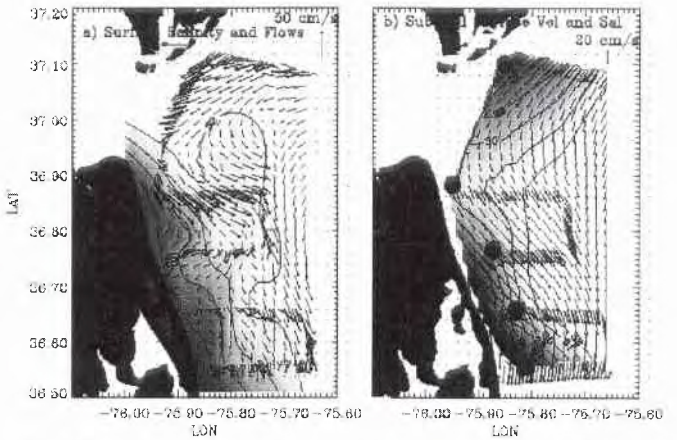

Figure 1. Study area off the mouth of the Chesapeake Bay. a) Istantaneous observations of near-surface flow (vectors) and salinity (shaded contours). b) Subdital near-surface flow and salinity. The Ship track is denoted by the closely spaced vectors. The gridded vectors are generated from interpolation. The location of the 1 nodes at which the least squares fit is performed is denoted by the filled circles in (b).

This weak salinity difference is quite contrasting to the salinity difference of September of 1996 when it was more than 10. Therefore, the buoyancy forcing was very weak and probably had a minor influence on the coastal circulation in the area at the time of the study. This idea is explored later by assessing the importance of wind forcing on the coastal circulation.

The instantaneous measurements of near-surface flow and salinity (Fig. 1a) showed spatial distributions that are typical of a plume influenced by downwelling winds as characterized in the modeling studies of [4] and [5]. These typical characteristics are: a region where the plume turns anticyclonically, the turning region; a transition region where the flow converges between the turning region and the coastal current as seen by the speed decrease in the alongshore flow south of the mouth of the bay; and the formation of a coastal current. Also, the freshest water remains constrained to a very narrow band, narrower than the internal radius of deformation of around 7 km, along the coast. These instantaneous measurements are, however, tidally aliased, i.e., they are biased by the different stages of the tidal cycle over which the observations were made. Then, in order to obtain a synoptic picture of the flow field, the influence of the tides on the instantaneous flow must be distinguished from the subtidal (or mean) current.

3.2. Fitting Technique

In order to separate the tidal signal from the instantaneous measurements, a least-squares technique was used. This technique has been used by [6] and assumes that each component of the current velocity observed $u_{ins}(x,y,t)$, where the subscript i denotes one component, has a contribution from a subtidal current u_{ini} plus one from a lunar semidiurnal (period of 12.42 h) tidal current, i.e.,

$$u_{ins}(x,y,t) = u_{ini}(x,y) + a_i(x,y)\cos(\omega_{M2}\, t) + b_i(x,y)\sin(\omega_{M2}\, t), \quad (1)$$

where ω_{M2} is the frequency of the lunar semidiurnal tidal component ($2\pi/12.42$ h). The subtidal flow component (or could also salinity), and the functions $a_i(x,y)$ and $b_i(x,y)$, are given by:

$$u_{ini}(x,y) = \Sigma_l\, \alpha_l(x,y)\, \phi_l(x,y),$$
$$a_i(x,y) = \Sigma_l\, \beta_l(x,y)\, \phi_l(x,y),$$
$$b_i(x,y) = \Sigma_l\, \gamma_l(x,y)\, \phi_l(x,y).$$

The parameters α_l, β_l, γ_l, are to be found by minimizing the least square error between observations and fit at each of the "l" nodes located at (x_l, y_l). The functions $\phi_l(x,y)$ are base functions that have been chosen as biharmonic splines [6], i.e.,

$$\phi_l(x,y) = \{(x - x_l)^2 + (y - y_l)^2\} \{\ln([(x - x_l)^2 + (y - y_l)^2]) - 1\}. \quad (2)$$

The least squares fit obtained with equations 1-2 and 5 nodes (Fig. 1b), reproduced the most prominent variations of both components of the observed flow (Fig. 2a, b). The goodness of fit depends on the position of the nodes, i.e., variations to the node location yield different subtidal and tidal flow fields. The node locations chosen here were optimized in such a way that

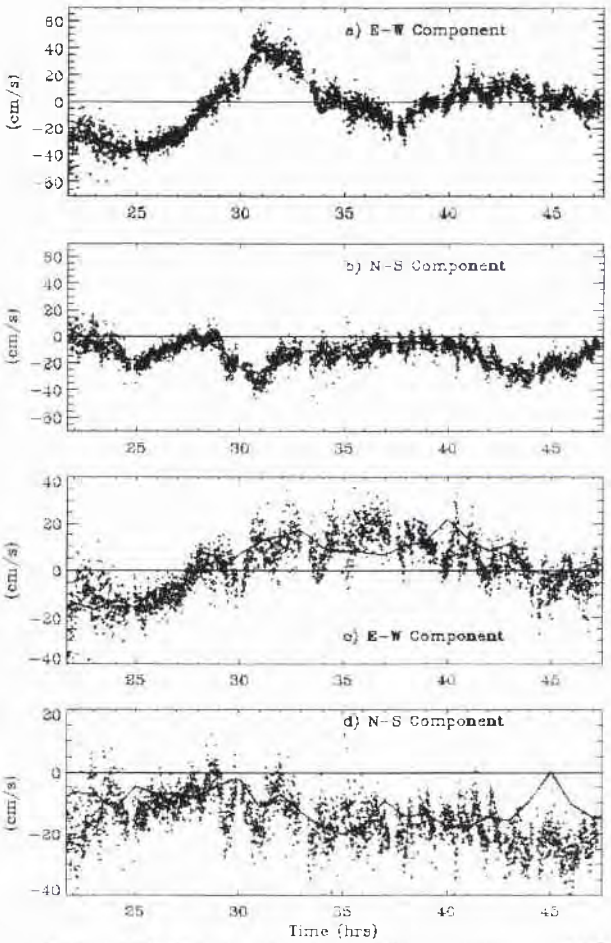

Figure 2. Istantaneous observations, represented by dots, compared to the least squares fit, denoted by continuous lines in (a) and (b). (c) and (d) present the subdital flow components, as dots, compared to the wind-induced flow (continuous lines) as explained by (3).

the noise (difference between observations and fitted values) had zero mean and variance that was a small fraction (less than 10%) of the variance of the observations. In addition, the optimal node locations were chosen for those that reproduced the tidal currents from moored current meters (data not presented here).

3.3. Subtidal Data

The subtidal flow obtained with the technique mentioned above reflects the contribution from wind forcing, from density gradients, and from forcing with periods greater than one tidal cycle (e.g. coastal waves). The resulting subtidal flow (Fig. 1b) showed a general tendency for southward flow throughout the domain. As seen later, this was due mostly to the forcing from the predominantly northerly winds. Another feature of the subtidal flow was the southward translation of the turning region of the Chesapeake Bay outflow. This turning region appeared to the south of the Chesapeake Bay mouth due to the interaction between the southward ambient flow and the estuarine outflow as suggested by the numerical results of [7]. The band of low salinity (Fig. 1b) remains very thin and close to the coast as a consequence of the weak buoyancy forcing from the estuary. An interesting question to answer is how much of the subtidal flow obtained from the least squares fit and shown in Figure 1b is due to wind forcing?

In order to assess the influence of wind forcing on the subtidal flow, a complex regression between the wind velocity and the detided velocity was performed. Hourly wind observations were interpolated to 30 s to match the sampling interval of the current velocities. This allowed the complex regression estimate to relate wind forcing to subtidal flow. The relationship between the wind and the subtidal flow was evident (Fig. 2c and 2d). In fact, the wind-induced flow produced a flow pattern that was very similar to the subtidal flow of Figure 1b according to the complex regression that yielded the following equations:

$$u = 0.04\ W_x$$
$$v = -0.04 + 0.04\ W_y \qquad (3)$$

These relationships explained 90% of the spatial variability of the subtidal flow. In (3), u and v were the east-west and north-south components of the current velocity, respectively, and W_x, W_y were the corresponding components of the wind velocity. This fit indicated that the north-south and the east-west components of the flow were approximately 4% of the north-south and the east-west components of the wind velocity, respectively. The -0.04 on the v component of the flow denoted a residual flow of 0.04 m/s directed to the south when the wind velocity is zero. This was consistent with the typical ambient coastal flow in this area of the Mid-Atlantic Bight [2]. The very high percentage of the subtidal flow variability explained by wind forcing was a consequence of the weak freshwater discharge onto the coastal ocean at the time of the study. This simple relationship between wind velocity and surface velocity allows the rapid assessment of the subtidal near-surface coastal circulation off the Chesapeake Bay only with wind velocity measurements. This assessment will, of course, be restricted to periods of weak freshwater discharge to the coastal ocean.

3.4. Tidal Data

The semidiurnal tidal contribution to the observations was obtained with the second and third terms on the right hand side of (1). The coefficients $a_1(x,y)$ and $b_1(x,y)$ were used to calculate the semidiurnal tidal ellipses following [8]. These ellipses are drawn in Figure 3 over the bathymetry of the study region. The orientation and ellipticity (ratio of the semi-minor axis of the ellipse to the semi-major axis) of the near-surface tidal currents appeared influenced by the coastline morphology. The ellipticity was lowest at the entrance to the Chesapeake Bay as the tidal currents were funneled into and out of the estuary. The ellipticity was greatest to the North and East as reflection of the rotary character of the tidal currents. The orientation of the ellipses suggested, once more, the funneling effect that the bay mouth has on the tidal currents entering and leaving the estuary. This orientation also suggested the influence of coastline morphology on the distribution of tidal currents. This representation of tidal properties was the first high-spatial resolution (less than 5 km) effort to characterize the distribution of the semidiurnal tidal ellipses off the Chesapeake Bay mouth. This is not the definitive distribution of tidal properties in the study area but offers an idea (and rapid assessment) of the spatial patterns that should prevail.

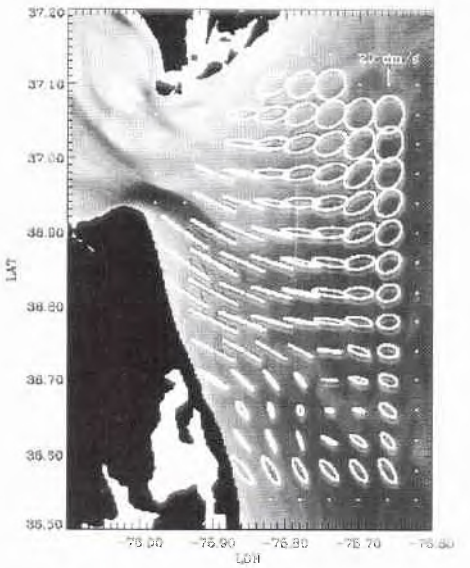

Figure 3. Near-surface semidiurnal tidal ellipses plotted over a regular grid of interpolates from the ship track shown in Figure 1. The bathymetry of the area is shown, for comparison with the orientation and ellipticity of the ellipses, as shaded contours. Deep areas are represented by darker shades.

4. Summary

Current velocity measurements with high spatial resolution were made off the mouth of the Chesapeake Bay in order to rapidly assess the coastal circulation off the mouth of an estuary under weak river discharge conditions. In particular, the influence of wind forcing on the coastal circulation was elucidated. The current velocity measurements were obtained with a towed acoustic Doppler current profiler during 25 hours between September 25 and 26, 1995. Ancillary measurements consisted of water temperature and salinity, and wind velocity. The current velocity measurements contained tidal and subtidal signals that were separated with a least squares technique as in [6]. The least squares fit was very good as it reproduced the salient temporal variations of the instantaneous measurements. The fit yielded a subtidal flow that featured a predominantly southward component and a turning region of the estuarine outflow that was advected southward by the coastal ambient flow. The latter feature

agreed with numerical results dealing with a similar problem of an estuarine outflow interacting with an ambient flow [7]. The subtidal flow field was mostly caused by wind forcing as buoyancy forcing was very weak. This subtidal velocity flowed at 4% of the wind velocity. In addition to the wind-induced component, the subtidal flow was influenced by a southward ambient flow of 0.04 m/s.

The least squares fit also identified a semidiurnal tidal flow contribution that showed influence of the coastal morphology on the orientation and ellipticity of the tidal ellipses. These tidal ellipses were more elliptic away from the mouth and became more rectilinear at the constriction of the estuary. The orientation of the ellipses roughly followed the morphology of the coastline. The spatial distribution of these tidal ellipse properties confirmed the expected funneling effect of the Chesapeake Bay entrance on the tidal flows entering and leaving the estuary.

The analysis technique used in this study allows the assessment of the coastal circulation of a region influenced by tidal and other forcings (e.g. wind and buoyancy) in approximately 30 hours: 25 hours of measurements and a few hours of data processing and analysis. The advantage of this technique is that it is relatively simple to apply to a data set and produces rapid results. The disadvantage is that it produces results that are statistically reliable but not dynamically reliable because the technique disregards any hydrodynamic aspect of the study area.

5. Acknowledgments

This study was funded by the U.S. Minerals Management Service under contract 14-35-0001-30807. The able command of Cdrs. Tim Tisch and Susan Mc. Kay, as well as the rest of the crew of the NOAA ship *Ferrel* allowed the success of the measurements presented here. Ship time was provided by Sea Grant. A. Münchow kindly provided information for the application of the least squares technique used. Thanks to R.C. Kidd, T.M. Wilson, K. Bock, D. Ruble, J. Miller, and N. Metzger for their help in collecting the data. J. Dixon from the NOAA office in Chesapeake, VA., kindly provided the wind data from the Chesapeake Bay Bridge Tunnel.

6. References

[1] Boicourt, W.C. 1973. The circulation of water on the continental shelf from Chesapeake Bay to Cape Hatteras. Johns Hopkins Univ. Ph.D. Dissertation. 183 pp.

[2] Boicourt, W.C. 1981. Circulation in the Chesapeake Bay entrance region: estuary-shelf interaction. In J. Campbell and J. Thomas (eds). Chesapeake Bay Plume Study: Superflux 1980. NASA Conference Publication 2188: 61-78.

[3] Boicourt, W.C., S.Y. Chao, H.W. Ducklow, P.M. Gilbert, T.C. Malone, M.R. Roman, L.P. Sanford, J.A. Fuhrman, C. Garside, and R.W. Garvine 1987. Physics and microbial ecology of a buoyant estuarine plume on the continental shelf. *Trans. Amer. Geophys. Union*. 68(31): 666-668.

[4] Chao, S.-Y. 1988. River-forced estuarine plumes. *J. Phys. Oceanogr.* 18: 72-88.

[5] Chao, S.-Y. and W.C. Boicourt 1986. Onset of estuarine plumes. *J. Phys. Oceanogr.* 16: 2137-2149.

[6] Wong, K.-C. and A. Münchow 1995. Buoyancy forced interaction between estuary and inner shelf: observation. *Cont. Shelf Res.* 15(1): 59-88.

[7] Valle -Levinson, A., J.M. Klinck, and G.H. Wheless 1996. Inflows/outflows at the transition between a coastal plain estuary and the coastal ocean. *Cont. Shelf Res.* 16, 1819-1847.

[8] Souza A. J. and J. H. Simpson 1996. The modification of tidal ellipses by stratification in the Rhine ROFI. *Cont. Shelf Res.*, 16, 997-1007.

The Use of Satellites to Detect Oil Slicks at Sea

David Bedborough

UK Department of Transport, The Coastguard Agency
Marine Pollution Control Unit (MPCU)
Spring Place, 105 Commercial Road
SOUTHAMPTON SO15 1EG, UK
Email: bedborough@tcahq.coastguard.gov.uk

Abstract

The area of sea patrolled by UK aircraft to detect and deter illegal discharges is extensive. To provide a complete coverage of these waters every day would require resources far in excess of those available. The use of satellite mounted SAR offers a possibility of increasing the detection of illegal discharges form shipping, which might in turn result in a reduction in the quantity of oil discharged illegally into UK waters.

1. Introduction

Oil pollution from ships (and offshore installations) poses a threat to the marine environment in two ways:

a) the accidental loss of crude oil due to accidents which can range in size from a few tens of tonnes to some hundreds of thousands of tonnes; and

b) the deliberate illegal discharge of oil, which can vary from a few litres to a few tonnes.

The effects of major spills have been well studied and the acute effects of the oil on the environment are fairly well understood. Illegal discharges pose a chronic threat and should be considered along with the other (greater) source of oil pollution which is land based, entering the marine environment via rivers.

This paper will concentrate on illegal discharges from ships and offshore installations and how we in the UK consider satellites might be of value in detecting and deterring illegal discharges.

2. The Role and Responsibilities of the Marine Pollution Control Unit (MPCU)

The MPCU was established to provide the UK Government's response to an oil or chemical spill from a ship at sea. It also provides assistance to Local Authorities who are responsible for cleaning oil from the coastline.

In order to conduct an effective at sea clean up operation it is necessary to have aircraft which are capable of directing the response into the thicker part of the oil. (As a rule of thumb 90% of the oil will be located in 10% of the slick area and it is not possible for a ship based observer to determine where the thicker parts of the slick are located.)

For this reason the MPCU has developed the use of aircraft remote sensing equipment. As this equipment is available on standby to respond to the relatively rare event of an oil spill it has been decided that this resource can provide a cost effective way of monitoring UK waters to detect illegal discharges of oil from ships.

3. Current Aerial Surveillance

The MPCU has two Cessna 404 aircraft on contract fitted with Side Looking Airborne Radar (SLAR), Ultraviolet and Infra Red detectors, a still camera and video

3.1. Side-way Looking Airborne Radar (SLAR)

This is an active device which measures the roughness of the sea surface. The surface is illuminated with microwaves with a wavelength in the region of 3 centimetres, and the reflection is used to build up a radar picture on both sides of the aircraft. Capillary waves on the sea surface will give a strong echo, and unusually smooth areas such as those caused by an oil slick, where the capillary waves have been damped, will show up against the background.

SLAR can provide an image of an oil slick from a distance of up to 20 km, even when the oil layer is thin. By scanning continuously to either side of the aircraft large areas of the sea can be checked for the presence of oil very quickly.

The main disadvantage of SLAR is that it responds to any phenomena that suppresses capillary waves. For example, certain current patterns, ice, and surface slicks associated with biological activity can all produce false targets. It is important, therefore, that SLAR targets be confirmed as oil by other means.

3.2. Ultra-violet Line Scanner (UV)

Oil is a good reflector of the ultraviolet component of sunlight. The UV a passive device which detects reflected ultraviolet with a wavelength of about 0.3 micrometers. It is mounted vertically beneath the aircraft, and can build up a continuous picture of an entire oil slick, even the extremely thin areas, as the aircraft passes over the oil. It cannot, though, distinguish between oil layers of different thickness.

3.3. Infra-red Line Scanner (IR)

The IR is very similar in operation to the UV, and the two are normally operated together. It detects infra-red radiation with a wavelength of about 10 micrometers emitted from the oil. Thin layers of oil radiate more slowly than the sea and show up as black patches on the display. Thicker layers (greater than about 0.5 millimetres) will warm up more rapidly than the surrounding sea and show up white on the display.

IR can therefore give some limited information about the relative thickness of the oil on the water surface. It is not as sensitive to oil as UV and so comparison of the outputs from the two sensors will show the position of those thicker parts of the slick where efforts should be concentrated. Infra-red systems can be mislead by other temperature effects, such as cooling-water discharges and should therefore always be used in conjunction with other sensors.

3.4. Photographic Camera

Conventional photography will not normally provide a clear and unambiguous image of an oil slick, but it can be valuable as a simple and readily understood record of the scene of an incident. When used to augment imagery from more sophisticated sensors, photographs can provide an on-scene commander with a better idea of the operations in progress around him. Also, in general the public and the Courts tend to be more receptive to photographic evidence than to imagery from less common devices.

3.5. Video Camera

Much the same applies to video recordings as to photography. The advantage of video is that it provides a more instant record and of course a moving picture. It does not have the same degree of resolution or clarity as a photograph and presentation is less convenient.

Cameras can be fitted either with a conventional data back, which will record date and time on the negatives, or with a data back which will accept information such as latitude and longitude from the remote sensing system computer.

3.6. Systems

The imagery from the remote sensors must be processed on board the aircraft if a display is to be available to the operator. This is done by means of a dedicated computer which accepts as input signals from the various sensors and information from the aircraft's navigation system, and presents it to the operator in the form of an annotated video display. If more than one sensor is operating, the operator can switch between the different images.

The computer can also provide some limited in-flight processing facilities, typically expanded views of areas of the screen, and facilities for selecting targets to provide navigational instructions for moving the aircraft to the target.

Output from the computer is recorded for future reference. There are several ways in which this is done. The raw information from the sensors and the navigation system are recorded digitally onto tape for further processing on the ground. The operator's display is recorded on to conventional video tape and it has been found useful in addition to provide an audio track on the video tape to record the operator's comments. The computer also provides navigational information (position, heading, altitude, time) to photographic and video cameras to be superimposed on to the pictures.

As data from the sensors are recorded digitally, it is necessary to have a ground-based computer system for further processing. This might simply be the production of hard copies - it has been found useful to augment flight reports by telefaxing hard copies of imagery from the operational airfield to the command post and to other appropriate centres. In addition, a ground-based computer provides digital video image enhancement to permit more accurate

measurements of the slick, and false colour displays to assist visualisation of the scene.

Some systems allow for the direct transmission of imagery from the aircraft to the ground station, using either fast but short-range VHF or slower but long-range HF radio, this has not been done in the UK.

3.7. Operational procedures

UK waters are divided into a number of patrol areas of roughly equal size. This areas are patrolled on a random basis but with more patrols in the areas of known activity, such as area M where most of the UK's oil production platforms are located and areas C, D, and E which cover the busy shipping lanes in the English Channel and Southern North Sea.

When on patrol the aircraft proceed at 290 km/hr at a height of 1000 meters using SLAR only. When an image is detected the aircraft drops to 300 meters and investigates the slick using UV and IR. If a vessel is associated with the slick the aircraft drops to 100 meters to identify the vessel and obtain pictures/ video.

Possible offenders are imaged and photographed using the techniques set out in Chapter 23 of the Bonn Agreement Counter-Pollution Manual. It is important that the photographs and the imagery show that the vessel is the only possible source of the oil. The vessel's name is photographed, if possible in a way which identifies it unambiguously as the offender, and recorded in the log. The master is contacted and invited to explain the discharge - his response is noted precisely, and if possible recorded on the remote sensing tape.

On return to base, the evidence from the offence is treated as evidence to court and all precautions required by the law are applied in securing it and transferring it to the responsible authorities. After each mission, routine tapes and logs (that is, those showing oil-like targets but with no potential as evidence) are taken for interpretation and statistical analysis and the results recorded in a database for use in periodic reports and future planning.

A SLAR image will give the location and area of the slick but UV will confirm that the slick is mineral oil and IR will show the thicker parts. The two images shown below are of a test spill of a approximately 10 tonnes, the IR shows the "structure" of the slick which has started to break down into windrows (wind is bottom right to top left).

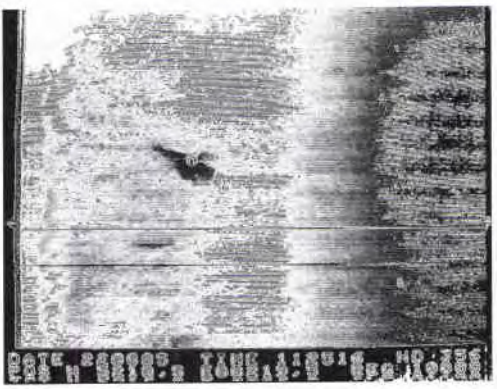

SLAR IMAGE

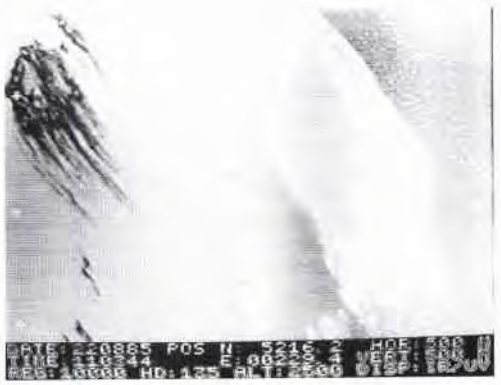

IR UV

3.8. BONN Agreement

The primary objective in routine patrolling is to encounter ships in the act of discharging oil illegally, and to gather sufficient evidence for a prosecution. Contracting parties to the BONN Agreement have agreed a co-operative approach to aerial surveillance, and this is set out in Chapter 4 of the Bonn Agreement Counter-Pollution Manual.

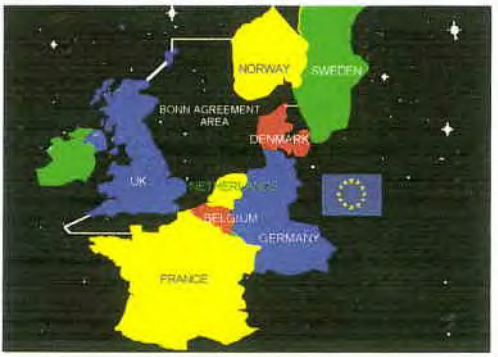

Over the years a large body of data has been collected which shows aerial surveillance in the North Sea and the number of detected oil slicks. The charts below show the data for individual BONN Agreement countries for 1994 (1995 figures are being compiled) and the total data for 1986 to 1994.

BONN AGREEMENT DATA

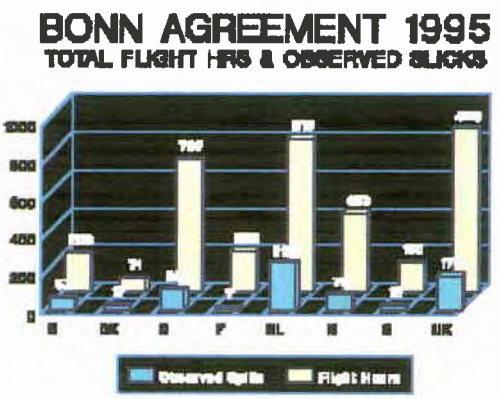

BY COUNTRY

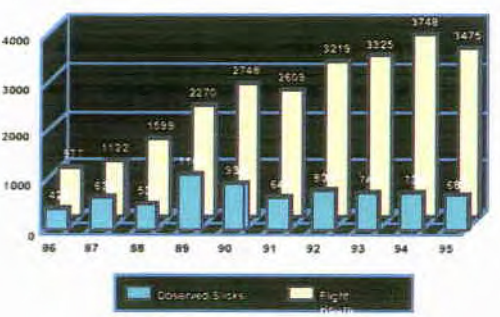

TREND

4. Perceived Weaknesses

4.1. Weather / Visibility

Weather and visibility will affect the ability of the remote sensing aircraft to detect slicks for two reasons.

Bad weather will restrict the ability of the aircraft to fly, although the North Sea can experience severe weather the percentage of times when the aircraft can not fly is quite small.

Weather conditions will affect the ability of the sensors to detect slicks and identify vessels.

SLAR is limited by very low wind conditions (calm). In near calm weather there are no capillary waves to be dampened by oil; at very high wind speeds any surface slick will be broken up and the lighter sheens will not be present.

IR will detect slicks for a few hours after sunset, and the UV can not be used during the hours of darkness, which is when many illegal discharges occur. Work is being carried out to develop a low light camera which can be used to identify the offender at night without the aircraft descending to an unsafe altitude.

4.2. Number of hours flown

The UK waters currently patrolled cover some 360,000 km^2. When on patrol the aircraft flies at 290 km/hr and covers 24 km on each side using SLAR. Therefore the aircraft can survey some 14,000 km^2/hr. Assuming a slick will persist for 24 hrs, then to ensure that all slicks are detected would require 26 hrs to be flown each day - assuming 6 hr patrols this would require some 4 aircraft.

The total yearly hours required would be some 9,400. Infact we fly some 800 hours (500 on ship patrols and 300 on offshore installation patrols). This represents around 10% of the requirement. It should be remembered that a form of "stratified sampling" is employed with more hours flown in some areas than in others.

The current cost of the 800 hrs is £ 320,000 and to give full coverage would require an expenditure in excess of £ 3.5 m.

5. Possible Uses of Satellite Mounted SAR

5.1. Collection of statistical data

A regular, thorough, coverage of UK waters would give sufficient data to show where slicks occur and when. Thus patrol flights could be focused in critical areas and at critical times. This would ensure that the aircraft had the maximum possibility of encountering an offender.

5.2. During major oil spills

It is unlikely that a major oil spill would occur without the relevant national authorities being aware (not least due to the search and rescue element which accompanies collisions, groundings, explosions etc). Therefore satellites will not help in the alerting process.

During a major incident remote sensing aircraft will be used to assess the spill and direct response operations. It is unlikely that satellites limited to SAR will assist. Indeed it is possible that a satellite image, which contains no internal structure showing where the thicker parts of the oil are located, could mislead and distract those carrying out clean-up operations.

SEA EMPRESS INCIDENT
IMAGE FROM RADARSAT FEBRUARY 21st 1996
at 06:45 UT(wind 5 to 8 m/s, Northerly)

During the recent SEA EMPRESS incident in Wales (15 February 1996) SAR images were obtained but were not used to direct response operations. Interestingly the image above does not indicate the main location of the slick and no significant oil was observed in the area shown as black on the image. Other images showed a mixture of "dark" areas where no significant oil had been detected and "dark" areas where oil could have been.

We will continue to look at ways in which the satellite images might be processed to determine if useful data can be abstracted for the responders.

5.3. Detection of illegal discharges

Satellites can detect slicks at sea, however they can not confirm that the slick is due to oil, nor can they identify any vessel causing the slick. It is unlikely that at present courts would prosecute on the evidence of satellite imagery alone. However, it is possible that satellites could prove a useful way of using remote sensing aircraft more effectively. This is currently being carried out in Norway.

From para 4.2 it can be seen that the probability of an aircraft encountering a ship discharging illegally is relatively low. If satellites could be used to direct the aircraft to probable offenders this would increase the detection rate and possibly the number of prosecutions. The increase in prosecutions, combined with the knowledge that satellites are being used, could increase the deterrent effect of the aircraft patrols and therefore reduce the total quantity of oil discharged.

6. User Requirements

For the aircraft to be directed to a possible offender in good time to ensure that the ship can be identified it will be necessary to receive notification from the satellite within 1 hour (it may take the aircraft upto to 2 hours to arrive on scene depending on distance from base). In order to avoid wasted effort the satellite should be correct in its identification of an oil slick at least 90% of the time.

It is not necessary to send detailed imagery in the first hour, this can follow in slower time and can be used in conjunction with data collected by the aircraft.

As mentioned in para 4.2, the UK currently spends some £ 320,000 each year on aircraft remote sensing. In order to improve the effectiveness perhaps some 20% of the budget could be directed to satellite detection. However, £ 60,000 will not buy much satellite time. It would appear that the best way forward would be some form of multi-user agreement based on a regional agreement such as the Bonn Agreement, or through a wider user group such as the EU.

The UK is currently running a nine month trial, for its sector of the North Sea, to determine whether satellite data can be integrated with the normal remote sensing operation. The cost is within the above parameters but actual satellite coverage is still relatively limited.

In situ Sensors

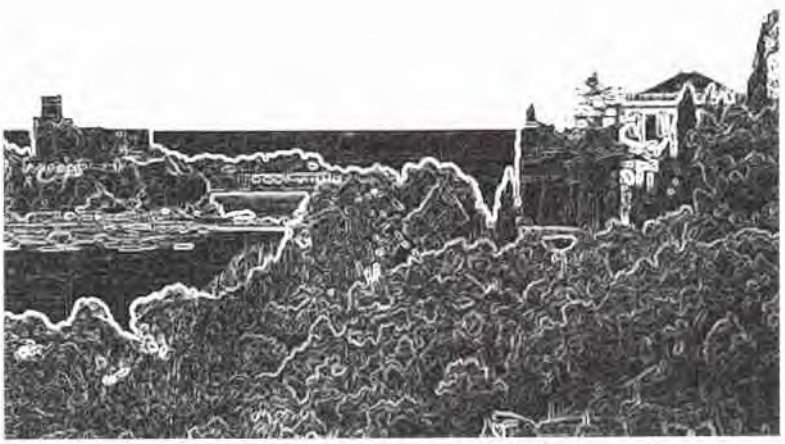

Acoustically Focused Oceanographic Sampling in Coastal Environments

Henrik Schmidt, James G. Bellingham and Pierre Elisseeff

Massachusetts Institute of Technology
Cambridge, MA 02139
USA
E-mail: henrik@keel.mit.edu

Abstract

A new oceanographic measurement concept, Acoustically Focused Ocean Sampling - AFOS, is presented, combining a tomographic network with small autonomous underwater vehicles. Using wireless local area network technology, the acoustic tomography data are recorded and processed in real time for achieving a low-resolution estimate of oceanographic parameters. The results are used to focus direct measurements by a network of small AUV's in areas of high spatial and temporal variability. By combining the high coverage but low resolution of the tomography with the high resolution capabilities of the AUVs, oceanographic phenomena with small scale dynamics controlled by large scale environmental forcing can be mapped. The feasibility of the new measurement concept has been demonstrated in a June 96 experiment in Haro Strait, BC, aimed at mapping coastal fronts driven by combined estuarian and tidal forcing.

1. Introduction

A fundamental problem facing oceanographic measurement techniques is a trade-off between coverage and resolution. Thus, a measurement system may cover a large area, but only provide coarse resolution, or provide much higher resolution over a smaller area. This problem occurs in particular in relation to oceanographic phenomenae which cannot be properly described at a single scale, but require consistent and coordinated measurement and analysis at a wide range of spatial and temporal scales. An example is coastal environments, where the estuarian and tidal driven oceanography interacts with medium and small scale topography to create an extremely dynamical oceanography with strong currents and distinct frontal structures. Such frontal structures are the main regions of mixing and upwelling, and are consequently of significance to the coastal ecosystem. They also provide one of the controlling factors for coastal transport processes.

Past studies of such frontal structures have focused either on high resolution volume measurements directly in the frontal region, or larger scale synoptic surface observations, but a measurement system accomplishing both simultaneously has been lacking.

Here we present a new approach to ocean sampling which combines the coverage capability of acoustic tomography with the high resolution capability afforded by mobile platforms. In this case the mobile platforms are small autonomous underwater vehicles (AUVs), operating in a moored acoustic communication and navigation network. The tomography component is achieved by adding a vertical hydrophone array to each of the network moorings, as illustrated in Fig. 1.

This *Acoustically Focused Ocean Sampling* concept uses the tomographic imaging capability to provide a low-resolution, but *synoptic* estimate of the frontal position. Using the acoustic communication network the AUVs are then guided into areas of high spatial variability to perform *high-resolution* direct measurements of currents, temperature, salinity, and other oceanographic parameters.

The feasibility of this new oceanographic measurement concept was demonstrated in a June 96 experiment carried out in Haro Strait, British Columbia. The scientific objective of the experiment was the mapping of a coastal front driven by combined estuarian and tidal forcing. The technological objectives was to determine the performance of the various components of the hybrid sampling network concept in a highly dynamic coastal environment, and through coordinated measurements with the various subsystems to determine the feasibility of the Acoustically Focused Ocean Sampling concept.

2. Littoral Environmental Assesment

2.1. Predictive Capabilities

Littoral oceanography is characterized by a high spatial and temporal variability, severely limiting the predictive capabilities which are essential to coastal environmental protection and operation of naval systems.

Oceanographic forecasting is an important tool for optimal distribution of protective resources in cases of severe oil spills, sewage leakages and other environmental hazards. Even though the fundamental equa-

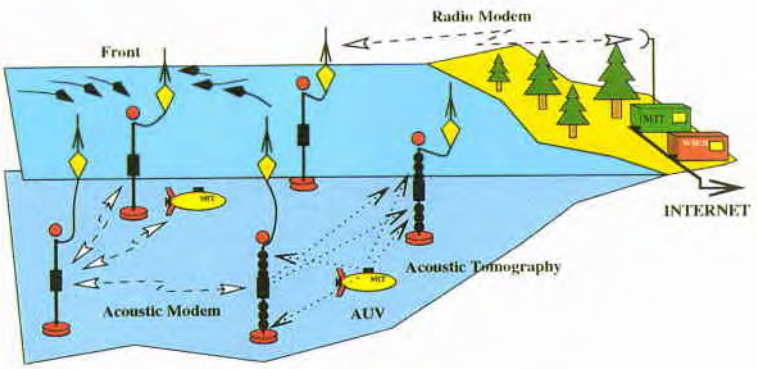

Figure 1: Acoustically Focused Oceanographic Sampling of coastal environments using a hybrid tomographic and autonomous vehicle network.

tions of the geophysical fluid dynamics may be reasonably well understood, the predictability of the oceanography is severely limited by the multi-scale nature of the forcing and the boundary conditions. Thus, for example, the formation and development of a coastal front may be driven by a combination of global tidal forces, estuarian processes such as fresh-water river run-off, and the local topography. In modeling such multi-scale phenomena, there is a trade-off between the size of the computational domain, i.e. the *coverage*, and the scale of the phenomenae modeled, the *resolution*. For coastal processes the small temporal and spatial scales are important, and consequently the computational domain that can be handled is severely limited. Because of the multi-scale forcing the boundary conditions are largely unknown, and accurate now- and forecasting only becomes possible if the models are constrained by in-situ measurements through data *assimilation*.

Acoustic modeling is crucial for high resolution sonar processing associated with acoustic imaging, passive and active matched field array processing, and acoustic communication. For example, modern communication technology uses channel equalization to adaptively adjust to the changing environment. Although very high data rates can be achieved using this approach in the open ocean, the short timescales of the ocean dynamics limit the performance of such systems in shallow water. Similar performance issues exist for the other acoustic systems of importance in shallow water. Thus, for example, matched field processing for source localization is highly sensitive to accurate modeling of the acoustic environment.

Unfortunately, even benign changes in the oceanography often have a dramatic effect on the acoustic environment. Thus, even though the oceanography may change at relatively low rate and linearly predictable manner, the associated acoustic environment may exhibit highly non-linear changes, such as shadow zone fading and the formation of caustic hot spots.

On the other hand, accurate modeling capabilities are readily available provided the environment is known, and consequently oceanographic predictability is the key to maintaining high performance of acoustic systems in shallow and littoral waters. The resolution of the oceanographic model is even more crucial here because of the non-linearity of the relation to the acoustic environment, and data assimilation becomes even more essential to the acoustic predictability than to the oceanographic equivalent.

Unfortunately the amount of data that can be assimilated has been severely limited for most acoustic systems of practical relevance, such as a handful of spatially and temporally "spotty" CTD or XBT casts, totally inadequate for acoustic prediction in littoral environments. However, recent progress in ocean sampling technology has yielded the possibility of vastly increasing the environmental data that can be assimilated into the oceanographic and acoustic models on a real-time basis, with the potential of dramatically improving the environmental prediction capabilities in shallow and littoral waters.

The Autonomous Ocean Sampling Network (AOSN) uses multiple Autonomous Underwater Vehicles (AUV) operating in an acoustic navigation and communication network to adaptively sample the oceanographic properties within the network, using a diverse suite of oceanographic and acoustic sensors. The adaptivity allows the AUVs to be focused in regions of high variability, thus allowing for adaptive distribution of resources in a manner which is optimal for real-time environmental assessment.

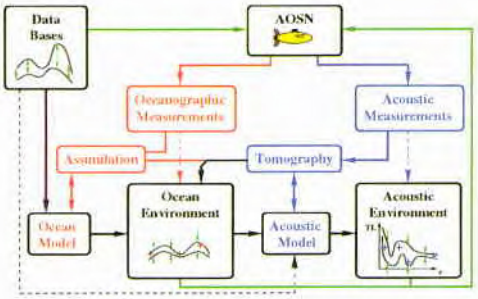

Figure 2: Real-time environmental assessment using the Autonomous Ocean Sampling Network

2.2. Autonomous Ocean Sampling Network

The explosive progress in recent years in developing small autonomous vehicles and underwater communication has provided the basis for a new paradigm for ocean measurements, the Autonomous Ocean Sampling Network (AOSN), [1]. The AOSN concept uses one or more inexpensive autonomous underwater vehicles (AUV) equipped with oceanographic sensors to make high resolution measurements in the ocean environment. A key component of the AOSN concept is the acoustic communication which is provided through a combined acoustic- and radio-modem network, Fig. 1.

The role of the AOSN in relation to real-time environmental assessment is shown schematically in Fig. 2. Traditional environmental assessment (red path) has been based on data collected by oceanographic instrumentation such as satelite imagery, current meters, CTD casts and XBTs. This data has been assimilated into environmental circulation models to provide now- and forecasting of the environment.

The oceanographic measurements can be augmented by by acoustic tomography estimates (blue path). The tomography provides *low resolution*, but *synoptic coverage*, while the oceanographic measurements provide high resolution, but very limited coverage. The AOSN allows combination of the two in an optimal way. Thus, the AUVs can be equipped with all traditional oceanographic sensors, and their mobility and acoustic communication capabilities allow them to be directed *adaptively* to regions of high variability or regions where the environmental properties are uncertain, with the potential of significantly improving the forecasting. In addition, the AUVs can be equipped with acoustic sources and receivers, enabling the addition of a moving source tomography component to the acoustic measurements, again improving the data available for assimilation into the forecasting.

An important component of the forecasting is the identification of areas of high variability or areas where the environmental properties are unknown or uncertain. This information provides the basis for the adaptive vehicle control.

2.3. Acoustically Focused Sampling

The main advantage of the AOSN concept is the adaptive, multi-scale sampling of the environment. Thus, some AUVs may be applied to provide coverage by sampling the environment using a large survey pattern, while other vehicles adaptively are applied to make high-resolution measurements in regions of strong variability detected by the survey vehicles, e.g. coastal fronts, Fig. 1.

Unfortunately, in coastal environments the temporal and spatial variability is such that a few survey vehicles cannot provide the synoptic measurement which is necessary to avoid time-space aliasing of the large-scale variability. However, by combining the AOSN with an acoustic tomography capability, a low resolution, but synoptic, map of the environment can be achieved, which is then used as a basis for adaptively directing the AUVs towards areas of high variability, Fig. 1. Consequently, this Acoustically Focused Ocean Sampling (AFOS) concept provides optimal use of the available AUV resources.

In addition to the AOSN, the key enabling technologies for AFOS are high-rate data telemetry, tomographic inversion algorithms, high-speed computers, all of which have undergone dramatic developments in recent years. On the other hand, the sampling strategies associated with AFOS are largely unknown, and require significant research effort for the concept to be developed into a robust and accurate measurement concept of general use to the oceanographic and naval communities. The *Haro Strait '96* experiment carried out in a joint effort between MIT, Woods Hole, and the Institute of Ocean Sciences, and with participation of Harvard University, and University of Victoria, was the first field deployment of the concept.

3. Haro Strait '96

3.1. Haro Strait Oceanography

Haro Strait and its adjacent channels (Fig. 3) form the most dynamically active portion of the fresh water estuary that extends from the mouth of the Fraser River through Juan De Fuca to the Pacific. It is in this area that tidal mixing is most intense, resulting in modification of the surface waters moving out of the system and also the two-way exchange. Accurate models of the circulation in this area, which includes such important deep water exchange with the Strait of Georgia and surface water flushing around Victoria, requires an adequate representation of the turbulent mixing [4].

Some of the mixing occurs in highly confined areas such as the tidal fronts, for example near Stuart Island

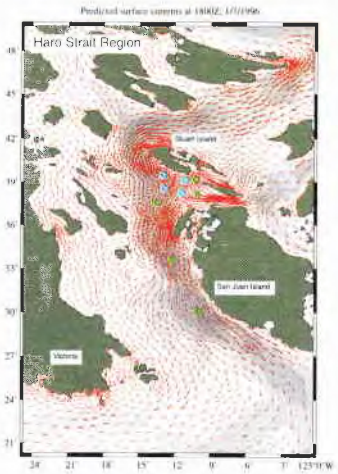

Figure 3: Topographic map of Haro Strait region, with predicted ebb tide currents during experiment. Tomography array (blue circles) is deployed to investigate the flow convergence of front south of Stuart Island.

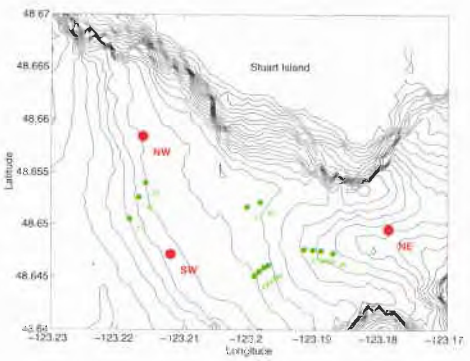

Figure 4: Acoustic array and source configuration in Haro Strait '96. Red dots indicate VLA moorings, while the green squares represent deployed ligh bulb sources.

(Fig. 3). These fronts may have a well defined surface expression. Tidal forcing is dominant, although meteorological effects, especially wind conditions over the southern Strait of Georgia, can be important in setting up the stratification at the northern boundary [5].

3.2. Haro Strait Sampling Network

The instrumentation applied to study the frontal dynamics in Haro Strait was a hybridization of traditional oceanographic floats and moorings, drifting instruments, autonomous underwater vehicles and a tomography network [6]. Using wireless and acoustic local area network technology one of the main objectives of the experiment was to demonstrate the combined, coordinated and adaptive use of all these systems within the AOSN.

3.3. Acoustic Network

The acoustic components of the network consisted of 3 moored nodes deployed South of Stuart Island as shown in Fig. 4. Each network node consisted of a U-shaped mooring, equipped with the following: GPS receiver, a 35 kbyte Radio Ethernet link to shore control station, 16 element vertical hydrophone array, 15 kHz Acoustic Communications Source, 1.5 kHz Tomography Source, and Array Tracking Sources. Each mooring was equipped with a 50 Mflop DSP based data logging computer with a 1 Gbyte hard disk.

In addition to the array mounted sources, a number of mobile tomography sources were applied to demonstrate the feasibility of the moving source tomography component of AFOS. Thus, one of the AUVs were equipped with a 15 kHz modem, and a 1.5 kHz tomography source identical to the array mounted ones. In addition, a low frequency CW source was towed from a surface vehicle by a participating group from University of Victoria, who also deployed a number of lightbulb sources within the network. The position of the lightbulb sources is shown by the green squares in Fig. 4.

The fully developed network infrastructure of the Haro Strait AOSN is shown in Fig. 5. All communication, whether hard-wired, wireless, or acoustic uses standard Internet protocols, with workstations, moorings and AUVs forming a selfcontained Internet domain, *haro.org*. The network was connected to the global Internet through a local provider via a fast modem line. This allowed optimal distribution of computational resources locally and at the various institutions for real-time data processing and modeling. Because of severe fluctuations, reverberation, and ambient noise, the acoustic link proved too unstable to allow full communication capability with the Odyssey AUVs. However, the remainder of the network was established and fully operational throughout the entire experiment. The control center was established in a couple of standard half-size containers, located on the shore in Sydney, BC.

3.4. Autonomous Underwater Vehicles

Two Odyssey IIb type AUVs (Fig. 6) were used for the *Haro Strait '96* experiment [2]. Derivatives of the original Odyssey design [3], the AUVs employ a fairing to obtain a low-drag configuration and are propelled by a single propulsor at the stern. The main pressure housings are glass spheres. The two vehicle used for this experiment each carried approximately 1 kW-hr of Ag-Zn batteries, which provided a maximum endurance of

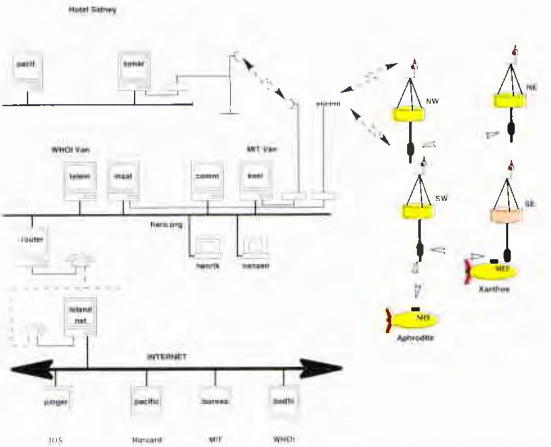

Figure 5: Internet architecture of the Autonomous Ocean Sampling Network in *Haro Strait '96*

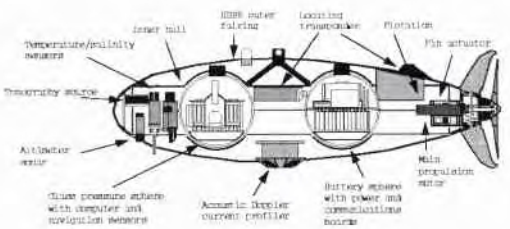

Figure 6: Odyssey class AUV used in Haro Strait '96

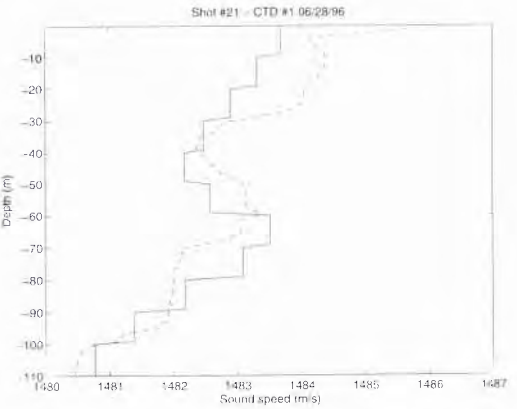

Figure 7: Sound speed profile inverted from light bulp source number 21 (solid), compared to CTD result (dashed) from a later date, measured at same point in tidal cycle

three hours at a speed of 1.6 m/s.

Measuring 2.2 m in length, and 0.6 m in diameter, the Odyssey fairing encloses a substantial wet volume for integrating various oceanographic payloads. One vehicle in this experiment carried a 300 kHz RDI Acoustic Doppler Current Profiler, an acoustic tomography source, and a WHOI acoustic modem. The ADCP was mounted in a downward looking configuration. The second vehicle carried a 100 kHz side-scan and 120 kHz upward looking sonar, developed by IOS as an integrated system. Both vehicles were equipped with Sea Bird conductivity and temperature sensors.

Navigation for the AUVs was provided by a long-baseline array. The vehicles were also tracked with a commercial USBL navigation system mounted on a DGPS equipped boat. For some of the experiments, the LBL system was used as a simple command link for sending heading commands to the vehicle from a deck unit on the tracking vessel.

4. Results

4.1. Acoustic Tomography

Several different acoustic tomography experiments were carried out, using both the 1.5 kHz and 15 kHz sources on the vertical arrays and and one of the AUV. A low frequency, moving source tomography component was added by deploying a series of light bulb sources in the network.

In AFOS the resolution of the tomography component is secondary to processing speed and robustness. A number of different tomographic inversion schemes

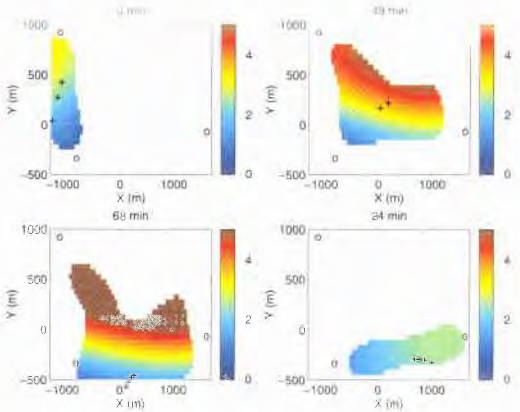

Figure 8: Contours of sound speed profile perturbation at 40-50 m depth, determined by tomographic inversion of light bulb data. The colours represent sound speed perturbation relative to a reference profile, in m/s, with red indicating higher, and blue lower speed.

have been applied to the lightbulb data, which is the dataset most thoroughly processed sofar. A layered algorithm using Gauss-Markov tomographic inversion for the direct and the surface reflected paths [7] have been developed, which provide real-time tomographic mapping of the sound speed profile throughout the network volume with a resolution of less than 1 m/s. The inversion simultaneously determines the source localization, a feature which may be applied for AUV navigation in future deployments. The source positions for the light bulb experiments are shown as green squares in Fig. 4.

The tomographically inverted sound speed profiles were verified by direct measurements by CTD and XBT. Fig. 7 shows a comparison of a tomographically inverted sound speed profile at the SW mooring, with a CTD measurement made at a later date, but at the same time in the tidal cycle.

The tomographic inversion was performed for each of four series of closely spaced sources. The inverted sound speed perturbation in the depth interval 40 - 50 m is shown in Fig. 8. The source and array positions are indicated by crosses and circles, respectively. Only results with an error estimate of less than 1 m/s are contoured, reflecting the coverage provided by the arrays and sources. The times stated above each frame represent a mean relative time at which each group of sources were deployed. The four frames therefore represent the time evolution of the oceanography.

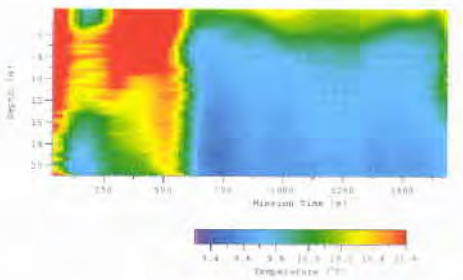

Figure 9: CTD measurement showing frontal crossing by AUV.

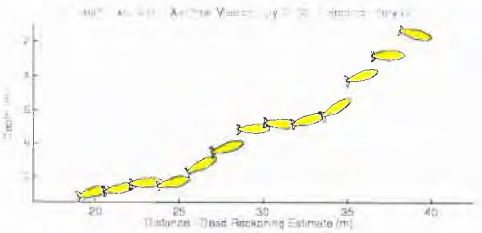

Figure 10: AUV pitch during survey mission, with pitch indicating attempt of compensating for large vertical velocities.

4.2. AUV Surveys

The AUV operations in Haro Strait had four basic objectives:

- Demonstrate moving source tomography from the AUV
- Take coordinated AUV-Sea Scan Drifter data sets
- Demonstrate model driven sampling with Harvard group data
- Take coordinated ADCP/CTD data sets for fast synoptic mapping test.

All four of the these objectives were met. Fig. 9 shows data for one of the 'front imaging experiments', in which AUV runs were designed to test model predictions of front location. For this experiment, the vehicle flew a yo-yo trajectory between 2 and 20 meters, completing 34 complete yo-yo cycles. Heading of the vehicle during the run was 90 m for the first 1200 seconds of the mission, followed by 900 seconds on a reciprocal heading. The trajectory carried the vehicle across the front twice, as illustrated by the strong horizontal temperature contrast observed at approximated 600 and 1700 seconds.

The more powerful fronts observed in the experiment had a strong influence on vehicle trajectory. Figure 10 shows the vehicle path during a mission in which the vehicle was attempting to hold a constant 10 m depth. Usually the vehicle is able to hold depth to within 0.2 m. However, this data set shows the vehicle apparently flying into a strong upwelling event. The event both deflect the vehicle to a pitch-up orientation, and physically lifts the vehicle to the surface. The maximum vertical velocity observed here is approximately 1.5 m/s.

Overall, AUV performance in Haro Strait was very reliable. Over 80 vehicle missions were run with no vehicle failures.

5. Conclusion

The *Haro Strait '96* experiment demonstrated the feasibility of Acoustically Focused Ocean Sampling in littoral environments. Using a network of small AUVs in conjunction with acoustic tomography AFOS was applied to measure the volumetric properties of estuarian and tidal driven coastal front systems. Even though the closed-loop connectivity of all the various measurement systems is yet to be achieved, the experiment demonstrated the feasibility of the concept by performing several combined experiments. Thus, the use of the AUVs for moving source tomography was demonstrated, and also the adaptive operation of multible AUVs in coordination with a free drifting oceanographic instrument was demonstrated. On the other hand, the experiment identified several fundamental, scientific and technological issues yet to be resolved before the new measurement concept can become of routine use. For example, the acoustic environment in such regions is a significant complicating factor, with extremely high ambient noise levels due to shipping and boating. Bottom reverberation is another limiting factor for acoustic systems and the extremely dynamic oceanography yields high scintillation indices. The operation of acoustic systems for communication and navigation is therefore non-trivial, and the experiment clearly identified a need for more robust acoustic systems and processing algorithms.

Acknowledgment

This work was supported by the Office of Naval Research, Codes 321HL and 322OM.

References

[1] T.B. Curtin, J.G. Bellingham, J.Catipovic and D. Webb, Autonomous Oceanographic Sampling Networks, *Oceanography*, Vol. 6, No. 3, 86–94, 1993.

[2] T.W.Altshuler, T.W.Vanek, and J.G. Bellingham, Odyssey IIb — Towards Commercialization of AUVs, *Sea Technology*, December 1995, 15–19.

[3] J.G. Bellingham, C.A. Goudey, T.R. Consi, and C. Chryssostomidis, A Small, Long-Range Vehicle for Deep Ocean Exploration, *Proceedings of the Second International Offshore and Polar Engineering Conference*, San Francisco, Vol. 2, 461–467, 1992.

[4] M.G.G. Foreman, R. A. Walters, R. F. Henry, C. P. Kellar, A. G. Dolling, A tidal model for eastern Juan de Fuca Strait and the southern Strait of Georgia, *J. Geophys. Res.* 100 (C1), 721–740, 1995.

[5] D. M. Farmer, E. D'Asaro, M. V. Trevorrow, G. T. Dairiki, Three dimensional structure in a tidal convergence front, *Cont. Shelf Res.* 15 (13), 1649–1673, 1995.

[6] H. Schmidt, J.G. Bellingham, M. Johnson, D. Herold, D.M. Farmer and R. Pawlowicz, Real-time frontal mapping with AUVs in a coastal environments, *Proceedings, Oceans'96, Ft. Lauderdale, FL*, 1996.

[7] P. Elisseeff, *Acoustic tomography of a coastal front in Haro Strait, British Columbia*, Massachusetts Institute of Technology, Internal Memo, 1996

AUTONOMOUS OCEANOGRAPHIC SAMPLING NETWORKS: STATUS REPORT THROUGH FY97/Q1

Thomas B. Curtin
U.S. Office of Naval Research

Introduction

A comprehensive modeling/sampling system is required for mapping littoral variability, validating high resolution ocean models and increasing forecasting skill. Mapping of temporal and spatial gradients in the ocean is accomplished through time constrained surveys designed to minimize temporal and spatial aliasing. Validating models involves assessing the accuracy of high resolution output fields of both basic and derived variables including dynamical balances. Forecasting skill is determined by the inherent limits of predictability of the underlying dynamical system together with the kind and method of data assimilation.

Systems for accurately nowcasting and forecasting ocean fields must have both modeling and sampling components. Here sampling is used synonymously but more aptly for measurement, observation or data. In advanced systems, modeling and sampling components are intimately linked by design. Sampling initializes the model which then produces diagnostic and prognostic fields. These fields including their error estimates are used to guide further sampling. This adaptive sampling is assimilated by the model in a feedback loop designed to minimize forecast error. Time delay, the content and the spatial structure of the sampling are critical factors in the performance of the system.

The system currently under development for nowcasting and forecasting functions as a hierarchical network. This architecture provides flexibility and timeliness in model-sampling interaction. Within the overall system, the sampling component is a subsystem called the Autonomous Ocean Sampling Network (AOSN). Advances in the modeling component (models capable of data assimilation and error estimation) are reviewed elsewhere. Here, the status of the AOSN through the first quarter of FY97 is reviewed.

Autonomous Ocean Sampling Network

Ocean nowcasting and forecasting problems are not new. What is new and exciting is the possibility for major advances enabled by recent technology. Current modeling capabilities reflect advances in CPU speed, parallel processing and mass storage. Sensors for various properties have improved steadily in recent years, capitalizing on advances in microprocessors, fiber optics, materials and microelectromechanical machining. In contrast, platforms necessary for measurement of spatial property gradients remain relatively primitive. With current trends, overall forecasting system advances will be increasingly platform limited. Thus an initial focus of the AOSN is on platform development and control. As network based sampling evolves, its most valuable component will shift from the hardware elements to the software operating system.

An AOSN consists of a number of fixed and mobile nodes with desired sensors configured to sample property gradients in an arbitrary ocean volume with a specified resolution and precision. The mobile nodes are small, smart, autonomous underwater vehicles (AUV's). In the near term, the fixed nodes are moorings. Most of these moorings are likely to be subsurface, but some surface expression is needed within the network for connectivity to the overall system. In the far term, current state-of-the-art moorings will disappear, and three classes of AUV will constitute an AOSN: temporary node vehicles, water column sampling vehicles and server-communication vehicles. Temporary node vehicles will be designed to perform the three principal functions of fixed nodes (subsurface moorings near term) in the network: navigation, energy storage, and time series/tomographic sampling. Water column sampling vehicles carry a variety of sensors to adaptively map evolving spatial gradients, functioning much as they do today. Server-communication vehicles will provide supervisory

intelligence and control and data storage for clusters of water column vehicles and higher level network connectivity for data and command interchange.

Initial network configuration for a specific sampling mission is a four step process. The measured variable(s) and resolution(s) are determined by identifying the phenomena of interest. The range is determined by the desired ocean volume coverage. Precision is specified by defining acceptable error bounds. Specific sensors, node distribution, number of vehicles and initial sampling strategy are determined to cover the range at the desired resolution and precision. Subsequently, the sampling strategy adapts to evolving conditions. Near term, spatial adaptation occurs through water column vehicle maneuvering. Far term, the network fixed nodes can also adapt since they possess inherent mobility.

Key network advantages include wide aperture volumetric sampling, adaptive sampling based on global as well as local knowledge, flexible control options, energy limitation management and robustness to component failure. Broad network implementation requires interoperability standards in four areas: communication, navigation, energy, and high level software.

Network sampling implies inexpensive, smart AUV's, precise subsurface navigation and reliable acoustic telemetry. The essence of the approach here is deployment of a flexible network of many, low-cost, lightweight vehicles with reliable navigation and communication skills versus using a few expensive, very sophisticated vehicles. To achieve a practical system, the AUV's must remain within a critical cost-size envelope. Large vehicles (greater than 10 m long, 1 m diameter) are too costly to build and operate; small vehicles (smaller than 1 m long, 0.1 m diameter) are too inflexible, at least at the prototype stage, in accepting off-the-shelf sensors and computer hardware. The best vehicle for the AOSN is moderate in size (1 to 3 m long, 0.2 to 0.8 m diameter) and cost ($10K to $50K), with a range exceeding hundreds of kilometers. Compared to larger vehicles, vehicles in this class can be deployed and recovered in rougher seas and off smaller vessels. Docks at nodes are compact with less drag. Low cost manufacturing techniques can be employed. They are more maneuverable in confined environments or near bottom. Higher thrust to mass ratios can be obtained for better control in current shear and turbulence. They are robust to collisions and cause less damage. To keep costs low and reliability high, a modular design is necessary. Modularity is equally important for electronics, intelligence and mechanical construction.

The quantitative advantages of a multiple vehicle approach for time and energy constrained surveys have been discussed in Curtin et al. (1993) and Bellingham (1995). To obtain synoptic data, a survey system must be capable of mapping an ocean structure faster than significant changes occur in that structure. For the coastal front example, tidal forcing may dictate a complete survey every six hours and typical cross-front gradients require a minimum spatial resolution of 0.5 km. Based on a minimum energy constraint, the optimum number of vehicles for surveying a given phenomenon scales as the area of the region surveyed and inversely with the required resolution and completion time. The optimum vehicle number increases weakly as vehicle size increases and as hotel load decreases. An assumption in the analysis is that the vehicle size remains constant. For the same total track coverage, the larger the vehicle number, the lower the expenditure of energy by a single vehicle. Therefore, smaller vehicles are possible as more vehicles are used, tilting the energy efficiency arguments even further in favor of multiple vehicles.

Technical issues in control, communication and navigation include integration of autonomous mission management and human supervisory control; performance predictability of autonomous mission management; integrated reliability within an adaptive control environment; control latency through long range acoustic communication links; arbitration of behaviors with competing objectives; gradient mapping, docking path optimization algorithms; collision resolution multiple access acoustic data transfer among multiple vehicles in close proximity; integrated undersea-satellite network communication architecture and protocols; optimum search strategies related to mission goals, sensor diversity, and communication constraints; measures of effectiveness in group performance; convergence of acoustic navigation precision by bootstrap methods; efficient stabilization in wave and turbulent environments; and optimal initial deployment of multiple vehicles for efficient adaptive behavior. Technical issues in propulsion and power include optimization of buoyancy driven vehicles; high pressure battery charging; and efficient, robust underwater power coupling. Technical issues in sensors include real time tomographic inversion techniques only for acoustically focused sampling.

AOSN System Elements

The principal AOSN system elements are AUV's (propeller-driven, buoyancy-driven), AUV docking, navigation, acoustic communication, radio communication, energy, network control and sensors. Progress in each of these elements is reviewed below.

AUV'S

Typical prototype small, high performance, propeller driven vehicles in this class are Odyssey, Ocean

Explorer and REMUS. Each is a mobile instrumentation platform with actuators, sensors, and on-board intelligence designed to complete sampling tasks autonomously. For example, Odyssey is 2.1 m long, has a maximum diameter of 0.6 m, and is rated to a depth of 6700 m. A free-flooded plastic shell shaped by vacuum forming provides a low-drag hull with a cost under $1K. Inside the hull is a selectable pressure case, standard glass instrumentation spheres for deep ocean work, and a variety of subsystems such as water property sensors, propulsion motor, control surface actuators, and sonar transducers. Figure x shows range versus speed curves (h = 0.35, D = 0.005 at 1.5 m/s). Note that as hotel load reduces, the maximum range is achieved at lower speed. Odyssey has been deployed in a variety of settings including the Arctic and Antarctic, Haro Strait near Vancouver Island and off New Zealand.

To improve the stability of propeller driven vehicles in a surface wave field, an accurate hydrodynamic model of an AUV thruster in being developed that provides accurate closed-loop thruster control in unsteady conditions with inputs of angular velocity and torque (Grosenbaugh, 1996). The model is being developed through both numerical simulations and experimental measurements under steady and unsteady operating conditions. The simulation will be based on the numerical vortex-lattice, lifting-surface theories developed at MIT and reported in Kerwin and Lee (1978) and Keenan (1989). Initial results show the significant effect of fluid dynamics on the thrust and torque. Because torque can be measured through motor current, current can be used to construct an accurate measure of the flow velocity at the propeller blades accounting for the hydrodynamic effects on the thrust.

Typical prototype buoyancy driven vehicles are Slocum and the virtual mooring glider. These small, near neutrally buoyant platforms move vertically and horizontally through the water as a result of small changes in buoyancy. Two versions of Slocum are under development. For the open temperate and tropical ocean, Slocum derives its propulsion power for a 2000 m deep sawtooth ascent/descent from a unique heat engine which utilizes heat flow from the warm surface to the cool deep water. By exploiting thermal energy from the environment, a 5 year, 40,000 km duration is feasible. An interactive network of such vehicles is particularly suitable for sampling large scale ocean processes. In areas of inadequate temperature differences to power propulsion, including shelf waters, the same vehicle is fitted with a battery operated buoyancy controller (similar to that used in ALACE) and can operate with a 40 day, 800 km duration. Gliders are slow speed AUV's and must be used with care in high current areas. They are quiet but not silent in operation. High efficiency (no external control surfaces) but slow rate maneuverability has been achieved with internal control of the center of gravity. This class of vehicle is poor at precision docking but excellent at station keeping within a given area, for example, sampling for years within a few kilometers of a fixed position.

Vehicles that are rugged and capable of complex missions with abstract goals (e.g., find and map the main convergence field in a coastal frontal zone) rely on a library of intelligent control algorithms. Capabilities that are becoming part of a vehicle's intelligence include rendezvous and docking, survey, gradient following, obstacle avoidance, adaptive sampling, terrain following and fault detection and recovery. Reconfiguring vehicle software for a range of missions, sensor types and performance must be straightforward since this reconfiguration will often be accomplished remotely through satellite or acoustic links.

New sensor technology may challenge onboard data management. The utility of continuous, non-linear, higher dimensional geometry in representing geophysical database information and managing uncertainty is being explored (Patrikalakis and Bardis, 1991). Such approaches are attractive where gradients are of primary interest.

AUV Docking

Docking is most important for energy management. Developing a reliable, low cost, universal docking system is a high priority for long term network operability. A number of methods are currently being investigated. Target geometries include a water column vertical stanchion with omnidirectional horizontal approach, a water column orienting cone with directional horizontal approach and a bottom mounted arresting deck with omnidirectional approach. Each geometry has its own precision latching mechanism for power and data transfer. Terminal homing has been achieved using high frequency acoustic, optical and electromagnetic systems. Sea trials are continuing with each of these approaches. It is not clear at this time which combination of techniques will be most cost-effective and robust. A goal is to converge on a common prototype system within the next year.

Optical docking hardware and software designed to sense and home to a 40 Hz chopped light source has been modified and integrated with an Odyssey test vehicle (Cowen, 1996). This docking system performed reliably: achieving acquisition ranges of up to 28 meters in the relatively clear, shallow water of Buzzard1s Bay. Various search strategies were attempted: the out-and-back and survey raster missions proving most successful, but even unsuccessful strategies provided valuable system performance data. Optical data couplers designed to

transfer data from the ULITE acoustic sensor array at its native rate of 1.1 Mbit/sec have been implemented. The new data coupler design utilized an array of IR-LED emitters, making it less sensitive to misalignment than the previous implementation. Tests in San Diego Bay have demonstrated autonomous handoff from acoustic to optical guidance. Latching and switching into data transfer mode were accomplished via manual switch over, and the vehicle's return to the pier was also accomplished under manual control. This is the first time that high speed digital data from an underwater surveillance array has been transferred in real time to a remote user with the data connections established after array deployment, broken off and reestablished multiple times. This demonstration represents a new benchmark in the capability of underwater surveillance technology and enables an entirely new data flow architecture based upon the agile establishment of fiber optic data links upon demand. Overall acoustic acquisition range of the prototype hardware is expected to approach 300-350 meters using the current 170 KHz acoustic homing system and the size of the sweet spot for acoustic-to-optical handoff is expected to become much larger, hence less critical, in typical coastal waters such as are located a few kilometers off the shoreline of Southern California.

Navigation

No single technique provides a broadly applicable navigation solution for small, long range AUV's. A variety of technologies exist today, including radio and satellite systems, long, short and ultra short baseline acoustic systems (Abbott, 1978; Baron, 1987; Bellingham, 1991, Jacobsen, 1985; Elliot, 1984), acoustic doppler and correlation speed logs (Dickey, 1978; Bookheimer, 1984), inertial systems (Johnstone, 1988) and terrain following techniques (Geyer, 1987). Radio and satellite navigation require the vehicle be at or close to the surface, long baseline acoustic navigation accuracy degrades at long ranges, and inertial systems have relatively high error levels for slow moving AUV's. Combining complementary techniques is one way to achieve improved performance, for example, using both Doppler sonar and inertial navigation (Hutchison, 1991). For long baseline acoustic navigation, accuracy is being iteratively enhanced through timely feedback of the measured sound speed field into onboard acoustic propagation models. Such approaches enable matched field processing to be used in real time by constraining the domain of the solution. In the Arctic, a location precision of 1 m over a range of 10 km has been achieved by capitalizing on multiple arrivals from navigation beacons (Deffenbaugh et al., 1993). Similar gains may be realized in shallow water environments by using multipath arrivals.

The efficacy of DGPS aided DVL based navigation of small AUV's in shallow water using commercial off the shelf systems has been demonstrated. This provides the potential for long range and long duration operation of AUV's without requiring pre-installation of an LBL beacon array. This mode of navigation requires the vehicle to surface periodically to get a GPS fix. This has been demonstrated in up to 3 foot seas with the AUV underway. GPS units that can take advantage of a 2-D sea level solution provide better accuracy than 3-D only solutions. Repeatable fixes are obtained with better than +- 1.5 meter accuracy. A simple sensor fusion scheme successfully combines dead reckoning position estimation with DGPS fixes without requiring a complicated Kalman filter, although at reduced accuracy. The DVL velocity measurements are adversely affected by vehicle self-motion when the vehicle is on or near the surface. More detailed analysis of the errors and navigation accuracy of the DVL in this application is underway (Smith, 1996).

Acoustic Communication

The network is linked underwater with acoustic modems on mobile AUV's and at stationary nodes. The modems communicate adaptively and establish routing in response to changes in acoustic paths and ambient noise (similar to RF cellular telephone systems). State-of-the-art acoustic modems are capable of 10 kbit/s data rates at 10 km range and 3 kbit/s at 90 km (Catipovic et al., 1993). Energy efficiency varies from 1 Kbit/joule/km with off-the-shelf commercial modems (e.g., Datasonics) to 100 Kbits/joule/km for research prototypes. These ranges and data rates enable efficient telemetry of commands to AUV's and transfer of modest amounts of data.

Efforts are underway to to determine the impact of inaccuracies in impulse response estimates on communication efficiency, such as equalizer divergence and bit error rate (Caimi, 1996). The closer to reality the initial estimate, the faster the convergence of an adaptive system. Knowledge of the impulse response will provide an estimate of system capacity, a necessary variable to adjust the transmission rate and the operational frequency of modems. An database of impulse responses from diverse shallow water environments of operational and scientific interest is being created as a resource for design of acoustic communication systems and for simulation and evaluation of their performance.

An adaptive beamformer front-end that can be used with most commercial modems to provide high data rate performance(>200 k baud) for transmission of video information from AUV's is being developed (LeBlanc, 1996). The method is based on separating signals received by an acoustic array into statistically uncorrelated components (Principal Components).

The Principal Component Beamformer is an array time series data reduction method that provides statistically uncorrelated components of wave energy arriving at an array of acoustic sensors. The method can be used to discriminate signal from noise, or interference by selecting the principal components of wave energy. Direction of the sources of wave energy are easily established by applying a beamforming vector to each principal component. Initially, the Principal Component Beamformer has been used to analyze experimental data taken in shallow water environments. Results indicate nearly complete separation of the coherent spatial components of the pulsed noise transmissions. The eigenvector beamformer collects correlated energy over a time scale corresponding to the inverse of the bandwidth. The eigenvectors can be calculated and updated on a continuous basis and utilized to spatially filter multipath corrupted transmissions. If the transmitted data is broad in bandwidth, it in itself can be used to provide the channel characterization and obtain the desired spatial transformation, all done without the use of special training sequences. This year, the Principal Component Beamformer will be used as a spatial filter for use with high performance modems.

For reliable AUV control and monitoring, a Utility Acoustic Modem (UAM) is being developed that adapts with a coherent equalizer algorithm and multicarrier modulation (Brady and Preisig, 1997) to maintain a fixed bit error rate (Johnson, 1996a). The UAM uses a TMS320c44 processor at 60 MHZ operating the Acoustic Modem System V3.0 (Johnson, 1996b) with 6 MB of static RAM and 1 MB of flash RAM. Included are two full duplex asynchronous serial ports, software selectable input and output lines, counter/timer and wake up lines, and analog input. Power consumption is typically 30 W transmit for 180 dB source level, 8 W receive for 60 MFLOP decoding, less than 30 mW standby (instant wakeup)and less than 1 mW hibernate (internal battery). The UAM is designed for a four element hydrophone array. UAM field testing is scheduled for Spring 1997. An automated underwater acoustic testbed has been designed and assembled (Brady and Preisig, 1996). Two mooring-deployed PC's control the single-source transmission and 8-channel reception of acoustic signals in the 10-22kHz band. These PC's are connected via radio ethernet to a ship-bound laptop PC. From the laptop, the user may control the transmission of signals, or allow the transmission and acquisition to run autonomously. Two trials of the testbed in Woods Hole Harbor have enabled coherence characterization of the shallow-water acoustic channel with 1-2 knot platform mobility. Results indicate that over the maximum array aperture possible with the Odyssey vehicle (approximately 1 meter), the different multipath arrivals are incoherent but arrivals of signals over the entire aperture via a common path are highly coherent, even with averaging windows of several seconds. This work will impact the structure of both modulation schemes and demodulation algorithms. Odyssey noise characterization has been performed and will be used to finalize communication signals and error-correction coding for reliable demodulation by the vehicle-bound modem. Several candidate modulation schemes for high reliability and reduced decoding complexity have been designed and signals using these schemes have been transmitted. A network modulation and demodulation algorithm will be implemented in the prototype UAM by March 1997 and a working version will be implemented in time for a May 1997 deployment.

A low cost means of providing multiple vehicle acoustic communications has been designed this is critical to cooperative sampling strategies and also for shepherding of multiple vehicles (Smith, 1996). The communications and control interface architecture on the Ocean Explorer provides a scalable approach to remote monitoring and control of AUV's. Placing the acoustic modem as a node on the LonTalk network allows for direct communication with any other node on the network without first passing through the main computer. This allows direct monitoring and control of vehicle subsystems and allows transparent diagnostics without rewriting main vehicle code every time a payload or subsystem is added or modified.

Low-to-medium data rate secure communications at speed and depth are important for current Naval operations. Gains of over 300 to 1 in data rate throughput over traditional (noncoherent) signaling methods have been demonstrated under non real-time experimental conditions. Signal processing improvements have been achieved using adaptive channel equalization techniques which permit multipath compensation in both deep and shallow water environments. An Advanced Technology Demonstration in Tactical Acoustic Communication will establish operational benchmarks using fleet assets. Reliable sub-to-ship and ship-to-sub communications will be demonstrated at 10 kbps over 2.5 nm and 2.4 kbps over 35 nm by 1999.

High-compression encoding transform(s) for transmitting multispectral image data across noisy, low-bandwidth acoustic uplinks are being developed (Caimi, 1996b). Two commonly-available image transforms (JPEG and VPIC) have been tested. JPEG exhibits insufficient image quality to support high compression (compression ratios CR > 40:1). In contrast, VPIC produces acceptable images up to CR = 50:1, but lacks the rigorous error control present in transforms such as vector quantization. Low-loss VPIC codebooks that have rigorous error bounds are

being derived. In addition, a fast high-compression transform called BLAST (Blur, Local Averaging, Sharpening, and Thresholding) has yielded visually acceptable underwater images at compression ratios of 75:1. BLAST produces mean-squared errors equivalent to EPIC (Efficient Pyramid Image Coder), a leading experimental compression method, but with much less computational overhead. Also, BLAST's output error is more uniformly distributed spatially. Plans are to use error-detecting and correcting codes, where feasible, together with a limited number of marker blocks to render the compressed image transmission robust in the presence of channel noise.

Radiofrequency Communication

A complete AOSN system includes a radio frequency (RF) link to the user, either satellite for long ranges or a line-of-sight RF modem for ranges of 10 to 20 km. The currently available ARGOS system will be supplanted by low earth orbiting microsats, C-band commercial communication satellites and/or the global cellular telephone satellites (Iridium), all with much higher data rates and downlink capabilities. For coastal work, 920 MHZ digital RF systems are capable of transmitting from 200 kbits/s to 2 Mbits/s at modest power levels using familiar TCP-IP protocols. This allows simple interfacing to commercially available workstations for data display, archiving, and adaptive experiment control.

A satellite datalink that supports global coverage using existing satellites, providing a two way capability with throughput 10 to 100 times that of ARGOS for the same cost, is being developed (Gamache, 1996). The system has a hub/spoke architecture with a forward and return link, both operating at C-band, using existing INTELSAT geosynchronous satellites and global beam transponders to provide global coverage with as few as 3 hubs. The system takes advantage of the latest digital signal processing technology, with most processing implemented in software including spectral spreading to prevent/minimize interference. The system also includes innovative RF and antenna technology in order to provide the small, low cost package envisioned. The low cost C-band patch antennas developed specifically for this effort can be as small as a quarter. Hardware system design has been completed. Software high and low level design is complete and being tested. The modem hardware is currently in fabrication. Special C-band patch antennas have been designed, built, and tested. The datalink receiver RF has been designed and is being tested; the transmitter design is complete pending further funding for implementation.

Energy

The network approach greatly reduces energy limitations through both platform diversity and cache storage capacity at docks. Although energy capacity (W-hr/kg) of an individual vehicle is an important variable, large energy capacity is useless without the required power delivery (W/kg). Currently, only electric batteries are practical for small, inexpensive AUV's, although other energy storage systems (e.g., fuel cells) may prove competitive. Although onboard battery capacity limits the sampling capability of individual AUV's, most sampling objectives can be achieved within the limitations of state-of-the-art battery technology by adjusting variables (e.g., number of nodes, number of vehicles, duty cycle, trackline traverse relative to existing currents). Cells with known recharge behavior, noncatastrophic failure and capacity at low temperature are desirable.

A number of technologies for AUV power management, power transfer, and in-situ recharge are being developed. The objectives of this work are to demonstrate in the field: (1) autonomous energy transfer from a mooring to an AUV at a high rate (200 W) and with high efficiency; (2) in-situ recharge of secondary cells in an unattended AUV operating within an AOSN; (3) intelligent power-management on both the stationary and mobile elements of an AOSN; and (4) performance the above technologies in a field deployment of a prototype AOSN.

An inductive coupling for power and data has been installed in an Odyssey-class AUV. Bench tests demonstrated a continuous transfer of over 200 W into the vehicle, with 84% overall power-transfer efficiency throughout a 10-hour test. The coupling simultaneously provided 10-base T ethernet performance, transferring over 7 million packets with no errors. A baseline design for the battery system has been developed. The possibility of pressure-compensating small Ag-Zn or Li-ion cells is currently under investigation. A novel, isolated method for measuring the voltage of individual cells in a series stack has been developed and demonstrated. The first set of field tests occurred in mid-November 1996. Future tests are scheduled for April 1997 (in-Situ recharge in shallow water), September 1997 (deep-water trials) and January-April 1998 (Deep-Convection ARI in the Labrador Sea).

Network Control

To support the development of an AOSN, an Ocean SAmpling MObile Network (SAMON) Controller is being developed as a hierarchically distributed command and control concept for a multi-vehicle tactical semiautonomous underwater oceanographic and environmental data collection system (Phoha,

1996). This effort involves the implementation of a simulation testbed facility for the design, analysis, and refinement of AOSN systems in a realistic environment. Objectives include: (1) implementation of a multi-vehicle self-organizing ocean sampling system simulator with a hierarchical autonomous control and inferencing architecture, (2) quantitative justification of intelligent inferencing at each of the layers of the control hierarchy to circumvent limitations of sensor data, communications and equipment failures, and (3) development of a simulation testbed facility, capable of interfacing with independently developed technologies for the simulation and evaluation of AOSN components. The Ocean SAMON Controller is conceived as a hierarchy of four operational levels: a Tactical Coordinator (TC) that sends commands to a collection of supervisory autonomous underwater vehicles (SAUV's), the second level, each of which in turn sends commands to a collection of autonomous underwater vehicles (AUV's) under its control, the third level. Each autonomous unit (SAUV or AUV) has responsibility to find and query fixed sensor packages (FSP's), the fourth level, fixed sensors that have been deployed in the area. The mathematical foundations of the hybrid hierarchical control architecture for the Ocean SAMON Controller stem from recent developments in systems theory [Phoha 92, Ozveren 92, Ho 89] which extend classical control theory concepts to characterize the time evolution of spatially distributed, interactive, discrete event driven, autonomous systems. In research funded by CECOM and the Army Research Office, this automaton-based approach was used to simulate digitized battlefield command and control models and was extended to multi-level hierarchies [Phoha 92, Peluso 94, Peluso 96]. The Perception/ Response controller architecture [Stover 92, Gibson 94, Stover 96] provides a hybrid (continuous/ discrete) vehicle controller architecture. This architecture, proven effective by in-water testing conducted at Dabob Bay and Nanoose in April-May 1995, incorporated new fuzzy logic technology for pattern recognition, classification and situation analysis, and a simplified architecture developed for on-board planning and plan execution. All nodes of the AOSN hierarchy are viewed as having a common component architecture. The Ocean SAMON Controller implements this commonality in a modular, configurable code, called the SAMON Intelligent Controller (SIC), that can be loaded into the on-board processors of each vehicle in the network. At deployment, each vehicle is configured either with or without the supervisory module activated. This approach provides for (1) ease of development and maintenance, in that only one controller needs to be designed, and (2) network reconfiguration flexibility, in that vehicles can assume various roles as necessary. A modular approach is being taken to the design of the simulation testbed facility to allow for the simulation and evaluation of independently developed AOSN components.

The hybrid hierarchical controller architecture has been implemented in a scalable nominal simulation, consisting of a Tactical Coordinator and two AUV's, one configured with the supervisory module activated. This simulation demonstrates the system's self-organizing capabilities and facilitates the study of observability issues. Appropriate interfaces have been implemented for the following simulation components: basic vehicle (autopilot, sonar communications package, radio communications package), environmental models, and sensor models. Graphical user interfaces include a Tactical Coordinator interface as well as Ground Truth. The Tactical Coordinator interface provides the ability to monitor and control the network from the Tactical Coordinator's point of view. The Ground Truth interface provides the user with various real-time displays of the simulated scenario information. Comparison of the Ground Truth data with the Tactical Coordinator's observed data provides a means for performance measurement and hypothesis testing. Additionally, a Ground Truth interface allows for the controlled perturbation of the system, thereby exercising the network's robustness.

Simulation testing has demonstrated the Ocean SAMON Controller's ability to provide AOSN vehicles with self-organizing capabilities. The SAMON architecture has been evaluated using development scenarios, and message passing capabilities among modules have been verified. The SAMON Intelligent Controller resident in the vehicles has been prototyped and debugged. Its ability to operate under self-organizing, nominal, and selected exceptional conditions has been verified. The controller software can be downloaded into AOSN vehicles, providing a robust and affordable approach to autonomous, distributed network operation and control. By augmenting the vehicles with an appropriate suite of sensors, this system offers a new approach to difficult problems as such mine hunting. The developing testbed facility can be utilized as a simulator for testing independently developed AOSN components. Simulation and evaluation of such components in the laboratory presents a cost effective method for the evaluation of component performance and the resolution of interoperability issues.

A complementary two-tiered approach to organization and reorganization of AOSN's that seeks to be both efficient and adaptable to changes is also being developed (Blidberg and Turner, 1996). Two organizations are used: a task-level organization

(TLO) that actually carries out the tasks of the mission, and a meta-level organization (MLO) that designs the appropriate TLO for the particular set of environmental, mission, and AOSN-related features present. The MLO provides flexibility and adaptability, freeing the TLO to be designed to be as efficient as possible. A major part of this work is designing the protocols and mechanisms necessary for control of an AOSN. In the MLO formation phase, each vehicle and instrument platform (VIP) that is capable of participating in a cooperative distributed problem solving system tries to find other, similar VIP's by broadcasting and waiting for replies. At the end of this phase, a loose, peer-to-peer organization has been formed comprised of these agents. During the next phase, the newly-formed MLO shares knowledge among its members about their own capabilities and broadcasts messages to determine what other resources are available. At the end of this phase, the MLO has information about the total capabilities and resources of the AOSN. Next, one or more of the MLO agents decides on an appropriate TLO for a desired mission by matching capabilities of the known agents with the task requirements. Initially, only hierarchical organizations are being considered. At this stage, control of the AOSN typically passes from the MLO to the TLO to carry out its mission. Errors and inefficiencies may be corrected by the TLO itself by reallocating its resources or by a re-formed MLO in extreme cases. Simple protocols for these phases have been implemented in a simulation testbed. Two kinds of MLO (hierarchical and "flat") are being investigated to examine the benefits and disadvantages of each (in terms of message traffic, time to create, etc.). Entry/exit protocols for VIP's and user control of some or all of the AOSN will also be implemented in the coming year.

Sensors

A 16 channel quantitative sonar has been developed for measuring buried target strengths and volume scattering strengths as well as for collecting data used in the developing 2D and 3D imaging and classification algorithms (Schock, 1996). This sonar is designed to measure target strengths with an accuracy of less than 1 dB. The two way transmission loss, used in the target strength measurement procedure, is calculated using sound speed and attenuation measurements directly estimated from the reflection data. The two way transmission loss and the measured aperture function of the transmitting and receiving arrays are used to measure volume scattering strengths as a function of depth under the seabed. The output of the beamformer is a vertical slice of the seabed. A vertical slice is generated immediately after each transmission. The pixel data in the 2D slice is placed in a 3D matrix at positions that account for along track translation between transmissions and vehicle pitch and roll. Targets are detected by searching for edges and increased regions of energy in the data set. The analysis of images will determine the target echo strength to scattering noise ratio that is required for automatic target logging and identification. Automatic target detection is critical for the buried object imaging application because 2D slices are being generated every 50 msec so the data rates are too high for real time visualization. The 3D data matrix of image pixels must be searched for targets and then each target must be displayed for the operator showing different slices of the target. Once a sonar model is developed for predicting buried object detection and classification and a database of volume scattering strengths and buried target strengths is collected, the sonar will be adapted for AUV operations. 2-D vertical slices of pipes buried under seabed have demonstrated the potential of this approach for locating buried objects. Reflection off the top and bottom of a 18' diameter pipe (lying horizontally) buried 1.5 meters under the seabed can be clearly detected in slices generated from a single 20 msec long 2-10 kHz FM transmission.

A chirp bathymetric sidescan sonar system for use on AUV's is being developed (Stewart, 1996). The new design will use low-cost, high-performance analog and digital electronics to minimize power consumption, reduce system noise, and maximize the dynamic range of the system. A variable number of modular digital signal processors (DSP's) will be used for environmental characterization, clutter rejection, and quantification of survey performance. Such performance metrics can be derived from environmental measurements (bathymetry and acoustic backscatter) combined with predictions from a real-time, onboard acoustic model. The new hardware design has been completed, and a prototype assembled and tested. Dockside trials included a test of all prototype hardware components and comparison of benchmark data collected simultaneously with the proven DSL-120 bathymetric sonar system. Data analysis confirms the validity of the hardware design and the expected advantages of new algorithms for multi-receiver chirp processing. The system will be tested on the Explorer AUV in 1997.

Two high resolution, high refresh rate, forward looking sonar systems (Forward Scan, FS; 3-D Forward Look, FL) for use on Ocean Explorer (OE) class AUV's are being developed (Cuschieri, 1996). The physical size is a compromise between required resolution and power consumption. Improved efficiencies in the power amplifiers on the source side and the conditioning amplifiers on the receiver side are being explored. Tank tests have verified the

operation of both sonar systems. The approach used is based on a theoretical model for a thin elastic shell in an unbounded fluid medium. Scattering results and target strength for incident plane waves in the frequency range of operation of the FS and 3-D FL sonar systems (200KHz - 250 KHz) have been developed. The FS sonar system is now being transitioned to at sea trials and AUV operation. AUV operation is at present limited by the data acquisition and processing hardware which will be addressed in the upcoming year. Significant improvement has also been achieved on the image quality of the 3-D FL system.

An ambient noise system (ANS) has been developed at for detecting passive targets and to obtain global directivity images of the ambient noise (Glegg, 1996). This system has proven to be a highly efficient low noise passive sonar and has a number of advantages which makes it ideal for AUV operations. First, it makes use of broadband signal processing so that only six transducers are needed to form an image. The low number of transducers reduces the complexity and power requirements which are important issues in AUV applications. Second, the sonar can produce 3D-global directivity images of the ocean noise. When this is coupled with the mobility of the AUV it allows for detailed mapping of the ocean ambient noise over extended area.

A Bottom Classification/Albedo Package (BCAP), a suite of optical instruments to acquire the hyper-spectral database required to deconvolve the components of the underwater and water-leaving light fields, is being adapted for network-class AUV's (Carder, 1996). In situ instrumentation includes a 512-channel upwelling radiometer, a 512-channel downwelling irradiometer, two, 6-channel, intensified bottom cameras, a dual-laser, optical altimeter/ chlorophyll probe, and instrumentation to measure attenuation, absorption, and fluorescence at various wavelengths. Three dimensional micro- topography is measured using a bi-static laser-line imaging system . BCAP has been integrated into Florida Atlantic University's Ocean Voyager II AUV. Eight missions have been performed in the Atlantic Ocean off the Coast of Boca Raton, Florida by the OV-II vehicle with BCAP aboard and activated. In the Coastal Benthic Optical Properties experiment in the Dry Tortugas during August 19-29, 1995, BCAP was deployed both aboard the OV-II AUV and the ROSEBUD ROV. Field exercises included a 3-day cruise in the Gulf of Mexico, TWIST I (Turbid Water Imaging of Submerged Targets) where the prototype micro-topography system was deployed using the ROV, participation in the 12-day CoBOP-96 exercise (with both the ROV and the AUV platforms), which provides baseline data for bottom discrimination, and participation in the 12-day COPE1 cruise (ROV platform) which tested instrument and vehicle performance in the rapidly changing environmental conditions of the Chesapeake Bay plume. The quantity of red light (solar stimulated fluorescence) measured near live bottoms and above sediments was sufficient to allow routine acquisition of fluorescence imagery at 670-700 nm and at 710-750 nm with an intensified (Gen-III-B), multi-channel, video camera. Animals and man-made objects are very distinct owing to their contrast with the bright fluorescent back- ground. Solar stimulated fluorescence was also apparent in hyper-spectral radiometric measurements over grass, sand, and various coral species. The effect of reflected light and fluorescence from the bottom have major impacts on the apparent optical properties near the bottom. This project has shown that the utilization of AUV's as platforms for optical oceanography is not only feasible but is, in many cases, the most effective method for the acquisition of certain measurements, especially near the bottom. The BCAP/OV-II, for example, performing bottom albedo/classification transects at 2 m altitude at a speed of three knots, can complete a one-kilometer, bottom-following, albedo mapping mission in about 11 minutes.

An in-situ sensor which will automatically quantify selected chemical species through existing spectrophotometric techniques is being developed (Byrne, 1996). The procedure will allow the detection of species such as iron, manganese, copper, total metals, phosphate, nitrate, silicate, and sulfide over an extended range of concentrations. The two key technical objectives are to, 'miniaturize' a one meter optical path and couple this optical path with a spectrometer for enhanced detection capability. A material with an index of refraction less than seawater has been identified. Preliminary experiments have confirmed the waveguide effect. Additional tests and modeling are required to determine how changes in refractive index due to temperature, salinity and other gradients can alter the waveguide effect. The amplitude of these effects will determine the liquid core waveguide's suitability with respect to the desired sensitivity. The experimental setup utilizes a fiber coupled pulsed broad band light source, a series of neutral density filters to simulate variable amounts of attenuation, and an Ocean Optics spectrometer. The light source is pulsed at 0.5 Hz and a number of spectrometer scans (i.e. 64, 128, 256, etc.) are acquired. The FFT and power spectral density of each of the 1024 spectrometer channels is computed. Currently, the signal sensitivity is equal to that of standard spectrometers. However, there are several digital signal processing techniques through which the signal can be enhanced.

A high sensitivity, multichannel fluorometric sensor capable of in situ operation for detection and

identification of natural and artificial organic components in seawater is being developed (Coble, 1996). Of particular interest are the fluorescence properties of material leached from samples of authentic plastic mines and various plastic ingredients. High resolution fluorescence spectroscopy results showed that epoxy resins and polyester ingredients used in manufacture of plastics have fluorescence fingerprints similar to mine leachate samples. Major excitation peaks were observed at 235 and 275 nm, resulting in emission between 300 and 410 nm. The double excitation maximum is characteristic of aromatic ring structures, and thus is consistent with mass spectrometry results. The fluorescence fingerprints of the epoxies and polyesters tested are distinct from that of natural organic matter present in seawater and they are, therefore, potential tracers of mines in the marine environment. More data are required to determine the detection range and feasibility of application of this technique outside the laboratory. The three optimal wavelengths determined in the laboratory will be used to design a sensor in 1997. Excitation at 250 nm can be produced by a KrF (krypton-fluoride) excimer laser, and excitation at 235 nm and 270 nm can be reached using a Raman shift of this laser in hydrogen and methane gas, respectively. A compact UV laser system that will use a waveguide excimer laser and be well-suited for use in an AUV is under construction. The size of the laser is about one cubic foot. The remainder of the system will include a spectrometer and silicon detector array to measure the emission spectrum. A Raman cell will be constructed to produce two other excitation wavelengths, if needed.

Small, power-efficient versions of laboratory fluorescent analytical methods are being developed that will enable measurement of nitrate (NO_3), nitrite (NO_2), and ammonia (NH_3)onboard network-class AUV's (Fanning, 1996). Laboratory methods currently achieve detection limits less than 5 nanomolar using standard fluorescence technology. These high sensitivity methods have been successfully applied to detailed investigations of coastal ocean water and have revealed structure considerably more complex than previously thought. These methods typically use flow-injection, wherein a sample is discharged into a reagent stream to react with aniline (or OPA in the case of ammonia analysis) before being pumped to a fluorometer for detection. Here, a three channel (three nitrogenous nutrients), reverse flow-injection method is used, in which reagents are injected into a sample stream, permitting correction for interference due to organic matter. State-of-the-art chromatography software for peak detection and analysis completes the system.

A comprehensive marine particle analysis system is being developed (Hopkins, 1996) The final system (High Resolution Sampler (HRS)) will encompass multiple sensors, both optical and acoustic. Developed sensors will, in the long term, be adapted to AUV platforms to characterize particle fields in estuaries, coastal and oceanic environments. The size spectrum characterized by the instrument suite ranges from submicron to centimeters. The small submicron to 50 um (spherical diameter, SD) size increment is measured with a multi angle-multi wavelength detector using a light- scattering and spectral deconvolution. Particles larger than 50 um SD are quantified with a non-intrusive laser light sheet-video system mounted at the entrance of a particle sampling tube. Also inserted within the sampling tube, down stream of the light sheet-video system, is a pair of collimated light sheets in tandem for size analysis of particles (>250 um SD). An angled, doubled laser, light-sensor will enable "shadowgramming" (identification) of larger (>250 um SD) particles moving through the sampling tube. Verification systems include a plankton cod end (162 um mesh) carousel (20 positions) at the effluent end of the sampling tube and a horizontal rosette of 500 cc water bottles to capture small particles.

Implementation

The implementation strategy is to capitalize on state-of-the-art technology and proceed systematically in a series of well-defined, progressively more complex basic and applied missions. Critical in this process are the experience and feedback gained from specific field experiments at each step. Success will lead to today's research vessel becoming the"mainframe" of ocean sampling and the AUV, the "PC", within reach of individual investigators and networkable in an open architecture established by AOSN development.

High Resolution Mapping of Coastal Fronts

A collaborative, multi-disciplinary experiment centering around the scientific problem of understanding the tidal and estuarine driven fronts in Haro Strait, British Columbia has been carried out (Schmidt, 1996). Participating institutions were MIT (AUV's, acoustic navigation and tomography), WHOI/AOPE (moorings, acoustic communication), and IOS (coastal oceanography),UVic (low-frequency acoustic tomography), WHOI/MB (marine mammals), and Harvard (circulation modeling and data assimilation). The Haro Strait experiment was successfully executed in June-July 1996. Four vertical acoustic arrays (nodes) were deployed, with 3 operating throughout the major part of the experiment. An Incidental Harassment Authorization was obtained form NMFS, allowing the experiment to operate the various acoustic sources in Haro Strait with its large Killer Whale and Porpoise population (Miller, 1996). A wireless LAN was established yielding real-time data rates of 35

kB/s with 1 Gb local storage capability in moorings. Tomography data were collected in three frequency bands, 0.5 kHz, 1.5 kHz, and 15 kHz. AUV transmitted tomography/navigation signals were recorded on vertical arrays. The central component of the acoustics effort was the development of robust matched field approaches for integrated source localization (navigation) and environmental tomography. Using fixed and moving AUV sources, the acoustic multipath signals were recorded on 3 or more vertical arrays, deployed around the frontal area, with a horizontal aperture of 1-2 km. A physics-based multipath identification approach is combined with a linear inversion procedure to yield simultaneous, high-resolution estimates of AUV position, and environmental parameters. These estimates were then used as a basis for real time adaptive control of vehicle sampling strategy. More than 60 AUV missions were successfully completed, with scientific data collected by on-board CTD, ADCP, and surface-imaging sidescan sonars. Adaptive sampling was further demonstrated using forecasts from the Harvard model with data assimilation. In support of the tomographic inversion effort new formulations for acoustic propagation in stratified flow have been developed and implemented in propagation codes such as KRAKEN and OASES, and new more robust parameterizations have been implemented. Analysis of the comprehensive data set continues through 1997.

Seafloor Acoustic Properties, Geologic Mapping and Sedimentary Processes

The objectives are to understand and quantify the natural geologic variability of the nearshore seafloor in different testbed geologic, hydrologic and energy environments (Indian Rocks Beach, Boca Raton, Dry Tortugas), and to assess the significant parameters which contribute to the acoustic response of the seafloor (Hine, et al., 1996). Real-time studies during the passage of a storm provide a measure of the episodic spatial and temporal changes that occur on the seafloor under high-energy conditions, and the potential impact on the burial or exposure of mines or other objects. The data contribute to the precise characterization of the seafloor by AUV acoustic remote sensing. The testbed sites have been investigated and defined in terms of the physical and acoustic properties of the sediments and rocks, and the general geology and geomorphology. These sites are now suitable as AUV test beds. The data acquired by towed vehicles (chirp sonar, sidescan sonar, seismic) using differential GPS provide a geologic, geographic and geoacoustic baseline for AUV testing and calibration. Off-nadir acoustic backscatter (sidescan sonar) is primarily a function of sediment characteristics (grain-size, mineralogy, bottom roughness) as opposed to simply bottom relief. The Ocean Voyager II AUV with a 60 kHz sidescan sonar will be deployed spring/summer 1997 in the Boca Raton and Indian Rocks Beach sites to evaluate navigation precision and the quality of AUV-acquired data compared to that acquired by towed platforms.

Deep Ocean Convection: Labrador Sea Experiment

A three month deployment in winter 97-98 of a three node AOSN in the Labrador Sea is planned as part of the ONR Deep Oceanic Convection ARI. While deep convection plays an important role in global heat transport between low and high latitudes, it is not well understood, in part because it has been poorly observed. Challenges to measurement of deep oceanic convection stem partly from the hostile conditions of the North Atlantic during February through April, the period in which convection reaches its peak, and partly from the episodic nature of the process. Thus the AOSN deployment in Labrador Sea, while extremely challenging, provides a previously unavailable ability to obtain both spatially and temporally distributed observations of convection events in a reactive, repetitive manner.

Conclusion

Nowcasting and forecasting ocean variability with demonstrable skill requires modeling and sampling systems designed to work together. A principal motivation for the AOSN is economically feasible ocean sampling for rapid environmental assessment, rigorous hypothesis testing and long term monitoring. The AOSN provides the mobility necessary to measure spatial gradients and the controllability necessary for adaptive sampling to bound errors and trigger on events. Recent advances in technology present an unprecedented opportunity to create a new generation of intelligent tools for ocean science, resource management and defense. A phased development plan is being pursued which coordinates government, industry and academic efforts. Success depends on sustaining three processes in parallel:

(1) Addressing specific science questions through a series of progressively more complex experiments. In-situ experience, persistence and feedback are essential. Results of these experiments must be published and have an impact.

(2) Evolving an engineering infrastructure that closely couples engineering research with science and operational missions. Since the network architecture will be an open one, consensus on some standardization for communication, navigation, energy and control algorithms will be necessary.

(3) Commercializing the tools to insure economical production and service of system components that can be readily networked. The AOSN approach

depends critically on low unit cost and high reliability.

References

Albus, J.S., 1988: System Description and Design Architecture for Multiple Autonomous Undersea Vehicles, NIST Tech. Note 1251.

Bellingham, J.G., R. Beaton, M. Triantafyllou, and L. Shupe, 1989: An autonomous submersible designed for software development, Proceedings, Oceans 89, Mar. Tech. Soc.,799-803.

Bellingham, J.G., T. Consi, R. Beaton, and W. Hall, 1990: Keeping layered control simple, Proceedings, AUV 90 Conference, 125-131.

Bellingham, J.G., C. Goudey, T.R. Consi and C. Chryssostomidis, 1992: A small long range vehicle for deep ocean exploration, Proceedings, Intern. Offshore & Polar Engineering Conf., San Francisco, 151-159.

Brooks, R.A., 1985: "A Robust Layered Control System for a Mobile Robot", Mass. Inst. Tech., Artificial Intelligence Memo #864.

Catipovic, J., D. Brady and S. Etchemendy, 1993: Development of underwater acoustic modems and networks, Oceanography, 6(3), 62-69.

Catipovic, J., L. Freitag and S. Merriam, August 1991: Underwater acoustic local area network for ROV and instrument communications, Proceedings, AUV-91 Conference, 447-461.

Curtin, T.B., J. Bellingham, J. Catipovic and D. Webb, 1993: Autonomous Oceanographic Sampling Networks, Oceanography, 6(3), 86-94.

Elliot, S. and R. Olson, 1984: Vehicle tracking using advanced acoustic technology in an ultra short baseline system, Proceedings, ROV 84, Mar. Tech. Soc., 42-44.

Geyer, E.M., P.M. Creamer, J.A. D'Appolito, and R.G. Rains, 1987: Characteristics and capabilities of navigation systems for unmanned untethered submersibles, Proceedings, Fifth International Symp. on Unmanned Untethered Submersible Technology, 320-347.

Huiyong, L., 1984: An auxiliary navigation system for an autonomous underwater vehicle, Proceedings, Oceans 89, Mar. Tech. Soc., 604-609.

Jacobsen, H.P., R.A. Klepaker, F.T. Knudsen, and K. Vestgard, 1985: A combined underwater acoustic navigation and control system, Proceedings, ROV 85, Mar. Tech. Soc., 52-56.

Johnson, M. Stojanovic, L. Freitag, 1997: Improved Doppler tracking and correction for underwater acoustic communications, ICASSP '97, Munich, April 1997.

Light R.D., and J. Morison, 1989: The autonomous conductivity-temperature vehicle: first in the SEASHUTTLE family of underwater vehicles for scientific payloads, Proceedings, Oceans 89, Mar. Tech. Soc., 793-798.

Loch, J., E. Waller, J.G. Bellingham, R. Beaton and M. Triantafyllou, 1988: Software development for the autonomous submersible program at MIT Sea Grant and Draper Laboratory, Sixth Int. Symp. on Unmanned Untethered Submersibles Technology, 92-98.

Patrikalakis, N.M. and L. Bardis, 1991: Localization of rational B-spline surfaces, Engineering with Computers, 7(4), 237-252.

Stojanovic, M., J. Catipovic and J. Proakis, 1993: Adaptive multichannel combining and equalization for underwater acoustic communication, J. Acous. Soc. Am., in press.

Stommel, H., 1989: The SLOCUM mission, Oceanography, 22-25.

Stutman, P.S., and R.H. Maloof, 1984: Synchronous pinger for range determination of underwater vehicles, Proceedings, ROV 84, 53-55.

Turner, R.M., J.S. Fox, E.H. Turner and D.H. Blidberg, 1988: Multiple autonomous vehicle imaging system (MAVIS), Proceedings, Sixth Int. Symp. on Unmanned Untethered Submersibles Technology, 526-536.

Triantafyllou, M.S. and K. Streitlien, 1988: Distributed control of multiple AUV's forming effective chains, Proceedings, Sixth Int. Symp. on Unmanned Untethered Submersibles Technology, 499-518.

A Prototype Autonomous Buoyed Environmental Measurement System

J. Mark Stevenson

Acoustic Branch, Code D881
Naval Command, Control and Ocean Surveillance Center
San Diego, CA 92152-6435
e-mail jms@nosc.mil

Abstract

A novel vertical line array (VLA) of relatively inexpensive oceanographic sensors is discussed. Many of the sensors themselves are adapted for oceanic use from other intended commercial applications (e.g., automobiles, factory assembly line monitoring). The intent of this device is to provide oceanographers with a low-cost, moderate-resolution sensor suite that affordably yields dense spatial sampling for a period of roughly one week in shallow-water applications, particularly in the context of mission planning or prospective surveillance system installation.

1. Background

For several years, the Acoustic Branch of NCCOSC RDT&E Div. has been developing very lightweight, low cost, low power acoustic arrays for ocean deployment, culminating in systems that collect at data rates of 2 Mbps with high reliability over optically-connected transmission paths of hundreds of km [1, 2, 3, 4]. In January 1996, work commenced on a departure from this high-data-rate family of research products, the Autonomous Buoyed Environmental Measurement System (ABES) [5, 6]. ABES is an integrated suite of oceanographic sensors that incorporates modern low power sensors that communicate on a single wire conductor to a buoy-based memory and RF (radio frequency) communications device.

The intent of this device is to provide to the oceanographic community a low-cost system of sensors that affordably yields dense spatial sampling for a period of roughly one week for shallow (depth<200 m) applications. The system would not replace existing high-resolution oceanographic instrumentation, but fill the niche for a low-cost, lower-resolution system that would provide the end user with the ability to achieve higher spatial sampling. For maritime forces that must be prepared to deploy on short notice and operate in unfamiliar coastal waters, the system would be capable of providing near real-time environmental support, particularly in oceanographically complex littoral settings.

2. Approach

The prototype system will demonstrate approximately 13 sensors spanning 100 m in a vertical array. Many of the sensors themselves are oceanic adaptations of devices primarily designed for other commercial applications (e.g., automobile airbag triggers, factory assembly line monitoring, handheld navigation devices). Data will be time-tagged by a microcontroller colocated at each sensor and then time-division multiplexed up to CMOS (complementary metal oxide semiconductor) memory in a buoy. The buoy is submerged until the data collection phase is complete. The buoy will then separate from the array, rise to the surface, and transfer data via RF.

This prototype will serve as the backbone configuration and demonstrate the time division analog electrical multiplexing data collection architecture. Other sensors can then be added as COTS (commercial off the shelf) refinements progress. The system will allow any variety of low-bandwidth (e.g., less than 100 Hz sampling frequency) sensors to input their output into the array backbone. Sensor electronics (e.g., preamplification, multiplexing, analog to digital (D/A) conversion) and mechanical issues (configuration, packaging, and sensor encapsulation) are being investigated on a case-by-case basis, as described below.

3. Sensor specifics

The ABES sensor list as of late 1996 includes 3 CTD (conductivity, temperature, pressure) modules, 5 temperature sensors, 1 wave height sensor, 1 tide height sensor, 1 tilt sensor, 1 current meter, and 1 accelerometer. With the advent of DC (direct current) response accelerometers, one of these may double as a tilt indicator. An optional acoustic ambient noise sensor is treated theoretically, but will not be implemented in hardware in the prototype.

3.1. Pressure sensor

In the ABES prototype, pressure sensors will be incorporated as depth sensors at the seafloor and at the

submerged buoy. We have breadboarded the IC Sensors model 1431 pressure sensor and verified through laboratory testing that it is suitable for the task. This sensor has a range of 0-2 MPa (a depth rating of about 300 m), good linearity, accepts potting well, 1 kPa accuracy, 70 Pa sensitivity, is consistant with 12 bit digitization, and costs about 20 US (United States) dollars. In subsequent hardware iterations, with some understanding between the spatial and temporal transfer functions between pressure at depth and swell, a pressure sensor mounted sufficiently shallow (just below the buoy) would measure surface waves and swell. A hydrophone may have sufficient sensitivity to make this measurement if located on the bottom. A pressure sensor mounted on the fixed anchor would remove data contamination induced by mooring motion. Examination of the attenuation curves for surface waves shows that measurable pressure signature from the dominant 12 second swell is available at 200 m [7]. The tidal heights and sensor depth could then be measured using a pressure sensor on the bottom package.

3.2. Thermistor

Several thermistors throughout the water column would provide a temperature profile. The technology here is straightforward and has been demonstrated previously [8].

3.3. Accelerometer

A first-order measurement of the sediment characteristics (i.e., rock, sand, or ooze) could be extracted from the deceleration of the package upon impacting the bottom. The output of an accelerometer similar to those used for automobile air bag sensors would be digitized for a few seconds after seafloor impact. We have investigated the performance of an Analog Devices solid-state accelerometer for this application.

3.4. Electromagnetic flowmeter

Building on an NRaD-patented design, testing is underway to determine if a coil-type electromagnetic flowmeter could be incorporated in the ABES anchor. This would require the measurement of extremely low voltage levels induced in coils of copper wire surrounding a pair of silver electrodes. Water current and direction could be obtained by installing this electromagnetic instrument in line or on the anchor without resorting to moving components. Several sensors distributed throughout the vertical array, together with the compass described below, would provide a water current profile to compare against the integrated current measurement derived from the tilt of the array.

3.5. Tiltmeter

Modern solid-state accelerometers available from IC Sensors and Analog Devices, Inc. have DC response that allows them to be used as tilt sensors. These sensors have sine and cosine outputs that facilitate true tilt measurement and are inexpensive (about 10 US dollars). Fluid-filled electrolytic tilt sensors made by The Frederics Co. and Spectrum, Inc. are other alternatives, but tend to cost more and require pressure protection for in-water use. Previous operational work in Arctic arrays has relied on the use of tilt measurements of vertical strings to verify acoustic element localization (active acoustic) schemes for pinpointing receiver elements [7]. In these vertical arrays, a tiltmeter measures tilt at the bottom of the array. An averaged current through the water column is calculated based on the hydrodynamic characteristics of the array system. We have mathematically modeled the signal available for hypothetical array profiles at a range of current speeds.

3.6. Compass

Located in each electromagnetic current meter package or with the tilt sensor, a compass would measure the current direction with respect to magnetic north. Three magnetometers would be used, two to measure the two horizontal components of the Earth's magnetic field, and one to correct for dip. Hall-effect magnetometers configured as compasses are capable of replacing more expensive fluxgate instruments, and are now in use in current meters built by Aanderaa. Advantages include low cost and low power. The cost of these sensors is around 4 US dollars per unit. Honeywell also makes a stand-alone compass module (HMC1002) that provides an attractive magnetoresistive alternative for a low-cost oceanographic system, however this compass requires a high current reset pulse to be provided occasionally, at a significant power drain. Precision Navigation, Inc. makes a very small coil-type sensor based on a relaxation oscillator technique that is also under investigation. Small fluid-filled compasses (e.g., Dinsmore) are attractively priced but unsuitable due to stress problems at pressure.

3.7. Four-electrode conductivity cell

This sensor provides measurement of water conductivity, from which salinity is inferred knowing temperature and depth. This could be one or several sensors distributed through the water column. The output of one sensor would be monitored continuously during the initial descent to provide a profile. Afterword, a time series would be collected at a fixed depth. For the initial prototype, the CTD sensor will measure in static mode. Three Ocean Sensors Inc. (San Diego, CA) conductivity, temperature, and depth modules will be used. These innovative sensors are included as an

outcome of a Cooperative Research and Development Agreement (CRADA) between Ocean Sensors, Inc. and NRaD. They feature a range from 0.1 mS/cm to 100 mS/cm with a sensitivity of 0.05 mS/cm. They required 5 mA at 5 V during their measurement period, with 0.5 second warmup time. The cost per cell is estimated at about 20 US dollars.

3.8. Optional Hydrophone

Although not included in the prototype ABES, an amplified hydrophone could theoretically be bandpass filtered, full-wave rectified, and low-pass filtered to provide a slowly varying DC signal proportional to the acoustic ambient noise. This signal could then be sampled at a very low rate. It may be possible to estimate variance between samples either through hardware or after some signal processing in the sensor microcontroller.

3.9. RF subsystem

The RF subsystem will use spread-spectrum wireless data transceivers that operate in the 902-928 MHz band. The subsystem is divided into two parts: (1) the buoy mounted transceiver and (2) the base station. The base station could be land-based or located aboard a vessel or aircraft. Freewave Technologies DGR-115 series transceivers will be used. These have a small footprint (OEM board size is 62 mm by 129 mm), 19.2 kband transfer rate and low power requirements (180 mA at 12 V in transmit, output power 0.3 W). The cost of a transceiver is about 700 US dollars.

3.10. Sensor Microcontrollers

Each ABES sensor will have associated with it a microcontroller, probably a Microchip, Inc. PC16C74, and a hardwire transceiver. This microcontroller will be the interface between the sensor analog-to-digital converter and the buoy-based microprocessor. The target controllers cost about 11 US dollars and operate on 50 μA at 3 V. They are digitally addressed by the buoy-based microprocessor and respond by putting a digital voltage value on the data line. Each microcontroller has an associated 32 kHz crystal clock that provides timing to the sensor analog-to-digital converter. The 32 kHz clock for the microcontroller will be provided by a Harris HA7210 oscillator circuit.

3.11. System Microprocessor

The buoy-based microprocessor and memory is based on the combination of an Onset Model-8 Tattletale computer and a Persistor Flash Card. The system microprocessor will accept mission configuration parameters (e.g., which sensors will be sampled and when, at what rates, for how long, and when the anchor should break away). It will also accept calibration, through a graphical user interface (GUI), from the topside interface computer in the form of look-up tables to compensate for sensor transfer function nonlinearities. The system microprocessor can also perform auxiliary functions, e.g., averaging, conversions, or computing integrated current speed and direction from various sensor outputs.

As of late 1996, an Onset Tattletale program has been produced up that writes a file of simulated data to the Flash memory card, and then re-opens the file, reads it and transfers it serially to a PC (personal computer). In addition, the module has been interfaced with a PCMCIA adapter to read the data on a laptop. One hardware/software interfacing inconvenience has been encountered with these new memory devices: the memory card has to be formatted while it is in the PCMCIA slot, and then written to by the Onset Model-8 Tattletale. If one uses the picodos initialization, the PCMCIA slot will not find the data.

The present topside interface computer is a laptop SHARP PC-8900. This computer will allow the user to display the output of the sensors, and modify calibration coefficients, sampling rates, and sleep cycles.

3.12. Riser Cable

Three Surlyn-coated 28 AWG copper stranded electrical wires (power, ground, and signal) sewn together with a Tex 210 4-strand Kevlar thread strength member comprise the riser cable. This cable has an overall outside diameter of about 2 mm and a measured breaking strength of 10 N. The weight per 100 m is 4.5 N in air and 1.5 N in water. Resistance per 100 m is 20 Ohms. The riser has excellent hockle resistance when packaged in a random layup inside the deployment container.

4. Future Work

Possible long-term applications for the outcome of this work include the monitoring of sewage outfalls, oceanographic fronts around offshore oil platforms, river estuaries, power plant discharge, mine reconnaissance and pre-surveillance for amphibious operations. There may be some commercial applicability as an alternative to expensive and relatively cumbersome systems now being marketed.

The inexpensive ABES connectivity scheme address another naval problem, that of bringing data to shore via a vulnerable fiber-optic trunk cable, that presents an ongoing problem for users of deployable underwater surveillance systems (e.g., Mobile Inshore Undersea Warfare (MIUW), Advanced Deployable System). In some circumstances, a buoyed RF data relay just outside the surf zone would mitigate much of the problem by not exposing the trunk cable to breaking surf. The Navy's progress in affordable wet-end sensor technology

Rapid Assessment of the Optical Attenuation Profile

M. R. Lewis[1,2], S. D. McLean[2], A. Weidemann[3]

[1]Department of Oceanography, Dalhousie University, Halifax, Nova Scotia, Canada B3H 4J1

[2]Satlantic Inc., 3295 Barrington St., Halifax, Nova Scotia, Canada B3K 5X8

[3]Naval Research Laboratory, Stennis Space Center, MS, USA

Abstract

Variability in the attenuation of visible radiation in the sea limits the skill in prediction of performance of many sensors and systems in the coastal waters. For example, the use of lidar bottom imaging is limited to depths order 6 attenuation length scales; for many coastal regions, this can vary between 0.5 and 150 meters, and is difficult to estimate with any accuracy from shallow-water climatologies. We report here the development of a small, air-deployable package which enables the rapid assessment of the optical attenuation profile in remote and denied access areas.

1. Introduction

The degree of penetration of visible light in the surface ocean is fundamental to a range of applied and basic oceanographic applications. For example, the rate of upper ocean heating, on both a diurnal and seasonal basis, is due in large part to the turbidity of the water column. The attenuation also limits and constrains the use of laser sounding for bathymetry, and laser imaging of underwater objects in mine countermeasure activities.

The attenuation coefficient can be considered as a summation of the attenuation due to water itself, and the dissolved and particulate matter contained in the water column. For waters removed from the coast, the principle determinant of variability in the attenuation is the concentration of phytoplankton pigment. In the more optically complex coastal regions, contributions from dissolved organic matter, and sediments from terrestrial sources also play a large role. The variability in the attenuation coefficient in these regions is large (2 orders of magnitude), and concentrated at much smaller space (<km) and time scales (<day) than that observed offshore. Furthermore, the vertical structure in the optical characteristics, such as intense layers of scattering and absorbing particulates, is highly pronounced in coastal regions. Consequently, it is extremely difficult to nowcast or forecast the attenuation coefficient with any confidence from climatologies, and to estimate the performance of various sensors and systems in the littoral environment that are sensitive to optical clarity of the sea.

Here we discuss the development of a novel optical instrument ("K-Chain") designed to measure the vertical profile of the attenuation coefficient in near-to-real-time, which can be either moored, or deployed as a drifting system from aircraft or ship into regions of interest.

2. Background.

The diffuse attenuation coefficient is used to describe the penetration of radiation in water. This equation has the form:

$$(1) \quad E_d(z,\lambda) = E_d(z_0,\lambda) * e^{-[(z-z_0)*K(z,\lambda)]},$$

where E_d is downwelling vector irradiance, z is the depth at which E_d is computed, z_0 is the depth at which E_{d0} was measured, λ is the wavelength of light and K is the average diffuse attenuation coefficient between z and z_0. Traditionally K is computed over some range of E_d values from a profiling instrument by solving equation 1 (e.g. Smith and Baker 1984, 1986). Profiling systems often have difficulty obtaining K within the top few meters of the water, usually due to effects from a nearby vessel. Using a freefall system, values of E_d can be obtained very close to the surface without ship effects (Waters et. al. 1990), but the computation of K using the Smith and Baker method results in the first value of K at a depth of the first sample plus half the number of bins used for the regression (usually 4-16 meters, depending on wave conditions). More sophisticated techniques have been developed (Mueller 1991)to eliminate this effect in profile data but currently processing is highly interactive.Profiling systems also require the presence of a vessel or other platform that make it not cost effective for long term monitoring of a given area or for use in denied access areas. Moored systems for open ocean use typically require large platforms to improve survivability in rough conditions. This often results in systems that contaminate the measurement due to shadowing, particularly if the measurement is made in shallow water. The goal of the development reported here is to produce a small freely drifting system that can be used to measure K in shallow waters with as little self contamination as

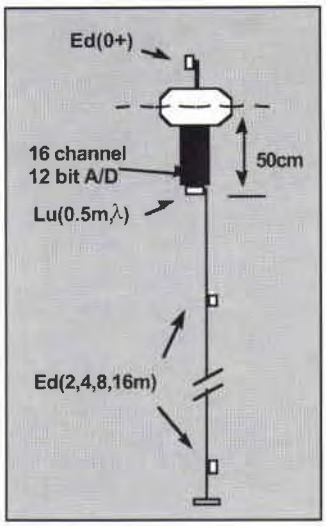

Figure 1 TACCS

possible, and which can be used for the rapid assessment of the underwater optical environment.

3. System Development

The K-Chain system that has resulted was developed for the Naval Research Laboratory (NRL) to allow the diffuse attenuation coefficient to be monitored in remote locations without manned presence, particularly in very shallow coastal waters (20-100m). The development of the K-Chain system is to lead to a fully air-launch capable system.

3.1 Heritage: CMOD-I/OCM (Compact Metcorological Oceanographic Drifter-I / Ocean Color Monitor)

Satlantic has been developing systems for remote monitoring of the apparent optical properties of water for seven years. Early projects developed for NRL in conjunction with MetOcean Data Systems Limited (Dartmouth, Canada) resulted in the CMOD-I/OCM buoy and the WOCE/OCM buoy. These are field proven air/ship launched buoys with an in-water seven channel upwelling radiance sensor and a single downwelling irradiance sensor. These buoys use the CLS/ARGOS system to send the data back to the user. The CMOD-I/OCM buoy (McLean and Lewis 1991) is a standard A-size sonobuoy which is certified for gravity tube air-launch. These buoys were successfully air-launched from the NASA P3B and ship-launched during JGOFS EqPac (Landry, et. al. 1997). As part of this development, Satlantic also produced the TSRB-I which is a tethered version of the same optical system which allow the user to obtain data in real time while the instrument drifts up to 100m away from the vessel. These instruments provided the development platforms for the K-Chain systems.

3.2 Heritage: TACCS (Tethered Attenuation Coefficient Chain System)

To expand on the ocean-color observing capability to retrieve the profile of attenuation, the TSRB-I tethered instrument was modified to accept a four (single wavelength) E_d sensor optical chain with sensors located at 2, 4, 8 and 16m below the TSRB-I. Initially designed as a proof of concept unit for the air-launch K-Chain, this instrument has subsequently become a commercial product referred to as TACCS. This system (shown in Figure 1) has a seven channel radiance sensor located at 50cm below the surface, a single E_d sensor above the surface, four E_d sensors (optionally 6) on a detachable chain (at user selectable depths - nominally 2, 4, 8 and 16m) and a sea surface temperature sensor. Using a Onset Tattletale Model 8 and a custom interface board, TACCS has a 16 channel 12 bit data acquisition system. The unit has a 100m tether which supplies power and allows the user to view (and log data) in real time at a rate of one sample from all channels once per second.

Figure 2 TACCS Chain Sensor

The chain sensors on the TACCS are Satlantic ED-20 vector irradiance sensors. Each sensor contains a custom interference /photodiode package, cosine diffuser and a preamplifier board which is optimized for the depth at which the sensor will be deployed. Each sensor is 3 cm in diameter and about 7.5 cm long. The sensors are potted onto a 1cm diameter polyurethane jacketed cable with 10 conductors (see Figure 3). A weight at the base of the chain provides stability. The entire chain can be detached from the instrument and interchanged with other chains if desired via an underwater connector on the bottom of the TACCS buoy.

K values are computed using the TACCS by different methods; for example, K can be computed by solving equation (1) for each combination of sensors on the chain. The $E_d(0+)$ sensor can be projected through the sea surface using the Fresnel reflectance losses to give $E_d(0-)$. Thus K can be computed at 1, 2, 3, 4, 5, 6, 8,

9, 10 and 12 m. Figure 4 is an example of some of the TACCS K values for 532nm plotted with a K profile from a freefall profiler (Satlantic SPMR). Note that the profiler cannot easily compute very near surface values of K using the Smith and Baker method and it does not detect the intensity of a near surface red tide.

TACCS also has a seven channel radiance sensor at 0.5m. Using this sensor and the computed K for 1m, K can be estimated for the other six wavelengths (Morel 1988) and the propagated to just below the surface to give $L_u(0-)$. The $L_u(0-)$ values are then projected through the sea surface (Mueller and Austin 1995). The $L_u(0+)$ values are then normalized using $E_d(0+)$ estimated for each wavelength from the E_d sensor and a solar model with the mean extraterrestial irradiance to give L_{wn} (Mueller and Austin 1995). The L_{wn} values are directly comparable to those derived from satellite ocean color measurements, and can then be used to evaluate the efficacy of satellite algorithms (e.g. Austin and Petzold 1981) for the retrieval of an average K for the upper layer of the ocean.

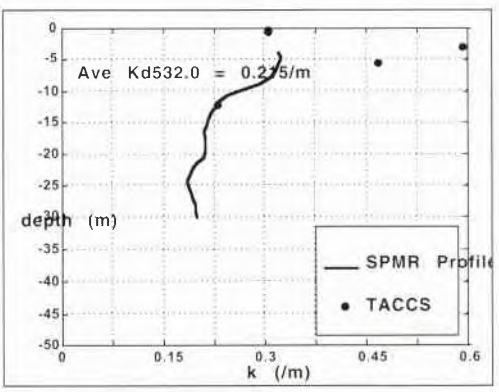

Figure 3 - TACCS and SPMR data

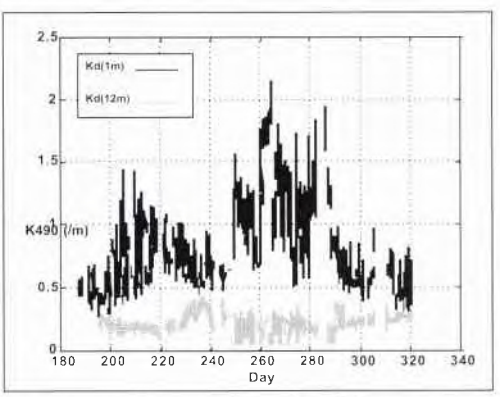

Figure 4 - TACCS Time Series for CESL

3.3 TACCS (Cellular Telephone Interface)

The TACCS design is very flexible and allows for numerous user interfaces. One such example was built for the Canadian Space Agency (CSA) to develop coastal K algorithms for the European Space Agency (ESA) MERIS sensor as part of the Canadian Expert Support Laboratory (CESL) Coastal Marine Algorithms Program (CoMAP). The system was designed for real-time monitoring of the coastal zone. This unique system uses the standard TACCS platform and cellular phone technology to interface with a totally automated acquisition and analysis system. During daylight hours TACCS collected data six seconds every 10 minutes for 6 months. Data was transmitted to shorebased computer via the cellular phone each morning at 3am. The system was moored from June to December in Bedford Basin, a 50m deep estuary near Halifax, Canada. Due to the power requirements of the system, a gel cell and a solar panel were added to the system (the latter attached to a nearby guard buoy to reduce shadowing). TACCS successfully monitored an intense red-tide which occurred in mid-September (see Figure 4).

3.4 CMOD-II/K-Chain

The final product of this development is an air-launched, A-size sonobuoy package which can be deployed in remote and denied access areas. A prototype system has been delivered to NRL configured as a TACCS with a MetOcean ARGOS/PTT (see Figure 8). This system was successfully used in a laser bathymetry experiment in Australia in January of 1996. Although the system was a ship-launched version, it allowed for testing of data formats which will be used on the final version (see Figure 5). A compact version of the chain sensor (ED-25) has also been developed which is 1.4 cm in diameter and 5 cm long. Along with a custom designed 0.5 cm cable with 15 conductors and 250 kg kelvar strength member, the cable has special breakouts at sensor nodes to allow the chain sensors to be attached in a minimal volume.

Figure 5
ARGOS TACCS

4. Summary

A flexible platform for the rapid assessment of the diffuse attenuation coefficient has been developed, which is capable of remote deployment and near-to-real-time data reporting. The system has been deployed in tethered, free drifting and moored applications. Using state-of-the-art technologies, the K-Chain, in its various configurations, can be deployed anywhere in the world to monitor the optical properties of the coastal zone.

5. Acknowledgments

Technical development of the K-Chain system was provided by the Naval Research Laboratory under contract N00014-94-C-6002. Funding for the Coastal Marine Algorithms Program was provided by the Canadian Space Agency under the Canadian Expert Support Laboratory (CESL) program.

6. References

Austin, R.W. and T.J. Petzold (1981), The determination of diffuse attenuation coefficient of seawater using the Coastal Zone Color Scanner, Oceanography from Space, J.F.R. Gower, Ed., Plenum Press, p239-256.

Landry, M., Barber, R., Bridigare, R., Chai, F., Coale, T., Dam, W., Lewis, M., Lindely, S., McCarthy, J., Roman, M., Stoecker, D., Verity, P., White, T. (1997), Iron and grazing constraints on primary production in the central equatorial pacific, An EqPac Synthesis, *Limnology and Oceanography, in press*.

McLean, S.D. and M.R. Lewis (1991), An expendable spectral radiometer drifter system, *IEEE Proceedings, OCEANS '91*.

Morel, A. (1988), Optical modeling of the upper ocean in relating to its biogenous matter content (Case I waters), *Journal of Geophysical Research*, **93 (C9)**, p10749-10768.

Mueller, J.L (1991), Integral method for irradiance profile analysis, CHORS Technical Memorandum 007-91, San Diego State University.

Mueller, J.L. and R.W. Austin (1995), SeaWiFS Technical Report Series (Vol. 25), Ocean Optics Protocols for SeaWiFS Validation, NASA Technical Memorandum 104566.

Smith, R.C. and K.S. Baker (1984), Analysis of ocean optical data, Ocean Optics VII, M. Blizzard, Ed., *Proceedings of the SPIE*,**478**, p119-126.

Smith, R.C. and K.S. Baker (1986), Analysis of ocean optical data, Ocean Optics VIII, P.N. Slater, Ed., *Proceedings of the SPIE*, **637**, p95-107.

Waters, K.J., R.C. Smith and M.R. Lewis (1990), Avoiding ship induced light field perturbation in the determination of oceanic optical properties, *Oceanography*, **3**, p18-21.

The Denied Area Measurement Processing System (DAMPS) and its Role in Rapid Environmental Assessment

J. Cartmill, J. Locklin, K. Walker, R. Hillyer

Planning Systems Incorporated
7923 Jones Branch Drive
McLean, VA 22102
Email: cartmill@plansys.com

Abstract

The Denied Area Measurement and Processing System (DAMPS) is a portable data acquisition and processing system, designed to achieve the mission of obtaining critical atmospheric, oceanographic and environmental acoustic data in denied areas. DAMPS is designed to utilize available and emerging sensor technologies, and be deployed from a variety of delivery platforms. DAMPS also provides a communications link to transmit data back to carrier battle groups, the Tactical Environmental Support System (TESS), and to operational centers (FNMOC and NAVOCEANO).

1. Introduction

DAMPS is the realization of a concept which provides the U. S. Navy with a "toolbox" of capabilities for measuring critical environmental factors in denied areas to increase the warfighters' effectiveness. This concept embodies:

- all available and emerging sensors,
- sensor delivery techniques,
- delivery platforms, and
- communication methodologies.

DAMPS is designed to "plugin" directly to existing Navy software, databases, hardware, and communications, yet still retain the flexibility required for littoral data collection.

The DAMPS paradigm of matching the platform and the sensor with the processing hardware is embodied in two configurations, the Portable Communications Processing Interface (PCPI) and MicroDAMPS. The PCPI is a "snap-on/snap-off", multiprocessor system that can be configured for up to 32 simultaneous channels of data acquisition and processing. The PCPI has flown aboard fleet P-3s during SHAREM 117, and on data collection exercises aboard the Force Warfare Ocean Water Lidar (OWL) aircraft. MicroDAMPS is a standalone receiver and processing unit designed to collect process and communicate a single channel of data from a tactical aircraft or AUV.

Another important facet of the DAMPS concept is automatic processing of the data. Raw data can be converted to standard Navy message formats and transmitted without the need for a specialized operator for the PCPI, and with no operator at all for MicroDAMPS.

In this paper the DAMPS / PCPI hardware and processing will described, results from data collection exercises will be presented and future developments of DAMPS capabilities will be detailed.

2. PCPI System Overview

The DAMPS PCPI consists of three TAC-4 Hewlett Packard (HP) 743/100 PA-RISC VME-Bus Single Board Computers (SBC) mounted in a custom ruggedized chassis. These computers make up the three DAMPS subsystems:

- Data Acquisition Subsystem (DAS)
- Data Processing Subsystem (DPS)
- Host Processing Subsystem (HPS).

The DAS runs under HPRT real time operating system and provides the interface with a VME analog to digital (A/D) conversion board. The DPS and HPS run under HPUX UNIX operating system Version 9.07, and provide the user interface and overall system control respectively. The three subsystems are connected with a VME backplane and use networking software to provide rapid interprocessor communications.

2.1. Data Acquisition Subsystem

The DAS is chiefly responsible for collecting the data digitized by the VME A/D board. The DAS is booted over the VME bus and runs the HPRT real-time operating system. It configures the A/D board, collects data, provides real-time processing of the data, and transfers the data to the HPS. Signals telemetered back to the aircraft are received and fed into a DAMPS docking station. Analog outputs from the signal conditioning unit, which provides low pass anti-aliasing filtering and amplification, are digitized at a maximum rate of 44 K samples per second (88 Kbytes/sec). Digital data is stored in shared memory buffers on the A/D board and then transferred via Ethernet or over the VME Bus.

2.2. Data Processing Subsystem

This subsystem transforms the raw data to tactical units, and configures the data for transmission. This subsystem is connected to the keyboard, pointing device (mouse), and the 1024 x 768 color Liquid Crystal Display. The DPS postprocesses the data using the National Instruments COTS software package LABVIEW which provides a visual interface to the DAMPS measured data stream. Using the LABVIEW virtual instrument interface, the user can configure the data collection system, select specific data channels to monitor as they are acquired, choose and perform onboard processing tasks. A built in P-coded GPS provides fixes which are used to provide aircraft position and time of instrument launch.

2.3. Host Processing Subsystem

The HPS manages the overall DAMPS system. The HPS is interfaced to the mass storage and backup devices. Serial data from other sensors may be input to this system and transferred to the DPS to provide additional information to the operator. The HPS also is responsible for the transfer and storage of raw and processed data. The HPS is connected to the disk drives and the 8mm tape backup system. Data is archived for backup and to preserve an adequate amount of available disk space for the raw and processed data.

3. Environmental Data Processing

The DAMPS approach to environmental data processing is comprised of three key ingredients:

- Automatic processing,
- Software in place of specialized hardware, and
- Data decimation that preserves features critical to system performance models.

Automatic processing eliminates the need for a special PCPI operator and assures a consistent data product. The use of software instead of specialized hardware has two advantages. First, it allows a wide variety of fleet assets to become data collection platforms and second, it reduces the risk of mechanical or electrical failure. Data decimation is required to conserve communications bandwidth and reduce data storage requirements. It is extremely important, however, to make sure that all of the data necessary to system performance modeling is communicated. Two examples are dropsonde and transmission loss messages. Dropsonde data is converted to a World Meteorological Organization (WMO) format at certain mandatory and significant levels. The criteria for the significant levels is based on the needs of weather forecasters, and is insufficient for high frequency radar propagation models. For acoustic transmission loss 1/3 octave levels are given for the entire frequency range, but near the cutoff frequencies of underwater sound ducts narrow band levels are also included.

3.1. Oceanographic Data Processing

The Navy has long made use of air deployable expendable sensors for measuring *in situ* ocean properties. DAMPS adds the advantages of automatic processing and communication of the data.

3.1.1 Air Expendable Bathythermograph (AXBT)

The AN/SSQ 36 AXBT provides temperature versus depth by using a thermistor probe that descends through the water column at a known fall rate. The data is transmitted as a frequency modulated (FM) signal that varies as a function of temperature. The conversion equation is

$$F = 1440. + 36 * T \qquad (1),$$

where F is the frequency in Hz and T is the temperature in °C. The range of the probe is -2° C to 35° C. The corresponding frequencies are 1368 Hz and 2700 Hz. The fall rate is 1.52 m/sec.

The processing consists of the following steps:

- Convert the digitized time series data to a frequency using FFT or zero crossing method. A 0.1 degree temperature resolution will require a 3.6 HZ frequency resolution.
- Apply equation (1) to convert the frequency to temperature.
- Convert the time samples to depth using the fall rate. A one meter depth resolution requires a sample every 0.66 seconds (1.52 samples/sec).

AXBT's are susceptible to noise and several types of failures. Common failure modes include: wirebreaks, probes hitting the bottom, and excessive electromagnetic interference. The software is able to filter the signal and provide sensor failure detection. Monitoring software is also included to provide a visual trace of temperature versus depth.

Post processing for AXBT data include reducing the data to inflection point data, and calculating water properties relevant to acoustic propagation. These properties include mixed layer depth, sonic layer depth, sound channel axis, and others critical to sonar system performance.

The basic communications processing requirements are to convert the data to JJXX message format for transmission.

3.1.2. Air expendable Current Profilers (AXCP)

AXCP's measure the vertical profile of current speed and direction with a constant bias or offset. This bias is dependent on the conductivity of the seafloor and is unknown. Because of the unknown bias, absolute velocities cannot be accurately determined, but current shear may be determined to a precision of 1 cm/sec (0.02 knots). Data is transmitted on three carrier frequencies, two of the frequencies are the current data U (East-West) and V (North-South), and the third carrier is temperature in a format similar to the AXBT. Data from the AXCP is sampled at 16Hz and provides a vertical resolution of 0.3 meters.

3.2. Acoustic Data Processing

DAMPS has the capability for processing three types of air launched sonobuoys the AN/SSQ-57, AN/SSQ-53(DIFAR) and the AN/SSQ-77(VLAD) buoy. The AN/SSQ-57 buoy provides an omni-directional signal of acoustic pressure versus time, while the other two buoys also transmit directional information.

3.2.1. Ambient noise processing

Ambient noise processing requires no additional assets to be deployed. The time series from the buoy is converted to calibrated frequency levels through the use of the Fast Fourier Transform (FFT), and the processed data are averaged to yield spectrum level versus frequency. Integration time and frequency bandwidth are the two major processing considerations for achieving consistent results. The stationarity of the noise establishes the desired integration time. If the desired result is average noise levels, a long integration time should be used. If noise level variability is needed, a shorter integration time is used. The frequency bandwidth chosen for processing is also dependent on the final product. If the noise is characterized by certain frequency lines or a system is sensitive only to a particular frequency, a narrow band processing method is used.

3.2.2. Transmission Loss

Transmission loss is the measurement of the attenuation of a signal from a source to receiver. Mechanisms for attenuation include spreading, scattering, and absorption. Transmission loss processing measures the received signal from a calibrated source a known distance away. The digitized time series of the initial arrival is windowed to remove contamination from reverberation, then Fast Fourier Transformed. The spectrum is summed over a 1/3 octave to obtain a receive level (RL). The transmission loss is then computed by,

$$TL = SL - RL \qquad (2)$$

where SL is the known calibrated source level.

Since there is no Navy standard format for transmission loss measurements a format has been developed. It is made up of the 1/3 octave band information with addition of narrow band 1/10 octave levels at the surface duct cutoff frequency. This message also includes source and receiver depths, source type, position and range.

3.2.3. Directional Sonobuoys

The AN/SSQ 53 is an uncalibrated sonobuoy that provides three signals for analysis, an omni-directional signal, a North-South Beam and an East-West Beam. These signals are frequency multiplexed at 0, 7.5 and 15 kHz; therefore, the frequency response is limited to a range of 0 to 2.4 kHz.

The AN/SSQ-77 sonobuoy uses a vertical line array that can be steered to the desired vertical directionality. This sonobuoy produces three output signals like the SSQ-53, and is also limited to the same 0 to 2.4 kHz frequency range. One reason for using directional receivers is to avoid the problems of hybrid path contamination when measuring bottom scattering.

3.3. Atmospheric Data Processing

The DAMPS atmospheric data collection process emphasizes the use of dropsondes, coupled with a communications network.

Dropsondes produce a vertical profile of atmospheric properties, typically temperature, humidity, and pressure. Initial processing requires the data from the dropsonde be Manchester decoded and converted to engineering units of millibars (mbar) for pressure, degrees C for temperature, and percent for relative humidity. By transmitting the position, determined from an onboard GPS sensor, a vertical profile of the wind field may be determined. Drop rates of 5 m/sec (1000 ft/min) provide ten minutes of data from an altitude of 10,000 feet. Sensor resolutions of 0.5 degrees C for temperature, 0.1% for relative humidity and 0.1 mbar for pressure are typical. Wind speeds can be resolved to 0.5m/sec using LORAN, and better accuracy is obtained with GPS.

Data from the dropsonde is converted to a WMO message format. Along with the meteorological standard and significant levels, data from levels important to electro-magnetic propagation models is included. This is done by calculating a profile of the index of refraction for the atmosphere and using the same inflection point method as the AXBT processing.

4. Communications

One great advantage of DAMPS is the ability to transmit critical environmental data to on scene battle groups and shore based operational centers. A flexible communication architecture enables the data to transmitted from the acquisition platform directly by line-of-sight or relayed by satellite. Provisions for secure communications using on board cryptographic equipment are built into the PCPI. DAMPS has demonstrated collection, processing and communication of atmospheric, oceanographic and acoustic environmental data aboard fleet and research aircraft. The capability to transmit digital images has also been demonstrated. A variety of transmission methods can be utilized to match the required data rates with communication equipment available on the delivery platform.

The PCPI provides three communication hardware interfaces: MIL-188 for serial data transmission through standard military cryptographic equipment, RS-232 for serial COTS equipment, and Ethernet for network communications. During SHAREM 117 DAMPS successfully transmitted data by satellite from a fleet P-3C aircraft using the ARC-187 transceiver to the METOC facility in Rota, Spain. Data has also been transmitted from aboard a research P-3A using a Motorola LST-5 radio to a ground facility at the Key West Naval Air Station. Line-of-sight data transmission was accomplished using the

OWL aircraft and a ground station at the Patuxent River Naval Air Station.

On the P3, the PCPI is attached internally by way of a serial cable to a MIL-188 converter board mounted in the docking station. The MIL-188 output controls the KY-58 cryptographic device and the ARC-187 satellite transceiver mounted in the P3. The ARC-187 transmits and receives via the Dorne & Margolin satellite antenna built into the top of aircraft.

A typical shore station has a laptop PC connected to an external MIL-188 converter which controls another KY-58. This is attached to a Motorola LST-5 lightweight satellite transceiver, which is connected to a portable satellite antenna.

The COTS software used by the PCPI and the receiving station is TTY-PLUS from Universal Data Link, Inc. of Jacksonville, Florida. Since TTY-PLUS is written for PC compatible computers, the UNIX based PCPI runs TTY-PLUS by way of SoftWindows PC emulation software. TTY-PLUS uses a compressed packet transmission scheme to provide transmission of digital data via satellite. The TTY-PLUS protocol is sufficiently robust that it can resume communications even after significant interruption or during periods of high electromagnetic noise.

5. Environmental Assessments

The DAMPS / PCPI has been deployed on a number of environmental data collection missions. Along with digital images, the PCPI has successfully acquired, processed and communicated ashore the data from the following expendable sensors:

- AN/SSQ-36 (AXBT)
- AN/SSQ-57 (Ambient Noise)
- AN/SSQ-53(DIFAR)
- AN/SSQ-77(VLAD)
- AN/SSQ-57 with the MK61 SUS and SSQ 110 for TL measurements
- L2D2 (Dropsonde)
- AXCP (Current Profiler)

5.1. Onslow Bay

In late January the PCPI flew aboard the OWL aircraft on an exercise designed to fully demonstrate the DAMPS concept. During the mission digital images, data messages from expendable sensors, and gridded fields of optical and bathymetric data from the OWL's Lidar system were relayed via satellite to the Warfighting Support Center at the Naval Oceanographic Office. Automatic data transfer procedures were in place that allowed these data to be browsed on the SIPRNET while the aircraft was still on station.

5.2. Additional Exercises

The DAMPS / PCPI was first deployed on a VP-45 P3 aircraft during the SHAREM 117 exercise last June. On-board real-time operations to acquire, process and communicate data from dropsondes and AXBT's were performed. Subsequent testing and exercise participation has been conducted aboard the OWL aircraft on three recent flights, one flown out of PAX River NAS and two out of Key West NAS. During December 1996, two more test exercise flights from Key West were conducted using the DAMPS / PCPI onboard the OWL aircraft over the Gulf of Mexico.

6. Future Development

Ongoing efforts to advance the DAMPS concept encompass three areas of development:

- MicroDAMPS,
- Additional and emerging sensors, and
- Additional processing capabilities

These developments will enhance the effectiveness of DAMPS for rapid environmental assessment.

6.1. MicroDAMPS

MicroDAMPS is a standalone single board processing unit with an onboard RF receiving unit. The prototype, currently under development, will include data acquisition, processing and communications software. Although constrained to a single data channel, a number of sensors of several different types may be deployed during a single mission. The target platforms for this unit are tactical aircraft or an AUV where available space is restricted.

6.2. Additional and Emerging Sensor Systems

The flexibility of the DAMPS system allows the rapid incorporation of new sensor technology for environmental data collection.

6.2.1. AXOTD Processing

The Air Expendable Optical-Temperature-Depth (AXOTD) - The AXOTD is an engineering prototype probe containing a light scattering sensor to measure water clarity at 880 nm and a temperature sensor. The probe has a drop rate of 2.5 meters/second and a depth capability to 300 meters.

6.2.2. AXSV Processing

Air Expendable Sound Velocimeters (AXSV) use a sing-around transducer to provide sound velocity data to a resolution of +/-0.25 meters per second. The sing-around frequencies are ~28 kHz for 52 mm separation, but are decimated by a factor of 128 to a range of 210 to 233 Hz. A frequency of 225.4 Hz corresponds to a sound velocity of 1500 meters/second.

6.2.3. Lidar Processing

Experience aboard the OWL aircraft has led to a laser bathymetry processing design concept that could be used to employ the DAMPS computers to perform some of the real-time tracking functions as well as many of the present ground processing functions onboard the aircraft while the survey was underway. The product being preliminary survey quality bathymetric charts and data to be communicated via JMCIS protocols.

6.3. Additional Processing

DAMPS sonobuoy data processing capabilities are an outgrowth of the SSQ-110 advanced air deployable source research performed by Planning Systems Incorporated. This research has identified several possible additions to the DAMPS processing repertoire.

Bottom scattering

Measurement of scattering strength requires the deployment of a calibrated source (SUS, SSQ-110, etc.) with the sonobuoy field. The general processing scheme for scattering measurements is to:

- Reduce the data to received level in the frequency bands of interest,
- Calculate the insonified area,
- Calculate the transmission loss to the area, and
- Determine the source level and the source beam pattern.

The bottom scattering strength (BS) can then be found from,

$$BS = RL - SL - EA, \qquad (3)$$

where RL is received level, SL is the source level and EA is the effective area. The effective area is 10logA - $TL_{two\text{-}way}$, where A is the area, and $TL_{two\text{-}way}$ is the two way transmission loss from the source to the insonified area. The transmission loss maybe estimated by a simple spherical spreading, or calculated by an eigenray analysis.

6.3.1. Bottom Loss

DAMPS bottom loss processing involves two distinct steps. The first is to measure the bottom loss directly as a function of frequency and grazing angle. The second is to convert these measurements into meaningful information on bottom and subbottom properties for use in propagation models.

Measurement of bottom loss requires a calibrated source at a known distance from the receiver, and proceeds similarly to transmission calculations. The difference is that the initial direct arrival is ignored and the bottom bounce time series are processed. The bottom loss is computed by calculating a transmission loss for a perfectly reflecting bottom, and the bottom loss is given by,

$$BL = TL_{perfect} - TL_{measured} \qquad (4)$$

The second phase of the bottom loss data processing employs the Automated Inversion algorithms developed under the SSQ-110 program. This technique optimizes the fit of Low Frequency Bottom Loss (LFBL) geoacoustic parameters by employing a simulated annealing method. The approach used constrains the parameters to realistic values and does not require an "expert" starting point for the optimization.

7. Conclusion

For the mission of rapid environmental assessment DAMPS is a proven total system concept that incorporates data collection from denied areas, pre-processing of sensor data, and communications. The system leverages existing software and is JMCIS compliant for connectivity to all users.

Rapid-Response Aircraft Surveys of Short-Lived Events in the Coastal Atmosphere

John M. Bane, Jr.

Marine Sciences Program
University of North Carolina
Chapel Hill, NC 27599-3300
Email: Bane@marine.unc.edu

Abstract

Two field measurement programs have been conducted off the west coast of the United States as part of the Coastal Meteorology Accelerated Research Initiative (ARI), sponsored by the U.S. Office of Naval Research. The objective of this ARI is to develop an understanding of the genesis, propagation and decay of coastally trapped "southerly surges" in the atmospheric marine layer along mountainous coastlines. The two field programs, which were conducted during the summers of 1994 and 1996, utilized measurements from coastal meteorological stations, coastal and inland wind profilers, moored and free-drifting offshore buoys, and an instrumented aircraft. A flexible, mobile and responsive measurement capability was required for the measurement of airflow and stratification over the normally data-sparse coastal ocean. A light twin-engined aircraft was specially instrumented and flown in order to meet this measurement objective. This aircraft system proved to be invaluable in obtaining data on the three-dimensional structure and evolution of several surges along the California and Oregon coasts. The views of southerly surge anatomy provided by the aircraft surveys have suggested an improved theory of surge dynamics.

1. Introduction

Two field measurement programs have been conducted off the west coast of the United States as part of the Coastal Meteorology Accelerated Research Initiative (ARI), sponsored by the U.S. Office of Naval Research. The objective of this ARI is to develop an understanding of the genesis, propagation and decay of coastally trapped "southerly surges" in the atmospheric marine layer along mountainous coastlines. The two field programs, conducted during the summers of 1994 and 1996, utilized measurements from coastal meteorological stations, coastal and inland wind profilers, moored and free-drifting offshore buoys, and an instrumented aircraft. A flexible, mobile and responsive measurement capability was required for the measurement of airflow and stratification over the normally data-sparse coastal ocean due to: (i) the short lifetimes of southerly surges (1-3 days), (ii) the speed at which surges propagate along the coast (several hundred km/day), and (iii) the difficulty in accurately forecasting a surge more than a day or so in advance of its initiation.

A light twin-engined aircraft was instrumented and used in this ARI to meet the following specific objective:

> "To determine the three-dimensional structure of a number of southerly surges propagating in the atmospheric marine layer off the U.S. West Coast during summer, with sufficient spatial and temporal resolution to differentiate between the candidate disturbance types or propose a new candidate process."

This aircraft system proved to be invaluable in obtaining data on the three-dimensional structure and evolution of several southerly surges along the California and Oregon coasts. Seven research flights were flown during 1994 and thirty-three research and two calibration flights were flown during summer 1996. The 1996 flights included five flight sequences in pursuit of southerly wind events. On two occasions we coordinated flights with the C-130 research aircraft operated by the National Center for Atmospheric Research, which was stationed in Monterey, California, during the month of June 1996.

2. Aircraft and Instrumentation

2.1 The Aircraft

A Piper Seneca III aircraft was used for the data collection program. The Seneca III is an all metal, low wing, non-pressurized, twin-engined aircraft capable of carrying six persons, including the pilot. It is powered by two Continental, turbocharged, 220-horsepower, piston engines and can cruise at altitudes up to 25,000 ft (7,625 m) above sea level. Typical flight speeds range from about 90 knots (46 m/sec) true airspeed during climbs, to a maximum of 190 knots (98 m/sec) true airspeed in cruise. Typical cruise configuration is 165 knots (85 m/sec) true airspeed at altitudes near 10,000 ft (3,050 m). For typical flights, the absolute endurance of the aircraft is just under six hours, and its maximum range is about 950 nautical miles (1,760 km). The

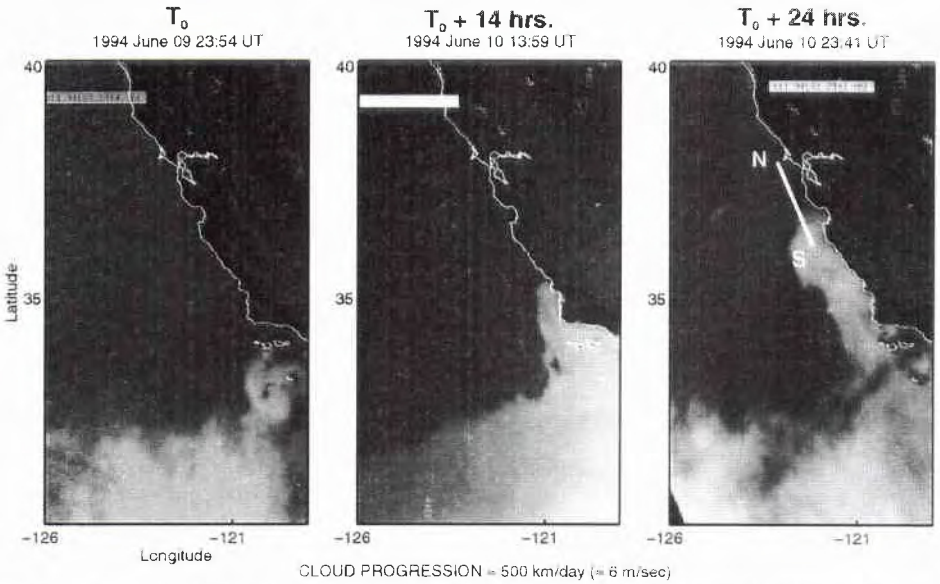

Figure 1. A sequence of three visible satellite images showing the northward progression of the clouds during the southerly surge of June 1994. The white line running alongshore in the rightmost panel is the flight track on which the vertical sections shown in Figure 5 were taken. The N (S) indicates the northern (southern) end of the aircraft sections, as seen in Figure 5.

aircraft, its normal systems and operating procedures are described in the *Seneca III Information Manual* [*Piper*, 1984]. During this research program, flights were made with three persons aboard, and flight speeds ranged from about 90 knots (46 m/sec) true airspeed during climbs to 125-155 knots (64-80 m/sec) true airspeed in level flight.

2.2 Sensors and Instruments

Several sensors and instruments were installed in the aircraft to measure the quantities required for computation of meteorologically relevant variables. Sensors that were installed are as follows: (1) a Rosemount Model 102E4AL total temperature sensor for measurement of atmospheric temperature; (2) a Vaisala Model 50U humidity sensor for measurement of atmospheric relative humidity; (3) a Setra Model 270 pressure sensor for measurement of *in situ* air pressure at the location of the aircraft; (4) a Setra Model 239 differential pressure sensor to measure the aircraft's indicated airspeed; and (5) a KVH Model C100 flux-gate compass for measurement of the aircraft's heading. Instruments that were installed in the aircraft for other measurements are: (6) a Garmin Model 150 GPS receiver, which measured the aircraft's horizontal position (latitude and longitude), ground speed and ground track; (7) a Terra Model TRA 3500 radar altimeter for measurement of the aircraft's absolute altitude above the ocean's surface [limited to an altitude of 2,500 ft (762 m)]; and (8) a Shadin Model 05-1-1-35 air-data computer, which is a commercially available unit designed for use in general aviation applications. The Shadin air-data computer received input from several of its own sensors (air temperature, static pressure, pitot pressure) as well as from the Garmin GPS-150 and the aircraft's King KCS-55A Compass System (which is part of the aircraft's autopilot system and determines aircraft heading). The Shadin air-data computer served as a backup to some of the sensors, since the accuracies of its sensors were, in general, lower than those of the comparable sensors described in (1) - (5) above. Sensor and instrument accuracies are given in *Bane et al.* [1995].

The Rosemount total temperature sensor and Vaisala humidity sensor were mounted on the underside of the aircraft, about 2 meters behind the nose. Each sensor is enclosed in a reverse-flow housing, and each was mounted about 0.2 m off the aircraft centerline. Each of the two reverse-flow housings protruded downward from the aircraft's fuselage about 7-8 cm. Each also protruded through a mounting hole in the aircraft skin, in order to provide an electrical connection within the fuselage. A Rosemount Model 510GA3A4 signal conditioning amplifier was mounted inside the aircraft fuselage within about 10 cm of where the total temperature sensor housing was mounted to the fuselage. The signal conditioning amplifier is a small electronics package that connects to the total temperature sensor, and it provides the analog voltage output that is proportional to the measured temperature.

Figure 2. The Piper Seneca III aircraft used in the measurement program.

The Vaisala barometer, Setra differential pressure sensor and Shadin air-data computer were mounted inside the aircraft adjacent to the control console (described below). The barometer was connected to the aircraft's static pressure line, and the differential pressure sensor and the Shadin were connected to the aircraft's static and pitot pressure lines. The KVH flux-gate compass was mounted at the outboard end of the right wing, inside the plastic wingtip. The Garmin GPS-150 was mounted in the aircraft's instrument panel, as was the Terra radar altimeter indicator. The GPS antenna was mounted on the upper fuselage centerline. The radar altimeter antennae were mounted on the underside of the fuselage just behind the trailing edge of the wing.

A control console was fabricated and installed in the passenger compartment of the aircraft. The console handled power distribution to the meteorological sensors and instruments, received output signals from them, and provided digital data through ports to the two microcomputers that received, stored and displayed the data. Several of the sensors provided analog voltage outputs, and these analog outputs were converted to digital signals by Keithley Model M1141 analog-to-digital conversion modules. One Keithley module was connected to each of the following: the Rosemount total temperature sensor, the Vaisala humidity sensor, the Vaisala barometer, the Setra differential pressure sensor, the KVH flux-gate compass, and the Terra radar altimeter. The six Keithley modules were mounted inside the control console.

An 8mm video camera/recorder was mounted atop the control console and aimed out a left-side window, looking slightly forward. The aircraft intercom was connected directly to the audio input of the video camera, so all radio transmissions and receptions as well as all cabin discussions over the intercom were recorded on the audio track of the video tape. The video camera recorded continuously throughout the flights, and thus provides a running view of the clouds and the sea surface, plus other visual information. The time stamp on the video recording provides correspondence with the computer-recorded data set.

2.2 Data Acquisition

Data were sent from the control console to two serial ports on each of two microcomputers through four RS-232 serial lines (two lines to each microcomputer). Apple Macintosh PowerBook microcomputers were used for this project. The first serial line to each microcomputer carried the digital data stream from the Shadin air-data computer. The Garmin GPS-150 sent its digital data to the Shadin air-data computer once per second, and all Garmin GPS-150 data were then incorporated into the Shadin serial output data stream. The second serial line to each computer carried information from the six Keithley modules. These modules were connected in serial fashion, and the computer system could interrogate the Keithley's in a pre-determined sequence. A data acquisition and display software system (referred to subsequently as the DAQ system) was written for the Macintosh microcomputers by S. M. Haines [*Haines and Bane*, 1994]. The DAQ system is based on LabVIEW, a commercially available software product that handles data input/output, processing, graphics and storage.

Every second during a flight, the data from all sources (Garmin, Shadin, and Keithley's) came to each computer through its two serial ports, were processed and stored. The first port received an ASCII burst of 205 characters from the Shadin every second. This burst contained the

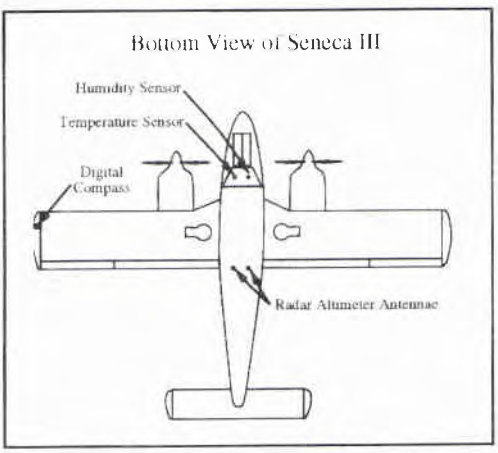

Figure 3. Schematic view of the underside of the Seneca III aircraft. The positions of the Rosemount temperature sensor, the Vaisala humidity sensor, the KVH digital compass and the Terra radar altimeter antennae are indicated. All of these were mounted on the exterior of the fuselage, except for the KVH compass which was mounted inside the wingtip.

Figure 4. The sensor and instrument control console, shown mounted in the interior of the Piper Seneca III aircraft just behind the pilot's seat.

Shadin data plus the Garmin GPS-150 data. The second port communicated through a daisy-chain accessing all six Keithley's. The Keithley's were polled in sequence for their data after the computer received a burst from the Shadin. Thus, each second the Shadin-plus-Garmin data were received, the data from the sensors connected via Keithley's read, all data values time-stamped with the computer system time, conversion equations applied where necessary, and all data arranged and stored to the hard drive in each computer.

For each variable whose value was transmitted via a Keithley module to the computer, a conversion from a digital voltage value to scientific units was performed prior to the value being writen to the disk or displayed. The conversion equations were applied to Rosemont temperature, Vaisala humidity, Setra pressure, Setra indicated airspeed, Terra radar altitude, and KVH aircraft heading [*Bane et al.*, 1995]. Data were logged into a LabVIEW log-file on each computer's hard drive after each second during the flight. After each flight, the DAQ system was stopped and the log-file was copied to a diskette for backup.

2.3 Inflight Data Display

Graphical displays and listings of the measured variables were produced in near-real time aboard the aircraft on each microcomputer using LabVIEW software. Presentation formats, which could be selected by the computer system operator aboard the aircraft, included the following: a current listing of values for the incoming variables; a time series presentation (a strip-chart-like display) of either one or two variables, with the specific variables to be displayed and the time interval visible in the strip-chart windows selectable by the operator; a variable *vs.* variable plot, which provided for display of vertical profiles when altitude or pressure was chosen as the vertical axis; and a map, which showed the flight track in real time. These onboard displays were crucial in executing the measurement flights efficiently, since a knowledge of the atmospheric structure being measured was needed to make informed inflight decisions, for example, where to position aircraft profiles and flight lines relative to the airflow pattern.

Several atmospheric variables were derived from the aircraft data set. The derived variables include atmospheric *in situ* temperature, potential tempera-ture, relative humidity, mixing ratio, air density, and horizontal wind velocity. These variables have been plotted in vertical and horizontal section format to gain an understanding of atmospheric structure.

3. Observations

Results from our 1994 flights defined the structure of one propagating, coastally trapped "southerly surge" event. We found that it was not a simple two-layer wavelike disturbance, nor was it a two-layer gravity current. The June 10-11, 1994 event was observed to have an overall wavelike character with an internal surface boundary layer imbedded within it, in which a very-near-surface cloud layer (or fog layer) formed. Vertical sections show that the airflow and stratification were clearly more complex than a two-layer system. Results from this work have appeared in a technical/ data report [*Bane et al.*, 1995] and in two articles [*Ralph et al.*, 1995; *Dorman et al.*, 1996], and a third article is soon to be submitted [*Ralph et al.*, 1996].

The data set we obtained in 1996 captured five southerly wind episodes, each one different from the other, and all somewhat different from the June 10-11, 1994, case. Three of the 1996 episodes had a surge component, one event was expected to produce a southerly surge but did not, and one event was a transition to synoptic scale southerlies without a surge component.

The four southerly surge cases that we now have measured include two surges between Point Conception and Point Reyes (June 1994 and June 1996; these are referred to as the "southern cases") and two surges between Point Reyes and Cape Blanco (July and September 1996; these are referred to as the "northern cases"). Temperature and velocity sections from these

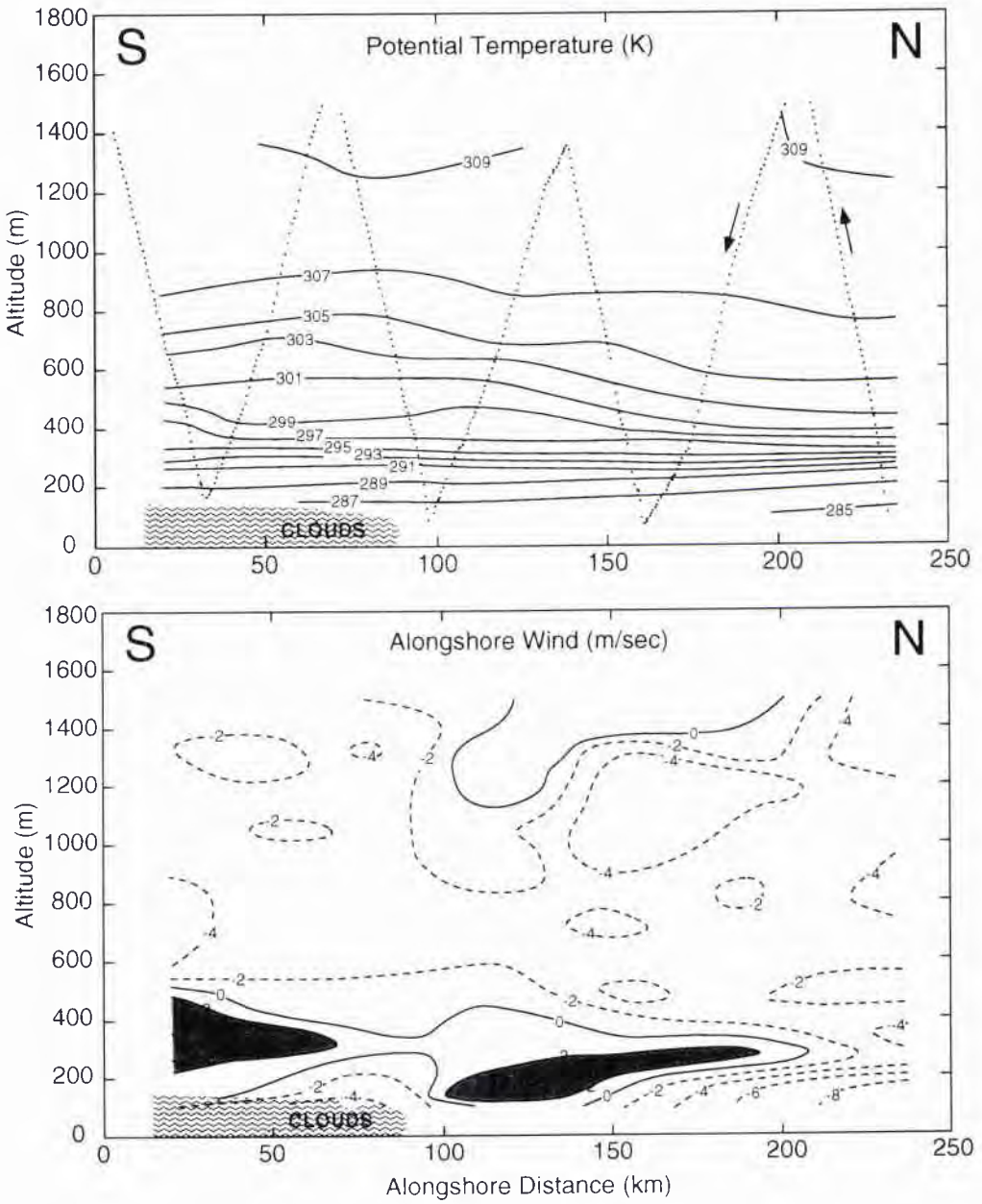

Figure 5 Vertical sections of potential temperature and alongshore airflow observed by the aircraft during the June 1994 southerly surge (refer to Figure 1). Note the following: (i) the wave pattern is only in the upper portion of the inversion; (ii) the marine layer itself (potential temperature less than 295 K) is of quite uniform thickness; (iii) the leading edge of the southerly alongshore airflow (speed > 0) is some 100 km ahead of the cloud front; and (iv) the cloud layer is at the ocean surface, *i.e.* it is a layer of fog.

surges suggest that each has a southerly flow leading edge above the MBL supporting the notion that the complex vertical structure observed in June 1994 is the typical situation as opposed to an isolated occurrence. A correct dynamical understanding must include an explanation of this structure.

Vertical sections of potential temperature and alongshore velocity through the 1996 surges show that the leading edge of the southerly wind flow is about 400 m above the surface, overlying northerly flow. There are distinct differences between the two northern cases and the two southern cases that warrant further investigation, including the greater vertical extent of the southerly airflow in the northern cases *vs.* the southern cases, and the stronger gradient between the southerlies and the northerlies in the northern cases.

Similarities exist between the structure of the June 1994 surge and that of the June 1996 surge, both of which propagated through the Pt. Conception-to-Pt. Reyes region. The intrusive nature of the southerly flow is apparent in each case, as is the general wavelike character of the inversion topography (*i.e.* elevated inversion top to the south). Differences include the fact that the southerly jet is more centered in the inversion in the 1994 case, while in the 1996 case the jet is at the transition between the mixed layer and the inversion.

It is apparent from these initial comparisons that the two southern cases look somewhat similar to each other and the two northern cases look somewhat similar to each other, while the northern cases differ from the southern cases in a number of ways. This leads to the question: Are these differences due to locational differences between the northern and southern domains (*e.g.* differing coastline geometry or terrain), is it something else (*e.g.* the strength of the synoptic forcing during the northern cases *vs.* the southern cases), or is it coincidence?

4. Conclusions

The objective of directly measuring three-dimensional airflow and stratification fields in the short-lived and difficult to predict southerly surges that were studied in the Office of Naval Research Coastal Meteorology ARI, was successfully met with the use of an instrumented, light, twin-engined aircraft. Keys to this success included: Choosing an economical aircraft with capabilities that matched the mission requirements (in this case, low to moderate altitudes and within about 200 km of the coastline); Continuous availability of the aircraft and flight/scientific crew over a several month period of time, with both on call to fly with as little as a few hours notice; Preparing the aircraft and its sensor and data systems so as to maximize reliability; Designing the aircraft data system so as to provide real-time views of the data being collected; Having the best possible forecasts of surge likelihood, even though these features remain a forecast challenge.

References

Bane, J.M., S.M. Haines, L. Armi and M.H. Sessions, 1995: *The California Coastal Marine Layer: Winds and Thermodynamics, June 1994 Aircraft Measurement Program.* Univ. North Carolina Report No. CMS-95-1, 289 pp.

Dorman, C.E., J.M. Bane, L. Armi and D. Rogers, 1996: Surface Boundary Layer during the June 10-11, 1994 California Coastally Trapped Event. *Mon. Wea. Rev.* (submitted).

Haines, S. M., and J. M. Bane, 1994: *Light Aircraft DAQ Software Manual.* Univ. North Carolina Report No. CMS-94-1, 20 pp.

Piper, 1984: *Seneca III Information Manual.* Handbook No. 761 756, Piper Aircraft Corp., Vero Beach, FL, 459 pp.

Ralph, F. M., P.J. Neiman, P.O. Persson, W.D. Neff, J. Miletta, L. Armi and J. M. Bane, 1995: Observations of an Orographically Trapped Disturbance along the California Coast on 10-11 June 1994. *Proceedings, Seventh Conference on Mountain Meteorology, Amer. Meteorol. Soc.*, Boston, pp. 204-211.

Ralph, F.M., L. Armi, J.M. Bane, C.E. Dorman, W.D Neff, P.J. Neiman, W. Nuss, and P.O.G. Persson, 1996: The Structure and Evolution of a Coastally Trapped Disturbance Observed along the California Coast on 10-11 June 1994. *Mon. Wea. Rev.* (submitted).

Assimilation, Modelling and Prediction

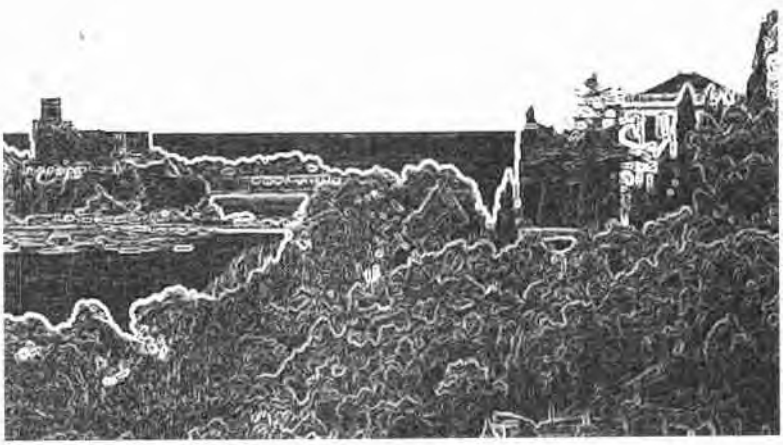

FORECASTING AND SIMULATING COASTAL OCEAN PROCESSES AND VARIABILITIES WITH THE HARVARD OCEAN PREDICTION SYSTEM

Allan R. Robinson

Division of Engineering and Applied Science
Department of Earth and Planetary Sciences
Harvard University
Cambridge, MA 02138 USA
E-mail: robinson@pacific.harvard.edu

Abstract

Sustained accurate and efficient oceanic field estimates are now feasible because of the advent of ocean prediction systems. Such systems produce nowcasts, forecasts and data-driven simulations by melding dynamics and observations via the assimilation of measurements into numerical models. The Harvard Ocean Prediction System is a flexible, portable and generic system for nowcasting, forecasting and simulations. Recent results from the application of HOPS in various coastal environments, including the Middle Atlantic Bight, Haro Straits and Strait of Sicily, are presented here.

1. Introduction

Accurate estimation of four dimensional interdisciplinary fields in the ocean is essential for modern ocean science and technology. For many applications the continuous time evolution of three dimensional synoptic realizations over a large regional domain with (sub) mesoscale resolution are required for physical, biological, chemical, acoustical and optical state variables, e.g., velocity, temperature, biomass, nutrients, sound speed, and radiation fields. There are many couplings and interactions among these fields which provide both challenges and opportunities for the use of interdisciplinary techniques. Field estimation in the ocean is complex and data sets are generally sparse compared to requirements. This is for the most part due to the presence of a large range of interactive space and time scales associated with the wide variety of oceanic phenomena. The coastal ocean is particularly challenging because of multiple forcings, complex geometries, and boundary interactions.

Sustained accurate and efficient oceanic field estimates are now feasible because of the advent of ocean prediction systems. Such systems produce nowcasts, forecasts and data-driven simulations by melding dynamics and observations via the assimilation of measurements into numerical models. Assimilation provides dynamical adjustment and dynamical interpolation. Error models play a critical role and the melded estimates should agree with the observations within observational errors and satisfy the dynamics within dynamical model error bounds. Ocean prediction systems provide mechanisms for important feedbacks including adaptive sampling for the observational component and improved dynamics for the model component.

An efficient and generally applicable coastal ocean prediction system must take into account the wide variety of coastal phenomena (currents, waves, tides, etc.) and forcings (buoyancy, wind, external) which occur over the multiplicity of time and space scales. The observational network will generally consist of a mix of platforms and sensors with real time telemetry deployed in nested domains of increasing resolutions. The set of coupled interdisciplinary models for assimilating the data will have compatible two-way nested computational domains. Prediction systems should accelerate scientific research progress in the multiscale intermittent ocean and important practical application areas include management of the multiuse coastal zone and naval and marine operations.

The development of specific regional predictive capabilities must take into account regional phenomena and the intended applications of the system. Accuracies must be determined and validation criteria established. It is useful to distinguish three phases [1]. In the first *descriptive* or *exploratory* phase dominant scales, processes and interactions are identified and a model is set up and *validated* as adequate to encompass the relevant dynamics. In the second, or *dynamical* phase, a definitive knowledge of the circulation structures and interactions must be achieved and the specific dynamical processes that govern synoptic feature evolution and events established. During this phase the regional predictive system is *calibrated*. In the third, or *predictive* phase real time forecast experiments with dense high quality data sets must be carried out to *verify* the sys-

tem. The final step is the design and verification of an efficient regional forecast system with minimal observational resources for the desired accuracies and applications.

In the remainder of this chapter we introduce the Harvard Ocean Prediction System (HOPS) and then illustrate its recent application to three diverse coastal and shelf regions with various forcings and phenomena: i) the Middle Atlantic Bight shelf/slope front driven by buoyancy effects and dominated by internal dynamical instabilities; ii) Haro Straits tidal fronts driven by the interaction of intense tides and an estuarine circulation in the presence of tidal and topographically induced mixing, and iii) the variability of the Atlantic Ionian Stream system in the Strait of Sicily and the western Ionian Sea driven by the general circulation, internal dynamics and regional atmospheric fluxes. The first example involves data-driven simulations carried out for fundamental dynamical process research. The second example was carried out as part of a proof of concept demonstration and involved providing real time frontal predictions as input to adaptive sampling mission design for deployments of autonomous underwater vehicles. The third example involved six weeks of real time nowcasting and forecasting, initiated on shipboard, which provided environmental guidance for NATO naval operations and maneuvers.

2. The Harvard Ocean Prediction System - HOPS

HOPS is a flexible, portable and generic system for nowcasting, forecasting and simulations. In addition to its use in fundamental process studies, HOPS can be rapidly deployed to any region of the world ocean, including the coastal and deep oceans and across the shelfbreak with open, partially open or closed boundaries. Real time and at sea forecasts have been carried out for more than a decade in fifteen sites in the Atlantic and Pacific Oceans and the Mediterranean Sea (*vid* Fig. 1). Recent reviews [2,1,3] provide a comprehensive presentation of the system and overview of its applications including coupled physical-acoustical [4] and physical-biological [5] studies. A rigorous quantitative verification has been achieved for the Iceland-Faeroe Islands frontal system [6]. Here we will only briefly highlight a few points and new developments.

The overall system schematic is shown on Fig. 2. The heart of the system for most coastal applications is a primitive equation physical dynamical model which has been specially structured for accurate and efficient calculations over steep topography [7,8]. Vertical coordinate options include sigma, hybrid and multiple sigma coordinate transformations which are calibrated for specific applications via sensitivity analyses to both vertical and horizontal resolutions [9]. Horizontal coordinate options include multiple two-way nests [9, *ibid.*]. A variety of physical, biological and acoustical, in situ and remotely sensed, data types have been assimilated in a variety of applications. The data analysis and management modules of HOPS represent a major resource of the Harvard system. HOPS methodology involves the construction of a best possible initial synoptic realization as a starting point for the assimilation of new synoptic data. There is an emphasis on the treatment of data prior to assimilation in order to maximize the impact of new data in the light of prior data. *Structured data models* [3] are utilized for this purpose, e.g., feature models or typical synoptic structures [10,11,12] and empirical orthogonal functions (EOFs) in one to three dimensions. Recent developments include: i) the use of temperature and salinity based, rather than velocity based, feature models which are more suitable over steep topography; ii) the addition of a dynamically balanced vertical velocity to the feature models for initialization and assimilations which will couple physics and biology; and, iii) the optical dynamical component (Fig. 2). For the construction of best possible synoptic realizations multiple data streams, including structured data models and seasonally adjusted historical synoptic realizations, are melded. The modularity of HOPS facilitates the selection of a subset of modules to form an efficient configuration for specific applications and also facilitates the addition of new or substitute modules.

A robust (suboptimal) optimal interpolation (OI) data assimilation scheme with weights set by simple engineering-type assumptions has been used in HOPS for several years [3]. OI, well understood by meteorologists, was adopted in order to focus research resources on the assimilation of real ocean data sets rapidly into the ocean dynamical models for a first round of impact studies. A second quasioptimal assimilation scheme option, Error Subspace Statistical Estimation (ESSE), has been developed and recently added to the system. A rational approach was used to identify an efficient statistical estimation scheme feasible for use in real time with real oceanic data sets. The ESSE goal is to determine the nonlinear evolution of the oceanic state by minimizing the most energetic errors under the constraints of the dynamical and measurement models and both of their uncertainties [13]. Error propagation is estimated via an ensemble forecast using the full nonlinear model. The evolving error subspace is characterized by singular error vectors and values, i.e., time evolving three dimensional error EOFs. Melding weights for assimilation are determined using a minimum error variance criterion. Importantly, melding occurs in the error subspace and is thus much less costly than a classical analysis with the full error covariances. The error subspace is updated at the melding step by combining the forecast principal errors, i.e., errors arising from the dynamical model and the loss of predictability, with the error co-

variances of the measurements. An example of ESSE assimilation is presented in Section 3.3.

3. Forecasts and Simulations

3.1. The Middle Atlantic Bight Shelf-Slope Front

The frontal boundary between colder, fresher shelf waters and warmer, saltier slope waters off the northeast coast of the United States, although partially density compensated, supports a frontal jet which exhibits vigorous submesoscale meandering and eddying variabilities. The dynamics of this frontal system, which is not yet well understood, is of interest not only in its own right, but also because the associated variabilities give rise to shelf-slope exchange processes for heat, nutrients, etc. The determination of the qualitative and quantitative characteristics of these exchange processes are important topics in research on deep sea/coastal ocean interactions. Dynamical studies via both idealized process studies and data driven simulations have been carried out [9] and nowcasting, forecasting and simulations of coupled physical and acoustical fields is currently in progress [14].

For initialization of the shelf-slope front a temperature and salinity based feature model was constructed which, under appropriate parameters, develops within a few days realistic variabilities. Shelf-slope interactions have been studied both in the absence and presence of warm core rings of Gulf Stream origin. Data sets assimilated were from the extensive synoptic hydrographic surveys with nominal 25km sampling of the MARMAP project [15] and the very high resolution hydrographic data taken from the RV Bear in 1958 in a one degree square centered at 39.5° N latitude and 70.5° W longitude. Fig. 3a shows an initialization field consisting of a feature model shelf break front and a feature model ring embedded into shelf MARMAP climatology and a uniformly stratified slope. MARMAP synoptic data from May, 1984 is assimilated into the initialization of the 30-day long simulation. A two-way nested inner grid of 3 km resolution is embedded in the larger regional domain of 9 km resolution. The simulation on day 24 (Fig. 3b) illustrates an interesting type of far field ring frontal interaction. Two long filaments of shelf water are being drawn out and an isolated shelf water eddy is present. Note that the nest successfully copes with the presence of a partial ring in the fine domain. A four day time series from a similar simulation with no ring but with RV Bear data assimilated is shown on Fig. 4 for the inner domain. Assimilation took place during days 3 and 6. Both shelf and slope waters intrude across the shelf-break and two way exchanges occur. Results of these studies indicate early growth of at least two types of unstable waves followed by spectral saturation at many scales, nonlinear wave steepening and nonlinear transfer to larger scales, events, vortices, and hammerheads. The front has been observed to reestablish itself from a turbulent variability field over steep topography.

3.2. Haro Straits Tidal Fronts

Haro Straits lie to the east of Vancouver Island between the Straits of Georgia and Juan de Fuca (Fig. 5). These straits constitute a large estuarine system in which salty water of North Pacific origin flows northward at depth and is mixed with fresher water primarily of riverine origin flowing above it seaward and southward. Haro Straits is believed to be the region where most of the mixing takes place, although the relative importance of possible mixing processes and locations has not been established [16]. The estuarine circulation is dynamically coupled to an energetic tidal flow with speeds in the region reaching 60 cm/s [17]. Driven by several tidal forcing constituents, the tidal circulation varies from day to day as well as on longer time scales, with maximum tides occurring in June and July. The complex topography and island geometry (Fig. 5) causes the flow to be accelerated through passages between islands and over sills which provides a mixing mechanism. A variety of tidal fronts occur in the region. In particular a tidal front with a generally north-south axis is often observed to occur to the south of Stuart Island.

In the summer of 1996 the Harvard group participated in a coupled physical and acoustical study of the Haro Straits tidal frontal phenomena in collaboration with scientists from the Institute of Ocean Science (Sidney), Massachusetts Institute of Technology, and the Woods Hole Oceanographic Institution [18,19,20]. The project objectives were oriented both towards: i) the investigation of basic scientific dynamical processes; and ii) the development of ocean predictive system methodology with adaptive sampling. Platforms included ships, aircraft, moorings, floats and autonomous underwater vehicles (AUVs). The HOPS participation focused on the ebb tidal front south of Stuart Island. Real time HOPS predictions with data assimilation carried out from 24 June to 3 July 1996 were supplied to the MIT AUV group, who took them to sea on operational work stations aboard the vehicle tender vessel. The forecasts were used to adapt the AUV mission tracks for efficient sampling of the front and for verification missions. HOPS functioned as the circulation model central to the AUV Laboratory's system schematic shown on Fig. 6. The decision to participate with HOPS in June 1996 was taken only in April 1996 and thus this exercise required a rapid setup of a forecast system for an unfamiliar region of highly complex and poorly understood phenomena and rugged geometry and topography. The main objective was to demonstrate the concept of real time predictions for adaptive sampling, with data assimilation and feedbacks between the model and observational components of the overall observational and predictive system.

The front south of Stuart is observed to form during ebb tide and to disappear flood. During ebb there is a flow from the north of the island around both the eastern and western sides of the island, which converges to the south of the island and continues to flow southward, e.g., (Fig. 7). At slack the flow reverses. A study of particle trajectories associated with the tidal circulation was carried out based on the IOS tidal flow model [17]. It was found that water parcels on either side of the ebb front had originated in close proximity to each other to the north of Stuart. Approximately two tidal cycles were required for the water to be transported permanently from the north of the island to the south of the island. There are two major channels to the west and south of Stuart (Fig. 5) (New and Speiden Channels). The hypothesis was introduced that mixing in the flow through these channels was much more intense than in the flow through Haro Straits to the west of Stuart, which together with the shear deformation and convergence in the tidal flow caused the front. A mixing model quadratic in the flow and inversely proportional to the depth was used. Because of the short time available a simple prototype version of HOPS was set up. Tracer fields were mixed and advected by the IOS tidal velocities in the upper layer of a conceptual two layer model. The primitive equation with combined tidal, wind and buoyancy driving and a more sophisticated mixing model is a natural extension. For the prototype model utilized, Fig. 8a shows a salinity initialization based on NODC historical data, 24 hours prior to the maximum ebb tide situation shown on Fig. 8b, which illustrates the frontogenetical mechanism.

The real time operational forecasts assimilated CTD data from both the prior day's AUV missions and a daily survey from a charter vessel. The charter vessel sampling was subjectively designed each day by the Harvard group based on the HOPS forecast. The daily AUV mission and CTD surveys were carried out nominally from 6 a.m. to 12 noon. Thus the daily forecasts were of 36 hours duration in order to allow the assimilation of the prior day's data and to extend into the forecast day's mission time. For each forecast, tracers were initialized by climatology. A systematic verification study is in progress. A successful example is presented on Fig. 9 for 25 June 1996. The initial temperature and salinity are shown on Fig. 9a,b and the predicted fronts during ebb and at about midpoint of the morning AUV operation are shown on Fig. 9c,d. Guided by this prediction CTD carried by an AUV accomplished a successful and detailed sampling of the front which also provided an excellent verification of the HOPS forecast. The AUV salinity section on Fig. 9e was obtained by the vehicle yo- yoing between the surface and 20 m along a 3 km track; the vehicle reversed direction half-way through the mission and thus crossed the front twice.

3.3. The Atlantic Ionian Stream in the Strait of Sicily and the Western Ionian Sea

South of the island of Sicily and north of the African coast, a narrow strait (Fig. 10) connects the western and eastern basins of the Mediterranean Sea. In the west there is a shallow (≈250m) sill and to the east a steep shelfbreak, past which the bottom plunges from only a few hundred meters to the depth of two to three thousand meters. The shelfbreak fans out to the south and the shelf-slope region north of Libya is broad and gentle. The flow in the region is driven both by Mediterranean general circulation features and local atmospheric fluxes. In the upper ocean, relatively fresh water of Atlantic origin flows eastward in a topographically controlled jet, the Atlantic Ionian Stream (AIS) (Fig. 11), which, after flowing northward along the narrow shelfbreak, separates into the western Ionian Sea. Wind-driving can maintain a coastal current off Sicily and can induce biologically important upwelling events. In 1994, the Harvard group undertook the development of a regional forecast system for this region in collaboration with SACLANT Undersea Research Centre scientists, led initially by Dr. Alex Warn-Varnas and subsequently by Dr. Jurgen Sellschopp. The region was chosen as a test bed for developing HOPS coastal capabilities because of its challenging geometry and topography and the variety of interactive processes and driving mechanisms. An exploratory cruise in November, 1994 (AIS 94) led to the design of a definitive survey for the regional circulation features, which was completed in October, 1995 (AIS 95) [21]. ¿From mid-August to early October in 1996, NATO navies carried out in this region an exercise in rapid environmental assessment called Rapid Response 96 (RR96) during which HOPS was used for real time operational nowcasts and forecasts [22].

HOPS was initialized and run at sea aboard the NRV Alliance from 12 to 22 August; subsequent forecasts were carried out at the SACLANT Centre. The nowcast and forecast maps shown on Figure 11 are taken directly from the RR96 web site, where they were made readily accessible to interested participants. Standard sound speed sections were prepared as indicated on Figure 10. At the start of the exercise, a first guess synoptic realization was prepared by warming the October 1995 realization to August conditions by artificial surface heating of the fields while under the constraint of primitive equation dynamics. As it was acquired by the ship, hydrographic data was assimilated into this circulation and by 24 August only contemporary data was utilized. Based upon subjective interpretation of the HOPS forecasts, adaptive sampling patterns were designed for the latter part of the ship's cruise and for the two to three AXBT flights per week throughout the duration of the exercise. The U.S. Navy's Fleet Numerical Meteorological and Oceanographi

Center products were used to prepare atmospheric momentum, heat and fresh water fluxes at Harvard, which were then relayed to the forecast center.

Figure 11 illustrates the nature of the mesoscale variabilities occurring in the main thermocline due to internal dynamics. The axis of the AIS is a thermal front at about 26°C. Notable features are the Adventure Bank Vortex (ABV) centered at ≈(37°N, 13°E), the Maltese Channel Crest (MCC) (37°N, 14°E) and the Ionian Shelfbreak Vortex (ISV) (36.5°N, 15.25°E). Comparing Figs. 11a and 11b, the extent, shape and configuration of these features are seen ot shift and vary over tens of kilometers on a time scale of three to four days. Additional near surface variabilities occur due to local atmospheric forcing, as shown on Figure 12. A shift of the wind from southerly and weak (12a) to westerly (12b) is accompanied by a significant shifting and strengthening of the surface currents (12c,d).

The ESSE methodology described at the end of Section 2 was used in real time for the first time to produce a research-operational forecast of fields and errors as a demonstration of concept and feasibility. Results are presented in Figure 12 for a three day forecast before assimilation (12a) and after (12b). The pattern of the expected error of the objectively analyzed AXBT data (12c) indicates a flight designed first to tie down the shape of the ISV and then to accurately map a local region of operational interest. The forecast error map after assimilation (12d) indicates error maxima which need to be sampled in future flights. Utilizing three SUN Ultra Sparc 2 CPUs and one Sparc 20 (4 CPU) workstations, the three day forecast took one day of wall clock time. Follow-up parameter sensitivity studies and considerations of improved networking of parallel computations [13] indicate that elapsed time for producing real time forecasts could be halved.

The time evolution of the regional circulation is driven by internal dynamical processes, inflow and outflow boundary conditions and surface atmospheric fluxes. Knowledge of internal dynamical processes and boundary conditions is affected byt he calibration and tuning of the ocean dynamical model and the quality, quantity and distribution of oceanic data. The knowledge of surface forcing is affected by the type, accuracy and quantity of atmospheric fluxes and the accuracy of the atmospheric weather forecasts. In addition, both the atmosphere and the ocean have predictability limits of a few dyas and a week or two, respectively, due to internal nonlinear dynamics. A quick-look verification comparison of HOPS RR96 forecasts with nowcasts and AVHRR composite SSTs indicated that variability indices for the location and shape of the ABV, MCC and ISV were predicted at a success rate of approximately 75%. Thus, RR96 indicates that a usefully accurate forecast capability for a few days has been achieved for the region.

4. Summary and Conclusions

The melding of data and dynamics via assimilation of observations into coastal ocean observing and prediction systems provides a powerful new methodology of field estimation. Such systems must be anticipated to significantly accelerate progress in coastal ocean science and to enhance capabilities for efficient and comprehensive coastal zone management and operations.

The Harvard Ocean Prediction System (HOPS) is a flexible, portable and generic system for nowcasting, forecasting and simulations which can be utilized in any region of the world ocean: coastal and deep ocean and across the shelf break. The physical dynamical model is primitive equation based and data assimilation schemes include optimal interpolation and a novel quasi-optimal algorithm (error subspace simulation estimation) which efficiently forecasts both errors and fields. A variety of physical, biological and acoustical, in situ and remotely sensed, data types have been assimilated in a variety of applications and regions. HOPS has recently been successfully applied to three diverse coast and shelf regions: the Middle Atlantic Bight shelf/slope front, Haro Straits tidal front, and the Atlantic Ionian Stream system in the Strait of Sicily and the western Ionian Sea. Qualitative and quantitative comparisons indicate that usefully accurate real time operational forecast capabilities have been achieved.

5. Acknowledgements

This research was supported at Harvard University by the Office of Naval Research under grants N0014: 90-J-1612, 95-1-0033, 95-1-0371, 95-1-0925, 97-1-0239. The author is pleased to acknowledge the useful collaborations with Dr. James G. Bellingham and Prof. Henrik Schmidt at the Massachusetts Institute of Technology in the Haro Straits and with Dr. Jurgen Sellschopp at the SACLANT Undersea Research Centre and Dr. Alex Warn-Varnas at the Naval Research Laboratory-Stennis in the Strait of Sicily. The author thanks the efforts of: Dr. Carlos J. Lozano, Mr. Wayne G. Leslie, Ms. Marsha A. Glass, Dr. Pierre F. J. Lermusiaux, Dr. N. Quincy Sloan, III, Dr. Patrick J. Haley, Jr., Dr. Lawrence A. Anderson and Dr. Jeffrey A. Dusenberry. Figure 5 is derived from the model of Foreman *et al.*, as modified for the Haro Strait Experiment by Dr. Richard Pawlowicz of the University of British Colombia, to whom we are grateful.

References

[1] Robinson, A.R., H.G. Arango, A. Warn-Varnas, W.G. Leslie, A.J. Miller, P.J. Haley, and C.J. Lozano, "Real-Time Regional Forecasting", *Modern Approaches to Data Assimilation in Ocean*

Modelling (P. Malanotte-Rizzoli, editor), Elsevier Oceanography Series, Elsevier Science, The Netherlands. 377–412, 1996b.

[2] Robinson, A.R, "Physical Processes, Field Estimation and Interdisciplinary Ocean Modeling", *Earth-Science Reviews* **40**, 3–54, 1996a.

[3] Lozano, C.J., A.R. Robinson, H.G. Arango, A. Gangopadhyay, N.Q. Sloan, P.J. Haley, and W.G. Leslie, "An Interdisciplinary Ocean Prediction System: Assimilation Strategies and Structured Data Models", *Modern Approaches to Data Assimilation in Ocean Modelling* (P. Malanotte-Rizzoli, editor), Elsevier Oceanography Series, Elsevier Science, The Netherlands. 413–452, 1996.

[4] Robinson, A.R. and D. Lee, "Ocean Variability, Acoustic Propagation and Coupled Models", *Oceanography and Acoustics: Prediction and Propagation Models* (A.R. Robinson and D. Lee, editors), American Inst. of Physics, New York, 1–6, 1994

[5] McGillicuddy, D.J., A.R. Robinson, and J.J. McCarthy, "Coupled Physical and Biological Modeling of the Spring Bloom in the North Atlantic, II: Three-Dimensional Bloom and Post-Bloom Effects", *Deep-Sea Research I*, 42(8), 1359–1398, 1995.

[6] Robinson, A.R., H.G. Arango, A.J. Miller, A. Warn-Varnas, P.-M. Poulain, and W.G. Leslie, "Real-Time Operational Forecasting on Shipboard of the Iceland-Faeroe Frontal Variability", *Bulletin of the American Meteorological Society* **72**(2), 243–259, 1996c.

[7] Lozano, C.J., P.J. Haley, Jr., H.G. Arango, N.Q. Sloan and A.R. Robinson, "Harvard coastal/deep water primitive equation model", *Harvard Open Ocean Model Reports*, **52**, 15pp., 1994.

[8] Haley, P.J., Jr., "GRIDS", *Harvard Open Ocean Model Reports*, **54**, 13pp., 1996.

[9] Sloan, N.Q., "Dynamics of a Shelf-Slope Front: Process Studies and Data-Driven Simulations in the Middle Atlantic Bight", Ph.D. Thesis, Harvard University, Cambridge, (MA), 1996.

[10] Gangopadhyay, A., A.R. Robinson, and H.G. Arango, "Circulation and Dynamics of the Western North Atlantic, I: Multi-Scale Feature Models", *Journal of Atmospheric and Oceanic Technology*, in press, 1997.

[11] Robinson, A.R. and A. Gangopadhyay, "Circulation and Dynamics of the Western North Atlantic, II: Dynamics of Meanders and Rings". *Journal of Atmospheric and Oceanic Technology*. In press, 1997.

[12] Gangopadhyay, A. and A.R. Robinson, "Circulation and Dynamics of the Western North Atlantic, III: Forecasting the Meanders and Rings" *Journal of Atmospheric and Oceanic Technology*, in press, 1997.

[13] Lermusiaux, P.F.J., "Data Assimilation via Error Subspace Statistical Estimation", Ph.D. Thesis, Harvard University, Cambridge, (MA), 1997.

[14] Robinson, A.R., C.J. Lozano, W.G. Leslie, L.A. Anderson, P.J. Haley, Jr. and J.A. Dusenberry, "Scientific objectives and plans for real-time simulation experiment and operations: Plankton Patchiness Studies by Ship and Satellite", *Harvard Open Ocean Model Reports*, **55**, 37pp., 1997b.

[15] Mountain, D.G. and T.J. Holzworth, *Surface and Bottom Temperature Distribution for the Northeast Continental Shelf*, Technical report, National Oceanographic and Atmospheric Administration, 1989.

[16] Farmer, D.M., E.A. D'Asaro, M.V. Trevorrow and G.Y. Dairiki, "Three dimensional structure in a tidal convergence front", *Cont. Shelf Res.*, 1649–1673, 1995.

[17] Foreman, M.G.H, R.A. Walters, R.F. Henry, C.P. Keller and A.G. Dolling, "A tidal model for eastern Juan de Fuca Strait and the southern Strait of Georgia", *J. Geophys. Res.*, **100**(C1), 721-740, 1995.

[18] Schmidt, H., J.G. Bellingham, M. Johnson, D. Herold, D.M. Farmer and R. Pawlowicz, "Real-time frontal mapping with AUVs in a coastal environment", *Proceedings, Oceans '96*, Ft. Lauderdale, FL, 1996

[19] Schmidt, H., J.G. Bellingham and P. Elisseeff, "Acoustically Focused Oceanographic Sampling in Coastal Environments", *Proc. Int. Conf. "Rapid Environmental Assessment"*, Lerici, Italy, Mar. 10-14, 1997.

[20] Nadis, S., "Real-Time Oceanography Adapts to Sea Changes", *Science*, **275**, 1881-1882, 1997.

[21] Robinson, A.R., J. Sellschopp, A. Warn-Varnas, W.G. Leslie, P.J. Haley, Jr., P.F.J. Lermusiaux and L.A. Anderson, "The Atlantic Ionian Stream", *Journal of Marine Systems*, In press, 1997a.

[22] Sellschopp, J. and A.R. Robinson, "Definition and Forecasting of Ocean Conditions During Rapid Response", *Proc. Int. Conf. "Rapid Environmental Assessment"*, Lerici, Italy, Mar. 10-14, 1997.

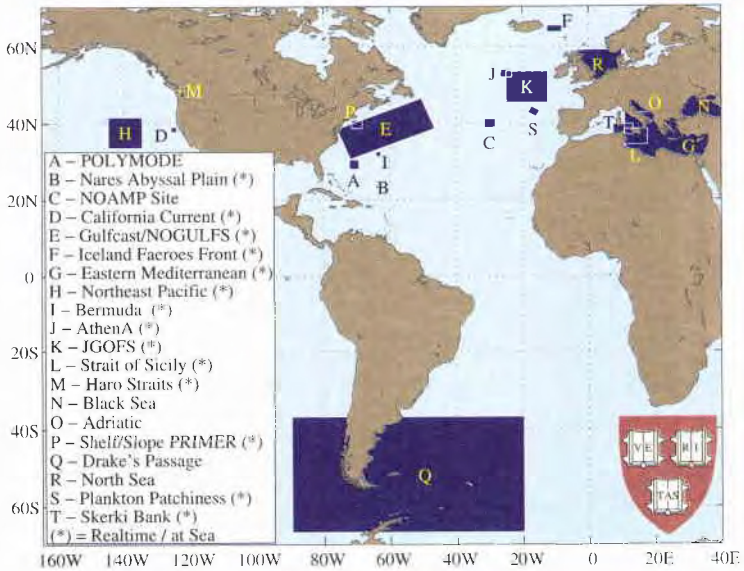

Fig. 1

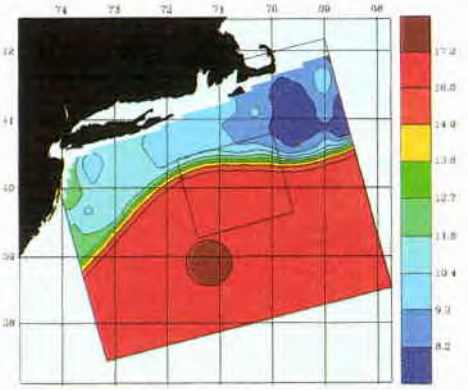

Fig. 3a

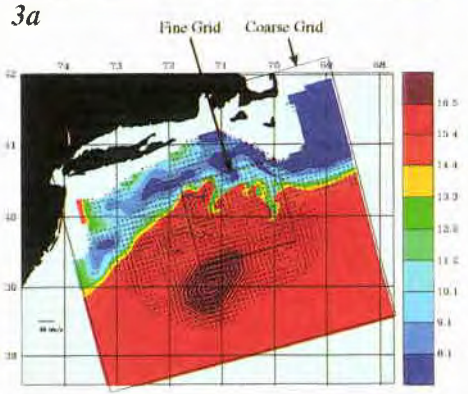

Fig. 3b

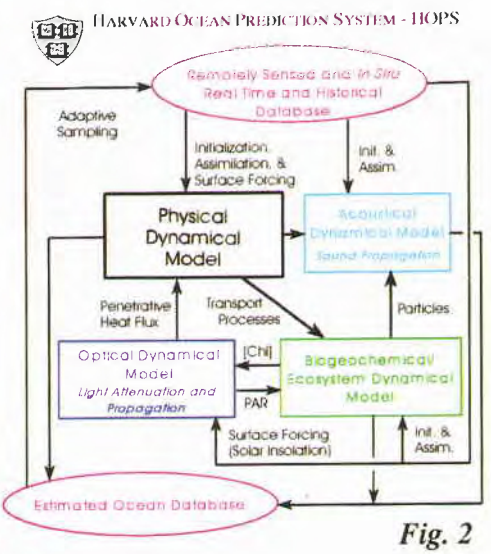

Fig. 2

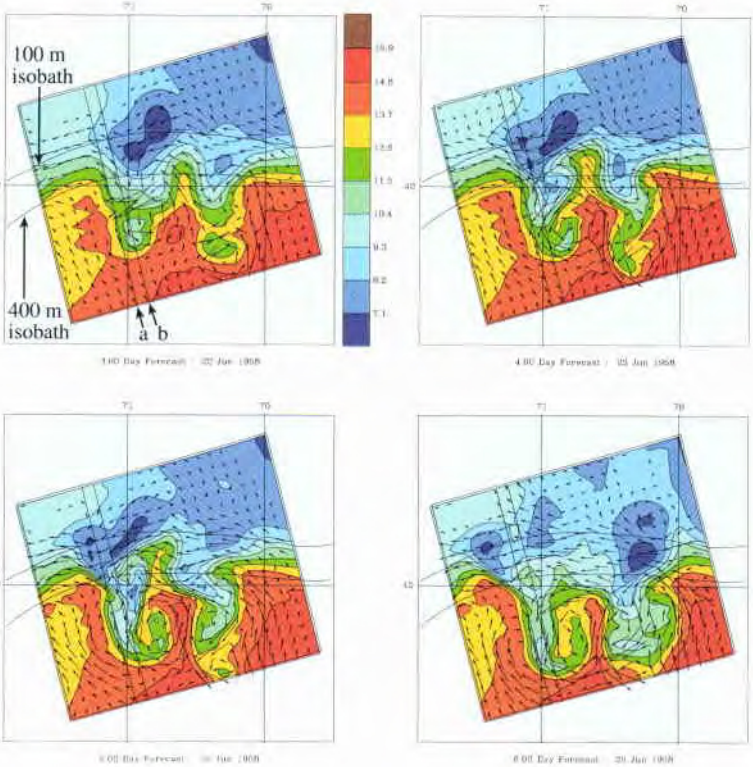

Fig. 4

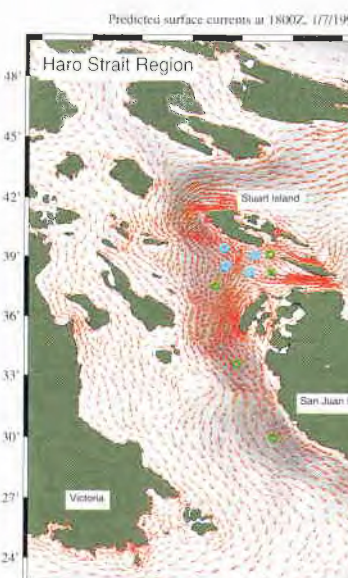

Fig. 5

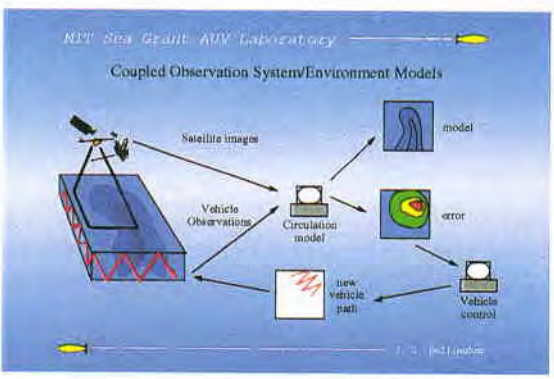

Fig. 6

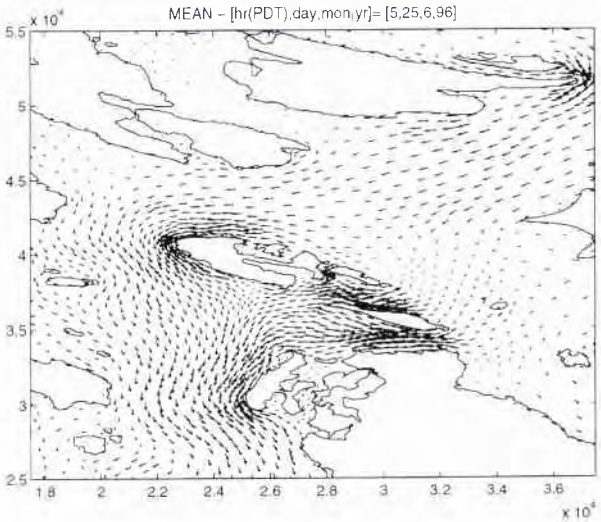
MEAN - [hr(PDT),day,mon,yr]= [5,25,6,96]
x 10^4
5.5
5
4.5
4
3.5
3
2.5
1.8
2
2.2
2.4
2.6
2.8
3
3.2
3.4
3.6
x 10^4

Fig. 7

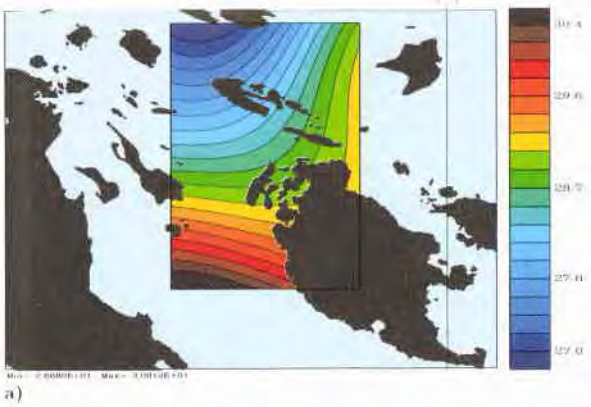
30.4
29.6
28.7
27.8
27.0

a)

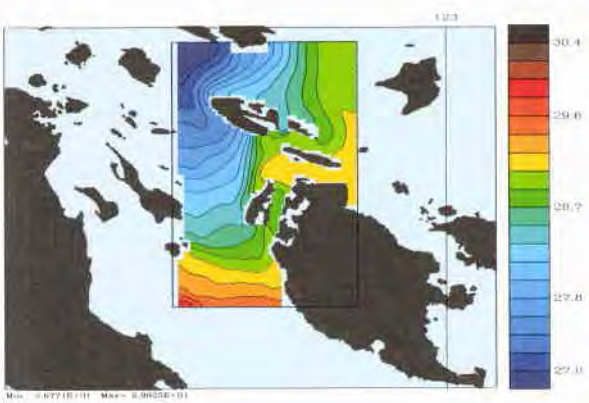
30.4
29.6
28.7
27.8
27.0

b)

Fig. 8

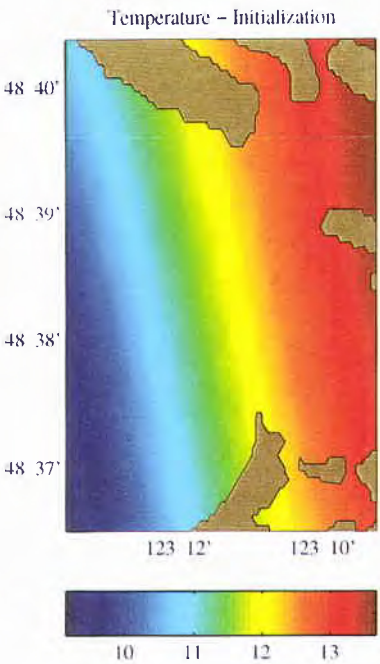

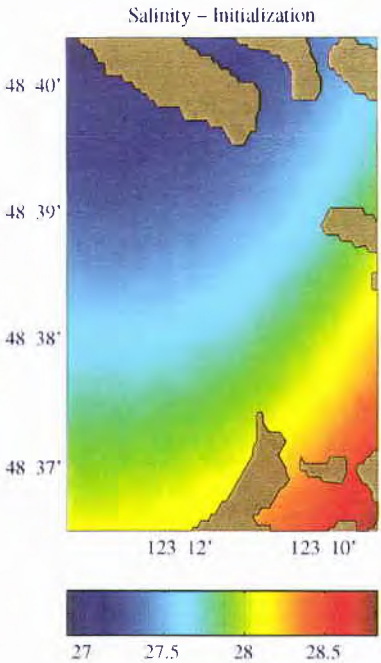

Fig. 9a,b

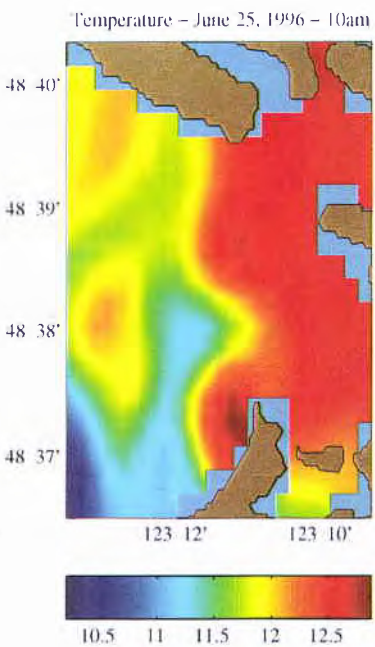

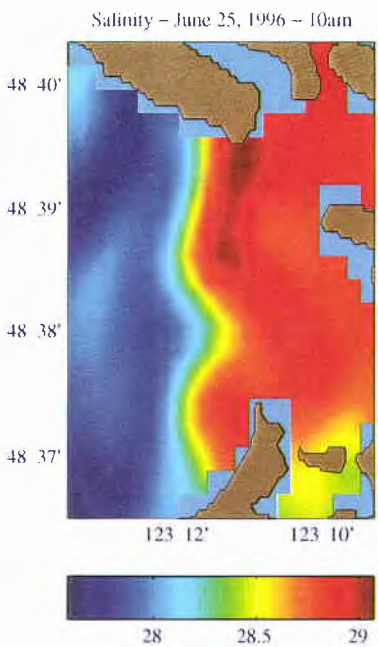

Fig. 9c,d

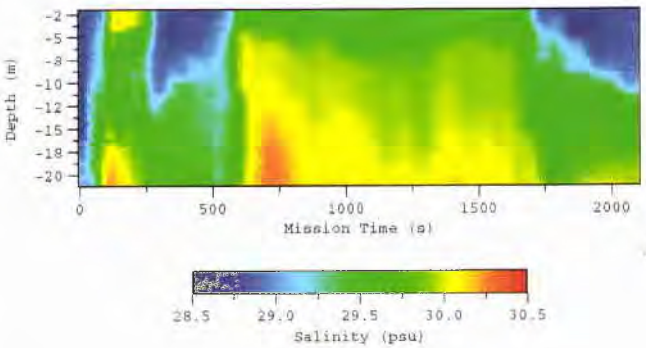

Fig.9e

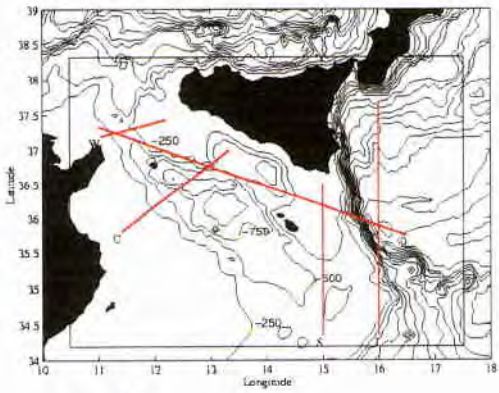

Fig. 10

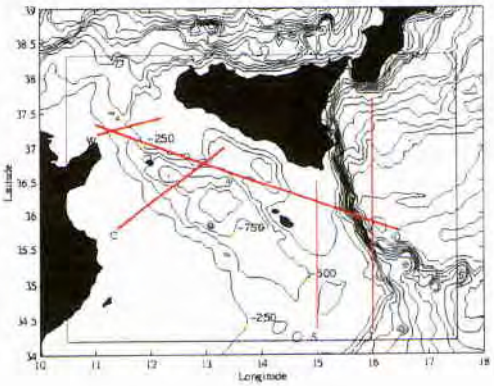

Fig. 11

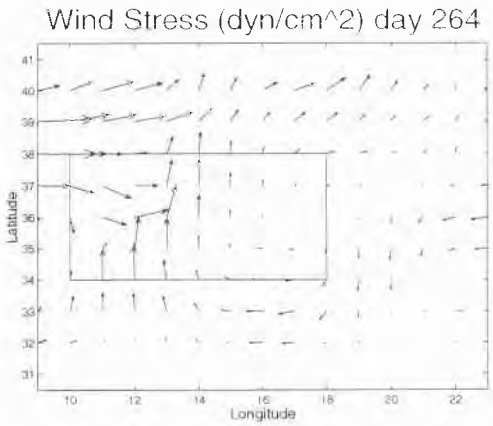

Fig. 12a

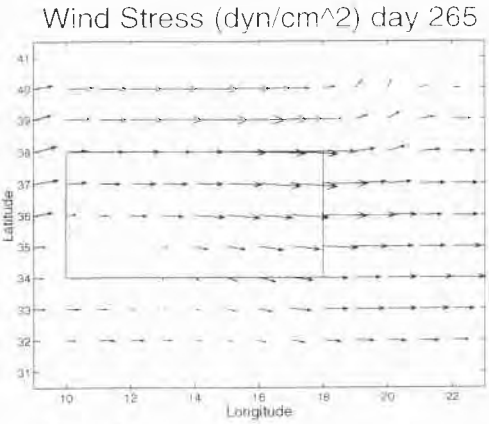

Fig. 12b

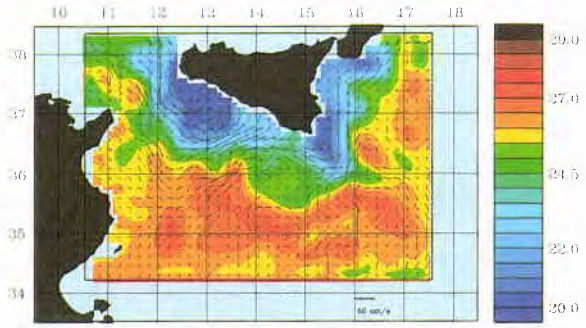

Fig. 12c

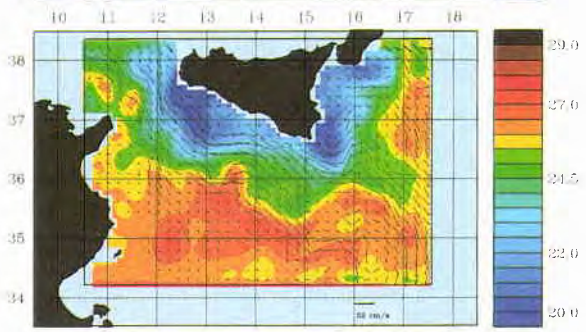

Fig. 12d

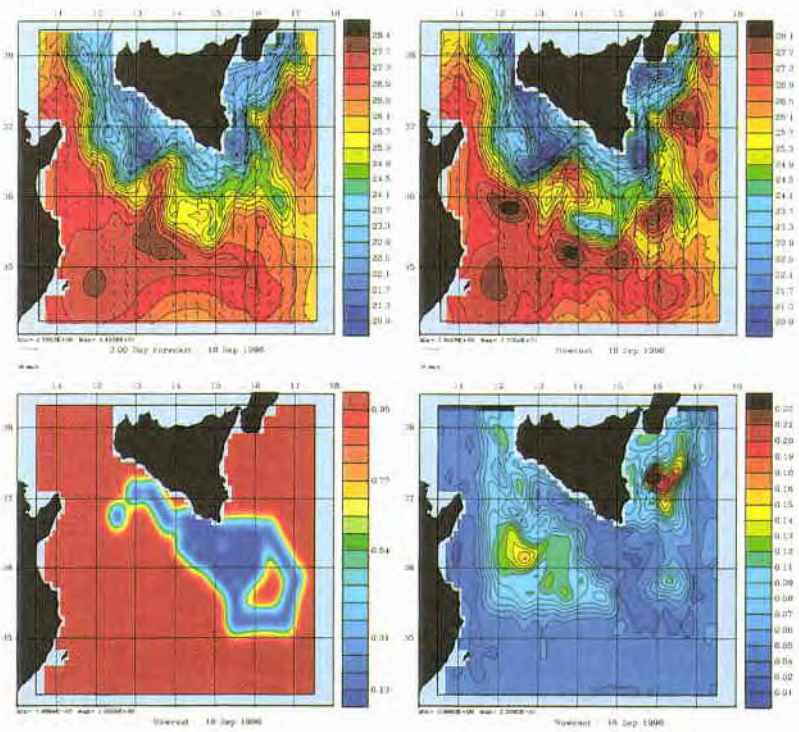

Fig. 13

Rapid Response to Geophysical Information Needs:Experience of establishing an Atmospheric and Ocean Forecast Model for the Olympic Games 1996

E. A. Martinsen and L. P. Røed

Norwegian Meteorological Institute (DNMI)
P.O.Box 43 - Blindern
0313 Oslo, NORWAY
Email: e.a.martinsen@dnmi.no; larspetter.roed@dnmi.no

Abstract

Shortly before the 1996 Olympics DNMI was asked to provide special forecasts for the Norwegian yachting team. The numerical model set-up was operational after three weeks. It delivered 24 hours forecasts of wind (five km grid) and currents (300 meter grid) for the race area. Valuable experience regarding methods and technical aspects of the set-up was gained. A major problem is the lack of real time ocean data for the ocean analysis.

1. Introduction

After the preolympic trials off Savannah, Georgia in 1995 the Norwegian Meteorological Institute (DNMI) was asked by the Norwegian Yachting Association if DNMI could provide special forecasts of wind and currents for the Norwegian yachting team during the sailing events of the Olympic Games in 1996. As late as mid June of 1996, i.e., only four weeks before the Olympics, DNMI formed a small group of meteorologists and oceanographers to provide the necessary information based on a setup of an automatic numerical modeling forecast of wind and currents. The system was up and running already after three weeks, one week before the Olympic sailing events was scheduled to take place.

The background for the request was that the Norwegian yachting team during the previous Olympics in Barcelona, Spain, had experienced that special detailed wind forecasts obtained directly from DNMI was of value. In particular they maintained that it was a crucial set of information and that it had helped the Norwegian team to win a gold medal in the Europe dinghy event. This time around they also asked for detailed current forecasts, in particular since large tidal currents had been observed during the preolympic trial events.

DNMI has for some time issued forecasts of currents and storm surges in Norwegian waters based on a fully three-dimensional, baroclinic numerical ocean model operating on a 20 km grid mesh (e.g., Figure 1). The model is a version of the Princeton Ocean Model (POM) and is called the Estuarine and Coastal Ocean Model - Three-Dimensional (ECOM3D). It was originally developed at Princeton University by G. L. Mellor and A. F. Blumberg (now at HydroQual Inc.) [1]. Its implementation at DNMI is described in [2].

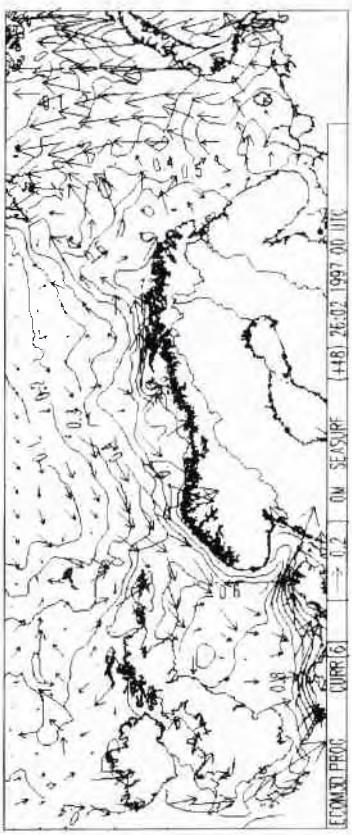

Figure 1: Example of a 48 hour current and sea level forecast valid for Norwegian waters on February 26, 1997. Solid curves show sea level in meters. Currents are represented as arrows. The arrow head points in the direction of the current and its length is proportional to the current speed. The scale (in m/s) is given in the figure.

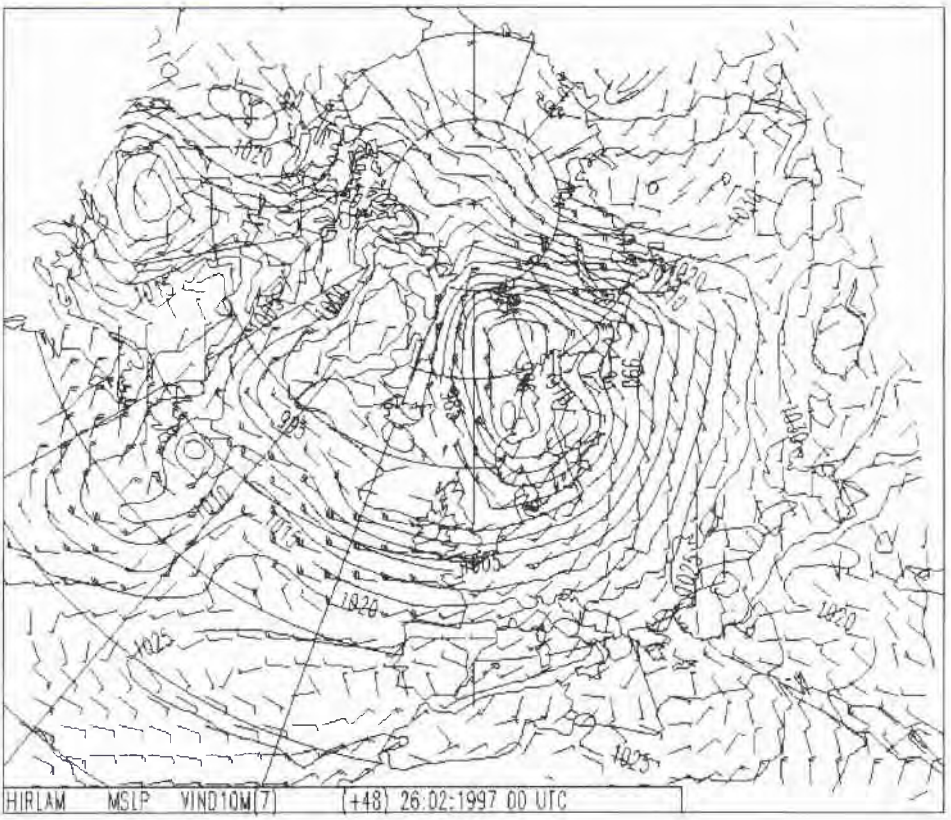

Figure 2: Example of a DNMI atmospheric forecast using the model HIRLAM. Shown is 48 hour forecast initiated at 00 hour UTC on February 24, 1997 for wind at 10 m and mean sea level pressure.

The ocean forecast takes its main driving forces such as wind, atmospheric pressure and heat fluxes from an atmosphere model forecast (e.g., Figure 2). Additional forcing is supplied by climatological (monthly mean) currents and sea level, including tidal information. These are specified at the models open boundaries. Finally, climatological (monthly mean) freshwater discharges from major rivers are supplied at the relevant locations.

The same model has also been used in various special projects which involves modeling of detailed currents in limited areas, e.g., the Vestfjorden in northern Norway and the Oslofjord in southeastern Norway. Through such projects DNMI has developed a system for which a limited area of smaller grid size may be nested into the coarse mesh grid of the forecast model area to provide more details. The nesting is one way, meaning that information is only submitted from the coarse mesh model to the fine mesh model. Such a nesting system is also implemented for the atmospheric model.

Below is presented the experience gained from the rapid response to the Norwegian Yachting Association. The forecast system is described in Section 2, while the experience gained is presented in Section 3.

2. The numerical modeling forecast system for the 1996 Olympics

In order to accommodate the needs for a detailed current forecast, i.e., a forecast that resolves the current changes over the race area, a triply nested ocean and atmosphere model system based on the operational systems at DNMI was employed.

Winds were forecasted using a five km grid version of the Norwegian limited area model (NORLAM5). This was nested into a 50 km version (NORLAM50), which in turn was nested into the European Center for Medium-Range Weather Forecast (ECMWF)'s global forecast model. In cooperation with HydroQual, Inc., USA, a 300 m grid version of DNMI's operational ocean model ECOM3D

(henceforth ECOM3D-300) was set up to cover the Wassaw Sound race area. This version was nested within a five km grid version of the same model (henceforth ECOM3D-5) which exactly matched the NORLAM5 area. The five km version was in turn nested into a 20 km grid version covering the US east coast from Florida to Long Island (henceforth ECOM3D-20). On the open boundaries the 20 km grid model was forced by monthly mean climatological values of salinity, temperature, current and sea level in addition to tidal motion from four tidal constituents. The set up of the system was made easier due to some precautions taken at DNMI in setting up it general operational modeling system. For instance the operational model setup allows the fine mesh area to be of any size and of any grid mesh. Further the orientation of the fine mesh grid can be skewed relative to the coarse mesh. All the meshes must, however, be regular with respect to a polar stereographic projection. All the nested models are identical except for the grid size and computational domain and contain routines that, when activated, automatically saves the information necessary for en even finer grid mesh model. This option was extremely useful in the triply nested approach taken here. The nesting of the various atmospheric and oceanographic models was accomplished through the use of the flow relaxation scheme (FRS) [3].

2.1. Model input

The topography and land contours for NORLAM50 and NORLAM5, were taken from the ETOPO5 database. The information was automatically interpolated to the model grid once the location of the grid was specified, and automatically generated the land/ocean matrix.

Since Norway is a member of the European Center for Medium-Range Weather Forecast (ECMWF) the sea surface temperature (SST) could be downloaded directly from the ECMWF SST analysis. In addition the necessary information at the open boundaries of the NORLAM50 was (by automatic routines) downloaded from the ECMWF global forecast and nested into the model employing the FRS technique. In turn NORLAM50 provided the necessary information at the open boundaries for the five km NORLAM5 model. It is important to realize that the two NORLAM models also contain automatic routines whereby available real time observations (through the world wide meteorological GTS system) is assimilated into the analysis which provides the initial conditions for each forecast.

Similar procedures were also followed regarding the triply nested oceanographic models. The bathymetry, except for ECOM3D-300, was again taken from the ETOPO5 database and automatically interpolated onto the respective model grids. For the ECOM3D-300 the topography was provided by HydroQual Inc. based on grid specifications from DNMI. Detailed information on topography is extremely important since it is well known that the tidal currents are strongly influenced by even small details in the topography. In addition it was known that the tides provided the dominant current component in the race area. This points to one of the major obstacles in setting up the fine mesh oceanographic model modules for a rapid response action. Detailed topography information is rarely available in digital form (see discussion below) and more often than not must be digitized for each application.

At the boundaries of the coarse mesh ECOM3D-20 model, the necessary information in terms of three-dimensional currents, temperature and salinity fields was taken from the climatological mean results for August. These data was provided by HydroQual Inc. in digital format through their access to the results from the diagnostic runs of T. Ezer and G. L. Mellor at the Princeton University [4].

Regarding tidal information only tidal amplitudes were available to us. They were again provided by HydroQual Inc. The amplitude originated from the model results of the global tidal model at Oregon State University. Since the FRS nesting approach employed also requires information on tidal currents, this problem was, due to the time constraints involved, solved in an ad hoc manner. To obtain the necessary tidal (kinetic) energy the tidal amplitude was increased by a certain factor. This amplitude factor was simply tuned based on experience from earlier North Sea tidal modeling efforts at DNMI.

Finally the freshwater discharge necessary for the most detailed model, i.e., the ECOM3D-300, was collected by and submitted to DNMI from HydroQual Inc. This included the discharge from two of the major rivers close to the Wassaw Sound race area.

2.2. Setup of the operational runs

In general the operational runs was done in a stepwise manner. First NORLAM50 was run and when completed then NORLAM5. Only when the atmospheric forecast was completed was ECOM3D-20 started. Thereafter ECOM3D-5 was run and then finally ECOM3D-300. Thus information from one module was only made available to the next model in line once its own forecast was completed. This way a forecast from the coarser meshes were always available even if one of the finer mesh model forecast runs should fail.

2.2.1. Winds

In order to provide a 24 hour detailed wind forecast starting at 00 hour UTC, the NORLAM50 model was run first. This run actually consists of four runs of which the first three were performed to provide initial values for the actual model forecast. This is part of what is referred to as the analysis. These runs consist of a sequence of three 6 hour forecast up to the analysis time.

During these runs all available observations (through GTS) within the area were assimilated into the model. In addition, as mentioned above, NORLAM50 was also forced at the boundaries of its computational domain by results from the ECMWF's global forecast. The fourth run then provided the 24 hour forecast.
Next, and as soon as NORLAM50 had completed its forecast, NORLAM5 was run in fashion similar to that described for NORLAM50, but without any data assimilation (only a very few observations were available). When NORLAM5 had finished its forecast the result was automatically submitted to a graphic package (see Section 2.3.3).

The atmospheric model modules were set in operation on July 8, 1996, i.e., one week prior to the first race.

2.2.2. *Currents*

The ocean forecasts were not that simple to initialize. One of the main problems in ocean forecasting is the provision of reasonably (dynamically) balanced initial fields. This problem stems from the fact that the ocean "memory" is much longer than the atmosphere one, and hence requires a much longer spinup time. This combined with the fact that no global forecast similar to the ECMWF atmospheric forecast exists for the ocean makes the initialization of the oceanographic models much more problematic. Commonly the ocean models have to be spun up for some length of simulated time well ahead of the actual forecasting time. To this end archived atmospheric analysis as well as other forcing data have to be used. The necessary spinup time is commonly determined by monitoring the time period it takes for the total kinetic energy to level off. Generally the larger the geographic domain covered the longer the spinup time.

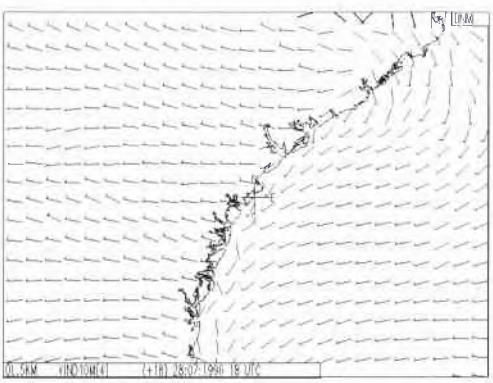

Figure 3: The NORLAM5 +18 UTC hour forecast issued based on the 00 UTC hour analysis on July 28, 1996. The wind is displayed as headless arrows where the feather indicates the wind strength. The arrow points in the direction of the wind. Note the influence of the land-sea matrix. The cross in the middle of the figure indicates the location of the race area along the eastern US coast

For the present application the ECOM3D-20 was spun up for a simulated period of about three month beginning May 10, 1996. For this purpose wind and other atmospheric driving forces were downloaded from the ECMWF analysis archives. The spinup was completed at the simulated time of 00 UTC July 9, 1996. The initial values for the spinup were taken from the August climatology given in [4]. ECOM3D-5 was spun up beginning June 15, 1996 while ECOM3D-300 was spun up beginning July 1, 1996. This way ECOM3D-5 could take its boundary and initial values directly from ECOM3D-20, and ECOM3D-300 in its turn could take the necessary data directly from ECOM3D5.

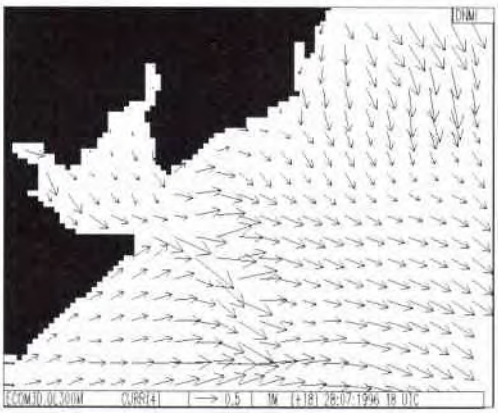

Figure 4: Example of current forecast concurrent with the atmospheric forecast shown in Figure 3. The forecast is from the ECOM3D-300 and covers the race area of Wassaw Sound. Currents are presented as explained in Figure 2. Note the influence of the detailed topography on the outgoing tide.

At the real time the spinup procedure was started (July 1, 1996) atmospheric analysis fields up to and including July 8, 1996 were for obvious reasons not available. Thus the spinup of the oceanographic model modules had to be made in two steps. One up to and including July 1, 1996 and a second from July 2, 1996 up to and including July 8, 1996, at which time the models were run in operational mode, i.e., the atmospheric forcing were then provided by NORLAM50 for the ECOM3D-20 and by NORLAM5 regarding the ECOM3D-5.

2.2.3. *Communication and presentation of the forecast*

Once the pertinent model forecasts were produced the results were automatically submitted to a graphic package for presentation. Two sets of products were automatically produced by this package. One was intended for the Internet and were in the form of animations for both winds and currents for the whole 24 hour forecast period. The animations were put on Internet by SchibstedNet (one of the major Internet providers in Norway).

The second product was an automatic generation of 18 paper plots showing wind respective currents one hour apart centered around the time of the races. This was made during the normal morning working hours in Norway and submitted to the Norwegian yachting team in the US via facsimile. Thus the forecasts were available to the team early in the morning US time (six hour time difference) and well before the races of that day.
A typical forecast made by NORLAM5 is shown in Figure 3, while a typical ocean forecast is shown in Figure 4. These plots are examples of the plots presented on the Internet.

3. Discussion and final remarks

The rapid response to the request from the Norwegian Yachting Association was made possible due to some general precautions made at DNMI in setting up its operational modelling system. However, the system at DNMI is not perfect. The experience gained from this exercise and similar applications leads us to conclude the following.

1) To respond to a rapid response request it is decidedly a major advantage to be within an operational institution (such as DNMI). It makes it easy to receive and arrange observations accessible over the GTS (even some oceanographic data are available over this net). Commonly also automatic systems for running models in operational mode already exist including graphical packages for presentation, i.e., the infrastructure is already in place.

2) The model system employed should be portable, i.e., no geographical information, such as grid orientation, size and location of computational domain, should be hard-coded in the models. All such information should be given through information on topography.

3) Different data archives should be collected and prepared for easy access in order to be able to rapidly extract the needed input to the models, i.e., archives of topography, monthly mean climatological values of salinity, temperature, sea ice, current and sea level, tidal motion, monthly mean freshwater run-off from rivers. In the example from the 1996 Olympics shown here too much time was wasted on arranging the tidal input. This was mainly due to the lack of appropriate tidal information for the given area, which clearly is outside the normal forecasting area for Norway. Nevertheless, the task would have been much easier if an appropriate global tidal information database had been in existence. For instance such a database exists for Norwegian waters and have been used to advantage for rapid responses in Norwegian waters.

4) A major problem pertaining to the oceanographic part of the rapid response is the lack of a real time oceanic observation system. It not only inhibits a proper initialization (data assimilation) of the model before each forecast, but also limits the possibilities of performing a meaningful validation of the model setup for a new area.

5) The results from NORLAM5 was subjectively validated against available observations over GTS and against special observations (downloaded via Internet) from automatic weather stations in the Savannah area. In particular the model was validated against known features such as coastal convergence and land-sea breeze effects. These effects seemed to be well captured by the model. A typical example is shown in Figure 3, taken from the 00 +18 UTC hour forecast using NORLAM5. As is evident from this figure that the above mentioned processes are prominent features of the model response.

6) The tidal currents produced by the model was (subjectively) validated against special buoy data provided by NOAA on Internet during the events. This showed that the tidal period in the model lagged about 90 minutes. The lag was probably due to the inadequate tidal information available and underscores the point made in 3) above.

Acknowledgment:

The authors are indebted to Anstein Foss and Harald Engedahl at DNMI. Without their efforts the rapid response to the request from the Norwegian Yachting Association would have been impossible. We would also like to thank Alan F. Blumberg and his colleagues at HydroQual Inc. for providing the various input data needed for the oceanographic models. It is also with gratitude we would like to thank many of our colleagues at DNMI for helping us with setting up the numerical modeling system. Thanks also goes to SchibstedNet for allowing us to "broadcast" the forecasts on Internet.

References

[1] Blumberg, A. F., and G. L. Mellor, A description of a three-dimensional coastal ocean circulation model. In: Three-Dimensional Coastal Ocean Models, ed. N. S. Heaps, AGU Coastal and Estuarine Ser., 4. American Geophysical Union, Washington D.C., 1987.

[2] Engedahl, H., 1995: Implementation of the Princeton Ocean Model (POM/ECOM3D) at the Norwegian Meteorological Institute (DNMI). Research Report No. 5, Norwegian Meteorological Institute, Oslo, Norway.

[3] Martinsen and Engedahl, 1987: Implementation and testing of a lateral scheme as an open boundary condition for a barotropic model. Coastal Engineering, **11**, 603-637.

[4] Ezer, T., and G. L. Mellor, 1994: Diagnostic and prognostic calculations of the North Atlantic Circulation and sea level using a sigma coordinate ocean model. *J. Geophys. Res.* **99**, 14,159-14,171

Determining the Coastal Environment by Data Assimilation using an Adjoint Technique

Pavel Pistek, Henry Perkins, Janice Boyd

Naval Research Laboratory, Code 7332
Stennis Space Center, MS, 39529, USA
Email: ppistek@nrlssc.navy.mil, hperkins@nrlssc.navy.mil, jboyd@nrlssc.navy.mil

Keith R. Thompson

Department of Oceanography, Dalhousie University
Halifax, Nova Scotia, Canada B3H 4J1
Email: keith@phys.ocean.dal.ca

Abstract

Data assimilation can provide detailed, accurate assessments of the ocean environment. This paper reports on an adjoint approach to data assimilation in coastal waters based on the shallow water equations of motion. Application of the method to a test data set from the California coast is described. The results provide insight into the type and quality of measurements required for wider application. Also noted are the instrument developments needed to use assimilation for real-time environmental assessments.

1. Introduction

Data assimilation techniques have been used for decades in meteorology and, more recently, in oceanography. A comprehensive review is given in [1]. A variant of this technique has been developed by Thacker and Long [2,3], who applied it to hypothetical data in the tropical ocean. It has been further advanced by Thompson and colleagues and applied to field data on the shelf east of Halifax [4, 5, 6]. Their domain was 60 km square with open boundary conditions on all sides and water depths varying from 40 to 100 m. Data was assimilated from bottom-mounted pressure gauges, moored current meters, a shipboard acoustic Doppler current profiler (ADCP) and surface drifters. They used the vertically averaged shallow water equations complemented by a spatially homogeneous slab-like surface layer and a geostrophic flow with polynomial dependence in the horizontal.

Success of the Scotian shelf work has prompted us to apply a similar technique to data collected in a setting on the California coast that included a coastal boundary. Results of that application are reported here along with a brief description of the technique. The paper concludes by discussing implications of the methodology for rapid environmental assessment.

2. Methodology

2.1. The Shallow Water Equations

The assimilation technique to be used requires the assumption of a system of equations that adequately represent the study area. Although a complete description might include a large number of processes, we argue that some of the complexity is already embodied in the data. For example, data collected in shallow water often shows spectral peaks whose frequencies are sums and differences of those in the tidal forcing potential. These are the hallmark of weak nonlinearities in the shallow water response dynamics. In the approach used here, we force the model not with the tidal potential, but with data itself in which the nonlinearities are already represented. To the extent that the nonlinearities are weak, the overall behavior can be represented adequately by linear equations. This approach is preferred over one that attempts to compute the nonlinear response from basic principles, for here it is the ocean itself that has provided the correct answer. Attention is further restricted, purely for the sake of simplicity, to the barotropic (vertically integrated) component of the current field. Thus the simplest credible dynamics have been adopted for the assimilation; that is, the linearized, vertically integrated, shallow water equations.

The assimilation equations are

$$u_t - f v + g \eta_x = \tau^{(S,x)} - \tau^{(B,x)} \tag{1a}$$

$$v_t + f u + g \eta_y = \tau^{(S,y)} - \tau^{(B,y)} \tag{1b}$$

$$\eta_t + (uH)_x + (vH)_y = 0 \tag{1c}$$

where u and v are vertically integrated horizontal ve-

locities in x and y directions respectively, and η is free surface elevation. Water depth is denoted by H and the Coriolis frequency by f. Surface and bottom stresses are represented by τ with various superscripts. The surface stresses in x and y directions, $\tau^{(S,x)}$ and $\tau^{(S,y)}$ respectively, are determined by the known wind field, which is negligible for the data to be presented here. Components of bottom stress are parameterized as functions of the currents:

$$\tau^{(B,x)} = \kappa u, \quad \tau^{(B,y)} = \kappa v \tag{2}$$

where κ is a constant.

2.2. Discrete Formulation

The above equations are solved on a rectangular grid in x and y and over uniformly spaced times. Specifically, a C grid with a total of M elevation points is used and the grid points are identified by a single index: x_j, y_j, $j = 1, \cdots, M$. Time is represented as N uniform time steps. Adopting the compact notation of [2,3], all dependent variables are represented at time t_n by a state vector:

$$x_n^T = [u_{1,n}, v_{1,n}, \eta_{1,n}, \cdots, u_{M,n}, v_{M,n}, \eta_{M,n}] \tag{3}$$

where the column vector x_n, represented here by its transpose, is of length $3M$. The dynamical equations, together with the coastal boundary conditions, can then be written as a matrix operator that advances x_n by one time step:

$$x_n = D_n x_{n-1} + f_n \qquad n = 1, \cdots, N \tag{4}$$

with f_n representing wind stress forcing over time interval (t_{n-1}, t_n).

Data is represented as a sequence of vectors d_n with components laid out corresponding to those of x_n. A measure of the mismatch between solution and data over all grid points and time can then be evaluated as

$$J_0 = \frac{1}{2\sigma_0^2} \sum_{n=0}^{N} (x_n - d_n)^T A_n (x_n - d_n) \tag{5}$$

Elements of matrix A_n give weights to the data values, possibly different for different types of data, at time t_n and are zero where there is no data. Here σ_0 is used as a scalar weight to adjust the influence of J_0 relative to other terms introduced later. For simplicity, it is assumed that all data lie at grid points, although the representation is general enough to allow other approaches.

In presenting results below, we will represent J_0 as the sum of contributions from different types of data, thus giving a measure of the success in assimilating a particular type of data. In particular we will take $J_0 = Ja + Jc$, where Ja and Jc, each of form (5), are respective contributions from ADCP and moored current meter data.

2.3. Solution Equations

As a solution for the assimilated fields that satisfies the dynamical equations (4) and minimizes the data mismatch (5) can be obtained by a standard constrained least squares fit. That is, by minimizing the cost function

$$J = J_0 + \sum_{n=1}^{N} \lambda_n^T (x_n - D_n x_{n-1} - f_n) \tag{6}$$

with respect to components of: the state vectors, $x_{i,n}$, and the Lagrange multiplier vectors, $\lambda_{i,n}$. The minimum of J is characterized by the vanishing of its derivatives with respect to each of these components. Application of this condition and some straightforward manipulations lead to the equations

$$x_n - D_n x_{n-1} - f_n = 0 \qquad n = 1, \cdots, N \tag{7a}$$

$$\lambda_n - D_{n+1}^* \lambda_{n+1} - A_n (d_n - x_n) = 0 \qquad n = 0, \cdots, N \tag{7b}$$

Equation (7a) repeats the dynamical equations (4), which the assimilation solution therefore must satisfy exactly. Matrix D_n^* is the adjoint of D_n, but for the linear dynamics used here it is simply the transpose of D_n. It steps the Lagrange multipliers backward in time. Finally, the two otherwise undefined Lagrange multiplier vectors are assigned the values

$$\lambda_0 = 0, \qquad \lambda_{N+1} = 0 \tag{7c, d}$$

The latter condition ensures that all the λ will be zero if the solution vectors x_n match all data points d_n.

The problem has now been solved in principle. There is the same number of unknown vectors as vector equations, so that (7) is a fully determined linear system. But for even a modest model domain, the system matrix is so large, typically having order 10^7, that a straightforward inversion is not possible.

Instead, a solution technique is developed in which some subset of the unknown quantities are selected and adjusted iteratively to steer the solution down the gradient of the cost function (6). The solution thus found is minimized with respect to these selected unknowns or control variables. For example, initial or final values (x_0 or x_N) might be chosen for controls (as in [2,3]) or values at lateral boundaries for some or all variables (as done in this paper). We consider next the selection of control variables before discussing further the iterative solution procedure.

2.4. Control Variables

Assignment of variables as controls is a matter of art, but subject to some general principles.

i) The model should depend strongly on their

value. Initial values alone will be a poor choice in a system with strong forcing and strong damping where the effect of initial conditions becomes irrelevant before the end of the model time. Similarly, if the model domain is so large that boundary forcing has little effect on the interior, then boundary values by themselves make poor control variables.

ii) They should be located away from data positions. Near data values, the solution is already constrained by the data values through (5). Hence, control values located there will have reduced ability to control the solution.

iii) There should be about the right number of them. If too few, they will not be able to control the solution. If too many, the iterative procedure will be unnecessarily slow, since it increases at least linearly with K.

As an example, consider a semi-enclosed bay that is strongly damped and forced through its entrance, across which there is a dense array of measurements. Then it would be inadvisable to use either the boundary or initial conditions for controls, and one might consider introducing a section of control values somewhere in the interior.

2.5. Solution Procedure

Define a collection C consisting of K integers, i_k and denote the controls as $v_{i,n} = v_{i,0}$ if $i \in C$, independent of the time step. One can thereby identify as control variables any of the dynamic variables $(u_{i,n}, v_{i,n}, \eta_{i,n})$ at any point in the model domain. Initially, all control variables $v_{i,n}$ and initial conditions $x_{i,0}$ are set to zero. The following steps are then carried out iteratively:

i) Forward time stepping is carried out using (7a), except that control variables are substituted for $x_{i,n}$ wherever one is defined; that is, set $x_{i,n} = v_{i,n}$ whenever $i \in C$. This practice amounts to forcing the model at the control points, and makes it attractive to choose those points to be initial or boundary values. Resulting solution vectors, call them $x_n^{(k)}$ after the k-th iteration, need not be stored except for those components that correspond to data values.

ii) Using (7b) and (7d), step backward to find estimates of the adjoint variables, say $\lambda_n^{(k)}$. Data-model differences are used whenever available and act as forcing for the adjoint equation.

iii) Adjust the control variables. The cost function gradient $\partial J / \partial x_{i,n}$ with respect to any variable can be found by differentiating (6). Here, it is evaluated at the control points using the approximate solution $x_n^{(k)}$, $\lambda_n^{(k)}$. The control variables can then be redefined to steer the solution towards a minimum of the cost function using, for example, the conjugate gradient method [7,8].

iv) Repeat steps *i-iii* until the procedure converges. A plot of the cost function versus iteration number is useful as a guide.

2.6. Further Constraints

Additional constraints on the solution may be used to induce desired properties. If these can be expressed as quadratic forms, say J_v or J_t as below, then it is straightforward to add them through a revised cost function, since their gradients with respect to the control variables can be evaluated as in of step *iii)* above. That is, (6) is replaced by

$$J = J_0 + J_v + J_t + \sum_{n=1}^{N} \lambda_n^T (x_n - D_n x_{n-1} - f_n) \qquad (8)$$

and the solution procedure remains otherwise unchanged.

2.6.1. Spatial smoothness

Smoothness may be imposed by minimizing mean square surface slope, vorticity, etc. In the results below, we have used a vorticity constraint to suppress spurious eddies and keep reflected waves to a minimum. Such constraints may be written as a quadratic form representing a contribution to the total cost function

$$J_v = \frac{1}{2\sigma_v^2} \sum_{n=0}^{N} v_n^T B_n v_n \qquad (9)$$

Elements of the weighting matrices B_n are constructed to evaluate the squared vorticity and, as before, σ_v is a weighting parameter. This could have been included in the original problem formulation, but it is conceptually and computationally simpler not to do so.

At step *iii)* of the above iterative scheme, it is sufficient to evaluate the gradients of J_v with respect to the control variables. This can be done by explicitly differentiating (9) and evaluating it at the control point using the solution x_n available at that iterative step.

2.6.2. Tidal periodicity

Tides often dominate the coastal environment and may not be adequately represented if the data is sparse in time -- as in the case below. The presumption of approximate tidal periodicity can be included in the solution in several ways. Here we make, at each iterative step, a regression of the control variables against a chosen set tidal frequencies, say ω_j, $j = 1, \ldots, J$. That is, after each iteration the solution at the i-th control point is a time series $y_{i,n}$. Each time series is approximated by an expression of the type

$$h_{i,n} = a_{i,0} + \sum_{j=1}^{J} (a_{i,j} \cos \omega_j t_n + b_{i,j} \sin \omega_j t_n) \qquad (10)$$

with the coefficients $a_{i,j}$, $b_{i,j}$ found by least squares regression. Thus the tidal coefficients are known at each control point.

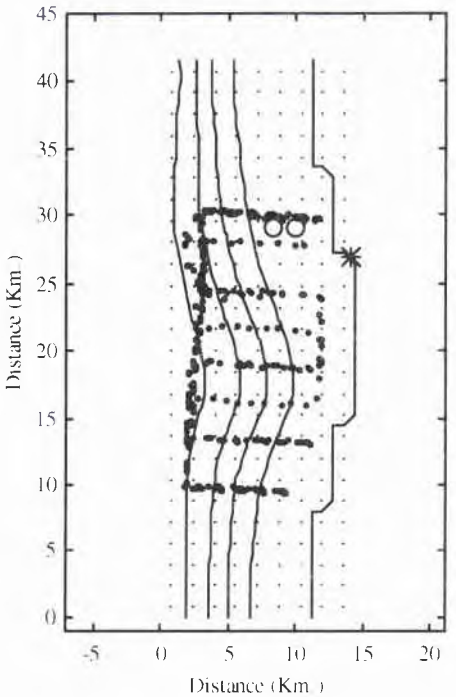

Figure 1 Plan view of the experiment. Model elevation points are shown as dots. The California coast, approximated by model velocity points, is at right, with an asterisk at Oceanside. Bathymetry within the gridded domain is given by contour lines at 100m intervals. Heavy dots mark underway ADCP current profiles from a series of surveys. Two circles near the upper trackline indicate surface current meters.

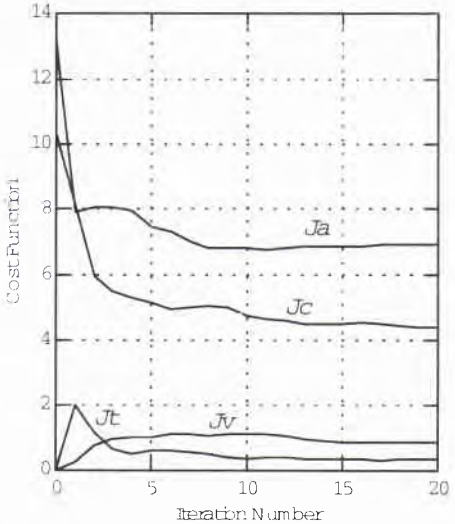

Figure 2 Values of the four components of the cost function associated with various data and other constraints. *Ja*: error in fitting the ADCP current data; *Jc*: error in fitting the current meter data; *Jv*: error in satisfying the vorticity constraint; *Jt*: error in satisfying the tidal constraint.

An additional cost function component is then taken in the form

$$J_t = \frac{1}{2\sigma_t^2} \sum_n \sum_i (v_{i,n} - h_{i,n})^T (v_{i,n} - h_{i,n}) \qquad (11)$$

where $h_{i,n}$ is a harmonic approximation of the tides and the sums are over all times and all control points. Finally, gradients of J_t with respect to the control variables can be evaluated explicitly making use of (11) and the solutions available at that iterative step. The effect is to penalize the cost function for non-tidal time dependence.

3. The Oceanside Experiment

3.1. Data

A test dataset was collected on the narrow shelf west of the town of Oceanside, California. A series of nine surveys was made over the eleven-day interval 17-27 October 1995 using a ship-mounted ADCP. Surveys were run along piecewise straight courses, either along the boxcar pattern evident in Fig. 1 or around the periphery of the survey area. Two surface current meters operated continuously during the experiment.

Current profiles from the ADCP survey were vertically integrated to create a barotropic field compatible with the equations of motion. The surface current meters were used as estimates of twice the barotropic component, based on the vertical structure of the ADCP profiles. Their role was most valuable in establishing the phase of the tidal currents.

3.2. Assimilation

The ADCP and surface current data were assimilated using the technique outlined above using (8) as cost function. Frequencies of the four dominant tides in the observing area, M_2, S_2, N_2, and K_1 were chosen for the tidal constraint. Control variables were taken along the lower and offshore sides of the model domain. A time step of 10 sec was used in accordance with the usual Courant-Friedrichs-Lewy stability criterion. In the interest of computational efficiency, certain quantities, most notably the control variables, were only evaluated at 15 min intervals with interme-

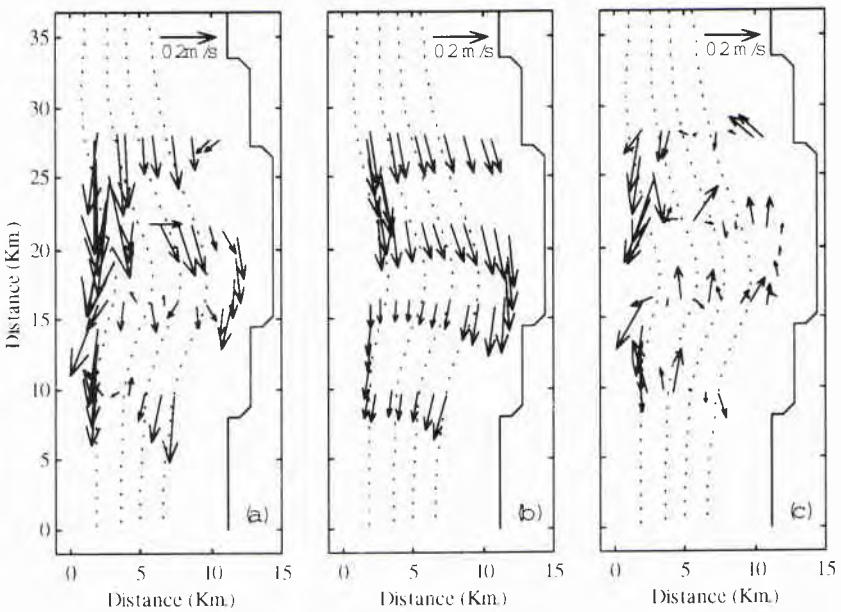

Figure 3 Comparison between original ADCP data and the final assimilated field during one of the ADCP surveys: (a) Measured current. (b) Currents from assimilation. (c) Difference. The survey started at upper right at 1600Z on 18 Oct 95 and required nearly 8 hr to complete, a substantial part of a tidal cycle. In this comparison the assimilated current vectors are shown at times that most nearly match the time and position of each measurement.

diate values found by interpolation when necessary.

Initial conditions were clearly irrelevant for this situation, since a southward-flowing current flushed the area daily. To avoid their formal appearance in the assimilation, a spin-up time was introduced at the start of which the initial conditions were set to zero. This two day interval before measurements started allowed the assimilation equations to adjust gradually toward the data values. Convergence of the iterative procedure was rapid, as seen in Fig. 2.

3.3. Results

In Fig. 3, result of the assimilation is compared directly with data from one of the ADCP surveys. Smoothness of the fitted solution compared with the observations is evident, as is a tendency of the flow to follow bathymetric contours. The substantial differences between observed and assimilated currents in the deeper portion of the domain we attribute to a deficiency in the ADCP measurements. The data extended only to a depth of 150 m; satisfactory estimates of barotropic current could not be made where the water was substantially greater.

Other discrepancies between fitted and measured currents have no satisfactory explanation since all the error sources common to ADCP observations have been treated. We cannot distinguish between measurement errors and the presence of small-scale variability not described by the presumed dynamics nor adequately sampled in the survey.

4. Discussion

4.1. Prospects for Rapid Assessment

Assimilation of the type we have described provides a virtually complete description of the variables described by the model providing that the model is appropriate to the area and that sufficient data is available. It combines data, dynamics, and preconceived ideas of what the environment is expected to look like in an optimum fashion to produce gridded fields in space and time of all the variables. Computational requirements are moderate. It may be thought of as a dynamically correct form of data interpolation. It may also serve for data extrapolation in either space or time since the domain of the model may be larger than the domain in which there is data. Forward time

extrapolation, or prediction, is simply a matter of continuing to step forward in time with the same equation (7a) used in the assimilation dynamics.

The initial assertion of the previous paragraph contains some major qualifications. Some variables of interest may not be described by the model; suitability of the model for use in a tactical area may not be known *a priori*; and it is not clear how much data is required. These issues are beyond the scope of this paper and the last will require further research. In the remaining paragraphs, we draw on experience gained from the Oceanside dataset to highlight some practical issues.

4.2. Data Requirements

Areas of tactical interest in the coastal zone have typical dimensions of only a few tens of kilometers. Two factors prevent this limited scale from translating into a correspondingly limited requirement for data. First is short flushing time. Alongshore currents often have speeds sufficient to flush the study area in less than one day. To capture advected features, frequent data updates are essential. Second is small space-time scales near coast. These arise from small bathymetric features combined with tidal-period variability, and can be accompanied by radiated waves. Time series data from fixed instruments is particularly valuable for process identification and for providing repeated data updates as the area is continually being flushed. For many purposes, a single instrumented site is as useful as a dedicated ship.

Good bathymetric data is critically important and that from conventional sources is often inadequate.

4.3. Instrumentation Requirements

We know what needs to be measured and how to measure it. Through such techniques as assimilation, we know how to make the most from the data. A modest array of bottom mounted ADCPs and tide gauges, perhaps accompanied by moored temperature and salinity measuring chains, can provide sufficient information for continuous updates of an assimilative tactical area model. The model can be generalized to treat three-dimensional, time varying fields. The challenge for rapid environmental assessment is in timely delivery of results. Present moored instrumentation records data internally, whereas the operational needs of tactical, assimilative models will require that data be reported in nearly real time.

Acknowledgments. Financial support of this work was provided by the Office of Naval Research through Program Element 602435N.

References

[1] M. Ghil and P. Manalotte-Rizzoli, "Data assimilation in meteorology and oceanography," *Adv. in Geophys.*, vol. 33, pp. 141-266, , 1991.

[2] W.C. Thacker, "Fitting models to data by enforcing spatial and temporal smoothness," *J. Geophys. Res.*, vol. 93, pp. 10655-10665, September, 1988.

[3] W.C. Thacker and R.B. Long, "Fitting dynamics to data," *J. Geophys. Res.*, vol. 93, pp. 1227-1240, February,1988.

[4] A.J. Bowen, D.A. Griffin, D.G. Hazen, S.A. Matheson, and K.R. Thompson, "Shipboard nowcasting of shelf circulation," *Cont. Shelf Res.*, vol. 15, pp.115-128, January, 1995.

[5] Griffin, D. A. and K. R. Thompson, "The adjoint method of data assimilation used operationally for shelf circulation," *J. Geophys. Res.*, vol. 101, pp. 3457-3478, February, 1996.

[6] K.R. Thompson and D. Griffin, "A model of the circulation on the outer Scotian shelf with open boundary conditions inferred by data assimilation," unpublished.

[7] P.E. Gill, W. Murray, and M.H. Wright, "*Practical Optimization*," London, Academic Press, 1981, ch. 4, p187.

[8] W.H. Press, B.P. Flannery, S.A. Teukolsky, and W.T. Vettering , "*Numerical Recipes*," Cambridge, Cambridge University Press, 1986, ch. 10, pp. 301-307.

Merging Disparate Oceanographic Data

B. L. Lipphardt, Jr.,* A. D. Kirwan, Jr.,* C. E. Grosch,* L. M. Ivanov,** J. K. Lewis***

*Center for Coastal Physical Oceanography
Old Dominion University
768 West 52nd Street
Norfolk, Virginia 23529
E-mail: bruce@ccpo.odu.edu

**Marine Hydrophysical Institute
Ukraine Academy of Sciences
Sevastapol, Ukraine
E-mail: ocean@mhi2.sebastopol.ua

***Ocean Physics Research & Development
207 S. Seashore Drive
Long Beach, Mississippi 39560

Abstract

Rapid Environmental Assessment (REA) exercises require data from a variety of disparate sources to be synthesized and integrated with numerical models. Here, a spectral method using basis functions satisfying Dirichlet or Neumann boundary conditions, as appropriate, is applied to the analysis of both scalar and vector oceanographic fields. When applied to velocity data, these basis sets exactly satisfy the no normal flow condition at solid model boundaries, and exactly ensure incompressibility. Applications of these basis sets to both scalar and velocity fields in the Black Sea and to the surface velocity field in Monterey Bay are discussed as examples of irregularly shaped, open and closed REA domains.

1. Introduction

In Rapid Environmental Assessment (REA) exercises, data from disparate sources must be merged, assessed and compared with numerical models. Consider one critical REA variable, velocity. Velocity observations may be obtained from current meter moorings, HF radar or drifters. Velocity is also a typical prognostic variable in a forecast model and thus must satisfy appropriate model slip and normal flow boundary conditions. For both observations and model results, the velocity field should be constrained to be incompressible. For variables other than velocity, different constraints may be appropriate.

A wide variety of methods are available for dealing with these issues. All have positive and negative attributes. Here we report on efforts to apply the method originally proposed by [1] to REA scenarios. This is a spectral approach which utilizes spatial basis functions which satisfy Dirichlet or Neumann boundary conditions. The basis functions are essentially the Fourier mode representation for the specified irregular boundary shape. They are generated numerically for any model grid and boundary, and observations or model results are projected onto them. Since the basis functions are known at every grid point, accurate interpolation to observation positions is straightforward. The recovery of the spectral amplitudes is also straightforward, but does require inverting large nonsparse matrices.

Since the method is applicable to arbitrary domain shapes, it is ideal for REA applications. Once an REA domain is specified, the Dirichlet and Neumann basis functions are calculated for the domain model grid. If the REA domain is contained in a basin scale model domain, the basin scale model can be used to specify boundary conditions for the REA domain. For multi layer problems, separate basis sets must be calculated for each layer.

The method has been applied to both scalar fields and Lagrangian velocity observations. For scalar fields, either Dirichlet or Neumann basis functions are required, depending on the boundary conditions appropriate for the scalar variable. Complete specification of the velocity field requires both basis sets.

The next section gives a synopsis of the theory, and section three provides some examples of applications. The last section summarizes the results and discusses potential problems.

2. Theory

2.1. Background

The theory behind our approach relies on representing data fields as a spectral expansion of basis functions which satisfy model boundary conditions appropriate for specific data sets. Typical boundary conditions are:

- **Dirichlet conditions** – values of the variable are prescribed as time varying quantities on the model boundary.
- **Neumann conditions** – values of the variable's flux at the model boundary are prescribed as time varying quantities.

Velocity is a particularly appropriate example. For solid boundaries, there should be no normal flow. For portions of the boundary that are open, the flow would be specified, either from observations or from a larger domain basin scale model. If a basin scale model is used to provide boundary velocities, our procedure permits large scale information to be incorporated into an REA subdomain in a dynamically consistent fashion. In this case, it is presumed that boundary information is at least as accurate as interior information.

Sections 2.2 and 2.3 describe the basis function representations for Dirichlet and Neumann boundary conditions, respectively. Both boundary conditions are needed to completely represent the velocity field, as discussed in section 2.4.

Since the data stream will, in general, be irregular in both space and time, some nuances in the spectral inversion of the data are required. These are discussed in section 2.5.

2.2. Dirichlet Boundaries

When values of the variable of interest are known on the REA boundary, the data should be represented as:

$$\Psi(\vec{x}, z, t) - \Theta_D(\vec{x}, z, t) = \sum_n \lambda_n(z, t)\, \psi_n(\vec{x}) \qquad (1)$$

where $\vec{x}$ is the horizontal position vector.

The left hand side of (1) is known from interior data (first term) and boundary data (second term). The right hand side is the representation of this data in terms of the Dirichlet basis functions.

This representation consists of an interior solution which satisfies homogeneous Dirichlet boundary conditions:

$$\nabla^2 \psi_n + \lambda_n \psi_n = 0, \quad \psi_n|_{boundary} = 0$$

and a boundary solution which satisfies Laplace's equation with inhomogeneous Dirichlet boundary conditions appropriate to a REA setting:

$$\nabla^2 \Theta_D = 0, \quad \Theta_D|_{boundary} = \Psi|_{boundary}$$

2.3. Neumann Boundaries

When values of the flux of a variable of interest are known on the REA boundary, the data should be represented as:

$$\Phi(\vec{x}, z, t) - \Theta_N(\vec{x}, z, t) = \sum_m B_m(z, t)\, \phi_m(\vec{x}) \qquad (2)$$

This representation consists of an interior solution which satisfies homogeneous Neumann boundary conditions:

$$\nabla^2 \phi_m + \mu_m \phi_m = 0, \quad \left.\frac{\partial \phi_m}{\partial \vec{x}}\right|_{boundary} = 0$$

and a boundary solution which satisfies Laplace's equation with inhomogeneous Neumann boundary conditions appropriate to a REA setting:

$$\nabla^2 \Theta_N = 0, \quad \left.\frac{\partial \Theta_N}{\partial \vec{x}}\right|_{boundary} = \left.\frac{\partial \Phi}{\partial \vec{x}}\right|_{boundary}$$

2.4. Velocity

Velocity represents an interesting combination of the Dirichlet and Neumann conditions. To see how the above spectral expansions can be applied to a velocity field, recall from [1] that an incompressible velocity field can be expressed in terms of two scalar potentials as:

$$\vec{u} = \nabla \times [n\Psi + \nabla \times (n\Phi)] \qquad (3)$$

Here, n is the unit vector in the vertical direction. It is important to note that this form ensures the velocity field is exactly incompressible in three dimensions.

In (3), Ψ may be thought of as the streamfunction. As shown in (1), the spectral portion of the Ψ field is composed of Dirichlet basis functions ψ_n. Note that, for each ψ_n, the horizontal divergence is zero and the vertical component of relative vorticity is generally nonzero, so that the Dirichlet modes might be interpreted as "rotational modes" for a velocity field.

Similarly, Φ in (3) may be interpreted as the velocity potential field. From (1), the spectral part of Φ is composed of Neumann basis functions ϕ_m. Each ϕ_m has a generally nonzero horizontal divergence and a zero vertical component of relative vorticity, so that the Neumann modes might be interpreted as "divergence modes" for a velocity field.

If the velocity field's boundary effects are associated only with the Ψ field, so that $\Theta_D \neq 0$ and $\Theta_N = 0$, the velocity components are expressed as:

$$u = -\sum_{n=1}^{N} A_n \frac{\partial \psi_n}{\partial y} + \sum_{m=1}^{M} \frac{\partial B_m}{\partial z} \frac{\partial \phi_m}{\partial x} - \frac{\partial \Theta_D}{\partial y}$$

$$v = \sum_{n=1}^{N} A_n \frac{\partial \psi_n}{\partial x} + \sum_{m=1}^{M} \frac{\partial B_m}{\partial z} \frac{\partial \phi_m}{\partial y} + \frac{\partial \Theta_D}{\partial x}$$

$$w = -\sum_{m=1}^{M} B_m \left(\frac{\partial^2 \phi_m}{\partial x^2} + \frac{\partial^2 \phi_m}{\partial y^2} \right)$$

2.5. Data Inversion

One application of this technique is to develop a two dimensional picture of the distribution of a scalar quantity over the REA domain. Here, if Dirichlet boundary conditions are appropriate, the scalar field ρ may be represented as:

$$\rho(\vec{x}_p, z_p, t) = \sum_{n=1}^{N} A_n(z_p, t)\, \psi_n(\vec{x}_p), \quad p = 1, \ldots, P$$

where ψ_n are the discrete set of N Dirichlet basis functions and P is the total number of locations of scalar observations.

Alternatively, if Neumann boundary conditions are more natural for the scalar quantity being considered, the field may be represented as:

$$\rho(\vec{x}_p, z_p, t) = \sum_{m=0}^{M} B_m(z_p, t)\, \phi_m(\vec{x}_p), \quad p = 1, \ldots, P$$

where ϕ_m are the discrete set of M Neumann basis functions.

Another application of this technique is to develop a two dimensional velocity field for an REA domain from a disparate set of P velocity observations. These observations may consist of a set of Lagrangian drifter trajectories, current meter observations, or satellite derived velocity estimates.

For this case, both Dirichlet and Neumann basis functions are required and the velocity components are represented as shown in section 2.4. Once the basis functions are known, and their gradients calculated, all that is required to describe the velocity field is the set of A_n and B_m amplitudes. Typically, for a set of P velocity observations, the "inversion" problem consists of a set of $2P$ equations, one for each velocity component observation (u and v components). The number of unknown amplitudes is $N + M$, where N is the maximum number of Dirichlet modes, and M is the maximum number of Neumann modes.

This linear least squares problem can be expressed in matrix form as:

$$\vec{U} = \tilde{L} \cdot \vec{C} \tag{4}$$

where $\vec{U}$ is the vector of *all* $2P$ velocity component observations, $\tilde{L}$ is the matrix of basis function gradients, and $\vec{C}$ is the vector of $N + M$ unknown amplitudes. Multiplying both sides of (4) by the transpose of $\tilde{L}$ yields:

$$\tilde{L}^T \cdot \vec{U} = \tilde{L}^T \cdot \tilde{L} \cdot \vec{C} \tag{5}$$

Note that this operation results in a square system of $N + M$ dimensions, which can be expressed more simply as:

$$\vec{Z} = \tilde{Q} \cdot \vec{C}$$

where $\vec{Z}$ and $\tilde{Q}$ are known and $\tilde{Q}$ is a square matrix. A least squares solution to this system is readily determined numerically, using any of a number of standard least squares solver packages.

3. Examples

In this section we present some examples of applications taken from the literature. We also describe an analysis of the surface velocity field in Monterey Bay, off the coast of California. The Monterey Bay domain is irregularly shaped and includes open boundaries, so that it provides a challenging example of a typical REA domain in a coastal region.

3.1. Distribution of Cesium nuclides in the Black Sea

In [2], the method described here was applied to develop a map of the concentration of a Cesium isotope (^{137}Cs) in the Black Sea from a set of observations. Because ^{137}Cs concentration is a scalar quantity that is assumed to have zero flux at land boundaries, Neumann basis functions was used for the spectral representation. Figure 1 shows the reconstructed ^{137}Cs concentration field from [2]. The authors note that 20 Neumann modes were required to accurately reconstruct this particular field.

3.2. Large Scale Circulation in the Black Sea

In [3], both Dirichlet and Neumann basis sets were used to develop spectra for a climatic Black Sea model surface velocity field for the month of July. The model used density observations for the period 1950–1987 to develop monthly climatic mean velocity fields.

The upper panel of Figure 2 shows the climatic velocity field at a depth of 10 m for the Black Sea in July. The middle panel of Figure 2 shows the A_n spectra (Dirichlet modes) for this field. The lower panel of Figure 2 shows the B_m spectra (Neumann modes) for the field.

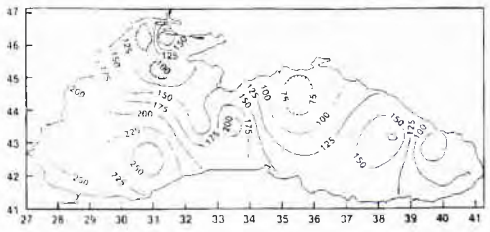

Figure 1: Reconstructed ^{137}Cs concentration field at a depth of 2.5 m in Becquerels (Bq) per cubic meter (1 Curie = $3.7 \times 10^{10} Bq$). From [2].

3.3. Surface Circulation in Monterey Bay

To illustrate how this technique might be applied to the surface velocity field in a coastal REA region, we applied the technique discussed in sections 2.4 and 2.5 to the surface velocity field in Monterey Bay, off the California coast. The Monterey Bay domain is irregularly shaped, and has open boundaries along the western side, and portions of the northern and southern sides.

Surface velocity observations from HF radar were made available to us by J. Paduan for the period August - December 1994. These observations were made with the Coastal Ocean Dynamics Application Radar (CODAR) and are described in detail in [4]. Our analysis used CODAR data for the period 1-27 August 1994. Velocity data was available at two hour intervals, with some short gaps in the data record. Typically, surface velocity was available for 500-600 locations in the domain at each two hour interval.

Our computational domain was chosen as a 40 by 40 grid with a uniform grid spacing of 2 km in both the east-west and north-south directions. For this domain, 32 Dirichlet basis functions (φ_n) and 39 Neumann basis functions (ϕ_m) were calculated. The first five φ_n and ϕ_m for Monterey Bay are shown in figure 3.

Our analysis consisted of treating each CODAR velocity observation as a group of 500-600 disparate velocity observations, and using this observation "set" to reconstruct the surface velocity field. Once the basis functions and their gradients were numerically determined, the "inversion" method described in section 2.5 was used to calculate the amplitudes A_n and B_m for each mode. Amplitudes were calculated for each two hour interval where at least 400 CODAR velocity observations were available. The calculations were performed on an IBM 6000 series computer, and each set of amplitudes took less than 5 seconds of CPU time to calculate. Although numerical model results were available to provide information about flow through the domains's open boundaries, the analysis results presented here are preliminary, and boundary data has *not* been

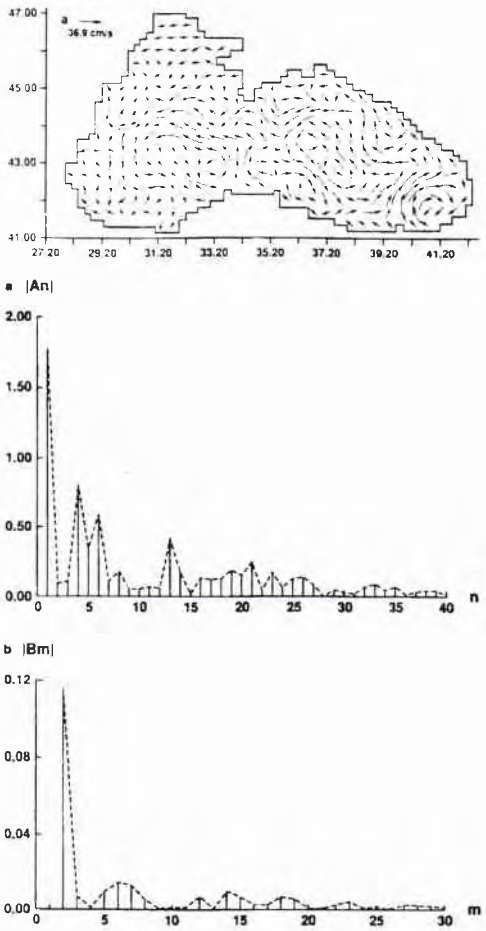

Figure 2: Mean Black Sea circulation at 10 m for July (top); Spectra of Dirichlet mode amplitudes A_n (middle); Spectra of Neumann mode amplitudes B_m (bottom). All taken from [3].

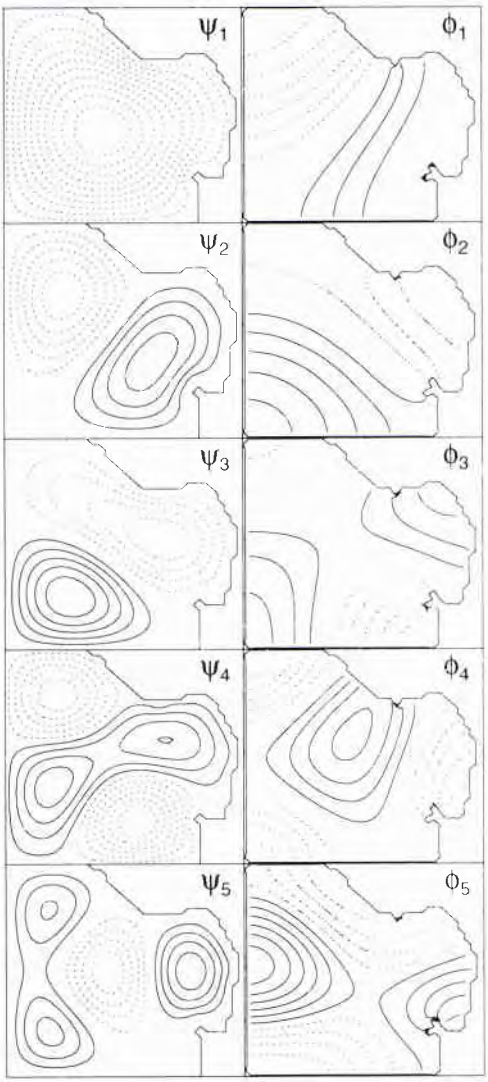

Figure 3: The first five Dirichlet modes (ψ_1 — ψ_5, left hand panels) and the first five Neumann modes (ϕ_1 — ϕ_5, right hand panels) for Monterey Bay.

incorporated into the velocity reconstructions.

Figure 4 shows the CODAR observed surface velocity for 0700, 1 August 1994 (upper panel), the reconstructed velocity using 32 Dirichlet and 39 Neumann modes (middle panel) and the difference between these two fields (CODAR minus reconstructed velocity, lower panel).

Figure 5 shows the CODAR observed surface velocity for 0700, 1 August 1994 (upper panel), the reconstructed velocity using 10 Dirichlet and 10 Neumann modes (middle panel) and the difference between these two fields (CODAR minus reconstructed velocity, lower panel).

The results shown in figures 4 and 5 are preliminary; velocity values were only recovered at each point where observations were already available, because boundary flow information has not yet been incorporated. We anticipate that, once boundary information is incorporated into the calculation, the method will yield useful velocity information at *all* points in the domain, if a sufficient number of velocity observations are available to constrain the amplitude calculation.

Figure 6 shows time series of horizontal divergence (in $10^{-5}\,s^{-1}$) at adjacent grid cells [20,21] and [21,20]. Divergence values are shown for the CODAR observations (upper panel), the velocity field reconstructed from 32 ψ_n and 39 ϕ_m (middle panel), and the velocity field reconstructed from 10 ψ_n and 10 ϕ_m (lower panel).

Generally divergence magnitudes of $10^{-5}\,s^{-1}$ or less would be typical for coastal flows like those in Monterey Bay. The upper panel of figure 6, then, suggests that the CODAR observations are rather noisy, with divergence magnitudes exceeding $1.6 \times 10^{-4}\,s^{-1}$. Additionally, there are several instances where the divergence magnitudes at the two adjacent grid cells were large, yet oppositely signed. For a shallow surface layer, large, oppositely signed divergences like those shown in the upper panel of figure 6 generated over a two hour period would result in sea level fluctuations of the order of $\sim 3\ m$. Such sea level fluctuations over a horizontal distance of about $2.8\ km$ are simply not realistic, and the actual divergence values at two adjacent grid cells are expected to be nearly in phase.

The middle and lower panels of figure 6 show that the horizontal divergence values at adjacent grid cells for the reconstructed velocity fields agree well with expected values. The time series of horizontal divergence based on the two reconstructed velocity fields exhibit less high frequency fluctuations, have peak values that are within the expected values, and have divergences at adjacent grid cells that are nearly always in phase. Note however, that the velocity reconstruction from 10 ψ_n and 10 ϕ_m (figure 6, lower panel) occasionally produces very large divergence magnitudes. This suggests that the reduced spectral basis set may not always be adequate to describe the horizontal divergence field ac-

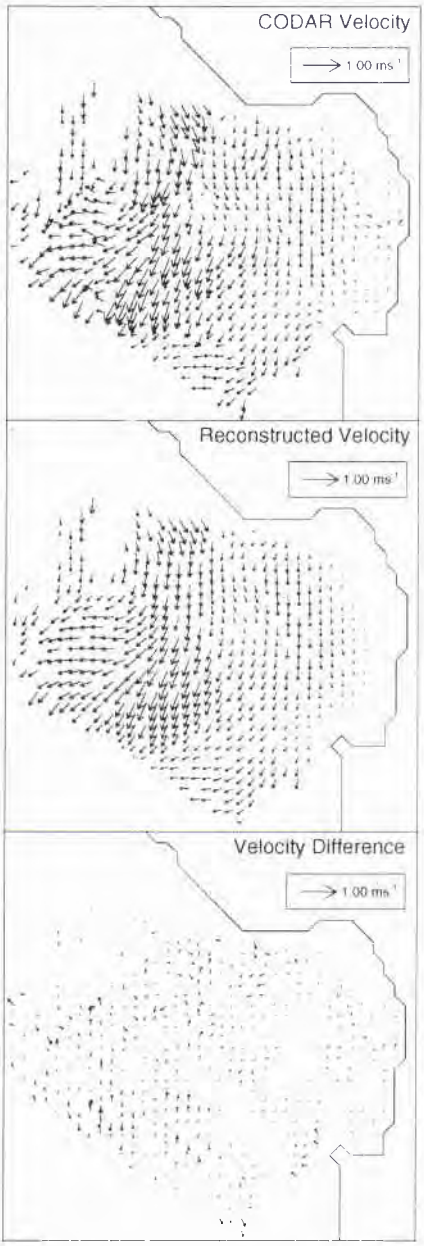

Figure 4: Surface velocity for 0700, 1 August 1994 for Monterey Bay. The velocity field shown in the middle panel was reconstructed from 32 ϕ_n and 39 ϕ_m.

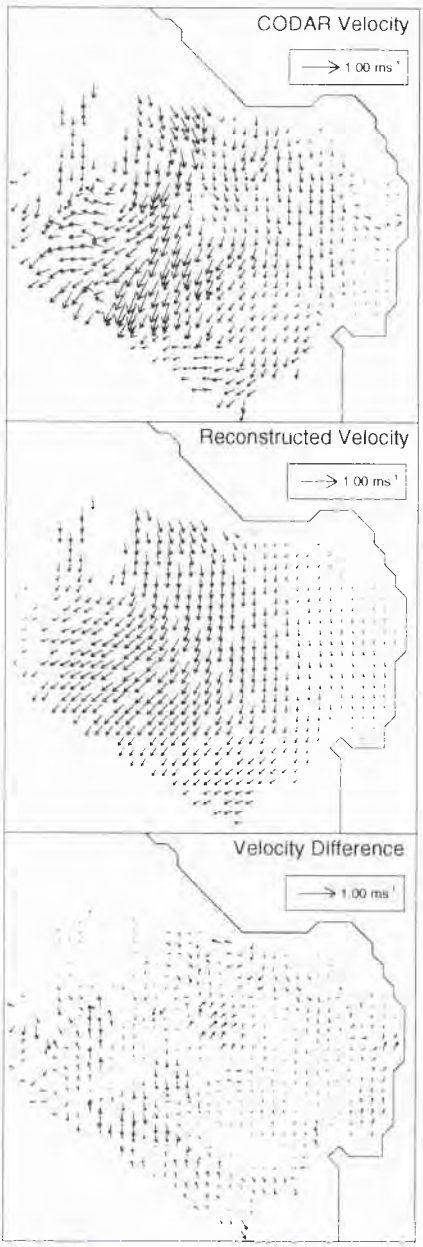

Figure 5: Surface velocity for 0700, 1 August 1994 for Monterey Bay. The velocity field shown in the middle panel was reconstructed from 10 ϕ_n and 10 ϕ_m.

curately.

These results demonstrate one useful aspect of the spectral reconstruction – it provides a method for filtering a disparate set of velocity observations while rigorously adhering to the constraints of three-dimensional incompressibility and model boundary conditions. Filtering velocity observations in this way will provide a more physically consistent velocity field for assimilation into a numerical model.

Spectral analysis of the time series of each A_n and B_m was performed for the case where all 32 ψ_n and all 39 ϕ_m were used to reconstruct the velocity field. The power spectral density for the first 10 ψ_n and ϕ_m was calculated. These spectra show that most of these modes contain significant spectral peaks at low frequencies only – the remainder of each spectrum is simply noise. In addition, the energy associated with the low frequency spectral peaks drops off sharply as mode number increases. This suggests that, for these surface velocity fields, variations occur over relatively long time and space scales, with most of the energy confined to the lowest modes. Consequently, we might expect that much of the variability in the data can be explained using some subset of the total number of available modes.

4. Discussion

The method described here is applicable to both layer and level models. It has been applied to both observations and model results with a variety of boundary geometries. Given a specific model boundary and grid spacing, the Dirichlet and Neumann basis functions are first calculated. Application to a layer or level model will require calculation of basis sets for each layer or level. Observations or numerical results are then projected onto the appropriate basis set. In the case of velocity, it is necessary to calculate the gradient of the basis functions. Since these functions are known at each grid point, the gradients can be readily evaluated by finite difference methods. Numerical interpolation can be used to evaluate the basis functions at off grid point locations.

We have calculated the basis functions numerically using both a direct method and a point iterative method (over relaxation). Both methods seem to be robust, although for large domains, the direct method requires inverting large matrices, and thus is limited by available memory. The point iterative method can be run in a workstation environment.

It should be stressed that the basis functions depend solely on the geometry of the domain boundary and the grid spacing. If either are altered during the course of an REA exercise, it is advisable to calculate new basis sets. We do not regard this as difficult.

Numerical errors accumulate as the order of the basis function (and the magnitude of its associated eigen-

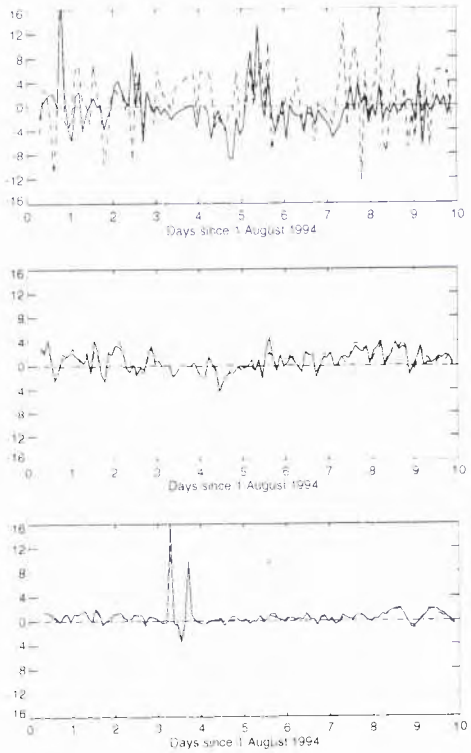

Figure 6: Time series of horizontal divergence (in $10^{-5}\ s^{-1}$) at grid cells [20,21] (solid lines) and [21,20] (dashed lines). The upper panel shows divergence for the CODAR observations. The middle panel shows divergence for the velocity field reconstructed from 32 ψ_n and 39 ϕ_m. The lower panel shows divergence for the velocity field reconstructed from 10 ψ_n and 10 ϕ_m.

value) increase. For the second order methods we use, approximately ten grid points per wavelength are required to resolve a given basis function. If greater resolution is required, grid refinement will be required, since the numerical methods are not reliable beyond this limit. In all applications we have attempted, we have been able to calculate more basis functions than required to accurately represent the data. However, we have not yet applied the method to high resolution data sets, and we have little experience with grids that contain subdomains of widely varying resolution.

5. Acknowledgments

The authors would like to acknowledge the support of the Office of Naval Research. A. D. Kirwan, Jr. also acknowledges the Samuel L. and Fay M. Slover endowment to Old Dominion University. We would also like to thank Dr. Jeffrey D. Paduan at the Naval Postgraduate School in Monterey, California for making the CODAR velocity observations available and for his help in understanding and interpreting the data.

References

[1] V. N. Eremeev, L. M. Ivanov, and A. D. Kirwan, Jr. "Reconstruction of oceanic flow characteristics from quasi Lagrangian data 1. Approach and mathematical methods", *J. Geophys. Res.*, vol. 97, pp. 9733–9741, June 1992.

[2] V. N. Eremeev, L. M. Ivanov, A. D. Kirwan, Jr, and T. M. Margolina, "Amount of ^{137}Cs and ^{134}Cs radionuclides in the Black Sea produced by the Chernobyl accident", *J. Environ. Radioactivity*, vol. 27, pp. 49–63, June 1994.

[3] V. N. Eremeev, L. M. Ivanov, A. D. Kirwan, Jr, O. V. Melnichenko, S. V. Kochergin, and R. R. Stanichnaya, "Reconstruction of oceanic flow characteristics from quasi Lagrangian data 2. Characteristics of the large scale circulation in the Black Sea", *J. Geophys Res.*, vol. 97, pp. 9743–9753, June 1992.

[4] J. D. Paduan and L. K. Rosenfeld, "Remotely sensed surface currents in Monterey Bay from shore based HF radar (Coastal Ocean Dynamics Application Radar)", *J. Geophys. Res.*, vol. 101, pp. 20,669–20,686, September 1996.

Data Input to Operational Sonar Forecast Models in Shallow Water.

Rolf Thiele, Dirk Tielbürger

Forschungsanstalt der Bundeswehr
für Wasserschall und Geophysik
(FWG)
Klausdorfer Weg 2-24
24148 Kiel, GERMANY
Email: fwg@fwg.ki.eunet.de

Abstract

Numerical modelling for sonar range predictions depends on correct input of depth profile, sound speed profile, bottom type and surface conditions. This is specifically a requirement in areas unfamiliar to the Navy. It is stated that the data of highest priority are bottom data. Necessary data transformations and problems of acquiring these data are discussed for the model MOCASSIN as an example.

1. Introduction

An important field of rapid environmental assessment is the assessment of the acoustical propagation conditions for sonar at a certain area of the continental shelf. The Navy operators are acquainted with the requirements in the deep sea. They know about the importance of the mixed layer depth, the critical depth, and if they are clever, they know also the propagation effects of cold or warm eddies. However, all these well known rules are not applicable in shallow water, coastal water, confined water, or how we might call the waters on the continental shelf significantly shallower than the critical depth (the depth where the pressure influence rules out the higher temperatures close to the sea surface, so that with more water depth propagation without bottom contact is possible). The critical depth is rather often more than 1000 m. Important places for rapid environmental assessment will have generally water depths less than critical depth, whether they are in the forefront of a certain country or at a choke point for sea passages.

2. Priorities of data input

The deep water rules about the environmental effects are not any more applicable in these waters. The main influences there are in the order of importance:

1. Water depth (and depth profile)
2. bottom characteristic
3. sound speed profile
4. sea surface characteristics

Furthermore the reverberation from the boundaries is crucial for any active sonar forecast.

It should be very clear that we should try to get with REA first the data of primary importance and then those of secondary importance. Therefore, I will discuss only very shortly the sound speed profile and the sea surface characteristics:

The sea surface characteristics, i.e. waves and swell are actually quite easy to assess, by satellite remote sensing and by the knowledge of the wind field that can be derived also from the pressure field. Certainly, it is difficult to make a forecast, but that is the same with all weather forecast. This will not be further discussed in this paper.

3. Sea surface and sound speed profiles

REA of the three-dimensional sound speed field is a very tough task. There will be a sufficient number of papers dealing with the profile compared to those with the water depth and the bottom characteristics. However, some words are required on the horizontal variability. We feel obliged to a short discussion, belonging to the team that produced MOCASSIN [1]. The quality of modern sonar range prediction models is assessed some times by their ability to handle horizontal variations of the sound speed. Because sonar ranges often are crossing „domains" of historical sound speed profiles, it is believed that the models should consider such a change - by whatever method. However, we should not forget, that even a front is not a vertical border separating two sections of water masses. The inclination of a front is normally about 1° out of the horizontal plane, more flat than a typical sound ray. The propagation depends than strongly on the type of transition, that is normally not available. We decided therefore, to abandon the existing version of MOCASSIN with range dependent sound speed profiles. We simply preserve the knowledge that the sound speed will be range dependent and will therefore produce forward scattering.

The comparative modeling for the MILOC survey Shallow Meadow in the Baltic was performed with two range dependent models and the range independent but forward scattering model MOCASSIN [2]. The results were that a deterministically range independent modeling was not acceptable, but that the range

depending calculation and the random forward scattering provided the same performance.

This concludes our discussion of the sound speed profiles. Certainly, it is nice to have the best knowledge about the profiles and even the three-dimensional sound field, but it is not the field of severe deficiencies of operational sonar forecast modeling.

4. Bathymetry

Now about water depth. The DBDB5 (Digitized Bathymetric Data Base 5 min. Grid) is public domain and available for the whole world. Considering the normal operating speed of a Navy vessel with let's say 10 kn, it passes one grid in a maximum of _ hour. No commander would like to get each half hour a new sonar range prediction forecast, especially not in range dependent environments with different propagation performance in different azimuths.

We have two concerns in this field:

- How reliable are the DBDB5 data points in front of some country of potential crises?
- Does not the undersampling of the depth have a smoothing effect, producing wrong forecasts by applying insufficient bottom scattering?

Bathymetry is therefore still a question of REA. In a model like MOCASSIN, that handles forward scattering, the grid size of DBDB5 will be sufficient any way, but the data in the database should be checked; and the effective roughness of the sea floor should be provided. This is a problem of bottom type (rock will be rough and mud will be smooth) and small scale bottom contours. It is necessary to provide such roughness maps, additionally to the bathymetry.

These parameters are also affecting reverberation. In addition we have to consider for that the „invisible" roughness, i.e. variations of surface impedance and inhomogeneities in the volume of the bottom. The advantage of reverberation is, that it can be measured ad hoc. Indeed the observed reverberation during sonar operation can be applied to get information about the acoustical behavior of an area[3].

5. Bottom characteristics

The most important and difficult task of REA for sonar forecast is the acquisition of the relevant bottom characteristics. At first we have to discuss the type and depth range of required data.

Usually the relevant depth of the bottom characteristics is up to some wavelengths, let's say between a quarter of a wave length and 10 wave lengths.

This means for an active sonar with a frequency of about 10 kHz, the relevant depth will be between 4 cm and 1.5 m. For typical passive sonar applications in shallow water we use about 200 Hz (the very much lower frequencies of modern passive sonar are only in deep water important). This results in a depth range of 2 m to nearly 100 m.

The other question is what the type of characterization is. It is rather well known that the reflectivity of the sea floor is primarily influenced by the compressional wave speed and secondary by the attenuation of the compressional wave speed per wave length.

Shear waves may also be of importance, but only at shear speeds of more than about 150 m/s. Low shear speeds only have the effect of a slight increase of the compressional wave attenuation; and the compressional attenuation is anyway not well known.

This means that - for unconsolidated sediments - the shear may be neglected. The problem is difficult enough without shear. You will very seldom find maps of surficial sediment sound speed and attenuation. We have to take an other way for REA. The relation between porosity and compressional wave speed is quite well confirmed. A first approach gives Wood's equation, if assuming a uniform grain density of the sediment [4]. A lot of empirical evaluations [5,6] and Biot-Stoll theory [7] modify the Wood's equation formula with rather good accuracy.

Biot-Stoll theory shows also - in good agreement with empirical data - a relation between grain size and compressional wave attenuation. And furthermore, there exists a relation between porosity and grain size for unconsolidated sediments.

Unfortunately, we find rather seldom maps of porosity and grain size in remote areas of the world. If any bottom map is available it is most likely one of the geological classification of the sediment or the type of surficial sediment. The age of a sediment is not a relevant acoustical parameter, except that all bottom types older than quaternary will most likely be consolidated to a certain amount. Consolidated sediments will have a rather high compressional and shear speed and are most likely not flat and smooth. These are characteristics that are not appreciated for our task. Fortunately, the sea floor is covered by quaternary sediments in most areas. For low frequency applications these maps may be useful to determine if the quaternary basis, so far the thickness of an intermediate layer is less than 100 m deep. The grain size and thereby the porosity of quaternary sediments is not ruled be the age of the sediment and is therefore not an acoustical relevant quantity

More useful are maps of the surficial sediment types. Is there mud, sand or rock at the sea floor? Information about these types is not only available in specific surficial sediment maps, but also in usual navigational maps (though the evaluation of such information may be tedious and uncertain).

A severe problem is the vertical distribution of the sediments in the depth interval mentioned. It appears that we may assume for the higher frequencies that there is only one sediment type in the relevant depth interval. There may be very thin layers of centimeters of soft sediments on more hard sediments, for example. It happens also that on the neighborhood of sand deposits thin sand layers on (and in) mud deposits may appear that were transported by single events of strong storms or so. More likely the upper few meters are of the same type, however.

This does not mean that the acoustical parameters will be independent of depth. Hamilton [8] gives typical empirical depth dependent compressional wave speeds as a consequence of the overburden pressure. This produces a frequency dependent reflection coefficient that results in perfect fitting with numerical modeling of sound propagation to measured data.

Altogether, information of the local type of sediment may be achieved in principle, that is sufficient for active sonar forecast for frequencies above 1 kHz.

MOC Nr	Description	NISSM II Nr	NISSM II Poros	MGS Nr
10	rock, gravel	9	0.30	1
9	coarse sand	8	0.39	
8	mid sand	7	0.47	2
7	fine sand	6	0.55	
6	silty sand	5	0.61	3
5	sandy silt	4	0.71	
4	silt	3	0.80	4
3	claiy silt	2	0.87	
2	silty clay			5
1	clay, mud, ooze	1	0.93	6,7,8,9

Table 1. Rentative relation of MOCASSIN bottom classes to those of NISSM II and MGS.

A collection of bottom types as in table 1 was tentatively established for the model MOCASSIN. Two further scales of bottom types were constructed by comparison of transmission loss measurements and model calculations. Fig. 2 and 3 show some tracks of transmission loss runs for this comparison. In addition profiling measurements of the angular reflectivity have been taken (fig. 1). The old NISSM II bottom formula gives a correct frequency dependence, while the GSM bottom formula provides an unrealistic reflectivity at small angles. It is assumed that this is a consequence of

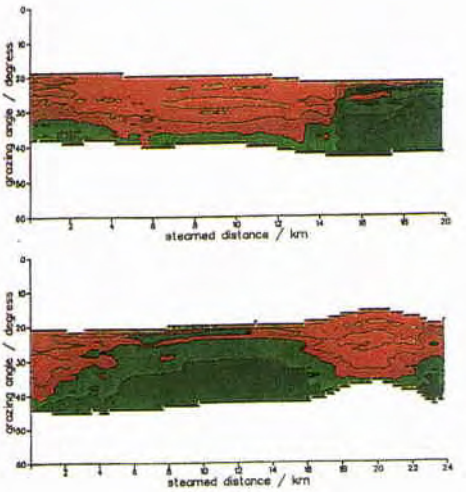

Fig. 1. Profiles of measured reflection coefficients. The ranges of measurement shifts to smaller angles at bottom elevations. Red meams high reflectivity, green low.

the measurement procedure and that the data were mainly for deep water applications assembled.
Producers of surficial sediment maps do not primarily focus on the acoustical characterization, and a standardized typification is not available. [9] e.g. provides 48 classes of sediment that have to be distributed properly to the MOCASSIN classes. The classes of sediment of [10] in the Baltic Sea are

- sand with minor soft bottom areas
- hard bottom (till, also bedrock)
- hard bottom and sand bottom equally distributed
- sand bottom with minor hard bottom areas
- sand bottom (sand and gravel)
- sand bottom and soft bottom equally distributed
- soft bottom (silt clay mud)
- soft bottom with minor hard bottom outdrops
- soft bottom and hard bottom equally distributed
- hard bottom with minor soft bottom areas.

The correspondence of these classes to the MOCASSIN classes is not obvious and must be tuned by empirical data.

A comparison of available data sources with own sample data indicated, that the accuracy of existing large area sediment type maps is rather low, mainly because of insufficient resolution of the bottom (the referenced data are exceptions in this respect, they appear to be quite reliable). This means that the grid is O.K., but that the data represent no such resolution as could be provided by the grid. Many maps appear to be a kind of „geopoetry", i.e. they do not correlate to reality and to more reliable maps. Therefore, we decided to take in all cases, where no quality proved data sources were available, a quite simple estimate for the databank of MOCASSIN:

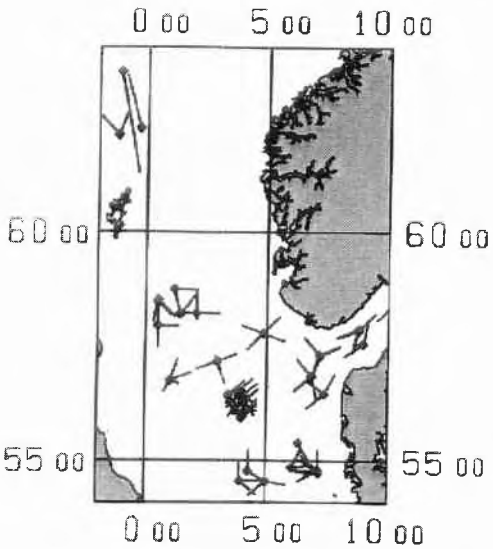

Fig. 2. Positions of transmission-loss measurements of FWG in the Northsea.

In flat areas, i.e. water depth less than 200 m weassume fine sand, so far there is no basin surrounded by shallower water. Such basins will contain clay. In deep water will be clay, and at the slopes coarse sand. This bottom type can be defined from the DBDB5 bathymetry map. If available, also hydrographic maps of current speed may be used for estimation of grain size distribution and by that of the bottom type. The map [9] shows a good example for this relation.

We see that we have a hierarchy of bottom data with increasing accuracy:

- estimate by bathymetry
- navigational maps and sporadic information, combined with the bathymetric information, or oceonagraphic current maps
- dedicated maps of surficial sediments
- direct reflectivity or transmission loss measurements.

The acoustical validation (fig. 2, 3) is achieved by TL-measurements of FWG in North and Baltic Sea. Reasonable map information is additionally available to us in certain areas.

6. Data acquisition

This discussion could tempt to the opinion that the problem of rapid bottom data input would be solved. True is only that a concept of data collection exists for high enough frequencies. The process of data conversion from a digitized map to a grid depends strongly on the strategy of data generation for example. Possibly, it is the simplest way to produce the required gridded data for the MOCASSIN MOCASSIN model by drawing the mapped and digitizing them in gridded form.

Another problem is the uncertain information about availability of data. For a certain area in Northern Europe we got once the information that reasonable bottom information should be available in 5 different datbases. One of them had for the whole area „data not available", the other posted at all places „sand", that will not be true for large parts of that area, the third appeared to be not existent, the forth indeed had already a number of a company for ordering, but it was not yet issued, and only the fifth was available with reasonable data. This map, however covered only some percentage of the area in question.

Nevertheless, this is a still better situation than having three maps of bottom type from one area that are absolutely uncorrelated.

7. Conclusion

Nowadays sonar range prediction accuracy is normally not anymore restricted by the quality of the applied algorithms, but by the information about the environment.

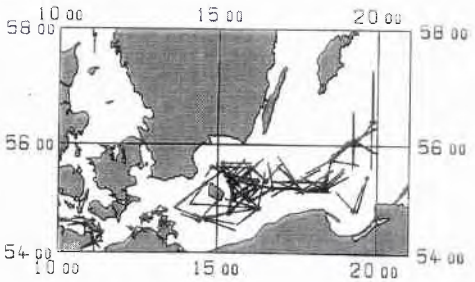

Fig. 2. Positions of transmission-loss measurements of FWG in the Northsea.

Though the sea floor does not vary critically with time, it is the limiting factor for shallow water predictions. The required bottom information for lower frequencies can only be estimated only by inverse modeling or very detailed studies of the 3 dimensional sediment distribution. The situation is easier for higher frequency sonar prediction, i.e. for frequencies higher than 1 kHz. For these frequencies just the upper few decimetres of the sea floor characterise the sea floor sufficiently. This remedy, however, makes REA of the sea floor not redundant but achievable. Even for places where maps are available, the application of REA is necessary. The available information has to be discovered, transformed into types of acoustical relevance, and validated by „majority decision" of information of independent sources or from direct REA measurements or inversion from available acoustical measurements.

References

[1] H. G. Schneider, *MOCASSIN, Sound Propagation and Sonar Range Prediction Model for Shallow Water Environments, User's Guide*, Kiel, FWG TR 1990-10, 1990

[2] H. G. Schneider, B. Damsgaard, T. Strarup, F. B. Jensen, *Modelling Results for Operation SHALLOW MEADOW: Acoustic Experiment in the Baltic Sea*, La Spezia, SCALANTCEN SR 169, 1990

[3] R. Thiele, H. Petersen, *„Ergebnisse von Nachhallmessungen mit Knallsignalen von den Fahrten PLANEX 74 und FLEX 76 (Results of reverberation measurements using explosives from the cruises PLANEX 74 AND FLEX 76)"*, Kiel, FWG report 1979-11

[4] A. B. Wood, *A Textbook of Sound*, London, G. Bell, 1911

[5] T. Akal, „Acoustical Characteristics of the Sea Floor: Experimental Techniques and Some Examples from the Mediterranean Sea", *Physics of Sound in Marine Sediments*, L. Hampton ed., New York, 1974, pp. 447-480

[6] P. J. Schultheiss, „The Influence of Packing Structure and Effective Stress on V_p, V_s, and the Calculated Dynamic and Static Moduli in Sediment", *Acoustics and the Sea-Bed"*, N. G. Pace Ed., Bath, Bath University Press, 1983, pp- 19-27

[7] R. D. Stoll, *Sediment Acoustics*, New York, Springer, 1989

[8] E. L. Hamilton, „Prediction of in-situ acoustic and elastic properties of marine sediments", *Geophysics*, vol. 36, pp. 579-604, 1971.

[9] C. Larsonneur e.a., *The Surficial Sediments of the British Channel*, , map, Orléans, Service Géologique National

[10] A. Voipio (ed.), *The Baltic Sea*, Amsterdam, Elsevier cientific Publishing Company, 1981, pp. 87-94

Assessing the Bottom-interacting Sonar Environment

David M.F. Chapman, Dale D. Ellis, and Philip R. Staal

Defence Research Establishment Atlantic
P.O. Box 1012, Dartmouth, Nova Scotia
B2Y 3Z7, CANADA
Email: dave.chapman@drea.dnd.ca

Abstract

Naval sonars operate in a variety of scenarios, and simulating sonar performance continues to be an art based on scientific principles. As it may be unrealistic to expect that sonar databases will exist for all possible naval theatres, an alternative solution is to attempt to quickly assess the sonar operating environment just prior to and/or during deployment. This paper presents the current DREA perspective on the requirements for Rapid Environmental Assessment in the sonar context, current methods and activities, and some suggestions regarding the way ahead, with emphasis on acoustic characteristics of the seabed.

1. Introduction

Many ocean acoustics laboratories—including DREA—have contributed to a large body of research that has explored the physics of bottom-interacting ocean acoustics, identifying the physical processes governing the propagation of sound in the ocean and its offshoots: ambient noise and reverberation. What remains to be done is to isolate the geo-acoustic parameters that really matter in a given scenario and to develop reliable techniques to measure them in unsurveyed areas. This requires not only a deep appreciation of the physics (theory), but also of what is technically feasible (practice). Models and modelling are a key element of Rapid Environmental Assessment (REA): they are an integral part of any inversion process. Environmental properties obtained through the application of scientific models can be used in operational sonar performance prediction models, and reverberation model-data differences can be used to map anomalous scattering features on the seabed.

Naval sonars operate in a variety of oceanographic and geophysical environments, and predicting or simulating sonar performance for both active and passive sonars continues to be an art based on scientific principles. Apart from the expected characteristics of sonar target and the specification of the sonar array, the sonar modeller needs to know much about the acoustic environment that conveys the desired signal and—at the same time—introduces noise and/or reverberation that clutter the display. We regard models as an essential component of any sonar system, but they must be used with care; the results of the most physically-correct and computationally-accurate ocean acoustic propagation models can be no more reliable than the inputs provided. As it may be unrealistic to expect that environmental databases will exist for all possible naval theatres, an alternative solution is to attempt to survey the operational area just prior to deployment, in attempt to quickly assess the sonar operating environment. As time will be precious, the goal of such a rapid environmental assessment (REA) would be to determine those features of the environment most important to the sonar modelling task, rather than to paint a comprehensive oceanographic and geophysical portrait of the area. This paper will review the highlights of DREA's foray into assessment of the seabed properties, including: matched-field inversion for geo-acoustic properties, seismo-acoustic inversion for shear wave properties, a temporal survey of shallow water ambient noise, and use of reverberation data to extract bottom loss and seabed scattering properties. Although oceanographic aspects will be touched upon, the emphasis will be on assessing the geo-acoustic environment presented by the ocean bottom and the layers of the seabed beneath.

2. The sonar oceanographic environment

The basic sonar problem is the detection of a signal masked by the presence of noise and/or reverberation. A passive sonar detects a target by sensing its self-generated sounds: the received signal depends on the source strength and the transmission loss; the masking noise is the ambient noise background. An active sonar "pings" on the target, the received echo level depends on the active source level, the two-way transmission loss, and the backscatter strength of the target; the masking ambient noise is augmented by the reverberant energy of the outgoing ping scattered back to the receiver by the environment.

The transmission loss, ambient noise, and reverberation can be considered as environmental quantities, and can be measured. Alternatively, they can be predicted, if more fundamental environmental quantities are known. Figure 1 illustrates the relationships between environmental, acoustic, and sonar models. Models for predicting transmission loss are relatively mature. Further models (usually built on propagation models) have been developed for ambient noise and reverberation, but they require many transmission loss

predictions from all directions. In addition, ambient noise models need information about the noise sources (such as ships, weather, and marine life); and reverberation models need information about scattering features (surface, volume, bottom, and sub-bottom).
Signal processing issues are important for sonar prediction models. A number of issues—such as noise and signal fluctuations, time spreading and frequency

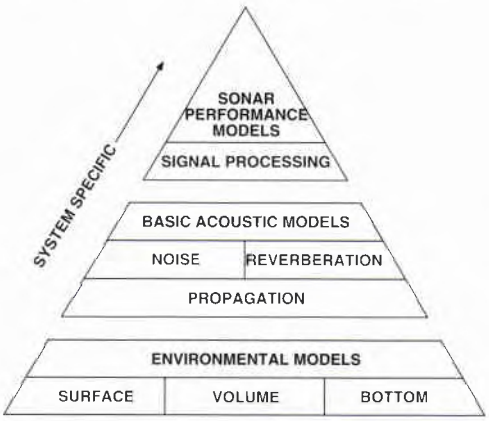

Figure 1. The pyramid showing the relationship between the environment and models, after Etter [1].

spreading—are related to the environment, but are research topics and beyond the current scope of DREA's REA activity.
Environmental properties of the ocean surface and water volume are reasonably accessible through remote sensing or direct measurement; seabed information is much harder to obtain, and often only available by acoustic means. Seabed properties are particularly important for shallow water, since acoustic propagation in much of the world's shallow ocean waters is dominated by bottom interaction. Also, seabed properties are more durable, in the sense that they do not need to be repeatedly re-surveyed, once measured. In this paper we concentrate on the assessment of seabed geo-acoustic properties important for ship sonar frequencies. (Although the bottom is even more important for mine countermeasures, we do not include MCM activities in our considerations.)

2.1 Sound speed

The most important oceanographic factor affecting sonar performance is the sound speed profile. Generally, the ocean is stratified, i.e. variations in depth are much more pronounced than lateral variations. The sound speed profile guides the transmission of acoustic energy from source to receiver, and controls whether the sound travels unimpeded, is refracted upwards towards the surface or downwards towards the bottom, or is even ducted by a sound speed minimum. It is essential to have a representative sound speed profile for the operational area—even if it is a single snapshot—and this is readily obtainable from ship-deployed or air-deployed expendable bathythermographs (XBTs). Multiple casts over an area would improve the assessment of prevailing conditions and may provide information on geographical variations that might interfere with sonar operations, such as ocean fronts, eddies, and currents.
To model such complications intensifies the task enormously. If the environment is geographically invariant (i.e. range-independent), acoustic propagation is cylindrically symmetrical, in effect reducing the computational problem to two dimensions. Lateral variation of the ocean water mass requires three-dimensional modelling capability, or serviceable approximations to this. As the complexity of the environment and modelling task grows, so does the susceptibility to error.

2.2 The role of ocean circulation models and remote sensing

Validated ocean circulation models—supplied with up-to-date temperature, current, and salinity profiles in an area of interest—may provide a forecast good for several days, but may only be useful in alerting the operators to sonar-unfriendly ocean features rather than providing precise inputs to sonar models [2]. In the same vein, remote sensing of ocean surface temperature may provide important background information, but it is not clear that these data can be mapped into sound speed profiles useful for sonar modelling.

2.3 Ocean surface roughness

An agitated ocean surface introduces loss (by scattering) for energy reflecting from the sea surface and creates reverberation through backscatter to the sonar (for an active sonar). The geometrical roughening of the surface is the principal physical factor leading to these phenomena, but clouds of micro-bubbles just beneath the surface may also contribute. Reflection loss and surface backscatter coefficients are typically correlated with ocean waveheight, "sea state" or local wind speed, estimates of which are readily available on-site or from remote sensors.

2.4 Acoustic ambient noise

As passive sonar detection is a signal-in-noise problem, estimating the ambient noise levels (for a single omnidirectional hydrophone) and the horizontal and vertical directionality (for hydrophone arrays or directional sensors) is just as important to the sonar prediction model as simulating the signal level. Statistical ambient noise data exist, but the coverage is spotty both in geography and season. A particular

problem is the influence of nearby shipping, which generates extra noise that is highly variable in time and direction. The changeable and unpredictable nature of ambient noise seems to dictate that an *in situ* measurement at the time would be the best estimate (if the sonar has provision for scientific data collection and reduction). Alternatively, one might consider signal processing techniques such as adaptive beamforming, whereby the signal processing algorithm attempts to account for the changing noise environment.

2.5 Ambient noise modelling

Models exist for simulating noise fields, but these are essentially variants of ocean acoustic propagation models. Assuming a distribution of sea surface sources and/or a distribution of ocean shipping, the propagation models sum up the contributions propagating from all sources to the receiver location, resulting in a simulation of the levels and directionality of the ambient noise field. Particularly in shallow water, the acoustic reflection characteristics of the seabed influence the properties of the noise field (and the signal field!). Also, three-dimensional propagation models may be required to model noise arriving from sources at any bearing or range.

2.6 Bathymetry

The depth of the ocean is another important oceanographic input, needed to account for acoustic energy reflected and scattered from the seabed. (If there is significant bottom interaction, it is the most important oceanographic input.) Echo sounders can provide depth under the vessel; multi-beam echo sounders produce swaths of bathymetric data. At a given geographical location, the ocean depth does not change significantly in time, so bathymetric databases are a reasonable source of data, provided the coverage and resolution are adequate. Even with a range-independent sound speed profile, a sloping or irregular ocean bottom introduces the need for range-dependent or three-dimensional propagation models. Water depth is crucially important in shallow water (i.e. on continental shelves), as the degree of bottom interaction is much greater for a given source-receiver range in shallow water than for the same range in deep water.

The bathymetry is a key feature in determining reverberation. Unless the sonar is very directional, bottom reverberation will dominate the reverberation field. In deep water multiple surface-bottom reflections (fathometer returns) dominate at short times, while feature scattering (e.g., basin margins and seamounts) dominates at long times; in shallow water backscattering from slopes (banks, islands or the coast) dominates. In addition to the large-scale bathymetric slopes, there is the small-scale roughness that determines the local scattering. Discussion of reverberation due to backscattering from the seabed is deferred to a later section.

3. The sonar geophysical environment

The role of the seabed as an acoustic reflector and scatterer has been mentioned. In a bottom-interacting acoustic multipath environment, the acoustic reflection and scattering properties of the seafloor influence sonar performance. Shallow water (continental shelves) could be considered an extreme multipath environment in which the acoustic influence of the seabed is paramount. There are almost as many ways to parameterize the acoustic effect of the seabed as there are computer models that claim to account for the effect.

As this is the main thrust of this paper, the parameters will be introduced first as a group, and the discussion of assessment methods will follow.

3.1 Geo-acoustic propagation parameters

Bottom-interacting ocean acoustic propagation models need several or all of the following seabed parameters as input data, either as constants, piecewise constant functions of depth, or continuous functions of depth, with lateral variations included, if appropriate:

- sound speed (pressure or compressional wave)
- density
- attenuation coefficient of compressional wave
- shear speed (transverse or rotational wave)
- attenuation coefficient of shear wave.

(Bottom or inter-layer roughness—in the context of reflection loss—is another important parameter, but many models are unable to handle it.)

Some models simply replace a detailed treatment of acoustic propagation within the seabed with a frequency-dependent and angle-dependent plane wave reflection coefficient. If the representation of the acoustic reflection process is accurate, this is all one needs, as the sonar and the target are in the water (a safe assumption). The details of the acoustical processes within the seabed are not needed, only their net effect on the sound field in the water column.

3.2 Acoustically equivalent seabeds

Enlarging on this last point, it may not be necessary to have a geophysically precise representation of the seabed at all, provided the net acoustic effect is modelled adequately for the sonar modelling task. To this end, for each real seabed, there exists a family of acoustically equivalent seabeds that produce the desired effect, but whose particular parameters may not match. For example, it has long been known that the contribution to near-grazing bottom loss by conversion of energy into low-speed shear waves in the seabed can be mimicked by slightly decreasing the density and slightly increasing the attenuation of the compressional wave. This technique is particularly helpful if the propagation model at the heart of the sonar simulator knows nothing about shear waves. The equivalent seabed is—in general—

frequency-dependent. The concept is similar to interpolating a curve of reflection loss vs. grazing angle, as used in many ray-trace models.

3.3 Scattering and reverberation parameters

The ocean bottom scatters sound in much the same way—and has much the same effect on sonar operations—as the ocean surface, with some important differences. Firstly, the scattering properties vary slowly with time and they are fixed in geographical location, so using databases to store and retrieve scattering parameters is a feasible option. Secondly, as sound penetrates to some extent into the seabed (more so at lower frequencies), the seabed structure beneath the water/seabed interface must be considered. Theoretical backscattering models based only upon scattering from rough surfaces do not seem to tell the full story: there is evidence that fine-scale variations of acoustic properties within the volume of the seabed just beneath the surface have a large influence. If this is so, then translating geophysical data from databases into scattering parameters may be overwhelmed by the considerable amount of high-resolution data required for the task. Alternatively, the scattering and backscattering properties of the seabed could be surveyed at the frequencies of interest and stored. Again, an *in situ* measurement at the time of deployment may be the best solution, although this would dictate that scientific reduction of acoustic data be included in the sonar processing software suite.

The vast literature on scattering attests to the difficulty in treating the process mathematically. For sonar modelling purposes, an empirical approach is generally used. Frequency- and angle-dependent scattering functions derived from measurements are used for surface and bottom scattering, and used in sonar models. The wind speed or sea state is the key parameter correlated to surface scattering. Bottom scattering is highly variable, and not readily deduced from fundamental physical quantities. It is therefore an important parameter for determination through REA techniques. The use of scattering functions to describe the effect of the environment is similar in principle to the equivalent seabed concept.

4.Assessing the geo-acoustic environment for sonar

4.1 Traditional survey methods (direct measurement)

Geophysical survey techniques developed for oil and gas exploration and other seabed activities have provided data relevant to bottom-interacting ocean acoustics. High-resolution vertical-incidence seismic profilers (i.e. echo sounders enhanced to process sub-bottom reflections) provide information on layering in surficial sediments, and have lately been improved to provide approximate sediment classification. However, these devices do not directly provide sediment geo-acoustic parameters, which must be extrapolated from direct measurements on associated core samples or boreholes. Deep-towed geophysical arrays can measure the compressional speed using critical-angle seismic refraction methods. Sidescan sonar provides a qualitative measure of seabed roughness; some multi-beam echo sounders can reduce returns to give seabed backscatter coefficients.

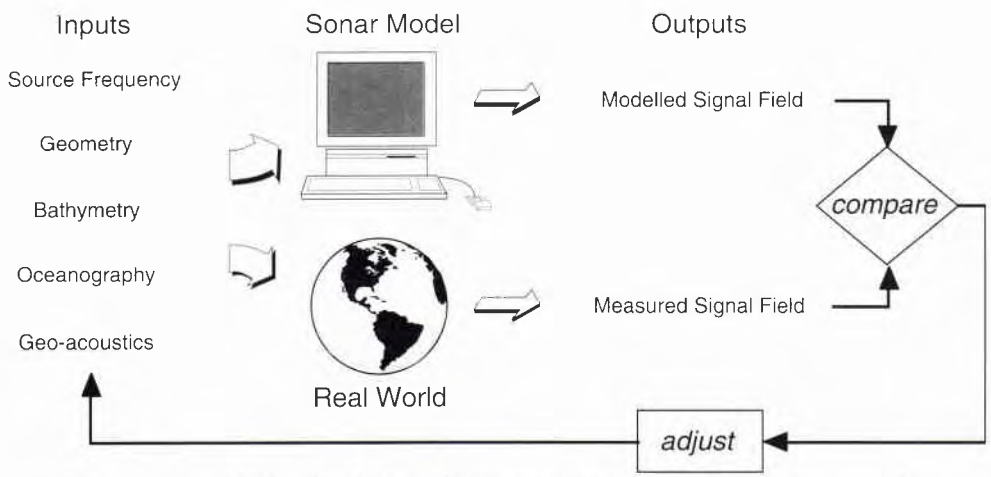

Figure 2. *An illustration of the concept of matched field processing for source localization or environmental inversion.*

4.2 Inversion techniques

In many cases the bottom is inaccessible to direct measurement and inversion techniques are used. The procedure involves making a measurement (such as transmission loss) then comparing to a model prediction based on some measured or assumed environmental inputs (perhaps from a database). The differences are then compared, and used to obtain improved estimates for the desired environmental inputs (such as geo-acoustic parameters). The conceptual procedure is illustrated in Figure 2.

Inversion can be done manually, whereby an expert makes some educated guesses and achieves reasonable agreement between model and data. An alternative is an inversion algorithm, where a parameter space is searched to find an optimum (or near optimum) fit to the data. This may be computationally intensive, and the physical solution may not be very realistic.

4.2.1 Repetitive forward modelling

To characterize the geo-acoustic environment more exactly, the ocean acoustician combines available information from traditional survey techniques or databases, makes an educated guess of the remaining parameters, and attempts to model measured acoustic propagation loss as a function of range at a series of frequencies, attempting to at least reproduce the trend of the data, if not the details. It is rare that the first try is even close, but this depends upon the experience of the modeller. Through a process that has come to be known as "repetitive forward modelling", an experienced modeller can refine the parameters of the input model to achieve reasonable agreement, provided that the propagation model has accounted for all the physical processes involved in the experiment.

4.2.2 Acoustic matched field inversion

Inversion techniques start with the measured data, apply them to a model, and provide estimates of model parameters using a disciplined and reproducible method implemented on a computer. Matched field inversion uses actual measurements of the ocean acoustic pressure field generated by a known source measured at an array over a short time interval: a small space-time "snapshot" of the field. This snapshot is compared with a replica of the same simulated with an ocean acoustic propagation model. The mismatch between experimental and simulated fields is quantified and—through a process of automated repetitive forward modelling—the mismatch is reduced to an acceptable level, producing a set of best-estimate geo-acoustic parameters.

4.2.3 Seismo-acoustic inversion

Using sources and receivers (geophones and/or hydrophones) on the seabed tens or hundreds of metres apart, one can generate and receive interface waves at the ocean/sediment boundary whose speed of advance is strongly dependent upon the depth profile of shear speed. In areas where bottom reflection loss due to excitation of shear waves is significant, this technique is an important investigative tool. For seismo-acoustic inversion, the speed of the interface waves is determined over a wide frequency band and matched to model predictions, either by repetitive forward modelling or by automated non-linear least-squares minimization.

4.2.4 Inversion of reverberation data

Inversion of reverberation data can be used to estimate geo-acoustic and scattering parameters. Reverberation data are compared to the prediction from a shallow water reverberation model for which the sound speed profile is known, and a reasonable geo-acoustic model is available. The bottom scattering characteristics are unknown, so Lambert's rule with an assumed backscatter coefficient is adopted. The prediction usually disagrees with the data, so the backscatter strength is adjusted manually to achieve acceptable agreement with the data. The procedure is typically repeated at a number of frequencies. These estimates can then be used in models for sonar performance predictions.

The resulting scattering strengths depend on the assumed geo-acoustic model, and consequently are sensitive to errors in it. Global inversion techniques developed for matched field processing can be used to simultaneously invert for the geo-acoustic parameters and bottom scattering. Due to the random nature of the reverberation data, there is no phase information and consequently there is less information about the environment. This may be beneficial if it leads to simple robust procedures.

5. REA and related activities by DREA and associates

Defence Research Establishment Atlantic has a long history of ocean acoustics research, including bottom-interacting ocean acoustics, particularly in shallow water [3]. DREA has several active sea-going research groups collecting environmental data, using a variety of research systems deployed from the acoustically-quiet research ships CFAV QUEST and CFAV ENDEAVOUR.

(Equally significant is work that was performed at Defence Research Establishment Pacific. Work at that laboratory continues at a reduced staffing level as Esquimalt Defence Research Detachment, a new division of DREA. EDRD also has an active ongoing research thrust on mine countermeasures. Other research activity has moved to industry and the Underwater Acoustics Chair at the University of Victoria.)

The fundamental goals of DREA's Rapid Environmental Assessment activity are:

- Timely products to support sea and air operations
- Improved measurement and inversion techniques
- Better inputs and models for Canadian naval and maritime air sonar simulators
- Support for in-house development projects

At present, DREA's emphasis is to validate the scientific

basis of techniques that would be included in an REA initiative, with a lower level of effort applied to creating REA products for operational use. Our investigations and model development continue to be guided by the requirements of the Canadian Navy and Air Force for sonar performance prediction.

5.1 Bottom-interacting ocean acoustics

DREA has favoured two shallow water sites on the Scotian Shelf for its shallow water acoustics experiments: one has 75 m water over a sand bank, the other has 210 m of water over a clay basin. Recent experiments have collected data for geo-acoustic inversion, matched field inversion, matched field localization, ambient noise studies, and adaptive beamforming with vertical arrays. In addition, we have sponsored a year-long ambient noise survey of 4 shallow water sites through monthly deployments of sonobuoys from aircraft. DREA collaborates with the Ocean Acoustics Chair at the University of Victoria and supervises contract work in these areas.

5.2 Matched field inversion (MFI)

This method of environmental assessment has made much progress in many directions, but is far from being a standard tool. There have been amazing successes and dismal failures, as reported at a 1996 workshop [4] at EDRD (to be repeated in 1997). Currently, DREA research is focussed on sensitivity studies to determine which seabed parameters have the most influence on the water-borne acoustic field, and hence which are most accessible through MFI. Also, DREA is participating in a challenge to invert a benchmark set of simulated matched field data of progressive difficulty, to test MFI algorithms. Through contracted research, two experimental data sets from the DREA test sites are being reduced using MFI. It is expected that MFI will eventually become an important tool for REA in support of sonar modelling, but not a panacea.

5.3 Seismo-acoustic inversion

As part of a study on the use of geophone sensors in underwater acoustics, DREA collected data on interface wave dispersion that was successfully inverted to provide shear speed profiles at the two DREA test sites. Figure 3 shows the results of interface wave dispersion experiments at sites with clay/silt bottoms [5]. In these cases, the "staircase" profile may be an approximation to a continuous power-law profile, as suggested in the figure. The experimental and data reduction methodology for this work removes it from the "rapid" category of techniques; however, researchers at the University of Victoria plan to compare these results with matched field inversion of acoustic data recorded at the same site on a vertical line array. This may be the first attempt at directly comparing results of seismo-acoustic inversion and acoustic matched field inversion.

5.4 Ambient noise studies

A year-long survey consisting of monthly snapshots of ambient noise at four shallow water sites will provide a useful database for sonar modellers. Further analysis of the results may provide insight into the relation between ambient noise levels and bottom type. A model for noise coherence at vertically-separated shallow-water sensors has shown the combined influence of the sound speed profile and the acoustic reflectivity for the sea floor on the vertical directionality of the noise field [6]. Figure 4 illustrates the influence of a downward-refracting sound speed profile on noise coherence. A survey of historical DREA ambient noise measurements has been performed and compiled in summary form.

5.5 Equivalent seabed models

Through contracted and in-house research, a search is underway for the optimal representation of the acoustical effect of the seabed in the context of sonar operation. The goal is to eliminate geo-acoustic parameters to which sonar operation is insensitive and to generate an irreducible set of robust geo-acoustic parameters. It may then be possible to devise experiments to rapidly and reliably assess these parameters in previously unsurveyed areas of interest (possibly using acoustic matched field inversion). An important complement to this work would be to develop translation algorithms that would generate the ideal parameter set from traditional geophysical databases.

5.6 Reverberation measurements and analysis

A large portion of DREA's effort is in support of integrated active and passive sonar systems. An active sonar system is under development for Canadian towed-array ships. For the patrol aircraft a processing system for sonobuoys is also being developed, with both monostatic and bistatic active sonar capability. Alongside this, a range-dependent shallow water active sonar modelling capability is being developed for

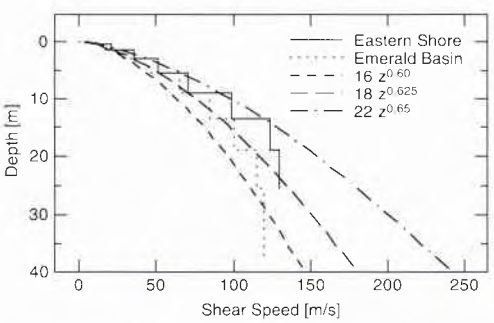

Figure 3. *Seismo-acoustic inversion: shear speed profiles determined from interface wave dispersion data measured with an ocean bottom seismometer.*

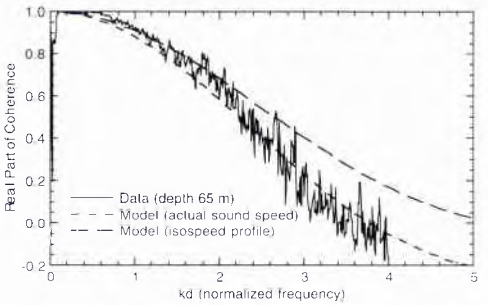

Figure 4. *Ambient noise studies: noise coherence between two sensors on a vertical array in shallow water. The downward-refracting sound speed profile has a profound effect on the noise coherence.*

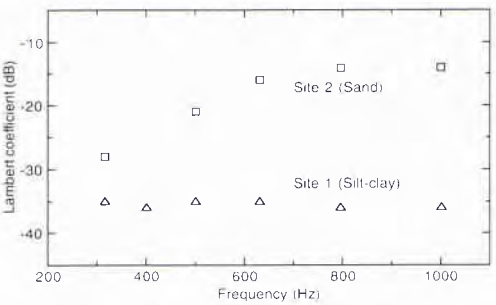

Figure 6. *Inversion of reverberation: Lambert coefficients for bottom backscattering*

DREA's research purposes and for incorporation in the Canadian version of the NATO prediction system AESS. We feel that integrated modelling capability is important for the sonar systems. The integration of AESS with the towed array development is also being investigated.

Figure 5 illustrates the very simple inversion procedure described above in Section 4.2.4. Experimental reverberation data (solid line) are compared to the prediction from a shallow water reverberation model with an assumed backscatter coefficient of –27 dB [7]. Adjusting this coefficient to -35 dB improves the fit. Figure 6 shows backscattering strengths obtained at several frequencies at two different sites. Results from applying global inversion techniques simultaneously to geo-acoustic parameters and backscatter parameters have been reported at a recent conference [8].

Collaborative work is important in developing REA techniques. Canada participated in the recent NATO MILOC exercise Rapid Response. Reverberation data were gathered on Alliance using the SACLANTCEN towed array. Software developed at the SACLANTCEN, DREA, and Penn State University was used to extract the reverberation time series and compare with model predictions. Key products are polar plots of towed array time series, which produce "maps" of the backscattering overlaid on the bathymetry. Examples of this type of polar plot are seen in references [9, 10]. We feel that no towed-array active sonar system should be without this feature.

In addition, estimates of bottom loss and scattering strength were obtained at several sites. This work is being supported by the (US) Office of Naval Research and further developments will be made in the 1997 exercise. The techniques will be used at DREA as well, through contracted and in-house effort.

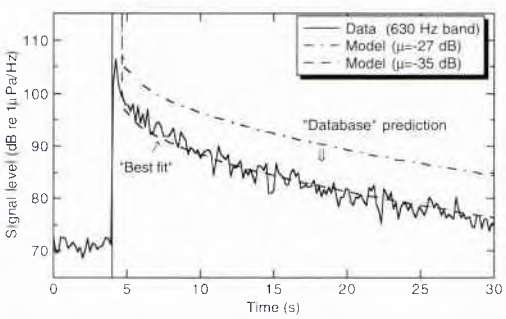

Figure 5. *Inversion of reverberation: "database" and "best fit" model-data comparisons.*

6. Conclusions

This article has presented the DREA view on the task of assessing the ocean environment in the context of sonar operations, with an emphasis on bottom interaction effects. Many issues have been raised, yet only touched upon in a superficial way. It is hoped that the article conveys the motivation for DREA (and associated) work in Rapid Environmental Assessment, the importance we place on various aspects of the research, and an indication of where we think it will lead.

In our research, we have found that the greatest delay in model-data comparisons has been in getting the data from the measurement devices to the model for inversion.

Models are mature; databases sparse or inaccurate; inversion techniques exist; and computational power is generally available. Integration with measurement systems needs to be done, and we feel progress can be made readily. Our goal is to develop robust techniques that will be able to provide useful, and reasonably

accurate, products in a timely manner.

References

[1] Paul C. Etter, *Underwater Acoustic Modeling: Principles, Techniques and Applications*, Elsevier, London (1991).

[2] D. Lee et al. (eds.), *Computational Acoustics: Ocean-Acoustic Models and Supercomputing (Vol. 1)*, North-Holland, Amsterdam (1990).

[3] David M.F. Chapman, Steven J. Hughes, and Philip R. Staal, "Shallow water acoustics: a review of DREA research," *Canadian Acoustics* **20**, 37–42 (1992).

[4] B. Sotirin and S. Hall, *Proceedings of the 8th Matched-Field Processing Workshop 12–14 June 1996*, (held at EDRD, Victoria, Canada), Naval Command, Control, and Ocean Surveillance Centre, RDT&E Division Technical Document 2932, October (1996).[5] John C. Osler and David M.F. Chapman, "Seismo-acoustic determination of the shear-wave speed of surficial clay and silt sediments on the Scotian Shelf", *Canadian Acoustics* **24**(4), 11–22 (1996).

[6] Francine Desharnais and David M.F. Chapman, "Shallow water inversion based on the vertical coherence of the ambient noise field", *Canadian Acoustics* **24**, 45 (1996).

[7] F. Desharnais and Dale D. Ellis, "Data-model comparisons of reverberation at three shallow-water sites," *IEEE J. Oceanic Engineering* (July, 1997), in press.

[8] Dale D. Ellis and Peter Gerstoft, "Using inversion techniques to extract bottom scattering strengths and sound speeds from shallow-water reverberation data," in *3rd European Conference on Underwater Acoustics Vol. 1*, (J. S. Papadakis, ed.), 557–562, FORTH, Heraklion, Crete, Greece (1996).

[9] Dale D. Ellis, F. Desharnais, R. H. Clarke, R. Hollett, E. Baglioni, and A. Legner, "Celtic Duet A Joint SACLANTCEN / NRL Shallow-Water Sea Trial in the Celtic Sea during July 1992: Data Summary," SACLANTCEN Memorandum, SM-307, (October 1996).

[10]J. Preston, T. Akal, and J. Berkson, "Analysis of backscattering data in the Tyrrhenian Sea", *J. Acoust. Soc. Am.*, **87**, 119-134 (1991).

Appendix: A comment on the utility of databases

Despite the sophistication of the computational acoustic models which form the kernel of sonar simulators, the predictions of such systems must be tempered by the GIGO rule: Garbage In, Garbage Out. It is tempting to think that marine geophysical databases will provide a basis for constructing geo-acoustic representations of the seabed for sonar modelling, but there are pitfalls on this path. Firstly, the relevant geophysical parameters must be understood and reliably measured. Secondly, these data must be inserted into the database and available! Thirdly, one has to have well-validated scientific models for translating the geophysical characteristics of the seabed into reasonable estimates of the acoustic effects. It is our experience that databases of marine geophysical data—however helpful they are to their designers—often lack parameters crucial to the sonar modeller. For example, a database containing the geographical extent, thickness, and classification of surficial sediments is of little use without the associated densities, sound speeds, and acoustic attenuation parameters. There is also a tendency for operators to trust data in databases without questioning the pedigree: where did the data originate? how did it get here? is it validated? how much of it has been invented or guessed? We must be wary of being fooled that we have solved our problems simply because we have technology that provides ready access to vast amounts of data.

Measuring and Predicting Ocean Circulation and Variability in Vestfjorden (Norway) - some experiences from the MILOC Survey Rocky Road

T. Jenserud[1], T. A. McClimans[2]

[1] FFI, N-3190 Horten, Norway
Email: tj@ffi.no

[2] SINTEF CEE/NTNU, N-7034 Trondheim, Norway

Email:thomas.mcclimans@civil.sintef.no

Abstract

The MILOC survey "Rocky Road" took place in the Lofoten region in northern Norway. The objective was to provide a foundation for operational oceanographic forecasting/nowcasting for naval operations in the region. A laboratory model provided a basis for choosing an effective measurement strategy. Several physical processes affecting the acoustic properties of Vestfjorden were observed.

1. Introduction

"Rocky Road" was a three-year (1993-95) NATO MILOC survey which took place in the shelf waters adjacent to the northwestern Norwegian coast, centered on Vestfjorden. The survey was planned to assess the effects of the environment on the performance of operational ASW sonar equipment. A principal aim was the improvement of monitoring and forecasting capabilities relevant to naval operations in the area.

Vestfjorden is considered to be a difficult area to perform ASW activities [1]. Although tidal currents through the Lofoten archipelago are likely to produce high spatial and temporal variability of the oceanographic conditions in the region, the observed acoustic propagation is also affected by the complex topography. The particular ambient noise characteristics inside the fjord pose a further problem.

Our work concentrated on

- improving the knowledge and understanding of the key oceanographic processes causing variability in the region. This included the use of a laboratory model [2] to (i) study cause/effect relationships, (ii) quantify current responses and variability, and (iii) devise an effective measurement strategy, and
- validating a numerical hydrodynamical model. An operational forecasting system for the Vestfjorden area can only be accomplished using an advanced numerical hydrodynamical model. In the Rocky Road project, the ECOM-3D model at DNMI was employed for trial forecasting during two field campaigns [3].

There were too few historical sets of field data available to capture the true natural variability within Vestfjorden, or to construct a monthly or weekly average hydrography [4]. With so little knowledge about the area it was difficult to devise a detailed field measurement program that would reveal important and representative information for the area. The laboratory model was used to fill in the gaps in our knowledge, and to provide a basis for choosing an effective measurement strategy. The model simulated the known currents and showed internal tidal amphidromes [5].

2. Developing a forecasting system for the region

Our objective is to provide a foundation for an operational forecasting/nowcasting system for the oceanographic properties in Vestfjorden.

The steps that lie behind our approach to developing an operational model are:

1. Search for cause/effect relationships.
2. Quantify algorithms.
3. Validate the model.
4. Check user responses.
5. Implement for operational forecasting.
6. Update the system.

We will concentrate on the first three steps here.

Vestfjorden is oceanographically very complex, and appears to be very difficult to predict because of high

variability on all time scales. Short-time variability comes mainly from tidal and meteorological forcing. Seasonal effects are particularly strong. Vestfjorden is influenced by three different water masses, the Coastal Water, the Atlantic Water and local freshwater runoff. The characteristics of all three of these water masses change throughout the year. Submerged, mesoscale eddies containing various combinations of these, for a week or two, are a prominent feature of the circulation in Vestfjorden.

During the early stages of planning the Rocky Road survey, it was realized that too little was known about the area to be able to devise adequate experiments and monitoring systems for the acoustics. Some of the needed inputs came from the oceanographic research at SINTEF Civil and Environmental Engineering (formerly the Norwegian Hydrotechnical Laboratory) and the Institute of Marine Research (IMR).

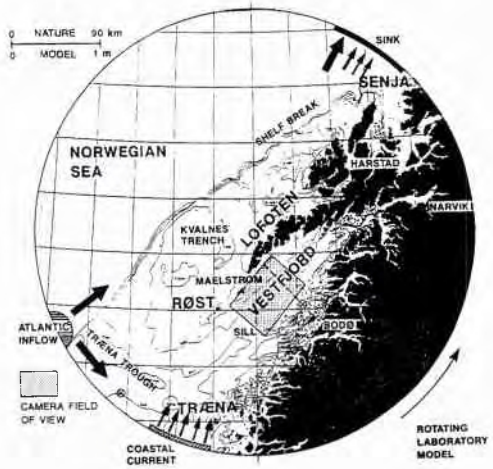

Figure 1. Extent of the laboratory model.

3. Laboratory simulation of the ocean circulation in Vestfjorden

A rotating laboratory model (Fig 1) was built to study the ocean circulation in the Lofoten region [3]. The model was forced by monthly averaged Atlantic Water and weekly averaged Norwegian Coastal Water inflows. Diurnal tidal currents through the Lofoten archipelago were calibrated into the model by tilting the axis of rotation. The energy flux in these currents is equal to that of gale force winds over the entire fjord. The shaded area in Fig 1 shows the region of photogrammetric analysis of the internal tides [5].

The laboratory results, simplified to two layers (Fig 2) agree well with known currents in the absence of extreme wind forcing [4]. The validation of the laboratory model to relevant field measurements shows deviations on the order of 25 %, which is typical for current models. A large part of the error is due to imperfect boundary conditions and noisy field data. The dashed line in Fig 2 shows the section where *in situ* velocity and tracer dye measurements were made.

The current jet in the Moskenes Sound is an important driving mechanism for the physics. We have called this the Maelstrom, although the classical Maelstrom is a frontal tornado at the edge of the jet.

The cartoon of the jet in Fig 3 shows how it promotes mixing of water masses and internal waves which propagate into the fjord.

A major result from the laboratory model was the observation of large amplitude (up to 15 m) internal tides to the east of Værøy. Here, the thermocline moves 30 m vertically within 6 hours.

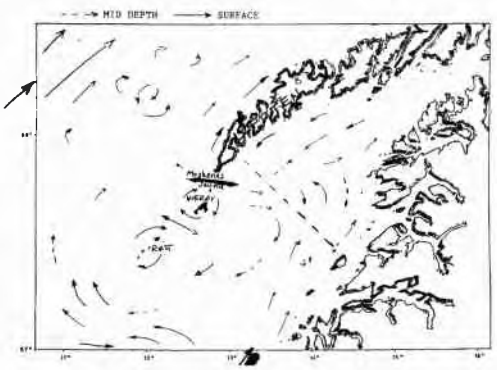

Figure 2. Modeled currents at the surface (line arrows) and at mid-depth (dashed arrows).

For the Rocky Road work, the variability caused by the internal tides, and the mesoscale eddies in the thermocline, and along the front between the Atlantic and coastal water masses, were of most interest. From the laboratory simulations, and available field data, an understanding was gained of the key oceanographic forcings which must be measured and/or modelled in order to develop a reliable forecasting capability of these features in the region: the inflows of Atlantic and coastal waters, the tidal currents through the Lofoten archipelago and winds. The variable response in Vestfjorden must also be measured to evaluate the model results and validate forecasting systems.

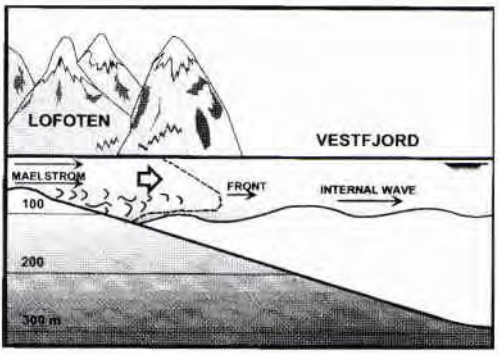

Figure 3. The tidal jet through Lofoten.

4. A field measurement program

We established the field measurement program in Fig 4 to quantifying the causes and effects seen in the laboratory model [6].

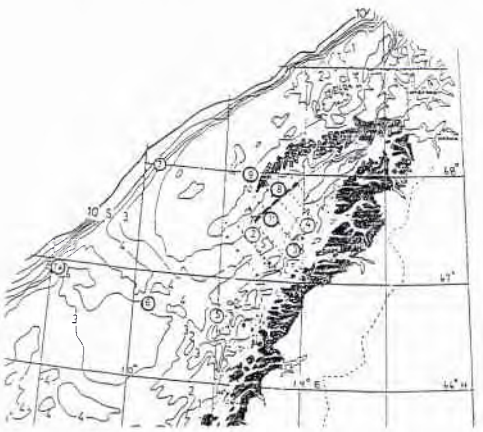

Figure 4. The field measurement program.

The Atlantic Water inflow and the Maelstrom jet were monitored by means of bottom pressure sensors at stations 7B,C and 8,9 respectively. The inflow of Atlantic Water was also monitored by current meters at stations 3, 6 and 7A, while the inflow of Coastal Water was monitored at Station 5. Station 1 was a current meter array consisting of five current meter moorings, placed in a region which showed interesting structures in satellite thermal images [7],[8]. A thermistor chain at Station 5 gave a measure of the available potential energy of the Norwegian Coastal Current.

In addition to this monitoring, over several months, there were two synoptic hydrographic surveys to obtain initializing data for numerical model forecasts.

4.1. Dedicated study of mesoscale eddies in the pycnocline

Quasistationary mesoscale eddies are an important feature for the acoustic properties of Vestfjorden. The results from the current meter array implied that large eddies east of the Moskenes Sound are formed by the tidal jet during spring tides, and are advected out of the fjord by the underflow of Atlantic Water. We therefore designed an intensive field study to the east of Værøy in May 1995 to study details of the response of this stratified geophysical system [9],[10].

The eddies appear to be swarms of filaments from several tidal injections to the pycnocline, as sketched in Fig 5. Frontal tornados at the edge of the inflowing tidal jet over the 50 m sill in the Moskenes Sound may lift water from 100 m depth, resulting in some strange temperature-salinity characteristics of the water masses observed inside the eddy [10]. This feature can effectively spread and destroy coherent acoustic signals.

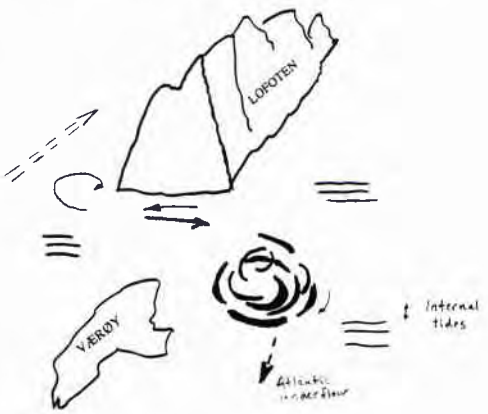

Figure 5. Rotating swarm of filaments in the pycnocline to the east of Værøy.

5. Predictability of the variability

The development of a reliable forecasting capability depends on the degree to which the processes *causing* the variability in the region can be monitored or predicted. The following conclusions on the predictability of the variability were presented at the Rocky Road Oceanography Workshop [11].

The most energetic variability which is relevant to ASW is due to internal tides. Tidal variability is predictable, but difficult because internal wave

propagation, both horizontally and vertically, depends on the changing density profiles.

Tidal jets introduce filaments of alien water masses at pycnocline depths. The fine structure is hard to predict but mesoscale eddies are formed which last over a week. Surface heating and wind-induced mixing and upwelling affect the characteristics of the surface waters and the tidal jet on most time scales.

The general circulation of the larger features, which are advected by the underflow, seems to be predictable over longer time, but we do not have enough data to quantify the details.

6. Monitoring key parameters

Operational forecasting models can be run only when the necessary forcing data can be acquired operationally. The models can, in turn, show the most cost effective combination of in situ and remotely sensed data which are needed to run the forecasts. The process is thus interactive.

The inflow of Atlantic Water to Vestfjorden is an important forcing for the transport of mesoscale eddies. For the purpose of modeling, we need an integrated value of the flux at a reasonable time resolution. An algorithm in which the Atlantic Water inflow can be computed from low-pass filtered coastal water level data, of the type used to monitor tides and surges, was suggested in [10]. The algorithm corrects for atmospheric pressure and the buoyancy of the Coastal Water in Vestfjorden, and is shown to predict the 5-day variability of the slope current with an accuracy of 15 %.

The daily changes of wind-induced upwelling and surge near Lofoten requires *in situ* monitoring and/or a high resolution numerical model [3].

7. Summary

There are several aspects of the physics of Vestfjorden that are either deterministic over extended periods or can be monitored with simple, cost-effective methods. These inputs are necessary for developing an operational forecasting system for the acoustic properties of the region. In addition, there are some stochastic parameters, like the atmospheric variables, which may have to be monitored with much higher spatial and temporal resolution than that which is available through the national monitoring network. Some of these details will be provided by fine resolution numerical models. From the above, it may be concluded that any operational forecasting system will involve some form of advanced hydrodynamical numerical model.

References

[1] T.Knudsen, FFI, Private communications, 1990.

[2] T.A. McClimans and J.H. Nilsen, "Laboratory simulation of the ocean circulation around Lofoten from October 1982 to June 1984", SINTEF Report STF60 A91027, 1991.

[3] V. Sveen and E.A. Martinsen, «Comparison of observed and modeled fields of temperature and salinity - Rocky Water 93/10», Norwegian Meteorological Institute Research Report 30, ISSN 0332-9879, 1996.

[4] S. Sundby, IMR, Private communications, 1991.

[5] J.H. Nilsen, "An experimental study of internal tidal amphidromes in Vestfjorden", Dr. ing Thesis, Civil and Environmental Engineering Faculty, NTNU, 1994.

[6] T.A. McClimans and B.O. Johannessen, "Rocky Road field measurement analysis: Vol. 1. The potential of a limited current meter array", SINTEF NHL Report STF60 F94050, 1994.

[7] J.C. Scott, «Animated NOAA thermal image sequence from Vestfjorden», Video presentation at the XVI General Assembly of the EGS, Wiesbaden, 1991.

[8] E.G. Mitchelson-Jacob, "A summary of AVHRR imagery of Vestfjorden during the period October 1982 - June 1984. Volume 1: AVHRR images", University College of North Wales, Marine Science Laboratories, UCES Report U93-6, 1993.

[9] T.A. McClimans and B.O. Johannessen, "Rocky Road: moored thermistor chain measurements east of Værøy", SINTEF Report STF22 F96208, 1996.

[10] T.A. McClimans, J.H. Nilsen, B.O. Johannessen and T. Jenserud, «Rocky Road data analysis: internal tides, eddies and underflows (Second Edition)», SINTEF Report STF22 F96234, 1996.

[11] T.A. McClimans, T. Jenserud and J.C. Scott, «Minutes of the Rocky Road Oceanography Workshop: 15-17 June 1996, Trondheim», SINTEF Report STF22 F96235, 1996.

Nonlinear Fourier Analysis with Cnoidal Waves

A. R. Osborne, M. Serio and L. Bergamasco

Dipartimento di Fisica Generale dell'Università
Via Pietro Giuria 1, Torino 10125, Italy
osborne@ph.unito.it

M. Petti

Dipartimento di Ingegneria Civile, Sezione Idraulica
Via Santa Marta 3, 50139 Florence, Italy

L. Cavaleri

Istituto Studio Dinamica Grandi Masse, CNR
Palazzo Papadopoli
Venice, Italy

Abstract

Fourier analysis is one of the most useful tools to the oceanographer and ocean engineer. The approach allows one to analyze wave data and thereby to describe them in terms of a linear superposition of ordinary sine waves. Furthermore, the Fourier technique allows one to compute the response function of a fixed or floating structure: each sine wave in the wave or force spectrum yields a sine wave in the response spectrum. However, nonlinearities in ocean waves deform the sinusoidal shapes into other kinds of waves such as the Stokes wave, cnoidal wave or solitary wave. A key question is: Does there exist a generalization of linear Fourier analysis which uses nonlinear basis functions rather than the familiar sine waves? Herein we address the dynamics of nonlinear wave motion in shallow water where the basis functions are cnoidal waves and discuss nonlinear Fourier analysis in terms of a linear superposition of cnoidal waves plus their mutual nonlinear interactions. We give a number of simple examples of nonlinear Fourier analysis and then analyze a surface-wave time series obtained on an offshore platform in the Adriatic Sea and a time series measured in a wave flume.

1. Introduction

In the last half of the twentieth century a number of important developments have been made with regard to the understanding of nonlinear wave propagation [1]. Of particular relevance to the present work has been the discovery of large classes of *nonlinear wave equations* whose solutions may be computed without approximation using a new technique referred to as the *inverse scattering transform (IST)*. IST may be viewed as a kind of *nonlinear Fourier analysis*, valid for fully nonlinear wave motion, which has many of the nice features that render ordinary Fourier analysis such a useful tool for the description of oceanic wave motions. Due to the complicated nature of the new theoretical formulations, however, many of these modern results have long remained in the domain of applied mathematics and theoretical physics. This paper constitutes an attempt to improve this unfortunate situation from a practical point of view. A number of known integrable waves equations are applicable to oceanographic situations and will eventually become important in the field of ocean engineering: 1) The Korteweg-deVries (KdV) equation describes unidirectional, shallow-water wave propagation. In this context IST provides an approach to nonlinearly Fourier analyze unidirectional waves in shallow water. 2) The Kadomtsev-Petviashvili (KP) equation describes two-dimensional, shallow-water wave propagation. Consequently, nonlinear Fourier analysis can be extended to include directional spreading of the wave components. 3) The nonlinear Schroedinger equation (NLS) describes the one-dimensional dynamics of the wave envelope function in both shallow and deep water. Hence IST provides a way to extend nonlinear Fourier analysis to deep-water situations.

This paper is intended to be a brisk introduction to the application of inverse scattering theory to the synthesis of shallow-water wave trains and to the analysis of data. A brief discussion of the application of the approach to the computation of the frequency response function of floating and compliant structures is also presented. Practical implementation of IST has been made possible by a number of theoretical advances [2-7] with regard to the case for *periodic boundary conditions* and by the recent paper of Osborne [8] in which techniques are developed for the simple exploitation of the method from physical, mathematical and numerical points of view. The approach has been

cast in terms of a kind of *nonlinear Fourier analysis* which, in the small amplitude limit, reduces to the ordinary, linear Fourier transform. It is for this reason that the nonlinear Fourier approach may be viewed as a generalization of linear Fourier analysis. The major difficulty with exploiting periodic inverse scattering theory in practical applications is that it is not normally studied outside of the curricula of mathematical physics and applied mathematics, i.e. oceanographers, fluid dynamicists and ocean engineers do not ordinarily study the theory of the periodic Schroedinger operator, hyperelliptic functions, θ-functions and algebraic geometry. The present paper avoids these mathematical difficulties and discusses primarily the physical results, which are, in an applications context, rather simple.

2. Linear Fourier Analysis

Fourier analysis allows the construction of linear wave trains, $\eta(x,t)$, by a linear superposition of sine waves:

$$\eta(x,t) = \sum_{n=1}^{N} \eta_n \sin\left(k_n x - \omega_n t + \phi_n\right) \qquad (1)$$

In the present case there are N sine waves which are interpreted as "degrees of freedom" or "Fourier components" in the wave train. In (1) the η_n are the Fourier amplitudes, the k_n are the wave numbers, the ω_n are the frequencies and the ϕ_n are the phases. The relationship between the frequencies ω_n and the wave numbers k_n is given by the dispersion relation, written symbolically: $\omega_n = \omega_n(k_n)$. The dispersion relation defines the physics via the correspondences

$$\frac{\partial}{\partial t} \leftrightarrow -i\omega, \qquad \frac{\partial}{\partial x} \leftrightarrow ik$$

For example the simple dispersion relation for *long waves in shallow water*

$$\omega = c_o k - \beta k^3 \qquad (2)$$

has the associated partial differential equation (the linearized Korteweg-deVries equation):

$$\eta_t + c_o \eta_x + \beta \eta_{xxx} = 0 \qquad (3)$$

The coefficients $c_o = \sqrt{gh}$, $\beta = c_o h^2 / 6$ are constants which depend upon the depth h and gravitational acceleration g. The simplest periodic solution to (3) is a travelling sine wave

$$\eta(x,t) = \eta_o \sin\left(k_o x - \omega_o t + \phi_o\right) \qquad (4)$$

from which the general Fourier solution for N components may be constructed by (1). The important point is that the *amplitudes of the sine waves and their phases are constants of the motion, provided that the motion is linear.* In oceanic applications one is often interested in the analysis of time series, i.e. measurements of the wave amplitude, $\eta(0,t)$, taken at a fixed spatial location over some convenient time interval, this implies setting $x = 0$ in (1) and (4).

3. Nonlinear Fourier Analysis

The Fourier transform is one of the most useful tools ever devised for the mathematical analysis of wave trains, for the analysis of experimental data and for engineering design purposes. Fourier analysis is, however, somewhat limited in its scope, primarily because ocean waves are effectively nonlinear. In sufficiently shallow water, where the waves may be considered long with respect to the depth, the waves 'feel' the presence of the bottom. Nonlinear effects typically manifest themselves by causing changes in the shape of the waves, i.e. nonlinear waves generally have crests which are higher and narrower than for a sine wave; likewise the troughs are less deep and broader than for a sine wave. The simplest nonlinear shallow water wave equation for which this occurs is the Korteweg-deVries equation [9]:

$$\eta_t + c_o \eta_x + \alpha \eta \eta_x + \beta \eta_{xxx} = 0 \qquad (5)$$

This equation is the same as (3) except for the presence of the nonlinear convective derivative term prefixed by the constant coefficient, $\alpha = 3c_o / 2h$. While the general solution of (3) for periodic boundary conditions is easily found using the linear Fourier transform, the general IST solution to the nonlinear equation (5) required an additional 170 years of mathematical progress! The simple travelling wave,

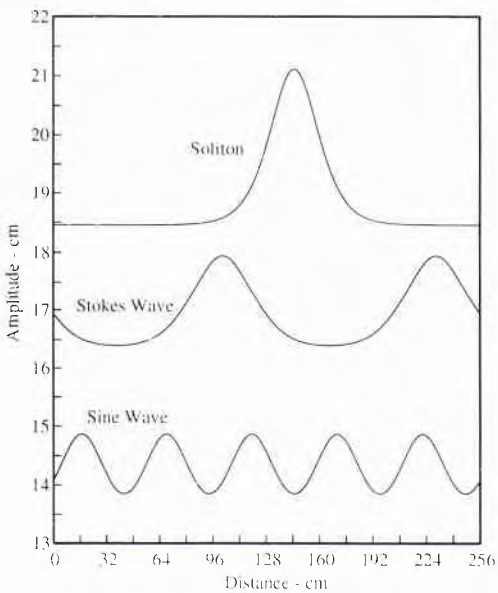

Figure 1. Examples of cnoidal waves. In vertical order are shown a solitary wave or soliton, a Stokes wave and a sine wave.

periodic solution of (5) is the *cnoidal wave*, well known in shallow water oceanography and offshore engineering [9-13]:

$$\eta(x,t) = \frac{4k^2}{\lambda}\sum_{n=1}^{\infty}\frac{n(-1)^n q^n}{1-q^{2n}}\cos[nk_o(x-Ct)+\phi_o] = \tag{6}$$

$$= 2\eta_o cn^2\left\{(K(m)/\pi)[k_o x-\omega_o t+\phi_o];m\right\}$$

where $\lambda = \alpha/6\beta = 3/2h^3$. The modulus, m, of the elliptic function cn, the nonlinear phase speed, C, and the nome, q, depend explicitly on the amplitude, η_o [14]; $\omega_o = Ck_o$. Note that the series in (6), suitably truncated to N terms, is the shallow-water, Nth order Stokes wave. In the limit as the modulus $m \to 0$ the cnoidal wave reduces to a sine wave; when $m \to 1$ the cnoidal wave approaches a solitary wave or soliton; intermediate values of the modulus correspond to the Stokes wave (see Fig. 1).

With regard to (5) and (6) an important problem in mathematical physics and related practical applications has remained open for a century. It is well known that linear Fourier analysis works well for linear wave equations with sine wave basis functions. The more difficult question as to whether there exists a generalization of linear Fourier analysis which uses cnoidal wave basis functions was resolved in reference [8]. This work formulates nonlinear Fourier analysis in a physical and mathematical form which is simple enough that practical oceanographic and engineering applications of the method can now be made. This approach is based upon the general periodic solution to the KdV equation (5) in terms of the so-called θ–*function representation* :

$$\lambda\eta(x,t) = 2\frac{\partial^2}{\partial x^2}\ln\Theta_N(x,t) \tag{7a}$$

where:

$$\Theta_N(x,t) = \sum_{M_1=-\infty}^{\infty}\cdots\sum_{M_N=-\infty}^{\infty}\mathrm{K} \tag{7b}$$

$$\exp\left[i\sum_{n=1}^{N}M_n\eta_n + \frac{1}{2}\sum_{m=1}^{N}\sum_{n=1}^{N}M_m B_{mn}M_n\right]$$

Here N is the number of cnoidal waves in a (broad-spectrum) solution to the KdV equation. The summation indices M_n $(1 \le n \le N)$ are simply integers summed from $-\infty$ to ∞. The θ–function phases have the same form as in linear Fourier analysis: $\eta_n = k_n x - \omega_n t + \phi_n$. Explicit computation of the period matrix, $\mathbf{B} = \{B_{mn}\}$, the wave numbers, k_n, the frequencies, ω_n and the phases, ϕ_n is discussed elsewhere [8]. The period matrix $\mathbf{B}$ is constant and negative definite and defines the cnoidal wave amplitudes and moduli (diagonal terms) and their nonlinear pair-wise interactions (off-diagonal terms). Equations (7) are discussed in detail for the particular case $N = 2$ in Boyd [2]. On the basis of the θ–function formulation (7) one can prove the following theorem [8]:

Fundamental Theorem of Nonlinear Fourier Analysis:

The θ–function solution (7) to the KdV equation (5) can be written in the following form:

$$\eta(x,t) = \frac{2}{\lambda}\frac{\partial^2}{\partial x^2}\ln\Theta_N(x,t) = \tag{8}$$

$$= \underbrace{\eta_{lin}(x,t)}_{\substack{\text{Linear superposition}\\ \text{of cnoidal waves}}} + \underbrace{\eta_{int}(x,t)}_{\substack{\text{Nonlinear interactions}\\ \text{among the cnoidal waves}}}$$

The theorem essentially states that *Shallow water wave trains can be represented by a linear superposition of cnoidal waves plus their mutual nonlinear interactions.* How is this formulation related to linear Fourier analysis? This is seen by letting the average wave amplitude become so small that the cnoidal wave components become sine waves and the nonlinear interactions tend to zero. In this way linear Fourier analysis is recovered from the nonlinear theory. An important aspect of the above theorem is that the *amplitudes of the cnoidal waves and their phases are constants of the motion, provided that the motion is governed by the KdV equation.*

4. The Synthesis of Nonlinear Wave Trains Using Nonlinear Fourier Analysis

In this Section we address the issue of synthesizing shallow-water wave trains from their constituent cnoidal waves. The approach adopted is to give several examples which illustrate the generality of the method. The N-cnoidal-wave solution to KdV is given by (8), which can be written:

$$\eta_{cn}(x,t) = 2\sum_{n=1}^{N}\eta_n cn^2\left\{(K(m_n)/\pi)[k_n x-\omega_n t+\phi_n];m_n\right\}$$

$$+\eta_{int}(x,t)$$

Here we consider an example with $N = 5$ cnoidal waves. The cnoidal wave spectrum is shown in Fig. 2; both the cnoidal wave amplitudes, η_n, and moduli, m_n, are graphed as a function of wave number, k_n, $1 \le n \le 5$. The first (leftmost) cnoidal wave, η_1, has a modulus near 1, $m_1 \sim 1$, and hence can be interpreted as a solitary wave. The next cnoidal wave has modulus 0.91 and is a Stokes wave. The remaining three waves may be thought of as small amplitude Stokes waves with moduli 0.51, 0.34 and 0.23. Note that the wave numbers of the various cnoidal waves have the values $k_n = n\Delta k = 2\pi n/L_*$ for $L_* = 256$ cm and $n = 1,2,\ldots,5$. The five cnoidal waves are shown at the top of Fig. 3 in

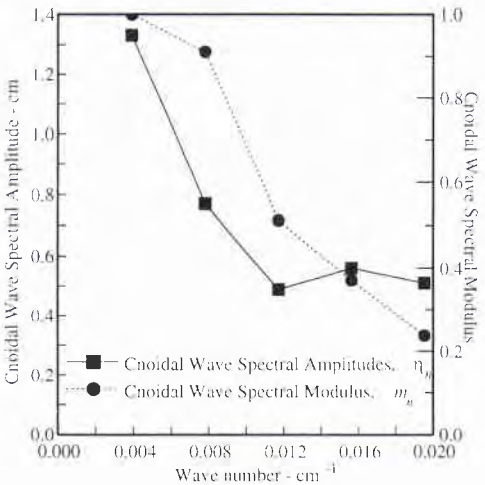

Figure 2. An example of nonlinear Fourier analysis using the inverse scattering transform. There are five cnoidal wave components in the spectrum. Shown are the amplitudes, η_n, and the moduli, m_n, of the cnoidal waves.

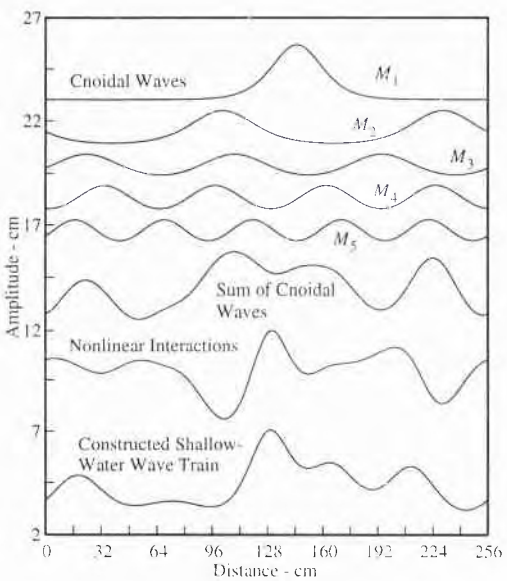

Figure 3. The cnoidal wave components in the spectrum of Fig. 2 are shown, together with the sum of the cnoidal waves, nonlinear interactions and synthesized five-component wave train. The linear superposition of the cnoidal waves plus interactions yields the synthesized wave train at the bottom of the panel.

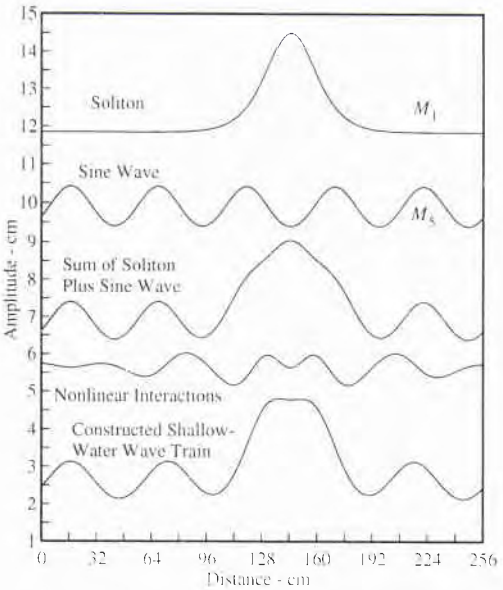

Figure 4. An example of the interaction between the soliton and a sine wave of Fig. 3.

vertical order from the lowest wave number to the highest. Below these are the 'sum of the cnoidal waves,' the 'nonlinear interaction contribution' and the constructed shallow-water wave train solution' of the KdV equation. The KdV solution consists of the summed cnoidal waves plus the nonlinear interactions. This example constitutes the direct application of Theorem (8) given above. In principle one can apply the theorem to an arbitrary number N of cnoidal waves.

We would now like to give several examples of *nonlinear filtering*. Recall that the simplest way to filter with the linear Fourier transform is simply to delete particular components from the Fourier sum (1), i.e. a low pass filter *deletes* all components with a wave number or frequency higher than some chosen cutoff value. This is the so-called 'perfect' low-pass filter. Due to limitations in length of the present paper we will not discuss other types of filters which, through various techniques, round off the shoulder of the perfect filter to minimize the Gibbs phenomenon. Nonlinear filtering using (7) is quite different from that for linear filtering using (1), primarily due to the presence of the nonlinear interactions. In practice, however, nonlinear filtering is implemented in a fashion similar to linear filtering, i.e. in order to delete a particular cnoidal wave from the spectrum it is enough that the particular component not be included in the sum (7). This is accomplished by not including the summation for a particular M_n: for example, if the third cnoidal wave is not wanted in the

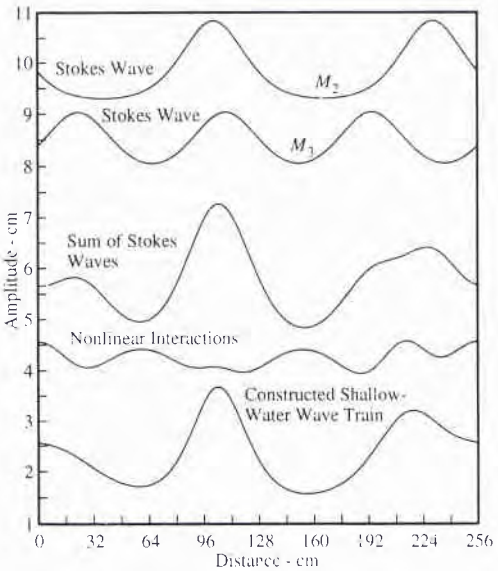

Figure 5. An example of the interaction between two Stokes waves of Fig. 3.

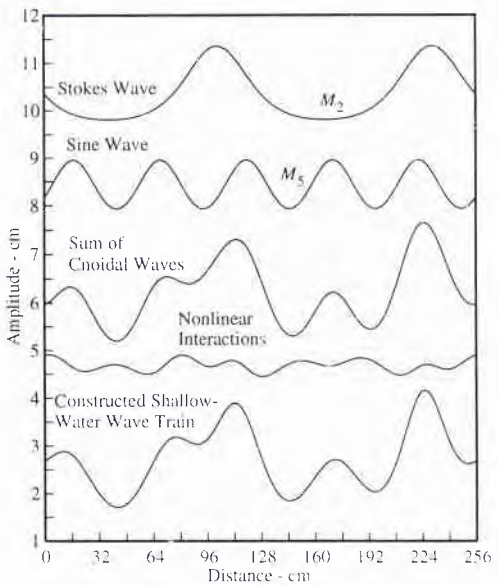

Figure 6. An example of the interaction between a sine wave and the Stokes wave of Fig. 3.

synthesized wave train one excludes the M_3 summation from (7b). A typical example is graphed in

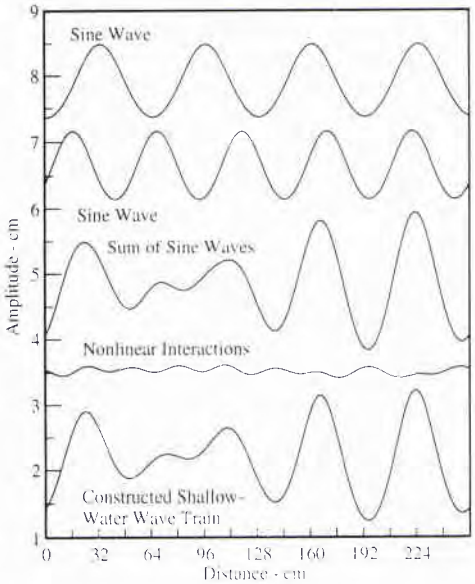

Figure 7. An example of the interaction between two (near) sine waves of Fig. 3.

Fig. 4 where we filter out the M_2, M_3 and M_4 components from the five-cnoidal-wave synthesis shown in Fig. 3. Thus only the M_1 (soliton) and M_5 (sine wave) components remain in the spectrum for Fig. 4. In vertical order we show the soliton, sine wave, sum of these two components, the nonlinear interactions and the synthesized wave train. Note that the nonlinear interaction contribution is a *localized packet wave centered on the soliton*. Note, further, that the nonlinear interactions provide a substantial contribution to the energetics of the wave train.

Fig. 5 shows the synthesis of two Stokes waves (components M_2, M_3 from Fig. 3). As before, the contributions are given in vertical order from top to bottom: the two Stokes waves, the sum of the Stokes waves, the nonlinear interactions and the constructed KdV wave train. The interactions in this example are rather small, due to the fact that the second Stokes wave is of relatively small amplitude. Fig. 6 gives the construction of a Stokes wave and a sine wave: here, again the interactions are small due to the small-amplitudes of the components. Fig. 7 synthesizes two components which are so small that they are nearly sine waves. The nonlinear interactions are seen to make an almost negligible contribution. We have selected the sine waves to differ in frequency by exactly Δk, a small number. We thus have a *small amplitude beat* for which nonlinear interactions are not very important. By studying the examples just given one begins to develop a feeling for the behavior of shallow-water, nonlinear wave trains which have only a few cnoidal wave

components. In the following Section we analyze ocean wave data for which the number of cnoidal wave components is instead large.

5. Analysis of Shallow-Water Ocean Waves

We now consider the analysis of a surface wave time series obtained from the Adriatic Sea in 16.5 m of water about 20 km from Venice [15]. In Fig. 8(a) we show the measured wave train for which the significant wave height is 2.0 m, the largest waves are about 3.5 m in height and the average zero- crossing period is 10.1 sec. The cnoidal wave spectrum is given in Fig. 8(b) where the cnoidal wave spectral amplitudes (solid line) and the moduli (dotted line) are shown. Note that the modulus is large at low frequency and then generally decreases with increasing frequency, but rises to a maximum (~ 0.27) near the peak of the spectrum ~ 0.1 Hz. The physical interpretation of these results is relatively simple: at low frequency there are several small-amplitude solitons in the spectrum, while at larger frequency the components are at most moderate-amplitude Stokes waves. We have applied the same spectral decomposition to the data that we previously applied to the numerically synthesized wave trains in the last Section. These results are shown in Fig. 9 where the first 50 cnoidal waves in the spectrum are given. We have truncated the number of cnoidal waves as an exercise in *low-pass filtering of the measured wave train* (the low-pass frequency range is 0 to 0.2 Hz). The sum of the 50 cnoidal waves is shown below the cnoidal waves in Fig. 9. Likewise, the nonlinear interactions have also been computed and this time series is graphed below the summed cnoidal waves. Finally the low-pass-filtered Adriatic Sea time series has been reconstructed at the bottom of the figure.

From the above results it is clear that the nonlinear effects in this particular Adriatic Sea wave train are relatively large. This is evidenced 1) by the values for the moduli for most of the cnoidal wave spectrum (note that many of the components are effectively sine waves while a few, near the spectral peak, are moderate amplitude Stokes waves; see Fig. 8(b)) and 2) by the fact that the nonlinear interaction contribution is large compared to the summed cnoidal waves (Fig. 9). However, in general the interactions can be even larger (see for example Fig. 3). One concludes that the effects of the nonlinearities in the present case are important and provide some insight into the behavior of the measured wave train. First, note that the summed cnoidal waves are larger than the measured wave train itself. By superposing the summation of the cnoidal waves with the nonlinear interactions we find that the measured wave amplitudes are *smaller* than the summed cnoidal waves. This occurs because the interactions are effectively *out of phase* with the measured time series. The phase shifting property is of course a well-known nonlinear physical phenomena; the present results demonstrate that this effect also occurs for *all* components in the IST spectrum. Due to the moderate size of the interaction contribution in the present case one might conceivably be able to construct a perturbation theory for nonlinear interactions; this is a topic for future consideration.

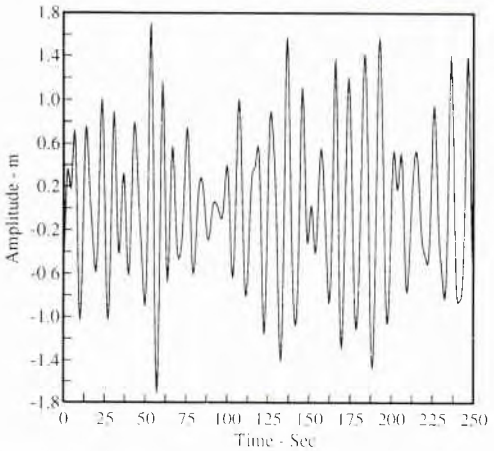

Figure 8(a). A measured surface wave time series from the Adriatic Sea.

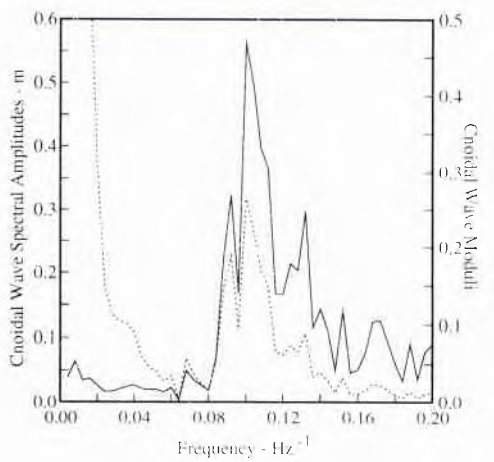

Figure 8(b). Nonlinear Fourier analysis of the Adriatic Sea time series of Fig. 8(a). Shown are the spectrum (solid line) and moduli (dotted line) as a function of frequency.

It is worthwhile noting at this point that the influence of nonlinear interactions in shallow-water, oceanic wave trains depends upon the Ursell number, $U = 3H_s L_z^2 / 32\pi^2 h^3$, where H_s is the significant wave height, L_z is the zero crossing wave length and h is the depth). Thus by increasing either the wave height or the wave length (or period, $T_z = L_z / c_{gr}$) or by decreasing

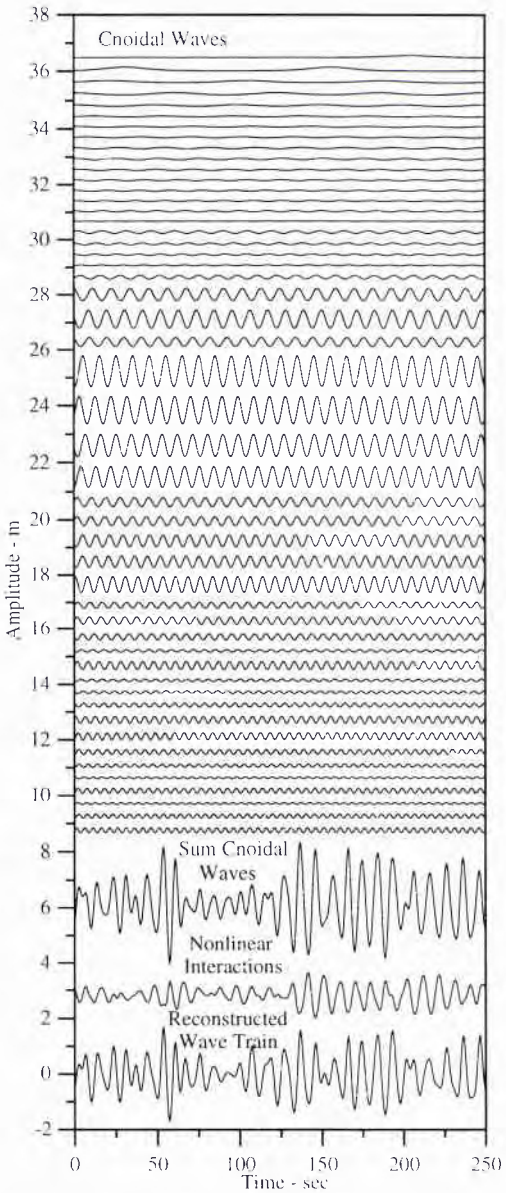

Figure 9. Nonlinear Fourier decomposition of the Adriatic Sea time series of Fig. 8. The first fifty cnoidal waves in the spectrum are shown (corresponding to nonlinear low-pass-filtering of the measured wave data from 0 to 0.2 Hz). Also shown are the wave trains corresponding to the sum of the cnoidal waves, the nonlinear interactions and the reconstructed low-pass-filtered input time series obtained from Fig. 8(a).

the depth, one increases the nonlinearity. In particular the $1/h^3$ dependence on depth can have a significant influence on nonlinear effects in shoaling wave trains. In general, one should not expect the influence of nonlinearity to be perturbative in nature, primarily because for sufficiently large Ursell number the nonlinear interactions can be roughly of the same size as the summed cnoidal waves.

6. Brief Discussion of Floating Body Motions

We would like to give a short overview of floating body motions under the influence of a nonlinear, shallow-water wave train. An important question is: How is the motion of a floating structure influenced by a broad-spectrum, cnoidal wave train? Under what conditions can one compute the frequency response function of the vessel in the presence of nonlinear wave forcing? we give a simple example to show how the method may be used. Assume that the equation of vertical motion of a floating object in a nonlinear sea state is given by

$$m\ddot{y} + c\dot{y} + ky = F(t) \tag{9}$$

where $F(t)$ is representable in terms of cnoidal waves plus interactions:

$$F = F_{cn1} + F_{cn2} + \ldots + F_{cnN} + F_{int} \tag{10}$$

The Fourier transform of this expression is then given by

$$\hat{F} = \hat{F}_{cn1} + \hat{F}_{cn2} + \ldots + \hat{F}_{cnN} + \hat{F}_{int} \tag{11}$$

where the over-symbol means "Fourier transform of." Then the frequency response function of the floating body is easily determined in at least two ways: 1) In terms of the response to each cnoidal wave plus the response to the nonlinear interactions or 2) In terms of the response to an ordinary Fourier series for $F(t)$ which is computed from IST variables. Hence the frequency response can be written in terms of the parameters m, c, k and *the nonlinear modes*. Therefore, vertical floating body motions, as governed by the dynamical equation (9), may be described in terms of the fundamental nonlinear components of the inverse scattering transform. The IST modes provide a new and unique way to study important problems in ocean engineering. Many more vessel-motion problems are discussed in detail elsewhere [16].

Expressions (10) and (11) are appropriate for addressing method (1) for computing the frequency response. To illustrate how the frequency response function may be computed we now discuss the second of the above two approaches, primarily because it is the simplest and also because it resembles the standard linear input/output method, i.e. for a sine-wave-input/sine-wave-output analysis. We assume that the force is proportional to a linear superposition of the wave height and its time derivatives, or alternatively of the velocity field and its time derivatives. Because of

limitations set on the length of this paper, we shall consider only the following case:

$$F(t) = K\eta(0,t) = \frac{2K}{c_o^2\lambda}\frac{\partial^2}{\partial t^2}\ln\Theta_N(0,t) \qquad (12)$$

where

$$\Theta_N(0,t) = \sum_{M_1=-\infty}^{\infty}\cdots\sum_{M_N=-\infty}^{\infty} \mathrm{K} \qquad (13)$$

$$\sum_{M_N=-\infty}^{\infty}\exp\left[-i\sum_{n=1}^{N}M_n(\omega_n t-\phi_n)+\frac{1}{2}\sum_{m=1}^{N}\sum_{n=1}^{N}M_m B_{mn}M_n\right]$$

K is a constant and $\eta(0,t)$ is the wave amplitude at some fixed spatial location, $x=0$. Thus in the present problem a floating object is subject to a *nonlinear, stochastic, vertical forcing which is proportional to the sea surface elevation*. Note that in the absence of dynamics ($m\sim0$) and drag ($c\sim0$), the vessel motion follows the surface elevation, $y(t)\sim\eta(0,t)$. Likewise, if we assume that $c=k=0$ we have only acceleration effects (a floating buoy) and the motion is given by:

$$y(t) = -\frac{2K}{c_o^2\lambda m}\ln\Theta_N(0,t)$$

which is merely the logarithm of a θ–function! This problem is given as a relatively simple example which can be used to provide insight into a large number of other important cases [16].

Recently Osborne [8,16] has shown that the θ–function (13) may be written in the following useful forms:

$$\Theta_N(0,t) = \sum_{l=1}^{\infty}C_l e^{-i(\Omega_l t-\Phi_l)} = \sum_{n=1}^{\infty}c_n e^{-i\omega_n t} \qquad (14)$$

where

$$C_l = \exp\left[\frac{1}{2}\sum_{i=1}^{N}\sum_{j=1}^{N}M_i^l B_{ij}M_j^l\right] \qquad (15)$$

In (14) we have written the N nested sums in the θ–function (13) as a single sum in terms of the "ordering parameter l". The frequencies, Ω_l, and phases, Φ_l, are defined by:

$$\Omega_l = \mathbf{M}_l\cdot\omega = \left[M_1^l, M_2^l, \ldots, M_N^l\right]\cdot[1,2,\ldots,N]\Delta\omega = \Delta\omega\sum_{j=1}^{N}jM_j^l$$

$$(16)$$

$$\Phi_l = \mathbf{M}_l\cdot\phi = \left[M_1^l, M_2^l, \ldots, M_N^l\right]\cdot\left[\phi_1,\phi_2,\ldots,\phi_N\right] = \sum_{j=1}^{N}M_j^l\phi_j$$

Note that the superscripts on the indices M_j^l simply refer to the sequential summation over the middle term in (14). Thus the vector of indices $\left[M_1^l, M_2^l, \ldots, M_N^l\right]$ is obtained and associated with a particular l *value* which is incremented each time one of the indices M_j^l is changed in the nested sum of (13). The first equation in (16) says that the frequencies in the θ–function are integer multiples of the lowest frequency, $\Delta\omega = 2\pi/T$, where T is the chosen period of the wave train forcing (12):

$$\Omega_l = l_l\Delta\omega; \qquad l_l = \sum_{j=1}^{N}jM_j^l \qquad (17)$$

Finally, the coefficients in the *second* summation in are given by the following *Poincaré series*:

$$c_n = \sum_{\substack{\text{sum over subset}\\ \text{of } l \text{ for which } l_l = n}} C_l e^{i\Phi_l}; \quad 1\le n\le\infty \qquad (18)$$

To compute the latter sum choose a value of n, say 3. Then compute the l_l by (17) for all l. Find the values of l for which $l_l = 3$. This is the subset of l for which $n=3$ and is hence the subset over which (18) is to be summed. Note that this point set is the intersection of a fractal curve [8] and a horizontal line at some chosen value of l_l. Hence, theoretically speaking, there are an infinite number of values of l to sum over for each value of n in the Poincaré series (18). Practically speaking, however, one of course sums over many fewer terms.

Now note what the above mathematical exercise has done for us, can be viewed as a small miracle because it has reduced the complicated θ–function (13) to an *ordinary Fourier series at the fixed spatial point*, $x=0$. The forcing function acting on the floating vessel is then computed by (12), from which it is straightforward to show that $F(t)$ *also has an ordinary Fourier series* and therefore the *equation of motion (9) has been fully linearized*. By introducing a linearization transformation of the θ–function using Poincaré series, the entire engineering procedure itself has been linearized. Why is this result so important? Because it says that by using the Fourier coefficients of the forcing function $F(t)$ (which have been derived from the complex machinery of inverse scattering theory (12), (13)) we can compute the frequency response function of (9) using *standard linear methods*, i.e. the usual sine-wave-in sine-wave-out approach.

It is also important to consider the dynamical problem for the case where *spatial evolution* is important. The equation of motion has the form:

$$m\ddot{\mathbf{x}} + c\dot{\mathbf{x}} + k\mathbf{x} = \mathbf{F}(t)$$

where $\mathbf{x}(t) = [x(t), y(t)]$ and the forcing function also has a horizontal part. In this case one finds it necessary to keep the spatial part of the θ–function, so that the counterpart of (14) becomes:

$$\Theta_N(0,t) = \sum_{l=1}^{\infty} C_l e^{i(K_l x - \Omega_l t + \Phi_l)} = \sum_{n=1}^{\infty} c_n(x) e^{-i\Omega_n t} \quad (19)$$

Thus the coefficient in the second sum depends on the space variable, x. One finds the generalization of the Poincaré series for these coefficients:

$$c_n(x) = \sum_{\substack{\text{sum over subset} \\ \text{of } l \text{ for which } I_l = n}} C_l e^{i(K_l x + \Phi_l)}; \quad 1 \le n \le \infty \quad (20)$$

The full space-time dynamics can therefore be determined using this latter formulation. The analysis approach just discussed works for a wide variety of vessel motion problems and should prove to be a useful tool in future analyses of nonlinear wave forcing on many types of fixed, floating and compliant structures.

7. Analysis of Data from a Wave Flume

We have performed several surface wave experiments in a wave tank facility located at the University of Florence in the Hydraulics Section of the Department of Civil Engineering. The wave tank is a long and narrow channel of dimensions 0.76 m x 0.8 m x 46 m, filled to a typical depth of about 50 cm. At one end of the tank a wave generator has been installed which consists of a vertical, computer-controlled paddle that occupies the entire channel cross section. The movement of the wave maker is fully programmable through a control and feedback system. A desktop computer with an Intel 80386 processor provides intelligent control of the paddle motion. Details of this system may be found elsewhere [42].

The first 19 meters of the tank has a flat bottom, while the remaining 31 meters is configured with a concrete ramp which has a 2% slope. This experimental configuration is motivated by two primary considerations: (1) the ramp provides an efficient way to minimize reflection, while (2) at the same time it offers the possibility of studying wave dynamics on the slope itself (the details of this latter study are delayed to a later publication). Minimization of reflected waves is of course an important consideration for the analysis considered herein, because the KdV equation and the scattering transform, assume unidirectional wave motion.

Eight resistance wave height gauges were placed at arbitrary spatial locations along the canal. For the present study five gauges recorded data in the initial 19 m section of the canal which was configured with a flat bottom. The outputs of the gauges were sampled and converted to digital form at a typical rate of 20 Hz; the data are then recorded on computer disk in real time. Both wave maker position and data recording are controlled by the 80386-based desktop computer which contains special acquisition, preliminary analysis and control software developed for this facility. The analog-to-digital/digital-to-analog electronic system has 12-bit resolution, with a sampling frequency of 10 Hz for the wave maker control signal and up to 40 Hz for the resistance wave gauge signals.

By choosing an appropriate wave height and dominant period for the wave maker (both parameters are adjustable over rather wide limits) we tuned the resultant wave trains in order to study KdV dynamics in the canal. Several experimental time series have been obtained in water depths of 30 and 50 cm for a number of different wave maker amplitudes generated with a fixed period of four seconds. All wave maker input signals were chosen to be sinusoidal with amplitudes varying from small (2.5 cm) up to large (6 cm) (Table I). Distortions of the measured wave trains from this simple sinusoidal shape (see experiments below) are indicative of the nonlinear nature of the wave motions studied herein. A battery of preliminary experiments was given in reference [17].

An example of an inverse scattering transform analysis of a particular wave tank experiment is shown in Fig. 10. The water depth was 40 cm and the waves were generated with a period of 4 sec. The measured wave train considered in this case is the lower curve in the figure. An IST analysis was conduced and the 12 degrees of freedom are shown in the upper 12 cnoidal waves in the spectrum. Below the cnoidal waves are curves for the 'sum of the cnoidal waves' and for the 'nonlinear interactions.' The sum of the cnoidal waves plus nonlinear interactions reproduces the measured wave train as shown in the bottom of the figure. Note that the wave train in Fig. 10 consists of two wave periods and hence a vertical line through the center of the figure would divide it into equal halves (for the even modes). The cnoidal waves toward the upper part of the figure are the most nonlinear, i.e. have the greatest departure from the sine wave. The three largest cnoidal waves dominate the motion and contain about 95% of the energy. There is no evidence of phase locking among the modes as computed by the IST. Documentation of a large number of experiments in terms of cnoidal wave spectra is forthcoming.

8. Summary and Discussion

The inverse scattering transform in the θ–function formulation is seen to provide new insight and perspective about the nonlinear dynamics of shallow-water wave trains. The propagation of shallow-water waves is found to be governed by two considerations, namely, the space/time evolution of individual cnoidal waves with particular amplitudes and moduli, plus their mutual nonlinear interactions. The actual spectrum of the cnoidal wave components is seen to depend on the period or interaction matrix, $\mathbf{B}$, whose *diagonal elements* define the cnoidal wave amplitudes and moduli and whose *off-diagonal elements* govern the nonlinear interactions. Both the synthesis of computer generated, shallow-water wave trains and the analysis of data are found to be feasible using recent methods the approach to ocean engineering will include the computation of nonlinear response functions of floating vessels, the reassessment of certain aspects of fatigue

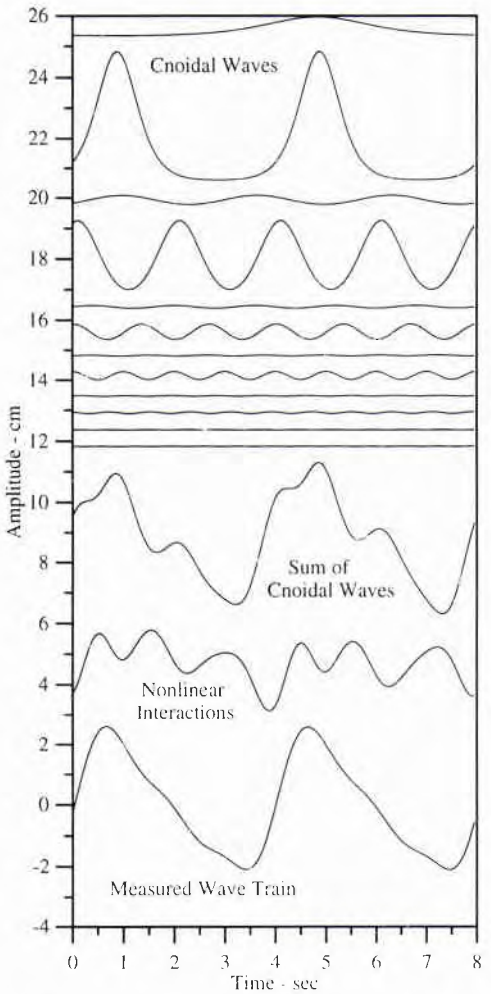

Figure 10. Results of inverse scattering transform analysis of wave data obtained in the wave tank in Florence. Shown in vertical order are the 12 cnoidal waves in the spectrum, the sum of the cnoidal waves, the nonlinear interactions and the measured wave train.

developed in Osborne [8]. A number of applications of analysis and the determination of the "maximum wave" in a nonlinear, shallow-water sea state.

References

[1] M. J. Ablowitz and H. Segur, *Solitons and the Inverse Scattering Transform*, 1981, Philadelphia, SIAM.

[2] J. P. Boyd, *Adv. Appl. Mech.*, vol. 10, pp. 1, 1990.

[3] E. Date and S. Tanaka, "Periodic multi-soliton solutions of Korteweg-deVries equation and Toda lattice," *Prog. Theoret. Phys. Supp.*, vol. 59, pp. 107-126, 1976.

[4] B. A. Dubrovin, V. B. Matveev and S. P. Novikov, "Nonlinear equations of Korteweg-deVries type, finite zoned linear operators, and Abelian varieties," *Russian Math. Surv.*, vol. 31, pp. 59-146, 1976.

[5] H. Flaschka and D. W. McLaughlin, "Canonically conjugate variables for KdV and Toda lattice under periodic boundary conditions," *Prog. Theoret. Phys.*, vol. 55, pp. 438-456, 1976.

[6] A. R. Its and V. B. Matveev, "The periodic Korteweg-deVries equation," *Func. Anal. and Appl.*, vol. 9(1), pp. 67ff, 1975.

[7] H. P. McKean and E. Trubowitz, "Hill's operator and hyperelliptic function theory in the presence of infinitely many branch points," *Comm. Pure Appl. Math.*, Vol. 29, pp. 143-226, 1976.

[8] A. R. Osborne, "Solitons in the periodic Korteweg-deVries equation, the θ-funtion representation, and the analysis of nonlinear, stochastic wave trains," *Phys. Rev. E*, vol. 52(1), pp. 1105-1122, 1995.

[9] D. J. Korteweg and G. deVries, "On the change of form of long waves advancing in a rectangular canal, and on a new type of long stationary waves," *Philos. Mag. Ser.*, vol. 5(39), pp. 422-443, 1895.

[10] J. W. Miles, "Solitary Waves," *Annual Rev. Fluid Mech.*, vol. 12, pp. 11-43, 1980.

[11] T. Sarpkaya and M. Isaacson, *Mechanics of Wave Forces on Offshore Structures*, New York, Van Nostrand Reinhold, 1981.

[12] R. Weigel, 1964, *Oceanographical Engineering*, Englewood Cliffs, N.J., Prentice-Hall, 1964.

[13] G. B. Whitham, *Linear and Nonlinear Waves*, New York, John Wiley, 1974.

[14] A. R. Osborne, "Numerical construction of nonlinear wave-train solutions of the periodic Korteweg-deVries equation," *Phys. Rev. E*, 48(1), pp. 296-309, 1993.

[15] A. R. Osborne, L. Bergamasco, M. Serio and L. Cavaleri, "Nonlinear shoaling of shallow-water waves: Perspective in terms of the inverse scattering transform," *Nuovo Cimento*, vol. 196, pp. 151-171, 1996.

[16] A. R. Osborne, unpublished, 1996.

[17] A. R. Osborne and M. Petti, 1994, "Laboratory-generated, shallow-water surface waves: Analysis using the periodic, inverse scattering transform," *Phys. Fluids*, vol. 6(5), pp. 1727-1744 1994.

Communications

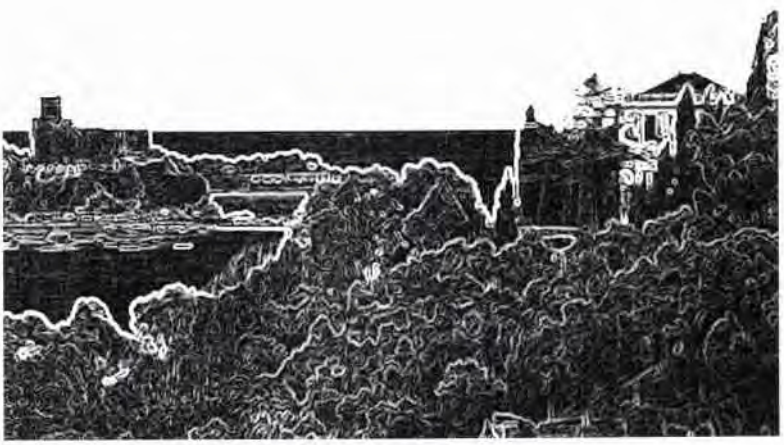

Inmarsat Mobile Satellite Comunications for Environmental Monitoring Applications

M. Mohindra

Maritime Applications Department INMARSAT
99 City Road
London EC1Y 1AX UK

Abstract

This paper provides an overview of communications via Inmarsat, inluding space segment, shore network and mobile terminals. Some institutional issues will be covered, such as the international nature of Inmarsat and use of Inmarsat systems for military purposes. The paper will offer some examples of data reporting applications in the environmental sciences and conclude with a look into the future of mobile satellite communications via Inmarsat.

2. Introduction

Crisis response operations, along with Joint military operations place unusual demands on military communications networks for wide area coverage. The need for true interoperability with other friendly forces as well as civil authorities and the Military Oceanographic support systems for Rapid Assessment capability becomes more imperative. Many of these requirements are incompatible with the design criteria for military communication satellites and systems. Appropriate use of commercial satellite systems can solve many of these problems.

The International Mobile Satellite Organization (Inmarsat) operates the space segment (satellites) for near-global mobile communications in the maritime, land-mobile and aeronautical sectors. Access to the space segment is offered to users through land earth station gateways, owned and operated by major telecommunications entities worldwide, and mobile earth stations of various types and capabilities.

As an intergovernmental organization established by Convention, Inmarsat is limited to the provision of communications "for peaceful purposes". Recent legal opinion permits the use of Inmarsat by armed forces not involved in armed conflict: UN peacekeeping or peacemaking forces acting under the auspices of the UN and for distress and safety communications by armed forces engaged in conflict.

Inmarsat mobile satellite communications capabilities offer a practical and cost-effective solution to the communications needs of Rapid assessment capabilities for forces providing near real-time environmental support . A full range of facilities is available, including voice, data, telex, fax, e-mail and emergency beacons. Mobile terminals can be fitted in ship, aircraft or vehicle or be fully man-portable. Compatible equipment and services can be obtained from a wide range of suppliers in most countries of the CIS and NATO Alliance.

3. Requirements

Based upon what I know about Environmental Monitoring systems and understanding of Military operations, I have identified the following possible requirements that will be required to be satisfied:

- Remote systems Management
- Wide Bandwidth options
- Global Coverage & High quality
- Relieve pressure on operational networks
- Interoperability & Secure Communications
- Range of Commercial-off-the-shelf equipment (COTS)
- Real-time or near real-time capabilities Available anytime and anywhere

4. Inmarsat: History & Evolution

Inmarsat is an inter-governmental organization, based in London, established by convention in 1979 and began operations in 1981. Inmarsat provides the 'space segment', that is the satellites, for world-wide mobile communications services and overall system integrity. It serves the Maritime, Landmobile and Aeronautical needs. 79 governments are party to the Inmarsat Convention (Parties). Individual countries (Parties) have the right to sit in the Inmarsat Assembly. The Parties each nominate a Signatory to be their representative shareholder in the Inmarsat organization.

The Signatories are telecommunications entities, normally PTTs, which contribute a share of the Organization's capital and undertake routine oversight of the Inmarsat Directorate through the Inmarsat

Council. It is usually the Signatories which act as service providers, offering commercial satellite communications services to customers via the Inmarsat satellites. Originally conceived to provide a global, internationally governed maritime communications facility, Inmarsat now offers services to land-mobile and aeronautical customers as well.

The system consists of the following components:

- Satellites
- Mobile Earth stations (MES)
- Land Earth stations (LES)

Full redundancy is built into all these components through the porvision of Backup satellites, over 30 LES's and offerings from a range of manufacturers & suppliers.

4.1. Satellites

Inmarsat provides near-global coverage through four geostationary satellites. Each of these provides cover to a large elliptical part of the globe known as an Ocean Region. The use of geostationary orbits does not allow the satellites to see the extreme polar regions but in the maritime context cover extends to all waters which are open to normal navigation

These are being replaced the 3rd generation system of satellites which offer:

- Higher power
- Larger number of channels
- Spot Beam capability

Navigational transponder to improve GPS accuracy.

The service will be complemented by the Intermediate Circular Orbit network of satellites to be operated by ICO for operation in 1999.

4.2. Land Earth Stations

These are characterised by huge (11-14 metre diameter) dish antennas pointed towards the satellites. They are operated by some Signatories and act as a gateway between the satellites and the terrestrial network. As well as performing this function, a special Network Control Station in each Ocean Region controls both access to the network and the flow of information through it. Figure 1 shows that many countries around the world, including CIS and NATO countries, have their own LES offering direct connection between mobile terminals and the terrestrial networks.

4.3. Mobile Earth Stations Inmarsat-A

This is the original Inmarsat ship terminal, in service since 1982. It provides:

- telephone / voice
- telex, (50 baud)
- fax (9600 bps)
- data (9600 bps)
- high speed data (HSD) (56/64 kbs).
- GMDSS Compliance

There are around 25,200 Inmarsat-A terminals in use at present. The maritime terminals tyicpally comprise of Above-deck and Below-deck equipments, with the dome-shaped antenna supporting a auto-stabilization so that it can track & stay locked onto the satellites even in very strong seas.

Inmarsat-B

This is the digital successor to Inmarsat-A. Offers the same services at the highest quality. Suitable for high volume users, Inmarsat-B was introduced in 1994 and there are already 1,040 terminals commissioned.

Both Inmarsat-A/B support a range of applications which include:

- Data Communications & Electronic Mail
- Electronic Data Interchange (EDI)
- Shipboard Integrated Systems
- Compressed Video
- Stu II/III Encryption etc

Inmarsat-M

This is a low-cost, lightweight mobile earth station using digital technology to offer telephone, medium-speed facsimile and data capabilities. Inmarsat-M entered service Spring 1993 and there are already 6,600 terminals in use. It provides:

- Medium quality digital voice

- Data (2400 bps)
- Facsimile (2400 bps)

Inmarsat-Mini-M:

This is equivalent to the Inmarsat-M but is smaller and lighter and works in the Spot beams offered by the 3rd generation satellite systems. Antenna size is 0.5 - 0.7 m in size and it weighs less than 2 kg.

Inmarsat-C

This is a basic telex-based satellite terminal, in service since January 1991 featuring low-cost and small size. Inmarsat-C is a messaging system offering :

1. Two-way Messaging for:
   - Telex, Facsimile, Data delivery
   - PSTN, PSDN, X.25, X.400, Internet access
   - Supports upto 32 kbytes per tx.
   - Provides a rate of 600 bps
2. Data Reporting & Polling:
   - individual, Group, area
   - Allows 32 bytes of packets
   - at pre-arranged intervals or triggered by polling anytime
3. Enhanced group calls
   - FleetNet (Commercial)
   - SafetyNet (Safety)
4. Position reporting
   - 100 m accuracy
   - near-real time
5. Distress alerting (GMDSS)

It incorporates the Enhanced Group Call (EGC) facility for receiving SafetyNET and FleetNET broadcast messages. FleetNET offers the option of broadcasting messages to pre-defined closed user groups.

Capable of transmitting automatic position reports and short (3-packet) data reports, Inmarsat-C is expected to be fitted in large numbers of trucks and almost all merchant ships. About 20,000 Inmarsat-C terminals are in use today.

Soon it will be complemented by Inmarsat-C3 which will be even smaller but still offer the same services. Target markets are the Transport industry, Caontainer Management and Coastal Waters.

Inmarsat-D/D+: is a new satellite paging service due to be introduced to the market in 1996. It offers:

- One-way delivery of messages upto 400 bytes
- D+ adds Acknowledgment of upto 8 bytes
- Global Coverage
- Built-in Error-Correction
- Digital Display
- Terminal prices $500-700
  AA battery powered

Inmarsat-E is the Inmarsat L-band Emergency Position Indicating Radio Beacon (EPIRB). Transmissions can be initiated manually, or automatically when the EPIRB floats free after a ship founders. The distress message contains all standard Distress Message Generator information, including position, updated continuously by an integrated GPS satellite navigation receiver.

4.4. Special And Value Added Services

- Group Calls
- Compressed Video TV
- Slow-scan TV
- Navigation information
- Subsscription News
- Electronic Mail with Gateways into the following networks
  - ♦ - PSTN / Fax
  - ♦ - PSDN (x.25)
  - ♦ - X.400
  - ♦ - Internet
- STU II/III Encryption capabilities
- FleetNet Services

International SafetyNET Service: is a special broadcast service provided through the Inmarsat satellites. It is part of the Enhanced Group Call (EGC) service which in turn is part of the Inmarsat-C System. SafetyNET is a maritime safety information broadcast service offering free reception on board any suitably equipped ship but with access restricted to internationally approved information providers. In the GMDSS, SafetyNET is used to broadcast navigational, meteorological and SAR information to ocean areas and to coastal areas not covered by NAVTEX

5. Peaceful Purposes

Having discussed the offerings by Inmarsat, it is important to point out the specific usage conditions that it holds for the Defence establishment. The overriding concept is "for Peaceful purposes".

Article 3, Paragraph 3 of the Inmarsat Convention states **"the Organization shall act exclusively for Peaceful Purposes"**. Under the guidelines issued on this , the following uses of Inmarsat are allowed:

(i) Use by armed forces (military use) not involved in armed conflict and any threat to or breach of the peace.

(ii) Use by UN peacekeeping or peacemaking forces acting under the auspices of the UN in implementation of UN Security Council decisions in order to maintain or restore international peace and security, irrespective of such UN forces becoming involved in armed conflict in the accomplishment of their UN mission; involvement in armed conflict is a possibility implicit in the maintenance or restoration of international peace and security by UN forces.

iii) Use of Inmarsat by armed forces engaged in armed conflict is permitted for distress and safety communications, and for communications relating to the protection of the wounded, sick, shipwrecked, prisoners of war and civilians, pursuant to the Geneva Red Cross Conventions, 1949, and the Protocols Additional to the Geneva Conventions, 1977. The same applies to personal and private, non-tactical communications by members of the armed forces that are not related to or in support of the war effort.

(iv) Use by armed forces - other than UN forces acting under the auspices of the UN Security Council - involved in international or non-international armed conflict is, in principle, not permitted under Convention, Article 3(3), without prejudice to the exceptional case of legitimate individual or collective self-defence against armed attack and within the limitations established by UN Charter, Article 51. The latter prohibit preventive action and self-help involving armed force in the absence of armed attack.

Inmarsat requires a governmental undertaking by a competent authority to guarantee adherence to these conditions. However, it is clear that use of Inmarsat is permitted for many peacekeeping, search and rescue (SAR) and humanitarian operations. By their very nature, these will often involve joint operations by the forces of more than one country.

6. Environmental / Remote Monitoring Examples

We will now look at some of the range of Remote & environmental Monitoring examples that use the Inmarsat systems in particular Inmarsat-C.

6.1. Supervisory Control And Data Acquisition systems (SCADA)

This is supported by Inmarsat-c which offers low capital costs, low power consumption, high integrity satellite link.

The system is linked to arrays of senssors, data loggers, remote control units and solar panels for power.

Data is encoded for optimisation / encryption and auto-transmitted at given intervals. Polling enables remote management and transmission at any other time if required.

Typical system implementations include the use of more than one of the Inmarsat system offerings.

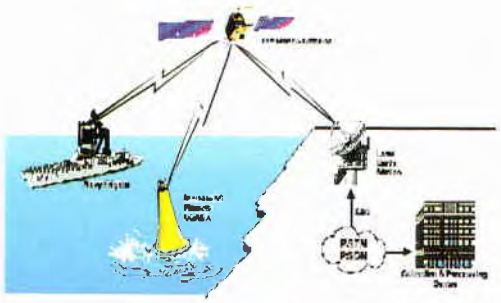

The figure above shows how:

- low-data rates are used for transmission over the Inmarsat-C network from Bouys, remote SCADA systems to a central processing centre.
- Where any of the complicated fusion / merging and model applications is carried out and the resulting data consequently transmitted
- over a high-data rate link over the Inmarsat-A/B HSD (64 kbps) to remote vessels etc.

This effectively demonstrates the ability of setting up and utilising a Wide Area Network system which enables the use of differing network options such as X.25, ISDN, X.400 and the Internet.

6.2. Water Resource Management

Public utility companies use Inm-C's capabilities to measure water levels, rainfall, evaporation and to also control sluice gates located in rural or remote areas of S.America and Africa.

6.3. Fisheries

All three parties involved in Fishing Government Agencies, Fishing fleets and Fisherman use/benefit from the information exchanged via the Inmarsat-C/B network. Fishing vessels in Argentina return sea temperature and salinity to shore-based scientific centres and receive data to enable optimal tracking of Tuna sholes etc

6.4. Others

Maritime navigational aids monitoring - such as remote management of Lighthouses, ligh buoys etc

Pipeline monitoring - collection of data from compressors, valves and metering stations.

Metrological monitoring - of wind, temperature and pressure in various remote locations of Land and Sea regions.

7. Why Inmarsat Meets Military Requirements ?

Bearing in mind the requirements detailed earlier, lets see how and why Inmarsat offerings meets them.

- Supports Secure Communications by using existing crypto standards
- Range of terminals and manufacturers providing COTS capability
- High-speed data available on demand, without pre-arrangement.
- Tried and tested and cheaper than milspec systems
- Access via Domestic network interfaces.
- MES's made in NATO and CIS countries
- Supports NATO recommended standards for data communications.
- Used as part of world-wide Oceanography and Metrological Monitoring projects.

8. Conclusion

Inmarsat mobile satellite communi-cations capabilities offer a practical and cost-effective solution to the communications needs of joint forces engaged in peacekeeping, Search and Rescue and humanitarian operations. A full range of facilities is available, including voice, data, telex, fax, e-mail and emergency beacons. Mobile terminals can be fitted in ship, aircraft or vehicle or be fully man-portable. Compatible equipment and services can be obtained from a wide range of suppliers in most countries of the CIS and NATO Alliance.

Inmarsat Delivers:

- Proven Technology
- Global Coverage
- COTS availability
- Interoperability
- Demand assigned usage
- Data rates of 600 bps upto 64,000 bps today.

9. Answers to questions

Any questions or requests for more information relating to this paper or Inmarsat services should be directed preferably via Email to:

Manoj Mohindra
Projects Manager
Maritime Applications Department
Inmarsat
99 City Road
EC1Y 1AX

Email: manoj_mohindra@Inmarsat.org
Phone: (44) 171-728-1432
Fax: (44) 171 728-1752

ARGOS SECOND AND THIRD GENERATIONS

Christian Ortèga

Collecte Localisation Satellites
18, Avenue Edouard Belin
31055 Toulouse, FRANCE
Email: ortega@cls.cnes.fr
Fax: +33 561 39 47 97
Telephone: +33 561 39 47 20

Abstract:

Since its inception, the Argos Data Collection and Location System has been providing on an operational basis in-situ environmental data for a broad range of applications. In late 1994 and in 1995, over one-half of the major User agencies were surveyed in an effort to obtain their perspective on Argos system capabilities. Users clearly defined several priorities for improving Argos. These were better satellite coverage, larger data volume transmission capability, increase of satellite receiver sensitivity, and two-way communication. The desirability of some of these improvements was anticipated by Argos, and plans for a second generation (Argos-2) are becoming reality, starting with the launch of NOAA-K and the Argos-2 instrument in 1997. Under a recently negotiated cooperative agreement with Japan, two-way communication with data collection platforms will be available in 1999, when Argos flies on ADEOS II. Beyond ADEOS II, a further advanced Argos instrument (Argos-3) is being designed for inclusion on NOAA-N' and O, P, Q, and on EUMETSAT's METOP-1 and METOP-2.

1 . The Argos System

The Argos Data Collection and Location Satellite System is operated under a partnership agreement between NOAA (National Oceanographic and Atmospheric Administration - USA) and CNES (Centre National d'Etudes Spatiales - France) to provide a worldwide in-situ environmental data collection and Doppler-derived location service.

The most significant use of Argos involves the location and collection of data associated with worlwide scientific programs that study oceans (buoys and floats), animals (birds, marine and terrestrial animals), atmosphere and earth.

Argos is a worldwide satellite-based system which locates fixed and mobile platforms and collects the data they transmit. It was developed in cooperation between the French Space Agency (CNES) and the National Oceanic and Atmospheric Administration (NOAA, USA).

The Argos instrument is flown on board NOAA satellites. Three are simultaneously in service at most times, at 850 km altitude on circular, polar orbits.

Together, they provide complete coverage of the Earth several times a day (figure 1).

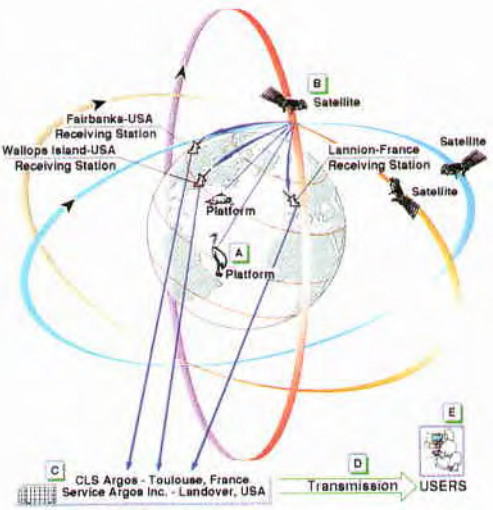

Figure 1 - The Argos system provides a global coverage

User relations and worldwide system operations are handled by CLS (*Collecte, Localisation, Satellites*) in Toulouse, France and Service Argos Inc in Largo, Maryland - USA. CLS is a subsidiary of CNES (the Space French Agency) and IFREMER (the French ocean agency)CLS uses a worldwide network of represent-atives, regional offices, subsidiaries and processing centers to make users' platform locations and data available.

2. Argos for the Earth environment

Due to the regulations governing the radio frequency which Argos transmitters use, the Argos system is designed and reserved for the studying, monitoring and protection of the earth's environment. Traditional Argos applications include oceanography,

meteorology, hydrology, fish stock management, monitoring vehicles carrying hazardous materials and animal tracking.

In December 1996, Argos tracked 5100 active platforms:

Drifting buoys	1805
Fixed stations	556
Moored buoys	405
Alace floats	396
Terrestrial animals	378
Birds	304
Subsurface floats	295
Fishing vessels	288
Marine animals	183
Containers	158
Miscellaneous	107
Manufacturers Tests	95
Terrestrial vehicles	86
Balloons	31
Orbitography platforms	13

Table 1: Active platforms in operation in December 1996

This table confirms the continued growth in the use of Argos for the studying, monitoring and protection of the earth's environment.

Design breakthroughs by manufacturers have fueled the demand, leading to ever-smaller, lighter transmitters for tracking more and more different types of measurement platforms.

3. Features of the Argos System

3.1 - Global coverage

Argos is the only satellite-based system of its kind offering full global coverage.

a) Polar orbits provide excellent visibility:

- 28 (42*) passes a day over polar regions
- 12 (18*) passes a day over Europe
- 7 (11*) passes a day at the Equator

* with three satellites

b) Tape recorders on board the satellites store data gathered along the whole orbital revolution

3.2 - Excellent sensitivity

High sensitivity to transmitter messages, one of the main features of the Argos system, results from:

- low satellite altitude (800 km),
- very little interference on the 401.65-MHz band used,
- sophisticated onboard receiver technology.

These basic features, together with deliberate limiting of the data transmission rate (400 bits per second), mean that transmitters can:

- be miniaturized: 15 to 25 grams, including batteries,
- operate on low radiated power, achieving good results with just 250 mW,
- use very low power, so that unattended platforms can be tracked over long periods (several years).

3.3 - Doppler location + GPS

The Argos processing centers normally use the Doppler effect to locate transmitters. In regular operating conditions, this provides accuracy of 350 meters. Argos uses a dedicated network of orbitography beacons, and location involves fairly complex calculations at the processing centers.

The advantages of Doppler location are:

- low transmitter power consumption,
- instant location opportunities throughout satellite passes, useful for intermittent transmitting platforms.

CLS has developed a dedicated processing system for low power transmitting platforms.

This supplies significant results even when a transmitter is operating in a difficult environment for radio transmission.

Some users are also starting to use GPS receivers, which have come down considerably in size, weight and cost. The GPS fixes provided by the receivers are included in the Argos messages and relayed to the Argos Processing Centers as if they were sensor data. Low Argos transmitter power consumption and efficient transmission remain the main attractions.

The processing systems have been modified to make the GPS positions available in the same format as that used for the regular Doppler-derived locations. Users can choose whichever form of location best suits their needs, and have a "spare" system.

3.4 - Reliability, simplicity, efficiency, ease of use

The features Argos users most appreciate are:

- operational service which has never been interrupted (Figure 2),
- antenna and transmitter needing no adjustment,
- transmit frequency (401.65 MHz) and sensitive onboard receivers which permit reception from primitive transmitters and in difficult conditions,
- automatic startup of service as soon as a transmitter is switched on.

4 . System enhancements

4.1 - Users' evolving needs

The above features meet the needs of a broad range of users in scientific and applied fields. We at

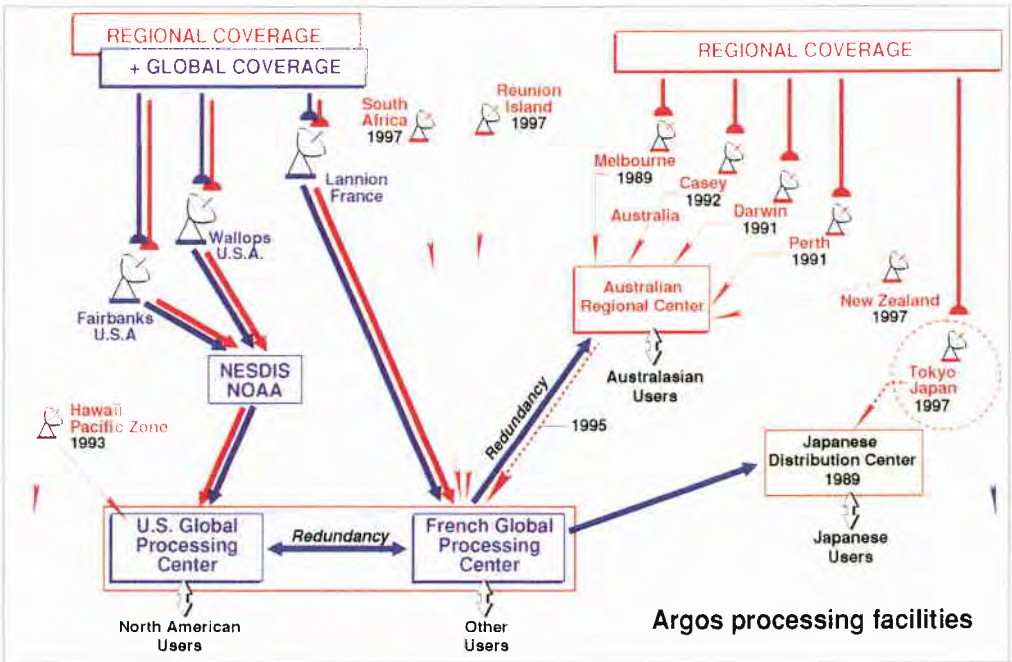

Figure 2 - Argos Processing facilities

A Broader International Cooperation

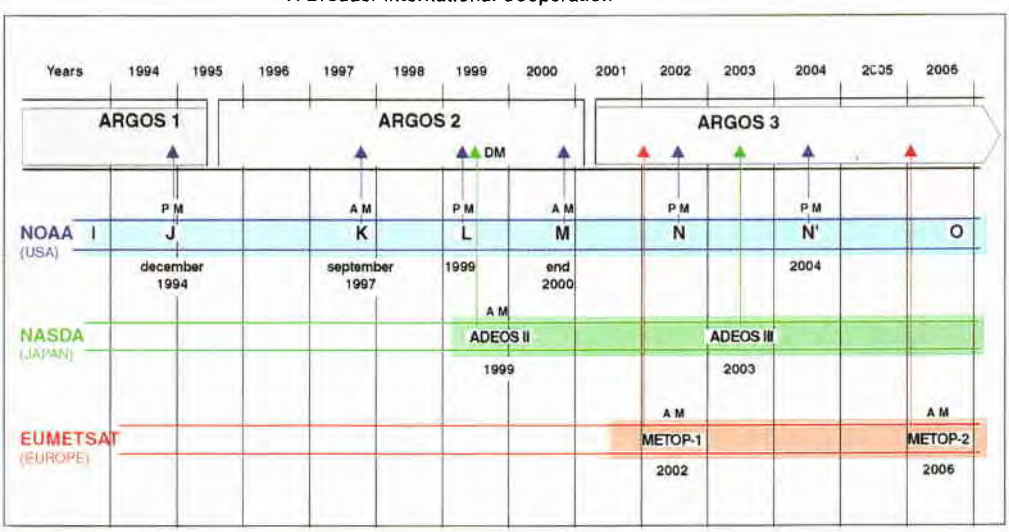

Figure 3 - A broader International Cooperation

CLS and Service Argos Inc. are constantly in contact with them either in person or through surveys, and record their feelings to make sure the Argos system keeps up with their requirements.

The four main areas in which Argos evolves are:

- satellite coverage: increasing the number of satellites,
- data volume: increasing the amount of data sent on each satellite pass,
- improving the transmitter-to-satellite link: obtaining better data, reducing transmitter power consumption, and continuing to miniaturize transmitters,
- implementing a return link back to transmitters to make the system more flexible and to remotely control transmitters.

4.2 - Worldwide cooperation

People around the world are becoming increasingly concerned about the need to study and monitor the environment. Governments are responding by implementing worldwide satellite networks through international cooperation. To better meet these needs, and consolidate the role of our system for observing and protecting the environment, Argos is becoming more internationally based (Figure 3).

In 1996 the initial program between France and the United States was extended to bring in Japan. From 1999 the Argos instrument will be flown on the ADEOS II satellite, operated by the National Space Development Agency of Japan (NASDA). This will be the first satellite launch in what is expected to be a long-term cooperation program.

We are also in the final phase of signing an agreement to fly Argos, from 2002, on the METOP satellites operated by the European Meteorological Satellite Organization (EUMETSAT).

More cooperation agreements will doubtless follow. Gradually they will help to increase the number of satellites in orbit, and contribute to meeting worldwide needs for protecting the environment of our planet.

4.3 - Higher performance equipment on board the satellites

The second generation of Argos instruments will gradually go into service from 1997, starting with satellite K in the NOAA series. The main enhancements are as follows:

- receiver bandwidth increased from 24 to 80 kHz,
- system capacity quadrupled,
- onboard receiver sensitivity increased by 2 dB.

The increase in receiver bandwidth means a new form of system management. To get the best out of the Argos system's high sensitivity, and reduce the risk of messages colliding, we plan to reserve a 24-kHz band (a width equivalent to that of the current Argos system) at the bottom end of the 80-kHz bandwidth for low-power transmitters. The remaining bandwidth will be for transmitters using normal power levels.

To take advantage of the quadrupling in system capacity with Argos-2, transmitters will be able to send higher volumes of data.

These changes in the management of the Argos system from the second-generation, in 1997, is part of our continuing efforts to meet users' new needs while retaining compatibility with their existing equipment. This is opening the way for third-generation Argos; the design phase started in September 1996.

The latest needs analysis was done through questionnaires sent to all users in 1995, and is continuing through direct contact. We can already see that the data collection channel needs splitting into three separate portions (Figure 4).

a) Standard ("center") channel, keeping the features of the Argos-1 system. This could cover the needs of traditional applications using primitive transmitters, requiring low cost and operating with standard radiated power.

b) Low-power channel, but still with today's modulation pattern and random access to the satellite receiver. There could be two types of transmissions:

- at 400 bits per second, with a 6-dB improvement over the Argos-1 link budget. A transmitter could provide the same performance as today with a quarter of the power.
- at 200 bits per second, with a 12-dB improvement over Argos 1. The data would have special additional encoding.

This channel would push miniaturization and low power consumption to their limits.

c) High-volume channel, with a new modulation pattern for data transmission, though still using random access. The data rate would increase from today's 400 bits per second to 5 kilo bits per second.

The new system would meet the increasing needs of today's scientific users while retaining the original features of Argos wherever possible.

Each of the three "separate" Argos systems on

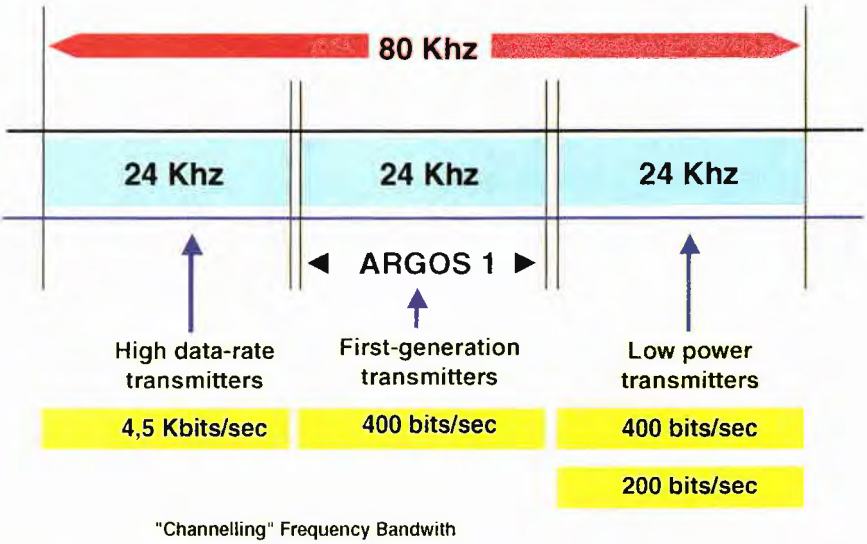

Figure 4 - Argos system "chanelling"

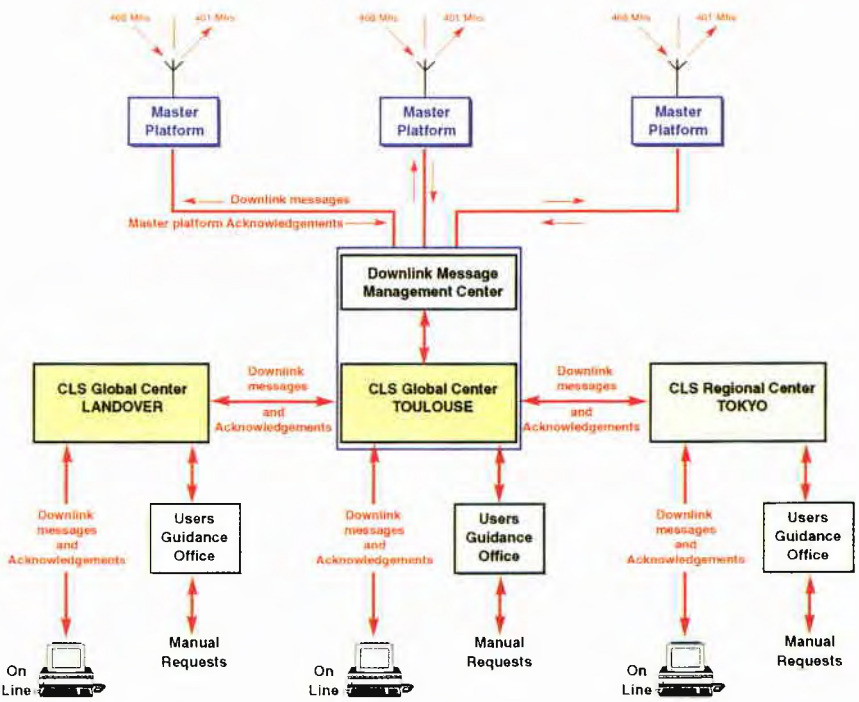

Figure 5 - Downlink Messaging Diagram function

board the satellites would keep up with a particular set of needs.

From now to the phase B of Argos-3 in September 1997, we will continue our meetings and talks with users to refine the concepts outlined above and better understand the changes needed and their impacts on applications.

4.4 - Downlink messaging

Downlink messaging, i.e. two-way capability, will be implemented from when Argos flies on NASDA's ADEOS satellite.

The main need is to make transmitters more flexible to use. The capability to send messages to any transmitter anywhere on Earth from a low-earth-orbiting (LEO) satellite will doubtless be unique to Argos for a long time. Argos will be able to send messages to transmitters anywhere on Earth.

Users messages to transmitters will first be uploaded by a master platform network for storage on board the satellite (Figure 5) They can then be sent to:

- **all transmitters "allcast" function**. This could be used to optimize transmissions by sending transmitters the times at which the satellites are to pass over them.
- **a set of transmitters: "multicast" function**. For example, a single group message could trigger an observation network into accelerated or routine observation mode.
- **a single transmitter: "monocast" function**. The many applications could include switching a transmitter on or off, changing the sampling rate, switching sensor configurations, sending numerical data, and so on.

Each message will have a useful length of 152 bits. This would be enough for the most complex applications.

As well as message transmission, the downlink could be used for:

- **detecting satellite passes**. A basic receiver will be able to detect a pass by picking up a special flag, repeated periodically in the data flow.
- **acknowledging reception of a transmitter message**. Once the satellite receives the message, error-free, it sends the Argos transmitter an acknowledgment over the downlink channel, so the transmitter can send the next message. This capability could be used to check on transmission quality and increase data volume.

To use the downlink function and still enjoy the advantages of today's Argos system, transmitters will need to be fitted with small, low-power receivers.

Models without receivers will still be compatible with Argos, and will be able to operate in the same way as today.

5 . Conclusion

Argos users' changing needs, as evidenced by studies, questionnaires and personal contact, have led to the decision to develop a third-generation system for the early 2000s.

The main enhancements will be:

- more capacity to handle low-power, "sub-miniature" transmitters,
- a tenfold increase in the amount of data a transmitter will be able to send on each satellite pass,
- a worldwide downlink messaging function, operating worldwide and matched to the way the Argos system works.

The Argos system is also opening up to broader international cooperation, under agreements with the United States, Japan and soon Europe. Argos is consolidating its role as a worldwide system designed and dedicated for studying, observing and protecting the Erth's.

Communication Technology in Support of SACLANTCEN Programme of Work

Edoardo Bovio , Michael D. Max [1] , Francesco Spina and Alessandro Berni [2]

SACLANT Undersea Research Centre
Viale San Bartolomeo, 400
19138 La Spezia, ITALY
Email: bovio@saclantc.nato.int
spina@saclantc.nato.int

1) now with Naval Research Laboratory,Washington DC 20375, max@qur.nrl.navy.mil

2) now with ITnet, Via Greto di Cornigliano 6 R, 16152 Genova, Italy, ab@it.net

Abstract

This paper presents the work carried out to connect SACLANTCEN to Internet and to extend the Centre's network to sea, enabling seamless communication with R/V Alliance and other mobile stations participating to sea trials. The security implications deriving from the connection to Internet are discussed and the solution adopted are described. Examples of the use of modern communication technologies and Geographical Information Systems during experiments at sea are also given.

1. Introduction

1.1. Requirements

SACLANTCEN is increasingly involved in activities that require fast (often real time) and reliable exchange of information with partners distributed all over the world. Scientists communicate daily with correspondents in Europe and the US and need to be able to access data available from different sources and locations. This applies also during sea trials, when data and information necessary to perform the mission are exchanged from ship to shore and viceversa. Furthermore, the improved communication facilities together with the capability of referencing data to precise geographical location, are very useful to coordinate complex sea tests involving multiple platforms.

1.2. COTS Technology

To satisfy the requirements for improved communication, SACLANTCEN has adopted solutions based on Commercial Off The Shelf (COTS) Internet technology.

Internet has undergone a dramatic growth in the past few years, and has become a de facto standard for scientific and business communication. It is based on well proven and open standards, and its diffusion has forced the development of very reliable low cost hardware and software products targeted to the mass market.

There are also some vulnerabilities, mainly related to security and availability, that prevent its use for mission critical (and military) applications, but they can also be minimized by taking appropriate solutions.

However, the cost saving and the seamless integration of widely dispersed resources achievable with Internet-based communication, outweigh by far its disadvantages.

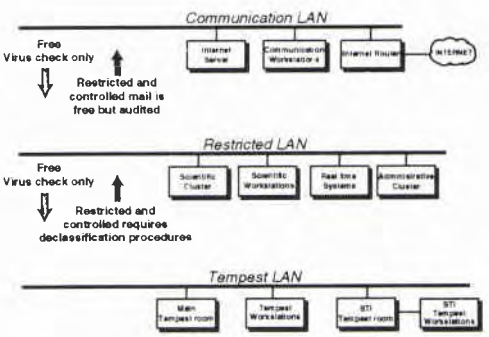

Figure 1 *SACLANTCEN Networks*

2. SACLANTCEN network infrastructure

2.1. The saclantcen.nato.int domain

SACLANTCEN has added to the existing Tempest and Restricted networks, a third network dedicated to communications that is physically separated from the others.

Although much can be done to prevent unauthorized access to SACLANTCEN networks, the complexity of the systems involved does not guarantee the full protection of a computer connected to Internet and therefore we have adopted a safe approach to keep our main networks separated from the communication network as shown in Fig. 1.

There are three aspects to consider the intrusion of external hackers, the unauthorized transfer of data and the diffusion of viruses in our networks.

These concerns have been addressed by separating the networks with sensitive information (this is in accordance with NATO regulations that limit the use of the worldwide Internet only to NATO UNLIMITED traffic), and by adopting a series of restrictive controls at the interfaces.

For example, the only connection requests we accept from the Internet are those to the electronic mail service and those to the World Wide Web service.

Virus checks are performed routinely on all imported files. All these activities are coordinated by the ADP security section.

The SACLANTCEN domain is connected to the Internet with a redundant 128Kbps connection managed through Cisco routers. The SACLANTCEN network

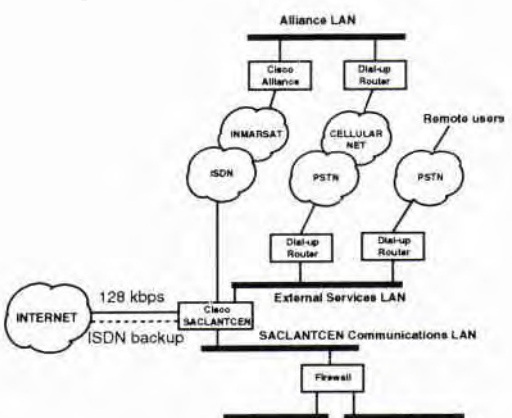

Figure 2 *The saclantc.nato.int domain*

infrastructure, shown in Fig. 2, is organized in different Ethernet networks (external transit, LANs in support of field work, WWW server network and SACLANTCEN communications LAN): tr exchanges between each of those networks and outside world are regulated by firewalls and r access control lists.

2.2. Networks for field work

The networking subsystem onboard R/V Allia shown on Fig 3, consists of two multiprotocol ro suitable for the management of on-demand di connections and three communication channel transmit data: TACS cellular phones and Inmars and B links.

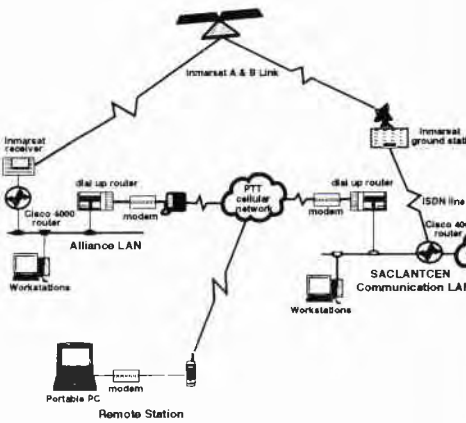

Figure 3 *The NRV Alliance Network*

The Inmarsat A system is an analog system for voice, fax and data transmission: sig transmitted from the ship are relayed by the Inm satellite to a ground station and from there they routed through the public switched telephone net to their final destination. A new digital sys Inmarsat B, has recently been installed and al fully digital communications at 64Kbps between s and ground stations; the ground link makes use o European ISDN digital network.

The cellular phone system installed on Allian connected to the analog cellular network of the It PTT, and can only be used close (up to approx. 8 distance) to the Italian coast, although ranges of Km have occasionally been achieved. The digital cellular network offers an alternativ Inmarsat connectivity when operating near the s of most European countries: however due to synchronization constraints imposed by communications between the mobile and the station, it will not be possible to use it operating far(i.e. more than 35 Km) from the sho

The analog cellular phone allows an average data rate of 4Kbps and has an operating cost of about $10 per Mbyte. However, due to the instability of the analog channel, we have found that a reliable data transmission at sea should not exceed approximately 5 minutes, thus limiting the practical size of data transfer to about 150KByte.

The digital GSM cellular service should allow a data rate of 8Kbps and will have an operating cost of $5 per Mbyte. As the GSM data service has just been introduced in Italy, we do not have yet sufficient experience about the maximum practical duration of the data transfer.

The Inmarsat A allows an average data rate of 4Kbps and has an operating cost of about $200 per Mbyte. The availability of the satellite channel is often very poor, and therefore Inmarsat A is a viable solution only for batch data services (typically is used for e-mail and short data transfer)

Inmarsat B supports a data rate of 64Kbps with an operating cost of about $50 per Mbyte. Due to the digital nature of the channel Inmarsat B guarantees error free data transmission.

Recently are appearing on the market spread spectrum radios that can connect LANs over short distances (few Km) and allow data rates up to one Mbps With appropriate antennas the range at sea could be extended up to about 20 Km.

2.3. Security considerations

Remote access to the Centre's resources is accomplished via the Internet itself or via the public switched telephone network (PSTN). A widespread concern associated with providing a remote access service is associated to user authentication: this becomes extremely important when access is made through the analog cellular phone network, which is particularly vulnerable to eavesdropping attacks.

For this reason, challenge-response authentication techniques based on cryptographic algorithms should be standard practice, to avoid the risk of passwork playback attacks.

Where data integrity and confidentiality is an important issue, the use of crypto technologies can be extended either at the network or at the application layer. Efficient solutions are available using standard government/military security tools or commercial products.

3. Data communications in support to the program of work

3.1. Communications and GIS

At SACLANTCEN E-Maps (Electronic Maps), composed of a Geographical Information System (GIS) linked to numerical data, text, image, and graphics of marine information, are used with relatively inexpensive transportable computers and commercial communication software [2] and [3].

E-Maps have been used to support planning and at-sea exercises and experiments, as well as providing a relational database [4].

The E-Map is an editable, expandable geographically referenced data set, with variable complexity and size. A simple map containing only bathymetry can be assembled in minutes to hours from existing digital bathymetry. Environmental data, such as bathymetry, bottom and water characteristics, and positions of artifacts such as wrecks, pipelines, and cables, are input and geographically linked to the digital chart. The map image is used directly to input, locate, and retrieve data and other information.

Used at sea, the E-Map functions as the repository for newly input real-time location and sensor information such as GPS position, radar, and experiment position data such as sonar contacts. New map overlays, for instance of bottom-reverberation character and bottom softness, can be compiled and edited in virtually real-time as the information becomes available.

The E-Map also allows complex geographically

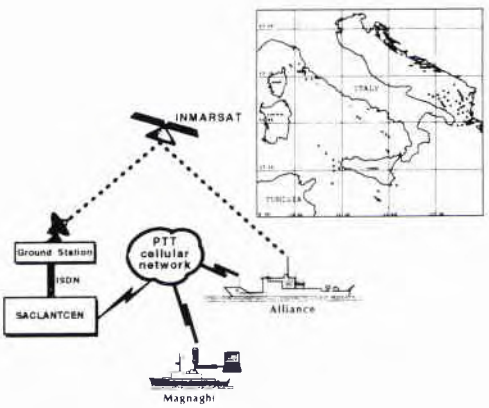

Figure 4 *Communications in Support to Oceanography*

referenced information to be shared rapidly. New map layers of positions, areas, and lines, as well as numerical data related to positions, have been electronically communicated and merged with duplicate copies of the E-Map at remote locations.

3.2. Communications in support to oceanography

As shown in Fig. 4, the E-Map was used as a primary means of communicating complex

geographically referenced information during several oceanographic experiments; new map layers were communicated electronically to SACLANTCEN, where they were merged with a duplicate copy of the prepared map taken on the ships. The dots on the map of Fig. 4 indicate the location of the experiments

Standard e-mail was used as a carrier for files of the new map layers, and the concept of allowing a remote site to view and have full GIS editing and other capabilities with the new map layers was proven.

3.3. Communications in support to MCM

As part of the Winter Sun-2 trial a realistic MCM environmental assessment of a small area was carried out. The main goal of this experiment was to test and evaluate the growth capabilities of the E-Map system with the Inmarsat B high speed digital data

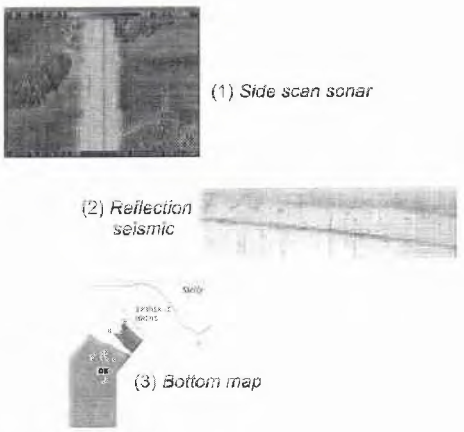

Figure 5 *MCM Experiment*

communication system.

As shown in Fig. 5, the experiment took place along the SE coast of Sicily and involved a first pass into the defined beach approach area, acquiring pictures from the side-scan sonar (1) in real time. Scans of the reflection seismic (2) were made and located along the track as segments and a bottom analysis for the line was extrapolated into a bottom map for the area (3) that contained bottom information according to ATP 24 standards.

The side scan pictures and the maps were then transmitted to SACLANTCEN as GIS map layers and merged with a duplicate copy of the map.

A team of MCM experts at SACLANTCEN chose a 1 km wide lane in what appeared to be the most favorable seafloor conditions. This information was sent to Alliance and a second survey took place to improve the knowledge of the lane. The results of the second survey were transmitted within 15 minutes of reaching the end of the survey line and available to SACLANTCEN team as soon as merged with their copy of the map.

3.4. Communications in support to Rapid Response

Communications for Exercise Rapid Response involved coordinating data exchanges between seven different locations, including 5 ships conducting sea trials, connected using cellular phones and the Internet protocol suite.

Data such as CTD, XBT, XCTD, XSV, satellite images and meteo observations were collected and uploaded to a central data fusion facility at SACLANCEN as shown in Fig.6.

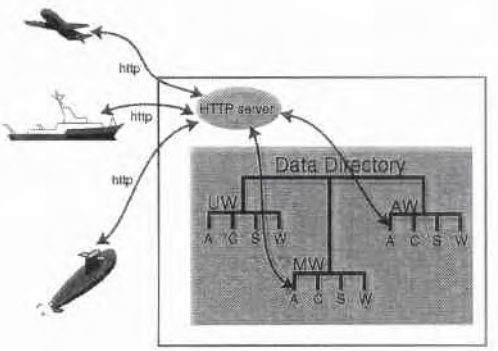

Figure 6 *SACLANTCEN Data Server for Rapid Response*

Data files were integrated by header files containing a description according to a predefined standard: header files were used to ease automatic archival of data. Data were then made available to all the ships participating in the experiment and to selected military commands and scientific institutes. Access to the data was restricted using access lists based on the TCP/IP address of the caller and on username/password couples. After a successful authentication, users were presented a query form to ease the extraction of data: interrogations were possible using limiting criteria such as geographical location (Latitude/Longitude), observation period or data type. New developments in communications in support of Rapid Response will focus on improving the mechanisms for data exchange and fusion, using distributed databases and higher speed communication links.

4. Future options

Advances in data communications technologies open new spaces and opportunities that can be exploited in support of scientific research.

SACLANTCEN is actively investigating new technologies to enable scientists involved in sea trials to interact with their colleagues ashore in a timely, cost effective and secure fashion.

4.1. Mobile communications

In the near future we will witness the rapid diffusion of cheap digital portable terminals, with world wide coverage, capable of transmitting voice, fax, images, video and data at low cost. At present, cellular phones which allow the transmission of voice, fax and data to remote locations, cover some of the communication needs of our scientific experiments, but are limited in speed and in coverage at sea.

For ship to shore communications, the Inmarsat satellite service is a de facto commercial standard.

Satellite capacity for the Inmarsat system consists of four operational satellites placed in geostationary orbits over the Atlantic (east and west), Pacific and Indian oceans. Calls to or from a terminal are relayed via satellite to one of 25 coastal earth stations, where they are patched directly into the international switched telecommunications networks. The Inmarsat B standard allows digital voice, fax, video and data communication at 64Kbps. Inmarsat offers also slower speed digital messaging systems, suitable for low-volume data transmissions, such as ship or buoy position information, at a speed of 600 bps.

Geostationary satellites are not well suited to interactive communications due to the wide distance covered in the uplink-downlink phase and the associated time delays. These problems can be overcome using low earth orbit satellites: the increased need for worldwide connectivity and the advances in electronic technology make now possible the establishment of complex networks of satellites, called constellations, offering high quality services for a convenient price, using compact subscriber units, about the size of a standard cellular phone.

Iridium, for example, is a project designed to enable anyone, anywhere on land, at sea, or in the air, to communicate directly with anyone else, using affordable handheld units with all the features of cellular phones, via a network of 77 small, smart low earth orbit (LEO) satellites, orbiting at an elevation of 413 n.mi. Unlike Inmarsat, these satellites would not be geosynchronous, but would be placed in a polar low earth orbit. Each satellite will communicate with users, ground station gateways, and the other satellites. Ground station gateways in various countries will interface with existing public telephone networks. In addition to the handheld units, units will also be available for cars, trucks, boats, ships and planes.

The LEO satellite market is appealing for both telecom operators and manufacturers, thus Iridium is not going to be the sole player: other operators such as Globalstar, Orbcomm or Teledesic will start offering their services in the next few years. Some players will concentrate in providing voice services, while others will specialize in data communications. If they will maintain the promises they are making today, we can expect to have as much bandwidth as we need, at a reasonable price

4.2. Wireless networks

To connect LANs over short distances (a few Km), it is possible to use spread spectrum radios designed to combat strong interference and to prevent message recovery by unauthorized receivers.

These radios allow data rates of some Mbps within line of sight and operate in the 2.4 GHz range with no licensing requirements. With appropriate antennas they can extend their operating range at sea to about 20 Km.

Preliminary tests have been conducted at SACLANTCEN to demonstrate the possibility of using spread spectrum radios as building blocks for point to point TCP/IP network connections: the results obtained so far have been very promising. Services such as file transfer and WWW access from a mobile PC have been demonstrated. Future work will concentrate on performance measurements under operational conditions.

Further experimentation will evaluate Time Division Multiplexing schemes as a more flexible alternative to point to point links whenever there is a need to exchange data from a cluster (e.g. a group of ships conducting a survey) to a central location (e.g. a centralized data fusion facility).

4.3. Encryption

Whenever there is the need to exchange data in a secure way (meaning that the data cannot be altered without detection and cannot be read by unauthorized recipients) via an exposed network, the only way to proceed is to make use of cryptography.

Today a great deal of COTS products exist to offer an excellent grade of protection for mission critical business applications. Although they are not yet endorsed for use with classified information, the algorithms they implement are well known for their robustness and many financial and industrial institutions already use them for real life corporate

applications.

In TCP/IP applications *tunnel managers* act just above the IP level, implementing "IP over IP" tunnels: for this reason, the tunnel software is absolutely application-independent and application - transparent, requiring no change to existing software other that installing a new software library.

Existing products use powerful RC4 encryption algorithms to ensure confidentiality and *message digest* (MD5) checksums to ensure data integrity. The initial key exchange is made using RSA (Rivest - Shamir - Adleman) public key exchange technology.

All traffic from the remote host to the internal host and viceversa is encrypted: no traffic travels in clear text, so passwords and data can be transmitted with no particular worry. Once negotiated for the first time, keys are changed every 30 minutes, using state of the art RSA public-key encryption techniques.

One important issue is the key size: the longer the key, the harder it is to break the code. Unfortunately, US regulations limit to 40 bits the key size of crypto products for the international market, while the domestic version can have keys of 128 bits, that grow to 512 bits for the key exchange phase, thus offering a much higher degree of protection.

It must however be noted that the RSA algorithms have been published since almost two decades: it will therefore be possible to write new code libraries based on RSA, using keys of arbitrary length and achieving the desired grade of coding complexity.

5. Conclusions

Advances in data communications technologies open new opportunities that can be exploited in support of scientific research.

SACLANTCEN is actively investigating new technologies to enable scientists involved in sea trials to interact with their colleagues ashore in a timely, cost effective and secure fashion.

Using modern communication techniques based on COTS Internet products, and commercially available Geographical Information Systems, data acquired at sea can be shared in real time with partners distributed world wide.

SACLANTCEN has demonstrated the effectiveness of such approach during several sea trials, and is monitoring the rapid hardware and software developments of the communication field.

Particular attention is given to commercial Spread Spectrum radios, operating in the 2.4 GHz band, and to services offered by Low Earth Orbiting satellites.

References

[1] E. Bovio and A. Berni,
Wide Area Networking at SACLANTCEN - A Case Study. SACLANTCEN M-118, Dec 1995

[2] M. D. Max, N. Vasseur, F. Spina, E. Bovio,
The E-Map, Innovative COTS Software for Data Fusion and Interactive Communication for Rapid Environmental Analysis, REA Conference Proc.

[3] M. D. Max, F. Spina, E. Bovio,
GIS and E-Maps as the Basis for Data Fusion and Near Real Time Information Distribution: Present Capabilities, REA Specific Requirements and Directions for Development, REA Conference Proc.

[4] M.D. Max, E. Bovio and F. Spina,
Two-way Rapid Response Communication of Geographically Complex Position and Numerical Data Using Internet via Cellphone from R/V Alliance. Abs. American Geophysical Union Fall meeting Dec. 11-15 1995

Geographic Information Systems

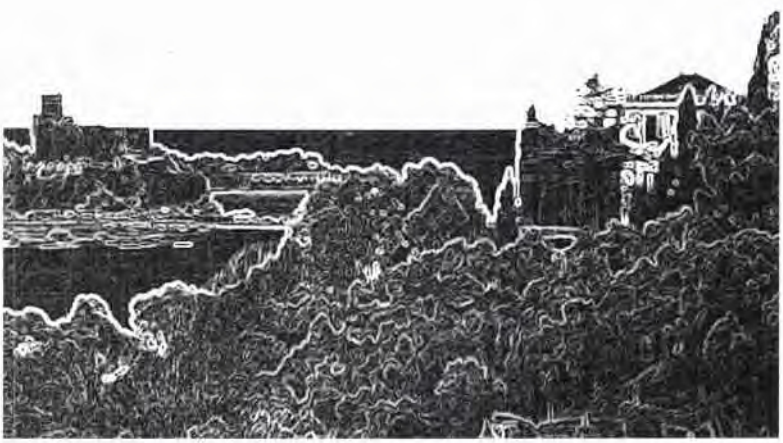

The E-Map, Innovative COTS Software for Data Fusion and Interactive Communication for Rapid Environmental Assessment

M. D. Max[1], N. Vasseur[2], F. Spina, E. Bovio

SACLANT Undersea Research Centre
Viale San Bartolomeo, 400
19138 La Spezia, ITALY

Abstract

E-Map software, originally produced to support marine scientific research, has been proven in a data fusion-communications role as the potential basis of a new means of interactive communication of geographically referenced information relevant to Navy operations. Rapid Environmental Assessment of an amphibious landing area was carried out as a structured exercise during 1996. With development, the E-Map methodology could be an information fusion and communication system for ships and other sites.

1. Introduction

The Littoral environment can be envisioned as extending from about 200 nautical miles offshore from a seacoast to at least the first line of communications inland. Within this shallow water-nearshore potential battlespace, increasingly precise positioning of a large number of seafloor and nearshore land attributes and objects is an emerging requirement for supporting Naval activities. The information required includes both environmental and man-made artifacts that are likely to be important during the progression of military response or intervention beginning with a perceived need for military activity and resulting in application of force (Table 1). In addition to a particular individual ship, or task force knowing where objects and reference points may be at sea with respect to their position (iso-spatial information), there is also an increasing need to be able to communicate as rapidly as possible not only where individual environmental elements or objects are, but where they are in geographical and temporal relation to each other.

Rapid Environmental Assessment (REA) is vital to carrying out operational planning (Table 1), which includes aspects such as force allocation and force level determinations on which all subsequent command and combat is based. By its nature, REA requires in-theater acquisition of relevant information, and rapid data fusion that extracts only the military relevant information for any set of requirements, and archives and optimizes them in such a way that they can be used with relative facility by the user. REA activities involves getting close to the military hot zone. The procedure for assembling REA datasets thus differs markedly from earlier data acquisition activity. Information datasets required for earlier response levels of readiness and response will be populated largely from information kept in existing national, local civilian, and military data repositories, such as National Geophysical and Bathymetric data and Mine Warfare Data Centers and from remote sensing capabilities that are mainly space borne satellite sensors. REA involves making a transition from covert to overt activities.

REA activities are carried out as a response to particular military requirements for critical information. Not only must the environmental and object information be clearly identified as a function of the military application, but its acquisition and fusion should be organized to minimize the time needed to both acquire and fuse the information while maximizing the quality of relevant information and presenting it in such a way that it can be used easily. An REA should be conceived of as a highly focused combined survey/analysis/presentation designed to produce Mission Specific digital Data Sets (MSDS). Because the acquisition of the information may take place under difficult, if not hostile conditions, and the lead time requirements are relatively short for the production of a useful REA data set prior to its use, new approaches to information acquisition, fusion, archiving, access, and use must be developed. This report outlines a new approach for integrated data fusion and communication suitable for REA, and describes its use in a short exercise designed to test itssuitability for development as a fundamental new REA tool.

1) Now at: Naval Research Laboratory, Washington DC 20375 <max@qur.nrl.navy.mil

2) (LtCdr) Now c/o Royal Netherlands Navy, Den Helder, The Netherlands

Level	Lead Time	Chart cover, km	Scale K=1,000	Bathy	Feature Resolve	Information Source	Use
Readiness	12 Days	300x300	1: 250k	50m	20 m	Available, Historical	All Planning
Response	72 Hours	90 X 90	**1:100k**	**10m**	10 m	+Remote sensing	OP AREA selection[3]
Operational	18 Hours	20 X 20	1:50k	5 m	5-<1m[4]4	+Survey,data fusion	OP Planning[5]
Combat	6 hours	2 X 2	1:5k	<1m	0.25 m	+Data assessment	Operations[6]3

Table 1. Character of required information as a function of: the military activity levels of a normal sequence of events leading to actual combat, lead time, required chart coverage in km, chart scale, bathymetric contour intervals (seafloor morphology detail), the likely source of the information and the use to which each chart will be put.

2. REA datasets

In addition to the scale and feature-specific nature of the type of information required for REA (Table 1), the nature of the environmental information required needs to be taken into consideration. This is both because current environmental sensing and measurement equipment can collect more data in a short time than can possibly be used operationally, when decision making is often focused on using simple but highly focused and relevant information to make relatively simple decisions rapidly, and because different military applications require different configuration or optimization of the data. Only the necessary information should be presented in the best way for rapid and easy use. REA information fills the data gap between major and more generalized data sets, and that which is necessary to commence military operations.

Environmental and other information must be acquired, assessed, reduced, and optimized for a user; this is data fusion. What data should be collected; how is it to be used; and where should resources be concentrated? These are basic questions that need to be addressed before tasking data acquisition assets. Because of limited REA time and resources, both the precise nature of what measurements and observations are being collected needs to be assessed for any particular REA, as well as considering how best to fuse and communicate the information for interactive use.

Traditional data collection, for example, often focuses on acquiring certain information simply because programs, agencies, and sea-going activities are well organized for carrying out the measurement programs. Extensive CTD measurements for instance, whose collection and averaging into huge historical data sets was originally of the utmost importance for carrying out Antisubmarine Warfare (ASW) in open ocean areas, are of only limited importance in the nearshore littoral where Mine Counter-measures (MCM) hunting and clearance for seafloor mines is carried out. This is because the water column properties are highly variable and normally one of the first actions of an MCMV (Mine Counter-Measure Vessel) upon reaching a route or lane to clear is to obtain a real-time CTD so that an current sound velocity profile can be obtained. Periodic CTDs are taken during the course of the MCM activity because the highly variable SVP will strongly affect all sonar use in the shallow water. Thus, efforts put into collecting more than a few CTDs as part of the MCM REA are probably largely redundant. With good foreknowledge of precisely the type of information that is required for any particular military application, effort can be focused on collecting only the most relevant information.

It is important to note that not all environmental and artifact information is equally likely to need acquisition or updating (Table 2). Operationally relevant information can be divided into three categories (Table 2), only one of which is normally of REA physical and temporal character. Intransient features are stable enough to not require extensive REA survey and data fusion, and transient features are too short-lived to make their surveying relevant to REA related planning activities. Metatransient features are of interest for REA.

1) e.g., select amphibious assault area (Readiness & Response).

2) Highest resolution is only required where the information will be included in combat-type charts. Readiness - Combat can also be expressed as 'Covert - Overt', and in a number of different ways.

3) e.g.,carry out multi-survey, Rapid Environmental Assessment of amphibious assault zone for MCM planning purposes, with feature resolution of less than 1 m to characterize mine-like objects (Operational).

4) e.g., commence MCM hunting, clearance operations using seafloor acoustic image navigational chart (Combat).

	Intransient	Metatransient	Transient
Areas	Seafloor types: e.g., muddy, sandy, seagrass, rocky, rough, smooth, current or biologically textured seafloors	Route selection for convoy or amphibious assault, beach gradients, current and biologically formed seafloor morphology, boundaries	Weather related
Objects & Features	Morphological and Geographical elements: e.g., Rock pinnacles, holes, floodplains, longshore bar islands, river mouths, delta and lagoon configuration,	Forebeach depressions, sand bars, storm birms, washouts on barrier bars, sandbars in rivers and estuaries, small seafloor area types, detailed boundaries, seagrass meadows, mine-like objects, oceanographic elements	Ripple marks, pockmarks, detailed oceanographic measurement character (CTD, SVP), sea state, surf, beach undertow, current pattern, state of tide
Artifacts	Harbors, levees, major roadworks and earthworks, habitations, Headquarters (e.g., the Pentagon)	Fixed bridges, tunnels, large constructions, minor roads, Major military forces, minefields	Operational force elements (tanks, trucks, artillery positions, etc.), temporary roads, Small military forces, minefields

Table 2. Nature of features. Not a comprehensive list of objects, areas, and artificial (man-made) artifacts, examples only. REA activities probably focus on the metatransient because data for intransient features may be available in historical or other existing datasets while transient information is liable to change between the REA and the Combat stage (Table 1).

Intransient features are those that are not likely to change position or character over a considerable period. Data relevant to these features is likely to be available from historical, military, and other existing data sources. For instance, bathymetry and local seafloor morphology change at a rate slow enough so that data sets collected years, and over a span of up to hundreds of years may remain relevant. Very detailed bathymetric data sets, with contour intervals as close as 1 m, also may remain valid on some types of seafloor regardless of their detailed nature, while they may need complete updating on other seafloor types under certain oceanographic conditions, usually where storms can alter the seafloor morphology on a 2-3 m scale. Transient features are those that are too small or short-lived to make their survey and recording in a data set of value because by the time that the next military intervention level is embarked upon, they may be significantly altered or absent. Effort spent mapping and acquiring the precise positions of all of these features may be largely wasted if the information is not used. Although the number and distribution of mine-like objects and their areal distribution is important to REA activities, the precise position of each is not. At the next level, however, when actual MCM hunting, classification, and clearance operations are embarked upon, some of the highly detailed data sets that can be acquired during the REA operations may be reconfigured for use. Because modern side-scan and other sonars that may be used in REA normally capture information at the detailed level, it can be archived so that it can be used later, if necessary, without further survey.

Metatransient features are of an intermediate physical and temporal scale and are by their nature significant for REA activities. They are more detailed than the those for which information is liable to be found in existing data sources, and usually hold the particular information necessary for operational planning. They are also less transient than individual natural features, such as the location of the crest of individual sand waves, and are liable to comprise a valid data set over the time span that encompasses their mapping and fusion, and initiation of military activity or data acquisition necessary for the next level of military intervention.

REA-significant features have a particular size range, degree of permanence, and significance for particular military operations. For instance, for a military operation where air cushion vehicles are to be used exclusively for amphibious assault, the precise location of a forebeach trough is of little significance, whereas for an assault with landing boats, the knowledge of the precise location is of great value at both the planning and combat levels.

3. The E-Map

The E-Map consists of computer software comprising a Geographical Information System (GIS) navigational chart containing map layers holding different types of geographically referenced point, line,

and area positions, which can be linked through object-defined file names to supporting text, numeric, and image information in a relational database [1]. It has been produced using new methodologies of opportunity, based on existing portable and desktop 4computers, Commercial, Off The Shelf (COTS) software, Internet technologies, and existing satellite-radio-cellphone systems. An early version of the E-Map was initially implemented as an aid to SACLANTCEN marine scientific research cruises. Its use has dramatically cut post-processing time and subsequent activities such as report and scientific paper presentation through integrated archiving of information gained on successive experiments and surveys. Because positions can be input directly from navigational systems (e.g. (D)GPS) at sea and some data can be input directly from environmental sensors without intermediate processing using AV (Audio-visual or multi-media) computers on which the E-Map is installed, the actual archiving does not impose an unmanageable work load. Information and position data entered into the E-Map are tagged with object identifiers for linking when, or shortly after they are acquired. New map overlays, for instance of bottom-reverberation, seafloor sample and classification, ship's tracks, route boundaries, core and sample locations, etc., can be compiled and edited in real-time, and oceanographic data positions can be linked with the verified data within minutes.

The E-Map provides a graphic interface, integrated archive for two-way real-time communications [2], now using both cellphone and Inmarsat-B links. A new level of extremely rapid communication of complex geographically-referenced information can be attained using the E-Map as the core of data fusion-communications activity. The basis of the rapid communication of edited, updated, and new positions and data is transfer of only the new information from where it has been generated to any or all other sites participating in the information sharing. New map layers and supporting data files are saved and exported, and then communicated electronically to other sites where they can be merged in duplicate copies of the area E-Map. When an information item is merged at a remote site, it is becomes part of that existing dataset with automatic geographical and relational database reference. Updated maps are normally archived on CD-ROM for internal SACLANTCEN use following each research cruise.

At present, the E-Map is a research tool suitable for supporting single ship marine research cruises and archiving the different types of data in an easily locatable and extractable manner. Archiving, linking and populating the GIS layers still requires scientists to be assisted on the research cruises by support staff with relevant computer skills familiar with the commercial software. This activity is presently carried out mainly during the scientific activities as normal SACLANTCEN practice. It was perceived, however, that the E-Map methodology might provide the basis for certain military activities, particularly those concerned with acquisition of environmental information for Rapid Environmental Assessment.

4. E-Map as a Prototype REA Tool

Rapid Environmental Assessment can best be conceived of as a response to particular military requirements. MCM activities, for instance, fall into two general categories, area assessment for planning purposes, and real-time operations. The E-Map was used in the course of a special and limited REA-type interactive exercise whose aim was selecting a nearshore route for MCM operations in an amphibious assault zone along the SE coast of Sicily. The coastal area selected was the site of a real amphibious invasion in 1943; thus these results thus can be judged against a real operational background. The E-Map was not reprogrammed or specially developed for operational application because of time and staff availability constraints, but by using extra personnel and with careful preparation that took into consideration existing E-Map limitations in its less-than-fully developed form, tested the concept of using the E-Map methodology as the basis for REA activity. Further details, including text of all message traffic, are available in the Cruise Report [3] that included this exercise.

High-resolution MCM seafloor characterization is mainly confined to waters shallower than 100 m, particularly between 50 m and the beach. Amphibious operations must have access to both nearshore land and marine information. Seafloor characterization on less than 1 meter scale is necessary, but for REA the information can be generalized. Broad area survey and data archiving methods are inappropriate. The E-Map has excellent possibilities for data fusion's because it is scale-independent. Linked, related charts of widely varying scales and information content, including very high-resolution, local scale and regional scale charts that may hold very different but related information, can form part of an integrated multi-level E-Map.

The main goal of this exercise was to more fully evaluate E-Map data fusion and communications using both cellphone and Inmarsat-B [4], the high speed digital data communication system [5]. High resolution seafloor images (side-scan, reflection seismic, video), image-based charts (registered side-scan), and frame-grabbed images as seafloor videos, could all be made part of the E-Map and communicated as part of an integrated information package. Duplicate charts of the area were established

on the NATO Research Vessel (RV) ALLIANCE and at SACLANTCEN. The shortest intervals between data capture, analysis, and E-Map updating using electronic communication were also determined.

Instructions as to which agencies were to be informed and what level of interaction was expected were issued by the C&C analogue immediately prior to beginning the exercise. The rules of the game, as such, were promulgated. A first operational tasking was then issued; this initiated the first environmental survey and response, which included communicating the integrated up-date information back to the C&C analogue. After merging and assessment at SACLANTCEN, a second operational tasking for more detailed information in an area selected on the basis of results gained during the first assessment was issued. This generated a second response, which was considered the close of the structured interactive REA exercise. Care was taken to insure that all information communicated was of operational quality

5. REA in an operational situation

5.1. I Exercise Setting

The operational scenario was based on the near-term possibility of a real operation in the eastern Adriatic, where NATO reinforcement by sea might be necessary. A mine threat in the landing area could be anticipated as a potential danger to any amphibious operation even though no shoreline there was presently hostile. The objective was to collect and interactively communicate environmental data relevant for planning MCM operations, modeling a future command and control - operational activity. In preparation for this possible event, the structured exercise was devised that consisted of 3 parts. 1. Rapid environmental assessment. 2. MCM operation advice. 3. Amphibious landing operation advice.

5.2. Exercise aims and organization

The methodology involved interactive E-Map communications using real datasets acquired, fused, and communicated under the pressure of time. A first survey into the beach approach area was followed by a second, more detailed investigation of a selected lane after re-tasking from SACLANTCEN. This follows the normal practice for picking the best narrow beach approach lane from an initial data set, and then assessing that in greater detail. On both surveys pictures were captured from the side-scan sonar in real time while the ship was moving; video images of a seagrass meadow fringing the surf zone were made at selected points. Scans of the reflection seismics were linked along the tracks, and a bottom analysis for the line was extrapolated into seafloor classification charts for the area based on standard NATO nomenclature. A seafloor chart of specific MCM attributes such as the anticipated number of mine-like objects per area, was also produced. Based on these charts and the associated images, which were merged with a duplicate copy of the chart at SACLANTCEN, a 1 kyd - wide lane was selected in what was judged to be the most favorable seafloor conditions for MCM activity.

5.3. Exercise Activity

First operational tasking and response

1. Conduct an MCM area survey along channel X (map layer and locations denoted).
2. The following environmental parameters should be reported to SACLANTCEN:

A. Water depth.
B. Seabed profile.
C. Seabed composition.
D. Likelihood of mine burial (scour and impact).
E. Incidence of Seagrass and other significant biological features.
F. General seafloor areas and density of naturally occurring mine-like sonar echoes.
G. Any other notable attributes.

1. Provide estimates for time to complete task and time to transfer processed data.

The area was entered twice: the first time with the RV ALLIANCE continuously sailing at 4 knots acquiring high-resolution reflection seismic records, side-scan sonar, multibeam (SWATH) bathymetry, and using expendable oceanographic measurement tools.

Wherever possible, text information was included directly on the chart layer to diminish possible confusion and enhance suability. The image data provided additional supporting information that was used at the Command and Control analoge to verify the at-sea interpretations. Although it would have been possible for the decision for the placement of the invasion lane to be made from the map layers of seafloor types alone, the ability to link the supporting information to the map layers, gave the C&C analogue increased confidence.

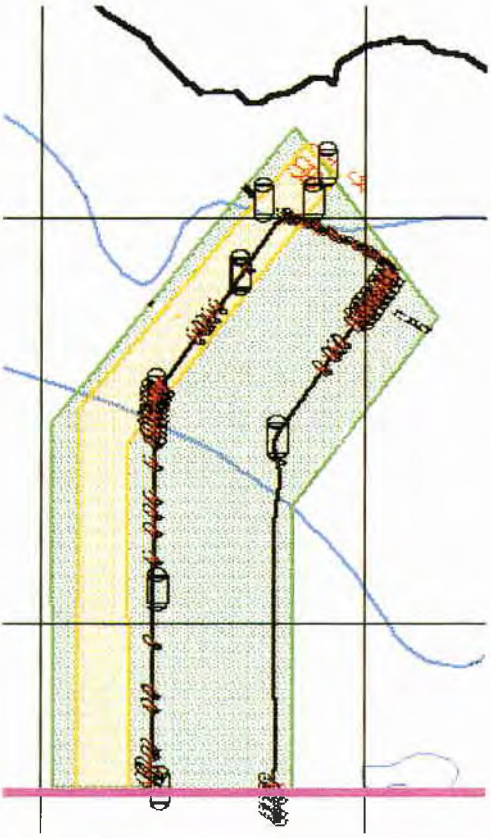

Figure 1. First survey area (Green pattern) and ship's track for the first survey entering on western line and proceeding clockwise to exit area. Second run of this survey phase from one core location to another, again counter clockwise. Large icons denote core positions, smaller icons show image positions from grabbed from video and side-scan sonar in real time. Scale and exact positions omitted on this and subsequent figures. Southern Sicily coastline at top.

The response to the first tasking consisted of 10-15 new map layers and hundreds of linked files consisting of text, tables, numercial data, and images. Images consisted of single frames selected from the seafloor videos of the core sites and the seagrass areas, side-scan sonar images unedited from the form of their original real-time capture, and scans of the reflection seismic sections along the track. In all cases, each image was linked through a file name to the location on the GIS side of the E-Map so that all images could be accessed directly through the map graphical interface using the mouse for selection. Numerical data from the oceanographic casts was placed in files within the appropriate folders on the realtional database side of the E-Map, and also linked to map layers for graphical selection. Some text was printed directly on map layers, while other text was contained in Word Processor files (later converted to HTML for direct internet access), and in tables that could be transmitted within a Word Processor document or as images saved using screen capture freeware.

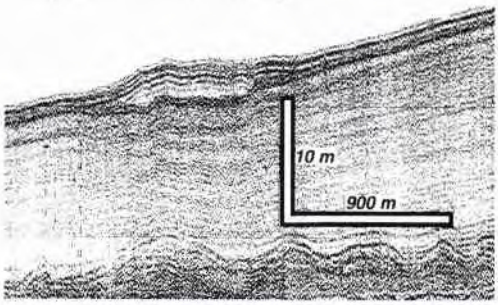

Figure 2. Reflection seismic image and scale from inner part of inbound leg showing a gravel or shell hash bar on otherwise featureless seafloor composed of marine muds a little over 10 m thick. Irregular surface below scale is an indurated calcareous sand sediment

The time required from the beginning of the survey to the communication of the integrated dataset was extremely short for this type of activity. 4 hours on the first survey run was followed by 3.5 hours of sampling and analysis of sediments and video inspections. 3.5 hours for completion of all chart layers and interpretation followed, intersperced with meals. The work began with putting the geophysical equipment in the water at about 08:00 and communicat was achieved by about 20:00. The communication times themselves were also short:

1. Small messages with attachments of data, charts, and instructions, etc., each took about 1 minute total from "send" to completion; total about 20 minutes.

2. 1 large message via Inmarsat-B of images, chart layers, data, and message. The transfer rate achieved using the Inmarsat-B was very close to the theoretical line speed of 64 Kbps. NRV ALLIANCE managed to transfer 56 files for a total of 5.3 MB of data in 13.8 min, at an average speed of 52 Kb/s

5.3.2. Second tasking and response

This was sent after an evaluation of the first response at SACLANTCEN following merging of the new E-Map data and analysis by Operational Research Group staff. The second, and narrower area was identified as being the probable invasion lane to the beach. A detailed survey of the 1,000 yard-wide channel was then initiated so that communication of new map layers to SACLANTCEN in an E-Map format could be made. The times for making the environmental description and times for accomplishment of objectives were also monitored as part of the experiment.

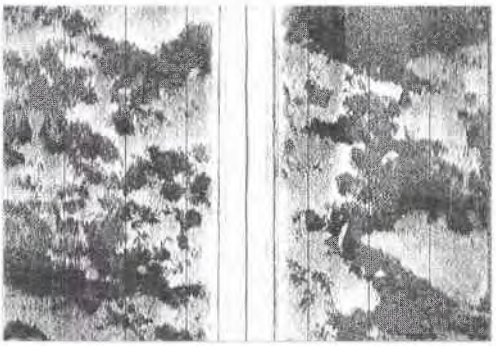

Figure 3. Image of side-scan sonargraph (green seafloor area on Fig. 4) showing irregularity of seafloor within the seagrass zone. 100 m each side from centre, equal area scale.

This survey was one pass only, with revision of the lane within the first surveyed area made on the fly from side-scan sonar, reflection seismics, and multibeam bathymetry, with additional cores and seafloor videos taken at the shoreward end of the run. The key to producing the interpretive bottom charts was to prepare chart layers with the anticipated information, with all polygons defined and text in place, by copying and clipping the chart layers created during the first survey. This reduced the data fusion to an editing process of modification, which can be done very quickly. The survey was completed to less than 12 m water depth just off the beach.

The response to this second tasking consisting of two chart layers containing the required information were completed and communicated to SACLANTCEN as files attached to an e-mail message sent from a portable computer near the E-Map computer within 15 minutes of reaching the end of the lane survey. In addition, 6 files for a total of 2.3 MB, were communicated in 5.6 min. from NRV ALLIANCE to the Naval Undersea Warfare Center (NUWC) in Newport RI, U.S.A., for assessment in the context of a joint LFAS program. A further large communication was made to the Dutch Navy research center.

Superimposed overlay of the second survey upon the first (Fig. 4) shows the slight but significant modification of area boundaries. Note that rock (red) in the shallowest area reached on the second line occurs on the seafloor; this is interpreted in the overall chart as a continuous rock ridge that follows a resistant geological unit. The results of this very detailed study were incorporated in the overall Sicilian-Tunisian Platform E-Map shortly after completion of the exercise. The map layers showing the sediment types and rocky seafloor were edited and updated. In principal, this attribute of updating could be carried out on copies of large map layers so that the original information, without the on-site presence of an environmentalist who could verify the new data and oversee the editing of the appropriate map layers, could be edited into the overall dataset without losing any of the original map layers. This selective edition is a feature of GIS and is one of the main reasons why a user front-end environmental information system should be GIS based, rather than being resident in single file-images or gridded databases.

Following the end of the second survey, video inspections of the outer surf zone (the shallowest reached by the RV ALLIANCE) were made, along with detailed inspection of the seagrass zone for about an hour. Color images were captured in real-time, using the same AV computer that was used to capture images from the side-scan sonar.

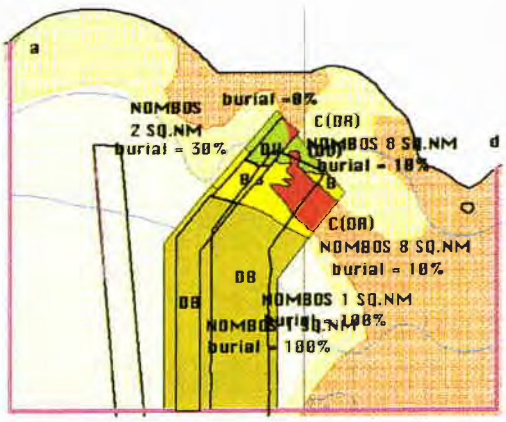

Figure 4. Bottom charts showing areas of different bottom types to NATO standard designations. Second survey, which contains two survey lines, shown superimposed on first survey. Note new rocky seafloor at north end of the lane not found by first survey links in a rocky ridge, isolating an area of sandy seafloor. Red margin of the sea area is the authorized exercise 'box'. MCM nomenclature included on map layers not explained here. Survey tracks to west of amphibious assault zone are part of other work. Sicily coastline is northern boundary.

6. Achievements

A realistic landing zone was surveyed by RV ALLIANCE, environmental information acquired, assessed, optimized, and fused, and a large integrated dataset communicated to SACLANTCEN using available commercial e-mail and internet software and networks. The exercise demonstrated the capability of the E-Map system to communicate "near" real time data.

The concept of using the E-Map as a primary means of communicating complex geographically referenced information was proven [6]. The present capabilities of the E-Map used in this experiment can archive and locate rapid environmental assessment information of operational character, appropriate for MCM activities. Interactive REA activities in a designated amphibious landing zone were successfully carried out as an interactive structured exercise.

The E-Map demonstrated its capability to communicate detailed and complex information relevant to MCM operations in a very short time. In fact, 2 chart layers constituted the entire reply to the second run into the beach. Once the attributes over a general approach area were known, good placement of a second line allowed a detailed picture to be gained in almost real-time.

Of course, dealing with a real threat by carrying out an REA where mines may have already been laid, a ship like the RV ALLIANCE probably would not be used. However, with emerging methodology and remote data acquisition systems within reach, the potential of the E-Map system demonstrated during the exercise is clear. The data collected was fused in the E-Map within a few hours and communciated immediately in such a way that it could be visuzalized and used very quickly.

7. Operational potential

An expanded E-Map communications concept may confir significant improvement in a number of operational areas, for instance, Mine Counter-Measures Vessels (MCMV), including drone-ships. MCMV units can use an E-Map as a Tactical Data System with the E-Map taking a feed from the ships' navigation system. In addition to the MCM data currently being acquired, the E-Map can be expanded to add linked sonar pictures of objects or video from ROVs, and text and numerical data, which is now kept on tape in their own archives. E-Map data is intended for use on small disc-type digital systems where direct access of position and supporting data are linked and held together. This information can be communicated in nearly real time within the task group and then forwarded to the Task Group Commander, the Area Commanders, and supporting activities, such as at-sea resupply. Mine Warfare Data Centers can quality control new E-Map revisions, which can then be communicated back down the operational chain to other data user sites.

E-Map communications for MCM purposes can encompass both area and route survey, as well as actual operations. The objective of an MCM-REA survey is to provide general both seafloor and oceanographic environmental data for an area to permit optimum route selection. Once the route has been selected, however, a more detailed E-Map application may be undertaken. The difference between the two levels of E-Map application may be illustrated using seabed contacts. For an REA survey, the objective is likely to determine and map the 'density' of mine-like objects on the seafloor in order to select routes that pass through areas of relatively 'low' clutter, whereas the objective of route clearanceis to locate precisel individual mine-like sonar echoes for mine investigation, classification, and, if necessary, clearance purposes.

E-Map allows for special information-rich navigational charts to be created for real-time MCM applications. This is regarded by us as a major development area, which has only been touched upon through the production of prototype seafloor acoustic image IIS navigational charts at SACLANTCEN. These image-based charts can provide a new means of showing precisely located detail of seafloor areas and offer opportunities that are not allowed by current practices. Side-scan images are used as the background of small-scale GIS charts and standard image-processing software can be used to edit the image. The images can also be processed using automatic target recognition software. These enhanced images can then be used in their E-Map configuration by operators MCM as the working navigational chart. Colored icons can be placed on objects in order to convey information about the nature of the object, the level of clearance, and indications for further activity.

8. E-Map development for REA

GIS-based (or E-Map) communications may not only have a major impact on Naval activities, but on other activities that require rapid interactive communication of these levels and volumes of information acquisition and exchange. At present, many military messages, which are low data volume printed documents whose form was originally defined by teletype technology, could be largely replaced by the E-Map interactive information-rich format, which is less prone to error, has a very low workload at the point of implementation, can be visualized rapidly following receipt, and will allow instructions to be acted upon very rapidly.

Further development of the software and optimization of existing communications capabilities should allow the E-Map methodology to become the basis for compiling and disseminating information among a fleet of vessels operating interactively in real-time, in concert with remote sites. E-Maps have the potential to provide a new communications medium in an interactive information-rich format.

The present capabilities of the E-Map used in this exercise allows for archiving and locating REA information appropriate for MCM activities.The demonstrated near real-time interactive communication capabilities would give an optimized and fully developed version of the system a near- operational capability at relatively low development costs. An

improved E-Map would give an MCM commander for carrying out command and control functions both better information and control.

The E-Map methodology thus shows promise for development as a means of fusing environmental information and archiving it for littoral Naval activities and for information exchange. Although the amphibious assault exercise showed that the E-Map methodology has exceptional potential for development as an operational tool, further development will be necessary. The E-Map approach to data fusion may have particular interest for military oceanographic programs, especially in an international environment where computer hardware and software is unlikely to ever be homolgated.

The development should include: 1. a very user-friendly information-layered E-Map relevant to Navy sponsor interests; different Navy activities may require somewhat different configurations of data capture and display but common object link file names can be used among a number of different implementations. 2. User-friendly and largely automatic file save, export, transfer, and merging modules must be developed for easy selection and visualization. 3. Internet technology must be optimized for the best communications. 4. The developed E-Map must be portable and robust. It must have the capability to take navigation from GPS, DGPS on any platform of opportunity or from a hand-held GPS unit. 5. A navigational interface for selecting automatic positional inputs and map layer-relational database file generation will greatly aid data fusion. Improve direct incorporation of images from high-resolution side-scan and reflection seismic equipment for digital input to an E-Map; position or file-at-a-time input automated. 6. Ship-to-ship and ship-to-shore interactive communication in near real-time should be equally smooth, with any communications system capable of delivering digital files. 7. Must be able to communicate between all sites in near real-time.

There is a further requirement for very high quality environmental information for shoaling and nearshore littoral areas. New methods need to be developed at low cost to recover this information, which can only be obtained by human intervention in the short term. At present, there is no systematic high resolution seafloor and nearshore mapping system in use. A prototype system based on operational scientific diving methods has been developed originally at SACLANTCEN, La Spezia, Italy in conjunction with Italian Navy MCM activities. It is presently under further development at NRL. It is a combined observational-measurement system for Diver characterization of oceanographic and seafloor sites to geotechnical standards with observations during the course of dives in which the recovered information can be input into a computer database visualization system for rapid communication. These data will provide for basic high resolution seafloor morphology and physical properties data, s well as very detailed oceanographic information that is useful in their own right and also will provide ground-truth to acoustic seafloor mapping techniques. Although the diver data information recording system is not yet under full development, it should be considered as a useful part of an overall E-Map system

A strong point of the E-Map system is its mobility. The software is presently implemented on desktop and portable computers. With suitable communication hardware and on-board GPS capability (presently available through PC card slot plug-in devices), communications sites can be hand-held, as well as fixed. With portability of mobile units supported by an operational theater or local area net of spread-spectrum radios for local communications, the E-map system would become a true user front-end for any major communications system that output its information in an Internet-type compatible format.

9. Conclusions

By combining the E-Map software operated in a 'shared' electronic communication framework and Internet technology, methodology has been developed that now allows for the real-time sharing of complex geographically-referenced data sets. This allows for real time data to be current on a number of platforms, including command centers, at almost the same time. The technology also allows for new operational procedures to develop based on the enhanced amount of useful information that can be communicated and the speed with which communicating sites can be easily updated.

For data fusion, the ability to both communicate not only a packet of information, but to edit it interactively at more than one place offers exciting possibilities. A fuller operational implementation, however, would probably not include the capability to directly edit map layers and files at every communicating site.

Although the focus of the development described here has been for a military application, the methodology can also be applied to non-military agencies such as law enforcement and civilian applications such as map and chart updating.

References

[1] Spina, F., Max, M.D. & Bovio, E. 1997. *GIS and E-Maps as the basis for data fusion and near-real time. In: Proceedings of the Rapid Environmental Assessment Conference, 10-13 March, 1997*, Lerici (La Spezia) Itlay. SACLANTCEN Special Publication (in press).

[2] Bovio, E. & Berni, A. 1996. Wide Area *Networking at SACLANTCEN - A case study.* NATO SACLANTCEN Report M-118, 21pp.

[3] Max, M. D. 1996. Cruise Report *'WINTER SUN-2'* Unpublished SACLANTCEN library open file report, 60pp.

[4] Bovio, E., Max, M.D, Spina, F. & Berni, A. 1997. *Communication Technology in Support of Saclantcen Program of Work.* In: Proceedings of the Rapid Environmental Assessment Conference, 10-13 March, 1997, Lerici (La Spezia) Itlay. SACLANTCEN Special Publication (in press).

[5] Max, M.D., Bovio, E. & Spina, F. 1996. *Shipping the news from the seabed.* GIS Europe 5-8, 16-18.

[6] Max, M.D., Bovio, E. & Spina, F. 1995. *Two-way rapid response communication of geographically complex position and numerical data using internet via cellphone from R/V ALLIANCE.* Abs. American Geophysical Union Fall meeting Dec. 11-15 1995, Proceedings

Acknowledgments

Special thanks to F. Turgutcan and R. Risso, who have contributed greatly to the development of the E-Map and its development into a prototype communications system.

GIS and E-MAPs as the basis for data fusion and near real-time information distribution: present capabilities, REA specific requirements and directions for development

F. Spina, M. D. Max and E. Bovio

SACLANT Undersea Research Centre
Viale San Bartolomeo, 400
19138 La Spezia, ITALY
Email: spina@saclantc.nato.int

Abstract

At SACLANTCEN the work done since 1993, and recently (1996) three cruises have demonstrated the validity of the use of a commercial GIS as the archive for marine scientific information in support of sea trials for REA. By definition GIS are the information systems for data which has significant geographic reference; The integration with communications makes the GIS the REA information system with no alternatives. Data from more than one ship or data source can be merged in the GIS in the course of a cruise. However, in general, the preparation of a GIS is often not at all a "rapid" job. REA in addition imposes specific constraints on timings for data acquisition and products distribution. This paper discusses what are the specific characteristics that make a GIS more suitable than others to be used in a rapid environmental assessment, both for military or civilian customers.

1. Introduction

The purpose of this paper is to discuss how a GIS should be made to meet the specific requirements of REA; to examine the existing systems and see how the they meet (or do not) the requirements; to see the technological evolution and guess what the future will offer, and to conclude with personal ideas on what we, users could do now.

2. A quick look at experiences at SACLANTCEN

The GIS appeared here in 1992, basically as a support for thematic maps compilation for a geophysical study in the Sicilian Tunisian platform. Soon data were added, and linked to map objects, the multilayer thematic map became a true GIS. The first GIS map used at sea by SACLANTCEN was in support of a Low Frequency Active Sonar (LFAS) exercise in the southwestern approaches to the British Isles (SWAPPS) in 1993.

The next step was the integration of communications and real time link to ship sensors. This became necessary very soon when we had experiments with multiple platforms doing data acquisition (South Adriatic, with our R.V. Alliance and the I.N. Hydrographic ship Magnaghi).We wanted a daily update of the experimental data base on our ship.

At that time the term D-Map (now evolved into E-Map) was adopted to identify the association of the three components: Maps data and communications, in a single system.

Since then, especially configured D-Maps have been used to support projects and experiments of

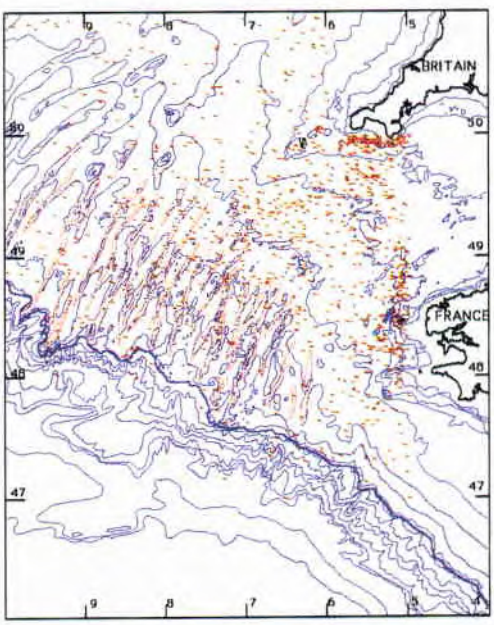

various types (Oceanographic, Acoustic, Geophysical) and in many places (SWAPPS in 1993, the Sicilian The GIS Map prepared for the LFAS experiments in the SWAPS in 1993.

Tunisian platform (STP) in 1995 and 1996, The South Adriatic in 1995, The Black sea and Bosphorus area in

1996, the North Tirrenian and Central Tirrenian seas in 1994, 1995, 1996, the South of Sardinia in 1996).

A specific evolution of the D-Map in support of LFAS experiments has led to its present version and it is worth to mentioning here as it is a good example of the use of GIS for real time data acquisition support and as an aid to data classification.

The GIS is interfaced with the sonar console (an UNIX workstation) where the acoustic echoes are displayed in polar coordinates relative to the ship.

The contacts found on the sonar display, on a ping-by-ping basis, are manually selected and possibly given a tentative classification, by the chief sonar operator, often in consultation with other operators and supervisory staff. After selection, the contacts are transformed into absolute geographical coordinates. These are transferred and altered into the geographical datum of the GIS using interface software, and are then passed via Ethernet to the GIS. The on-screen contact classification is depicted using colored icons.

An interface to the ships radar provides information about surface ships in the area, that may generate acoustic echoes. At the end of each run, as well as prior to, during, and after formal exercise phases, a basic acoustic reflection map is produced, based on NRV Alliance's movements. The union of all the layers of bottom acoustic response data allows the creation of a series of sonar response charts. These charts, and the positions of non-bottom echo responses, representing the position of an underwater object, i.e., a submarine, with time, are both produced in real time, being finished within minutes of the close of exercises. Real positions of detections could be compared with reconstructed tracks, where known.

3. The REA life cycle

At the cost of an oversemplification of what REA is, at least for the purpose of this paper, the REA life cycle could be considered as composed of four phases: the preparation phase, the data acquisition phase, the "event" phase, and the post exercise analysis. The GIS has a role during all the phases.

3.1. The preparation phase

During this phase all the pertinent historical information available for the area of the exercise or "event" is collected and placed on the map or loaded into the database. This is typically the time when coast lines, bathymetry, bottom types, bottom features, statistical water column data are collected.

The preparation phase may be a relatively long period but may also not exist at all: the possibility to have such a phase is depending upon the ability to know in advance that a REA will occurr and where. This assertion is true for military exercises, it is partially true for real military events, it may be totally false for civilian events. So the preparation phase may be short, or just merged into the data acquisition phase.

3.2. The data acquisition phase

Shortly before the occurrence of the event the time-dependent data, or the area specific data are collected with in situ measurements. This is a short, intensive period during which the data processing time is critical. Data fusion and data modelling begin and data products start to be available and ready for distribution.

3.3. The event phase

During this period all the data acquisition, data modelling and products distribution activities continue.

3.4.The post-event analysis

During this phase there is no more data acquisition: the data collected are used for some more modelling or re-modelling of the data, new data products are generated and distributed.

4.Important issues

The above model of activity needs to be supported by an information system with different entities responsible for collection, validation, uploading, processing, and utilization of data. This is similar to almot all Information systems. What is specific for the REA information system is it is never in a stationary status, and that during part of its life (the most critical part) the entities providing data and those using them are far away scattered in the field. The time required to exchange information is an important factor. There is a clear requirement for an information system with distributed access. As all the data are geographically referenced, the REA information system shall be by definition a distributed geografic information system

4.1. Client server model

Distributed access is today synonimous of client server. Between clients and server there is a set of communication facilities and this is normally referred to as an Intranet.

The Intranet technology for a system that must be accessed by multi platform clients is without doubt the collection of TCP/IP based Internet protocols. As a result of these simple considerations there is a simple

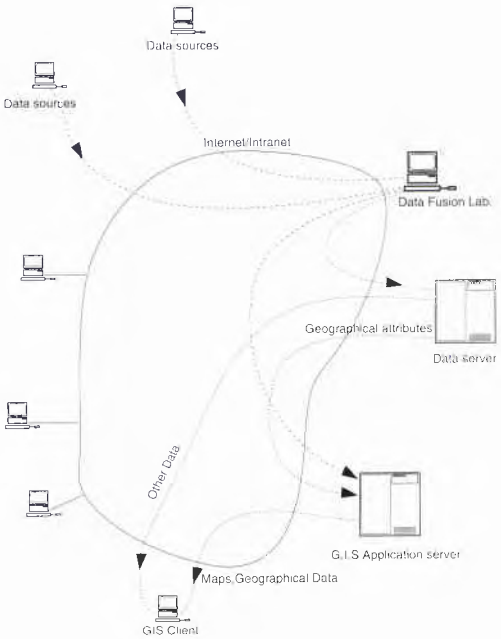

A Scheme for a Client-Server GIS

statement: The ideal REA Information system is a GIS that is based on separate clients and servers communicating using internet protocols. The client/server model however is a very generic representation: Questions are: Which format for the geographic maps (Raster, vector or both?); Which local functions should the client be able to perform (Pan and zoom? Switch on/off , activate layers?) Which kind of client software will be used? (a standard browser, a browser with specific extensions, or a specific GIS client?)

These alternatives will be considered later in this paper.

4.2. The Multiple Communicating GIS model

The alternative to the Internet Client -Server model is the Multiple, communicating GIS systems. Data are sent from data sources to a central site which is responsible for data uploading. Data base and map updates are sent periodically in batch mode to all GIS sites in the field. This model has a number of disadvantages, the first of them being that similar systems (hardware and software) are required on all locations where the G.I.S is to be used, clients will not be multi-platform,and software licences must be purchased. The advantage is however that even with limited communication capabilities at all locations the G.I.S. is available with all its functionalities and fully interactive. This is the model adopted by Saclantcen for the experiments and demonstrations made up to now.

4.3. Data formats

The choices about data formats have an impact on data flow and are another very important issue. In a complex system "standardize" the software may help to solve the data exchange problems, but it is neither the only nor the best solution. Standardization of the data formats is a requirement for both the information system models: while for the client/server model the main problem is to define standards for the data sent from the data sources to the data fusion laboratory (from the data servers to the clients the format is depends upon the selected client software), for the multiple GIS model there is the freedom (and the need) to define the data formats both between the data sources and the central GIS and between this and the systems in the field.

The point here is not the absence of standards, but indeed the existence of too many standards. In principle the spread of Internet has pushed common, multiplatform formats for data; in addition there are specific GIS exchange standard that must be considered. An alternative solution (both models, data formats both between the data sources and the data fusion laboratory) is to give the originators the total freedom to decide the formats for the data they are sending. This approach was adopted at Saclantcen for REA 96, with some interesting results.

4.3.1. GIS exchange standard

There is an approved Nato GIS data exchange standard (STANAG 7074) that could be used with both models and for the multiple GIS model both between the data sources and the data fusion lab and from this to the systems in the field. The problem is that this standard is not likely to be widespread as long as it takes so much effort to obtain its description.

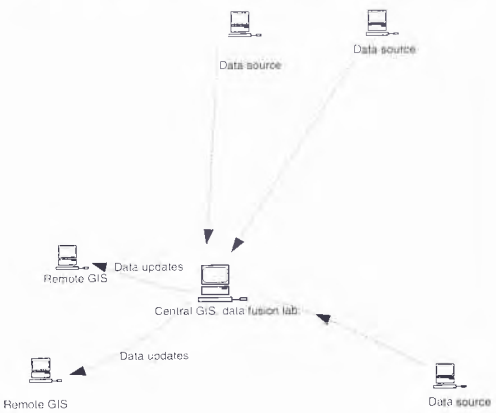

Fig 2. Multiple GIS Sylsems, periodically updated from a central system

Other standards are the STANAG 1116, and the old NODEF (Nato data exchange format). Apparently in practice these standards are not much used yet.

4.3.2. Internet standatrds(Images and graphics)

While GIF and JPEG are well established formats for rasterized images, there is no equivalent for vector plots. The various PS, EPS formats are often not compatible, and therefore my preference here is for pdf, the industry standard promoted by Adobe. Acrobat readers are free and exists for most Unix platforms, Windows and Mac; the pdf writers are also available for the same platforms, are not free but certanly affordable. The integration of Acrobat reader with Netscape is an important asset.

4.4. Users

For all information systems, including geographic information systems, there are different categories of users:who is loading the data, and who is accessing them making interrogations at various level of complexity, or just requesting and receiving the result of standard queries. For a Rea information system however there is a specific requirement: a simple interface as none of the user will be professionally involved with this system for a long period. There is little time for training, and in any case no convinience in it. The system must therefore be suitable for use by a large number of people with no specific experience who could receive as a maximum a training class of one day.

5. Solutions based on commercial systems

Having seen the requirements, let us have a look at what is commercially available to set up a system meeting these requirement. What follows is the result of an investigation that does not pretend to be complete; in addition the evolution of what is offered is so quick that whatever may be completed today, may not be so in two weeks time. In any case at the moment this is the situation.

5.1. The GIS

All major vendors of GIS software are offering or soon will offer systems based on Internet technology, as described in the client-server model above

ArcView Internet Map server:[1] It is the simplest technical solution: the maps are raster active image; the object selection is done as traditionally with active maps. A basic browser acts as client; zooms and pan are the result of interactions with the server. The client does very little, and the load imposed on communication lines continuosly resending raster images is high. My impression is that at this stage the product cannot be used in a complex application unless unlimeted bandwidth is available on the communication lines.

Intergraph GeoMedia Web Map[2] uses vector maps coded in "Active CGM." CGM is an old ISO standard for graphics, that has been enhanced to allow the definition of active objects. The Netscape browser may display active CGM coded maps and allow to interact with them if provided with a specific plug-in. The problem is that the plug-in is at the moment only available for Windows platforms.

Mapinfo MapInfo Proserver.[3] The client is a standard browser, with the same advantages and limitations of the ESRI (Arc view) solution.

None of these solutions seems to me satisfactory; The requirement to use vector maps seems to be understood (except by ESRI). Intergraph gives me the impression of moving in the right direction, but there is still a lot of work to do to improve the functionalities given to the client (zoom and pan, layers interaction, data requests validation,..); the client programmability is potentially available (Java and Javascript) but still is not offered, and therefore the interactivity that could be achieved with voice grade communication lines is limited.

5.2. The GIS building blocks.

While an effective Internet based GIS is still to come, some promising components of a future system are already on the market. One of these is Acrobat 3.0 and the related format (pdf) for vector based graphics. Being able to work in intimate connection with the browser (There is a Netscape plug-in to access Acrobat Reader 3.0), to handle active objects and vector maps, and to take advantage of servers capable of byte serving mode, it seems to have most of the functionalities required to display an interactive map on an Internet client.[4]

Another possible building block for an Internet based GIS is Quarck Immedia. Like Acrobat reader, its client is able to display vector based images with active objects. Opposite to Acrobat the client is an application specific browser; this is an advantage as the generic buttons, icons, windows of the Netscape browser do not occupy the screen of the GIS client. The disadvantage of Quarck Immedia software is that its client is at the moment only available for PC and Mac computers[5].

A third component is Netscape communicator with its ability to handle html documents structured in layers. It is at beta version level now, and demo's are available on Internet.[6]

5.3. The Data base

The alternative here is between GIS that use internal tables as relational data bases, and others that have the ability to relate geographical objects of the map to information in tables maintained by a conventional relational data base system, external to

the GIS. Most GIS offer both possibilities. I believe that the capabilities of traditional SQL based relational data base systems, and the complexity of some of the data we use make the linked exrternal data base a better choice. It is however desirable that the data base system has the specific ability to organize data geographically (such as the Oracle 7 Multidimension.) A considerable advantage of the internet technology is that there is no need to have on a single system the data server and the geographic server.

5.4. Data validation and uploading: Operational considerations

The data must be validated on the field, as close as possible to the acquisition; however the conversion made at the source of format to a common standard suitable for automatic upload is beyond what could be requested (given the time frame, the number of data sources and the limited amount of training that could be given, see the previous section). It is rather safer to agree to have the data sent in wathever format they are at the origin and have a central team who will take care of conversions and uploading. This operation may also include a second data validation phase.

5.5. The communication facilities

There is a separate presentation about communication facilities[1]; at the moment the two systems are Inmarsat B and cellular telephone. About cellular telephones the bad new is that what does the job better for us, due to its better range is the "old" analogue standard (TACS) GSM coverage at sea is much more limited.

The usable data rate is 9,6 k for Cellular telephone links and 64k (ISDN-like) for Inmarsat B.

6. Conclusions

The GIS is indeed an ideal information system, for information support to REA.

In a situation where data sources and users are distributed a client-server IS is the answer as it allows geographic information distribution to a large number of users. At the moment an emerging GIS that meets the REA requirements and in particular is suitable to work int server mode is not on the market, but the components are here, and the picture is changing every day. For the time being the multiple communicating GIS is an excellent alternative, better perhaps as long as the number of sites using GIS is limited.

---

[1] [3]http://www.esri.com/base/products/internetmaps/internetmaps.html

[2] [2] http://www.intergraph.com/iss/geomedia/webmap/

[3] [3]http://www.mapinfo.com/events/prosrv/proserver.html

[4] [4]http://www.adobe.com/prodindex/acrobat/main.html

[5] [5] http://www.quark.com/glry003.htm

[6] [6]http://home.netscape.com/comprod/products/communicator/index.html

[7] M.Max, E.Bovio, F.Spina "The shipping news from the seabed" GIS Europe, Vol 5, no.8, pp 16-18

[8] [7] E.Bovio, M.Max, F. Spina Communication technology in support to SACLANTCEN program of work In: Proceedings of the Rapid Environmental Assessment Conference, 10-13 March, 1997, Lerici (La Spezia) Itlay. SACLANTCEN Special Publication (in press).

[9] M.Max, F. Spina, E.Bovio The E-Map, Innovative COTS Software for Data Fusion and Interactive Communication for Rapid Environmental Assessment In: Proceedings of the Rapid Environmental Assessment Conference, 10-13 March, 1997, Lerici (La Spezia) Itlay. SACLANTCEN Special Publication (in press).

A NETWORK-BASED GIS FOR SUPPORT OF RAPID RESPONSE ENVIRONMENTAL ASSESSMENT.

Farid Askari[1*] and Erick Malaret[2]
[1] Naval Research Laboratory, Washington, D.C. 20375
Currently at
*SACLANT Undersea Research Centre
Email: askari@saclantc.nato.int

[2] ACT Corp, Herndon, VA, USA
Email: malaret@actgate.com

Abstract

An operational Rapid Environmental Assessment (REA) system requires timely access to geospatial information from multiple sensors and platforms. We describe an interactive network-based near-real-time image processing system that relies on high speed access to remotely stored data and processing power. The oceanographic and atmospheric applications of spaceborne synthetic aperture radar (SAR), and the various algorithms that are under development for extracting geophysical products from the imager will also be discussed briefly.

1. Background

This article presents an overview of a network-based Geographic Information System (GIS) architecture and its applications that is currently under development for support of NATO's rapid environmental assessment efforts. The objective is to demonstrate near real-time image processing capabilities, and interactive exchange of data between multiple, distributed users.

To address one of the central objectives of Rapid Response (RR) which is the dissemination of time-critical data and information, we have implemented an interactive network-based image processing system that relies on high speed access to remotely stored data and processing power.

The types of satellite data collected during RR-96 included: ERS-2 and RADARSAT synthetic aperture radar (SAR), NOAA Advanced Very High Resolution Radiometer (AVHRR), DMSP special sensor microwave imager (SSM/I) and the French SPOT multi-spectral imagery. The core of the remote sensing data for RR-96, however, consisted of AVHRR and ERS-2/SAR imagery. RADARSAT imagery, however, was not utilized during the experiment due to delays in receiving the data.

In support of RR-96, a total of 40 ERS-2 and one RADARSAT SAR images were acquired during the period August 12 to 5 October, 1996. The raw SAR data stream was first down-linked in real-time to the receiving station in West Freugh in UK. From there, the data was routed via high speed links to DRA Farnborough remote sensing facilities for image formation. Then, high resolution (150m) SAR images were sent via the INTERNET to Naval Research Laboratory (NRL) in Washington, D.C. for post-processing and image interpretation. Finally, the annotated feature maps were sent via the INTERNET from NRL to the SACLANTCEN World Wide Web (WWW) homepage. The approach used during the exercise by the image analyst was to view the low resolution (1.5 km) imagery, select regions and features of interest, and post the final products on the home page for the operator. While this approach served the demonstration purpose of the RR-96 which was the dissemination of data over the WWW, it severely restricted the end-user from interacting with the data or from choosing his/her own regions of interest. Thus it became clear that a new approach for information extraction was needed in order to realize the full benefits of high speed networking and to transform RR from a experimental concept to operational status.

In this initial phase, for demonstration purposes, we use only the ERS-2/SAR imagery, which because of it's high spatial resolution, is by far the most computationally demanding sensor, requiring massive amounts of storage, network throughput and processing power. A separate GIS module for multi-layered data integration and sensor fusion has been developed which uses a "hypercube" architecture (Figure 1), the details of which are given in [1].

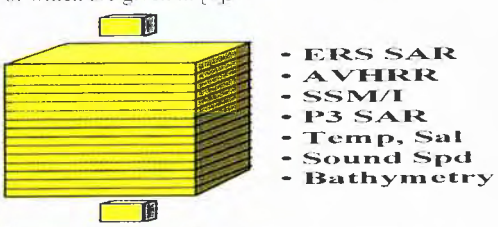

Figure (1) Multi-layered geo-referenced data

Here, we focus on the networked-based image browser that was developed for the ERS-2/SAR system.

2. The Architecture

The basic components of the architecture consist of

the image server (IS) system, the network, and the applications and tools for the client (Figure 2). It is assumed that all clients have access to the IS via a modem (14.4 kb/s) or a high speed network, and interact with the host using a WEB browser. Once connection is established with the server, two possible scenarios exist. In the first scenario it is assumed that client A has limited computing power in terms of speed, memory, and storage. In this case we have configured a system in which the data, the computing power, and algorithms all reside on the host/server side. The data sets and client/applications are not collocated. The satellite imagery is located and stored remotely on the server, and is supplied to the client/application on as needed basis by means of a modem or high speed-network. In the second scenario, client B has significantly more computing power allowing downloading and use of locally resident processing tools.

In the operational environment, the first scenario is more likely to occur. As most field operators do not have access to high speed computing or large storage devices, it is often impractical to transfer large volumes of data. For example, the SAR data storage requirements collected during RR-96 exceeded 5 GB of disk space. The other consideration is that there may be multiple sources of data which may need maintenance and updates. These tasks are typically performed at a fusion center and should not involve or put unnecessary burdens on the client. Given these constraints, an innovative approach to distributed computing is required in order to provide the user with maximum flexibility and interactions.

2.1. Hardware/software Configuration

The IS system which stores, retrieves, and processes the client-supplied queries consists of the following hardware and software components:

- 200 MHz Pentium Pro operating with single or multiple processors.
- ProView image processing software and ProViewWeb server.
- CD-ROM jukebox.
- Two 9 GB hard drives.

The IS may consist of a single Pentium Pro machine with one or multiple processors, or a series of coordinated platforms operating in parallel. The main engines for image processing and hyper text markup language (HTML) file generation are the ProView and ProViewWeb software systems. All the applications, including sensor fusion, multi-layered data synergism, automatic feature detection, and extraction of geophysical parameters from remotely sensed imagery were developed using ProView and ProViewWeb which are available commercially. These are highly versatile, PC-based languages (developed by ACT), that operate under the MS Windows 3x and NT, as 32 bit application. One of the unique capabilities of ProView is that it permits the processing of large volumes of data using virtual image variable, that is, images can be large as the disk space.

Also ProViewWeb allows for interactive image processing, user defined products, visualization, data queries, and HTML file generation

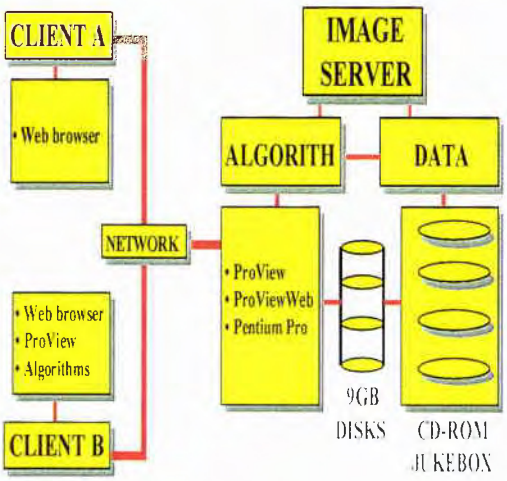

Figure (2) The system architecture

On the server side, SAR data is organized in three layers and in two different spatial resolutions. In the first layer, the data is organized as a series of mosaics covering the RR operating areas (Figure 3).

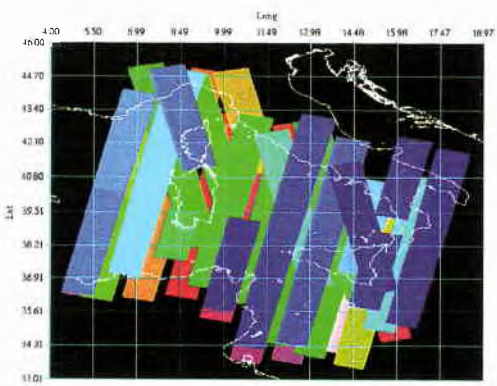

Figure (6) Edge-enhanced image

In this layer, the client can choose imagery by date, by geographic coordinates, or by specifying the satellite orbit number. In the second layer, the client can access low resolution (1.5 km) SAR maps that are georeferenced and are individually stored on SCSI disks. The low resolution images (Figure 4) provide a synoptic view of the regions and features of interest

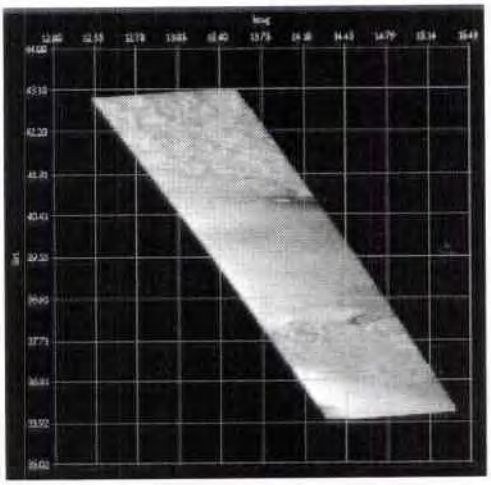

Figure (4) Low resolution synoptic SAR image. ESA/Copyright

In the third layer, the client specifies a sub-region (512x512) of his choice which is located within the low resolution image. At this point the IS retrieves high resolution (150 m) image subsets from a CD-ROM jukebox. Figure 5 is an example of a sub-region from the southern tip of Sicily. If the clients have the computing capabilities they can download raw data and proceed with their own applications. However, if there are minimal computing capabilities, clients can utilize the remote image processing power that resides on the server side. For both cases, several image processing algorithms have been developed for the client.

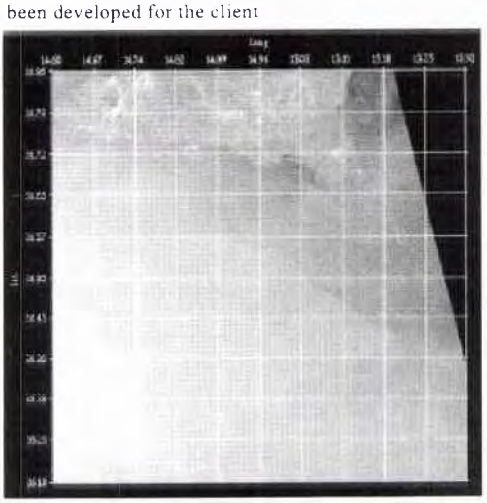

Figure (5) High resolution sub-mage ESA/Copyright

2.2. Algorithms

Improvements in satellite technology have significantly affected our ability to assess the environment. At the same time, however, the complexities and the volume of information that can be processed by human interpreters have dramatically increased. To tackle this complex, multidimensional problem some degree of automation is required. Here we have designed a series of algorithms to assist in extracting quantitative information.

- Edge detection.
- Two-dimensional directional spectra.
- Cluster seeking.
- Wind vector retrieval.
- Sensor fusion.
- Automatic shape detection.

Figure 6 is a result of applying a edge-detection filter to the previous image (figure 5).

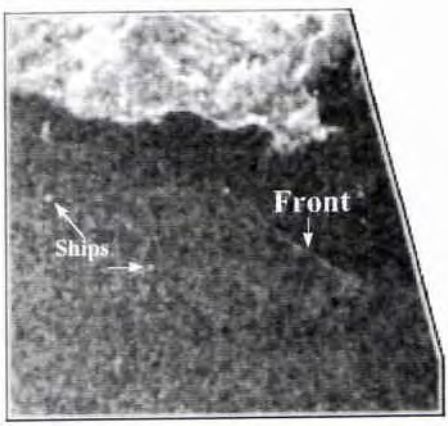

Figure (6) Edge-enhanced image

3. Applications

SAR imagery can provide rapid assessment of the background oceanographic and atmospheric environment over a variety of spatial and temporal scales. Because of its high spatial resolution and all-weather capabilities, SAR can also detect manmade features such as oil spills and ships/wakes. Below is a partial list of oceanographic and atmospheric features that are readily identifiable in SAR imagery [2]:

- Internal and surface waves.
- Current boundaries and types.
- Fronts and eddies.
- Bottom signatures.
- Wind/Gust fronts.
- Atmospheric internal gravity waves.
- Katabatic winds.
- Cellular convection cells.

Thunderstorms, rain cells, and squall lines.

For tactical applications, however, one must go beyond simple feature identifications and detection. The goal is to derive as much quantitative information and geophysical products from a combination of sensors as possible given the spatial, spectral, and temporal constraints of the sensors. Some of the SAR-derived geophysical products include: locations and types of oceanic/atmospheric fronts, wind speed and direction, propagation direction and height of shoaling waves, magnitudes of littoral currents, and locations of coastal geomorphological features such as submarine sand waves and sand banks, beach berms and troughs, submarine canyons and headlands. More importantly, subsequent to detection and identification, the characteristic time scales for the various physical processes must be defined. The ultimate goal is to provide the end-user with information within tactically usable time scales. The usable-time-scale is, however, a function of two temporal variables; the "delivery-time" through the network, and the "age" or "life-span" of the physical processes. The "delivery-time" can vary for each client depending on the system's communication bandwidth and throughput requirements. Assuming that an atmospheric gust front and an oceanic front have been identified in a SAR image. We know from dynamical principals that atmospheric gust fronts can form and dissipate over periods of several minutes, while oceanographic fronts can last over periods of several days. Operationally, it takes about four to five hours from the time of down-link to digitally process a SAR image. Hence, from the standpoint of the end-user, information regarding the gust front may be tactically useless, while the information regarding the oceanic front remains tactically useful. A strategy for defining the "life-span" or "age" of the features seen in the imagery must be devised in accordance with physically-derived scaling parameters [3].

4. Conclusions

With the recent advances in high-speed networking technology, it is now possible to deliver to the end-user time-critical oceanographic/atmospheric information on a variety of spatial scales. An operational REA system requires timely access to geospatial information from a multitude of sensors and platforms. Here, we implemented the framework for a near real-time image processing architecture that allows high-speed access to information which is stored on a remote host. The challenge is to deliver to the end-user useful information faster and in a more automatic fashion using multiple distributed data sources.

5. Acknowledgments

This work was sponsored by SPAWAR. The authors wish to thank DRA/UK for supplying the ERS-2/SAR imagery which made this work possible.

References

[1] F. Askari, et. al."A PC-based remote sensing system for detection and classification of oceanic fronts", Proceeding of IGARSS, Lincoln, Nebraska, May, 1996.

[2] W. Alpers, "Measurement of meso-scale oceanic and atmospheric phenomena by ERS-1 SAR" The Radio Sci. Bull., No 275, Dec 1995.

[3] I. Orlanski, "A rational subdivision of scales for atmospheric processes," *Bull. Amer Meteoro. Soc.*, vol. 56, pp.527-530, May 1975.

Author Index

SACLANTCEN CONFERENCE PROCEEDINGS SERIES CP-44

Rapid Environmental Assessment

edited by

E. POULIQUEN
North Atlantic Treaty Organization
SACLANT Undersea Research Centre, La Spezia, Italy

A.D. KIRWAN,Jr
Old Dominion University, Norfolk, VA, USA

and

R.T. PEARSON
Supreme Allied Command Atlantic (SACLANT) , Norfolk, VA, USA

The 40 papers presented at this conference, describe rapid environmental assessment in the specific context of oceanography and marine geology applied to antisubmarine, mine and amphibious warfare. The systems described include: remote sensing, geographical information systems, measurement systems, assimilation and modelling. A synopsis of the conference is presented as a nine-page executive summary.

ISBN 88-900194-0-9

9 788890 019401

NATO SACLANT Undersea Research Centre